DESIGN AND SCREENING OF BIARYL PHOSPHITE-BASED LIGAND LIBRARIES FOR ASYMMETRIC REDUCTION AND C-C AND C-X BOND FORMING REACTIONS

Javier Mazuela Aragón

Dipòsit Legal: T.1471-2012

UNIVERSITAT ROVIRA I VIRGILI
DESIGN AND SCREENING OF BIARYL PHOSPHITE-BASED LIGAND LIBRARIES FOR ASYMMETRIC REDUCTION AND C-C AND C-X BOND FORMING REACTIONS
Javier Mazuela Aragón
Dipòsit Legal: T.1471-2012

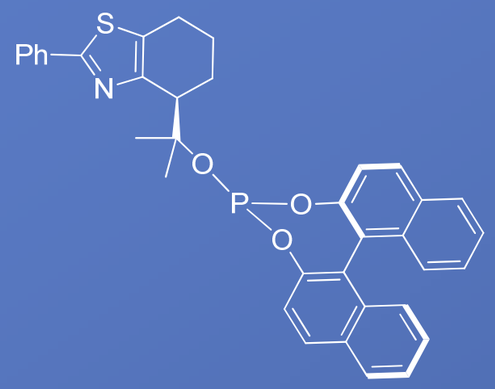

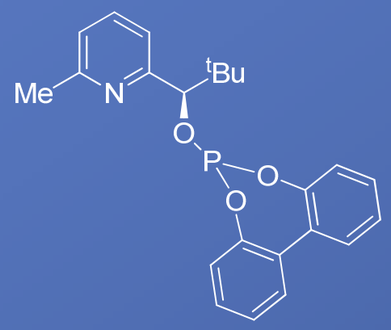

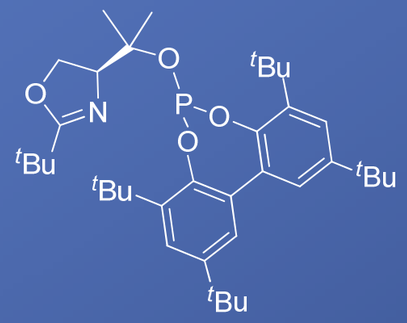

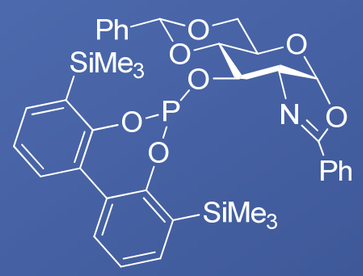

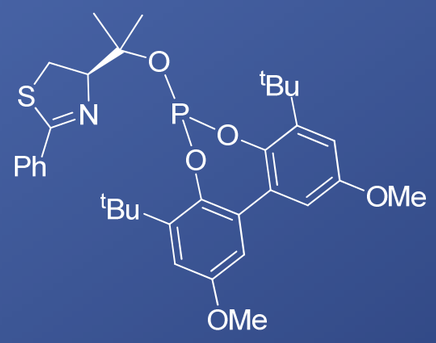

Design and screening of biaryl phosphite-based ligand libraries for asymmetric reduction and C-C and C-X bond forming reactions

Design and screening of biaryl phosphite-based ligand libraries for asymmetric reduction and C-C and C-X bond forming reactions

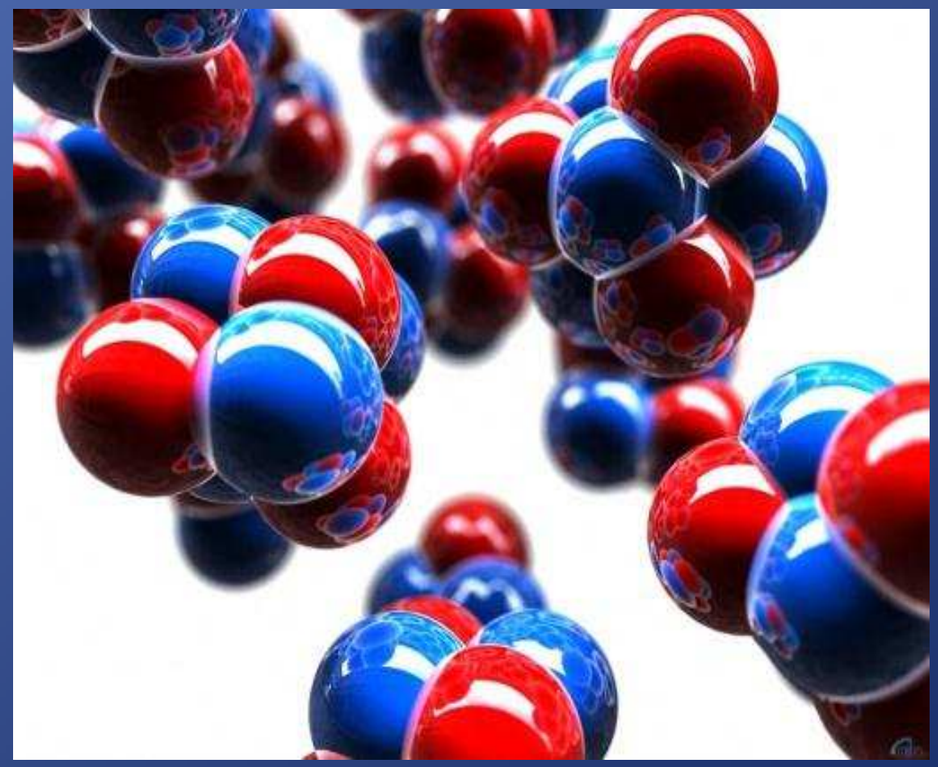

Javier Mazuela
Ph. D. Thesis
October 2012

Javier Mazuela Aragón

Design and screening of biaryl phosphite-based ligand libraries for asymmetric reduction and C-C and C-X bond forming reactions

PhD-Thesis

Supervised by Prof. Montserrat Diéguez

and Dr. Oscar Pàmies

Departament de Química Física i Inorgànica

UNIVERSITAT ROVIRA I VIRGILI

TARRAGONA

Octubre 2012

UNIVERSITAT ROVIRA I VIRGILI
Departament de Química Física i Inorgànica

PROF. MONTSERRAT DIÉGUEZ FERNÁNDEZ i DR. OSCAR PÀMIES OLLÉ, Catedràtica i Professor Agregat del Departament de Química Física i Inorgànica de la Facultat de Química de la Universitat Rovira i Virgili

FEM CONSTAR:

Que la present memòria que porta per títol "**DESIGN AND SCREENING OF BIARYL PHOSPHITE-BASED LIGAND LIBRARIES FOR ASYMMETRIC REDUCTION AND C-C AND C-X BOND FORMING REACTIONS**", que presenta JAVIER MAZUELA ARAGÓN per a obtenir el grau de Doctor en Química, ha estat realitzada sota la nostra direcció al Departament de Química Física i Inorgànica de la Universitat Rovira i Virgili i compleix amb els requeriments per a poder optar a Menció Europea.

Tarragona, Octubre de 2012

Prof. Montserrat Diéguez Fernández Dr. Oscar Pàmies Ollé

Agraïments/Agradecimientos/Acknoledgment/Erkännande

Después de sangre, sudor y lágrimas (sobretodo sangre, que no he parado de cortarme…) he acabado mi tesis. Sé que prometí que no iba a agradecer a nadie esta tesis, al fin y al cabo es mía; pero sería faltar a la realidad ya que durante este periodo de tiempo (5 años, un lustro completo) muchísima gente me ha apoyado y sin ellos todo esto no hubiera sido posible. Como bien sabéis, no soy hombre de muchas palabras y mis dedicatorias son míticas (Suerte!...Javi).

Para empezar, agradecer su apoyo mis directores de tesis la Prof. Montserrat Diéguez y el Dr. Oscar Pàmies que confiaron en mí incluso antes de que yo mismo estuviera decidido a hacer el doctorado (recuerdo una mañana haciendo RMN's de ligandos durante el proyecto de final de carrera cuando Oscar me dijo que tenía potencial de sobra para hacer el doctorado y todo lo que me propusiera. Sin su ayuda, apoyo y motivación no hubiera sido capaz de acabar esta tesis.

También quiero agradecer su apoyo al resto de profesores del grupo: a Carmen y Sergio y las cenas de grupo míticas en Altafulla; a Aurora, a Núria, a Anna, a Pilar, a Yolanda y, especialmente a Elena (que ha tenido que "soportar" a Amadeu, un buen elemento). También agradezco a los doctores Cyril Goddard y Henrik Gulyás por toda la ayuda durante estos años. Ha sido un placer trabajar en equipo con todos vosotros durante estos años.

A María José, Josep María, Arantxa (siempre estará entre nosotros), Jordi (que Cthulhu te salve) y, especialmente, a Raquel, que nos habéis tenido que soportar (tarea difícil en muchas ocasiones) para que siguiéramos todas las normas del laboratorio. Un agradecimiento especial a Ramón, que ha sufrido todas las horas de RMN conmigo.

During this thesis, I have been for really long time in Sweden working in PGA's group (Prof. Pher G. Andersson in Uppsala) and PON's group (Prof. Per-Ola Norrby in Gothenburg). The first time I moved to Uppsala I was a Master student in 2007, and I was completely lost (my first time in a foreign lab). I really want to thank all the people that helped me during my period there: Johan, Alex, Païvi, Tamara, Jia-Qi, Taigang and Lina and, of course, Prof. Pher G. Andersson. I have done several trainings in Gothenburg with Prof. Per-Ola Norrby (4 times there, for nearly 7 months in total). I learned a lot of new things there, and Prof. Norrby introduced me to the computational chemistry. I want to thank Prof. Norrby for all his patience and help also to all the people in Gothenburg Jonathan, Charlotte, Petra and Sten.

A las doctoras Yvette y Eva por enseñarme a trabajar en el laboratorio durante los primeros meses de doctorado. Yvette, me enseñaste a trabajar en el laboratorio, fuimos a un congreso increíble en Estocolmo con Marta y Amadeu y ahora puedes ser miembro del tribunal de mi tesis (se buena por favor…). Eva, tu eres la responsable que me integrara en el grupo lanzándome corchos y siempre con una sonrisa en la cara, como nos hemos divertido en el laboratorio.

También quiero recordar a todos los doctores que presentaron tesis durante este periodo de tiempo: Aitor (la jipa será recordada), Jesús, Bianca, Isa, Clara y Vanesa. Os he admirado mucho durante estos años. También a Ali que siempre estuvo dispuesto a echar una mano cuando se le necesitaba.

Durante estos años muchos doctorandos han pasado por el grupo de visita, cada uno aportando su granito de arena, así que también me acuerdo de Benjamin, Francesca, Lina y Matteo que han compartido laboratorio conmigo. Y especialmente a Olivier, que bien nos lo pasamos en Florencia y Roma.

Quiero recordar a todos los que han compartido el camino del doctorado conmigo y que han apoyado en el día a día.

Primeramente, a Carol, Martha, Ariadna y, especialmente, Verónica, la persona más implicada en la química que conozco y con un conocimiento increíble; los congresos han sido inolvidables. A todo el grupo del boro, Cristina S, Jessica C, Cristina P (animo que ya estas acabando, solo falta lo último) y a los "novatos" Gerard y Xavi (para la próxima vez leeros el manual de calidad del grupo). Al Dr. Manuel, que eres un espejo en el que todos nos queremos reflejar. También a Marlene y Laia, que han compartido conmigo estos últimos meses. A todo el grupo de heterogéneas que ha compartido el camino conmigo, Dra. Dolores y Dra. Tati.

¿Personaje (o Nanomarquesa), que te pensabas que me iba a olvidar de ti? Oyeeeeee!! Me he divertido muchísimo contigo y nos hemos reído juntos hasta no poder más (no sé cómo te lo montas que todas las desgracias te pasan a ti). Elí, todo este tiempo contigo ha sido increíble, eso sí, cuando se te mente algo en la cabeza se transforma en un caso perdido… Sin vosotras dos el laboratorio no habría sido el mismo y, cuando no estáis, os echamos de menos (es que no sabemos de qué hablar). También quiero recordar a Javier, Bernabé, Alberto, Jamin y Jorge, por las risas que hemos compartido. Y a Oriol (ahora refugiado en el ICIQ) con el que me he reído mirando FC hasta no poder mas (y con los piques en el Striker, ya pronto te tocara a ti….).

Los siguientes son los que han estado día a día compartiendo conmigo proyectos, grupo y laboratorio (os tendría que hacer un monumento por soportarme). A la doctora Mercé, empezamos juntos en el labo (y el primer día ya la estábamos liando) y hemos compartido muchísimos momentos juntos. Acabaremos los dos al mismo tiempo y te deseo toda la suerte del mundo una vez acabes en la universidad. A Sabina, ha sido un placer trabajar contigo (aunque tus compuesto eran apestosos) y haber compartido tiempo y trabajo contigo; que te vaya bien por Sassari. Los novatos (bueno no tan novatos ya, que tienen que ascender rápido) Marc y Jéeessica (sí, con tres e's, que se note la pronunciación "vallenca") ha sido un placer trabajar con vosotros; espero que hayáis aprendido mucho, yo he intentado enseñaros tanto como he podido de química (al final todo depende de los resultados jejeje).

A todos los orgánicos con los que he compartido este viaje. Suerte a todos!!

Sr. y Sra. Bonet, como iba a olvidarme de vosotros, sois los mejores amigos que puedo tener. Amadeu, hemos compartido juntos 10 años (que se dice rápido) y me has demostrado día a día que siempre puedo contar contigo cuando te necesite. No creo que haga falta que te lo digo, pero tienes un amigo para toda la vida y cuando me necesites allí estaré (Estocolmo no esta tan lejos de Bristol, en el mapa solo son unos pocos centímetros. Angy (ex-señorita Balanta, actualmente señora Bonet jejeje) ha sido un placer haberte conocido. Simplemente no tengo palabras para describir el aprecio que os tengo. Muchas gracias por ser como sois (lo bueno si breve, dos veces bueno).

Finalmente, quiero agradecer su apoyo a todos los amigos de toda la vida que han estado a mi lado siempre que los he necesitado (no hace falta que os nombre, todos sabéis quien sois y no nos van estas cursiladas), a mi familia, que ha sido un pilar básico en mi vida que me han enseñado que desde la humildad, el esfuerzo y el respeto se puede conseguir cualquier cosa y a todos los miembros del AJJRR (que Cthulhu, la muerte de warhammer y los dados de Gary Gygax os guíen).

Tan solo me falta una persona a la que agradecer su apoyo durante los mejores años de mi vida, la más importante de todas. Merian, Sin ti la tesis nunca hubiera sido posible. Petarda, todo lo que pueda escribir aquí no representa ni una ínfima parte de lo que siento por ti. Juntos hemos compartido muchísimos buenos momentos y vamos a seguir compartiéndolos durante toda la vida, porque para mí no existe la posibilidad de otra persona que no seas tú. Te quiero.

Gràcies/Grácias/Thanks/Tack

Table of contents

Structure of the thesis

The thesis is divided into nine chapters.

- Chapter 1. *Introduction*. This chapter first presents the importance of metal asymmetric catalysis in the synthesis of enantiomerically pure compounds. An important step in this synthesis is the design and preparation of chiral ligands. Among them, several families of heterodonor P-N containing ligands (mainly phosphine and phosphinite) are presented. These ligands are applied to four asymmetric catalytic reactions, which are reviewed in detail in this chapter. For each reaction, the antecedents, performance and main achievements are discussed. The state-of-the-art and current needs in this field justify the objectives of the thesis.

- Chapter 2. *Objectives*. Based on the aspects discussed in chapter 1, this chapter presents the objectives of the thesis. These involve the synthesis and application of several large modular phosphite-containing ligand libraries in asymmetric catalysis.

- Chapter 3. *Asymmetric hydrogenation of minimally functionalized olefins*. This chapter contains five sections on the development and application of five large modular phosphite-nitrogen ligand libraries in Ir-hydrogenation of minimally functionalized olefins. The first section, *pyranoside phosphite/phosphinite-oxazoline ligands for the highly versatile and enantioselective Ir-catalyzed hydrogenation of minimally functionalized olefins. A combined theoretical and experimental study*, includes the first successful application of a phosphite-oxazoline ligand library, derived from D-glucosamine, in the Ir-hydrogenation of a wide range of *E*- and *Z*- trisubstituted and 1,1-disubstituted alkenes. The results compete favorable with the best ones reported in the literature. This section also includes DFT calculation in order to explain the origin of enantioselectivity. The second section, *iridium phosphite-oxazoline catalysts derived from hydroxyl amino acids for the highly enantioselective hydrogenation of minimally functionalized alkenes*, describes the successful application of a new phosphite-oxazoline ligand library, derived from available hydroxyl amino acids, in the Ir-hydrogenation of minimally functionalized olefins, including the use of propylene carbonate as environmentally friendly solvent. Comparable excellent enantioselectivities than previous pyranoside phosphite-oxazoline ligands were obtained. The third section, *expanded scope of the asymmetric Ir-catalyzed hydrogenation of minimally functionalized olefins using phosphite-thiazoline ligands*, describes the synthesis and application of phosphite-thiazoline ligands in the Ir-hydrogenation of minimally functionalized olefins. These phosphite-thiazoline ligands are based on previous hydroxyl-aminoacid derived phosphite-oxazoline ligands, in which thiazoline moiety was used instead of an oxazoline motif. In the next two sections we focus our research in the application of heterodonor-phosphite-nitrogen ligands that include more robust N-donor groups than oxaxolines. In this respect, the fourth section, *adaptative biaryl phosphite-oxazole and phosphite-thiazole ligands for asymmetric Ir-catalyzed hydrogenation of alkenes*, describes the synthesis and application of a new phosphite-oxazole/thiazole ligand library in the Ir-hydrogenation of minimally functionalized alkenes. The fifth section, *a phosphite-pyridine/iridium complex library as highly selective catalysts for the hydrogenation of minimally functionalized olefins*, describes the first successful application of a phosphite-pyridine ligand library in the present process.

- Chapter 4. *Asymmetric allylic substitution reactions.* This chapter contains three sections, on the application of three phosphite-nitrogen ligand libraries for asymmetric Pd-catalyzed allylic

substitution reactions. The first section, *phosphite-thiazoline versus phosphite-oxazoline for Pd-catalyzed allylic substitution reactions. A case for comparison*, compares the application of the phosphite-thiazoline ligand library, previously synthesized in chapter 3, with related phosphite-oxazoline ligands in the Pd-allylic substitution of a wide range of mono-, di- and trisubstituted substrates using several carbon nucleophiles, including the less studied α-substituted malonates and β-diketones. This section also discusses the synthesis and characterization of the Pd-π-allyl intermediates in order to provide greater insight into the origin of enantioselectivity. In the next two sections we focus our research in the application of heterodonor-phosphite-nitrogen ligands that include more robust N-donor groups than oxaxolines. Thus, the second section, *a new class of modular P,N-ligand library for asymmetric Pd-catalyzed allylic substitution reactions. A study of the key Pd-π-allyl intermediates*, includes the successful evaluation of the phosphite-oxazole/thiazole ligand library, previously synthesized in chapter 3, in the Pd-allylic substitution of mono-, di- and trisubstituted substrates. This section also includes NMR and DFT studies on the Pd-π-allyl intermediates. The third section, *a new modular phosphite-pyridine ligand library for asymmetric Pd-catalyzed allylic substitution reactions. A study of the key Pd-π-allyl intermediates*, discusses the first successful application of the phosphite-pyridine ligand library, previously synthesized in chapter 3, in the Pd- allylic substitution reactions of di- and trisubstituted substrates using C-, N- and O-nucleophiles.

- Chapter 5. *Asymmetric Heck reaction.* This chapter contains two sections on the application of two phosphite-nitrogen ligand libraries for asymmetric Pd-catalyzed intermolecular Heck reaction. The first section, *biaryl phosphite-oxazolines from the chiral pool: Highly efficient ligands for the asymmetric Pd-catalyzed Heck reaction*, discusses the successful application of a phosphite-oxazoline ligand library in the Pd-catalyzed Heck reaction of several substrates and triflates under thermal and microwave conditions. This large modular ligand library contains three main ligand structures that have been designed by systematic modifications of one of the most successful ligand family (PHOX). The results compete favorably with the best ones reported. The second section, *phosphite-oxazole/thiazole ligands in asymmetric intermolecular Heck reaction*, describes the first application of phosphite-oxazole/imidazole ligands in the intermolecular Pd-catalyzed Heck reaction.

- Chapter 6. *Asymmetric hydroformylation*. This chapter contains three sections. The first section, *Rh-catalyzed asymmetric hydroformylation of heterocyclic olefins using chiral diphosphite ligands. Scope and limitations*, discusses the successful application of a large series of diphosphite ligands in the Rh-catalyzed asymmetric hydroformylation of several heterocylic olefins. The second section, *fine-tunable monodentate phosphoroamidite and aminophosphine ligands for Rh-catalyzed asymmetric hydroformylation*, describes the application of a biaryl-based monophosphoroamidite and aminophosphine ligand library in the asymmetric hydroformylation of several vinylarenes and heterocyclic olefins. In the third section, *Rh-catalyzed hydroformylation of 1,1'-disubstituted terminal enol esters*, we report our preliminary results on the Rh-catalyzed hydroformylation of isopropenyl acetate.

- Chapter 7. *Conclusions*. This chapter presents the conclusions of the work presented in this thesis.

- Chapter 8. *Resum (Summary)*. This chapter contains a summary of the thesis in catalan.

- Chapter 9. The *Appendix* contains the list of papers and meeting presentations given by the author during the period of development of this thesis. This chapter also includes the reprint of one paper, "*Furanoside phosphite-phosphoroamidite and diphosphoroamidite ligands applied to asymmetric Cu-catalyzed allylic substitution reactions*" not discussed in this thesis, in which I have participated during my PhD with the synthesis and evaluation of some substrates.

Chapter 1

Introduction

1. Introduction

Fine chemicals and natural product chemistry rely on enantiomerically pure compounds. The growing demand for enantiomerically pure compounds has stimulated the search for highly efficient asymmetric processes that display high selectivity and activity, minimum consumption of energy and minimum generation of byproducts.[1] There are many applications in which only one of the enantiomers has the desired properties while the other enantiomer is either inactive or has undesirable side-effects. The discovery of synthetic routes for preparing enantioenriched compounds is therefore one of the most persistently pursued goals in chemistry. Asymmetric catalysis is one of the most attractive approaches, because it can provide very high reactivity and selectivity, and is environmentally friendly.[1] Usually with this strategy, a transition-metal complex containing a chiral ligand catalyzes the transformation of a prochiral substrate to one enantiomer as major product.The importance of asymmetric catalysis is reflected by the many publications in this field and the Nobel Prize award in 2001 to W. S. Knowles, K.B. Sharpless and R. Noyori and in 2010 to E. Negishi, R. F. Heck and A. Suzuki.[1]

To reach the highest levels of reactivity and selectivity in catalytic enantioselective reactions, several reaction parameters must be optimized. Of these, the selection and design of the chiral ligand is perhaps the most crucial step.[1] In this respect the use of highly modular ligand scaffolds is desirable, because it facilitates the synthesis and screening of series of chiral ligands (ligand libraries) in the search for high activities and selectivities for each particular asymmetric catalytic reaction. One of the simplest ways to obtain chiral ligands is to transform or derivatize natural chiral compounds, thus making tedious optical-resolution procedures unnecessary.[1]

In this context, this thesis focuses on the development of new chiral ligand libraries, the synthesis of new catalyst precursors and their application in the enantioselective Ir-catalyzed hydrogenation, asymmetric Pd-catalyzed allylic substitution, asymmetric Pd-catalyzed Heck reactions and Rh-catalyzed hydroformylation. In following sections, we describe the background of each of the catalytic reactions studied in this thesis.

1.1. Asymmetric hydrogenation of minimally functionalized olefins

Because of its high efficiency, atom economy and operational simplicity, the metal-catalyzed asymmetric hydrogenation using molecular hydrogen of properly selected prochiral olefins can be a sustainable and direct synthetic tool for preparing enantiopure compounds (Scheme 1.1).[1]

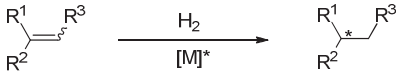

Scheme 1.1. Asymmetric M-catalyzed hydrogenation of prochiral olefins.

Whereas the reduction of olefins containing an adjacent polar group (i.e. dehydroamino acids) by Rh- and Ru-catalyst precursors modified with phosphorus ligands has a long history, the asymmetric hydrogenation of minimally functionalized olefins is less developed because they have no adjacent polar group to direct the reaction.[2] Iridium complexes with chiral P,N-ligands have

become established as one of the most efficient catalysts for the hydrogenation of minimally functionalized olefins, and their scope is complementary to those of Rh- and Ru-diphosphine complexes.[1]

1.1.1. Mechanism

Although the mechanism of olefin hydrogenation by Rh-catalysts is well understood,[3] the mechanism that uses chiral Ir-catalysts is not, despite having been investigated both experimentally and computationally. In the first case, there is enough evidence to support a Rh^{I}/Rh^{III} mechanism in which substrate chelation to metal plays a pivotal role in stereodiscrimination, but in the second four different pathways have been proposed (two of them involving Ir^{I}/Ir^{III} intermediates[4] and the other two Ir^{III}/Ir^{V} species[5]). Andersson and coworkers have recently used DFT calculations and a full, experimentally tested combination of ligands (mainly phosphine/phosphinite,N) and substrates to study all of the possible diastereomeric routes of the four different mechanisms.[6] Their studies agree with the two already proposed catalytic cycle involving Ir^{III}/Ir^{V} intermediates;[5] however, they fail to distinguish the two Ir^{III}/Ir^{V} mechanisms. One of the mechanisms involves an Ir^{III}/Ir^{V} migratory-insertion/reductive-elimination pathway (labeled as 3/5-MI in Scheme 1.2)[5c] whereas the second mechanism uses an Ir^{III}/Ir^{V} σ-metathesis/reductive-elimination pathway (labeled as 3/5-Meta in Scheme 1.2).[5a,b]

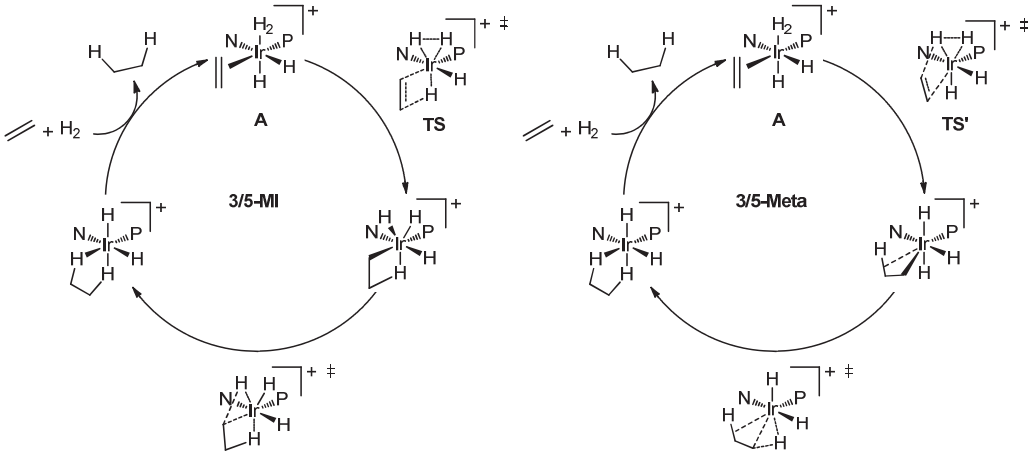

Scheme 1.2. 3/5-MI and 3/5-Meta catalytic cycles for the Ir-hydrogenation of unfunctionalized olefins.

From these cycles, it has been demonstrated that the π-olefin complex **A** and the transition states for the migratory-insertion in 3/5-MI (**TS**) and the σ-metathesis in 3/5-Meta (**TS'**) are responsible for the enantiocontrol in iridium hydrogenation.[6] It has been demonstrated that the enantioselectivity can be reliably obtained from the calculated relative energies of migratory insertion transition states.[6] Very recently Hopmann and coworkers performed a computational study using a phosphine-oxazoline (PHOX)-based iridium catalyst.[7] At the same time our group, in conjunction with Norrby's and Andersson's groups have also performed DFT calculation using Ir-phosphite-oxazoline ligands (see Chapter 3, Section 3.2). Both studies confirm that the hydrogenation of unfunctionalized olefins follows the 3/5-MI pathway.

1.1.2. Ligands

A breakthrough in the hydrogenation of unfunctionalized olefins came in 1997 when Pfaltz and coworkers used phosphine-oxazoline ligands PHOX **1**[8] (Figure 1.1) to design [Ir(PHOX)(cod)]PF_6 (cod = 1,5-cyclooctadiene), a chiral analogue of Crabtree's catalyst ([Ir(py)(PCy_3)(cod)]PF_6)[9] that enantioselectively hydrogenated prochiral imines.[10] Although this catalyst also hydrogenated prochiral olefins highly enantioselectively, it was unstable under the reaction conditions. Pfaltz and coworkers overcame this problem by changing the catalyst anion to [(3,5-$(F_3C)_2$-$C_6H_3)_4B]^-$ ($[BAr_F]^-$). The result was [Ir(PHOX)(cod)]BAr_F (Figure 1.1), an active, enantioselective, and stable catalyst library for olefin hydrogenation. These catalysts have been successfully used for the asymmetric hydrogenation of a limited range of alkenes (mainly trisubstituted *E*-olefins, Figure 1.1).[8,11] Bolm's group have recently successfully applied Ir-PHOX catalytic systems in the hydrogenation of α,β-unsaturated ketones (ee's up to 99%, Figure 1.1).[12] Hydrogenation of α,β-unsaturated ketones leads to the formation of ketones with α-chiral carbon centers; which are an important group of compounds in organic synthesis.[13]

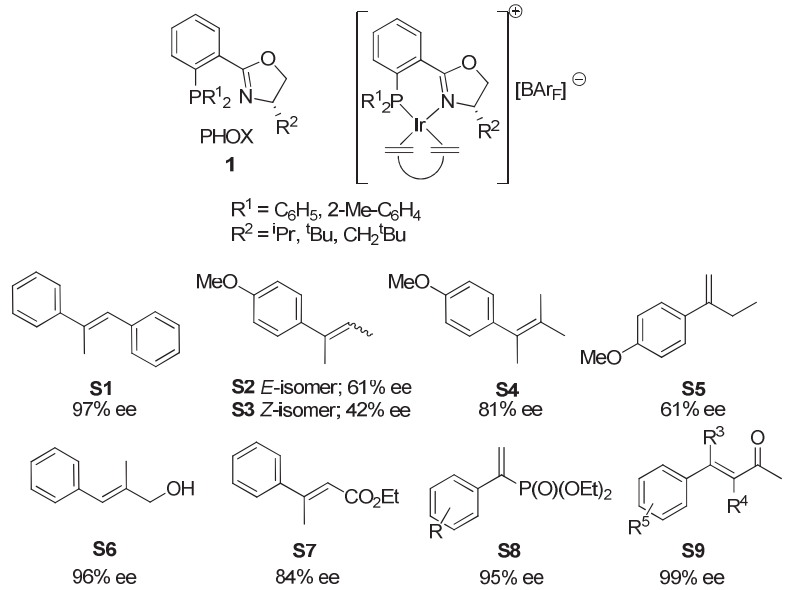

Figure 1.1. Selected Ir-hydrogenation results using PHOX ligands **1**.

Since then, the composition of the ligands has been extended by initially replacing the phosphine moiety with a phosphinite or a carbene group, and the oxazoline moiety with other N-donor groups (such as pyridine, thiazole and oxazole).[2] The structure of the chiral ligand's backbone has also been modified. More recently, the use of iridium catalysts containing P,S[14] and P,O[15] heterodonor ligands have been also developed. All, these modifications have led to the discovery of new ligands that have considerably broadened the scope of Ir-catalyzed hydrogenation. Of them all, chiral Ir-P,N compounds have been the most studied and they have therefore become extremely useful catalytic precursors for the hydrogenation of unfunctionalized tri- and tetra-substituted olefins.[2] The most successful P,N-ligands contain a phosphine or

phosphinite moiety as P-donor group and either an oxazoline, pyridine, oxazole, or thiazole as N-donor group.

In the next sections we summarized the most relevant catalytic data published for asymmetric hydrogenation of minimally functionalized olefins with P,N-ligands.

1.1.2.1. Phosphorus-oxazoline ligands

Inspired by the work of Pfaltz and coworkers using PHOX ligands, several other successful phosphorus-oxazoline compounds have been developed for this process (Figure 1.2). Most of them are phosphine-oxazoline, *N*-phosphine-oxazoline and phosphinite-oxazoline ligands and to a lesser extent phosphite/phosphoroamidite-oxazoline ligands.

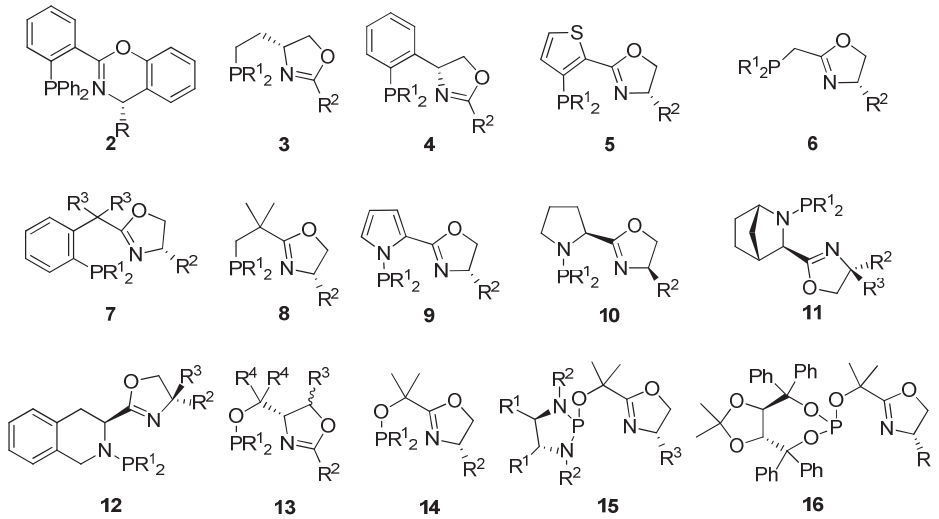

Figure 1.2. Phosphorus-oxazoline ligands applied in the Ir-catalyzed hydrogenation.

Phosphine-oxazoline ligands

In 2001, Kündig and coworkers reported a modification in the oxazoline moiety of the PHOX ligands, with the development of a phosphine-benzoxazine analogues **2** (Figure 1.2, R = ^{t}Bu, ^{i}Pr).[16] These ligands provided somewhat lower enantioselectivities than the PHOX ligands **1**.

Then, the new phosphine-oxazoline ligands developed for this process are based on modifications on the ligand backbone. In this respect Burgess' group also reported the synthesis of ligands **3** and applied them in the Ir-catalyzed hydrogenation of several aryl-alkyl alkenes (Figure 1.2, R^1 = Ph, *o*-Tol, R^2 = Me, ^{t}Bu, 1-adamantyl, CPh_3).[17] These ligands proved to be superior than the PHOX ligands in the hydrogenation of *Z*-alkenes (i.e. 75% ee for substrate **S3**), while ee's for the hydrogenation of *E*-alkenes were lower. Later, Zhang and coworkers further modified ligands **3**, by introducing again the *ortho*-phenylene tether backbone motif of the PHOX ligand.[18] The new ligands **4** proved to be excellent (ee's up to 99%) in the hydrogenation of *trans*-methylstilbene derivatives (i.e. substrate **S1**) and α-methylcinnamic esters (i.e. substrate **S7**).

In 2003, Cozzi and coworkers reported the application of ligands **5** (Figure 1.2, R^1 = Ph, *o*-Tol, Cy, R^2 = ^{i}Pr, ^{t}Bu), in which the phenyl ring of the PHOX has been replaced by thiophene, in the

hydrogenation of *trans*-methylstilbene (ee's up to 99%) and α-methylcinnamic alcohol (ee's up to 94%).[19]

In 2007, Pfaltz and coworkers disclosed a series of simple and readily accesible phosphine-oxazolines **6** which form a 5-membered chelate ring when coordinated to iridium (Figure 1.2, R^1 = Ph, *o*-Tol, Cy, ^{t}Bu, R^2 = ^{i}Pr, ^{t}Bu, Ph, Bn).[20] Surprisingly this motif has proved to be the most efficient ligand family for the hydrogenation of challenging tetrasubstitued alkenes (Figure 1.3).

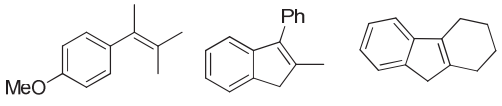

S4 97% ee **S10** 95% ee **S11** 96% ee

Figure 1.3. Selected Ir-hydrogenation results of tetrasubstituted olefins with ligands **6**.

In 2008, Hou and coworkers developed new phosphine-oxazoline ligands **7** based on the PHOX ligands, in which the flat *ortho*-phenylene tether is replaced by benzylic type group (Figure 1.2 , R^1 = Ph, *o*-Tol, *p*-Tol, R^2 = Me, ^{i}Pr, ^{t}Bu, R^3 = H, Me).[21] These ligands were successfully applied in the Ir-asymmetric hydrogenation of a range of *E*-aryl alkenes, α,β-unsaturated esters and allylic alcohols (ee's up to 98%).[21b] Interestingly, these ligands also provided excellent enantioselectivities in a range of α,β-unsaturated ketones (Figure 1.4; ee's up to 98%).[21a]

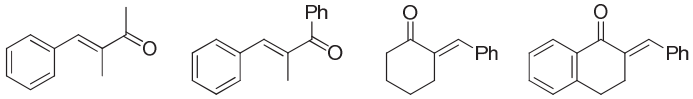

S12 98% ee **S13** 98% ee **S14** 98% ee **S15** 98% ee

Figure 1.4. Selected Ir-hydrogenation results of α,β-unsaturated ketones with ligands **7**.

Finally, Pfaltz and coworkers have modified PHOX ligands by replacing the *ortho*-phenylene tether by a branched alkyl chain. Ligands **8** (Figure 1.2**,** R^1 = Ph, *o*-Tol, Xyl, R^2 = ^{i}Pr, ^{t}Bu, Bn) provided higher enantioselectivities in the hydrogenation of trisubstituted *E*- and *Z*-aryl alkenes than the PHOX ligands (ee's up to 98%).[22] The potential utility of these new ligands was demonstrated in the synthesis of *(R)*-7-demethyl-2-methoxycalamenene an antitumor natural product (Scheme 1.3).

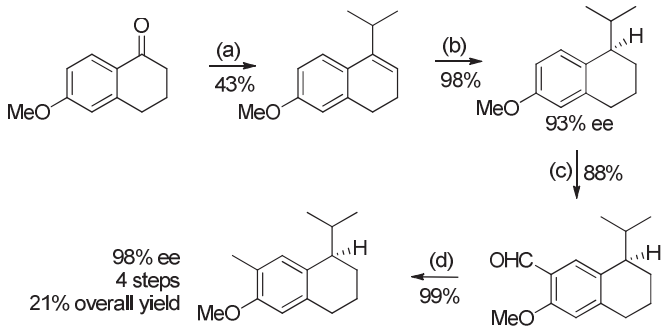

Scheme 1.3. Total synthesis of *(R)*-7-demethyl-2-methoxycalamenene.

N-Phosphine-oxazoline ligands

In 2001, the Pfaltz's group modified the PHOX ligands by introducing a pyrrole group. These new ligands **9** proved to be highly efficient in the hydrogenation of trisubstituted alkenes (Figure 1.2, R^1 = Ph, *o*-Tol, Cy, R^2 = ^{i}Pr, ^{t}Bu).[23] Enantiomeric excesses surpassed those previously obtained with the PHOX ligands (Figure 1.5).

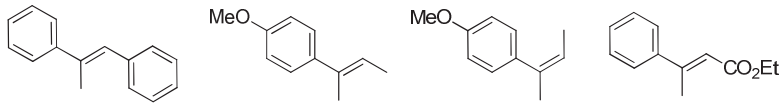

S1 99% ee | **S2** 75% ee | **S3** 70% ee | **S7** 92% ee

Figure 1.5. Selected Ir-hydrogenation results of unfunctionalized olefins with ligands **9**.

Later, Gilberston and coworkers developed the proline derived N-phosphine-oxazoline ligands **10** (Figure 1.2, R^1 = Ph, *o*-Tol, R^2 = ^{i}Pr, ^{t}Bu) that provided lower enantioselectivities than previous pyrrole-based ligands **9**.[24]

Andersson's group developed ligands **11** and **12** for the Ir-catalyzed hydrogenation of alkenes (Figure 1.2, **11**; R^1 = Ph, *o*-Tol, Cy, R^2 = H, ^{t}Bu, Ph, R^3 = H, Ph and **12**; R^1 = Ph, R^2 = H, ^{i}Pr, Ph, R^3 = H, ^{i}Pr, Ph).[25a,26] Ligands **11**, containing a chiral rigid bicyclic backbone, provided higher enantioselectivities than ligands **12**, with a more flexible backbone. Ir-**11** catalysts provided for the first time high enantioselectivities in the hydrogenation of enol phosphinates,[25b,c] vinyl silanes,[25d] fluorinated olefins[25e] and vinyl boronates[25f] (Figure 1.6).

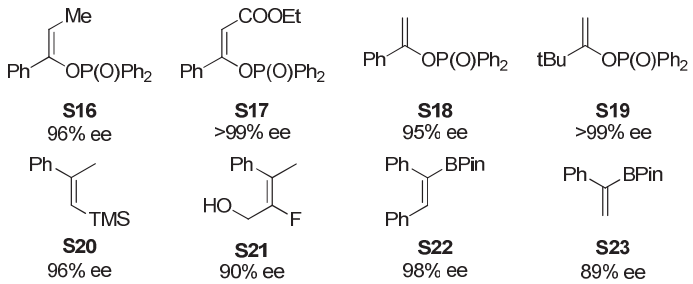

S16 96% ee | **S17** >99% ee | **S18** 95% ee | **S19** >99% ee

S20 96% ee | **S21** 90% ee | **S22** 98% ee | **S23** 89% ee

Figure 1.6. Selected results of the Ir-hydrogenation of olefins with non-traditional functional groups with ligands **11**.

Phosphinite-oxazoline ligands

Two families of phosphinite-oxazoline ligands have been developed for this process. Phosphinite-oxazolines **13** (Figure 1.2, R^1 = Ph, *o*-Tol, Cy, R^2 = ^{t}Bu, Ph, ferrocenyl, 2-Napht, R^3 = H, Me, R^4 = Me, ^{i}Pr, ^{i}Bu, Bn), reported by Pfaltz's group soon after the development of the PHOX ligands **1**, constitutes one of the most privileged ligands for this transformation.[27] These ligands provided excellent enantioselectivities in the hydrogenation of a broad range of both *E*- and *Z*-trisubstituted olefins, including α,β-unsaturated esters (Figure 1.7).[27a,b] Interestingly, these ligands also provided high enantioselectivities in the hydrogenation of a limited range of more challenging terminal olefins (Figure 1.7).[27c]

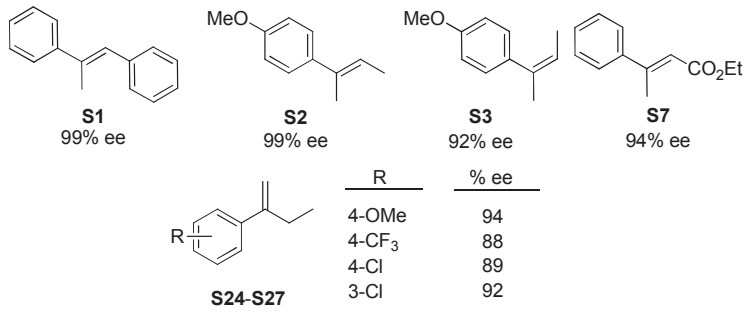

Figure 1.7. Selected Ir-hydrogenation result of trisubstituted and terminal olefins with ligands **13**.

The second family of phosphinite-oxazoline ligands **14** (Figure 1.2, R^1 = Ph, *o*-Tol, R^2 = ^{i}Pr, ^{t}Bu) is based on previously mentioned phosphine-oxazoline ligands **8** in which the phosphine group has been replaced by a phosphinite moiety.[28] The scope of these ligands is narrower in comparison with the phosphinite-oxazolines ligands **13**, however, they are complementary. Ligands **14** provided therefore high enantioselectivities for allylic alcohols (ee's up to 97%) and alkenes bearing heteroaromatic substituents (ee's up to 99%), for which the privileged ligands **13** provided moderate enantioselectivities.

Phosphoroamidite/Phosphite-oxazoline ligands

Despite the advantage of phosphite/phosphoroamidite ligands in asymmetric catalysis,[29] only two families of phosphite/phosphoroamidite-oxazoline ligands **15** and **16** have been applied (Figure 1.2, **15**; R^1 = Ph, *p*-Tol, Cy, 3,5-Xyl-$(CH_2)_4$, R^2 = SO_2-R, 3-OMe-Ph, 4-OMe-Ph, 4-^{t}Bu-Ph, 4-Ph-Ph, 2-Napht, R^3 = ^{t}Bu, Ph and **16**; R= Ph, ^{t}Bu).[30] However, their substrate range limitation was higher and enantioselectivities and activities lower than their related phosphinite/phosphine-oxazoline ligands (**13** and **14**). They also required higher catalyst loadings (4 mol %) and higher pressures (100 bar) to achieve full conversions.

1.1.2.2. Phosphorus-pyridine ligands

The intention to mimic the coordination sphere of Crabtree's catalyst motivated Pfaltz's group to prepare a new kind of P,N-ligand that incorporate a pyridine as a N-donor group. In this context they developed phosphine-pyridine ligands **17** (Figure 1.8).[31] These ligands contain several silyl ether substituents (R= Si(^{t}Bu)Me_2, Si(^{i}Pr)$_3$, Si(^{t}Bu)Ph_2) at the alkyl chain bridge with the aim to increase the rigidity and to provide a similar steric environment than the PHOX ligands **1**. Despite this, a worst catalytic performance was obtained than the previously commented PHOX ligands. In the same report, it was also tested the phosphinite version of ligands **17** (ligands **18**, R^1= Ph, *o*-Tol, Cy, ^{t}Bu and R^2= Me, ^{t}Bu, Ph, CPh_3; Figure 1.8).[31] The presence of a phosphinite moiety had a positive effect in terms of catalytic performance; i.e. the enantiomeric excess in the Ir-hydrogenation of *trans*-α-methylstilbene (**S1**) increased from 88% to 97%.

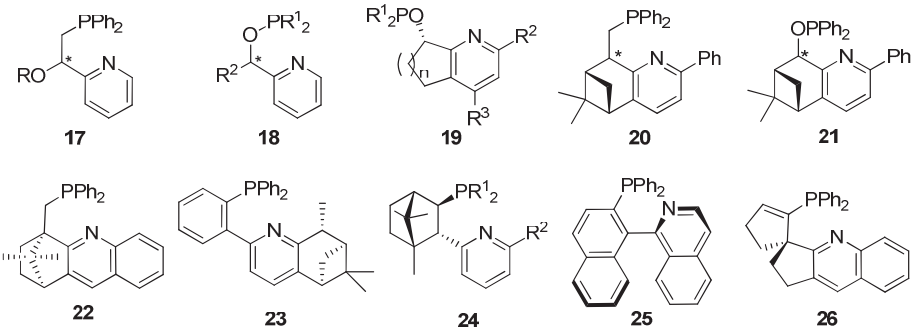

Figure 1.8 Phosphorus-pyridine ligands applied in the Ir-catalyzed hydrogenation.

Later, other groups developed new phosphorus-pyridine ligands. In this respect, Moberg's group prepared a series of phosphinite-pyridine ligands related to **18** in which an enantiomerically pure (-)-menthol moiety was introduced at the R^2 position. However these ligands were less enantioselective (ee's up to 84%).[32]

In order to increase the rigidity in the alkyl bridge moiety, ligands **19** were developed (Figure 1.8; R^1= Ph, *o*-Tol, Cy, ^{t}Bu ; R^2= H, Ph, Me; R^3= H, Me).[33,34] Ligands **19** became one of the most privileged ligand family applied in the Ir-hydrogenation of unfunctionalized olefins obtaining excellent enantioselectivities (ee's up to >99%). These ligand family were especially efficient in the hydrogenation of trisubstituted olefins including furanes and benzofurane derivates[33,34] and pure alkyl trisubstituted olefins[35] (ee's up to >99%) (Figure 1.9). The potential utility of these iridium catalytic systems have been demonstrated with the hydrogenation of γ-tocotrienyl acetate to obtain γ-tocopherol with enantioselectivity >98% towards the *RRR* enantiomer. It should be noted that tocopherols are the principal component of vitamin E (Figure 1.10).[36]

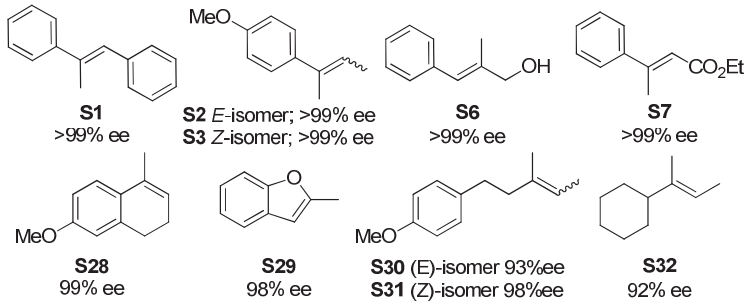

Figure 1.9. Selected Ir-hydrogenation results with ligands **19**.

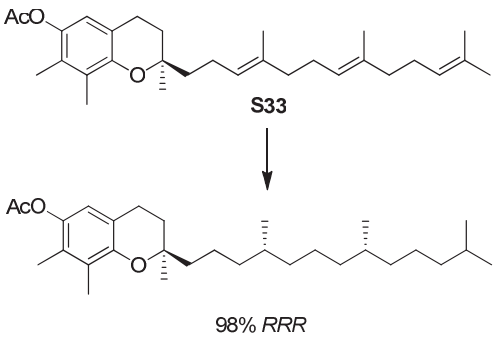

Figure 1.10. Hydrogenation of γ-tocotrienyl acetate.

Andersson's group synthesized phosphine-pyridine ligand **20** and phosphinite-pyridine ligands **21** (Figure 1.8) with the aim to increase even more the rigidity of ligands **17** and **18** by the introduction of an enantiomerically pure bicyclic moiety.[37] These ligands, derived from readily available α-pinene, showed high enantioselectivities (ee's up to 97%) but poor activities. Very recently, Chelucci and coworkers increased the range of phosphine-pyridine ligands derived from α-pinene with the synthesis of compounds **22** and **23** (Figure 1.8). However, these ligands provided lower enantioselectivities than ligand **20**.[38]

Knochel's group reported the application of phosphine-pyridine ligands **24** (Figure 1.8; R^1= Ph, Cy; R^2= H, Ph), obtained from readily available D-(+)-camphor, in the hydrogenation of trisubstituted olefins obtaining moderate-to-high enantioselectivities (ee's up to 96% for **S2**).[39]

In 2007, Li's group applied the axially chiral phosphine-quinoline ligand **25** (Figure 1.8) in the Ir-hydrogenation of unfunctionalized trisubstituted olefins obtaining promising results (ee's up to 96%).[40] The same concept of axial chirality was followed by Ding's group with the preparation of the spiro phosphine-quinoline ligand **26** (Figure 1.8). This ligand showed low enantioselectivities in the Ir-hydrogenation of **S1** (48% ee).[41]

1.1.2.3. Phosphorus-other nitrogen donor ligands

Although most of the ligands developed for the Ir-hydrogenation of unfunctionalized olefins contain either an oxazoline or a pyridine, other nitrogen donor groups have also been developed and successfully used in this process. The first application of this type of ligands in Ir-hydrogenation was reported by Pfaltz's group with phosphine-imidazoline ligands **27** (Figure 1.11, R^1 = Ph, *o*-Tol; R^2 = ^{i}Pr, ^{t}Bu; R^3 = ^{i}Pr, ^{t}Bu, Cy, Ph, Bn, *p*-Tol).[42] The advantage of the imidazoline moiety over the oxazoline is the possibility to introduce a new substituent R^3 at the nitrogen that could serve as a linker for attaching the ligand to a solid support. In several cases higher enantiomeric excesses were obtained than with analogues phosphine-oxazoline PHOX ligands (i.e. enantioselectivities for Z-2-(4-methoxyphenyl)-2-butene ee's increased from 42% to 88%). Very recently, Pfaltz and coworkers prepared zwitterionic iridium complexes by introducing an anionic moiety at R^3 position of the imidazole group. However, the presence of the anionic derivatization has a negative influence on the asymmetric induction of the iridium complex.[43]

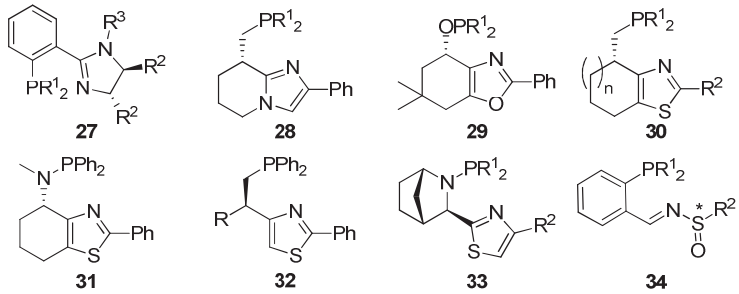

Figure 1.11. Phosphorus-other nitrogen donor ligands applied in the Ir-hydrogenation.

Andersson's group developed phosphine-imidazole ligands **28** (Figure 1.11; R^1 = Ph, *o*-Tol, 3,5-diMe-Ph) for the Ir-hydrogenation of unfunctionalized olefins obtaining excellent results (ee's up to 98%).[44] The same group developed related phosphinite-oxazole ligands **29** (Figure 1.11; R^1 = Ph, *o*-Tol, 3,5-diMe-Ph).[45] These new ligands provided also high enantioselectivity in the hydrogenation of trisubstituted olefins (ee's up to >99%) (Figure 1.12).

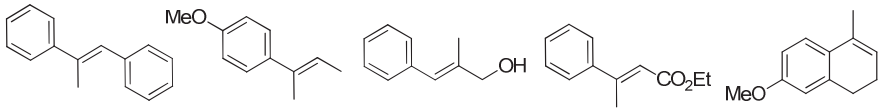

Figure 1.12. Selected Ir-hydrogenation results of trisubstituted olefins with ligands **29**.

Andersson's group also developed several families of phosphine/N-phosphine-thiazole ligands **30**-**33** (Figure 1.11). Phosphine-thiazole ligands **30** (R^1 = Ph, *o*-Tol; R^2 = H, Ph) provided high enantioselectivities in the Ir-hydrogenation of trisubstituted unfunctionalized olefins,[46] vinylsilanes,[25d] trifluoromethyl-containing olefins[47] and triaryl-substituted olefins.[48] Related N-phosphine-thiazole ligand **31** allowed to expand the range of substrates that can be hydrogenated. Therefore, high enantiomeric excess were achieved in the hydrogenation of fluorinated olefins,[25e] diphenylphosphine oxides and vinylphosphonates[49] becoming one of the most privileged ligands for the Ir-hydrogenation of olefins (Figure 1.13).

Ligands **32**, in which the rigid cyclic backbone were eliminated, were less successful (Figure 1.11, R= Me, Bn, allyl).[50] Recently, Andersson's group wanted to increase the rigidity in the ligand backbone by introducing a bicyclic moiety with the synthesis of N-phosphine-thiazole ligands **33** (Figure 1.11, R^1 = Ph, *o*-Tol; R^2 = Me, ^{t}Bu, Ph).[51] Moderate-to-high enantioselectivities were obtained in the hydrogenation of trisubstituted olefins. Interestingly, Ir-**33** catalysts provided excellent enantioselectivities in the hydrogenation of vinyl boronates (Figure 1.14). These results complement perfectly with the results obtained in the hydrogenation of monoborated substrates with the previously commented ligands **11** (Figure 1.2).[25f]

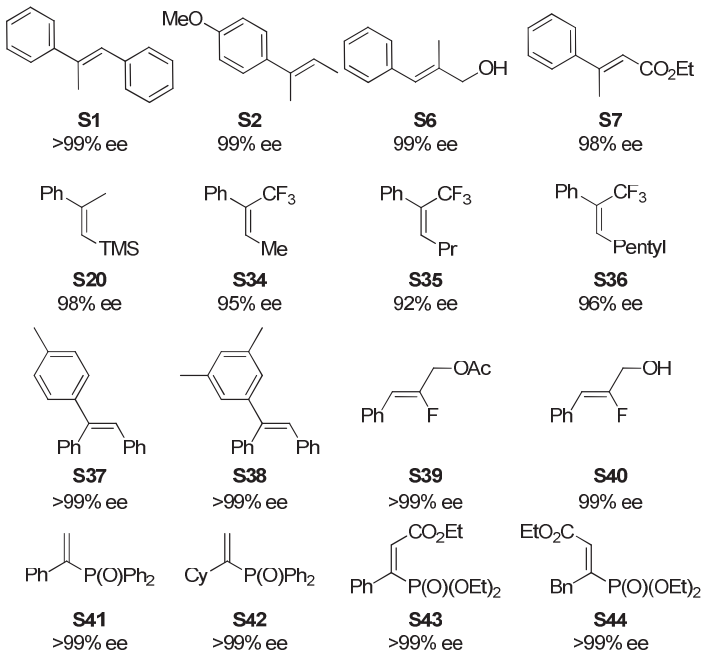

Figure 1.13. Selected Ir-hydrogenation results using the N-phosphine thiazole ligands **31**.

Finally, Ellman's group developed the chiral sulfinyl imine ligands **34** (Figure 1.11; R^1= Ph, *o*-Tol, Mes; R^2= ^{t}Bu, 1-adamantyl, *p*-Tol). These ligands were applied in the Ir-catalyzed hydrogenation of several trisubstituted olefins. However, high enantioselectivities (up to 94%) were only obtained using the standard substrate **S1**.[52]

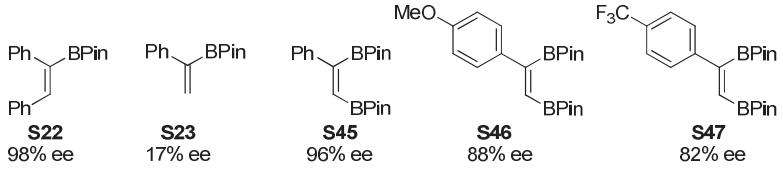

Figure 1.14. Selected Ir-hydrogenation results of vinyl boronates with ligands **33**.

1.2. Asymmetric allylic substitution reactions

Enantioselective Pd-catalyzed allylic substitutions represent a synthetically valuable strategy for the construction of asymmetric carbon-carbon and carbon-heteroatom bonds. The mild reaction conditions and the compatibility with many functional groups make this method attractive for the application in the synthesis of drugs and natural products.[1,53]

Scheme 1.4 shows two important classes of Pd-catalyzed allylic substitutions that can be carried out enantioselectively with chiral catalysts. Type A reactions start from a racemic substrate (linear or cyclic) and proceed via symmetrical allyl systems. In this case, the enantioselectivity is determined by the regioselectivity of nucleophilic attack and therefore depends on the ability of the chiral ligand to differentiate between the two allylic termini.[53] In type B reactions, racemic or prochiral substrates possessing two identical geminal substituents at one of the allylic termini

react via π-allyl intermediate which can isomerize via the well-established π–σ–π mechanism.[53] In this case, enantioselection can occur either in the ionisation step, leading to the allyl intermediate, or in the nucleophilic addition step.[53] For these later substrates, not only does the enantioselectivity of the process need to be controlled, but the regioselectivity is also a problem because a mixture of regioisomers may be obtained. Most Pd-catalysts developed to date favor the formation of achiral linear product rather than the desired branched isomer.[53] Therefore, the development of highly regio- and enantioselective Pd-catalysts is still a challenge. In contrast to Pd-catalytic systems, Ir-, Ru-, W-, Mo- and Cu-catalysts provide very high selectivity for the attack at the non-terminal carbon to give the chiral product.

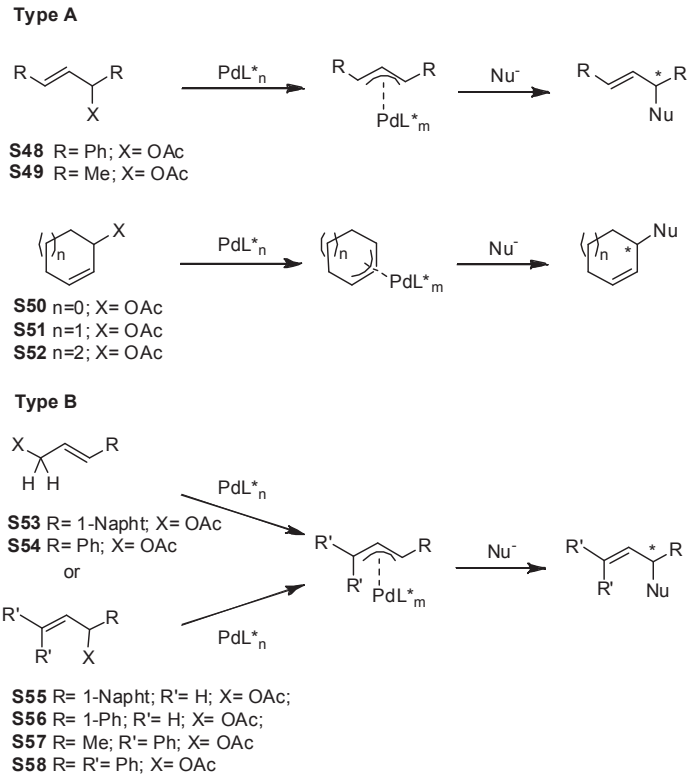

Scheme 1.4. Two classes of asymmetric Pd-catalyzed allylic substitution reactions.

The allylic substrates tested in this process can be linear or cyclic, although *rac*-1,3-diphenylprop-2-enyl acetate (**S48**, Scheme 1.4) is considered as the model substrate for testing the new catalytic systems. With regard to the metal source, a variety of transition metal complexes derived from Pd, Ni, Ru, Rh, Ir, Mo, W, Cu and other elements are known to catalyze allylic substitutions.[53] However, the most widely used catalysts are palladium complexes.[53] A wide range of carbon and heteroatom stabilized nucleophiles (those derived from conjugate acids with pKa < 25) have been employed in this process. Besides dimethyl malonate, which has become the standard nucleophile for testing new catalysts, many other stabilized carbanions bearing carbonyl, sulfone, nitrile or nitro groups have also been used. There are less examples of enantioselective

reactions with non-stabilized nucleophiles such as diorganozinc or Grignard reagents, and those are mainly limited to the use of Cu-catalysts.[54]

1.2.1. Mechanism

The catalytic cycle for Pd-catalyzed allylic substitution reactions with stabilized nucleophiles is well established and involves four main steps (Figure 1.15).[53]

The first step of the catalytic cycle is the coordination of an allylic substrate **B** to the catalyst precursor **A**, which enters the cycle at the Pd(0) oxidation level. Both Pd(0) and Pd(II) complexes can be used as precatalysts due to Pd(II) is easily reduced *in situ* by the nucleophile to the Pd(0) form. The most widely used precursors are $Pd_2(dba)_3$•dba, (dba = dibenzylidenacetone), $Pd(OAc)_2$ and $[Pd(\eta^3\text{-}C_3H_5)(\mu\text{-}Cl)]_2$. Next step is the oxidative addition of complex **C** to form the π-allyl intermediate **D**, which is usually the rate-determining step of the reaction.[53] The product of this oxidative addition has two susceptible positions for receiving nucleophilic attack (C-1 and C-3). After nucleophilic addition, an unstable Pd(0)-olefin complex **E** is produced, which readily releases the final product **F**.

It is accepted, that the enantioselectivity of the process is controlled by the external nucleophilic attack on the most electrophilic allylic carbon terminus of the π-allyl intermediate **D**.[53] Therefore, the π-allyl intermediate **D** plays an important role in the catalytic cycle and it is recognized as the intermediate which controls regio- and enantioselectivity. This intermediate can be isolated in the absence of nucleophiles. It is known, that allyl complex type-**D** can show a dynamic behavior in solution, which results in a mixture of isomers (Figure 1.16).

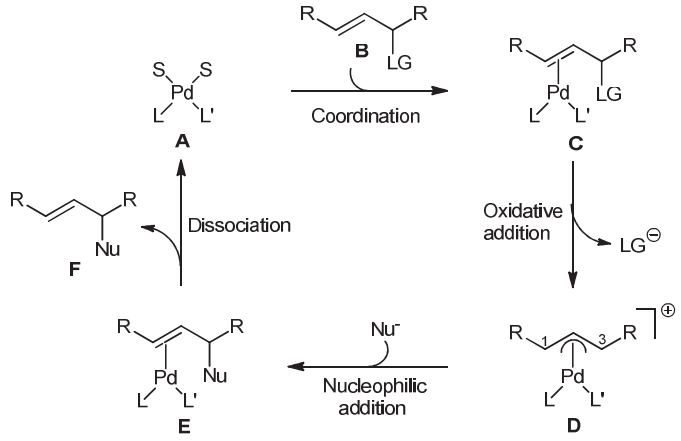

L,L'= mono- or bidentate ligand; S= solvent or vacant; LG= leaving group; Nu= nucleophile

Figure 1.15. Accepted catalytic cycle for Pd-catalyzed allylic substitutions.

To achieve high enantioselectivities, the formation of a single isomer is necessary, if we assume that the reaction rates are similar for all possible isomers. Both oxidative addition and nucleophilic attack usually occurs stereoselectively with inversion of the configuration. Therefore, if the intermediate allyl complex **D** does not undergo any isomerization that changes its

configuration, the overall process **A** to **F** proceeds with the retention of the configuration, i. e. the nucleophile is introduced at the same side of the allyl plane that occupied by the leaving group.

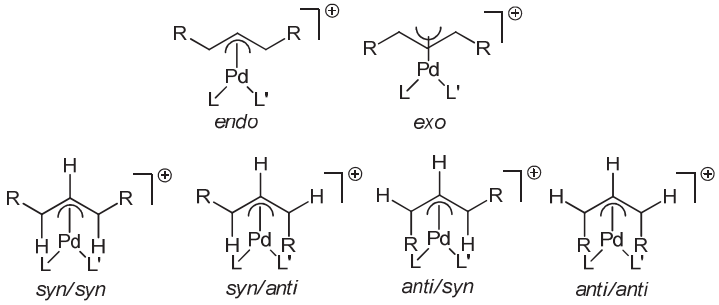

Figure 1.16. Possible isomers adopted by the π-allyl palladium complex **D**.

1.2.2. Ligands

Unlike asymmetric hydrogenation process, few diphosphines have provided good enantioselectivities in allylic substitutions. Though high ee's could be obtained in certain cases for instance, with BINAP **35** and CHIRAPHOS **36**, the scope of standard diphosphines in this process seems limited (Figure 1.17).[1,53]

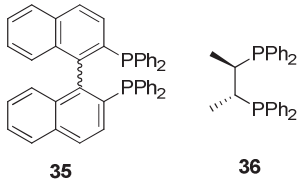

Figure 1.17. BINAP and CHIRAPHOS ligands.

Most of the successful ligands reported to date for this process have been designed using three main strategies. The first one, developed by Hayashi and coworkers, was the use of a secondary interaction of the nucleophile with a side chain of the ligand to direct the approach of the nucleophile to one of the allylic terminal carbon atoms (Figure 1.18).[55] The second one, developed by Trost and co-workers, was to increase the ligand's bite angle in order to create a chiral cavity in which the allyl system is perfectly embedded (Figure 1.18). This idea paved the way for the successful application of ligands with large bite angles for the allylic substitution of sterically undemanding substrates.[56] The third strategy, developed by groups led by Helmchen, Pfaltz and Williams, was the use of heterodonor ligands that result in an electronic discrimination of the two allylic terminal carbon atoms due to the different *trans* influences of the donor groups (Figure 1.18).[57] This made it possible to successfully use a wide range of heterodonor ligands (mainly P,N-ligands) in allylic substitution reactions.[1,53] More recently, we found that the use of biaryl phosphite-containing heterodonor ligands is highly advantageous by overcoming the most common limitations of this process, such as low reaction rates and high substrate specificity.[58] Introducing a biaryl phosphite in the ligand design was beneficial because of its larger π-acceptor ability, which increases reaction rates, and because of its flexibility that allows the catalyst chiral

pocket to adapt to both hindered and unhindered substrates. In addition, the presence of a biaryl phosphite moiety was also beneficial in the allylic substitution of more challenging monosubstituted substrates. Regioselectivity towards the desired branched isomer in this substrate class increases thanks to the π-acceptor ability of the phosphite moiety, which decreases the electron density of the most substituted allylic terminal carbon atom via the *trans* influence, favoring the nucleophilic attack to this carbon atom.[58]

The first successful P,N-ligands developed for the Pd-allylic substitution reaction were the phosphine-oxazoline PHOX ligands **1** (Figure1.18), developed simultaneously by Pfaltz, Helmchen and Williams.[57] Excellent enantioselectivities were obtained in the Pd-allylic alkylation of the model substrate **S48**, but poor-to-moderate enantioselectivities were obtained with unhindered linear (**S49**) and cyclic (**S51**) substrates (ee's up to 71%). Since then, the composition of the ligands has been extended by initially replacing the phosphine moiety with a phosphinite or a phosphite group, and the oxazoline moiety with other sp^2- or sp^3-N-donor groups (such as pyridine, imines, pirrolidines, etc.). The structure of the chiral ligand's backbone has also been modified. In next sections, the most successful P,N-ligands applied in the Pd-allylic substitution reaction will be discussed.

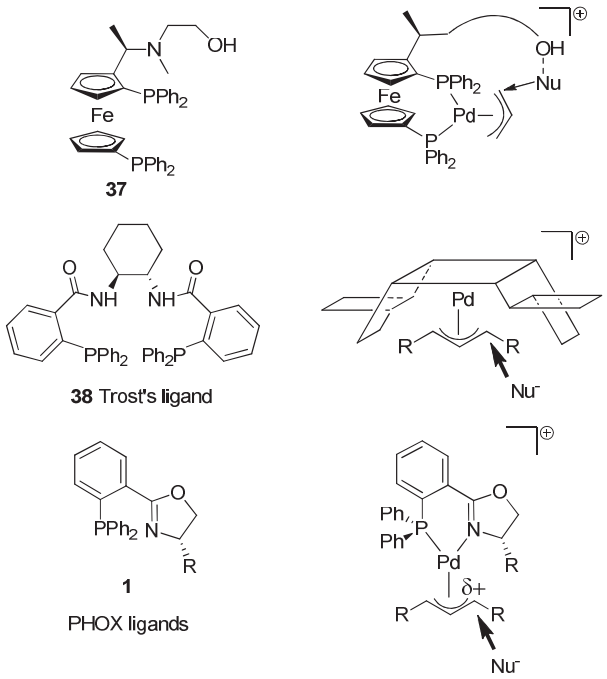

Figure 1.18. Representative ligands developed for the Pd-catalyzed allylic substitution reactions.

1.2.2.1. Phosphorus-oxazoline ligands

Inspired by the early work done by Pfaltz, Helmchen and Williams, several successful phosphorus-oxazoline ligands have been developed for this process. Most of them are phosphine-oxazoline and to a lesser extend phosphinite- and phosphite-oxazoline ligands.

Phosphine-oxazoline ligands

In 1998, Kunz and coworkers developed the phosphine-oxazoline ligand **39** (Figure 1.19) derived from the carbohydrate *D*-glucosamine.[59] Although high conversions and enantioselectivities were obtained in the Pd-allylic substitution reaction of the model substrate **S48** with dimethyl malonate (ee's up to 98%), only moderate enantioselectivities were obtained for unhindered linear substrate **S49** (ee's up to 69%) and long reaction times were needed to obtain high yields. This ligand was also tested in the Pd-allylic alkylation of the trisubstituted allylic acetate **S55** obtaining high enantioselectivities (ee's up to 88%).

Moyano and coworkers introduced a ferrocenyl substituent at the oxazoline ring with ligand **40** (Figure 1.19).[60] Although enantioselectivities were comparable with those of PHOX ligands **1** in the Pd-allylic alkylation of model substrate **S48**, the activities were much worse (7 days were needed to obtain 63% of yield). Ligand **40** was also tested in the Pd-allylic alkylation of unhindered linear substrate **S49** and the cyclic substrate **S51** obtaining poor enantioselectivities (44% ee for **S49** and 12% ee for **S51**).

Moberg and coworkers also studied the effect of the substituent at the oxazoline ring by introducing a new stereogenic center with the synthesis of ligands **41** (Figure 1.19, R^1 = Me, Ph; R^2 = H, Me).[61] While, similar high enantioselectivities than PHOX ligands were obtained in the Pd-allylic substitution of model substrate **S48**, in the allylic substitution of cyclic substrate **S51** enantioselectivities were higher but still low (ee's up to 59%).

Zehnder and coworkers replaced the oxazoline group by a oxazine ring with the synthesis of ligand **42** (Figure 1.19). The application of ligand **42** in the Pd-allylic alkylation of model substrate **S48** provided similar enantioselectivities than the PHOX ligands **1**, but much lower activity.[62]

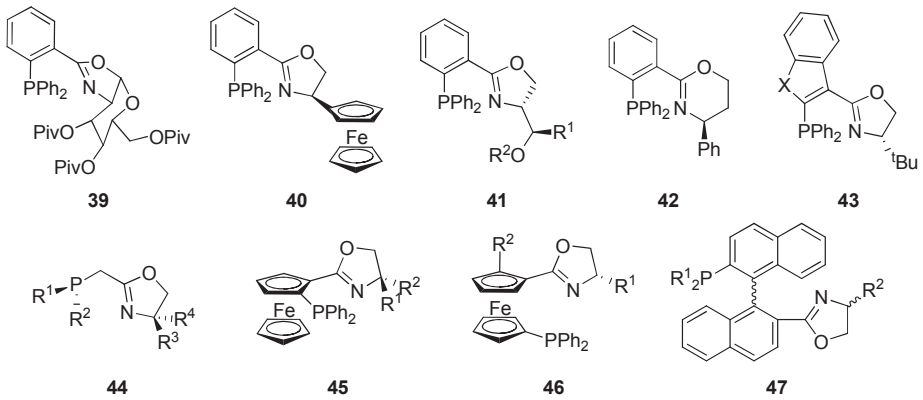

Figure 1.19. Selected phosphine-oxazoline ligands applied in the Pd-allylic substitution reaction.

The next families of ligands are modifications on the ligand backbone of PHOX type ligands. In this context, Tietze and coworkers replaced the benzene ring backbone by a benzothiophene or benzofuran moiety with the synthesis of ligands **43** (Figure 1.19, X= S, O).[63] These ligands provided somewhat lower enantioselectivities than the PHOX ligands **1** (ee's up to 97%). Later, Imamoto's group replaced the benzene ring by a methylene bridge and introduced a stereogenic phosphine moiety with ligands **44** (Figure 1.19, R^1 = Cy, ^{t}Bu, Ph, 1-adamantyl, CpFeCp; R^2 = Me,

Cy; R^3 = H, Me, ^{i}Pr; R^4 = H, Me, ^{i}Pr, ^{t}Bu).[64] These modifications had a negative effect on both enantioselectivity and activity (ee's up to 96%).

The next modification was to introduce a ferrocene moiety in the ligand backbone with ligands **45** (Figure 1.19, R^1 = H, Me, Bn; R^2 H, Me, ^{t}Bu, Bn). These ligands provided excellent results in the Pd-allylic alkylation of model substrate **S48** with dimethyl malonate (ee's up to 99%).[65] Several other groups studied the effect of replacing the position of the phosphine moiety in the ferrocene backbone. In this context, ligands **46** (Figure 1.19, R^1 = ^{i}Pr, ^{t}Bu; R^2 = H, Me, Bn, $SiMe_3$)[66] provided similar results than with ligands **45**. The authors found that the planar chirality is decisive in exerting control over both absolute configuration and enantiomeric excess.

The groups of Ikeda and Pregosin developed ligands **47** by introducing an enantiomericallyl pure binaphthyl moiety (Figure 1.19, R^1 = Ph, 3,5-diMe-Ph; R^2 = ^{i}Pr, ^{t}Bu). These ligands provided excellent enantioselectivities (ee's up to 97%) in the Pd-allylic substitution reaction of model substrate **S48**.[67] They found that the configuration of the substituted product was mainly determined by the configuration of the binaphthyl moiety.

Finally, the previously described ligands **3** and **4** (Figure 1.2) were also successfully applied in the Pd-allylic alkylation reaction of model substrate **S48** (ee's up to 98%).[68,69] Ligand **3** also provided promising enantioselectivities in the allylic substitution of unhindered substrate **S49** (ee's up to 80%) and the cyclic substrate **S51** (ee's up to 79%).[68]

Phosphinite-oxazoline ligands

Two families of phosphinite-oxazoline ligands have been developed for the Pd-allylic substitution reaction. In this context, Uemura and coworkers reported the synthesis of a pyranoside phosphinite-oxazoline ligand family **48** (Figure 1.20). These ligands provided high enantioselectivities for the model substrate **S48** (ee's up to 96%), but moderate enantioselectivities for unhindered linear and cyclic substrates **S49** and **S51** (ee's up to 57% and 74%, respectively).[70]

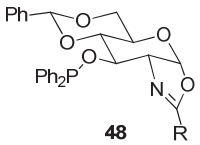

48

R= Me, ^{i}Pr, ^{t}Bu, Ph, Bn

Figure 1.20. Phosphinite-oxazoline ligands **48** applied in the Pd-allylic alkylation reaction.

The second family applied is the previously mentioned phosphinite-oxazoline ligands **13** (Figure 1.2).[71] These ligands provided somewhat lower enantioselectivities than their phosphine-oxazoline analogues **3** (ee's up to 96% at 0 ºC in the substitution of model substrate **S48**).

Phosphite-oxazoline ligands

The first successful application of phosphite-oxazoline ligands **49** (Figure 1.21, R^1= ^{i}Pr, ^{t}Bu, Ph; R^4= H, Me; R^5= H) in this process was achieved by Pfaltz and co-workers.[72] Ligands **49** were designed to overcome the problem of regioselectivity in the allylic alkylation of monosubstituted linear substrates **S53**-**S56** (Scheme 1.4). Pfaltz et al. found that regio- and enantioselectivities

were affected by substituents in the oxazoline moiety and by the substituents/configuration of the phosphite moiety. An excellent combination of regioselectivities (up to 95%) in the desired branched isomer and enantioselectivities (up to 94%) were achieved. The success of these ligands is due to the combination of two ligand parameters that direct the nucleophilic attack to the most substituted allyl terminus (Scheme 1.5).[72] The first one is the π-acceptor capacity of the phosphite moiety, which decreases the electron density of the most substituted allylic terminal carbon atom via the *trans* influence. The second one is the introduction of bulky biaryl phosphite moiety which shifts the equilibrium to the desired Pd-π allyl intermediate. Despite this success these ligands produced moderate results for hindered (ee's up to 60% for **S48**) and unhindered (ee's up to 70% for **S51**) disubstituted substrates. Later, the same group applied the previously mentioned phosphite-oxazoline ligands **16**, derived from TADDOL (Figure 1.2).[30b] These ligands also provided high regio- (up to >99%) and enantioselectivities (ee's up to 99%) in the allylic substitution of monosubstituted substrates, but again low enantioselectivities (ee's up to 56%) were achieved for disubstituted substrates.

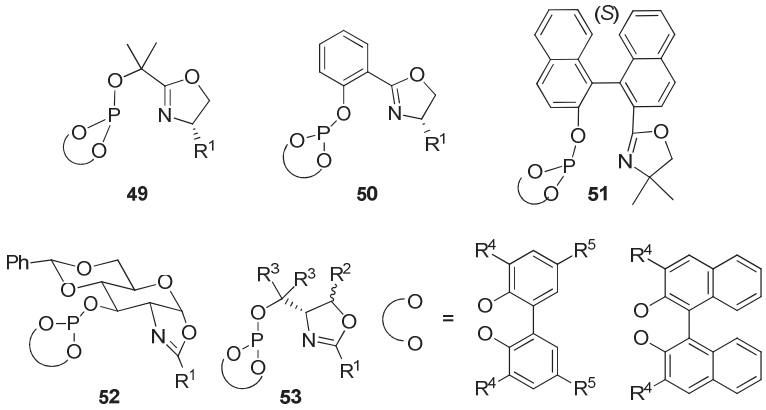

Figure 1.21. Selected phosphite-oxazoline ligands applied in the Pd-allylic alkylation reaction.

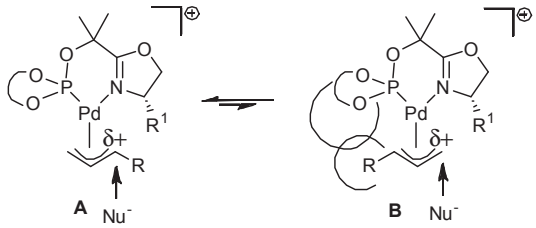

Scheme 1.5. Key Pd-allyl intermediates containing monosubstituted substrates.

With the aim of finding a more versatile phosphite-oxazoline ligand, a decision was made to take one of the most successful ligand families for this process, the phosphine-oxazoline PHOX ligands, and replace the phosphine group with a bulky diphenyl phosphite moiety (Figure 1.21, ligands **50**, R^1 = Et, ^{i}Pr, ^{t}Bu, Ph; R^4 = H, ^{t}Bu; R^5 = H, ^{t}Bu, OMe).[29f] The application of these ligands in the asymmetric Pd-catalyzed allylic substitution reactions was very successful. Therefore, excellent activities (TOF's > 2400 mol substrate * (mol Pd * h)$^{-1}$), regio- (up to 99%) and enantioselectivities (ee's up to >99%) were obtained for hindered and unhindered disubstituted

and also monosubstituted substrates (Figure 1.22). It is noteworthy that these ligands show higher versatility than their phosphine-oxazoline PHOX analogues.

S48 > 99% ee

S49 93% ee

S50 n = 0; 97% ee
S51 n = 1; 99% ee
S52 n = 2; 98% ee

S55 92% ee, 99% regio
S56 86% ee, 68% regio

Figure 1.22. Summary of the best results obtained in the Pd-catalyzed allylic substitution using ligands **50**.

Following these significant contributions come the developments of three new biaryl phosphite-oxazoline ligand libraries. The first of these, developed by Gladiali and co-workers, described the application of chiral (*S*)-binaphtalene-core ligands **51** (Figure 1.21) in the Pd-catalyzed asymmetric allylic substitution of **S48**, albeit with moderate results (100% conv, ee's up to 43% in 7 h).[73]

The second contribution reported the development of a pyranoside phosphite-oxazoline ligand library **52** (Figure 1.21, R^1 = Me, ^{i}Pr, ^{t}Bu, Ph, Bn; R^4 = H, Me, ^{t}Bu, $SiMe_3$; R^5 = H, Me, ^{t}Bu, OMe), related to previous phosphinite-oxazoline **48** (Figure 1.20).[74] High enantioselectivities (ee's up to 99%) and good activities (TON's up to 10000 mol substrate x (mol Pd)$^{-1}$) were achieved in a broad range of mono- and disubstituted linear hindered and unhindered linear and cyclic substrates (Figure 1.23). In addition, the efficiency of this ligand design is corroborated by the fact that these Pd-phosphite-oxazoline catalysts provided higher enantioselectivity than their phosphinite-oxazoline analogues **48** in several substrate types.

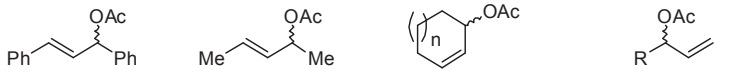

S48 99% ee

S49 81% ee

S51 n = 1; 45% ee
S52 n = 2; 92% ee

S55 90% ee, 80% regio

Figure 1.23. Summary of the best results obtained in the Pd-catalyzed allylic substitution using ligands **52**.

The third contribution appeared more recently and reported the synthesis and screening of a highly modular phosphite-oxazoline ligand library **53** in the Pd-catalyzed allylic substitution reactions of several substrate types (Figure 1.21, R^1 = ^{t}Bu, Ph, *p*-Tol, *o*-Tol, 2,6-diMe-Ph; R^2 = H, Me; R^3 = H, Me, Ph; R^4 = H, Me, ^{t}Bu, $SiMe_3$; R^5 = H, Me, ^{t}Bu, OMe).[75] This ligand library was a modification of previously mentioned ligands **13** (Figure 1.2) in which the phosphinite moiety was replaced by a phosphite group. High regio- and enantioselectivities (ee's up to 99%) were achieved in a broad range of mono- and disubstituted linear hindered and unhindered linear and cyclic substrates (Figure 1.24).

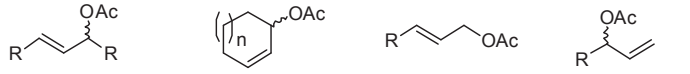

S48 R= Ph; 96% ee
S49 R= Me; 96% ee

S51 n = 1; 75% ee
S52 n = 2; 83% ee

S53 96% ee, 95% regio

S55 95% ee, >95% regio

Figure 1.24. Summary of the best results obtained in the Pd-catalyzed allylic substitution using ligands **53**.

1.2.2.2. Other sp^2-nitrogen-phosphorus ligands

Although most of the P,N ligands applied in the palladium allylic alkylation contain an oxazoline as nitrogen donor group, heterodonor ligands with other sp^2-nitrogen donor group than oxazoline have also been applied. Next, the most relevant other sp^2-nitrogen-phosphorus ligands will be discussed.

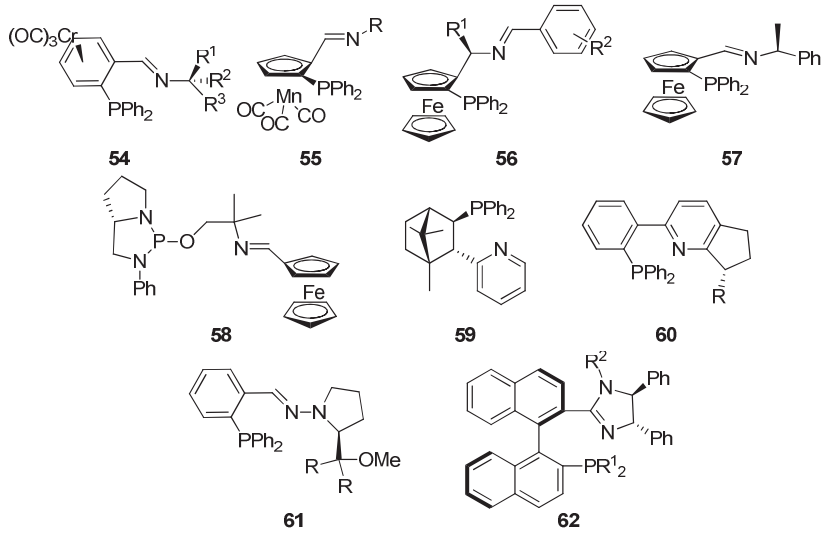

Figure 1.25. Selected sp^2-nitrogen-phosphorus ligands applied in the Pd-allylic alkylation reaction.

Several phosphorus-imine ligands have been developed and showed to be efficient in the Pd-allylic substitution reactions. In this context, Chung and coworkers reported the application of optically active Cr-complexed phosphine-imine ligands **54** (Figure 1.25, R^1 = Me, Ph; R^2 = H, Me, Ph; R^3 = H, Me). Excellent enantioselectivities were obtained in the Pd-allylic alkylation of model substrate **S48** (>98% ee).[76] Later, the groups of Chung and Zheng developed planar chiral cyclopentadienyl manganese ligands **55** and ferrocene derivatives **56** (Figure 1.25, R= ^{t}Bu, Ph, Bn, CHPh$_2$, R^1= Me, Cy, Ph; R^2= H, *p*-OMe, *p*-Cl, *p*-Me, *p*-NO_2, *m*-OMe, *m*-Cl, *m*-NO_2, *o*-NO_2). These ligands provided comparable results than those with ligands **54**.[77,78] Recently, Attar and coworkers developed ferrocene-based phosphine-imine ligands **57** (Figure 1.25) obtaining somewhat lower enantioselectivities than previous ligands **54**-**56** (ee's up to 94%).[79] Finally, Gavrilov and coworkers developed the P-chiral ferrocenylimino diamidophosphite ligand **58** (Figure 1.25) for its application in the Pd-allylic substitution reaction of model substrate **S48** obtaining enantioselectivitites up to 98%.[80]

Phophorous-pyridine ligands have also been applied in Pd-allylic alkylation reactions, but enantioselectivities have been only high for model substrate **S48**. [81,82,83] In this context, phosphine-pyridine ligands **59** and **60** (Figure 1.25, R= Me, ^{i}Pr, ^{t}Bu) provided enantioselectivities up to 96% in the allylic substitution of model substrate **S48**.[81,82]

Other sp^2-nitrogen donor groups have also been incorporated in heterodonor P,N-ligands. In this respect, phosphine-hydrazone ligands **61**,[84] (Figure 1.25, R = H, Me, Et) and the more recently phosphine-imidazoline ligands **62**,[85] (Figure 1.25, R^1 = Ph, 3,5-diMe-Ph, *p*Tol; R^2 = Ts,

Ms) have been successfully applied in the allylic substitution of model substrate **S48** (ee's up to 98%).

1.2.2.3. *sp*^{3}-Nitrogen-phosphorus ligands

Heterodonor ligands containing an *sp*^{3}-nitrogen donor group have been also applied in the Pd-allylic alkylation reaction with great success. Next, the most representative sp^3-nitrogen-phosphorus ligands will be discussed.

The first sp^3-nitrogen containing ligands developed for the Pd-allylic substitution reaction were variations of the PHOX ligands **1**, where the oxazoline was replaced by other heterocycles, such as oxazolidines **63-64** (Figure 1.26, R^1 = Me, Bu; R^2 = ^{i}Pr, Ph),[86,87] oxazinanes **65** (Figure 1.26, R = Et, Pr, Bu, Bn),[88] imidazolidines **66** (Figure 1.26, R = Me, Et)[89] and pyrrolidines **67** (Figure 1.26, R^1 = H, $SiMe_3$; R^2 = Me, Et, Ph, OMe).[90] All these ligands provided similar high enantioselectivities in the Pd-allylic alkylation of model substrate **S48** (ee's up to 99%).

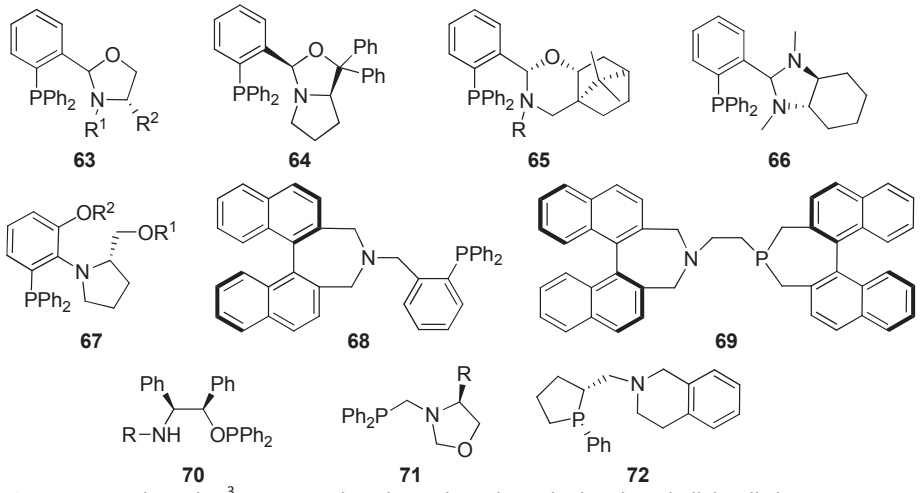

Figure 1.26. Selected sp^3-nitrogen-phosphorus ligands applied in the Pd-allylic alkylation reaction.

In 2002, the azepine-type P,N ligand **68** were applied in the Pd-allylic alkylation of several substrates (Figure 1.26).[91] Although excellent enantioselecetivities were obtained with model substrate **S48** (ee's up to 97%), poor results were obtained for unhindered substrates. Moberg and coworkers also developed the azepine-type P,N ligand **69** (Figure 1.26) containing a phospholane moiety with similar results.[92]

Phosphinite-amine ligands **70** (Figure 1.26, R= ^{i}Pr, ^{n}Bu, Bn) have also been applied in the allylic substitution of model substrate **S48** (ee's up to 95%).[93]. The authors found that the presence of a secondary amine was crucial to achieve good enantioselectivities. The use of related ligands with tertiary amines led therefore to poor enantioselectivities.

In 2005, Braga and coworkers reported the application of phosphine-oxazolidine ligands **71** (Figure 1.26, R = Me, ^{i}Pr, Ph, Bn) in the Pd-allylic substitution reaction of model substrate **S48** with dimethyl malonate obtaining enantioselectivities up to 97%.[94]

Finally, Kobayashi and coworkers developed the phospholane-amine ligand **72** for its application in the Pd-allylic alkylation of model substrate **S48** (Figure 1.26), achieving enantioselectivities up to 96%.[95]

1.3. Asymmetric Heck reaction

The palladium-catalyzed asymmetric Heck reaction, that is, the coupling of an aryl or alkenyl halide or triflate to an alkene (Scheme 1.6), is a powerful and highly versatile procedure for preparing enantioenriched compounds since it tolerates several functional groups.[1,96] This process has found extensive applications in asymmetric synthesis. Shibasaki and Overman have convincingly demonstrated the value of such transformation in the synthesis of complex natural molecules.[1,96] In addition, the importance of this C-C forming reaction has been established with a recent Nobel Prize (2010).

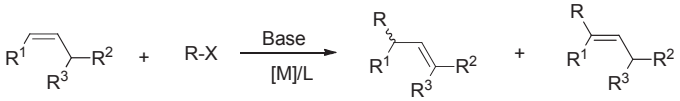

Scheme 1.6. Pd-catalyzed Heck reaction. X= Halide or triflate.

Heck reaction has been known to synthetic chemists since the late 1960's. However, reports of successful examples of the asymmetric Heck reaction were not published until the end of 1980's. The bulk of the reported examples involve intramolecular reactions, where the alkene regiochemistry and the geometry of the product can be easily controlled.[1b] Firstly, the scope of the intermolecular reactions were limited to O-, N-heterocycles substrates to simplify the alkene regiochemistry.[1b,96] Nowadays several substrates have been applied in the intermolecular asymmetric Heck reaction. Most of them are cyclic substrates (Figure 1.27); although, 2,3-dihydrofuran **S59** has been selected as benchmark substrate for testing new chiral ligands. A wide variety of aryl or vinyl halides or triflates have been applied, but phenyl triflate have been used as standard. The base is also an important parameter to be controlled that affects both activity and selectivity. *N*,*N*-diisopropylamine and proton sponge are the standard bases used for testing new catalysts.[1b,96]

S59 **S60** **S61** **S62** **S63**

Figure 1.27. Most common substrates applied in the asymmetric Pd-Heck reaction.

It should be noted that not only the enantioselectivity of the process has to be controlled, also the regioselectivity, because a mixture of regioisomers can be obtained. For example, in the asymmetric Heck reaction of 2,3-dihydrofuran with phenyl triflate, a mixture of two products can be obtained: the expected 2-phenyl-2,5-dihydrofuran **74** and 2-phenyl-2,3-dihydrofuran **73**, formed due to an isomerization process (Scheme 1.7).[1b,96]

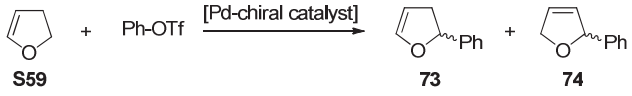

S59 **73** **74**

Scheme 1.7. Model Pd-catalyzed intermolecular Heck reaction.

1.3.1. Mechanism

Figure 1.28 illustrated a proposed catalytic cycle for the phenylation of 2,3-dihydrofuran.[1b,96,97] The catalytic cycle starts with the oxidative addition of the organic triflate to a Pd(0)-complex **A** to produce a Pd(II)-complex **B**. Since the triflate ligand is a good leaving group, coordination of the 2,3-dihydrofuran on **B** induces dissociation of the triflate ligand to give the cationic phenylpalladium olefin species **C**, which a 16-electron square-planar structure convenient for the subsequent enantioselective insertion of olefins. The resulting alkyl palladium (II) complex **D** undergoes β-hydride elimination leading to a hydrido-palladium olefin complex **E**. Dissociation of this π-complex leads to the product **74** and a hydrido-palladium species **H**. Finally, the catalytic Pd(0) complex **A** is regenerated by reductive elimination of HOTf.

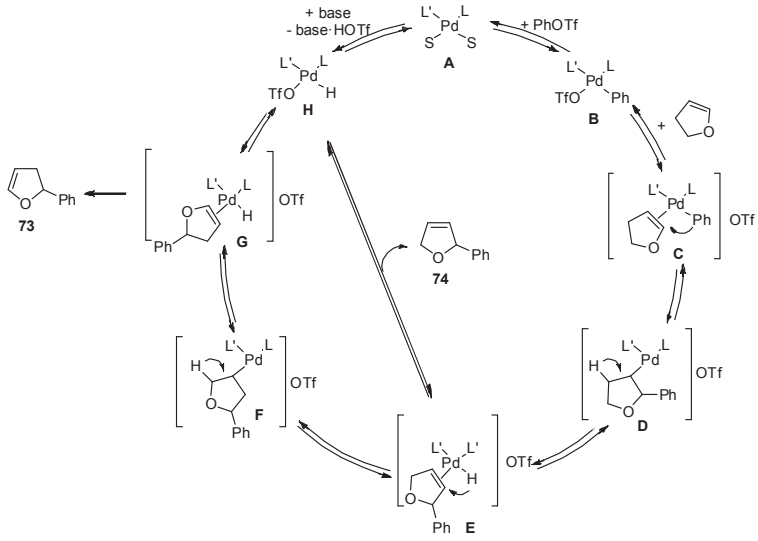

Figure1.28. Proposed mechanism for the catalytic Pd-catalyzed arylation of 2,3-dihydrofuran with phenyl triflate.

Depending on the ligand, catalyst precursor and reaction parameters, the palladium complex **E** can also undergo re-insertion of the hydride, which leads to the alkyl palladium (II) complex **F**. β-hydride elimination of **F** followed by dissociation of the resulting Pd-π-complex **G** lead to isomer **73** and hydride **H**. Reductive elimination of HOTf in **H** regenerates active species **A**.

1.3.2. Ligands

The first ligands developed for this process were diphosphines. Although Pd-diphosphine catalyst systems provided high enantioselectivities, there were still major problems of

regioselectivities and activities.[96] For instance, the diphosphine BINAP provided an enantioselectivity of 96% but the major product was the isomerized 2-phenyl-2,3-dihydrofuran **73** (71% regioselectivity) and the reaction time was 9 days.[98]

An important breakthrough in this area came with the use of heterodonor P,N ligands. Several phosphine/phosphinite-nitrogen ligands were therefore developed. However, although some of them have provided high regio- and enantioselectivities, there was still a problem of low reaction rates and substrate versatility.[96]

The first success in the Pd-catalyzed asymmetric intermolecular Heck reaction was reported by Pfaltz and coworkers using heterodonor phosphine-oxazoline PHOX ligands **1** (Figure 1.1).[99] These ligands were successfully applied in the intermolecular Heck reaction of several substrates and triflate sources (Figure 1.29, ee's up to 98%). Results also indicate that the presence of a *tert*-butyl group in the oxazoline moiety was crucial for obtaining the highest levels of enantioselectivity. The main limitation of these catalytic systems was the long reaction times (reactions usually take 3-7 days to complete). Hallberg and coworkers decided to apply the benefits of microwave irradiation using PHOX ligands **1** observing a considerable decrease in reaction times (from 4 days to 1 hour) but lower enantioselectivities were obtained (from 97% ee to 90% ee).[100]

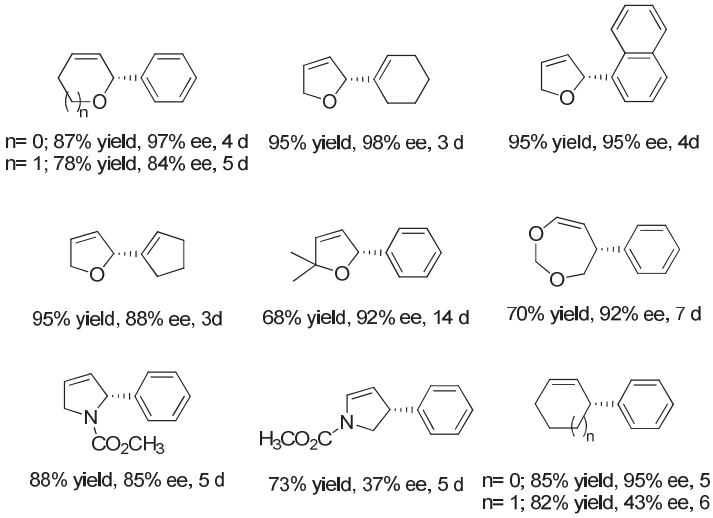

Figure 1.29. Yields, enantioselectivities and reaction times using Pd/**1** catalytic systems in the intermolecular Heck reaction.

Next, the most representative P,N-ligands applied in the Pd-Heck coupling will be discussed.

1.3.2.1. Phosphorus-oxazoline ligands

Phosphine-oxazoline ligands

Figure 1.30 collects the most representative phosphine-oxazoline ligands for this process. In 2000, Hayashi and coworkers reported a modification in the oxazoline moiety of the PHOX ligands with the development of an indane-fused ligand **75** (Figure 1.30).[101] Ligand **75** was successfully applied in the Pd-asymmetric Heck coupling of the model substrate **S59** obtaining ee's up to 98%.

Later in 2009, Paquin and coworkers reported ligand 5,5-(dimethyl)-^{i}Pr-PHOX **76** (Figure 1.30), which behaves similarly in terms of enantioselectivity (ee's up to 92% in the phenylation of **S59**) to PHOX.[102]

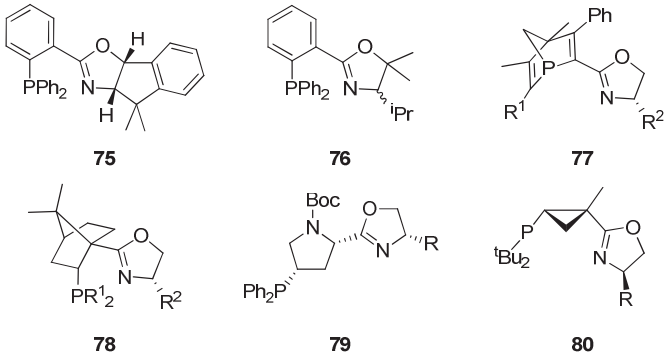

75 **76** **77**

78 **79** **80**

Figure 1.30. Selected phosphine-oxazoline ligands applied in the Pd-catalyzed intermolecular Heck reaction.

Next, the modifications focused on the ligand backbone. In this context, Hayashi's group reported the application of (*S*,*R*)- and (*S*,*S*)-2-[4-(isopropyl)oxazol-2-yl)]-2'-diphenylphosphino-1,1'-binaphthyl ligands **47** (Figure 1.19) in the Pd-catalyzed asymmetric arylation of **S59**, obtaining enantioselectivities up to 88%.[103] The authors found that the axial chirality in ligands **47** regulates the chiral environment around the palladium center and has therefore a greater influence on the stereochemical outcome than the central chirality of the corresponding oxazoline unit.

Gilbertson developed bicyclic phosphine-oxazoline **77** and **78** and proline-derived phosphine-oxazoline **79** ligands (Figure 1.30) that were successfully screened in the Pd-catalyzed intermolecular Heck reaction of several substrates with several aryl- and alkenyl-triflates (Figure 1.31).[104]

Several planar chiral ferrocene phosphine-oxazoline ligands have been developed.[99c,105] Two of the most successful families are ligands **45** and **46** (Figure 1.19). Ligands **45** provided good yields and enantioselectivities (up to 90% yield and 98% ee) in the arylation of 2,2-dialkyl-2,3-dihydrofurans.[105a] Hou and coworkers replaced the position of the phosphine moiety in ligands **45** with the synthesis of ligands **46**. This modification leads to an increase in the activity of the system (full conversion in 8 h) while maintaining the excellent enantioselectivities (ee's up to 99%).[105b-c]

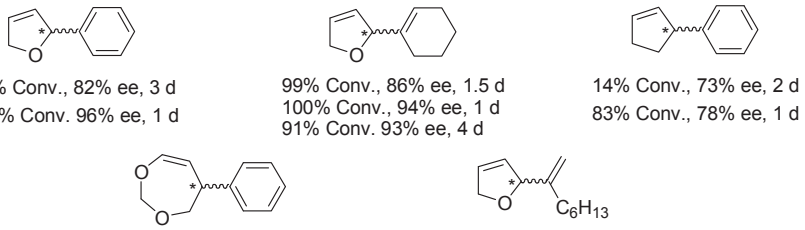

85% Conv., 82% ee, 3 d
100% Conv. 96% ee, 1 d

99% Conv., 86% ee, 1.5 d
100% Conv., 94% ee, 1 d
91% Conv. 93% ee, 4 d

14% Conv., 73% ee, 2 d
83% Conv., 78% ee, 1 d

50% Conv., 96% ee

83% Conv., 23% ee, 1 d
85% Conv., 93% ee, 1.5 d

Figure 1.31. Summary of the best results obtained in the Pd-catalyzed Heck reaction using ligands **77**-**79**.

Guiry, Cozzi and coworkers reported the application of ligands **5** and **43** (Figure 1.2 and Figure 1.19, respectively) in which the phenyl ring of the PHOX has been replaced by thiophene moieties, in the arylation and cyclohexenylation of model substrate **S59**.[106] Ligand **5**, containing bulky substituents at both oxazoline and phosphine moieties provided the best results for the arylation (ee's up to 96%) and cyclohexenylation (ee's up to 95%).

Recently two new studies on the development of new phosphine-oxazoline ligands have appeared. One of them reports the synthesis of a new type of PHOX ligand with a rigid chiral cyclopropyl backbone (ligands **80**, Figure 1.30, R = ^{t}Bu, Ph).[107] The introduction of this rigid cyclopropyl fragment lowered the degrees of freedom in the catalyst and led to an efficient catalyst, which demonstrates excellent enantioselectivities in the asymmetric arylation of dihydrofuran with various aryl triflates (yields up to 85 and ee's up to 99%). The second study reports the application of the previously mentioned phosphine-oxazoline ligands **7** (Figure 1.2) based on the PHOX ligands, in which the flat *ortho*-phenylene tether is replaced by benzylic type groups. The authors found that simply by changing the substituent of the benzylic group of the ligand backbone both enantiomers of the arylated products can be obtained in high regio- and enantioselectivities (ee's up to 95%).[108]

Finally, Zhang's group applied the previously mentioned phosphine-oxazoline ligand **4** (Figure 1.2).[69] High yields and enantioselectivities were achieved in the arylation of the model substrate **S59** (ee's up to 94%).

Phosphinite/phosphite-oxazoline ligands

Although most of the phosphorus-oxazoline ligands developed for the Pd-catalyzed asymmetric Heck coupling contain a phosphine group, there are two reports in the literature where this group have been replaced by a phosphinite or a phosphite group.

In 2000, Uemura and coworkers developed a new type of P,N-ligand for this process: the previously mentioned phosphinite-oxazoline **48** (Figure 1.20).[109] These ligands were successfully applied in the arylation of model substrate **S59** (ee's up to 96%). In contrast to the results obtained using PHOX-type ligands and the vast majority of the phosphine-oxazoline ligands, results were best with a benzyl oxazoline substituent. In addition, these ligands were also tested in the phenylation of *cis*- and *trans*-crotyl alcohols (ee's up to 17%).

The latest innovation in the design of ligands for this process was the replacement of the phosphine/phosphinite moiety by a biaryl phosphite group. The previously mentioned phosphite-oxazoline ligands **52** (Figure 1.21), related to **48**, were therefore successfully applied for the first time with a broad range of substrates and triflate sources (Figure 1.32).[29g,110]

R	% Conv	% regio	% ee
C_6H_5	100	97	99
4-CH_3-C_6H_4	100	85	96
4-NO_2-C_6H_4	100	>99	91
1-Naphthyl	100	95	99
C_6H_9	100	98	99

R	% Conv	% regio	% ee
C_6H_5	100	94	96
C_6H_9	100	95	96

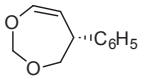

100% Conv, 92% ee

Figure 1.32. Summary of the best results obtained in the Pd-catalyzed Heck reaction using ligands **52**.

1.3.2.2. Phosphorus-other nitrogen donor ligands

The effectiveness of the phosphine-oxazoline ligands in the Pd-catalyzed asymmetric Heck coupling suggested that other nitrogen donor groups could be also introduced in the ligand design. In this context, several new heterodonor P,N-ligands in which the oxazoline have been replaced by other nitrogen donor groups have been developed (Figure 1.33).

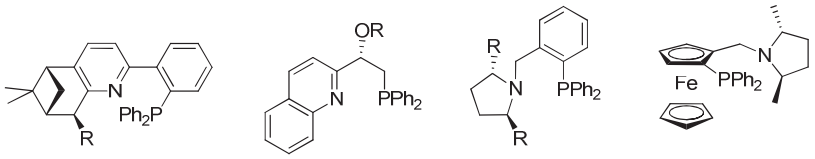

81 **82** **83** **84**

Figure 1.33. Phosphorus-other nitrogen donor ligands **81**-**84** applied in the Pd-catalyzed Heck reaction.

Phosphine-pyridine ligands **81**, **82** (Figure 1.33, **81**: R= H, Me; **82**: R= Si(^{t}Bu)Me$_2$, Si(^{i}Pr)$_3$, Si(^{t}Bu)Ph$_2$) and previously mentioned **17** (Figure 1.8) have been successfully applied to the phenylation of **S59** (regio's up to 98% and ee's up to 99%).[31,111] The results using ligands **17** and **82** showed that the structure of the remote silyl group has a small but significant influence on the enantioselectivity. Enantioselectivities (ee's up to 99%) were therefore best using ligands with a *tert*-butyldiphenylsilyl group. The reaction rates were similar to those observed with the above mentioned Pd-phosphine-oxazoline catalysts.[31]

Guiry and coworkers developed new phosphine-amine ligands **83**-**84** (Figure 1.33) for the arylation and cycloalkenylation of the standard substrate **S59** but with little success.[112] These ligands proved to be considerably less reactive (<25% after several days) and enantioselective (ee's up to 17%) than analogous phosphine-oxazoline ligands.

The previously mentioned phosphine-phenylbenzoxazine **2** (Figure 1.2), in which the oxazoline group of the PHOX ligands has been replaced by an oxazine moiety, provided slightly lower enantioselectivities than those obtained using PHOX ligands in the phenylation and cycloalkenylation of **S59** (ee's up to 94%).[16]

More recently, Andersson and coworkers successfully screened the previously mentioned phosphine-imidazole **28** and phosphine-thiazole **30** (Figure 1.11) in the arylation of **S59** under microwave conditions (ee's up to 98%).[113] Results indicated that the presence of a bulky mesityl substituent at the thiazole group has a positive effect on selectivity. They also found that catalysts could be prevented from deteriorating with no decrease in selectivity by adding triphenylphosphine.[113b]

1.4. Asymmetric hydroformylation

Hydroformylation is an important and extensively studied process for the functionalization of carbon-carbon bonds.[1] In this process, alkenes are converted into aldehydes by reaction with CO/H$_2$ via the addition of a formyl group to the double carbon-carbon bond (Scheme 1.8).

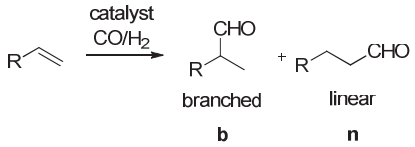

Scheme 1.8. Hydrofomylation of olefins

The regioselectivity is given by the ratio between the branched **b** and linear **n** aldehydes. The linear aldehydes **n** are preferred in industry because aldehydes are mostly made to react to the corresponding alcohols, which are used as solvents, detergents or plasticizer components. Extensive research aimed at producing only linear aldehydes has provided impressive results. The application of phosphines with a wide bite angle in the Rh-catalyzed hydroformylation of terminal alkenes enables regioselecitivity to be practically totally controlled.[1,114]

The branched aldehydes **b** are the product of interest in the asymmetric hydroformylation version. Chiral aldehydes are an important pool for the preparation of fine chemicals (high-value-added compounds) such as flavors, fragances, pharmaceuticals and agrochemicals.[1,114] However, despite these advantages the hydroformylation reaction has been little used in the synthesis of fine chemicals. This may be due to the difficulty in simultaneously controlling chemo-, regio- and enantioselectivity. To date, much effort in this field has concentrated on the hydroformylation of styrene and other vinylarenes.[114] The conversion into enantiomerically pure (*S*)-2-phenylpropanol derivatives is of considerable interest because it is a straightforward route to enantiomerically pure non-steroidal anti-inflammatory drugs. Oxidation of the branched aldehydes provides the desired enantiopure 2-arylpropionic acids, such as cetoprofen, fenoprofen, naproxen and ibuprofen. In the last few years, however, researchers have become significantly more interested in the asymmetric hydroformylation of vinyl acetate, unsaturated nitriles and heterocyclic substrates.

Typically, catalysts for this process are complexes of a transition metal atom (M) that enables the formation of mononuclear metal-carbonyl hydride species. These complexes may be modified by additional ligands (L). The general composition is represented by the structure $HM(CO)_xL_n$. Most of the transition-metal complexes used in asymmetric hydroformylation have been based on Rh and Pt. The best results, however, have been achieved with the Rh-systems.[114]

1.4.1. Mechanism

The accepted mechanism for the Rh-catalyzed hydroformylation of olefins is illustrated in Figure 1.34.[115] The catalytic cycle begins with the dissociation of a carbon monoxide molecule from the catalyst precursor $[HRhL_2(CO)_2]$ (18-electron) intermediate **A**, which has a trigonal bipyramidal structure. Next, the alkene substrate is added to a vacant coordination site of the metal, which generates a π-bonded alkene rhodium complex (**C** or **C'**). The hydride then migrates towards alkene and a 1,2-insertion or 2,1-insertion takes place and a linear (**D'**) or branched (**D**) rhodium alkyl complex is formed. The rhodium-alkyl complexes can also undergo β-hydride elimination, which, in the case of the branched alkyl complex, can lead to isomerized alkenes. In the insertion step, a 16-electron species is formed. This rhodium alkyl species is electronically unsaturated and reacts with carbon monoxide to generate an 18-electron species (**E** or **E'**). At low temperature and a sufficiently high carbon monoxide pressure, the insertion reaction is usually irreversible, so the regioselectivity of the reaction is fixed in this reaction step. The preference for

the hydride migration to form the linear and branched alkyl toward the β-hydride elimination is a key step in the determination of the regioselectivity. There is then the migratory insertion of the alkyl group to one of the coordinated carbon monoxides (complexes **F** or **F'**), the oxidative addition of molecular hydrogen (compounds **G** or **G'**), the reductive elimination of the product aldehyde, and the regeneration of the species [$HRhL_2(CO)$] (**B**), which completes the catalytic cycle.

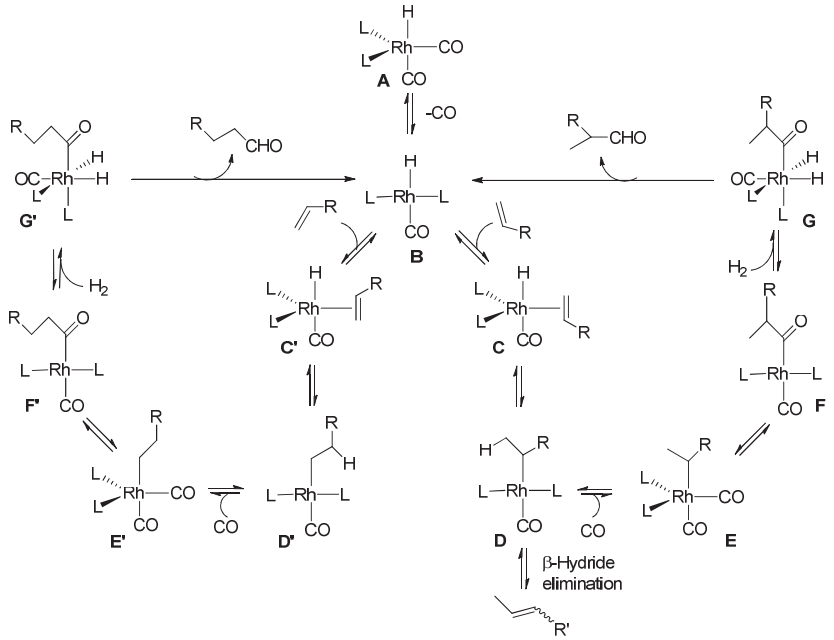

Figure 1.34. Accepted mechanism for the Rh-catalyzed hydroformylation of olefins.

Asymmetric hydroformylation with transition metals is based on the modification of the catalytic system by bidentate phosphorus chiral ligands, which, to obtain high enantioselectivities, must be coordinated throughout the catalytic steps. The solution structures of the trigonal bipyramidal hydrodorhodium complexes with bidentate phosphorus ligand (P-P) [$HRh(P\text{-}P)(CO)_2$] (**A**), which are the resting states in the hydroformylation reaction, have been analyzed in detail.[115] These complexes are generally assumed to have a trigonal bipyramidal structure. Two isomeric structures of these complexes are possible. These contain the bidentate ligand coordinated in a bis-equatorial (**ee**) or an equatorial-axial (**ea**) fashion (Figure 1.35). In certain cases, ^{31}P and ^{1}H NMR spectroscopy studies at variable temperature, together with IR studies, establish a relation between the results from catalysis, the coordination mode of the bidentate phosphorus ligand to the rhodium, and the selectivity of the hydride rhodium intermediates.[115] The excellent selectivities obtained using some diphosphite and phosphine-phosphite ligands have been mainly attributed to the presence of only one active diastereoisomeric hydridorhodiumcarbonyl species.[115] To design and synthesize chiral ligands is therefore a fundamental research subject in asymmetric hydroformylation.

Figure 1.35. Equatorial-equatorial (**ee**) and equatorial-axial (**ea**) [HRh(P-P)$(CO)_2$] species.

1.4.2. Ligands

Although the first highly enantioselective example of hydroformylation was carried out with a Pt-Sn system by Consiglio et al. in 1991, the most successful asymmetric hydroformylation catalysts are based on rhodium.[116] Platinum catalysts have several disadvantages: low reaction rates, low chemoselectivity and low selectivity to the branched product. After the discovery of the high enantioselectivity provided by Rh/diphosphite and Rh/phosphine-phosphite systems, with total conversions in aldehydes and high regioselectivities towards the branched product, rhodium systems became the catalyst of choice for the asymmetric hydroformylation.[1,115] Next, we describe the most important ligands developed for this process.

1.4.2.1. Diphosphite ligands

The initial success in the Rh-catalyzed asymmetric hydroformylation came when Babin and Witheker at the Union Carbide patented the application of the bulky diphosphites ligands **85a-b** derived from (2*R*,4*R*)-pentane-2,4-diol in the asymmetric hydroformylation of vinylarenes with ee's up to 90% (Figure 1.36).[117a] Inspired by these results, van Leeuwen and coworkers found a cooperative effect between the chiral ligand bridge and the axially chiral binaphthyl phosphite moieties, which led to a matched combination for ligand **85d** with (S^{ax}, 2*R*, 4*R*, S^{ax}) configurations.[117b]

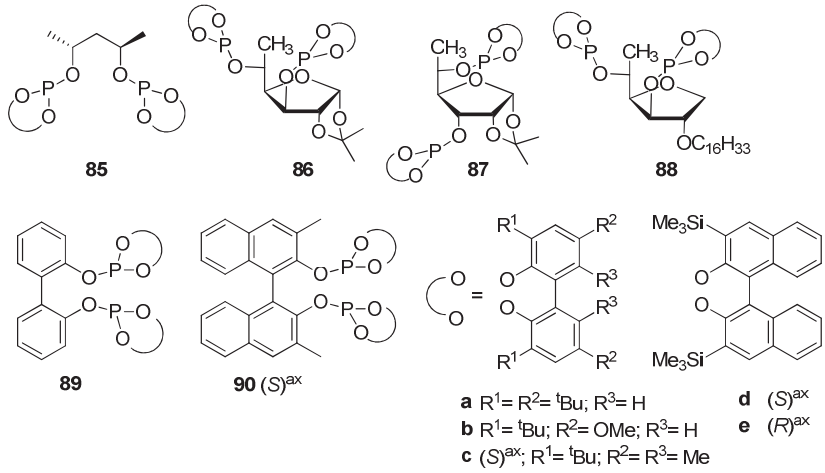

Figure 1.36. Diphosphite ligands **85-90** developed for the Rh-catalyzed hydrofomylation.

Later, 1,3-furanoside diphosphite ligands **86**-**87a-b**,**d-e**, derived from D-glucose, were successfully applied in the Rh-catalyzed asymmetric hydroformylation of styrene derivatives achieving both enantiomeric products in high enantioselectivities (ee's up to 93%) and

regioselectivities (up to 98,8%) under mild conditions (Figure 1.36).[118] These ligands were also successfully used in the hydroformylation of 2,3- and 2,5-dihydrofuran (ee's up to 74%).[119] Ligand **88a**, a further modification of ligand **86a**, has recently afforded enantioselectivities up to 88% in the hydroformylation of 2,3- and 2,5-dihydrofuran.[120]

Through all these years, several authors have developed new diphosphite ligands with biaryl, spiro, pyranoside, mannitol, macrocylic and ferrocene backbones for the Rh-asymmetric hydroformylation of mainly vinylarenes.[121] Only diphosphite ligands **89c** and **90a** have been successfully applied in the Rh-hydroformylation of vinyl acetate obtaining excellent enantioselectivities (ee's up to 88%).[121j-l]

1.4.2.2. Phosphine-phosphite/phosphoroamidite/phosphonite ligands

The first report on asymmetric catalysis using phosphine-phosphite ligands was carried out by Takaya and co-workers in 1993 using the BINAPHOS ligands **91**-**92** (Figure 1.37), obtaining high enantioselectivities in the Rh-hydroformylation of styrene (ee up to 95%).[122]

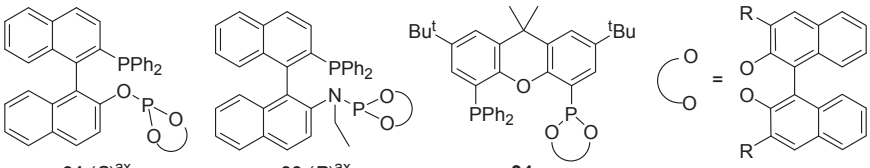

91 $(S)^{ax}$
92 $(R)^{ax}$
93 $(R)^{ax}$
94
a $(S)^{ax}$; R= H
b $(R)^{ax}$; R= H
c $(S)^{ax}$; R= Ph

Figure 1.37. Phosphine-phosphite/phosphoroamidite/phosphonite ligands applied in the Rh-catalyzed hydroformylation.

Later, a wide range of structural variations on the BINAPHOS ligands has been reported.[123] In this context, Nozaki and coworkers found that the sense of enantioselectivity is governed by the configuration of the binaphthyl bridge, whereas the enantiomeric excess depends strongly on the configuration of both binaphthyl moieties. Enantioselectivity is therefore higher when the configurations of the two binaphthyl moieties are opposite (i.e. diastereoisomers *R*,*S* or *S*,*R*; ligands **92a** and **91b**). Over the years, BINAPHOS has been established the most important ligand for asymmetric hydroformylation. Thus, this ligand provides higher enantioselectivities than diphosphine and diphosphite ligands for a wide variety of alkenes, including vinylarenes (ee's up to 98.5%)[122,123], vinyl acetate (ee's up to 92%)[124] and heterocyclic olefins (ee's up to 97%)[125] among others.

Inspired by the excellent results using the BINAPHOS ligands, new phosphine-phosphite ligands with different backbones have been developed in the last years. Unfortunately, their Rh-hydroformylation provided low-to-moderate enantioselectivities (ee's from 20 to 71%).[126]

In 2006, phosphine-phosphoroamidite ligand **93a**, related to BINAPHOS, has also been successfully applied in the Rh-catalyzed asymmetric hydroformylation of vinylarenes and vinyl acetate (ee's up to 99% and 96%, respectively).[127]

In 2010, the group of Reek reported the successful application of phosphine-phosphonite ligand **94c** in the Rh-catalyzed asymmetric hydroformylation of dihydrofurans (ee's up to 91%).[128]

1.4.2.3. Diphosphines and other ligands

Several diphosphine ligands have been applied to this catalytic process. In general, they do not achieve ee's as high as the Rh-system with diphosphite or BINAPHOS.[115] However, recently bisphosphacyclic ligands have emerged as interesting alternatives.[129] For example, ligands **95**-**97** (Figure 1.38) afforded excellent enantioselectivities in the asymmetric hydroformylation of vinylarenes (ee's up to 94%), vinyl acetate (ee's up to 96%%) and allyl cyanide (ee's up to 96%).[129] It should also be noted that bis-(diazaphospholodine) ligand **98** provided high regio- and enantioselectivity in the Rh-catalyzed hydroformylation of vinyl acetate (ee's up to 89%).[130]

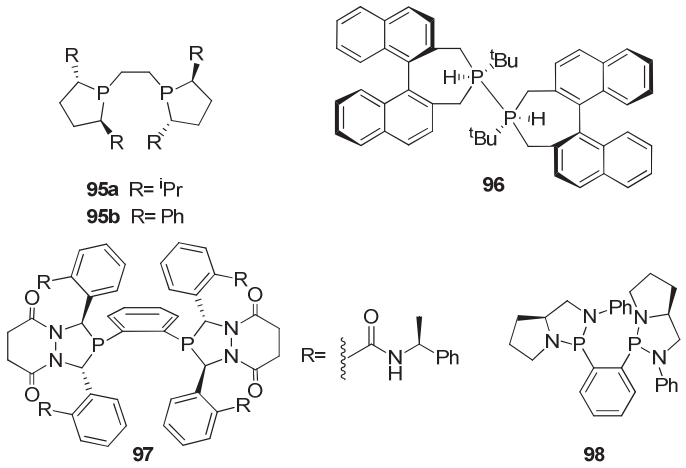

Figure 1.38. Bisphophacyclic ligands applied in the Rh-catalyzed hydroformylation.

1.5. References

[1] a) *Asymmetric Catalysis in Industrial Scale: Challenges, Approaches and Solutions*; Blaser, H. U, Schmidt, E., Eds.; Wiley: Weinheim, 2003. b) *Comprehensive Asymmetric Catalysis*; Jacobsen, E. N., Pfaltz, A., Yamamoto, H., Eds.; Springer-Verlag: Berlin, 1999. c) *Asymmetric Catalysis in Organic Synthesis*; Noyori, R., Ed.; Wiley: New York, 1994. d) *Applied Homogeneous Catalysis with Organometallics Compounds*, 2nd ed.; Cornils, B., Hermann, W. A., Eds.; Wiley-VCH: Wienhein, 2002. e) *Catalytic Asymmetric Synthesis;* Ojima, I., Ed.; Wiley: New Jersey, 2010.

[2] For recent reviews, see: a) Källström, K.; Munslow, I.; Andersson, P. G.; *Chem. Eur. J.* **2006**, *12*, 3194. b) Roseblade, S. J.; Pfaltz, A. *Acc. Chem. Res.* **2007**, *40*, 1402. c) Church, T. L.; Andersson, P. G. *Coord. Chem. Rev.* **2008**, *252*, 513. d) Cui, X.; Burgess, K. *Chem. Rev*. **2005**, 3272. e) Pàmies, O.; Andersson, P. G.; Diéguez, M. *Chem. Eur. J.* **2010**, *16*, 14232. f) *Modern Reduction Methods*; Andersson, P. G.; Munslow, I. J., Eds.; Wiley-VCH: Wienhein, 2008. g) Woodmansee, D. H.; Pfaltz, A. *Chem. Commun.* **2011**, *47*, 7912.

[3] See, for example: a) Halpern, J.; Riley, D. P.; Chan, A. S. C.; Pluth, J. J. *J. Am. Chem. Soc.* **1977**, *99*, 8055. b) Chan, A. S. C.; Pluth, J. J.; Halpern, J. *J. Am. Chem. Soc.* **1980**, *102*, 5952. c) Feldgus, S.; Landis, C. R. *J. Am. Chem. Soc.* **2000**, *122*, 12714. d) Donoghue, P. J.; Helquist, P.; Norrby, P. – O.; Wiest, O. *J. Am. Chem. Soc.* **2009**, *131*, 410.

[4] a) Roseblade, S. J.; Pfaltz, A. *C. R. Chim.* **2007**, *10*, 178. b) Vazquez-Serrano, L. D.; Owens, B. T.; Buriak, J. M. *Chem. Commun.* **2002**, 2518. c) Dietiker, R.; Chen, P. *Angew. Chem. Int. Ed.* **2004**, *43*, 5513.
[5] a) Cui, X.; Fan, Y.; Hall, M. B.; Burgess, K. *Chem. Eur. J.* **2005**, *11*, 6859. b) Fan, Y.; Cui, X.; Burgess, K. *J. Am. Chem. Soc.* **2004**, *126*, 16688. c) Brandt, P.; Hedberg, C.; Andersson, P. G. *Chem. Eur. J*. **2003**, *9*, 339.
[6] Church, T. L.; Rasmussen, T.; Andersson, P. G. *Organometallics*, **2010**, *29*, 6769.
[7] Hopmann, K. H.; Bayer, A. *Organometallics*, **2011**, *30*, 2483.
[8] a) Lightfoot, A., Schnider, P., Pfaltz, A*., Angew. Chem. Int. Ed.* **1998**, *37*, 2897. b) Blackmond, D. G.; Lighfoot, A.; Pfaltz, A.; Rosner, T.; Schnider, P.; Zimmermann, *Chirality* **2000**, *12*, 442. c) Zimmermann, N. *Dissertation*, University of Basel, **2001**.
[9] Crabtree, R. H. *Acc. Chem. Res.* **1979**, *12*, 331.
[10] Schnider, P.; Koch, G.; Prétôt, R.; Wang, G.; Bohnen, F. M.; Krüger, C.; Pfaltz, A. *Chem. Eur. J.* **1997**, *3*, 887.
[11] Goulioukina, N. S.; Dolgina, T.; M.; Bondarenko, G. N.; Beletskaya, I. P.; Ilyin, M. M.; Davankov, V. A.; Pfaltz A. *Tetrahedron: Asymmetry* **2003**, *14*, 1397.
[12] a) Lu, S.–M.; Bolm. C. *Angew. Chem. Int. Ed* **2008**, *47*, 8920. b) Lu, S.–M.; Bolm. C. *Chem. Eur. J.* **2008**, *14*, 7513.
[13] a) Nicolau, K. C.; Edmonds, D. J.; Li, A.; Tria, G. S. *Angew. Chem. Int. Ed*. **2007**, *46*, 3942. b) Lim, S. H.; Curtis, M. D.; Beak, P. *Org. Lett*. **2001**, *3*, 711. c) Schneider, U.; Pannecoucke, X.; Quirion, J. C. *Synlett* **2005**, 1853.
[14] Coll, M.; Pàmies, O.; Diéguez, M. *Chem. Commun.* **2011**, *47*, 9215.
[15] Rageot, D.; Woodmansee, D. H.; Pugin, B.; Pfaltz, A. *Angew. Chem. Int. Ed.* **2011**, *50*, 9598.
[16] Bernardinelli, G. H.; Kündig, E. P.; Meier, P.; Pfaltz, A.; Radkowski, K.; Zimmermann, N.; Neuburger-Zehnder, M. *Helv. Chim. Acta.* **2001**, *84*, 3233.
[17] Hou, D. –R.; Reibenspies, J.; Calacot, T. J.; Burgess, K. *Chem. Eur. J*. **2001**, *24*, 5391.
[18] Liu, D.; Tang, W.; Zhang, X. *Org. Lett*. **2004**, *4*, 513.
[19] Cozzi, P. G.; Menges F.; Kaiser, S. *Synlett*. **2003**, 833.
[20] Schrems, M. G.; Neumann, E.; Pfaltz, A. *Angew. Chem. Int. Ed.* **2007**, *46*, 8274.
[21] a) Lu, W.–J.; Chen, Y.–W.; Hou, X.–L. *Angew. Chem. Int. Ed* **2008**, 47, 10133. b) Lu, W. J.; Chen, Y.–W.; Hou, X.–L. *Adv. Synth. Catal.* **2010**, *352*, 103.
[22] Schrems, M. G.; Pfaltz, A. *Chem. Commun*. **2009**, 6210.
[23] Cozzi, P. G.; Zimmermann, N.; Hilgraf, R.; Schaffner, S.; Pfaltz, A. *Adv. Synth. Catal.* **2001**, *343*, 450.
[24] Xu, G.; Gilbertson, S. R. *Tetrahedron Lett.* **2003**, *44*, 953.
[25] a) Trifonova, A.; Diesen, J. S.; Andersson, P. G. *Chem. Eur. J.* **2006**, *12*, 2318. b) Cheruku, P.; Diesen, J.; Andersson, P. G. *J. Am. Chem. Soc.* **2008**, *130*, 5595. c) Cheruku, P.; Gohil, S.; Andersson, P. G. *Org. Lett.* **2007**, *9*, 1659. d) Källström, K.; Munslow, I. J.; Hedberg, C.; Andersson, P. G. *Adv. Synth. Catal.* **2006**, *348*, 2575. e) Engman, M.; Diesen, J. S.; Paptchikhine, A.; Andersson, P. G. *J. Am. Chem. Soc.* **2007**, *129*, 4536. f) Paptchikhine, A.; Cheruku, P.; Engman, M.; Andersson, P. G. *Chem. Commun.* **2009**, 5996.
[26] Chakka, S. K.; Peter, B. K.; Andersson, P. G.; Maguire, G. E. M.; Kruger, H. G.; Govender, T. *Tetrahedron: Asymmetry* **2010**, *21*, 2295.

[27] a) Blankenstein, J.; Pfaltz A. *Angew. Chem. Int. Ed.* **2001**, *40*, 4445. b) Menges, F.; Pfaltz, A. *Adv. Synth. Catal.* **2002**, *344*, 40. c) McIntyre, S.; Hörmann, E.; Menges, F.; Smidt, S. P.; Pfaltz, A. *Adv. Synth. Catal*. **2005**, *347*, 282.
[28] Smidt, S. P.; Menges, F.; Pfaltz, A. *Org. Lett,* **2004**, *12*, 2023.
[29] For some representative examples see: a) Peña, D.; Minnaard, A.; de Vries, J. G.; Feringa, L. J. *J. Am. Chem. Soc.* **2002**, *124*, 14552. b) Reetz, M. T.; Sell, T.; Meiswinkel, A.; Mehler, G. *Angew. Chem. Int. Ed.* **2003**, *42*, 790. c) Claver, C.; Fernandez, E.; Gillon, A.; Heslop, K.; Hyett, D. J.; Martorell, A.; Orpen, A. G.; Pringle, P. G. *Chem. Commun*. **2000**, 961. d) Claver, C.; Diéguez, M.; Pàmies, O.; Castillón, S. in *Catalytic Carbonylation Reactions*; Beller, M., Ed.; Springer-Verlag: Berlin, 2006; pp 35-64. e) Yan, M.; Zhou, Z.-Y.; Chan, A. S. C. *Chem. Commun*. **2000**, 115. f) Pàmies, O.; Diéguez, M.; Claver, C. *J. Am. Chem. Soc.* **2005**, *127*, 3646. g) Mata, Y.; Pàmies, O.; Diéguez, M. *Chem. Eur. J.* **2007**, *13*, 3296.
[30] a) Hilgraf, R.; Pfaltz, A. *Synlett* **1999**, 1814. b) Hilgraf, R.; Pfaltz, A. *Adv. Synth. Catal.* **2005**, *347*, 61. c) Schönleber, M.; Hilgraf, R.; Pfaltz, A. *Adv. Synth. Catal.* **2008**, *350*, 2033.
[31] Drury, W. J. III; Zimmerman, N.; Keenan, M.; Hayashi, M.; Kaiser, S.; Goddard, R.; Pfaltz, A. *Angew. Chem. Int. Ed.* **2004**, *43*, 70.
[32] Zalubovskis, R.; Hörmann, E.; Pfaltz, A.; Moberg, C. *ARKIVOC* **2008**, *14*, 58.
[33] a) Kaiser, S.; Smidt, S. P.; Pfaltz A. Angew. *Chem. Int. Ed.* **2006**, *45*, 5194. b) Woodmansee, D. H.; Müller, M.–A.; Neuburger, M.; Pfaltz A. *Chem. Sci*. ***2010***, *1*, 72.
[34] Liu, Q. –B.; Yu, C. –B.; Zhou, Y. –G. *Tetrahedron Lett*. **2006**, *47*, 4733
[35] a) Bell, S.; Wüstenberg B.; Kaiser, S.; Menges, F.; Netscher, T.; Pfaltz, A. *Science* **2006**, *311*, 642. b) Wang, A.; Fraga, R. P. A.; Hörmann, E.; Pfaltz, A. *Chem. Asian J.* **2011**, *6*, 599.
[36] Netscher, T. *Chimia* **1996**, *50*, 563.
[37] Verendel, J. J.; Andersson, P. G. *Dalton Trans.* **2007**, 5603.
[38] Chelucci, G.; Marchetti, M.; Malkov, A. V.; Friscourt, F.; Swarbrick, M. E.; Kocovsky, P. *Tetrahedron*, **2011**, *67*, 5421.
[39] Bunlaksananusorn, T.; Polborn, K.; Knochel, P. *Angew. Chem. Int. Ed.* **2003**, *42*, 3941.
[40] Li, X.; Kong, L.; Gao, Y.; Wang, X. *Tetrahedron Lett.* **2007**, *48*, 3915.
[41] Han, Z.; Wang, Z.; Zhan, X.; Ding, K. *Tetrahedron: Asymmetry* **2010**, *21*, 1529.
[42] Menges, F.; Neuburger, M.; Pfaltz, A. *Org. Lett*. **2002**, *26*, 4713.
[43] Franke, A.; Pfaltz, A. *Chem. Eur. J*. **2011**, *17*, 4131.
[44] Kaukoranta, P.; Engman, M.; Hedberg, C.; Bergquist, J.; Andersson, P. G. *Adv. Synth. Catal.* **2008**, *350*, 1168.
[45] Källström, K.; Hedberg, C.; Brandt, P.; Bayer, A.; Andersson, P.G. *J. Am. Chem. Soc.* **2004**, *126*, 14308
[46] Hedberg, C.; Källström, K.; Brandt, P.; Hansen, L. K.; Andersson, P. G. *J. Am. Chem. Soc.* **2006**, *128*, 2995.
[47] Engman, M.; Cheruku, P.; Tolstoy, P.; Bergquist, J.; Völker, S. F.; Andersson, P. G. *Adv. Synth. Catal.* **2009**, *351*, 375.
[48] Tolstoy, P.; Engman, M.; Paptchikhine, A.; Bergquist, J.; Church, T. L.; Leung, A. W. –M.; Andersson, P. G. *J. Am. Chem. Soc*. **2009**, *131*, 8855.
[49] Cheruku, P.; Paptchikhine, A.; Church, T. L.; Andersson, P. G. *J. Am. Chem. Soc.* **2009**, *131*, 8285.
[50] Cheruku, P.; Paptchikhine, A.; Ali, M.; Neudörfl, J. –M.; Andersson, P. G. *Org. Biomol, Chem.* **2008**, *6*, 366.

[51] Li, J. –Q.; Paptchikhine, A.; Govender, T.; Andersson, P. G. *Tetrahedron: Asymmetry* **2010**, *21*, 1328.
[52] Schenkel, L. B.; Ellman, J. A. *J. Org. Chem.* **2004**, *69*, 1800.
[53] a) *Palladium Reagents and Catalysis, Innovations in Organic Synthesis*; Tsuji, J., Ed.; Wiley: New York, 1995, b) Trost, B. M.; van Vranken, D. L. *Chem. Rev.* **1996**, *96*, 395. c) Johannsen, M.; Jorgensen, K. A. *Chem. Rev.* **1998**, *98*, 1689. d) Trost, B.; Crawley, M. L. *Chem. Rev*. **2003**, *103*, 292. e) Helmchen, G.; Pfaltz, A. *Acc. Chem. Res.* **2000**, *33*, 336. f) Lu, Z.; Ma, S. *Angew. Chem. Int. Ed*. **2008**, *47*, 258.
[54] a) Yorimitsu , H.; Oshima, K.; *Angew. Chem. Int. Ed*. **2005**, *44*, 4435. b) Alexakis, A.; Bäckvall, J.-E.; Krause, N.; Pàmies, O.; Diéguez, M. *Chem. Rev.* **2008**, *108*, 2796. c) Karlström, A. S. E.; Bäckvall, J. E. in *Modern Organocopper Chemistry*; Krause, N., Ed.; Wiley-VCH: Weinheim:, 2002.
[55] Hayashi, T.; Yamamoto, A.; Ito, Y.; Nishioka, E.; Miura, H.; Yanagi, K. *J. Am. Chem. Soc.* **1989**, *111*, 6301.
[56] a) Trost, B. M.; van Vranken, D. L.; Bingel, C. *J. Am. Chem. Soc.* **1992**, *114*, 9327. b) Trost, B. M. *Acc. Chem. Res.* **1996**, *29*, 355.
[57] a) Von Matt, P., Pfaltz, A., *Angew. Chem. Int. Ed.* **1993**, *32*, 566. b) Sprinz, J., Helmchen, G., *Tetrahedron Lett.* **1993**, *34*, 1769. c) Dawson, G. J., Frost, C. G., Williams, J. M. J, Coote, S. J., *Tetrahedron Lett.* **1993**, *34*, 3149.
[58] Diéguez, M.; Pàmies, O. *Acc. Chem. Res.* **2010**, *43*, 312.
[59] Gläser, B.; Kunz, H. *Synlett* **1998**, 53.
[60] Moreno, R. M.; Bueno, A.; Moyano, A. *J. Organometal. Chem.* **2002**, *660*, 62.
[61] Frölander, A.; Lutsenko, S.; Privalov, T.; Moberg, C. *J. Org. Chem.* **2005**, *70*, 9882.
[62] Liu, S.; Müller, J. F. K.; Neuburger, M.; Schaffner, S.; Zehnder, M. *Helv. Chem. Acta.* **2000**, *83*, 1256.
[63] Tietze, L. F.; Lohmann, J. K. *Synlett* **2002**, 2083.
[64] Danjo, H.; Higuchi, M.; Yada, M.; Imamoto, T. *Tetrahedron Lett.* **2004**, *45*, 603.
[65] a) Ahn, K. H.; Cho, C. –W; Park, J.; Lee, S. *Tetrahedron: Asymmetry* **1997**, *8*, 1179. b) You, S. –L.; Hou, X. –L.; Dai, L. –X.; Yu, Y. –H.; Xia, W. *J. Org. Chem.* **2002**, *67*, 4684.
[66] a) Zhang, W.; Yoneda, Y. –I.; Kida, T.; Nakatsiju, Y.; Ikeda, I. *Tetrahedron: Asymmetry* **1998**, *9*, 3371. b) Parl, J.; Quan, Z.; Lee, S.; Ahn, K. H.; Cho, C. –W. *J. Organometal. Chem*. **1999**, *584*, 140. c) Deng, W. –P.; Hou, X. –L.; Dai, L. –X.; Yu, Y. –H.; Xia, W. *Chem. Commun*. **2000**, 185. d) Deng, W. –P.; You, S. –L.; Hou, X. –L.; Dai, L. –X.; Yu, Y. –H.; Xia, W.; Sun, J. *J. Am. Chem. Soc*. **2001**, *123*, 6508.
[67] a) Imai, Y.; Zhang, W.; Kida, T.; Nakatsuji, Y.; Ikeda, I. *Tetrahedron Lett.* **1998**, *39*, 4343. b) Selvkumar, K.; Valentini, M.; Pregosin, P. S. *Organometallics* **2000**, *19*, 1299.
[68] a) Hou, D. –R.; Burgess, K. *Org. Lett.* **1999**, *11*, 1745. b) Hou, D. –R.; Reibenspies, J. H.; Burgess, K. *J. Org. Chem.* **2001**, *66*, 206.
[69] Liu, D.; Dai, Q.; Zhang, X. *Tetrahedron* **2005**, *61*, 6460.
[70] a) Yonehara, K.; Hashizume, T.; Mori, K.; Ohe, K.; Uemura, S. *Chem. Commun*. **1999**, 415. b) Yonehara, K.; Hashizume, T.; Mori, K.; Ohe, K.; Uemura *J. Org. Chem.* **1999**, *64*, 9374.
[71] a) Jones, G.; Richards, C. J. *Tetrahedron Lett.* **2001**, *42*, 5553. b) Jones, G.; Richards, C. J. *Tetrahedron: Asymmetry* **2004**, *15*, 653.
[72] a) Prétôt, R.; Pfaltz, A. *Angew. Chem. Int. Ed.* **1998**, *37*, 323. b) Prétôt, R.; Lloyd-Jones, G. C.; Pfaltz, A. *Pure Appl. Chem*. **1998**, *70*, 1035.
[73] Gladiali, S.; Loriga, G.; Medici, S.; Taras, R. *J. Mol. Cat. A: Chem*. **2003**, *196*, 27.

[74] a) Mata, Y.; Diéguez, M.; Pàmies, O.; Claver, C. *Adv. Synth. Catal.* **2005**, *347*, 1943. b) Mata, Y.; Pàmies, O.; Diéguez, M. *Adv. Synth. Catal.* **2009**, *351*, 3217.
[75] Diéguez, M.; Pàmies, O. *Chem. Eur. J*. **2008**, *14*, 3653.
[76] Jang, H. –Y.; Seo, H.; Han, J. W.; Chung, Y. K. *Tetrahedron Lett* **2000**, *41*, 5083.
[77] Lee, J. H.; Son, S. U.; Chung, Y. K. *Tetrahedron: Asymmetry* **2003**, *14*, 2109.
[78] a) Hu, X.; Dai, H.; Hu, X.; Chen, H.; Wang, J.; Bai, C.; Zheng, Z. *Tetrahedron: Asymmetry* **2002**, *13*, 1687. b) Hu, X.; Dai, H.; Chen, H.; Wang, J.; Bai, C.; Zheng, Z. *Tetrahedron: Asymmetry* **2004**, *15*, 1065.
[79] Thiesen, K. E.; Maitra, K.; Olmstead, M. M.; Attar, S. *Organometallics* **2010**, *29*, 6334.
[80] Tsarev, V. N.; Lyubimov, S. E.; Bondarev, O. G.; Korlyukov, A.; Antipin, M. Y.; Pretovskii, P. V.; Davankov, V. A.; Shiryaev, A. A.; Benetsky, E. B.; Vologzhanin, P. A.; Gavrilov, K. N. *Eur. J. Org. Chem.* **2005**, 2097.
[81] Bunlaksananusorn, T.; Luna, A. P.; Bonin, M.; Micouin, L.; Knochel, P. *Synlett* **2003**, 2240.
[82] Ito, K.; Kashiwagi, R.; Iwsaki, K.; Katsuki, T. *Synlett* **1999**, 1563.
[83] For other recent applications, see: a) Goldfuss, B.; Löschmann, T.; Rominger, F. *Chem. Eur. J.* **2004**, *10*, 5422. b) Liu, Q.-B.; Zhou, Y.-G. *Tetrahedron Lett.* **2007**, *48*, 2101. c) Meng, X.; Gao, Y.; Li, X.; Xu, D. *Cat. Commun.* **2009**, *10*, 950. d) Leca, F.; Fernández, F.; Muller, G.; Lescop, C.; Réau, R.; Gómez, M. *Eur. J. Inorg. Chem.* **2009**, 5583.
[84] a) Mino, T.; Shiotsuki, M.; Yamamoto, N.; Suenaga, T.; Sakamoto, M.; Fujuta, T.; Yamashita, M. *J. Org. Chem.* **2001**, *66*, 1795. b) Mino, T.; Imaya, W.; Yamashita, M. Synlett **1997**, 583.
[85] Mei, L.-Y.; Yuan, Z.-L.; Shi, M. *Organometallics* **2011**, *30*, 6466.
[86] Jin, M. –J.; Jung, J. –A.; Kim, S. –H. *Tetrahedron Lett.* **1999**, *40*, 5197.
[87] Okuyama, Y.; Nakano, H.; Hongo, H. *Tetrahedron: Asymmetry* **2000**, *11*, 1193.
[88] a) Mino, T.; Tanaka, Y.; Akita, K.; Sakamoto, M.; Fujita, T. *Heterocycles* **2003**, *60*, 9. b) Mino, T.; Hata, S.; Ohtaka, K.; Salamoto, M.; Fujita, T. *Tetrahedron Lett*. **2001**, *42* 4837.
[89] a) Jin, M.-J.; Kim, S.-H.; Lee, S.-J.; Kim, Y.-M. *Tetrahedron Lett*. **2002**, *43*, 7409. b) Lee, E.-K.; Kim, S.-H.; Jung, B.-H.; Ahn, W.-S.; Kim, G.-J. *Tetrahedron Lett.* **2003**, *44*, 1971.
[90] Tanaka, Y.; Mino, T.; Akita, K.; Sakamoto, M.; Fujita, T. *J. Org. Chem.* **2004**, *69*, 6679.
[91] a) Kubota, H.; Koga, K. *Heterocycles* **1996**, *42*, 543. b) Widhalm, M.; Nettekoven, U.; Kalchhauser, H.; Mereiter, K.; Calhorda, M. J.; Félix, V. *Organometallics* **2002**, *21*, 315.
[92] Vasse, J.-L.; Stranne, R.; Zalubovskis, R.; Gayet, C.; Moberg, C. *J. Org. Chem*. **2003**, *68*, 3258.
[93] Chen, G.; Li, X.; Zhang, H.; Gong, L.; Mi, A.; Cui, X.; Jiang, Y.; Choi, M. C. K.; Chan, A. S. C. *Tetrahedron: Asymmetry* **2002**, *13*, 809.
[94] Braga, A. L.; Sehnem, J. A.; Lüdtke, D. S.; Zeni, G.; Silveira, C. C.; Marchi, M. I. *Synlett* **2005**, 1331.
[95] Sun, X.-M.; Koizumi, M.; Manabe, K.; Kobayashi, S. *Adv. Synth. Catal*. **2005**, *347*, 1893.
[96] For recent reviews, see: a) Tietze, L. T.; Ila, H.; Bell, H. P. *Chem. Rev.* **2004**, *104*, 3453. b) Dai, L. X.; Tu, T.; You, S. L.; Deng, W. P.; Hou, X. L. *Acc. Chem. Res*. **2003**, *36*, 659. c) Bolm, C.; Hildebrand, J. P.; Muñiz, K.; Hermanns, N. *Angew. Chem. Int. Ed.* **2001**, *44*, 3284. d) Loiseleur, O.; Hayashi, M.; Keenan, M.; Schemees, N.; Pfaltz, A*. J. Organometal. Chem.* **1999**, *576*, 16. e) Beller, M.; Riermeier, T. H.; Stark, G. in *Transition Metals for Organic Synthesis;* Beller, M., Bolm, C., Eds.; Wiley-VCH: Wienheim, 1998. f) Dounay, A. B.; Overman, L. E. *Chem. Rev.* **2003**, *103*, 2945. g) Mc-Cartney, D.; Guiry, P. J. *Chem. Soc. Rev.* **2011**, *40*, 5122.
[97] Ozawa, F.; Kubo, A.; Matsumoto, Y.; Hayashi, T. *Organometallics* **1993**, *12*, 4188.

[98] a) Ozawa, F.; Kubo, A.; Hayashi, T. *J. Am. Chem. Soc*. **1991**, *113*, 1417. b) Ozawa, F.; Hayashi, T. *J. Organomet. Chem*. **1992**, *428*, 267.
[99] a) O. Loiseleur, P. Meier, A.; Pfaltz, *Angew. Chem.* **1996**, *108*, 218; *Angew. Chem. Int. Ed. Engl.* **1996**, *35*, 200. b) O. Loiseleur, M. Hayashi, N. Schmees, A. Pfaltz, *Synthesis* **1997**, 1338. c) A. J. Hennessy, Y. M. Malone, P. J. Guiry, *Tetrahedron Lett*. **1999**, *40*, 9163. d) A. J. Hennessy, D. J. Connolly, Y. M. Malone, P. J. Guiry, *Tetrahedron Lett*. **2000**, *41*, 7757.
[100] P. Nilsson, H. Gold, M. Larhed, A. Hallberg, *Synthesis* **2002**, 1611.
[101] Hashimoto, Y.; Horie, Y.; Hayashi, M.; Saigo, K. *Tetrahedron: Asymmetry* **2000**, *11*, 2205.
[102] Bélanger, E.; Pouliot, M.-F.; Paquin, J.-F. *Org. Lett.* **2009**, *11*, 2201.
[103] Ogasawara, M.; Yoshida, K.; Hayashi, T. *Heterocycles* **2000**, *52*, 195.
[104] a) Gilbertson, S. R.; Xie, D.; Fu, Z. *J. Org. Chem.* **2001**, *66*, 7240. b) Gilbertson, S. R.; Fu, Z. *Org. Lett.* **2001**, *3*, 161. c) Gilbertson, S. R.; Genov, D. G.; Rheingold, A. L. *Org. Lett.* **2000**, *2*, 2885.
[105] a) Deng, W.-P.; Hou, X.-L.; Dai, L.-X.; Dong, X.-W. *Chem. Commun.* **2000**, 1483. b) Tu, T.; Deng, W.-P.; Hou, X.-L.; Dai, L.-X.; Domg, X.–C. *Chem. Eur. J*., **2003**, *9*, 3073.
[106] a) Kilroy, T. G.; Cozzi, G. P.; End, P. J.; Guiry, P. J. *Synlett* **2004**, 106. b) Kilroy, T. G.; Cozzi, G. P.; End, P. J.; Guiry, P. J. *Synthesis* **2004**, 1879. c) Fitzpatrick, M. O.; Müller-Bunz, H.; Guiry, P. J. *Eur. J. Org. Chem.* **2009**, 1889.
[107] Rubina, M.; Sherrill, W. E.; Rubin, M. *Organometallics*, **2008**, *27*, 6393.
[108] Wu, W.-Q.; Peng, Q.; Dong, D.-X.; Hou, X.-L.; Wu, Y.-D. *J. Am. Chem. Soc.* **2008**, *130*, 9717.
[109] Yonehara, K.; Mori, K.; Hashizume, T.; Chung, K.-G.; Ohe, K.; Uemure, S. *J. Organometal. Chem*. **2000**, *603*, 40.
[110] Mata, Y.; Diéguez, M.; Pàmies, O.; Claver, C. *Org. Lett.* **2005**, *7*, 5597.
[111] Malkov, A. V.; Bella, M.; Stará, I. G.; Kocovsky, P. *Tetrahedron Lett*. **2001**, *42*, 3045.
[112] Kilroy, T. G.; Hennessy, A. J.; Connolly, D. J.; Malone, Y. M.; Farrell, A.; Guiry, P. J. *J. Mol. Chem. Cat. A.* Chem **2003**, *196*, 65.
[113] a) Kaukaronta, P.; Källström, K.; Andersson, P. G. *Adv. Synth. Catal.* **2007**, *349*, 2595. b) Henriksen, S. T.; Norrby, P.-O.; Kaukaronta, P.; Andersson, P. G. *J. Am. Chem. Soc.* **2008**, *130*, 10414.
[114] For reviews, see: a) *Aldehydes: synthesis by hydroformylation alkenes. In Science of synthesis*; Breit, B., Eds.; Thieme: Stuttgart, 2007. b) *Rhodium catalyzed Hydroformilation*; van Leeuwen, P. W. N. M.; Claver, C., Eds.; Kluver Academic Press: Dordrecht, 2000. c) *Homogeneous catalysis "Understanding the Art"*; van Leeuwen, P. W. N. M., Ed.; Elsevier: Amsterdam, 2004.
[115] See, for instance: a) Heck, R. F. *Acc. Chem. Res.* **1969**, *2*, 10. b) Evans, D. A.; Osborn, J. A.; Wilkinson, G. *J. Chem. Soc. A* **1968**, 3133. c) Evans, D.; Yagupsky, G.; Wilkinson G.; *J. Chem. Soc. A,* **1968**, 2660. d) Young, J. F.; Osborn, J. A.; Jardine, F. A.; Wilkinson, G. *J. Chem. Soc. Comm.* **1965**, 131. e) Agbossou, F. F.; Carpentier, J. F.; Mortreux, A. *Chem. Rev.* **1995**, *95*, 2485. f) Gladiali, S. Bayón, J. C.; Claver, C. *Tetrahedron: Asymmetry* **1995**, *7*, 1453. g) Consiglio, G. in *Catalytic Asymmetric Syntheses;* Ojima, I., Ed.; VCH: New York, 1993, 273. h) Claver, C.; Diéguez, M.; Pàmies, O.; Castillón, S. in *Topics in Organometallic Chemistry;* Beller, M., Ed.; Springer: Berlin, 2006, 35. i) Nozaki, K. in *Comprehensive Asymmetric Catalysis;* Jacobsen, E. N., Pfaltz, A., Yamamoto, H., Eds.; Springer: Berlin; 1999, 382. j) Breit, B *Top. Curr. Chem.* **2007**, *279*, 139. k) Klosin, J.; Landis, C. R. *Acc. Chem. Res.* **2007**, *40*, 1251
[116] a) Stille, J. K.; Su, H.; Brechot, P.; Parrinello, G.; Hegedus, L. S. *Organometallics*, **1991**, *10*, 1183. b) Consiglio, G.; Nefkens, S. C. A. *Tetrahedron: Asymmetry*, **1990**, *1*, 417. c) Consiglio, G.;

Nefkens, S. C. A.; Borer, A. *Organometallics*, **1991**, *10*, 2046. d) Cserépi-Szücs, S.; Bakos, J. *Chem. Commun.* **1997**, 635.

[117] a) Babin, J. E.; Witheker, G. T. (Union Carbide Chem. Plastics Tech. Co.) WO 93/03839, 1993, Chem. Abs., **1993**, *119*, P159872h. b) Buisman. G. J. H.; van der Veen, L. A.; Klootwijk, A.; de Lange, W. G.; Kamer, P. C.; van Leewuen, P. W. M. N.; Vogt, D. *Organometallics*, **1997**, *16*, 2929.

[118] a) Diéguez, M.; Pàmies, O.; Ruiz, A.; Castillón, S.; Claver, C. *Chem. Commun.* **2000**, 1607. b) Diéguez, M.; Pàmies, O.; Ruiz, A.; Castillón, S.; Claver, C. *Chem. Eur. J*., **2001**, *7*, 3086. c) Diégiez, M.; Pàmies, O.; Ruiz, A.; Castillón, S.; Claver, C. *New. J. Chem*., **2002**, *26*, 827.

[119] Diéguez, M.; Pàmies, O.; Claver, C. *Chem. Commun.* **2005**, 1221.

[120] Gual, A.; Godard, C.; Castillón, S.; Claver, C. *Adv. Synth. Catal.* **2010**, *352*, 463.

[121] See for instance: a) Cserépi-Szûcs, S.; Huttner, G.; Zsolnai, L.; Bakos, J. *J. Organometal. Chem.* **1999**, *586*, 70. b) Cserépi-Szûcs, S.; Huttner, G.; Zsolnai, L.;Szölösy, A.; Hegebüs, C.; Bakos, J *Inorg. Chem. Acta* **1999**, *296*, 222. c) Vegehetto, V. Scrivanti, A.; Matteoli. U. *Catal. Commun.* **2001**, *2*, 139. d) Jiang, Y.; Xue, S.; Li, Z.; Deng, J.; Mi, A.; Chan, A. S. C. *Tetrahedron: Asymmetry* **1998**, *9*, 3185. e) Jiang, Y.; Xue, S.; Li, Z.; Deng, J.; Mi, A.; Chan, A. S. C *J. Organomet. Chem*. **1999**, *586*, 159. f) Kadyrov, R.; Heller, D.; Selke, R. *Tetrehedron: Asymmetry* **1999**, *9*, 329. (g) Freixa, Z.; Bayón, J. C. *J. Chem. Soc., Dalton Trans*. **2001**, 2067. h) Wang, L. L.; Guo, E. –W.; Li, Y. –M.; Chan, A. S. C. *Tetrahedron: Asymmetry* **2005**, *16*, 3198. i) Cobley, C. J.; Froese, R. D.; Klosin, J.; Qin, C.; Witheker, G. T.; Abboud, K. A. *Organometallics* **2007**, *26*, 2986. j) Cobley, C. J.; Klosin, J.; Qin, C.; Witheker, G. T. *Org. Lett.* **2004**, *6*, 3277. k) Zou, Y.; Yna, Y.; Zhang, X. *Tetrahedron: Asymmetry* **2007**, *48*, 4781. l) Peng, X.; Wang, Z.; Xia, C.; Ding, K. *Tetrahedron Lett*. **2008**, *49*, 4862.

[122] Sakai, N.; Mano, S.; Nozaki, K.; Takaya, K.; *J. Am. Chem. Soc*. **1993**, *115*, 7033.

[123] a) Nozaki, K.; Sakai, N.; Nanno, T.; Hagashijima, T.; Mano, S.; Horiuchi, T.; Takaya, H. *J. Am. Chem. Soc*. **1997**, *16*, 5681. b) Nozaki, K.; Matsuo, T.; Shibahara, F.; Hiyama, T. *Adv. Synth. Catal.* **2001**, *343*, 61.

[124] Higashizima, T.; Sakai, N.; Nozaki, K.; Takaya, H. *Tetrahedron Lett.* **1994**, *35*, 2023.

[125] Horiuchi, T.; Ohta, T.; Shirakawa, E.; Nozaki, K.; Takaya, H. *J. Org. Chem.* **1997**, *62*, 4285.

[126] See for example: a) Deeremberg, S.; Kamer, P. C. J.; van Leewuen, P. W. M. N. *Organometallics* **2000**, *19*, 2065. b) Pàmies, O.; Net, G.; Ruiz, A.; Claver, C. *Tetrahedon: Asymmetry* **2001**, *12*, 3441. c) Arena, C. G.; Faraone, F.; Graiff, C.; Tiripicchio, A. *Eur. J. Inorg. Chem*. **2002**, 711. d) Rubio, M.; Suárez, A.; Álvarez, E.; Bianchini, C.; Oberhauser, W.; Peruzzini, M.; Pizzano, A. *Organometallics* **2007**, *26*, 6428.

[127] Yan, Y.; Zhang, X. *J. Am. Chem. Soc.* **2006**, *128*, 7198.

[128] Chikkali, S. A.; Bellini, R.; Berthon-Gelloz, G.; van der Vlugt, J. I.; de Bruin, B.; Reek, J. N. H. *Chem. Commun.* **2010**, *46*, 1244.

[129] See for instance: a) Clark, T. P.; Landis, C. R.; Freed, S. L.; Klosin, J.; Abboud, K. A. *J. Am. Chem. Soc*. **2005**, *127*, 5040. b) Axtell, A.; Cobley, C. J.; Klosin, J.; Whiteker, G. T.; Zanotti-Gerosa, A.; Abboud, K. A. *Angew. Chem. Int. Ed*. **2005**, *44*, 5834. c) Axtell, A. T.; Klosin, J.; Abboud, K. A. *Organometallics*, **2006**, *25*, 5003. d) Thomas, P. J.; Axtell, A. T.; Klosin, J.; Peng, W.; Rand, C. L.; Clark, T. P.; Landis, C. R.; Abboud, K. A. *Org. Lett.* **2007**, *9*, 2665.

[130] a) Breeden, S.; Cole-Hamilton, D. J.; Foster, D. F.; Schwarz, G. J.; Wills, M. *Angew. Chem. Int. Ed.* **2000**, *39*, 4106. b) Clarkson, G. J.; Ansel, J. R.; Cole-Hamilton, D. J.; Pogorzelec, P. J.; Whittell, J.; Mills, M. *Tetrahedron: Asymmetry* **2004**, *15*, 1787.

Chapter 2

Objectives

2. Objectives

The objective of this thesis is to develop new chiral compounds for their application as chiral ligands in several important asymmetric catalytic reactions.

The more specific aims are:

1. To synthesize and apply a pyranoside phosphite/phosphinite-oxazoline ligand library (**L1**-**L5a**-**m**) in the asymmetric Ir-catalyzed hydrogenation of minimally functionalized olefins (Figure 2.1).

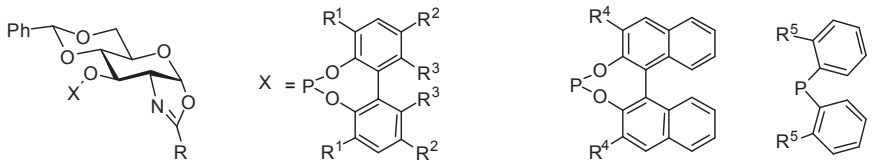

L1 R= Me
L2 R= ^{i}Pr
L3 R= ^{t}Bu
L4 R= Bn
L5 R= Ph

a $R^1 = R^2 = {}^{t}Bu$; R^3= H
b $R^1 = {}^{t}Bu$; R^2 = OMe; R^3= H
c $R^1 = SiMe_3$; $R^2 = R^3$= H
d $R^1 = R^2 = R^3$= H
e $R^1 = R^2$ = Me; R^3= H
f $(S)^{ax}$; $R^1 = {}^{t}Bu$; $R^2 = R^3$= Me
g $(R)^{ax}$; $R^1 = {}^{t}Bu$; $R^2 = R^3$= Me

h $(S)^{ax}$; R^4= H
i $(R)^{ax}$; R^4= H
j $(S)^{ax}$; $R^4 = SiMe_3$
k $(R)^{ax}$; $R^4 = SiMe_3$

l R^5= H
m R^5= Me

Figure 2.1. Pyranoside phosphite/phosphinite-oxazoline ligand library **L1**-**L5a**-**m** developed for this thesis.

2. To synthesize and apply a phosphite-oxazoline ligand library (**L6**-**L26a**-**k**) in the asymmetric Ir-catalyzed hydrogenation of minimally functionalized olefins and in the Pd-catalyzed allylic substitution and intermolecular Heck reactions. For purposes of comparison we have also prepared and screened phosphite-thiazoline analogues (**L27**-**L28a**-**k**) (Figure 2.2).

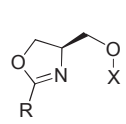
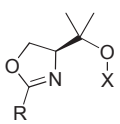
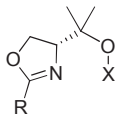
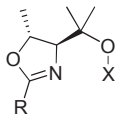
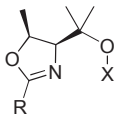

L6 R= C_6H_5
L7 R= $C(CH_3)_3$
L8 R= 4-CH_3-C_6H_4
L9 R= 2-CH_3-C_6H_4

L10 R= C_6H_5
L11 R= 4-CH_3-C_6H_4
L12 R= 4-CF_3-C_6H_4
L13 R= 2-CH_3-C_6H_4
L14 R= 2,6-di-CH_3-C_6H_3
L15 R= $C(CH_3)_3$
L16 R= $FeCp(C_5H_4)$

L17 R= C_6H_5

L18 R= C_6H_5

L19 R= C_6H_5

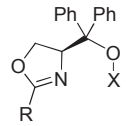
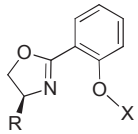
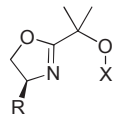
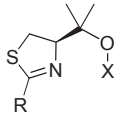
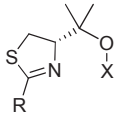

L20 R= C_6H_5
L21 R= 4-CF_3-C_6H_4

L22 R= C_6H_5
L23 R= $C(CH_3)_3$
L24 R= $CH(CH_3)_2$
L25 R= CH_2CH_3

L26 R= C_6H_5

L27 R= C_6H_5

L28 R= C_6H_5

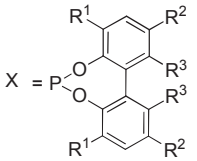

a $R^1 = R^2 = {}^tBu$; R^3= H
b $R^1 = {}^tBu$; R^2 = OMe; R^3= H
c $R^1 = SiMe_3$; $R^2 = R^3$= H
d $R^1 = R^2 = R^3$= H
e $R^1 = R^2$ = Me; R^3= H
f $(S)^{ax}$; $R^1 = {}^tBu$; $R^2 = R^3$= Me
g $(R)^{ax}$; $R^1 = {}^tBu$; $R^2 = R^3$= Me

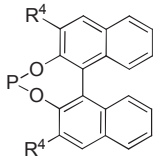

h $(S)^{ax}$; R^4= H
i $(R)^{ax}$; R^4= H
j $(S)^{ax}$; $R^4 = SiMe_3$
k $(R)^{ax}$; $R^4 = SiMe_3$

Figure 2.2. Phosphite-oxazoline/thiazoline ligand library **L6**-**L28a-k** developed for this thesis.

3. To synthesize and apply a phosphite/phosphinite-oxazole/thiazole/imidazole ligand library (**L29**-**L37a**-**h**) in the asymmetric Ir-catalyzed hydrogenation of minimally functionalized olefins and in the Pd-catalyzed allylic substitution and intermolecular Heck reactions (Figure 2.3).

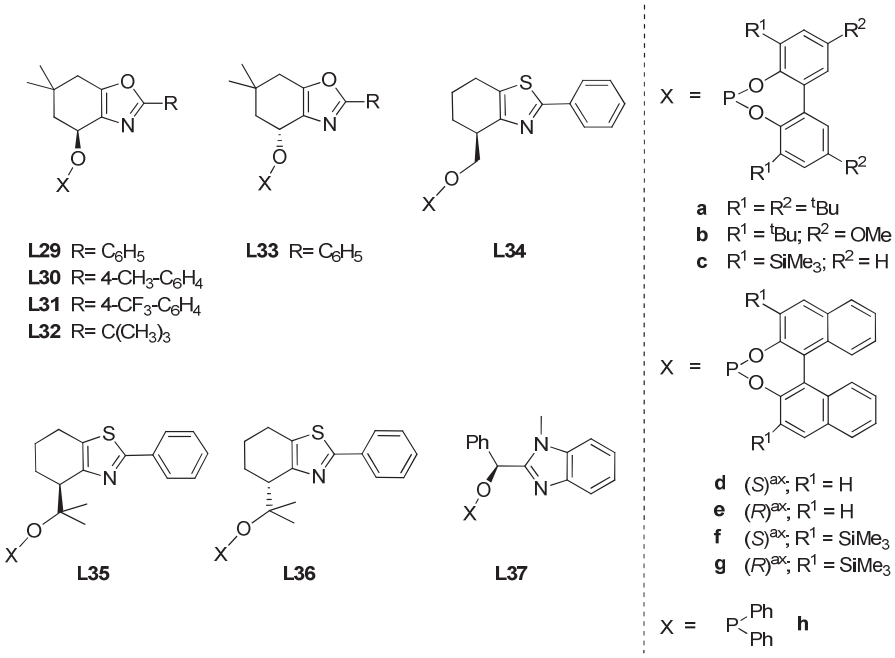

Figure.2.3. Phosphite/phosphinite-oxazole/thiazole/imidazole ligand library **L29**-**L37a**-**h** developed for this thesis.

4. To synthesize and apply a phosphite-pyridine ligand library (**L38-L49a-g**) in the asymmetric Ir-catalyzed hydrogenation of minimally functionalized olefins and in the Pd-catalyzed allylic substitution reactions (Figure 2.4).

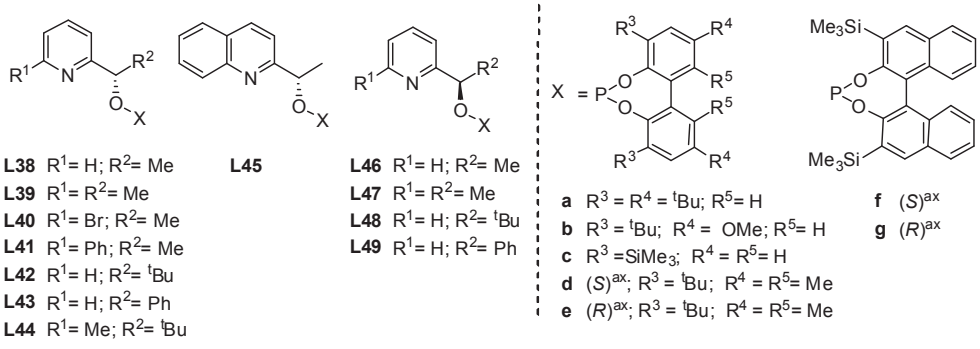

Figure 2.4. Phosphite-pyridine ligand library **L38**-**L49a**-**g** developed for this thesis.

5. To apply diphosphite (**L50**-**L66a**-**f**, Figure 2.5), phosphoroamidite and N-phosphine ligands (**L67-L73a-f**, Figure 2.6) in the asymmetric Rh-catalyzed hydroformylation of heterocyclic olefins and styrene.

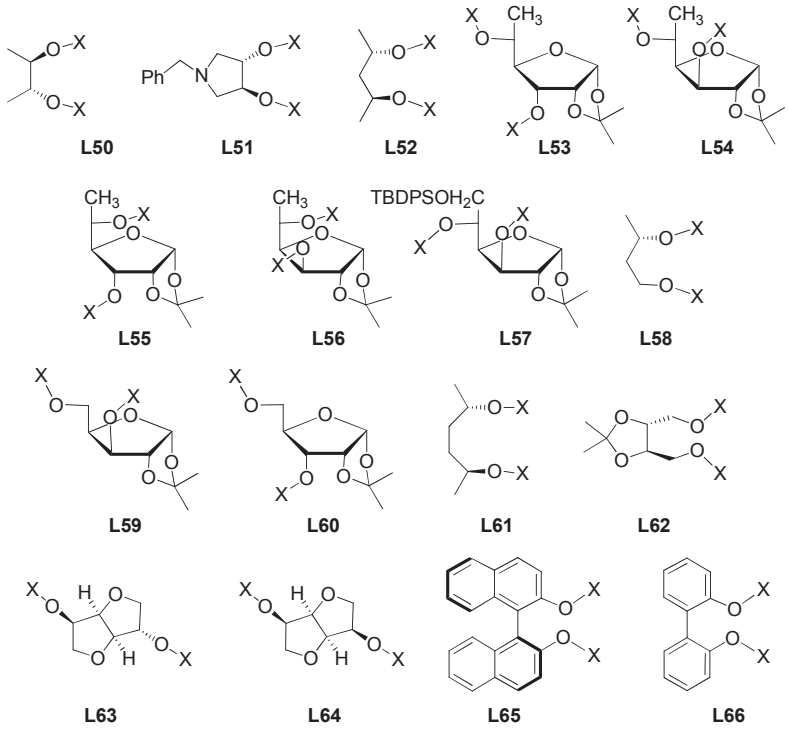

Figure 2.5. Diphosphite ligand library **L50**-**L66a**-**e** screened in this thesis.

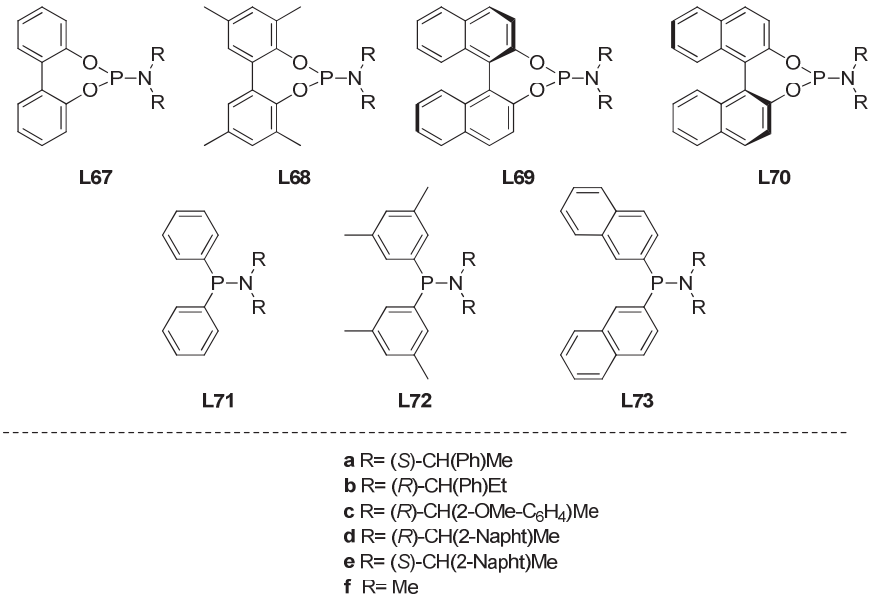

Figure 2.6. Monodentate phophoroamidite/N-phosphine ligand library **L67**-**L73a**-**f** screened in this thesis.

6. To study the Rh-catalyzed hydroformylation of isopropenyl acetate (Figure 2.7).

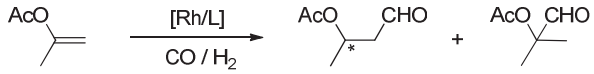

Figure 2.7. Hydroformylation of isopropenyl acetate studied in this thesis.

Chapter 3

Asymmetric hydrogenation of minimally functionalized olefins

3. Asymmetric hydrogenation of minimally functionalized olefins

3.1. Background

The enantioselective hydrogenation of olefins is one of the most powerful and sustainable transformations in asymmetric catalysis for preparing optically active compounds due to its high efficiency, atom economy and operational simplicity.

As we discussed in the introduction, whereas the reduction of olefins containing an adjacent polar group (i.e. dehydroamino acids) by Rh- and Ru- catalysts has a long history, the asymmetric hydrogenation of minimally functionalized olefins is less developed. Iridium complexes with chiral P-N ligands have become established as one of the most efficient catalyst types for the hydrogenation of minimally functionalized olefins. In this respect, the most successful P-N ligands contain a phosphine or phosphinite as P-donor group and either an oxazoline, oxazole, thiazole or pyridine as N-donor group. However, these Ir-P,N catalysts are still highly substrate dependent. Despite the successful early use of phosphite ligands in the Rh-catalyzed hydrogenation of dehydroamino acid derivatives, only one report has been published on phosphite ligands, TADDOL-based phosphite-oxazoline ligands, in the Ir-hydrogenation of alkenes. However, their substrate range limitation was higher and enantioselectivities lower than their related phosphinite/phosphine-oxaline ligands. They also required higher pressure and catalyst loading. More research is therefore needed to study the possibilities of phosphite-N ligands in this process.

In this chapter, we therefore report the synthesis and screening of 5 large modular phosphite-nitrogen ligand libraries in Ir-catalyzed hydrogenation of minimally functionalized olefins. The modular ligand design has shown to be crucial in finding highly selective catalytic systems for each substrate type. More specifically, in section 3.2 we describe the first successful application of a phosphite-oxazoline ligand library, derived from D-glucosamine, in the Ir-hydrogenation of a wide range of *E*- and *Z*- trisubstituted and 1,1-disubstituted alkenes. The results compete favorable with the best ones reported in the literature. This section also includes DFT calculation in order to explain the origin of enantioselectivity. This study agree with an Ir(III/V) catalytic cycle with migratory insertion of a hydride as selectivity-determining step. In next section 3.3, we report the successful application of a new phosphite-oxazoline ligand library, derived from readily available hydroxyl amino acids, in the hydrogenation of a wide range of minimally functionalized olefins. By appropriate tuning of the ligand parameters comparable excellent enantioselectivities than previous pyranoside phosphite-oxazoline ligands (section 3.2) have been achieved in a wide range of *E*- and *Z*- trisubstitued olefins and challenging 1,1-disubstituted terminal olefins, including examples with neighboring polar groups (allylic alcohols, acetates, α,β-unsaturated esters and ketones, allylic silanes and vinylboronates). The asymmetric hydrogenation was also performed using propylene carbonate as solvent, which allowed the Ir-catalysts to be reused and maintained the excellent enantioselectivities. On the basis of the previous ligand library, in next section 3.4, we designed a new phosphite-N ligand family (phosphite-thiazoline) in which the oxazoline moiety is replaced by a thiazoline group. We have found that the replacement of the oxazoline by a thiazoline moiety in the ligand design has been beneficial in terms of substrate scope. Thus, the

ranges of substrates that can be hydrogenated in excellent enantioselectivities have been extended. In next section 3.5, we synthesized a library of phosphite-oxazole/thiazole ligands with the aim to study whether biaryl phosphite groups maintain its effectiveness in combination with N-donor group other than oxazolines/thiazolines. We were pleased to see that again excellent activities and enantioselectivities were obtained in a wide range of *E*- and *Z*- trisubstitued olefins and challenging 1,1-disubstituted terminal olefins, including examples with neighboring polar groups. The efficiency of this ligand design is also corroborated by the fact that these phosphite-oxazole/thiazole catalytic systems provided higher enantioselectivities than their related phosphinite-oxaxole/thiazole counterparts. Finally, in section 3.6, we reported the first successful application of a phosphite-pyridine ligand library in the Ir-catalyzed hydrogenation of minimally functionalized olefins. These ligands combine the advantages of both phosphite and pyridine moieties. By carefully selecting the ligand components we obtained excellent enantioselectivities in a wide range of *E*- and *Z*-trisubstituted alkenes, including more demanding triarylsubstituted olefins and dihydronaphthalenes. The good performances extend to the very challenging class of terminal disubstituted olefins. Both enantiomers of the hydrogenation product can be obtained in high enantioselectivity, simply by changing the configuration of the carbon next to the phosphite moiety.

3.2. Pyranoside phosphite/phosphinite-oxazoline ligands for the highly versatile and enantioselective Ir-catalyzed hydrogenation of minimally functionalized olefins. A combined theoretical and experimental study

Javier Mazuela, Per-Ola Norrby, Pher G. Andersson, Oscar Pàmies and Montserrat Diéguez in J. Am. Chem. Soc. ***2008**, 130,* 7208*; J. Am. Chem. Soc.* **2011**, *133*, 13634 and manuscript to be submitted.

3.2.1. Abstract

A modular set of phosphite/phosphinite-oxazoline (P,N) ligands has been applied to the title reaction. Excellent ligands have been identified for a range of substrates, including challenging terminally disubstituted olefins, where we have reached enantioselectivities of 99% for a range of substrates. The selectivity is best for minimally functionalized substrates with at least a moderate size difference between geminal groups. A DFT study has allowed identification of the preferred pathway. Computational prediction of enantioselectivities gave very good accuracy.

3.2.2. Introduction

Pharmaceuticals, agrochemicals, fragrances, fine chemicals, and natural chemicals all rely on the preparation of enantiomerically enriched compounds.[1] Because of its high efficiency, atom economy and operational simplicity, the asymmetric hydrogenation of properly selected prochiral starting materials can be a sustainable and direct synthetic tool for preparing these compounds.[1]

Whereas the reduction of olefins containing an adjacent polar group (i.e. dehydroamino acids) by Rh- and Ru- catalyst precursors modified with phosphorus ligands has a long history, the asymmetric hydrogenation of minimally functionalized olefins is less developed because these substrates have not adjacent polar group to direct the reaction.[1] Iridium complexes with chiral P,N ligands have become established as one of the most efficient catalyst types for the hydrogenation of minimally functionalized olefins, and they complement Rh- and Ru-diphosphine complexes.[2,3] The first successful P,N ligands[4] contained a phosphine or phosphinite moiety as P-donor group and either an oxazoline,[4b,g,j] oxazole,[4d] thiazole[4i] or pyridine[4c] as N-donor group. However, these iridium-phosphine/phosphinite,N catalysts were still highly substrate-dependent and the development of efficient chiral ligands that tolerate a broader range of substrates remained a challenge.

In the last few years, a group of less electron-rich phosphorus compounds–phosphite containing ligands–have demonstrated their huge potential utility in many transition-metal catalyzed reactions.[5] Their highly modular construction, facile synthesis from readily available chiral alcohols and greater resistance to oxidation than phosphines have proved to be highly advantageous. Despite the successful early use of phosphite ligands in the Rh-catalyzed hydrogenation of dehydroamino acid derivatives,[6] only one report has been published on phosphite ligands–TADDOL-based phosphite-oxazoline ligands–in the Ir-catalyzed hydrogenation of alkenes.[7] However, their substrate range limitation was higher and enantioselectivities and

activities lower than their related phosphinite/phosphine-oxazoline ligands. They also required higher catalyst loadings (4 mol%) and higher pressures (100 bars) to achieve full conversions. More research is therefore needed to study the possibilities of phosphite-oxazoline ligands in this process. For this purpose in this chapter, we present the application of a phosphite-oxazoline ligand library (**L1**-**L5a**-**k**, Figure 3.2.1) in the asymmetric Ir-catalyzed hydrogenation of several unfunctionalized olefins. For comparative purposes, we also evaluated phosphinite-oxazoline analogues (**l**-**m**). These ligands are derived from natural D-glucosamine so they also have the advantages of carbohydrates: that is to say, they are cheap and can be easily constructed in modules. With this library we therefore investigated the effects of systematically varying the electronic and steric properties of the oxazoline substituents (**L1**-**L5**) and different substituents/configurations in the biaryl phosphite moiety (**a**-**k**). By carefully selecting these elements, we achieved high enantioselectivities and activities in a wide range of *E*- and *Z*-trisubstituted and 1,1-disubstituted alkenes.

In this chapter, we have also performed DFT calculations in order to explain the origin of enantioselectivity for these highly versatile pyranoside Ir/phosphite-oxazoline catalytic systems. It should be noted, that we have also elucidated a computational model that can explain the enantioselectivities obtained with 1,1-disubstituted substrates, which was lacking in the literature.

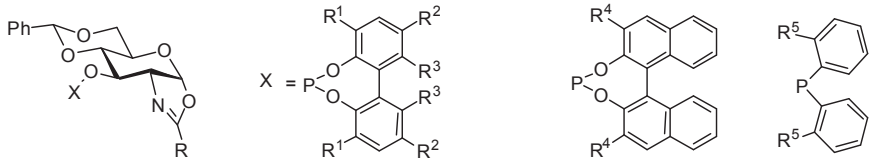

L1 R= Me
L2 R= ^{i}Pr
L3 R= ^{t}Bu
L4 R= Bn
L5 R= Ph

a $R^1 = R^2 = {}^{t}Bu$; R^3= H
b $R^1 = {}^{t}Bu$; R^2 = OMe; R^3= H
c $R^1 = SiMe_3$; $R^2 = R^3$= H
d $R^1 = R^2 = R^3$= H
e $R^1 = R^2$ = Me; R^3= H
f $(S)^{ax}$; $R^1 = {}^{t}Bu$; $R^2 = R^3$= Me
g $(R)^{ax}$; $R^1 = {}^{t}Bu$; $R^2 = R^3$= Me

h $(S)^{ax}$; R^4= H
i $(R)^{ax}$; R^4= H
j $(S)^{ax}$; $R^4 = SiMe_3$
k $(R)^{ax}$; $R^4 = SiMe_3$

l R^5= H
m R^5= Me

Figure 3.2.1. Pyranoside phosphite/phosphinite-oxazoline ligand library **L1**-**L5a**-**m**.

3.2.3. Results and discussions

3.2.3.1. Synthesis of ligands

The synthesis of the new pyranoside phosphite-oxazoline ligands (**L5f**-**g** and **L5j**-**k**) and phosphinite-oxazoline ligands (**L5m**) is straightforward following the procedure previously described for ligands **L1**-**L4a** and **L5a**-**e**,**h**-**i**,**l** (Scheme 3.2.1).[8,9] They were therefore efficiently synthesized in one step by reacting the corresponding sugar oxazoline-alcohols (**1** and **2**) in the presence of base with 1 equiv of either the corresponding biaryl phosphorochloridite ($ClP(OR)_2$; $(OR)_2$=**a**-**k**) to achieve phosphite-oxazoline ligands or chlorodi(*o*-tolyl)phosphine to provide phosphinite-oxazoline ligands. Oxazoline-alcohols **1** and **2** are easily prepared from inexpensive D-glucosamine on a large scale.[9] All the ligands were stable during purification on neutral alumina under an atmosphere of argon and isolated in moderate-to-good yields as white solids. They were

stable at room temperature and very stable to hydrolysis. The elemental analyses were in agreement with the assigned structure. The ^{1}H, ^{13}C and ^{31}P NMR spectra were as expected for these C_1 ligands.

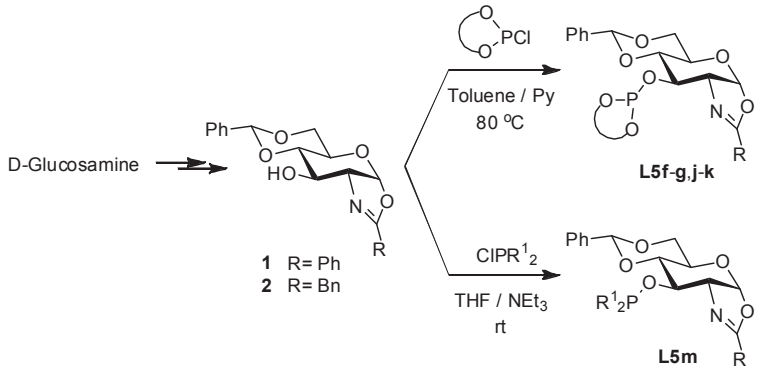

Scheme 3.2.1. Synthesis of new pyranoside phosphite/phosphinite-oxazoline ligands

3.2.3.2. Synthesis of the Ir-catalyst precursors

The catalyst precursors were made by refluxing a dichloromethane solution of the appropriate ligand (**L1**-**L5a**-**m**) in the presence of 0.5 equivalent of $[Ir(\mu\text{-}Cl)cod]_2$ for 1 h and then exchanging the counterion with sodium tetrakis[3,5-bis(trifluoromethyl)-phenyl]borate ($NaBAr_F$) (1 equiv), in the presence of water (Scheme 3.2.2). All complexes were isolated as air-stable orange solids and were used without further purification.

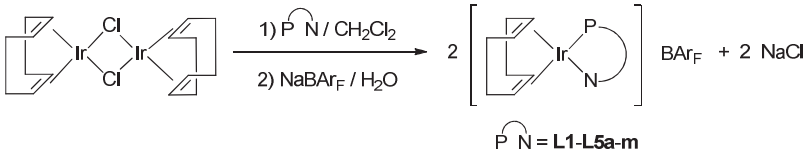

Scheme 3.2.2. Synthesis of catalyst precursors [Ir(cod)(P-N)]BAr_F (P-N = **L1**-**L5a**-**m**).

The complexes were characterized by elemental analysis and ^{1}H, ^{13}C, and ^{31}P NMR spectroscopy. The spectral assignments were based on information from ^{1}H–^{1}H and ^{13}C–^{1}H correlation measurements and were as expected for these C_1 iridium complexes. The VT-NMR spectra indicate that only one isomer is present in solution. One singlet in the ^{31}P-{^{1}H} NMR spectra was obtained in all cases.[10]

3.2.3.3. Asymmetric hydrogenation of trisubstituted olefins

Asymmetric hydrogenation of minimally functionalized trisubstituted olefins

In a first set of experiments we used the Ir-catalyzed hydrogenation of substrates *trans*-α-methylstilbene **S1** and *Z*-2-(4-methoxyphenyl)-2-butene **S2** to study the potential of ligands **L1**-**L5a**-**m**. Substrate **S1** was chosen as a model for the hydrogenation of *E*-isomers because it has been reduced with a wide range of ligands, which enable the efficiency of the various ligand systems to be compared directly.[2] In order to assess the potential of the ligand library **L1**-**L5a**-**m**

for the more demanding *Z*-isomers, which are usually hydrogenated less enantioselectively than the corresponding *E*-isomers, we chose substrate **S2** as a model. The reactions proceeded smoothly at room temperature. Excellent activities and enantioselectivities (up to >99% for **S1** and up to 95% for **S2**) were obtained. The results, which are summarized in Table 3.2.1, indicate that activity is mainly affected by the steric properties of the oxazoline substituent and by the substituents at the *ortho* positions of the biaryl phosphite moiety.

Table 3.2.1. Ir-catalyzed asymmetric hydrogenation of **S1** and **S2** using ligands **L1**-**L5a**-**m**[a]

		 **S1**		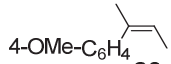 **S2**	
Entry	Ligand	% Conv[b]	% ee[c]	% Conv[b]	% ee[c]
1	**L1a**	100	92 (*R*)	100	69 (*S*)
2	**L2a**	98	95 (*R*)	100	73 (*S*)
3	**L3a**	40	99 (*R*)	44	75 (*S*)
4	**L4a**	100	98 (*R*)	100	85 (*S*)
5	**L5a**	100	99 (*R*)	100	95 (*S*)
6	**L5b**	100	98 (*R*)	100	79 (*S*)
7	**L5c**	100	>99 (*R*)	100	78 (*S*)
8	**L5d**	32	96 (*R*)	58	75 (*S*)
9	**L5e**	<5	-	<5	-
10	**L5f**	100	38 (*R*)	56	34 (*S*)
11	**L5g**	100	99 (*R*)	100	91 (*S*)
12	**L5h**	50	20 (*R*)	59	44 (*S*)
13	**L5i**	45	98 (*R*)	67	74 (*S*)
14	**L5j**	23	32 (*R*)	39	38 (*S*)
15	**L5k**	100	99 (*R*)	100	79 (*S*)
16	**L5l**	100	95 (*R*)	100	78 (*S*)
17	**L5m**	100	96 (*R*)	100	89 (*S*)
18[d]	**L5a**	100	99 (*R*)	100	95 (*S*)
19[d]	**L5c**	100	>99 (*R*)	100	78 (*S*)

[a] Reactions carried out at room temperature by using 1 mmol of substrate and 2 mol% of Ir-catalyst precursor at 50 bar of H_2 using dichloromethane (2 mL) as solvent. [b] Conversion measured by ^{1}H-NMR after 2 h. [c] Enantiomeric excess determined by HPLC (**S1**) and GC (**S2**). [d] Reaction carried out at 0.2 mol% of Ir-catalyst.

Bulky substituents need to be present in the biaryl phosphite and less sterically demanding substituents in the oxazoline if activities are to be high. Enantioselectivity, on the other hand, is affected by the electronic and steric properties of the substituents in the oxazoline moiety and by the substituents/configuration in the biaryl phosphite moiety. However, the effect of these ligand parameters on enantioselectivity depends on the substrate type (*E*- or *Z*-isomers). Thus, while for the *E*-substrate **S1** the enantioselectivity was best with ligand **L5c** (>99% ee), enantioselectivities for the more demanding *Z*-substrate **S2** were best with ligand **L5a** (95% ee). For both type of substrates, we also found a cooperative effect between the configuration of the biaryl phosphite moiety and the configuration of the sugar backbone on enantioselectivity. This led to a matched combination for ligands **L5g**, **L5i** and **L5k**, which contain an *R*-biaryl moiety (entries 11, 13 and

15). In addition, a comparison of the absolute stereochemistry obtained by using tropoisomeric biphenyl ligands **L5a**-**e** with those obtained with the related atropoisomeric biaryl ligands (**L5f**-**k**) shows that the tropoisomeric biphenyl moiety in ligands **L5a**-**e** adopts an *R*-configuration when complexed with iridium.[10] Replacing the biaryl phosphite moiety by a phosphinite group (ligands **L5l**-**m**) lead to lower enantioselectivities (Table 3.2.1, entries 16 and 17).

Next, we used the ligands that provided the best results (ligands **L5a** and **L5c**) to study these reactions at a low catalyst loading (0.2 mol%). In these conditions, the excellent enantioselectivities and activities were maintained (Table 3.2.1, entries 18 and 19).

We then studied the asymmetric hydrogenation of other *E*- and *Z*-trisubstituted olefins (**S3**-**S10**) by using the pyranoside phosphite/phosphinite-oxazoline ligand library **L1**-**L5a**-**m**. The most noteworthy results are shown in Scheme 3.2.3. The enantioselectivities are among the best observed for these substrates.[2,4]

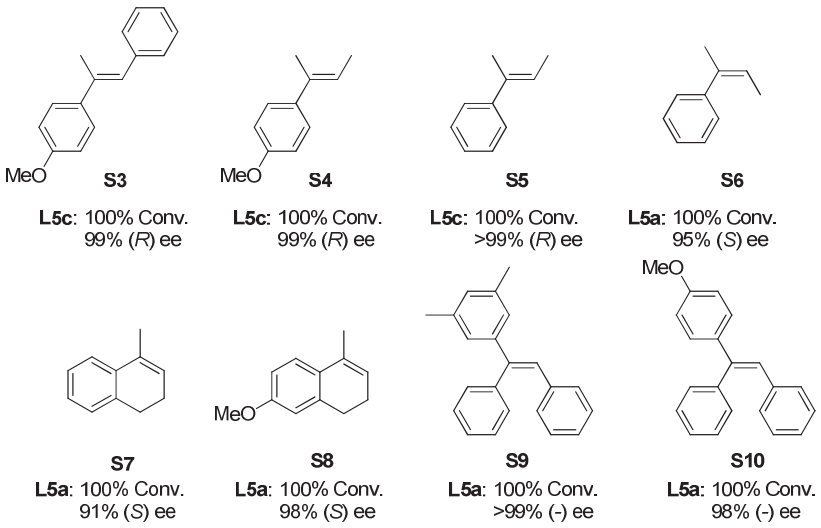

Scheme 3.2.3. Selected hydrogenation results of trisubstituted olefins using [Ir(cod)(**L1**-**L5a**-**m**)]BAr_F catalyst precursors. Reaction conditions: 1 mol % catalyst precursor, CH_2Cl_2 as solvent, 50 bar H_2, rt, 2 h.

In general, the Ir-**L5c** catalyst precursor provides the best enantioselectivities for the hydrogenation of *E*-trisubstituted olefins (**S1**, **S3**-**S5**), while ligand **L5a** gives best enantioselectivities for *Z*-trisubstituted olefins (**S2**, **S6**-**S8**). Our results also indicated that enantioselectivity (ee values up to >99%) is relatively insensitive to the electronic nature of the substrate phenyl ring (i.e substrates **S1**, **S5** and **S6** vs **S3**, **S4** and **S2**, respectively). Notably the [Ir(cod)(**L1**-**L5a**-**m**)]BAr_F catalyst precursors also proved to be highly active and enantioselective in the reduction of triarylsubstituted substrates **S9** and **S10** (Scheme 3.2.3, ee's ranging from 98% to >99%). This latter substrate class provides an easy entry point to diarylmethine chiral centers, which are present in several important drugs and natural products.[11] Despite this, only one previous study has been made.[12]

Asymmetric hydrogenation of trisubstituted olefins containing a neighboring polar group

To further study the potential of the pyranoside phosphite/phosphinite-oxazoline ligand library **L1**-**L5a**-**m** in the reduction of minimally functionalized trisubstituted olefins, we screened it in the Ir-catalyzed hydrogenation of trisubstituted alkenes containing a neighboring polar group. These substrates are interesting because they allow for further functionalization and they are important intermediates for the synthesis of high-value chemicals. The results are summarized in Scheme 3.2.4. Again, excellent enantioselectivities (ee values up to >99%) for a range of substrates were obtained under mild reaction conditions.

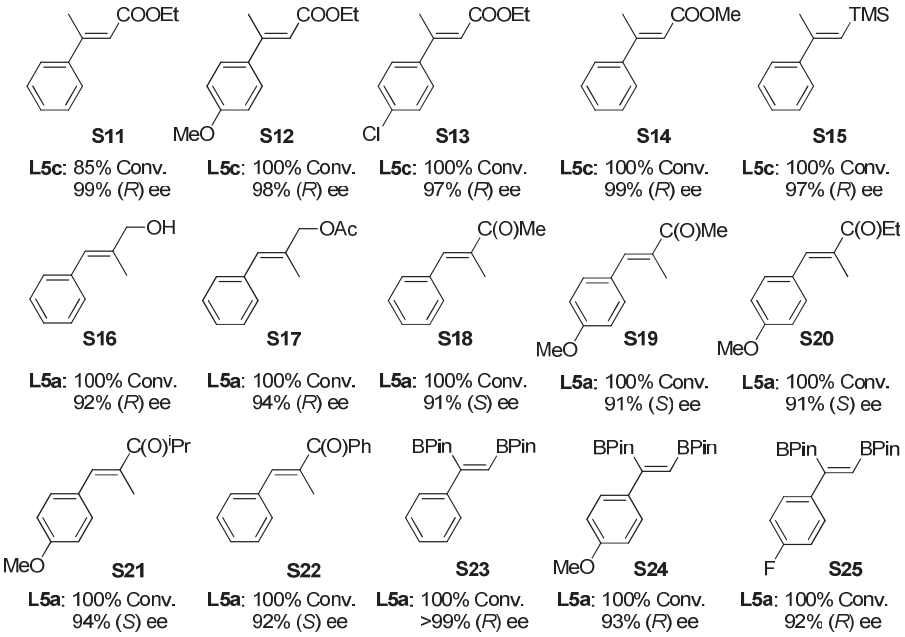

Scheme 3.2.4. Selected hydrogenation results of trisubstituted olefins bearing a neighboring polar group using [Ir(cod)(**L1**-**L5a**-**m**)]BAr_F catalyst precursors. Reaction conditions: 1 mol % catalyst precursor, CH_2Cl_2 as solvent, 50 bar H_2, rt, 2 h.

The reduction of several α,β-unsaturated esters (**S11**-**S14**) followed the same trends as those observed for the previous *E*-trisubstituted substrates. Therefore, enantioselectivities were best using ligand **L5c**. It should be noted that ee's are highly independent of the electronic nature of the substrate phenyl ring and the substituent in the ester functionality. As expected, the hydrogenation of vinylsilane **S15** was also best using ligand **L5c**. However, for trisubstituted allylic alcohol **S16**, allylic acetate **S17**, several α,β-unsaturated ketones **S18**-**S22** and vinylboronates **S23**-**S25**, enantioselectivities were best with ligand **L5a**. It should be pointed out the unprecedented excellent enantioselectivities obtained in the hydrogenation of vinylboronates (ee's ranging from 92% to >99%). The hydrogenation of vinylboronates provides an easy access to chiral borane compounds, which are useful building blocks in organic synthesis because the C-B bond can be readily converted to C-O, C-N and C-C bonds with retention of the chirality. For α,β-unsaturated ketones and vinylboronates, ee's are again highly independent on the electronic

properties of the phenyl substrate ring. Moreover, our results indicate that for enones **S18**-**S22** the substituent linked to the ketone functionality has little effect on enantioselectivity. This is therefore one of the few catalytic systems that can hydrogenated a wide range of trisubstituted olefins in high activities and enantioselectivities.[4]

3.2.3.4. Asymmetric hydrogenation of 1,1-disubstituted terminal olefins

We next screened ligands **L1**-**L5a**-**m** in the asymmetric hydrogenation of more demanding terminal olefins. Enantioselectivity is more difficult to control in these substrates than in trisubstituted olefins. There are two main reasons for this:[2d,e] a) the two substituents in the substrate can easily exchange positions in the chiral environment formed by the catalysts, thus reversing the face selectivity (Scheme 3.2.5(a)) and b) the terminal double bond can isomerize to form the more stable internal alkene, which usually leads to the predominant formation of the opposite enantiomer of the hydrogenated product (Scheme 3.2.5(b)). Few known catalytic systems provide high enantioselectivities for these substrates, and those that do are usually limited in substrate scope.[2e,13,14] In contrast to the hydrogenation of trisubstituted olefins, the enantioselectivity in the reduction of terminal alkenes is highly pressure dependent. Therefore, hydrogenation at an atmospheric pressure of H_2 gave, in general, significantly higher ee values than at higher pressures.[13]

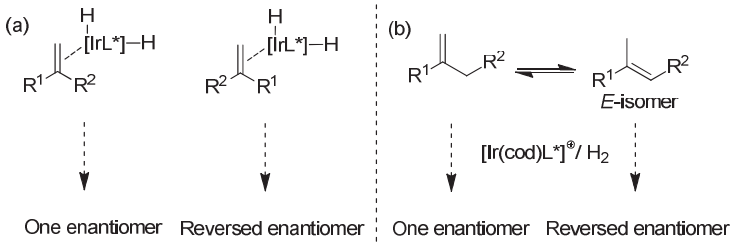

Scheme 3.2.5. Isomerization in the hydrogenation of terminal olefins.

Asymmetric hydrogenation of unfunctionalized 1,1-disubstituted terminal olefins

In a first set of experiments we used the Ir-catalyzed asymmetric hydrogenation of 2-phenylbut-1-ene **S26**. The results obtained using the ligand library **L1**-**L5a**-**m** in optimized conditions are shown in Table 3.2.2. We were again able to fine-tune the ligand parameters to produce high activities and enantioselectivities (ee's up to 99%) in the hydrogenation of this substrate using low catalyst loadings (0.2 mol%) and hydrogen pressures (1 bar). Enantioselectivities were affected by the electronic and steric properties of the oxazoline moiety and by the substituents/configurations of the biaryl phosphite group. In general, the effect of these ligand parameters on enantioselectivity followed the same trend as for the reduction of trisubstituted olefins. However, the effect of the substituents at the *para* positions of the biaryl phosphite moiety is different. Therefore, in contrast to the previous trisubstituted olefins, enantioselectivities increased if the steric bulk of the substituent at the *para* position of the biaryl phosphite moiety decreased (i.e. **L5c** (H)> **L5b** (OMe)> **L5a** (^{t}Bu)).

Table 3.2.2. Selected results for the Ir-catalyzed hydrogenation of **S26** using the ligands **L1**-**L5a**-**m**[a]

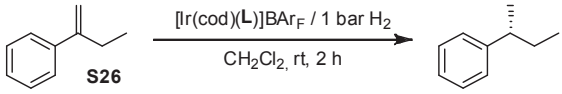

Entry	Ligand	% Conv[b]	% ee[c]
1	**L1a**	100	76 (*S*)
2	**L2a**	100	84 (*S*)
3	**L3a**	100	89 (*S*)
4	**L4a**	100	87 (*S*)
5	**L5a**	100	92 (*S*)
6	**L5b**	100	97 (*S*)
7	**L5c**	100	99 (*S*)
8	**L5d**	99	97 (*S*)
9	**L5e**	<5	-
10	**L5f**	100	39 (*S*)
11	**L5g**	100	94 (*S*)
12	**L5h**	95	34 (*S*)
13	**L5i**	100	97 (*S*)
14	**L5j**	100	23 (*S*)
15	**L5k**	100	98 (*S*)
16	**L5l**	100	93 (*S*)

[a] Reactions carried out using 1 mmol of **S26** and 0.2 mol% of Ir-catalyst precursor at 1 bar of H_2.[b] Conversion measured by GC after 2 hours. [c] Enantiomeric excesses determined by chiral GC.

In summary, enantioselectivities were best (99% ee) when phosphite–oxazoline ligand **L5c**, which contains a phenyl group in the oxazoline moiety and bulky *ortho* trimethylsilyl groups at the biphenyl phosphite moiety, was used. This result, which again clearly shows the efficiency of using modular scaffolds in ligand design, is among the best that have been reported for this demanding substrate.[2e]

We then studied the asymmetric hydrogenation of other 1,1-disubstituted aryl-alkyl substrates (**S27**-**S34**), 1,1-disubstituted heteroaryl-alkyl olefins (**S35**-**S37**) and 1,1-diaryl terminal alkenes (**S38**-**S40**) by using the phosphite/phosphinite-oxazoline ligand library **L1**-**L5a**-**m**. The most noteworthy results are shown in Table 3.2.3. Again these results are among the best reported for these substrates.[2e] For aryl-alkyl and heteroaryl-alkyl substrates (**S27**-**S37**), the results follow the same trends as the hydrogenation of **S26**. Again, the catalyst precursor containing the phosphite-oxazoline ligand **L5c** provided the best enantioselectivities (ee's up to 99%). However, for the hydrogenation of the diaryl terminal alkenes enantioselectivities were best using ligand **L5k**, which differs from **L5c** in the biaryl phosphite group.

Our results with several 1,1-disubstituted aryl-alkyl substrates (**S26**-**S32**) indicated that enantioselectivity is affected by the nature of the alkyl chain (ee's ranging from 83% to 99%, Table 3.2.2, entry 7 and Table 3.2.3, entries 1-6). One plausible explanation for this can be found in the competition between direct hydrogenation *vs* isomerization for the different substrates. This is supported by the fact that the hydrogenation of substrate **S32** bearing a *tert*-butyl group, for which

isomerization cannot occur, provides high levels of enantioselectivity (ee's up to 97%; Table 3.2.3, entry 6), while the lowest enantioselectivity of the series (ee's up to 84%; Table 3.2.3, entries 4-5) is found for substrates **S30** and **S31** which form the most stable isomerized tetrasubstituted olefins.

Table 3.2.3. Selected results for the Ir-catalyzed hydrogenation of minimally functionalized 1,1-disubstituted terminal olefins using ligands **L1**-**L5a**-**m**[a]

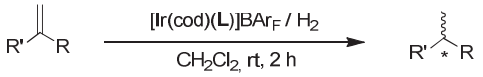

R' = aryl, 2-thiophene, 2-pyridine
R = alkyl, aryl

Entry	Substrate	L	% ee[b]	Entry	Substrate	L	% ee[b]
1	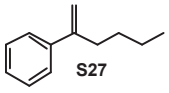 **S27**	**L5c**	90 (*S*)	8	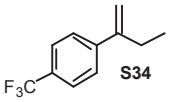 **S34**	**L5c**	99 (*S*)
2	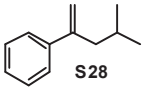 **S28**	**L5c**	93 (*S*)	9	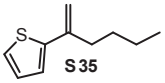 **S35**	**L5c**	90 (-)
3	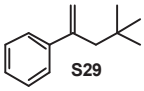 **S29**	**L5c**	93 (*S*)	10	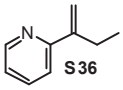 **S36**	**L5c**	99 (+)
4	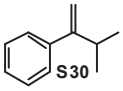 **S30**	**L5c**	83 (*S*)	11	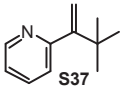 **S37**	**L5c**	99 (+)
5	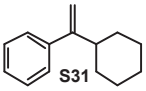 **S31**	**L5c**	84 (*S*)	12[c]	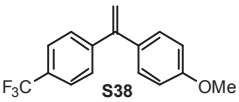 **S38**	**L5k**	65 (+)
6	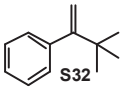 **S32**	**L5c**	97 (*S*)	13[c]	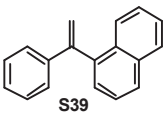 **S39**	**L5k**	70 (+)
7	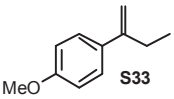 **S33**	**L5c**	98 (*S*)	14[c]	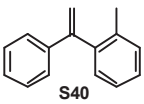 **S40**	**L5k**	68 (+)

[a] Reactions carried out using 1 mmol of substrate and 0.2 mol% of Ir-catalyst precursor at 1 bar of H_2. Full conversions were achieved in all cases. [b] Enantiomeric excesses determined by chiral GC (except for entries 12-14 that were measured by HPLC). [c] Reaction carried out at 50 bar of H_2.

The hydrogenations of several *para*-substituted 2-phenylbut-2-enes with different electronic properties (**S26**, **S33** and **S34**) all gave similar high activities and enantioselectivities (full conversion, ee's up to 99%; Table 3.2.2, entry 7 and Table 3.2.3, entries 7 and 8).

We next decided to apply this ligand library in the asymmetric hydrogenation of 1,1-heteroaromatic alkenes (**S35**-**S37**, Table 3.2.3, entries 9-11). Even though heterocycles are used in industry and the heterocyclic part can be modified post-hydrogenation, very few previous studies have been made.[2e] Under standard conditions, our catalyst systems were also able to hydrogenate this type of substrate with excellent activities and enantioselectivities (ee's up to 99%).

Encouraged by the excellent results we decided to study the hydrogenation of several diaryl terminal alkenes (**S38**-**S40**; Table 3.2.3, entries 12-14). Enantiopure diarylalkanes are important intermediates for the preparation of drugs and research materials.[15] They have traditionally been prepared using rather laborious approaches.[15,16] Interestingly, both substrate types differing electronically (**S38**) and sterically (**S39**-**S40**) were hydrogenated with fair enantioselectivities (ee's up to 70%) using ligand **L5k**.

Asymmetric hydrogenation of 1,1-disubstituted terminal olefins containing a neighboring polar group

To further determine the scope of this ligand library we also examined the asymmetric hydrogenation of 1,1-disubstituted terminal olefins containing a polar neighboring group (**S41**-**S44**). The results are summarized in Scheme 3.2.6.

We initially tested the ligand library in the hydrogenation of the allylic alcohol **S41** and allylic acetate **S42**. Derivatives of the hydrogenation of these products are important intermediates for the synthesis of high-value cosmetics, natural products and drugs.[17] Enantioselectivities up to 70% were obtained using ligand **L5a**. We then turned our attention to the asymmetric reduction of the trifluoromethyl olefin **S43** and allylic silane **S44**. The hydrogenation of these compounds gave rise to important organic intermediates and a number of innovative new organofluorine[18] and organosilicon[19] drugs are now being developed. The enantioselectivities (71% ee for **S43** and 96% ee for **S44**) were best with ligands **L5k** and **L3a**, respectively. These results, which again clearly shown the efficiency of using modular scaffolds in ligand design, are among the best that have been reported for these demanding substrate classes.[2e]

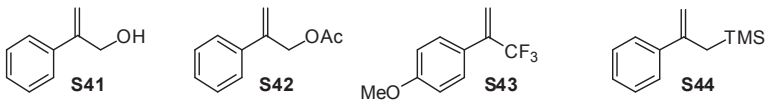

L5a: 100% Conv. 70% (*R*) ee | **L5a**: 100% Conv. 69% (*R*) ee | **L5k**: 100% Conv. 71% (-) ee | **L3a**: 100% Conv. 96% (*S*) ee

Scheme 3.2.6. Selected hydrogenation results of 1,1-disubstituted terminal olefins containing a neighboring polar group using [Ir(cod)(**L1**-**L5a**-**m**)]BAr_F catalyst precursors. Reaction conditions: 0.5 mol % catalyst precursor, CH_2Cl_2 as solvent, 50 bar H_2, rt, 2 h.

3.2.3.5. Origin of enantioselectivity. Computational studies

Although the mechanism of olefin hydrogenation (and consequently of stereocontrol) by Rh catalysts is well understood,[20] the mechanism when chiral iridium catalysts are used is not, despite having been investigated both experimentally and computationally.[1,2] In the first case, there is enough evidences to support a Rh^{I}/Rh^{III} mechanism in which substrate chelation to metal

plays a pivotal role in stereodiscrimination, but in the second four different mechanisms have been proposed (two of them involving Ir^{I}/Ir^{III} intermediates[21] and the other two Ir^{III}/Ir^{V} species[22]). Andersson and coworkers have recently used DFT calculations and a full, experimentally tested combination of ligands (mainly phosphine/phosphinite,N) and substrates to study all of the possible diastereomeric routes of the four different mechanisms.[23] Their studies agree with the two already proposed catalytic cycles passing through Ir^{III}/Ir^{V} intermediates;[22] however, they failed to distinguish the two Ir^{III}/Ir^{V} mechanisms.[24] One of the mechanisms involves an Ir^{III}/Ir^{V} migratory-insertion/reductive-elimination pathway (labeled 3/5-MI in Scheme 3.2.7)[22c] whereas the second mechanism goes through an Ir^{III}/Ir^{V} σ-metathesis/reductive-elimination pathway (labeled 3/5-Meta in Scheme 3.2.7)[22a,b]. From these cycles, it has been demonstrated that the π-olefin complex **C** and the transition states for the migratory-insertion in 3/5-MI (**TS**) and the σ-metathesis in 3/5-Meta (**TS'**) are responsible for the enantiocontrol in the iridium hydrogenation.[23] It was demonstrated that the enantioselectivity could be reliably obtained from calculated relative energies of migratory insertion transition states.[23]

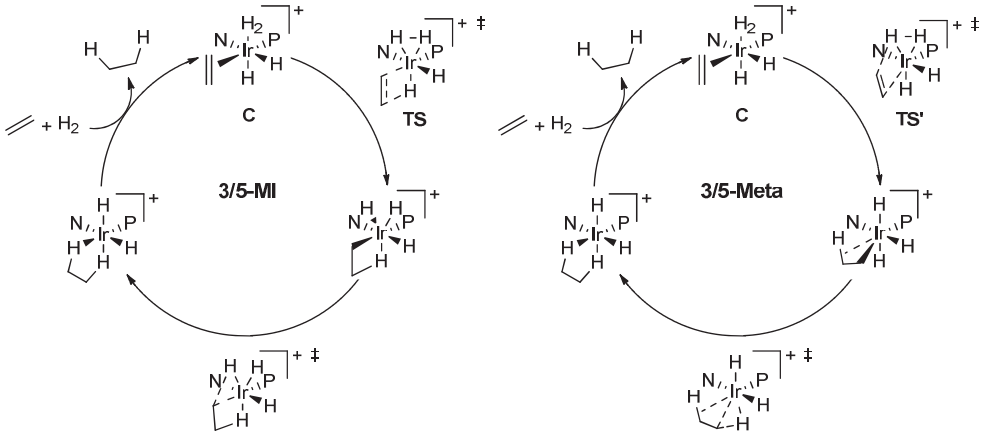

Scheme 3.2.7. 3/5-MI and 3/5-Meta catalytic cycles for the Ir-hydrogenation.

On the basis of these previous studies and in an attempt to rationalize the enantioselectivity obtained with the iridium/phosphite-oxazoline catalyst library reported in this paper, we performed a computational study of the complexes **C** and transition states (**TS** and **TS'**) most commonly involved in the enantiocontrol of the iridium-catalyzed hydrogenation reaction (Scheme 3.2.7).

All geometries were optimized in the gas phase using the Jaguar program[25] and both the B3LYP hybrid density functional[26] and the LACVP* basis set. Termochemical data was computed at 298.15 K for all optimized geometries. Energies in CH_2Cl_2 solution were calculated as single-point energies from optimized structures at the B3LYP/LACVP* level of theory using a Poisson-Boltzmann continuous field. Final energies were retrieved from single-point calculations at the B3LYP/LACV3P++* level of theory and corrected by inclusion of the van der Waals repulsion energy calculated by DFT-D3.[27] Reported energies (in kJ/mol) are the Gibbs free energy, including thermodynamic and solvation contributions. For more computational details see the experimental section and supporting information.

This computational study has been performed with two different types of substrate: **S1** as a model substrate for trisubstituted olefins and **S26** as a model for 1,1-disubstituted olefins. We chose to study the catalyst precursor Ir/**L5c** since for both substrates **L5c** proved to have the best combination of ligand parameters for high enantioselectivity. For preliminary calculations, the ligand was simplified by removing the benzylidene protecting group (Figure 3.2.2) in an attempt to accelerate the DFT calculation and verify whether the method gave satisfactory results. Then the method was used to explore the reactions involving the complete ligand.

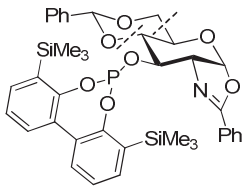

Figure 3.2.2. Ligand truncation used for preliminary DFT calculations.

Initially, we applied the calculation for the trisubstituted olefin **S1**. Table 3.2.4 shows the calculated energies for the most stable isomers of complex **C** and for the most stable isomers of the transition states (**TS** and **TS'**) with the truncated ligand.

Table 3.2.4. Calculated energies for the most stable isomers of complex **C** and transition states **TS** and **TS'** with substrate **S1** using the truncated ligand system

Starting geometry	**3/5-MI cycle C** energy (kJ/mol)	**TS** energy (kJ/mol)	**Starting geometry**	**3/5-Meta cycle C** energy (kJ/mol)	**TS'** energy (kJ/mol)
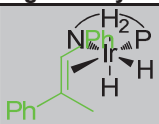 **C1**$_{3/5\text{-MI}}$	-45.6	0 (ref)	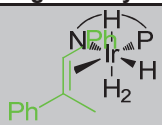 **C1**$_{3/5\text{-Meta}}$	-41.2	20.2
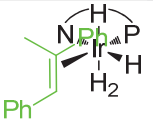 **C2**$_{3/5\text{-MI}}$	-47.4	51.6	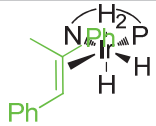 **C2**$_{3/5\text{-Meta}}$	-47.2	26.5
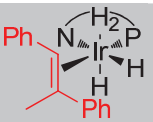 **C3**$_{3/5\text{-MI}}$	-32.5	15.6	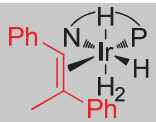 **C3**$_{3/5\text{-Meta}}$	-47.9	64.0
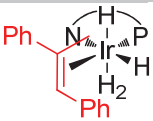 **C4**$_{3/5\text{-MI}}$	-28.3	61.5	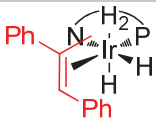 **C4**$_{3/5\text{-Meta}}$	-59.4	27.9

These key isomers are the result of varying the relative coordination of the substrate (*si* face or *re* face) and the relative position of the hydride (up or down).[28] The olefins coordinated on the *si* face are shown in green and are hydrogenated to (*R*)-product, whereas those coordinated on the *re* face are shown in red and are hydrogenated to the (*S*)-product. The results show that the most stable transition state (**C1$_{3/5\text{-MI}}$**, Table 3.2.4) matches the major product obtained experimentally (*R* product, Table 3.2.1, entry 7). We also found that the hydrogenation of olefins **S1** by Ir/**L5c** follows the 3/5-MI mechanism (the energies for hydrogenation pathway 3/5-MI, in both the major and minor configuration, are around 15 kJ/mol more stable than those for the 3/5-Meta pathway, see Table 3.2.4). In addition, the difference in energy between the most stable transition state for the major and the minor product is 15.6 kJ/mol, which agrees with the excellent enantioselectivity obtained experimentally using the Ir/**L5c** catalyst system (Table 3.2.1, entry 7).

Since the method gives satisfactory results, we next applied it to the reaction of **S1** with the full ligand structure. The difference in energy of 22.9 kJ/mol between the most stable transition states (Figure 3.2.3) matches well with the excellent enantioselectivities obtained experimentally (>99% ee, Table 3.2.1, entry 7).

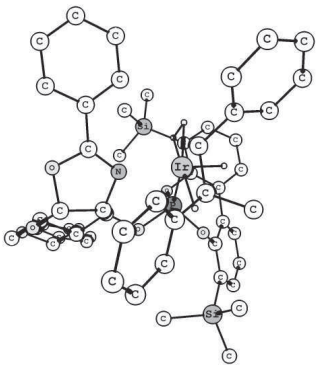

Major pathway
0 kJ/mol

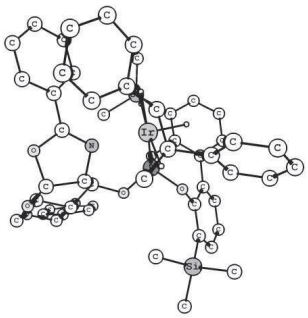

Minor pathway
22.9 kJ/mol

Figure 3.2.3. Calculated transition states (**TS**) for the major and the minor pathway with the full ligand. Hydrogen atoms of the ligand **L5c** and substrate **S1** have been omitted for clarity.

The optimized DFT structure shows a quadrant diagram (depicted in Figure 3.2.4), a model already used by Andersson and coworkers to describe the steroselectivity in the Ir-catalyzed hydrogenation of trisubstituted olefins.[4d] In this quadrant model, we found that the phenyl group of the oxazoline substituent blocks the upper left quadrant and one of the aryls of the biaryl phosphite group partly occupies the lower right quadrant making it semi-hindered (Figure 3.2.4(a)). The other two quadrants, which are free from bulky groups, are open (Figure 3.2.4(a)). Therefore, the calculated structure clearly shows a chiral pocket that is well suited to olefins with large *trans* substituents (*E*-olefins). In the case of the trisubstituted *E*-olefin **S1** the smallest substituent (H atom of **S1**) will face the steric bulk of the ligand and the olefin will preferentially coordinate to the catalyst from the *si* side (Figure 3.2.4(b)), as the opposite coordination mode will result in unfavorable interactions between one of the large *trans*-substituents and the steric bulk of the ligand.

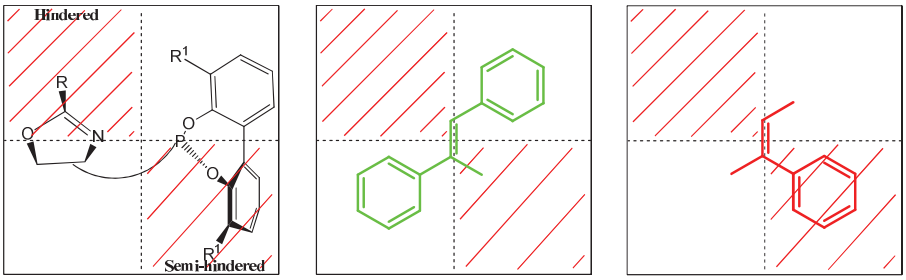

Figure 3.2.4. Quadrant diagram describing the enantioselective substrate-ligand interactions.

This model also explains the lack of enantioselectivity observed when ligands **L5f**, **L5h** and **L5j** were used (Table 3.2.1, entries 10, 12 and 14). In all these ligands the biaryl phosphite group has an *S*-configuration, which is opposite to the configuration adopted by ligand **L5c** when coordinated to the Ir, as shown by the catalytic results and the DFT calculation (Figures 3.2.3 and 3.2.4(a)). This change in the configuration moves the previously found semi-hindered quadrant from the lower right to the upper right. Therefore, the favorable chiral pocket generated by the Ir/**L5c** catalyst, which can accommodate large *trans* substituents, is lost and consequently Ir/**L5f**, Ir/**L5h** and Ir/**L5j** catalysts fail to control the face coordination preference of the olefin.

Using this quadrant model we can also predict the change in the sense of enantioselectivity observed experimentally when *E*-trisubstituted olefins (i.e. **S1**) change to *Z*-olefins (i.e. **S2**). The lowest energy transition state, then, will be achieved with the *Z*-olefin coordinated through the *re* face, opposite face to that of the *E*-olefin, with the hydrogen atom positioned in the hindered upper left quadrant and the aryl substituent in the semi-hindered lower right quadrant (Figure 3.2.4(c)). The catalytic results also show that in order to obtain high enantioselectivity in the reduction of *Z*-olefins we have to switch to ligand **L5a**. This is not unexpected since the DFT calculations have shown that the catalytic system Ir/**L5c** generated a pocket that is well suited to *E*-olefins. Ligand **L5a** differs from the previous ligand **L5c** in the presence of bulky substituents at the *para* position of the biphenyl group. These substituents increase the dihedral angle of the biaryl group, which results in lower occupancy of the lower right quadrant than with the previous Ir/**L5c** catalytic system. So, the substituents of the biphenyl moieties can tune the steric hindrance of the lower right quadrant so that it can accommodate the phenyl substituent of *Z*-substrates and led to high enantioselectivity. The same explanation may account for the excellent enantioselectivities obtained with triarylsubstituted olefins **S9** and **S10**.

Finally, we did the calculation for the 1,1-disubstituted olefin **S26**, using first the truncated ligand structure of **L5c** without the benzylidene protecting group (Figure 3.2.2). We found that the results followed the same trend as for the trisubstituted olefin (Table 3.2.5). Therefore, the most stable transition state observed matches the major product and the preferred pathway is the 3/5-MI with an energy difference of 15 kJ/mol with respect to the 3/5-Meta pathway.

Using the full structure of ligand **L5c** we observe that the difference in energy between the transition states for the major and the minor products is 9.5 kJ/mol (Figure 3.2.5). Thus, not only is the major isomer correctly identified for this challenging system, but the quantitative prediction of 96% ee at ambient temperature matches well with the enantioselectivity obtained experimentally (99% ee, Table 3.2.2, entry 7).

Table 3.2.5. Calculated energies for the most stable isomers of complex **C** and transition states **TS** and **TS'** with substrate **S26** using the truncated ligand system

3/5-MI cycle			3/5-Meta cycle		
Starting geometry	**C** energy (kJ/mol)	**TS** energy (kJ/mol)	**Starting geometry**	**C** energy (kJ/mol)	**TS'** energy (kJ/mol)
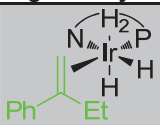 **C5**$_{3/5\text{-MI}}$	-45.0	0 (ref)	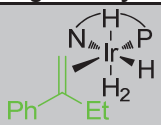 **C5**$_{3/5\text{-Meta}}$	-36.1	20.1
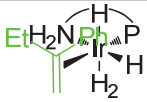 **C6**$_{3/5\text{-MI}}$	-44.0	7.4	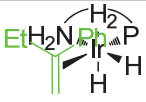 **C6**$_{3/5\text{-Meta}}$	-40.9	21.9
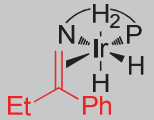 **C7**$_{3/5\text{-MI}}$	-40.3	11.4	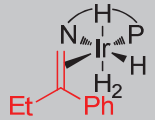 **C7**$_{3/5\text{-Meta}}$	-41.4	27.6
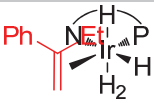 **C8**$_{3/5\text{-MI}}$	-39.5	59.2	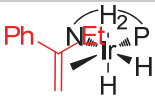 **C8**$_{3/5\text{-Meta}}$	-38.0	40.9

In summary, the substrate versatility of our Ir/phosphite-oxazoline catalytic system is higher than that of related Ir-phosphine/phosphinite-nitrogen catalysts because the biaryl phosphite moiety makes the catalyst more flexible. Therefore, subtle variations in the dihedral angle of the biaryl phosphite moiety, which may arise from changing the biaryl substituents and/or be imposed by the substrate itself, lead to a different occupancy of the semi-hindered quadrant. As a result, the catalyst can adapt its chiral environment to a range of substrate types.

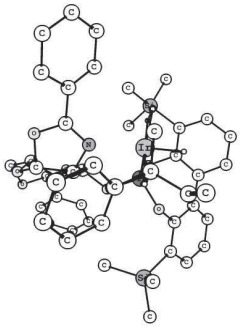

Major pathway
0 kJ/mol

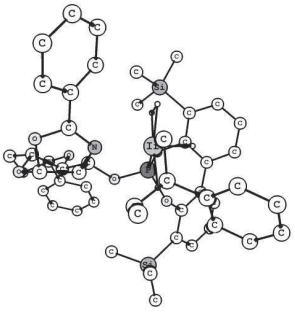

Minor pathway
9.5 kJ/mol

Figure 3.2.5. Calculated transitions states (**TS**) for the major and the minor pathway with the full ligand. Hydrogen atoms of the ligand **L5e** and substrate **S26** have been omitted for clarity.

3.2.4. Conclusions

The modular ligand design has been shown to be highly successful, both in finding highly selective ligands for each substrate, and in identifying two general ligands (**L5a** and **L5c**) with good performance over the entire range of substrates. The good performance extends even to the very challenging class of terminally disubstituted olefins. The enantioselectivity was below 90% for olefins with two similarly sized substituents, such as aryl *vs* aryl or *s*-alkyl, but even a moderate size difference like aryl *vs n*-alkyl allowed good enantioselectivities in the range 90-99%. It should be pointed out that these catalysts are also very tolerant to the presence of neighboring polar group. Thus, a range of allylic alcohols, acetates, α,β-unsaturated ketones, α,β-unsaturated esters and vinylboronates were hydrogenated in high enantioselectivities (ee's up to >99%).

The computational study allowed identification of the preferred reaction path, an Ir(III/V) cycle with migratory insertion of a hydride as selectivity-determining step.[23] The alternative metathesis mechanism[22a,b] was consistently higher in energy. For selected models, the DFT calculations allowed computational determination of the observed selectivities with high accuracy. Both the favored enantiomer and the effect of ligand modifications could be rationalized in terms of the previously proposed quadrant model.

3.2.5. Experimental section

3.2.5.1. General considerations

All reactions were carried out using standard Schlenk techniques under an argon atmosphere. Solvents were purified and dried by standard procedures. Phosphorochloridites are easily prepared in one step from the corresponding biaryls.[29] ^{1}H, $^{13}C\{^{1}H\}$, and $^{31}P\{^{1}H\}$ NMR spectra were recorded using a 400 MHz spectrometer. Chemical shifts are relative to that of $SiMe_4$ (^{1}H and ^{13}C) as internal standard or H_3PO_4 (^{31}P) as external standard. ^{1}H, ^{13}C and ^{31}P assignments were made on the basis of ^{1}H-^{1}H gCOSY, ^{1}H-^{13}C gHSQC and ^{1}H-^{31}P gHMBC experiments. All catalytic experiments were performed three times.

3.2.5.2. Computational details

Geometries of all substrates were optimized using the Jaguar program[25] and both the B3LYP hybrid density functional[26] and the LACVP* basis sets. The complexes were treated with charge = +1 and in the singlet state. In some cases, structures were first optimized using geometric constraints in order to generate starting structures that were subsequently optimized without geometric constraints. No symmetry constraints were applied. Normal-mode analysis of stable structure revealed no imaginary frequencies or a single imaginary frequency with negligibly low frequency ($v < 100$ cm^{-1}); those of transition states had a single imaginary frequency of higher negative frequency (usually $v < -500$ cm^{-1}). Reported energies are the Gibbs free energy at 298.15 K. LACVP in Jaguar defines a combination of the LANL2DZ basis set[30] for iridium and the 6-31G basis set for other atoms. Final energies were retrieved from single-point calculations at the B3LYP/LACV3P++* level of theory. LACV3P++* differs from LACVP* because it uses the 6-311++G* basis set instead of 6-31G*, one additional p function and two additional d functions on Ir. Energies in CH_2Cl_2 solution were calculated as single-point energies from optimized structures

at the B3LYP/LACVP* level of theory using a Poisson-Boltzmann continuous field with ε = 8.93 and F = 1.3266 g/mL to calculate the solvent radius (2.33 Å).[31] Final energies were corrected by inclusion of the Van der Waals repulsion energy calculated by DFT-D3.[27] All structures and energies for complexes **C1**-$\mathbf{8}_{3/5\text{-MI - }3/5\text{-Meta}}$ and transitions states **TS1**-$\mathbf{8}_{3/5\text{-MI - }3/5\text{-Meta}}$ can be found in http://pubs.acs.org/doi/suppl/10.1021/ja204948k.

3.2.5.3. General procedure for the preparation of the phosphite-oxazoline ligands

The corresponding phosphorochloridite (3.0 mmol) produced *in situ* was dissolved in toluene (12.5 mL) and pyridine (1.14 mL, 14 mmol) was added. The corresponding hydroxyl-oxazoline compound (2.8 mmol) was azeotropically dried with toluene (3 x 2 mL) and then dissolved in toluene (12.5 mL) to which pyridine (1.14 mL, 14 mmol) was added. The oxazoline solution was transferred slowly at 0 ºC to the solution of phosphorochloridite. The reaction mixture was stirred overnight at 80 ºC, and the pyridine salts were removed by filtration. Evaporation of the solvent gave a white foam, which was purified by flash chromatography in alumina to produce the corresponding ligand as a white solid.

L5f. Yield: 1.0 g (48 %). ^{31}P NMR ($CDCl_3$), δ: 147.3 (s). ^{1}H NMR (C_6D_6), δ: 1.44 (s, 9H, CH_3, ^{t}Bu), 1.69 (s, 9H, CH_3, ^{t}Bu), 1.74 (s, 3H, CH_3-Ar), 1.81 (s, 3H, CH_3-Ar), 2.09 (s, 3H, CH_3-Ar), 2.11 (s, 3H, CH_3-Ar), 3.52 (m, 1H, H-6'), 3.67 (m, 1H, H-5), 3.78 (m, 1H, H-4), 4.11 (m, 1H, H-2), 4.27 (m, 1H, H-6), 4.92 (m, 1H, H-3), 5.52 (d, 1H, H-1, $^{3}J_{1\text{-}2}$= 7.6 Hz), 5.57 (s, 1H, H-7), 7.14-7.83 (m, 12H, CH=). ^{13}C NMR (C_6D_6), δ: 16.1 (CH_3-Ar), 16.4 (CH_3-Ar), 19.8 (CH_3-Ar), 20.0 (CH_3-Ar), 32.9 (CH_3, ^{t}Bu), 33.1 (CH_3, ^{t}Bu), 35.9 (C, ^{t}Bu), 36.0 (C, ^{t}Bu), 64.5 (C-5), 70.3 (C-6), 70.5 (C-2), 79.1 (C-3), 81.0 (C-4), 102.9.0 (C-7), 103.2 (C-1), 125.7 (CH=), 125.8 (CH=), 127.0 (CH=), 128,1 (CH=), 128.4 (CH=), 128.6 (CH=), 129.1 (CH=), 129.4 (CH=), 129,6 (CH=), 129.7 (CH=), 129.9 (CH=), 130.4 (CH=), 130.7 (CH=), 130.9 (C), 131.8 (C), 132.1 (C), 132.2 (C), 132.5 (C), 134.4 (C), 135.2 (C), 137.3 (C), 137.6 (C), 138.0 (C), 144.6 (C), 145.3 (C), 165.7 (C=N). Anal. calcd (%) for $C_{44}H_{50}NO_7P$: C 71.82, H 6.85, N 1.90; found: C 71.87, H 6.93, N 1.88.

L5g. Yield: 1.1 g (52 %). ^{31}P NMR ($CDCl_3$), δ: 147.8 (s). ^{1}H NMR (C_6D_6), δ: 1.43 (s, 9H, CH_3, ^{t}Bu), 1.63 (s, 9H, CH_3, ^{t}Bu), 1.71 (s, 3H, CH_3-Ar), 1.83 (s, 3H, CH_3-Ar), 2.11 (s, 6H, CH_3-Ar), 3.53 (m, 1H, H-6'), 3.68 (m, 1H, H-5), 3.73 (m, 1H, H-4), 4.14 (m, 1H, H-2), 4.25 (m, 1H, H-6), 4.75 (m, 1H, H-3), 5.51 (d, 1H, H-1, $^{3}J_{1\text{-}2}$= 7.6 Hz), 5.58 (s, 1H, H-7), 7.14-7.83 (m, 12H, CH=). ^{13}C NMR (C_6D_6), δ: 16.1 (CH_3-Ar), 16.4 (CH_3-Ar), 19.9 (CH_3-Ar), 33.1 (CH_3, ^{t}Bu), 35.9 (C, ^{t}Bu), 36.0 (C, ^{t}Bu), 64.6 (C-5), 70.2 (C-6), 71.2 (C-2), 79.8 (C-3), 80.5 (C-4), 102.9 (C-7), 103.1 (C-1), 125.8 (CH=), 125.9 (CH=), 126.8 (CH=), 128,0 (CH=), 128.6 (CH=), 128.9 (CH=), 129.5 (CH=), 129.7 (CH=), 129.8 (CH=), 130.7 (CH=), 130.9 (CH=), 131.7 (CH=), 131.9 (C), 132.3 (C), 132.5 (C), 132.8 (C), 134.5 (C), 135.2 (C), 137.3 (C), 137.6 (C), 138.0 (C), 144.6 (C), 145.3 (C), 165.9 (C=N). Anal. calcd (%) for $C_{44}H_{50}NO_7P$: C 71.82, H 6.85, N 1.90; found: C 71.85, H 6.89, N 1.89.

L5j: Yield: 0.40 g, 17 %. ^{31}P NMR (400 MHz, C_6D_6) δ: 150.5 (s). ^{1}H NMR (400 MHz, C_6D_6) δ: 0.41 (s, 9H, $Si(CH_3)_3$), 0.55 (s, 9H, $Si(CH_3)_3$), 3.18 (m, 1H, H-6'), 3.49 (m, 1H, H-5), 3.66 (m, 1H, H-4), 3.90 (m, 1H, H-6), 4.41 (dd, 1H, H-2, $^{3}J_{2\text{-}1}$= 8.0 Hz, $^{3}J_{2\text{-}3}$= 2.4 Hz) 5.00 (s, 1H, H-7), 5.04 (m, 1H, H-3), 5.64 (d, 1H, H-1, $^{3}J_{1\text{-}2}$= 8.0 Hz), 6.80-8.01 (m, 22H, CH=). ^{13}C NMR (400 MHz, C_6D_6) δ= 0.5 ($Si(CH_3)_3$), 0.9 ($Si(CH_3)_3$), 63.4 (C-5), 69.0 (C-6), 70.9 (C-2), 77.1 (d, C-3, $^{2}J_{c\text{-}p}$= 9.1 Hz), 81.0 (C-4), 101.7 (C-1), 102.0 (C-7), 124.4 (C), 124.7 (C), 125.4 (CH=), 126.0 (CH=), 127.2 (CH=), 127.3 (CH=), 127.6 (CH=), 127.7 (CH=), 127.8 (CH=), 128.1 (CH=), 128.4 (CH=), 128.6 (CH=),

128.7 (CH=), 128.8 (CH=), 128.9 (CH=), 129.0 (CH=), 129.1 (CH=), 129.2 (CH=), 129.6 (C), 131.6 (CH=), 131.9 (CH=), 132.3 (CH=), 133.1 (CH=), 134.9 (C), 135.1 (C), 137.3 (CH=), 137.8 (CH=), 138.0 (C), 152.8 (C), 153.0 (C), 164.3 (C). Anal. calcd (%) for $C_{46}H_{46}NO_7PSi_2$: C 68.04, H 5.71, N 1.72; found: C 68.23, H 5.84, N 1.63.

L5k: Yield: 0.40 g, 17 %. ^{31}P NMR (400 MHz, C_6D_6) δ: 151.7 (s, 1P). ^{1}H NMR (400 MHz, C_6D_6) δ: 0.57 (s, 9H, $Si(CH_3)_3$), 0.65 (s, 9H, $Si(CH_3)_3$), 3.37 (m, 1H, H-6'), 3.52 (m, 1H, H-5), 3.91 (m, 1H, H-4), 4.02 (m, 1H, H-6), 4.23 (m, 1H, H-2), 5.12 (m, H-3), 5.40 (d, 1H, H-1, $^{3}J_{1-2}$= 8.0 Hz), 5.47 (s, 1H, H-7), 6.86-8.19 (m, 22H, CH=). ^{13}C NMR (400 MHz, C_6D_6) δ: 0.6 ($Si(CH_3)_3$), 0.9 ($Si(CH_3)_3$), 63.1 (C-5), 69.1 (C-6), 70.1 (C-2), 77.0 (d, C-3, $^{2}J_{c-p}$= 13.6 Hz), 80.5 (d, C-4, $^{2}J_{c-p}$= 4.1 Hz), 101.8 (C-7), 102.2 (C-1), 110.4 (C), 124.4 (CH=), 124.7 (CH=), 125.5 (CH=), 126.0 (CH=), 127.1 (CH=), 127.3 (CH=), 127.4 (CH=), 127.6 (CH=), 127.8 (CH=), 127.9 (CH=), 128.1 (CH=), 128.4 (CH=), 128.6 (CH=), 128.8 (CH=), 129.1 (CH=), 129.1 (CH=), 129.3 (CH=), 129.3 (CH=), 129.7 (CH=), 130.2 (C), 131.7 (C), 132.0 (C), 132.8 (C), 135.0 (C), 135.1 (C), 135.4 (C), 137.4 (CH=), 138.0 (CH=), 138.2 (CH=), 138.6 (CH=), 152.5 (C), 152.9 (C), 163.6 (C). Anal. calcd (%) for $C_{46}H_{46}NO_7PSi_2$: C 68.04, H 5.71, N 1.72; found: C 68.12, H 5.78, N 1.69.

3.2.5.4. Synthesis of phosphinite-oxazoline ligand L5m

Chlorodi(*o*-tolyl)phosphine (136.5 mg, 0.55 mmol) was slowly added at -40 °C to a solution of **1** (176.6 mg, 0.5 mmol) and DMAP (5.7 mg, 0.05 mmol) in THF (3.3 mL) and triethylamine (1.7 mL). The reaction mixture was stirred for 15 minutes at room temperature. Diethyl ether was then added and the salts were removed by filtration. The residue was purified by flash chromatography (eluent: Toluene/NEt_3= 100/2) to produce the corresponding ligand as a colorless oil. Yield: 152 mg (54%). ^{31}P NMR ($CDCl_3$), δ: 106.6 (s). ^{1}H NMR ($CDCl_3$), δ: 2.25 (s, 3H, CH_3-Ph), 2.69 (s, 3H, CH_3-Ph), 3.28 (m, 1H, H-6'), 3.45 (m, 2H, H-4 and H-5), 3.97 (dd, 1H, H-6, $^{2}J_{6-6'}$= 10.8 Hz, $^{3}J_{6-5}$= 3.6 Hz), 4.13 (dd, 1H, H-2, $^{3}J_{2-1}$= 8.0 Hz, $^{3}J_{2-3}$= 3.6 Hz), 4.43 (m, 1H, H-3), 5.02 (s, 1H, H-7), 5.58 (d, 1H, H-1, $^{3}J_{1-2}$= 8.0 Hz), 6.8-7.2 (m, 12H, CH=), 7.25 (m, 2H, CH=), 7.64 (m, 1H, CH=), 7.88 (m, 1H, CH=), 8.08 (m, 2H, CH=). ^{13}C NMR ($CDCl_3$), δ: 20.8 (d, CH_3-Ph, J_{C-P}= 21.4 Hz), 21.5 (d, CH_3-Ph, J_{C-P}= 20.6 Hz), 63.6 (C-5), 68.8 (C-6), 70.1 (d, C-2, J_{C-P}= 4.6 Hz), 80.2 (C-4), 83.8 (d, C-3, J_{C-P}= 22.1 Hz), 101.7 (C-7), 103.4 (C-1), 126.9 (CH=), 128.8 (CH=), 128.9 (CH=), 129.0 (CH=), 129.1 (CH=), 129.6 (CH=), 130.2 (CH=), 130.5 (CH=), 130.6 (CH=), 130.8 (CH=), 130.9 (CH=), 131.2 (CH=), 131.3 (CH=), 131.4 (CH=), 131.5 (CH=), 132.1 (CH=), 138.2 (CH=), 140.3 (C), 140.4 (C), 140.6 (C), 141.3 (C), 141.6 (C), 142.2 (C), 142.5 (C), 163.6 (C=N). Anal. Calc (%) for $C_{34}H_{32}NO_5P$: C 72.20, H 5.70, N 2.48; found: C 72.17, H 5.72, N 2.43.

3.2.5.5. Typical procedure for the preparation of [Ir(cod)(L)]BAr_F

The corresponding ligand (0.074 mmol) was dissolved in CH_2Cl_2 (2 mL) and [Ir(μ-Cl)cod]$_2$ (25 mg, 0.037 mmol) was added. The reaction was refluxed at 50 °C for 1 hour. After 5 min at room temperature, $NaBAr_F$ (77.1 mg, 0.082 mmol) and water (2 mL) were added and the reaction mixture was stirred vigorously for 30 min at room temperature. The phases were separated and the aqueous phase was extracted twice with CH_2Cl_2. The combined organic phases were filtered through a celite plug, dried with $MgSO_4$ and the solvent was evaporated to give the product as an orange solid.

[Ir(cod)(L1a)]BAr$_F$. Yield 130 mg (93 %). ^{31}P NMR ($CDCl_3$), δ: 102.2 (s). ^{1}H NMR ($CDCl_3$), δ: 1.28 (s, 9H, CH_3, ^{t}Bu), 1.36 (s, 9H, CH_3, ^{t}Bu), 1.49 (s, 9H, CH_3, ^{t}Bu), 1.61 (s, 9H, CH_3, ^{t}Bu), 1.71 (b, 3H, CH_2, cod), 1.93 (m, 1H, CH_2, cod), 2.08 (m, 2H, CH_2, cod), 2.21 (s, 3H, CH_3-N), 2.28 (b, 2H, CH_2 cod), 3.30 (b, 1H, CH=, cod), 3.70 (m, 1H, H-4), 3.78 (m, 1H, H-6'), 3.90 (m, 1H, H-5), 4.10 (b, 1H, CH= cod), 4.21 (m, 1H, H-3), 4.36 (dd, 1H, H-6, $^2J_{6\text{-}6'}$ = 10.4 Hz, $^3J_{6\text{-}5}$ = 5.6 Hz), 4.40 (m, 1H, H-2), 4.67 (m, 1H, CH=, cod), 5.29 (b, 1H, CH=, cod), 5.48 (s, 1H, H-7), 6.05 (d, 1H, H-1, $^3J_{1\text{-}2}$ = 6.4 Hz), 7.0-7.8 (m, 21H, CH=, aromatics). ^{13}C NMR ($CDCl_3$), δ: 16.3 (s, CH_3-N), 25.8 (b, CH_2, cod), 29.4 (b, CH_2, cod), 31.5 (s, CH_3, ^{t}Bu), 32.4 (b, CH_2, cod), 32.7 (s, CH_3, ^{t}Bu), 34.9 (s, C, ^{t}Bu), 35.0 (s, C, ^{t}Bu), 35.6 (s, C, ^{t}Bu), 36.1 (b, CH_2 cod and C, ^{t}Bu), 65.2 (b, CH=, cod), 66.6 (s, C-5), 67.4 (s, C-2), 67.6 (s, C-6), 70.4 (b, CH=, cod), 74.4 (d, C-4, $J_{C\text{-}P}$= 8.3 Hz), 79.2 (s, C-3), 95.9 (d, CH=, cod, $J_{C\text{-}P}$= 20.5 Hz), 101.9 (s, C-7), 104.6 (s, C-1), 105.7 (d, CH, cod, $J_{C\text{-}P}$ = 12.1 Hz), 117.7 (b, CH= BAr$_F$), 120-132 (aromatic carbons), 135.0 (b, CH= BAr$_F$), 135.5-150 (aromatic carbons), 161.9 (q, C-B BAr$_F$, $^1J_{C\text{-}B}$ = 50 Hz), 174.8 (s, C=N). Anal. calc (%) for $C_{83}H_{80}BF_{24}IrNO_7P$: C 52.65, H 4.26, N 0.74; found: C 53.91, H 4.33, N 0.71.

[Ir(cod)(L2a)]BAr$_F$. Yield 126 mg (89 %). ^{31}P NMR ($CDCl_3$), δ: 103.2 (s). ^{1}H NMR ($CDCl_3$), δ: 1.22 (d, 3H, CH_3, ^{i}Pr, $^3J_{H\text{-}H}$= 7.2 Hz), 1.31 (s, 9H, CH_3, ^{t}Bu), 1.35 (m, 3H, CH_3, ^{i}Pr), 1.37 (s, 9H, CH_3, ^{t}Bu), 1.49 (s, 9H, CH_3, ^{t}Bu), 1.61 (s, 9H, CH_3, ^{t}Bu), 1.98 (m, 1H, CH_2, cod), 2.11 (m, 3H, CH_2, cod), 2.34 (m, 4H, CH_2, cod), 2.76 (m, 1H, CH, ^{i}Pr), 3.41 (b, 1H, CH=, cod), 3.74 (m, 1H, H-4), 3.79 (m, 1H, H-6'), 3.88 (m, 1H, H-5), 4.16 (m, 2H, H-3 and CH= cod), 4.39 (dd, 1H, H-6, $^2J_{6\text{-}6'}$ = 10.8 Hz, $^3J_{6\text{-}5}$ = 4.8 Hz), 4.40 (dd, 1H, H-2, $^3J_{2\text{-}3}$ = 8.4 Hz, $^3J_{2\text{-}1}$ = 6.8 Hz), 4.71 (m, 1H, CH=, cod), 5.28 (b, 1H, CH=, cod), 5.49 (s, 1H, H-7), 6.10 (d, 1H, H-1, $^3J_{1\text{-}2}$ = 6.8 Hz), 7.1-7.8 (m, 21H, CH=, aromatics). ^{13}C NMR ($CDCl_3$), δ: 18.7 (s, CH_3, ^{i}Pr), 20.5 (s, CH_3, ^{i}Pr), 25.9 (b, CH_2, cod), 29.2 (b, CH_2, cod), 30.9 (s, CH, ^{i}Pr), 31.5 (s, CH_3, ^{t}Bu), 31.6 (s, CH_3, ^{t}Bu), 31.7 (s, CH_3, ^{t}Bu), 32.6 (b, CH_2, cod), 32.7 (s, CH_3, ^{t}Bu), 34.9 (s, C, ^{t}Bu), 35.0 (s, C, ^{t}Bu), 35.6 (s, C, ^{t}Bu), 36.1 (s, C, ^{t}Bu), 36.2 (b, CH_2, cod), 64.4 (s, CH=, cod), 66.4 (s, C-2), 67.1 (s, C-5), 67.6 (s, C-6), 70.4 (s, CH=, cod), 74.3 (s, C-4), 79.6 (s, C-3), 96.1 (m, CH=, cod), 101.7 (s, C-7), 104.4 (s, C-1), 105.9 (d, CH=, cod, $J_{C\text{-}P}$ = 13.4 Hz), 117.7 (b, CH=, BAr$_F$), 120-132 (aromatic carbons), 135.0 (b, CH=, BAr$_F$), 135.5-150 (aromatic carbons), 161.9 (q, C-B, BAr$_F$, $^1J_{C\text{-}B}$ = 49 Hz) 181.4 (s, C=N). Anal. calc (%) for $C_{85}H_{84}BF_{24}IrNO_7P$: C 53.13, H 4.41, N 0.73; found: C 53.21, H 4.47, N 0.72.

[Ir(cod)(L3a)]BAr$_F$. Yield 136 mg (95 %). ^{31}P NMR ($CDCl_3$), δ: 106.9 (s). ^{1}H NMR ($CDCl_3$), δ: 1.16 (s, 9H, CH_3, ^{t}Bu), 1.36 (s, 9H, CH_3, ^{t}Bu), 1.54 (s, 9H, CH_3, ^{t}Bu), 1.55 (s, 9H, CH_3, ^{t}Bu), 1.57 (s, 9H, CH_3, ^{t}Bu), 1.65 (m, 2H, CH_2 cod), 2.05 (m, 1H, CH_2, cod), 2.20 (m, 2H, CH_2, cod), 2.34 (m, 2H, CH_2, cod), 2.53 (m, 1H, CH_2, cod), 3.59 (m, 1H, H-4), 3.75 (m, 2H, H-6' and H-5), 3.97 (m, 1H, H-3), 4.21 (m, 1H, CH=, cod), 4.32 (m, 1H, H-6), 4.36 (m, 1H, H2), 4.49 (b, 1H, CH=, cod), 4.72 (b, 1H, CH=, cod), 5.40 (s, 1H, H-7), 5.42 (b, 1H, CH=, cod), 5.99 (d, 1H, CH, H1, $^3J_{1\text{-}2}$ = 6 Hz), 7.1-7.8 (m, 21H, CH=, aromatics). ^{13}C NMR ($CDCl_3$), δ: 24.2 (b, CH_2, cod), 28.3 (b, CH_2, cod), 28.6 (s, CH_3, ^{t}Bu -N), 31.4 (s, CH_3, ^{t}Bu), 31.6 (s, CH_3, ^{t}Bu), 31.8 (s, C, ^{t}Bu), 34.8 (s, C, ^{t}Bu), 35.0 (s, C, ^{t}Bu), 35.1 (b, CH_2, cod), 35.4 (s, C, ^{t}Bu), 36.1 (s, C, ^{t}Bu), 37.4 (b, CH_2, cod), 66.2 (s, C-5), 67.5 (s, C-6), 68.4 (s, C-2), 69.8 (s, CH=, cod), 70.1 (s, CH=, cod), 74.1 (m, C-4), 79.8 (s, C-3), 90.8 (m, CH=, cod), 101.2 (s, C-7), 103.5 (s, C-1), 104.3 (m, CH=, cod), 117.7 (b, CH= BAr$_F$), 120-132 (aromatic carbons), 135.0 (b, CH= BAr$_F$), 135.5-150 (aromatic carbons), 161.9 (q, C-B, BAr$_F$, $^1J_{C\text{-}B}$ = 50 Hz) 183.6 (s, C=N). Anal. calc (%) for $C_{86}H_{86}BF_{24}IrNO_7P$: C 53.37, H 4.48, N 0.72; found: C 53.42, H 4.53, N 0.69.

[Ir(cod)(L4a)]BAr$_F$. Yield: 138 mg (95%). ^{31}P NMR ($CDCl_3$), δ: 104.3 (s). ^{1}H NMR ($CDCl_3$), δ: 1.36 (s, 9H, CH_3, ^{t}Bu), 1.41 (s, 9H, CH_3, ^{t}Bu), 1.65 (s, 2H, CH_2), 1.70 (s, 9H, CH_3, ^{t}Bu), 1.73 (s, 9H, CH_3, ^{t}Bu), 1.8-2.2 (b, 8H, CH_2, cod), 3.48 (m, 1H, H-6'), 3.65 (m, 2H, CH=, cod and H-5), 3.84 (m, 1H, H-4), 4.13 (m, 1H, H-2), 4.15 (b, 1H, CH=, cod), 4.24 (dd, 1H, H-6, $^2J_{6\text{-}6'}$= 10.0 Hz, $^3J_{6\text{-}5}$= 4.8 Hz), 4.79 (b, 1H, CH= cod), 4.92 (m, 1H, H-3), 5.18 (b, 1H, CH= cod), 5.49 (d, 1H, H-1, $^3J_{1\text{-}2}$= 7.6 Hz), 5.53 (s, 1H, H-7), 7.1 – 8.5 (m, 26H, CH= aromatics). ^{13}C NMR ($CDCl_3$), δ: 15.3 (CH_2), 22.8 (b, CH_2, cod), 28.9 (b, CH_2, cod), 31.3 (CH_3, ^{t}Bu), 31.4 (CH_3, ^{t}Bu), 31.6 (CH_3, ^{t}Bu), 32.4 (b, CH_2, cod), 32.9 (b, CH_2, cod), 34.9 (C, ^{t}Bu), 35.1 (C, *t*Bu), 35.5 (C, ^{t}Bu), 36.0 (C, ^{t}Bu), 64.7 (C-5), 67.1 (CH=, cod), 70.4 (C-2), 70.7 (C-6), 72.3 (CH=, cod), 79.5 (d, C-3, $^2J_{C\text{-}P}$= 20.5 Hz), 80.3 (C-4), 99.6 (b, CH=, cod), 103.0 (C-7), 103.2 (C-1), 104.1 (d, CH=, cod, $J_{C\text{-}P}$= 12.2 Hz), 117.7 (b, CH=, BAr$_F$), 119-134 (aromatic carbons), 135.0 (b, CH=, BAr$_F$), 136-149 (aromatic carbons), 161.9 (q, C-B, BAr$_F$, $^1J_{C\text{-}B}$= 49.6 Hz), 168.7 (C=N). Anal. Calc (%) for $C_{89}H_{84}BF_{24}IrNO_7P$: C 54.27, H 4.30, N 0.71; found: C 54.32, H 4.35, N 0.68.

[Ir(cod)(L5a)]BAr$_F$. Yield 131 mg (91 %). ^{31}P NMR ($CDCl_3$), δ: 102.9 (s). ^{1}H NMR ($CDCl_3$), δ: 1.21 (s, 9H, CH_3, ^{t}Bu), 1.38 (s, 9H, CH_3, ^{t}Bu), 1.59 (s, 9H, CH_3, ^{t}Bu), 1.63 (s, 9H, CH_3, ^{t}Bu), 1.67 (m, 4H, CH_2, cod), 2.22 (m, 2H, CH_2, cod), 2.41 (m, 2H, CH_2, cod), 3.69 (m, 1H, H-4), 3.79 (m, 1H, H-6'), 3.93 (b, 2H, CH= cod and H-5), 4.27 (m, 1H, H-3), 4.39 (b, 2H, CH= cod and H-6), 4.52 (b, 2H, CH= cod and H-2), 5.43 (b, 1H, CH=, cod), 5.44 (s, 1H, H-7), 6.32 (d, 1H, H-1, $^3J_{1\text{-}2}$ = 6.4 Hz), 7.1-8.5 (m, 26H, CH= aromatics). ^{13}C NMR ($CDCl_3$), δ: 25.1 (b, CH_2, cod), 29.3 (b, CH_2, cod), 31.2 (s, CH_3, ^{t}Bu), 31.5 (s, CH_3, ^{t}Bu), 31.6 (s, CH_3, ^{t}Bu), 33.2 (b, CH_2, cod), 34.9 (s, C, ^{t}Bu), 35.0 (s, C, ^{t}Bu), 35.4 (s, C, ^{t}Bu), 36.1 (s, C, ^{t}Bu), 36.9 (b, CH_2, cod), 66.4 (s, CH=, cod), 67.6 (s, C-5), 67.9 (s, C-2), 68.6 (s, C-6), 70.4 (s, CH=, cod), 74.2 (d, C-4, $J_{C\text{-}P}$= 8.4 Hz), 79.5 (s, C-3), 94.9 (d, CH=, cod, $J_{C\text{-}P}$ = 22.3 Hz), 101.4 (s, C-7), 104.4 (s, C-1), 107.5 (m, CH=, cod), 117.7 (b, CH=, BAr$_F$), 119-132 (aromatic carbons), 135.0 (b, CH=, BAr$_F$), 135.5-150 (aromatic carbons), 161.9 (q, C-B, BAr$_F$, $^1J_{C\text{-}B}$ = 49 Hz) 171.4 (s, C=N). Anal. calc (%) for $C_{88}H_{82}BF_{24}IrNO_7P$: C 54.05, H 4.23, N 0.72; found: C 54.21, H 4.28, N 0.68.

[Ir(cod)(L5b)]BAr$_F$. Yield 125 mg (89 %). ^{31}P NMR ($CDCl_3$), δ: 104.4 (s). ^{1}H NMR ($CDCl_3$), δ: 1.57 (s, 9H, CH_3, ^{t}Bu), 1.58 (s, 9H, CH_3, ^{t}Bu), 1.80 (b, 4H, CH_2, cod), 2.31 (b, 3H, CH_2, cod), 2.52 (m, 1H, CH_2, cod), 3.67 (m, 1H, H-4), 3.76 (m, 3H, CH_3-O), 3.78 (m, 1H, H-6'), 3.82 (s, 3H, CH_3-O), 3.91 (m, 1H, H-5), 4.02 (m, 1H, CH=, cod), 4.24 (m, 1H, H-3), 4.38 (dd, 1H, H-6, $^2J_{6'\text{-}6}$ = 10.4 Hz, $^3J_{6\text{-}5}$ = 4.8 Hz), 4.44 (b, 1H, CH=, cod), 4.51 (dd, 1H, H-2, $^3J_{2\text{-}3}$ = 7.6 Hz, $^3J_{2\text{-}1}$ = 6.4 Hz), 5.38 (b, 1H, CH=, cod), 5.46 (s, 1H, H-7), 6.31 (d, 1H, H-1, $^3J_{1\text{-}2}$ = 6.4 Hz), 7.1-7.8 (m, 26H, CH=, aromatics). ^{13}C NMR ($CDCl_3$), δ: 25.2 (b, CH_2, cod), 29.4 (b, CH_2, cod), 31.1 (s, CH_3, ^{t}Bu), 31.4 (s, CH_3, ^{t}Bu), 32.9 (b, CH_2, cod), 35.5 (s, C, ^{t}Bu), 36.0 (s, C, ^{t}Bu), 36.5 (b, CH_2, cod), 55.7 (s, CH_3-O), 55.8 (s, CH_3-O), 66.8 (s, CH=, cod), 67.6 (s, CH, C-2), 67.9 (s, CH, C-5), 68.2 (s, CH, C-6), 70.0 (s, CH=, cod), 74.4 (d, C-4, $J_{C\text{-}P}$ = 8.3 Hz), 79.0 (s, C-3), 96.3 (d, CH=, cod, $J_{C\text{-}P}$= 21.2 Hz), 101.2 (s, C-7), 104.4 (s, C-1), 107.3 (d, CH=, cod, $J_{C\text{-}P}$ = 12.1 Hz), 112-116 (aromatic carbons), 117.7 (b, CH=, BAr$_F$), 120-132 (aromatic carbons), 135.0 (b, CH=, BAr$_F$), 135.5-160 (aromatic carbons), 161.9 (q, C-B BAr$_F$, $^1J_{C\text{-}B}$ = 49.2 Hz) 171.4 (s, C=N). Anal. calc (%) for $C_{82}H_{70}BF_{24}IrNO_9P$: C 51.74, H 3.71, N 0.74; found: C 51.69, H 3.80, N 0.79.

[Ir(cod)(L5c)]BAr$_F$. Yield 127 mg (92 %). ^{31}P NMR ($CDCl_3$), δ: 100.9 (s). ^{1}H NMR ($CDCl_3$), δ: 0.40 (s, 9H, CH_3-Si), 0.56 (s, 9H, CH_3-Si), 1.64 (m, 4H, CH_2, cod), 2.22 (m, 2H, CH_2, cod), 2.56 (m, 2H, CH_2, cod), 3.65 (m, 1H, H-4), 3.76 (m, 1H, H-6'), 3.85 (m, 1H, H-5), 3.98 (m, 1H, CH=

cod), 4.27 (m, 1H, H-3), 4.37 (b, 2H, H-6 and CH= cod), 4.51 (dd, 1H, H-2, $^3J_{2\text{-}3}$ = 8.4 Hz, $^3J_{2\text{-}1}$ = 6.8 Hz), 4.66 (b, 1H, CH= cod), 5.42 (s, 1H, H-7), 5.54 (b, 1H, CH=, cod), 6.32 (d, 1H, H-1, $^3J_{1\text{-}2}$ = 6.8 Hz), 7.0-8.5 (m, 28H, CH=, aromatics). ^{13}C NMR ($CDCl_3$), δ: 0.26 (s, CH_3-Si), 0.61 (s, CH_3-Si), 24.8 (b, CH_2, cod), 29.1 (b, CH_2, cod), 33.8 (b, CH_2, cod), 37.2 (b, CH_2, cod), 66.9 (s, C-5), 67.6 (s, C-6), 67.8 (s, C-2), 68.9 (s, CH=, cod), 69.0 (s, CH=, cod), 74.3 (m, C-4), 79.1 (s, C-3), 95.0 (d, CH=, cod, $J_{C\text{-}P}$= 22.7 Hz), 101.9 (s, C-7), 104.4 (s, C-1), 107.2 (m, CH=, cod), 117.7 (b, CH BAr_F), 120-134 (aromatic carbons), 135.0 (b, CH BAr_F), 135.5-137 (aromatic carbons), 161.9 (q, C-B BAr_F, $^1J_{C\text{-}B}$ = 49 Hz), 171.5 (s, C=N). Anal. calc (%) for $C_{78}H_{66}BF_{24}IrNO_7PSi_2$: C 49.95, H 3.55, N 0.75; found: C 50.11, H 3.61, N 0.72.

[Ir(cod)(L5d)]BAr_F. Yield: 118 mg (92%). ^{31}P ($CDCl_3$), δ: 112.7 (s). ^{1}H ($CDCl_3$), δ: 1.7-2.4 (b, 8H, CH_2, cod), 3.73 (m, 2H, H-5, H-6'), 3.81 (m, 2H, CH=, cod and H-4), 4.24 (b, 1H, CH= cod), 4.41 (m, 2H, H-6, H-2), 4.71 (b, 1H, CH= cod), 4.77 (m, 1H, H-3), 5.33 (b, 1H, CH= cod), 5.69 (s, 1H, H-7), 6.03 (d, 1H, H-1, $^3J_{1,2}$= 7.2 Hz), 7.1-8.2 (m, 30H, CH=). ^{13}C ($CDCl_3$), δ: 22.4 (b, CH_2, cod), 23.1 (b, CH_2, cod), 31.9 (b, CH_2, cod), 32.3 (b, CH_2, cod), 63.2 (C-5), 68.9 (C-6), 70.2 (C-2), 76.7 (C-3), 80.0 (C-4), 100.5 (d, CH=, cod, $J_{C\text{-}P}$= 18 Hz),101.6 (C-7), 102.7 (C-1), 103.3 (d, CH=, cod, $J_{C\text{-}P}$= 22 Hz), 117.8 (b, CH=, BAr_F), 119-134 (aromatic carbons), 135.1 (b, CH=, BAr_F), 136-149 (aromatic carbons), 161.7 (q, C-B, BAr_F, $^1J_{C\text{-}B}$= 49.6 Hz), 170.3 (C=N). Anal. Calc (%) for $C_{72}H_{50}BF_{24}IrNO_7P$: C 49.95, H 2.91, N 0.81; found: C 50.02, H 2.93, N 0.79.

[Ir(cod)(L5e)]BAr_F. Yield: 134 mg (93%). ^{31}P NMR ($CDCl_3$), δ: 113.5 (s). ^{1}H NMR ($CDCl_3$), δ: 1.8-2.1 (b, 6H, CH_2, cod), 2.19 (s, 3H, CH_3), 2.28 (b, 5H, CH_2, cod and CH_3), 2.34 (s, 3H, CH_3), 2.39 (s, 3H, CH_3), 3.54 (m, 2H, CH=, cod and H-6'), 3.63 (m, 1H, H-4), 3.68 (m, 1H, CH=, cod and H-5), 4.21 (m, 1H, H-6), 4.33 (m, 1H, H-2), 4.39 (b, 1H, CH= cod), 4.81 (m, 1H, H-3), 5.11 (b, 1H, CH= cod), 5.46 (s, 1H, H-7), 5.71 (d, 1H, H-1, $^2J_{1\text{-}2}$= 7.5 Hz), 7.1 – 8.5 (m, 26H, aromatics). ^{13}C NMR ($CDCl_3$), δ: 17.2 (CH_3), 17.4 (CH_3), 21.1 (CH_3), 21.3 (CH_3), 23.1 (b, CH_2, cod), 25.4 (b, CH_2, cod), 33.4 (b, CH_2, cod), 33.6 (b, CH_2, cod), 68.9 (C-6), 68.4 (CH=, cod), 69.5 (C-2), 70.5 (CH=, cod), 78.6 (d, C-3, $^2J_{c\text{-}p}$= 12 Hz), 78.4 (C-4), 99.9 (d, CH=, cod, $J_{C\text{-}P}$= 22.2 Hz), 102.1 (C-7), 103.2 (C-1), 104.3 (d, CH=, cod, $J_{C\text{-}P}$= 16 Hz), 117.6 (b, CH=, BAr_F), 119-134 (aromatic carbons), 135.1 (b, CH=, BAr_F), 136-149 (aromatic carbons), 161.6 (q, C-B, BAr_F, $^1J_{C\text{-}B}$= 49.6 Hz), 170.4 (C=N). Anal. Calc (%) for $C_{76}H_{58}BF_{24}IrNO_7P$: C 51.07, H 3.27, N 0.78; found: C 51.11, H 3.32, N 0.80.

[Ir(cod)(L5f)]BAr_F. Yield: 134 mg (94%). ^{31}P NMR ($CDCl_3$), δ: 108.4 (s). ^{1}H NMR ($CDCl_3$), δ: 1.41 (s, 9H, CH_3, ^{t}Bu), 1.57 (s, 9H, CH_3, ^{t}Bu), 1.69 (s, 3H, CH_3-Ar), 1.77 (s, 3H, CH_3-Ar), 1.8-2.1 (b, 7H, CH_2, cod and CH_3-Ar), 2.14 (s, 3H, CH_3-Ar), 2.2-2.4 (b, 4H, CH_2, cod), 3.52 (m, 1H, H-6'), 3.65 (m, 1H, CH=, cod), 3.68 (m, 1H, H-5), 3.82 (m, 1H, H-4), 4.08 (b, 2H, CH= cod and H-2), 4.23(m, 1H, H-6), 4.79 (b, 1H, CH= cod), 4.83 (m, 1H, H-3), 5.32 (b, 1H, CH= cod), 5.49 (d, 1H, H-1, $^3J_{1\text{-}2}$= 7.6 Hz), 5.59 (s, 1H, H-7), 7.1 – 8.3 (m, 24H, aromatics). ^{13}C NMR ($CDCl_3$), δ: 16.1 (CH_3-Ar), 16.4 (CH_3-Ar), 17.8 (CH_3-Ar), 19.1 (CH_3-Ar), 26.8 (b, CH_2, cod), 27.6 (b, CH_2, cod), 31.3 (CH_3, ^{t}Bu), 31.4 (CH_3, ^{t}Bu), 33.7 (b, CH_2, cod), 34.9 (C, ^{t}Bu), 35.1 (C, ^{t}Bu), 64.7 (C-5), 68.8 (CH=, cod), 70.5 (C-2), 71.1 (CH=, cod), 79.2 (C-3), 81.3 (C-4), 100.4 (d, CH=, cod, $J_{C\text{-}P}$= 21.8 Hz), 102.7 (C-7), 103.1 (b, CH=, cod),103.6 (C-1), 117.4 (b, CH=, BAr_F), 119-134 (aromatic carbons), 135.1 (b, CH=, BAr_F), 136-149 (aromatic carbons), 161.6 (q, C-B, BAr_F, $^1J_{C\text{-}B}$= 49.6 Hz), 169.4 (C=N). Anal. Calc (%) for $C_{82}H_{74}BF_{24}IrNO_7PSi_2$: C 50.99 H 3.86, N 0.73; found: C 51.02, H 3.92, N 0.72.

[Ir(cod)(L5g)]BAr_F. Yield: 142 mg (95%). ^{31}P NMR ($CDCl_3$), δ: 107.6 (s). ^{1}H NMR ($CDCl_3$), δ: 1.40 (s, 9H, CH_3, ^{t}Bu), 1.55 (s, 9H, CH_3, ^{t}Bu), 1.78 (s, 3H, CH_3-Ar), 1.81 (s, 3H, CH_3-Ar), 1.8-2.1

(b, 7H, CH_2, cod and CH_3-Ar), 2.2-2.4 (b, 7H, CH_2, cod and CH_3-Ar), 3.57 (m, 2H, H-6' and CH=, cod), 3.69 (m, 1H, H-5), 3.95 (m, 1H, H-4), 4.11 (b, 2H, CH= cod and H-2), 4.19 (m, 1H, H-6), 4.27 (b, 1H, CH= cod), 4.79 (m, 1H, H-3), 5.28 (b, 1H, CH= cod), 5.32 (d, 1H, H-1, $^3J_{1-2}$= 7.6 Hz), 5.57 (s, 1H, H-7), 7.1 – 8.3 (m, 24H, aromatics). ^{13}C NMR ($CDCl_3$), δ: 16.3 (CH_3-Ar), 16.5 (CH_3-Ar), 18.4 (CH_3-Ar), 18.9 (CH_3-Ar), 27.2 (b, CH_2, cod), 27.4 (b, CH_2, cod), 31.6 (CH_3, ^{t}Bu), 31.9 (CH_3, ^{t}Bu), 32.4 (b, CH_2, cod), 32.8 (b, CH_2, cod), 34.9 (C, ^{t}Bu), 35.1 (C, ^{t}Bu), 64.9 (C-5), 71.3(CH=, cod), 71.6 (CH=, cod), 71.9 (C-2), 79.4 (C-3), 80.4 (C-4), 100.9 (b, CH=, cod), 102.7 (C-7), 103.3 (b, CH=, cod), 103.7 (C-1), 117.5 (b, CH=, BAr_F), 119-134 (aromatic carbons), 135.1 (b, CH=, BAr_F), 136-149 (aromatic carbons), 161.7 (q, C-B, BAr_F, $^1J_{C-B}$= 49.6 Hz), 169.1 (C=N). Anal. Calc (%) for $C_{82}H_{74}BF_{24}IrNO_7PSi_2$: C 50.99 H 3.86, N 0.73; found: C 51.09, H 3.96, N 0.71.

[Ir(cod)(L5h)]BAr$_F$. Yield 126 mg (93 %). ^{31}P NMR ($CDCl_3$), δ: 108.3 (s). ^{1}H NMR ($CDCl_3$), δ: 1.74 (b, 4H, CH_2, cod), 2.00 (m, 1H, CH_2, cod), 2.13 (m, 2H, CH_2, cod), 2.21 (m, 1H, CH_2, cod), 3.90 (b, 2H, CH=, cod and H-4), 3.94 (m, 1H, H-6'), 4.06 (m, 1H, H-5), 4.11 (b, 1H, CH=, cod), 4.31 (m, 3H, CH=, cod, H-6 and H-3), 4.67 (m, 1H, H-2), 5.44 (b, 1H, CH=, cod), 5.51 (s, 1H, H-7), 6.41 (d, 1H, H-1, $^3J_{1-2}$ = 6.4 Hz), 6.9-8.7 (m, 34H, CH=, aromatics). ^{13}C NMR ($CDCl_3$), δ: 25.4 (b, CH_2, cod), 29.3 (b, CH_2, cod), 32.1 (b, CH_2, cod), 36.7 (b, CH_2, cod), 66.7 (s, CH=, cod), 67.1 (s, C-5), 67.4 (s, C-2), 67.9 (s, C-6), 68.4 (s, CH=, cod), 74.3 (m, C-4), 80.1 (s, C-3), 99.4 (m, CH=, cod), 100.8 (s, C-7), 104.7 (s, C-1), 110.4 (m, CH=, cod), 117.8 (b, CH=, BAr_F), 119-134 (aromatic carbons), 135.2 (b, CH=, BAr_F), 135.5-151 (aromatic carbons), 162.4 (q, C-B, BAr_F, $^1J_{C-B}$ = 50 Hz) 172.5 (s, C=N). Anal. calc (%) for $C_{80}H_{54}BF_{24}IrNO_7P$: C 52.47, H 2.97, N 0.76; found: C 52.53, H 3.02, N 0.79.

[Ir(cod)(L5i)]BAr$_F$. This compound has been prepared following a slight modification of the general procedure. The anion exchange has been therefore performed at low temperature (0 ºC) without the presence of water. Yield 115 mg (91 %). ^{31}P NMR ($CDCl_3$), δ: 107.7 (s). ^{1}H NMR ($CDCl_3$), δ: 1.6-2.5 (m, 8H, CH_2 cod), 3.85 (b, 3H, CH=, cod, H-5 and H-6'), 3.91 (m, 1H, H-3), 3.98 (b, 2H, CH= cod and H-4), 4.01 (b, 1H, CH=, cod), 4.33 (m, 1H, H-6), 4.71 (m, 1H, H-2), 4.99 (b, 1H, CH=, cod), 5.45 (s, 1H, H-7), 5.51 (b, 1H, CH= cod), 6.31 (d, 1H, H-1, $^3J_{1-2}$ = 6.4 Hz), 7.1-8.3 (m, 32H, CH=, aromatics). ^{13}C NMR ($CDCl_3$), δ: 26.3 (b, CH_2, cod), 28.5 (b, CH_2, cod), 32.3 (b, CH_2, cod), 34.5 (b, CH_2, cod), 64.5 (CH=, cod), 65.9 (C-5), 69.8 (C-6), 70.8 (CH=, cod), 70.9 (C-2), 74.3 (C-4), 80.3 (C-3), 98.4 (d, CH=, cod, J_{C-P}= 22 Hz), 101.8 (s, C-7), 102.9 (d, CH=, cod, J_{C-P} = 12.2 Hz), 103.8 (s, C-1), 117.7 (b, CH= BAr_F), 120-134 (aromatic carbons), 135.0 (b, CH= BAr_F), 135-137 (aromatic carbons), 161.7 (q, C-B BAr_F, $^1J_{C-B}$ = 49 Hz) 170.3 (s, C=N). Anal. calc (%) for $C_{72}H_{52}BF_{24}IrNO_5P$: C 50.83, H 3.08, N 0.82; found: C 51.02, H 3.14, N 0.80.

[Ir(cod)(L5j)]BAr$_F$. All attempts to prepare this compound using different reaction conditions were unsuccessful. In all the cases decomposed product was obtained even at low temperature.

[Ir(cod)(L5k)]BAr$_F$. Yield 126 mg (86 %). ^{31}P NMR ($CDCl_3$), δ: 108.3 (s). ^{1}H NMR ($CDCl_3$), δ: 0.56 (s, 9H, CH_3-Si), 0.65 (s, 9H, CH_3-Si), 1.63 (b, 2H, CH_2, cod), 1.79 (m, 2H, CH_2, cod), 2.20 (m, 2H, CH_2, cod), 2.39 (b, 1H, CH_2, cod), 2.49 (m, 1H, CH_2, cod), 3.72 (m, 1H, H-4), 3.76 (m, 1H, H-6'), 3.92 (b, 2H, CH= cod and H-5), 4.36 (b, 4H, H-3, H-6 and 2 CH= cod), 4.64 (m, 1H, H-2), 5.37 (s, 1H, H-7), 5.59 (b, 1H, CH=, cod), 6.35 (d, 1H, H-1, $^3J_{1-2}$ = 6.8 Hz), 6.7-8.5 (m, 32H, CH=, aromatics). ^{13}C NMR ($CDCl_3$), δ: 0.58 (s, CH_3-Si), 1.77 (s, CH_3-Si), 24.6 (b, CH_2, cod), 29.9 (b, CH_2, cod), 33.7 (b, CH_2, cod), 37.4 (b, CH_2, cod), 66.5 (s, CH=, cod), 67.5 (s, C-5), 68.0 (s, C-2), 69.4 (s, C-6), 70.8 (s, CH=, cod), 74.2 (d, C-4, J_{C-P}= 8.4 Hz), 79.1 (s, C-3), 93.6 (m, CH=, cod, J_{C-}

$_P$= 22.7 Hz), 100.9 (s, C-7), 104.1 (s, C-1), 107.6 (d, CH=, cod, J_{C-P} = 12.1 Hz), 117.6 (b, CH=, BAr_F), 120-134.5 (aromatic carbons), 135.0 (b, CH=, BAr_F), 135.5-152 (aromatic carbons), 161.9 (q, C-B, BAr_F, $^1J_{C-B}$ = 50 Hz) 171.3 (s, C=N). Anal. calc (%) for $C_{86}H_{70}BF_{24}IrNO_7PSi_2$: C 52.28, H 3.57, N 0.71; found: C 53.11, H 3.64, N 0.67.

[Ir(cod)(L5l)]BAr$_F$. Yield 115 mg (91 %). ^{31}P NMR ($CDCl_3$), δ: 107.5 (s). ^{1}H NMR ($CDCl_3$), δ: 1.61 (b, 1H, CH_2, cod), 1.80 (b, 1H, CH_2, cod), 1.93 (b, 1H, CH_2, cod), 2.16 (b, 1H, CH_2, cod), 2.25 (b, 1H, CH_2, cod), 2.40 (m, 1H, CH_2 cod), 2.55 (m, 1H, CH_2, cod), 2.67 (m, 1H, CH_2, cod), 3.69 (b, 1H, CH, cod), 3.85 (m, 2H, H-5 and H-6'), 3.90 (m, 2H, H-3 and H-4), 3.98 (b, 2H, CH=, cod), 4.31 (m, 1H, H-6), 4.71 (m, 1H, H-2), 5.08 (b, 1H, CH=, cod), 5.58 (b, 2H, H-7 and CH= cod), 6.37 (d, 1H, H-1, $^3J_{1-2}$ = 6.4 Hz), 7.1-8.3 (m, 32H, CH=, aromatics). ^{13}C NMR ($CDCl_3$), δ: 26,1 (b, CH_2, cod), 29.8 (b, CH_2, cod), 31.7 (b, CH_2, cod), 36.2 (b, CH_2, cod), 63.6 (s, CH=, cod), 66.6 (s, C-5), 67.7 (s, C-6), 67.9 (s, CH, C-2), 69.3 (s, CH=, cod) 74.7 (d, C-4, J_{C-P}= 12.4 Hz), 79.8 (s, C-3), 95.5 (d, CH=, cod, J_{C-P}= 12.8 Hz), 101.9 (s, C-7), 103.7 (d, CH=, cod, J_{C-P} = 12.2 Hz), 104.1 (s, C-1), 117.7 (b, CH= BAr_F), 120-134 (aromatic carbons), 135.0 (b, CH= BAr_F), 135-137 (aromatic carbons), 161.9 (q, C-B BAr_F, $^1J_{C-B}$ = 49 Hz) 170.8 (s, C=N). Anal. calc (%) for $C_{72}H_{52}BF_{24}IrNO_5P$: C 50.83, H 3.08, N 0.82; found: C 51.10, H 3.14, N 0.81.

[Ir(cod)(L5m)]BAr$_F$. Yield: 122 mg (96%). ^{31}P NMR ($CDCl_3$), δ: 116.2 (s). ^{1}H NMR ($CDCl_3$), δ: 1.6-1.8 (m, 4H, CH_2, cod), 1.89 (s, 3H, CH_3-Ph), 1.8-2.2 (b, 4H, CH_2, cod), 2.48 (m, 1H, CH=, cod), 2.99 (s, 3H, CH_3-Ph), 3.6-3.8 (m, 4H, H-3, H-4, H-5, H-6'), 3.86 (m. 1H, CH=, cod), 4.28 (dd, 1H, H-6, $^2J_{6-6'}$= 10.0 Hz, $^3J_{6-5}$= 4.0 Hz), 4.58 (m, 1H, H-2), 5.02 (m, 1H, CH=), 5.47 (m, 1H, H-7), 6.28 (d, 1H, H-1, $^3J_{1-2}$= 6.06.5 (m, 1H, CH= aromatic), 7.0-7.8 (m, 26H, CH= aromatic), 8.32 (m, 2H, CH= aromatic), 8.73 (m, 1H, CH= aromatic). ^{13}C NMR ($CDCl_3$), δ: 21.6 (CH_3-Ph), 23.0 (d, CH_3, J_{C-P}= 6.0 Hz), 25.6 (b, CH_2, cod), 29.0 (b, CH_2, cod), 29.9 (b, CH_2, cod), 32.3 (b, CH_2, cod), 65.9 (CH), 66.4 (CH), 67.7 (CH), 69.3 (CH=, cod), 75.1 (CH=, cod), 80.7 (CH), 93.0 (d, CH=cod, J_{C-P}= 13.8 Hz), 101.8 (d, CH=cod, J_{C-P}= 12.6 Hz), 102.2 (C-7), 104.4 (C-1) 117.7 (b, CH=, BAr_F), 120-134 (aromatic carbons), 135.0 (b, CH=, BAr_F), 136-145 (aromatic carbons), 161.9 (q, C-B, BAr_F, $^1J_{C-B}$= 49.6 Hz), 170.5 (C=N). Anal. Calc (%) for $C_{74}H_{56}BF_{24}IrNO_5P$: C 51.40, H 3.26, N 0.81; found: C 51.35, H 3.24, N 0.77.

3.2.5.6. General procedure for the preparation of terminal alkenes S35-S37

To a suspension of methyltriphenylphosphonium bromide (5.7 g, 15.9 mmol, 1.5 equiv.) in THF (400 mL) at 0 ºC under Ar was added *n*-butyllithium (2.5 M, 5.9 mL, 14.8 mmol, 1.4 equiv.) dropwise. The resulting orange solution was stirred at 0 °C for 30 minutes. A solution of the corresponding ketone (10.6 mmol, 1.00 equiv.) in THF (10 mL) was added dropwise and the resulting yellow solution was left overnight at room temperature. The reaction was quenched with water (10 mL), extracted with Et_2O and dried over $MgSO_4$. The precipitate was removed by filtration through a silica plug. The collected solids were washed with pentane (3x10 mL) and the filtrate was concentrated *in vacuo*.

S35. The crude product was purified on silica eluting with pentane. Colorless liquid (1.30 g, 7.80 mmol, 73% Yield). ^{1}H-NMR (400 MHz, $CDCl_3$): δ = 0.94 (t, 3H, CH_3, ^3J = 7.7 Hz), 1.41 (m, 2H, CH_2), 1.57 (m, 2H, CH_2), 2.48 (t, 2H, CH_2, ^3J = 7.2 Hz), 4.96 (s, 1H, CH_2=), 5.40 (s, 1H, CH_2=), 6.97 (m, 1H, CH=), 7.05 (m, 1H, CH=), 7.18 (m, 1H, CH=) ppm. ^{13}C-NMR (100 MHz,

$CDCl_3$): 14.1 (CH_3), 22.7 (CH_2), 30.8 (CH_2), 35.4 (CH_2), 110.8 (CH_2=), 123.4 (CH=), 124.2 (CH=), 127.5 (CH=), 142.1 (C), 145.7 (C)

S36. The crude product was purified on silica eluting with pentane/ethyl acetate (99:1). Pale-yellow liquid (0.9 g, 6.8 mmol, 65% Yield). ^{1}H-NMR (400 MHz, $CDCl_3$): δ = 1.17 (t, 3H, CH_3, ^3J = 7.6 Hz), 2.66 (q, 2H, CH_2, ^3J = 7.4 Hz) 5.29 (s, 1H, CH_2=), 5.77 (s, 1H, CH_2=), 7.17 (m, 1H, CH=), 7.47 (m, 1H, CH=), 7.66 (m, 1H, CH=), 8.61 (m, 1H, CH=) ppm.

S37. The crude product was purified on silica eluting with pentane/ethyl acetate (99:1). Pale-yellow liquid (1 g, 6.2 mmol, 59% Yield). ^{1}H-NMR (400 MHz, $CDCl_3$): δ = 1.21 (s, 9H, CH_3 ^{t}Bu), 5.00 (s, 1H, CH_2 =), 5.31 (s, 1H, CH_2 =), 7.17 (m, 2H, Ar), 7.62 (m, 1H, Ar), 8.58 (m, 1H, Ar) ppm. ^{13}C-NMR (100 MHz, $CDCl_3$): 30.1 (CH_3), 36.4 (C), 113.5 (CH_2=), 121.6 (CH=), 123.9 (CH=), 136.0 (CH=), 148.4 (CH=), 159.1 (C), 162.5 (C) ppm.

3.2.5.7. Preparation of S43

To a suspension of methyltriphenylphosphonium bromide (1.33 g, 3.72 mmol, 1.5 equiv.) in Et_2O (20 mL) under Ar was added potassium *t*-butoxide (0.39 g, 3.47 mmol, 1.4 equiv.) dropwise. The resulting orange solution was stirred at 0 °C for 30 minutes. A solution of 2,2,2-trifluoro-1-(4-methoxyphenyl)ethanone (0.51 g, 2.48 mmol, 1.00 equiv.) in Et_2O (10 mL) was added dropwise and the resulting yellow solution was left for 72 hours at room temperature. The reaction was quenched with water (10 mL), extracted with Et_2O and dried over $MgSO_4$. The crude product was purified on silica eluting with petroleum ether/ethylacetate (99:1) to obtain a colorless liquid (350 mg, 1.74 mmols, 70% yield). The characterization data is in agreement with the previously published.[32]

3.2.5.8. Typical procedure for the hydrogenation of olefins

The alkene (1 mmol) and Ir complex (0.2 mol%) were dissolved in CH_2Cl_2 (2 mL) in a high-pressure autoclave, which was purged four times with hydrogen. Then, it was pressurized at the desired pressure. After the desired reaction time, the autoclave was depressurized and the solvent evaporated off. The residue was dissolved in Et_2O (1.5 ml) and filtered through a short celite plug. The enantiomeric excess was determined by chiral GC or chiral HPLC and conversions were determined by ^{1}H NMR. The enantiomeric excesses of hydrogenated products were determined using the conditions previously described.[4d,4q,4s,13a,33]

(4-Methylpentan-2-yl)benzene. For characterization details see ref. 34. *Rt* (GC, Chiraldex β-DM, isotherm 75 °C, 100 Kpa H_2) = 17.3 min (*S*), 18.1 min (*R*).

2-(Hexan-2-yl)furan. ^{1}H-NMR: ^{1}H-NMR (400 MHz, $CDCl_3$): δ: 0.92 (t, 3H, CH_3, ^3J = 7.7 Hz), 1.32 (m, 7H, 2x CH_2 and CH_3), 1.63 (m, 2H, CH_2), 3.45 (m, 1H, CH), 6.98 (m, 1H, CH=), 7.15 (m, 1H, CH=), 7.28 (m, 1H, CH=). *Rt* (GC, Chiraldex β-DM, 50 °C for 30 min, 2 °C/min until 175 °C, 100 Kpa H_2) = 36.3 min (+), 37.2 min (-).

2-(Hexan-2-yl)thiophene. ^{1}H-NMR (400 MHz, $CDCl_3$): δ: 0.89 (t, 3H, CH_3, ^3J = 7.7 Hz), 1.31 (m, 7H, 2x CH_2 and CH_3), 1.62 (m, 2H, CH_2), 3.03 (m, 1H, CH), 6.83 (m, 1H, CH=), 6.94 (m, 1H, CH=), 7.14 (m, 1H, CH=). *Rt* (GC, Chiraldex β-DM, 50 °C for 30 min, 2 °C/min until 175 °C, 100 Kpa H_2) = 53.7 min (+), 54.2 min (-).

2-(Butan-2-yl)pyridine. For characterization details see ref. 35. *Rt* (GC, Chiral β-Dex, 50 °C for 60 min, 3 °C/min until 150 °C, 120 Kpa H_2) = 75.1 min (-), 75.4 min (+).

2-(3,3-Dimethylbutan-2-yl)pyridine. For characterization details see ref. 36. *Rt* (GC, Chiral β-Dex, 60 °C for 60 min, 3 °C/min until 150 °C, 120 Kpa H_2) = 63.5 min (-), 65.4 min (+).

1-(1-Phenylethyl)naphthalene. For characterization details see ref. 37. *Rt* (HPLC, Chiracel OD-H, hexane/2-propanol=98/2, 0.5 mL/min, 254 nm) = 11.0 min (+), 12.2 min (-).

1-Methyl-2-(1-phenylethyl)benzene. For characterization details see ref. 38. *Rt* (HPLC, Chiracel IB, hexane/2-propanol=99.8/0.2, 0.5 mL/min, 220 nm) = 8.9 min (+), 9.3 min (-).

1-Methoxy-4-{1-[4-(trifluoromethyl)phenyl]ethyl}benzene. ^{1}H-NMR (400 MHz, $CDCl_3$): δ: 1.62 (d, 3H, CH_3, ^3J = 7.2 Hz), 3.77 (s, 3H, CH_3-O), 4.28 (q, 1H, CH, ^3J = 7.2 Hz), 6.81 (m, 2H, CH=), 7.15 (m, 2H, CH=), 7.32 (m, 2H, CH=), 7.56 (m, 2H, CH). *Rt* (GC, Chiraldex β-DM, 50 °C for 30 min, 2 °C/min until 175 °C, 100 Kpa H_2) = 90.1 min (+), 90.4 min (-).

2-Phenylpropyl acetate. ^{1}H-NMR (400 MHz, $CDCl_3$): δ: 1.34 (d, 3H, CH_3, ^3J = 6.4 Hz), 2.00 (s, 3H, CH_3, OAc), 3.09 (m, 1H, CH), 4.17 (m, 2H, CH_2), 7.21 (m, 3H, CH=), 7.32 (m, 2H, CH=) ppm. For ee determination, the sample was hydrolyzed to the corresponding alcohol by adding 1 mL of methanol and 50 mg of LiOH.

1-Methoxy-4-(1,1,1-trifluoropropan-2-yl)benzene. ^{1}H-NMR (400 MHz, $CDCl_3$): δ: 1.42 (d, 3H, CH_3, ^3J = 7.2 Hz), 3.41 (q, 1H, CH, ^3J = 7.2 Hz), 3.74 (s, 3H, O-CH_3), 6.81 (m, 2H, CH=), 7.18 (m, 2H, CH=). *Rt* (GC, Chiraldex β-DM, 50 °C for 30 min, 2 °C/min until 175 °C, 100 Kpa H_2) = 9.2 min (-), 9.6 min (+).

3.2.6. Acknowledgements

We would like to thank the COST D40, the Spanish Government for providing grants Consolider Ingenio Intecat-CSD2006-0003, CTQ2010-15835, 2008PGIR/07 to O. Pàmies and 2008PGIR/08 to M. Diéguez, the Catalan Government for grant 2009SGR116, and the ICREA Foundation for providing M. Diéguez and O. Pàmies with financial support through the ICREA Academia awards.

3.2.7. References

[1] a) *Asymmetric Catalysis in Industrial Scale: Challenges, Approaches and Solutions*; Blaser, H. U., Schmidt, E., Eds.; Wiley: Weinheim, 2003. b) *Catalytic Asymmetric Synthesis*; Ojima, I., Ed.; Wiley-VCH: New York, 2000. c) Brown, J. M. in *Comprehensive Asymmetric Catalysis*; Jacobsen, E. N., Pfaltz, A., Yamamoto, H., Eds.; Springer-Verlag: Berlin:, 1999; Vol. I, pp 121-182. d) *Asymmetric Catalysis in Organic Synthesis*; Noyori, R., Ed.; Wiley: New York, 1994. e) *Applied Homogeneous Catalysis with Organometallic Compounds*, 2nd edition; Cornils, B., Herrmann, W. A., Eds.; Wiley-VCH: Weinheim, 2002.

[2] For recent reviews, see: a) Källström, K.; Munslow, I.; Andersson, P. G. *Chem. Eur. J.* **2006**, *12,* 3194. b) Roseblade, S. J.; Pfaltz, A. *Acc. Chem. Res.* **2007**, *40*, 1402. c) Church, T. L.; Andersson, P. G. *Coord. Chem. Rev.* **2008**, *252*, 513. d) Cui, X.; Burgess, K. *Chem. Rev.* **2005**, *105*, 3272. e) Pàmies, O.; Andersson, P.G.; Diéguez, M. *Chem. Eur. J.* **2010**, *16*, 14232.

[3] Chelating oxazoline-carbene ligands, mainly developed by Burgess and coworkers, have also been successful used and also to a less extent chiral diphosphines. See for instance: a) Perry, M. C.; Cui, X.; Powell, M. T.; Hou, D. R.; Reibenspies, J. H,.; Burgess, K. *J. Am. Chem. Soc.* **2003**, *125*, 113. b) Cui, X.; Burgess, K. *J. Am. Chem. Soc.* **2003**, *125*, 14212. c) Cui, X.; Ogle, J. W.; Burgess, K. *Chem. Commun.* **2005**, 672. d) Zhao, J.; Burgess, K. *J. Am. Chem. Soc.* **2009**, *131*, 13236. (e) Co, T. T.; Kim, T. J. *Chem. Commun.* **2006**, 3537. f) Forman, G. S.; Ohkuma, T.; Hems, W. P.; Noyori, R. *Tetrahedron Lett.* **2000**, *41*, 9471.

[4] See for instance: a) Perry, M. C.; Cui, X.; Powell, M. T.; Hou, D. –R.; Reibenspies, J. H.; Burgess, K. *J. Am. Chem. Soc.* **2003**, *125*, 5391. b) Blankestein, J.; Pfaltz, A. *Angew. Chem. Int. Ed.* **2001**, *40*, 4445. c) Kaiser, S.; Smidt, S.P.; Pfaltz, A. *Angew. Chem. Int. Ed.* **2006**, *45*, 5194. d) Källström, K.; Hedberg, C.; Brandt, P.; Bayer, P.; Andersson, P. G. *J. Am. Chem. Soc.* **2004**, *126*, 14308. e) Engman, M.; Diesen, J. S.; Paptchikhine, A.; Andersson, P. G. *J. Am. Chem. Soc.* **2007**, *129*, 4536. f) Trifonova, A.; Diesen, J. S.; Andersson, P. G. *Chem. Eur. J.* **2006**, *12*, 2318. g) Menges, G.; Pfaltz, A. *Adv. Synth. Catal.* **2002**, *334*, 4044. h) Drury III, W. J.; Zimmermann, N.; Keenan, M.; Hayashi, M.; Kaiser, S.; Goddard, R.; Pfaltz, A. *Angew. Chem. Int. Ed.* **2004**, *43*, 70. i) Hedberg, C.; Källström, K.; Brandt, P.; Hansen, L. K.; Andersson, P. G. *J. Am. Chem. Soc.* **2006**, *128*, 2995. j) Franzke, A.; Pfaltz A. *Chem. Eur. J.* **2011**, *17*, 4131. k) Tang, W.; Wang, W.; Zhang, X. *Angew. Chem. Int. Ed.* **2003**, *42*, 943. l) Hou, D. –R.; Reibenspies, J.; Colacot, T. J.; Burgess, K. *Chem. Eur. J.* **2001**, *7*, 5391. m) Cozzi, P. G.; Menges, F.; Kaiser, S. *Synlett* **2003**, 833. n) Lightfoot, A.; Schnider, P.; Pfaltz, A. *Angew. Chem. Int. Ed.* **1998**, *37*, 2897. o) Menges, F.; Neuburger, M.; Pfaltz, A. *Org. Lett.* **2002**, *4*, 4713. p) Liu, D.; Tang, W.; Zhang, X. *Org. Lett.* **2004**, *6*, 513. q) Lu, S.-M; Bolm, C. *Angew. Chem. Int. Ed.* **2008**, *47*, 8920. r) Lu, W.-J.; Chen, Y.-W.; Hou, X.-L. *Adv. Synth. Catal.* **2010**, *352*, 103. s) Paptchikhine, A.; Cheruku, P.; Engman, M.; Andersson, P. G. *Chem. Commun.* **2009**, 5996.

[5] For some representative examples see: a) Claver, C.; Diéguez, M.; Pàmies, O.; Castillón, S. in *Catalytic Carbonylation Reactions*; Beller, M. Ed.; Springer-Verlag: Berlin, 2006, pp 35-64. b) Diéguez, M.; Pàmies, O.; Ruiz, A.; Claver, C. in *Methodologies in Asymmetric Catalysis*; Malhotra, S. V. Ed.; ACS: Washington:, 2004, pp 161-174. c) Yan, M.; Zhou, Z.-Y.; Chan, A. S. C. *Chem. Commun*. **2000**, 115. d) Pàmies, O.; Diéguez, M.; Claver, C. *J. Am. Chem. Soc.* **2005**, *127*, 3646. e) Mata, Y.; Pàmies, O.; Diéguez, M. *Chem. Eur. J.* **2007**, *13*, 3296.

[6] See for instance: a) Reetz, M. T.; Neugebauer, T. *Angew. Chem. Int. Ed.* **1999**, *38*, 179. b) Diéguez, M.; Ruiz, A.; Claver, C. *Chem. Commun.* **2001**, 2702.

[7] Hilgraf, R.; Pfaltz, A. *Adv. Synth. Catal.* **2005**, *347*, 61.

[8] a) Mata, Y.; Pàmies, O.; Diéguez, M.; Claver, C. *Adv. Synth. Catal.* **2005**, *347*, 1943. b) Mata, Y.; Pàmies, O. Diéguez, M. *Chem. Eur. J.* **2007**, *13*, 3296. c) Mata, Y. Pàmies, O.; Diéguez, M. *Adv. Synth. Catal.* **2009**, *351*, 3217.

[9] Yonehara, K.; Jashizume, T.; Mori, K.; Ohe, K.; Uemura, S. *J. Org. Chem*. **1999**, *64*, 9374.

[10] The rapid ring inversions (tropoisomerization) in the biaryl phosphite moiety is usually stopped upon coordination to the metal center. See for example: a) Buisman, G. J. H.; van der Veen, L. A.; Klootwijk, A.; de Lange, W. G. J.; Kamer, P. C. J.; van Leeuwen, P. W. N. M.; Vogt, D. *Organometallics* **1997**, *16*, 2929. b) Diéguez, M.; Pàmies, O.; Ruiz, A.; Claver, C.; Castillón, S. *Chem. Eur. J.* **2001**, *7*, 3086. c) Pàmies, O.; Diéguez, M.; Net, G.; Ruiz, A.; Claver, C. *Organometallics* **2000**, *19*, 1488. d) Pàmies, O.; Diéguez, M.; Net, G.; Ruiz, A.; Claver, C. *J. Org. Chem.* **2001**, *66*, 8364. e) Pàmies, O.; Diéguez, M. *Chem. Eur. J.* **2008**, *14*, 944.

[11] (a) Rovner, E. S.; Wein, A. *J. Eur. Urol.* **2002**, *41*, 6. (b) Wefer, J.; Truss, M. C.; Jonas, U. *World J. Urol.* **2001**, *19*, 312. (c) Hills, C. J.; Winter, S. A.; Balfour, J. A. *Drugs* **1998**, *55*, 813. (d) McRae, A. L.; Brady, K. T. *Expert Opin. Pharmacother.* **2001**, *2*, 883.
[12] Tolstoy, P.; Engman, M.; Paptchikhine, A.; Bergquist, J.; Church, T. L.; Leung, A. W. –M.; Andersson, P. G. *J. Am. Chem. Soc.* **2009**, *131*, 8855.
[13] For successful application of Ir-catalysts, see: a) McIntyre, S.; Hörmann, E.; Menges, F.; Smidt, S. P.; Pfaltz, A. *Adv. Synth. Catal.* **2005**, *347*, 282. b) ref. 4b.
[14] For successful applications of Sm-, Ru- and Rh-complexes, see: a) Conticello, V. P.; Brard, L.; Giardello, M. A.; Tsuji, Y.; Sabat, M.; Stern, C. L.; Marks, T. J. *J. Am. Chem. Soc.* **1992**, *114*, 2761. b) Giardello, M. A.; Conticello, V. P.; Brard, L.; Gagné, M. R.; Marks, T. J. *J. Am. Chem. Soc.* **1994**, *116*, 10241. c) ref. 3e. d) ref. 3f.
[15] a) Fessard, T. C.; Andrews, S. P.; Motoyohsi, H.; Carreira, E. *Angew. Chem. Int. Ed.* **2007**, *46*, 9331. b) Prat, L.; Dupas, G.; Duflos, J.; Quéguiner, G.; Bourguignon, J.; Levacher, V. *Tetrahedron Lett.* **2001**, *42*, 4515. c) Wilkinson, J. A.; Rossington, S. B.; Ducki, S.; Leonard, J.; Hussain, N. *Tetrahedron* **2006**, *62*, 1833.
[16] a) Okamoto, K.; Nishibayashi, Y.; Uemura, S.; Toshimitsu, A. *Angew. Chem. Int. Ed.* **2005**, *44*, 3588. b) Hatanaka, Y.; Hiyama, T. *J. Am. Chem. Soc.* **1990**, *112*, 7793.
[17] See for instance: a) Abate, A.; Brenna, E. Fuganti, C.; Gatti, G. G.; Givenzana, T.; Malpezzi, L.; Serra, S. *J. Org. Chem.* **2005**, *70*, 1281. b) Drescher, K.; Haupt, A.; Unger, L.; Rutner, S. C.; Braje, W:; Grandel, R.; Henry, C.; Backfisch, G:; Beyerbach, A.; Bisch, W. *WO Patent* 2006/040182 A1.
[18] See for instance: a) Schlosser, M. *Angew. Chem. Int. Ed.* **1998**, *37*, 1496. b) Smart, B. E. *J. Fluorine Chem.* **2001**, *109*, 3. c) *Asymmetric Fluoroorganic Chemistry: Synthesis, Application and Future Directions;* Ramachandran, P. V., Ed.; American Chemical Society: Washington DC, 2000. d) A special issue has been devoted to "Fluorine in the Life Sciences" *ChemBioChem* **2004**, *5*, 559.
[19] See for instance: a) Fleming, I.; Barbero, A.; Walter, D. *Chem. Rev.* **1997**, *97*, 2063. b) Jones, G. R.; Landais, Y. *Tetrahedron* **1996**, *52*, 7599. c) Bains, W.; Tacke, R. *Curr. Opin. Drug Discv. Dev.* **2003**, *6*, 526.
[20] a) Feldgus, S.; Landis, C. R. *J. Am. Chem. Soc.* **2000**, *122,* 12714. b) Donoghue, P. J.; Helquist, P.; Norrby, P.-O.; Wiest, O. *J. Am. Chem. Soc.* **2009**, *131,* 410.
[21] a) Roseblade, S. J.; Pfaltz, A. *C. R. Chim.* **2007**, *10*, 178. b) Vazquez-Serrano, L. D.; Owens, B. T.; Buriak, J. M. *Chem. Commun.* **2002**, 2518.
[22] a) Cui, X.; Fan, Y.; Hall, M. B.; Burgess, K. *Chem. Eur. J.* **2005**, *11*, 6859. b) Fan, Y.; Cui, X.; Burgess, K.; Hall, M. B. *J. Am. Chem. Soc.* **2004**, *126*, 16688. c) Brandt, P.; Hedberg, C.; Andersson, P. G. *Chem. Eur. J.* **2003**, *9*, 339.
[23] Church, T.L.; Rasmussen, T.; Andersson, P.G. *Organometallics* **2010**, *29*, 6769.
[24] Very recently the group of Hopmann et al. has performed a computationally study using a phosphine-oxazoline (PHOX)-based iridium catalyst, which indicates that the hydrogenation of **S1** follows the 3/5-Meta pathway. See: Hopmann, K. H.; Bayer, A. *Organometallics* **2011**, *30*, 2483.
[25] Jaguar, version 7.0, Schrödinger, LLC, New York, NY, 2010. http://www.schrodinger.com/
[26] a) Becke, A. D. *J. Chem. Phys.* **1993**, *98*, 5648. b) Lee, C.; Yang, W.; Parr, R. G. *Phys. Rev.* B **1988**, *37*,785.
[27] Grimme, S.; Antony, J.; Ehrlich, S.; Krieg, H *J. Chem. Phys.* **2010**, 132, 154104.

[28] The rest of possible isomers generated from considering the hydride attack to the less substituted carbon of the olefin have not been considered, since it has been previously demonstrated that they proceed with higher energies. See ref. 4i.

[29] Buisman, G. J. H.; Kamer, P. C. J.; van Leeuwen, P. W. N. M. *Tetrahedron: Asymmetry* **1993**, *4*, 1625.

[30] Hay, P. J.; Wadt, W.R. *J. Chem. Phys.* **1985**, *82*, 299.

[31] a) Tannor, D. J.; Marten, B.; Murphy, R.; Friesner, R. A.; Sitkoff, D.; Nicholls, A.; Honig, B.; Ringnalda, M.; Goddard, W. A. *J. Am. Chem. Soc.* **1994**, *116,* 11875. b) Marten, B.; Kim, K.; Cortis, C.; Friesner, R. A.; Murphy, R. B.; Ringnalda, M. N.; Sitkoff, D.; Honig, B. *J. Phys. Chem.* **1996**, *100,* 11775.

[32] Koshy, K. M.; Roy, D.; Tidwell, T. T. *J. Am. Chem. Soc.* **1979**, *101*, 357

[33] a) Ohta, T.; Ikegami, H.; Miyake, T. Takaya, H. *J. Organomet. Chem.* **1995**, *502*, 169. b) Inagaki, K.; Ohta, T.; Nozaki, K.; Takaya, H. *J. Organomet. Chem.* **1997**, *531*, 159. c) Källström, K.; Munslow, I. J.; Hedberg, C.; Andersson, P. G. *Adv. Synth. Catal.* **2006**, *348*, 2575. d) Deerenberg, S.; Kamer, P. C. J.; van Leeuwen, P. W. N. M. *Organometallics* **2000**, *19*, 2065.

[34] Fraenkel, G.; Geckle, J. M. *J. Am. Chem. Soc.* **1980**, *102*, 2869.

[35] Guanti, G.; Narisano, E.; Riva, R. *Tetrahedron: Asymmetry* **1997**, *8*, 2175.

[36] Salvadori, P.; Rosini, C.; Bertucci, C.; Pini, D.; Marchetti, M. *J. Chem. Soc. Perkin Trans. 2*, **1983**, *3*, 399.

[37] Díaz Gómez, E.; Albert, D.; Mattiza, J.; Duddeck, H.; Chojnowsky, J.; Cypryk, M. *Tetrahedron: Asymmetry* **2006,** *17*, 1743.

[38] Miyai, T.; Onishi, Y.; Baba, A. *Tetrahedron* **1999**, *55*, 1017.

3.2.8. Supporting Information

Table 3.2.6. Ir-catalyzed asymmetric hydrogenation of trisubstituted olefins using ligands **L1**-**L5a**-**m**[a]

Entry	Ligand	Substrate	% Conv[b]	% ee[c]	Entry	Ligand	Substrate	% Conv[b]	% ee[c]
1	**L1c**	**S3**	100	91 (*R*)	20	**L4c**	**S6**	100	81 (*S*)
2	**L2c**	**S3**	98	92 (*R*)	21	**L5a**	**S6**	100	95 (*S*)
3	**L3c**	**S3**	40	97 (*R*)	22	**L5d**	**S6**	100	77 (*S*)
4	**L4c**	**S3**	100	98 (*R*)	23	**L5e**	**S6**	100	79 (S)
5	**L5c**	**S3**	100	98 (*R*)	24	**L1c**	**S7**	100	58 (S)
6	**L5d**	**S3**	100	96 (*R*)	25	**L3c**	**S7**	64	84 (*S*)
7	**L5e**	**S3**	100	99 (*R*)	26	**L5a**	**S7**	100	91 (*S*)
8	**L5k**	**S3**	100	98 (*R*)	27	**L5e**	**S7**	100	74 (*S*)
9	**L1c**	**S4**	100	93 (*R*)	28	**L1a**	**S8**	100	64 (S)
10	**L3c**	**S4**	67	98 (*R*)	29	**L3c**	**S8**	64	93 (*S*)
11	**L5c**	**S4**	100	97 (*R*)	30	**L5a**	**S8**	100	98 (*S*)
12	**L5e**	**S4**	100	99 (*R*)	31	**L5e**	**S8**	100	81 (*S*)
13	**L1c**	**S5**	100	92 (*R*)	32	**L1c**	**S9**	100	90 (-)
14	**L3c**	**S5**	71	97 (*R*)	33	**L4c**	**S9**	100	98 (-)
15	**L5c**	**S5**	100	98 (*R*)	34	**L5a**	**S9**	100	>99 (-)
16	**L5e**	**S5**	100	99 (*R*)	35	**L5e**	**S9**	100	98 (-)
17	**L1c**	**S6**	100	68 (*S*)	36	**L1c**	**S10**	100	79 (-)
18	**L2c**	**S6**	100	72 (*S*)	37	**L5a**	**S10**	100	98 (-)
19	**L3c**	**S6**	44	73 (*S*)	38	**L5e**	**S10**	100	91 (-)

[a] Reactions carried out by using 1 mmol of substrate and 1 mol% of Ir-catalyst precursor at 50 bar of H_2 using dichloromethane (2 mL) as solvent. [b] Conversion measured by ^{1}H-NMR after 2 h. [c] Enantiomeric excess determined by GC.

Table 3.2.7. Ir-catalyzed asymmetric hydrogenation of trisubstituted olefins bearing a neighboring polar group using ligands **L1**-**L5a**-**m**[a]

Entry	Ligand	Substrate	% Conv[b]	% ee[c]	Entry	Ligand	Substrate	% Conv[b]	% ee[c]
1	**L1c**	**S11**	100	94 (*R*)	26	**L1c**	**S18**	100	76 (*S*)
2	**L2c**	**S11**	56	92 (*R*)	27	**L2c**	**S18**	100	84 (*S*)
3	**L3c**	**S11**	22	97 (*R*)	28	**L3c**	**S18**	92	86 (*S*)
4	**L4c**	**S11**	100	98 (*R*)	29	**L4c**	**S18**	100	90 (*S*)
5	**L5c**	**S11**	84	98 (*R*)	30	**L5c**	**S18**	100	91 (*S*)
6	**L5d**	**S11**	78	97 (*R*)	31	**L5d**	**S18**	100	90 (*S*)
7	**L5e**	**S11**	85	99 (*R*)	32	**L5e**	**S18**	100	89 (*S*)
8	**L5e**	**S12**	100	98 (*R*)	33	**L5c**	**S19**	100	91 (*S*)
9	**L5e**	**S13**	100	97 (*R*)	34	**L5e**	**S19**	100	88 (*S*)
10	**L5e**	**S14**	100	99 (*R*)	35	**L5c**	**S20**	100	91 (*S*)
11	**L1c**	**S15**	100	53 (*R*)	36	**L5e**	**S20**	100	87 (*S*)
12	**L2c**	**S15**	100	88 (*R*)	37	**L5c**	**S21**	100	94 (*S*)
13	**L3c**	**S15**	100	97 (*R*)	38	**L5e**	**S21**	100	91 (*S*)
14	**L4c**	**S15**	100	76 (*R*)	39	**L5c**	**S22**	100	92 (*S*)
15	**L5c**	**S15**	100	95 (*R*)	40	**L5e**	**S22**	100	86 (*S*)
16	**L5e**	**S15**	100	97 (*R*)	41	**L5c**	**S23**	100	>99 (*R*)
17	**L1c**	**S16**	100	52 (*R*)	42	**L5e**	**S23**	100	94 (*R*)
18	**L2c**	**S16**	100	20 (*R*)	43	**L1c**	**S24**	100	62 (*R*)
19	**L3c**	**S16**	100	80 (*R*)	44	**L2c**	**S24**	100	67 (*R*)
20	**L4c**	**S16**	100	51 (*R*)	45	**L3c**	**S24**	100	43 (*R*)
21	**L5c**	**S16**	100	92 (*R*)	46	**L4c**	**S24**	100	88 (*R*)
22	**L5d**	**S16**	100	90 (*R*)	47	**L5c**	**S24**	100	93 (*R*)
23	**L5e**	**S16**	100	88 (*R*)	48	**L4c**	**S25**	100	90 (*R*)
24	**L5c**	**S17**	100	94 (*R*)	49	**L5c**	**S25**	100	92 (*R*)
25	**L5e**	**S17**	100	91 (*R*)					

[a] Reactions carried out by using 1 mmol of substrate and 1 mol% of Ir-catalyst precursor at 50 bar of H_2 using dichloromethane (2 mL) as solvent. [b] Conversion measured by ^{1}H-NMR after 2 h. [c] Enantiomeric excess determined by GC or HPLC.

Table 3.2.8. Ir-catalyzed asymmetric hydrogenation of 1,1-disubstituted olefins using ligands **L1**-**L5a**-**m**[a]

Entry	Ligand	Substrate	% Conv[b]	% ee[c]	Entry	Ligand	Substrate	% Conv[b]	% ee[c]
1	**L1c**	**S27**	100	72 (*S*)	26	**L5c**	**S32**	100	93 (*S*)
2	**L2c**	**S27**	100	84 (*S*)	27	**L5e**	**S32**	100	97 (*S*)
3	**L3c**	**S27**	100	86 (*S*)	28	**L1c**	**S33**	100	76 (*S*)
4	**L4c**	**S27**	100	82 (*S*)	29	**L2c**	**S33**	100	84 (*S*)
5	**L5c**	**S27**	100	89 (*S*)	30	**L3c**	**S33**	100	88 (*S*)
6	**L5d**	**S27**	100	89 (*S*)	31	**L4c**	**S33**	100	85 (*S*)
7	**L5e**	**S27**	100	90 (*S*)	32	**L5c**	**S33**	100	94 (*S*)
8	**L5j**	**S27**	100	45 (*S*)	33	**L5d**	**S33**	100	96 (*S*)
9	**L5k**	**S27**	100	89 (*S*)	34	**L5e**	**S33**	100	98 (*S*)
10	**L5c**	**S28**	100	90 (*S*)	35	**L5j**	**S33**	100	32 (*S*)
11	**L5e**	**S28**	100	93 (*S*)	36	**L5k**	**S33**	100	97 (*S*)
12	**L5c**	**S29**	100	89 (*S*)	37	**L5c**	**S34**	100	93 (*S*)
13	**L5e**	**S29**	100	93 (*S*)	38	**L5d**	**S34**	100	96 (*S*)
14	**L1c**	**S30**	100	51 (*S*)	39	**L5e**	**S34**	100	99 (*S*)
15	**L2c**	**S30**	100	45 (*S*)	40	**L5c**	**S35**	100	87 (-)
16	**L3c**	**S30**	100	62 (*S*)	41	**L5e**	**S35**	100	90 (-)
17	**L4c**	**S30**	100	49 (*S*)	42	**L5c**	**S36**	100	97 (+)
18	**L5c**	**S30**	100	78 (*S*)	43	**L5e**	**S36**	100	99 (+)
19	**L5d**	**S30**	100	82 (*S*)	44	**L5c**	**S37**	100	97 (+)
20	**L5e**	**S30**	100	83 (*S*)	45	**L5e**	**S37**	100	99 (+)
21	**L5j**	**S30**	100	38 (*S*)	46	**L5c**	**S38**	100	60 (+)
22	**L5k**	**S30**	100	80 (*S*)	47	**L5k**	**S38**	100	65 (+)
23	**L5c**	**S31**	100	79 (*S*)	48	**L5c**	**S39**	100	23 (+)
24	**L5e**	**S31**	100	84 (*S*)	49	**L5k**	**S39**	100	70 (+)
25	**L5k**	**S31**	100	81 (*S*)	50	**L5k**	**S40**	100	68 (+)

[a] Reactions carried out by using 1 mmol of substrate and 1 mol% of Ir-catalyst precursor at 50 bar of H_2 using dichloromethane (2 mL) as solvent. [b] Conversion measured by ^{1}H-NMR after 2 h. [c] Enantiomeric excess determined by GC or HPLC.

Table 3.2.9. Ir-catalyzed asymmetric hydrogenation of 1,1-disubstituted olefins bearing a neighboring polar group using ligands **L1**-**L5a**-**m**[a]

Entry	L	Substrate	% Conv[b]	% ee[c]	Entry	L	Substrate	% Conv[b]	% ee[c]
1	**L1c**	**S41**	100	37 (*R*)	11	**L5e**	**S43**	100	62 (-)
2	**L2c**	**S41**	100	34 (*R*)	12	**L5k**	**S43**	100	71 (-)
3	**L3c**	**S41**	100	32 (*R*)	13	**L1c**	**S44**	100	87 (*R*)
4	**L4c**	**S41**	100	65 (*R*)	14	**L2c**	**S44**	100	90 (*R*)
5	**L5c**	**S41**	100	70 (*R*)	15	**L3c**	**S44**	100	96 (*R*)
6	**L5d**	**S41**	100	64 (*R*)	16	**L4c**	**S44**	100	94 (*R*)
7	**L5e**	**S41**	100	40 (*R*)	17	**L5c**	**S44**	100	95 (*S*)
8	**L5c**	**S42**	100	69 (*R*)	18	**L5d**	**S44**	100	92 (*S*)
9	**L5d**	**S42**	100	63 (*R*)	19	**L5e**	**S44**	100	90 (*S*)
10	**L5e**	**S42**	100	47 (*R*)	20	**L5k**	**S44**	100	89 (*S*)

[a] Reactions carried out by using 1 mmol of substrate and 1 mol% of Ir-catalyst precursor at 50 bar of H_2 using dichloromethane (2 mL) as solvent. [b] Conversion measured by ^{1}H-NMR after 2 h. [c] Enantiomeric excess determined by GC.

3.3. Iridium phosphite-oxazoline catalysts derived from hydroxyl amino acids for the highly enantioselective hydrogenation of minimally functionalized alkenes

Javier Mazuela, Johan J. Verendel, Mercedes Coll, Benjamín Schäffner, Armin Börner, Pher G. Anderson, Oscar Pàmies and Montserrat Diéguez in *Chem. Commun.* **2008**, 3888 and *J. Am. Chem. Soc.* **2009**, *131*, 12344

3.3.1. Abstract

High enantioselectivities and activities are achieved in the Ir-catalyzed hydrogenation of several unfunctionalized olefins using modular biaryl phosphite-oxazoline ligands (**L6**-**L21a**-**i**) from hydroxyl amino acid derivatives; whereby the presence of a biaryl phosphite group is crucial in this success.

3.3.2. Introduction

The asymmetric hydrogenation of olefins has been widely used in stereoselective organic synthesis and some processes have found industrial applications. In this respect, the asymmetric hydrogenation of unfunctionalized olefins still represents a challenge class of substrates.[1] Iridium complexes with chiral P,N ligands have become established as efficient catalysts for the hydrogenation of unfunctionalized olefins, with complementary scope to Rh- and Ru-diphosphine complexes.[2] Unlike Rh- and Ru-catalysts, they do not require a coordinating polar group adjacent to the C=C group. The first chiral ligands developed for this process were the phosphine-oxazolines, which are chiral mimics of Crabtree's catalyst. These ligands have been successfully used for the asymmetric hydrogenation of a limited range of alkenes.[3] Recently, the composition of the ligands has been extended by the discovery of new mixed P,N ligands that have considerably broadened the scope of Ir-catalyzed hydrogenation.[4] Of them all, the most successful ligands contain a phosphinite moiety as P-donor group and either an oxazoline, oxazole or pyridine as N-donor group.[4b-d,g]

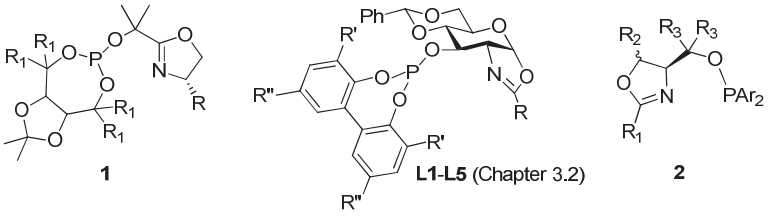

Figure 3.3.1. Phosphite-oxazoline ligands **1** and **L1-L5** and phosphinite-oxazoline ligands **2**.

In the last few years, phosphite-containing ligands have demonstrated that they are potentially extremely useful in many transition-metal catalyzed reactions.[5] Their highly modular construction, facile synthesis from readily available chiral alcohols, greater resistance to oxidation than phosphines and π-acceptor capacity have proved to be highly advantageous. Despite this, they have rarely been used in the Ir-catalyzed hydrogenation of olefins. So far, only two reports have

been published that use phosphite ligands.[6] One of these reports described the application of TADDOL-based phosphite-oxazoline ligands **1** (Figure 3.3.1).[6a] However, their substrate range was more limited and their enantioselectivities and activities were lower than those of their related phosphinite/phosphine-oxazoline ligands. They also required higher catalyst loadings (4 mol%) and higher pressures (100 bars) to achieve full conversions. The second report is the successful application of pyranoside phosphite-oxazoline ligands **L1-L5a-k** previously discussed in Chapter 3.2 (Figure 3.3.1).[6b-c] However it is unclear whether this success is due to the pyranoside-sugar backbone or the introduction of a biaryl-phosphite moiety.

To address this point, we took one of the most successful ligand families for this process (ligands **2**, Figure 3.3.1) and replaced the phosphinite moiety with a biaryl-phosphite group (**L6**-**L21a**-**i**; Figure 3.3.2). In this chapter we present the application of this phosphite-oxazoline ligand library (**L6**-**L21a**-**i**, Figure 3.3.2) in the asymmetric Ir-catalyzed hydrogenation of several unfunctionalized olefins.

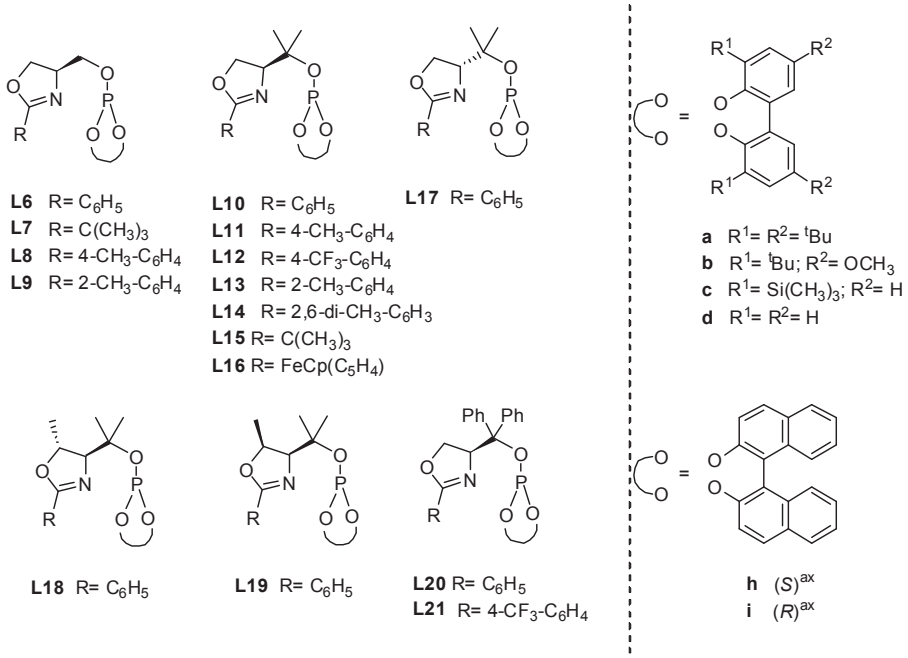

Figure 3.3.2. Phosphite-oxazoline ligand library **L1**-**L21a-i**

Another advantage of this ligand library design is its highly modular construction which enables a systematic study of the ligand parameters on catalytic performance. With this library, we investigated the effect of systematically varying the substituents in the oxazoline (R) moiety and in the alkyl backbone chain (H, **L6**-**L9**; Me, **L10**-**L16** and Ph, **L20**-**L21**). We also studied the configuration of the alkyl backbone chain (ligands **L10** and **L17**), the presence of a second stereogenic centre in the heterocycle ring and its configuration (ligands **L18** and **L19**) and the substituents and configurations in the biaryl phosphite moiety (**a**-**i**). By carefully selecting these elements, we achieved high enantioselectivities and activities in a wide range of minimally functionalized alkenes.

3.3.3. Results and discussions

3.3.3.1. Synthesis of the Ir-catalyst precursors

The catalyst precursors were made by refluxing a dichloromethane solution of the appropriate ligand (**L6**-**L21a**-**i**) in the presence of 0.5 equivalent of $[Ir(\mu\text{-}Cl)cod]_2$ for 2 h followed by counterion exchange with sodium tetrakis[3,5-bis(trifluoromethyl)-phenyl]borate ($NaBAr_F$) (1 equiv), in the presence of water (Scheme 3.3.1). All complexes were isolated as air-stable orange solids and were used without further purification.

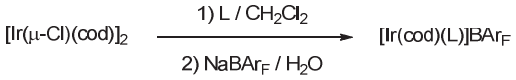

Scheme 3.3.1. Synthesis of iridium catalyst precursors $[Ir(cod)(L)]BAr_F$ (L= **L6**-**L21a**-**i**).

The complexes were characterized by elemental analysis and ^{1}H, ^{13}C, and ^{31}P NMR spectroscopy. The spectral assignments (see experimental section) were based on information from ^{1}H-^{1}H and ^{13}C-^{1}H correlation measurements and were as expected for these C_1 iridium complexes. The VT-NMR spectra indicate that only one isomer is present in solution. One singlet in the ^{31}P-{^{1}H} NMR spectra was obtained in all cases. We were able to obtain $[Ir(cod)(\mathbf{L11c})]BAr_F$ crystals that were suitable for X-ray analysis (Figure 3.3.3).[7] The crystal structure confirmed the expected boat conformation of the chelate ring. It also showed that the biphenyl-phosphite moiety adopts an *R*-configuration when coordinated to the iridium center.[8]

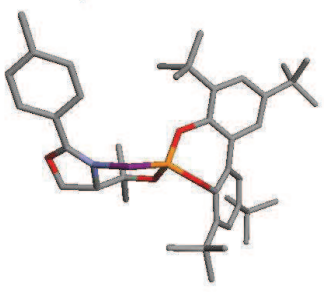

Figure 3.3.3. Structure of the [Ir(cod)(**L11a**)]BArF in the crystal (H atoms, BAr_F ion and cod ligand have been omitted for clarity).

3.3.3.2. Asymmetric hydrogenation of trisubstituted olefins

To make the initial evaluation of this new type of ligands (**L6**-**L21a**-**i**), we chose the Ir-catalyzed hydrogenation of *trans*-α-methylstilbene **S1** (Table 3.3.1). As this reaction was carried out with a wide variety of ligands carrying different donor groups, we were able to compare the efficacy of the various ligand systems.

The results (Table 3.3.1) indicate that enantioselectivity is affected by the substituents at the oxazoline and in the alkyl backbone chain, the presence of a second sterogenic center in the oxazoline ring and the substituents/configuration in the biaryl phosphite moiety. The best result (100% conversion; 99% ee) was therefore obtained with ligand **L6h** (entry 4), which contains the

optimal combination of ligand parameters. These results show the efficiency of using highly modular scaffolds in the ligand design.

We also performed the reaction at low catalyst loading (0.2 mol%) using ligand **L6h** (entry 11). The excellent enantioselectivity (99% (*R*) ee) and activity (100% conversion after 2 hours at room temperature) were maintained.

Table 3.3.1. Selected results for the Ir-catalyzed asymmetric hydrogenation of **S1** using ligands **L6**-**L21a**-**i**[a]

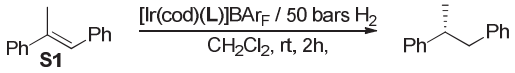

Entry	L	mol% Ir	% Conv.[b]	% ee[c]
1	**L6a**	2	100	97 (*R*)
2	**L6b**	2	100	94 (*R*)
3	**L6c**	2	100	98 (*R*)
4	**L6h**	2	100	99 (*R*)
5	**L6i**	2	100	94 (*R*)
6	**L11a**	2	100	95 (*R*)
7	**L12a**	2	100	90 (*R*)
8	**L18a**	2	100	92 (*R*)
9	**L8a**	2	100	91 (*R*)
10	**L21a**	2	80	81(*R*)
11	**L6h**	0.2	100	99 (*R*)

[a] Reactions carried out using 1 mmol of **S1**. [b] Conversion measured by ^{1}H-NMR. [c] Enantiomeric excesses determined by chiral HPLC.

The subsequent screening of other potential substrates showed that these catalysts also allow the asymmetric hydrogenation of several other trisubstituted unfunctionalized linear **S2**-**S4** and cyclic **S5** olefins, α,β-unsaturated ester **S6**, allylic alcohol **S7** and acetate **S8** (Figure 3.3.4).

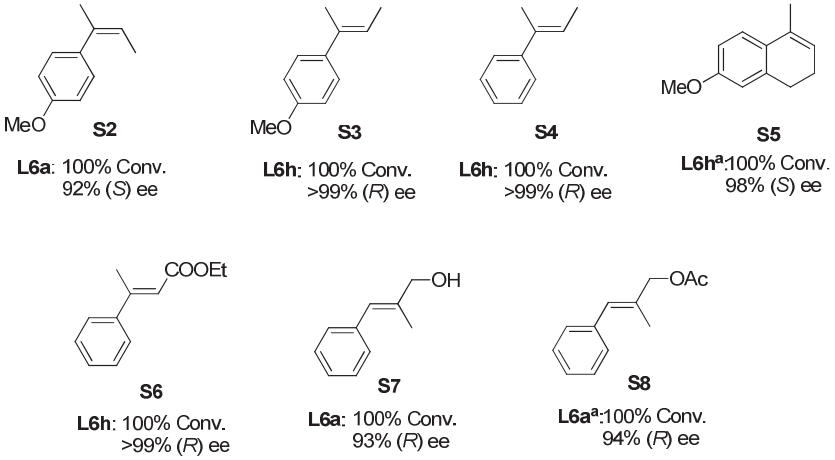

Figure 3.3.4. Selected hydrogenation results. Reactions conditions: 0.2 mol% catalyst, CH_2Cl_2 as solvent, 50 bar H_2, rt, 2 h. [a]1 mol% catalyst.

The enantioselectivities are among the best observed for these substrates.[2] It should be noted that if ligands are appropriately tuned, high enantioselectivities can also be obtained for the more demanding *Z*-isomer **S2**, which usually reacts with a lower enantioselectivity than that of the corresponding *E*-isomer **S3**. These phosphite-oxazolines also provided higher enantioselectivities in a wider range of trisubstituted substrates at lower catalyst loadings than their related phosphinite-oxazoline counterparts **2**, which are one of the most successful ligand class.[9]

3.3.3.3. Asymmetric hydrogenation of 1,1-aryl-alkyl terminal olefins

In the first set of experiments, we used the Ir-catalyzed hydrogenation of 2-phenylbut-1-ene **S9** to study the scope of ligands **L6**-**L21a**-**i**. The results are summarized in Table 3.3.2. The reaction proceeded smoothly at room temperature under 1 bar of H_2 at low catalyst loading (0.2 mol%). The results indicate that enantioselectivity is affected by the substituents at the oxazoline and in the alkyl backbone chain, the presence of a second sterogenic center in the oxazoline ring and the substituents/configuration in the biaryl phosphite moiety.

The effect of the substituents and the configuration at the alkyl backbone chain was studied with ligands **L6a**, **L10a**, **L17a** and **L20a** (Table 3.3.2, entries 1, 5, 17 and 20). Our results showed that introducing bulky substituents into the alkyl backbone chain has a positive effect on enantioselectivity (i.e. Ph > Me > H) and that the sense of enantioselectivity is governed by the absolute configuration of the alkyl backbone chain (Table 3.3.2, entries 5 *vs* 17). Both enantiomers of the hydrogenation product can therefore be accessed with high enantioselectivity by changing the absolute configuration of the alkyl backbone chain.

We studied the effect of the oxazoline substituent using ligands **L10**-**L16a** (Table 3.3.2, entries 5, 11-16). Our results showed that enantioselectivity is dependent on both the electronic and steric properties of the substituents in the oxazoline moiety. Therefore, either bulky or electron-withdrawing substituents in this position decreased enantioselectivities. Enantioselectivities were best with ligand **L10a**, which contains a phenyl-oxazoline group (Table 3.3.2, entry 5).

To study how a second stereogenic centre in the oxazoline and its configuration affect the catalytic performance, we also tested ligands **L18a** and **L19a** (Table 3.3.2, entries 18 and 19). The results show a cooperative effect between the configuration of this second stereocentre and the configuration of the alkyl backbone chain on enantioselectivity that results in a matched combination for ligand **L18a**, which contains an *R*-configuration at the second stereocentre and an *S*-configuration at the alkyl backbone chain (Table 3.3.2, entries 18 *vs* 19).

Finally, the effects of the biaryl phosphite moiety were studied using ligands **L10a-i** (Table 3.3.2, entries 5-10). The results indicated that enantioselectivity is mainly affected by the configuration of the biaryl phosphite moiety (Table 3.3.2, entries 9 and 10), while the substituents at both *ortho* and *para* positions of the biphenyl phosphite moiety has little effect on enantioselectivity (Table 3.3.2, entries 5-8). The best enantioselectivities were therefore obtained when an enantiopure *S*-binaphthyl phosphite moiety was present in the ligand (Table 3.3.2, entry 9). Moreover, comparing the results of using tropoisomerically flexible biphenyl phosphite based ligands (**a**-**d**) with enantiopure binaphthyl phosphite ligands (**h** and **i**), we can conclude that the biphenyl phosphite moiety in ligands **L10a-d** and **L11c** adopts an *R*-configuration upon complexation to the iridium.[8] This is in agreement with the configuration of the biphenyl phosphite moiety observed in the X-ray structure of the [Ir(cod)(**L11a**)]BAr_F (*vide supra*).

Table 3.3.2. Selected results for the Ir-catalyzed hydrogenation of **S9** using the ligand library **L6**-**L21a-i**[a]

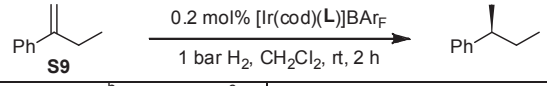

Entry	Ligand	% Conv[b]	% ee[c]	Entry	Ligand	% Conv[b]	% ee[c]
1	**L6a**	100	67 (*S*)	13	**L13a**	100	53 (*S*)
2	**L7a**	100	14 (*S*)	14	**L14a**	100	35 (*S*)
3	**L8a**	100	65 (*S*)	15	**L15a**	100	46 (*S*)
4	**L9a**	100	24 (*S*)	16	**L16a**	100	50 (*S*)
5	**L10a**	100	88 (*S*)	17	**L17a**	100	87 (*R*)
6	**L10b**	100	85 (*S*)	18	**L18a**	100	85 (*S*)
7	**L10c**	100	87 (*S*)	19	**L19a**	100	62 (*S*)
8	**L10d**	100	89 (*S*)	20	**L20a**	100	92 (*S*)
9	**L10h**	100	95 (*S*)	21	**L20a**	100	91 (*S*)
10	**L10i**	100	88 (*S*)	22	**L20h**	100	99 (*S*)
11	**L11a**	100	85 (*S*)	23	**L21a**	100	78 (*S*)
12	**L12a**	100	60 (*S*)				

[a] Reactions carried out using 1 mmol of **S1** and 0.2 mol% of Ir-catalyst precursor at 1 bar of H_2.[b] Conversion measured by ^{1}H-NMR after 2 hours. [c] Enantiomeric excesses determined by chiral GC.

In summary, phenyl substituents need to be present in the oxazoline and in the alkyl backbone chain and there must also be an enantiopure (*S*)-binaphthyl phosphite moiety if enantioselectivities are to be excellent. The best result (100 % conversion; 99% ee) was therefore obtained with ligand **L20h** (Table 3.3.2, entry 22), which contains the optimal combination of the ligand parameters. Moreover, both enantiomers of the hydrogenation product can be accessed in high enantioselectivity simply by changing the absolute configuration of the alkyl backbone chain. These results clearly show the efficiency of using highly modular scaffolds in the ligand design.

We then studied the asymmetric hydrogenation of other 1,1-disubstituted aryl-alkyl substrates (**S9**-**S18**) using the phosphite-oxazoline ligand library **L6**-**L21a-i**. The most noteworthy results are shown in Table 3.3.3. In general, they follow the same trends as for the hydrogenation of **S9**. Again, the catalyst precursor containing the phosphite-oxazoline ligand **L20h** provided the best enantioselectivities (ee's up to >99%).

Our results using several *para*-substituted 2-phenylbut-2-enes (**S9**-**S11**) indicated that enantioselectivity is relatively insensitive to the electronic effects in the aryl ring (Table 3.3.3, entries 1-4). However, the enantioselectivity (up to >99%) was highest with electron-rich alkene **S10** (Table 3.3.3, entry 3), and lowest (up to 96%) with the electron-deficient alkene **S11** (Table 3.3.3, entry 4). A similar trend was obtained using the previously published Ir/phosphinite-oxazoline (ee's up to 94% for **S10**)[6] and Ru/Me-Duphos (ee's up to 86% for **S10**)[10] catalysts.

Several α-alkylstyrenes bearing increasingly sterically demanding alkyl substituents (**S12**-**17**) were equally reactive and were hydrogenated with similar results using the Ir-**L20h** catalytic system (full conversion, 90-99% ee; Table 3.3.3, entries 5-12). This represents one the first catalysts able to hydrogenate **S12**-**S17** with high enantioselectivities.

Table 3.3.3. Selected results for the Ir-catalyzed hydrogenation of aryl-alkyl terminal olefins using the ligand library **L6-L21a-i**[a]

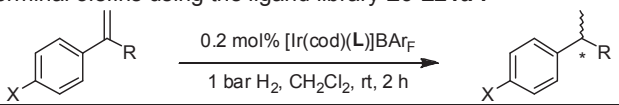

Entry	Substrate	Ligand	% Conv[b]	% ee[c]
1	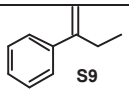 **S9**	**L20h**	100	99 (*S*)
2	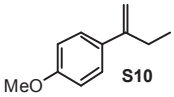 **S10**	**L10h**	100	97 (*S*)
3		**L20h**	100	>99 (*S*)
4	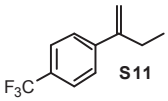 **S11**	**L20h**	100	96 (*S*)
5	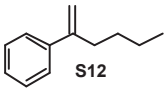 **S12**	**L20h**	100	94 (*S*)
6	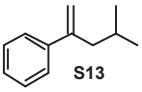 **S13**	**L20h**	100	93 (*S*)
7		**L20h**	100	93 (*S*)
8	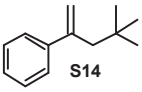 **S14**	**L20h**	100	90 (*S*)
9	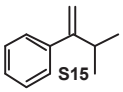 **S15**	**L10h**	100	88 (*S*)
10		**L20h**	100	97 (*S*)
11	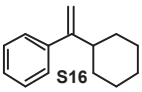 **S16**	**L20h**	100	97 (*S*)
12	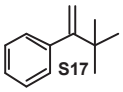 **S17**	**L20h**	100	>99 (*S*)
13	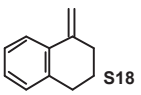 **S18**	**L20h**	100	25 (*R*)
14[d]		**L20h**	99[e]	87 (*R*)

[a] Reactions carried out using 1 mmol of substrate and 0.2 mol% of Ir-catalyst precursor at 1 bar of H_2. [b] Conversion measured by ^{1}H-NMR or GC. [c] Enantiomeric excesses determined by chiral GC. [d] Reaction carried out at 100 bar of H_2 and 1 mol% of catalyst precursor using PC as solvent at 40 °C for 10 hours. [e] 8% of non-hydrogenated isomerized trisubstituted olefin observed by ^{1}HNMR.

Under standard conditions, our catalyst systems were unable to hydrogenate 1-methylene-1,2,3,4-tetrahydronaphthalene **S18** with high enantioselectivities (Table 3.3.3, entry 13). This has been attributed to the fact that this olefin easily isomerizes to the trisubstituted internal olefin under reaction conditions. The hydrogenation of the trisubstituted olefin produces the opposite configuration of the hydrogenated product than when **S18** is hydrogenated, which results in low enantioselectivities.[11] Recently, Börner and coworkers discovered that the use of propylene carbonate (PC) as solvent reduces the isomerization considerably so **S18** can be hydrogenated in

high enantioselectivities (up to 85% ee).[11] Using this strategy we also managed to hydrogenate **S18** in high enantioselectivity (ee's up to 87%, Table 3.3.3, entry 14).

In conclusion, our Ir-phosphite-oxazoline catalytic system is highly tolerant to the steric and electronic properties of the α-alkylstyrene derivatives so enantioselectivities can be high in the asymmetric hydrogenation of this type of aryl-alkyl 1,1-disubsituted alkenes.

3.3.3.4. Asymmetric hydrogenation of 1,1-heteroaromatic-alkyl terminal olefins

We then applied this ligand library in the asymmetric hydrogenation of 1,1-heteroaromatic alkenes. This is interesting because heterocycles are used in industry and because the heterocyclic part can be modified post-hydrogenation. The results are summarized in Table 3.3.4. Again enantioselectivities were excellent under mild reaction conditions (ee's up to >99%). Even though it has been reported that the catalytic activity using Ir complexes with P,N ligands can be diminished in the presence of coordinating groups (or solvents),[2d,12] the heteroaromatic alkenes **S19**-**S22** were hydrogenated in 100% conversion using 1 bar of H_2. Hydrogenation of alkenes with thiophene **S20** and pyridyl **S21**-**S22** substituents followed the same trends as those observed for the previous substrates **S9**-**S17**. Therefore, enantioselectivities were best when ligand **L20h** was used (Table 3.3.4, entries 2-4). However, for furan-substituted substrate **S19** the enantioselectivity was best with ligand **L10a** (Table 3.3.4, entry 1). Once again, these results clearly show the efficiency of using highly modular scaffolds in the ligand design.

Table 3.3.4. Selected results for the Ir-catalyzed hydrogenation of heteroaryl-alkyl terminal olefins using the ligand library **L6-L21a-i**[a]

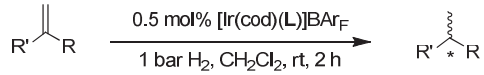

R' = 2-furan, 2-thiophene, 2-pyridine
R = alkyl

Entry	Substrate	Ligand	% Conv[b]	% ee[c]
1	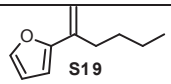 **S19**	**L10a**	100	99 (-)
2	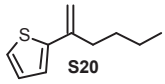 **S20**	**L20h**	100	96 (-)
3	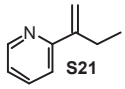 **S21**	**L20h**	100	99 (+)
4	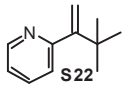 **S22**	**L20h**	100	>99 (+)

[a] Reactions carried out using 1 mmol of substrate and 0.5 mol% of Ir-catalyst precursor at 1 bar of H_2. [b] Conversion measured by ^{1}H-NMR. [c] Enantiomeric excesses determined by chiral HPLC.

3.3.3.5. Asymmetric hydrogenation of 1,1-diaryl terminal olefins

To further study the potential of this ligand library, we also screened **L6**-**L21a**-**i** in the Ir-catalyzed hydrogenation of 1,1-diaryl terminal olefins (**S23**-**S25**). Enantiopure diarylalkanes are important intermediates for the preparation of drugs and research materials.[13] To date optically active diarylalkanes can be prepared through some rather laborious approaches.[13,14] The asymmetric hydrogenation can provide a more efficient approach to prepare these compound. However, to our knowledge there is no successful enantioselective hydrogenation of this kind of substrates.

In a first set of experiments we examined the Ir-catalyzed asymmetric hydrogenation of diaryl alkenes **S23** and **S24**. In contrast to the previous aryl-alkyl substrates **S9**-**S22**, enantioselectivities are slightly better at higher pressures (i.e. using Ir/**L10a**; 26% ee at 1 bar and 30% ee at 50 bar). The enantioselectivity is also mainly affected by the substituents at the oxazoline and at the biaryl phosphite moieties, while the substituents in the alkyl backbone chain have little effect. Although high enantioselectivities (ee's up to 90%) can be obtained by replacing the bulky tetra *tert*-butyl substituted biphenyl phosphite moieties by less sterically demanding *S*-binaphtyl phosphite moieties (Table 3.3.5, entries 2, 4, 5 and 8 *vs* 3, 7 and 9), the enantiocontrol is highest (>99% ee) with bulky substituents on the oxazoline ring (ligand **L14a**, Table 3.3.5, entries 6 and 10).

Table 3.3.5. Selected results for the Ir-catalyzed hydrogenation of 1,1-diaryl terminal alkenes **S23**-**S25** using the ligand library **L6**-**L21a**-**i**[a]

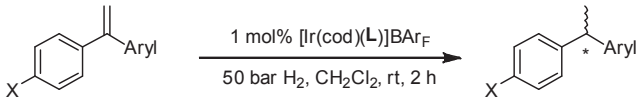

Entry	Substrate	Ligand	% Conv[b]	% ee[c]
1	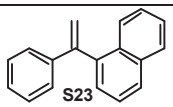	**L6a**	100	26 (+)
2		**L10a**	100	30 (+)
3		**L10h**	100	90 (+)
4		**L11a**	100	31 (+)
5		**L12a**	100	30 (+)
6		**L14a**	100	>99 (+)
7		**L20h**	100	90 (+)
8	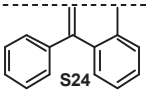	**L10a**	100	23 (+)
9		**L10h**	100	64 (+)
10		**L14a**	99	99 (+)
11	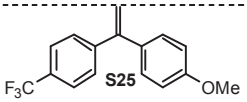	**L6a**	100	43 (+)
12		**L10a**	100	61 (+)
13		**L10h**	100	38 (+)
14		**L11a**	100	60 (+)
15		**L12c**	100	65 (+)
16		**L14a**	100	39 (+)
17		**L20a**	100	63 (+)

[a] Reactions carried out using 1 mmol of substrate and 1 mol% of Ir-catalyst precursor at 50 bar of H_2.
[b] Conversion measured by ^{1}H-NMR. [c] Enantiomeric excesses determined by chiral HPLC.

We also tested the Ir/phosphite-oxazoline catalytic systems in the asymmetric hydrogenation of **S25**. We anticipated that for this substrate enantiodiscrimination would be more difficult to control because it would be mainly due to the electronic differentiation of both phenyl substituents.[15] While the effect of the pressure dependence on enantioselectivity is similar to that observed for **S23** and **S24**, the effect of the ligand parameters on enantioselectivity is different. Therefore, the presence of bulky oxazoline substituents and/or the replacement of a bulky tetra *tert*-butyl-phenyl phosphite moiety by an *S*-binaphyl moiety has a negative effect on enantioselectivity (Table 3.3.5, entry 11 *vs* 13 and 16). Enantioselectivity is highest (ee's up to 65%) using ligand **L12c** (Table 3.3.5, entry 15).

3.3.3.6. Asymmetric hydrogenation of 1,1-disubstituted terminal olefins containing a neighboring polar group

Encouraged by the excellent results obtained up to this point, we examined the asymmetric hydrogenation of 1,1-disubstituted terminal olefins containing a polar neighboring group (**S26**-**S29**). The results are summarized in Table 3.3.6.

Table 3.3.6. Selected results for the Ir-catalyzed hydrogenation of 1,1-disubstituted terminal olefins containing a neighboring polar group using the ligand library **L6-L21a-i**[a]

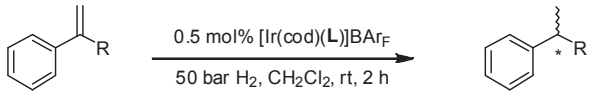

Entry	Substrate	Ligand	% Conv[b]	% ee[c]
1	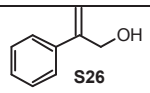 **S26**	**L20h**	100	95 (*R*)
2	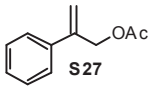 **S27**	**L20h**	100	91 (*R*)
3	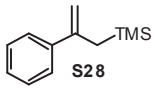 **S28**	**L20h**	100	96 (*S*)
4	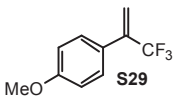 **S29**	**L20h**	100	75 (-)

[a] Reactions carried out using 1 mmol of substrate and 0.5 mol% of Ir-catalyst precursor at 50 bar of H_2. [b] Conversion measured by ^{1}H-NMR. [c] Enantiomeric excesses determined by chiral GC.

We initially tested the ligand library in the hydrogenation of the allylic alcohol **S26**. Derivatives of the hydrogenation product 2-phenylpropanol are frequently used as components of fragrance mixtures (i.e. commercial odorants Muguesia and Pamplefleur) and also as intermediates for the synthesis of natural products and drugs (i.e. modulators of dopamine D3 receptors).[16] Complex Ir-**L20h** proved to be the most selective catalyst, giving 95% ee at room temperature (Table 3.3.6, entry 1). This result competes favorably with the results obtained using related phosphinite-

oxazoline ligands.[6b] In addition, the enantioselectivities and activities obtained are higher than those reported in the asymmetric Zr-catalyzed methylalumination of α-olefins[17] and the lipase-mediated kinetic resolution of racemic 2-phenyl propanol.[16a] Similarly, the hydrogenation of the allylic acetate **S27** also proceeds with high activity and enantioselectivity with the catalyst system Ir-**L20h** (Table 3.3.6, entry 2).

We next screened ligands **L6**-**L21a**-**i** in the asymmetric hydrogenation of the allylic silane **S28** and the trifluoromethyl olefin **S29**. The hydrogenation of these compounds gave rise to important organic intermediates and a number of innovative new organosilicon[18] and organofluorine[19] drugs are being developed. The enantioselectivities (96% ee for **S28** and 75% ee for **S29**) were best with ligand **L20h** (Table 3.3.6, entries 3 and 4).

3.3.3.7. Recycling experiments

Encouraged by the excellent results obtained, we decided to go one step further and to study the recycling of our catalyst systems. For a practical application, catalyst recycling is an extremely important topic because of the very high price of iridium. Recently, propylene carbonate (PC) has emerged as an environmentally friendly alternative to standard organic solvents that allow catalyst to be repeatedly recycled by a simple two phase extraction with an apolar solvent.[11] For this purpose, substrates **S17**, **S22** and **S23** were hydrogenated in PC with the catalyst precursor [Ir(cod)(**L20h**)]BAr_F (substrates **S17** and **S22**) and [Ir(cod)(**L14a**)]BAr_F (substrate **S23**) and the products were removed by extraction with hexane (Table 3.3.7). Catalysts can be used up to five times with no significant losses in enantioselectivity, although the reaction time increased. This is probably due to the iridium catalyst partially passing into the hexane phase.[11]

Table 3.3.7. Recycling experiments with the catalyst [Ir(cod)(**L**)]BAr_F and **S17**, **S22** and **S23** as substrates in PC[a]

Cycle	Substrate	Ligand	% Conv (h)[b]	% ee[c]
1	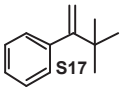	**L20h**	98 (4)	99 (S)
2			98 (4)	99 (S)
3			94 (6)	98 (S)
4			95 (10)	97 (S)
5			82 (12)	97 (S)
1[d]	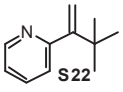	**L20h**	98 (12)	99 (+)
2[d]			94 (12)	99 (+)
3[d]			84 (18)	97 (+)
1[d]	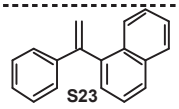	**L14a**	100 (12)	99 (+)
2[d]			95 (15)	99 (+)
3[d]			93 (24)	99 (+)

[a] Reactions carried out using 1 mmol of substrate and 1 mol% of Ir-catalyst precursor at 50 bar of H_2. [b] Conversion measured by ^{1}H-NMR. [c] Enantiomeric excesses determined by chiral GC. [d] Reaction carried out at 100 bar and 40 °C.

3.3.4. Conclusions

A library of readily available phosphite-oxazoline ligands (**L6**-**L21a**-**i**) has been applied in the Ir-catalyzed asymmetric hydrogenation of several *E*- and *Z*-trisubstituted and 1,1,-disubstituted terminal minimally functionalized alkenes. We found that their effectiveness at transferring the chiral information in the product can be tuned by correctly choosing the ligand components. Enantioselectivities were therefore excellent (ee's up to >99%) in a wide range of substrates. These Ir-phosphite-oxazoline catalytic systems, then, compete favorably in terms of enantioselectivity and, more important, in terms of substrate versatility with a few other ligand series that also have provided high ee's for a limited range of substrates. Of particular note are the unprecedented excellent enantioselectivities (ee's up to > 99%) obtained with 1,1-diaryl substrates. It should be noted that these catalytic systems also have high tolerance to the presence of a neighboring polar group and therefore several allylic alcohols, acetates and silanes can be hydrogenated in high enantioselectivities (ee's up to 96%). The asymmetric hydrogenations were also performed using propylene carbonate as solvent, which allowed the Ir-catalyst to be reused and maintained the excellent enantioselectivities. These results open up a new class of Ir-catalysts for the highly enantioselective Ir-catalyzed hydrogenation of minimally functionalized 1,1-disubstituted terminal alkenes, which is of great practical interest.

3.3.5. Experimental section

3.3.5.1. General considerations

All reactions were carried out using standard Schlenk techniques under an atmosphere of argon. Solvents were purified and dried by standard procedures. Phosphite-oxazoline ligands **L6**-**L21** were prepared as previously described.[20] ^{1}H, ^{13}C-{^{1}H}, and ^{31}P-{^{1}H} NMR spectra were recorded using a 400 MHz spectrometer. Chemical shifts are relative to that of $SiMe_4$ (^{1}H and ^{13}C) as internal standard or H_3PO_4 (^{31}P) as external standard. ^{1}H and ^{13}C assignments were made on the basis of ^{1}H-^{1}H gCOSY and ^{1}H-^{13}C gHSQC experiments.

3.3.5.2 Typical procedure for the preparation of [Ir(cod)(L)]BAr$_F$

The corresponding ligand (0.074 mmol) was dissolved in CH_2Cl_2 (2 mL) and $[Ir(COD)Cl]_2$ (25 mg, 0.037 mmol) was added. The reaction was refluxed at 50 °C for 1 hour. After 5 min at room temperature, $NaBAr_F$ (77.1 mg, 0.082 mmol) and water (2 mL) were added and the reaction mixture was stirred vigorously for 30 min at room temperature. The phases were separated and the aqueous phase was extracted twice with CH_2Cl_2. The combined organic phases were filtered through a celite plug, dried with $MgSO_4$ and the solvent was evaporated to give the product as an orange solid.

[Ir(cod)(L6a)]BAr$_F$. Yield: 125 mg (95%). ^{31}P NMR ($CDCl_3$), δ: 103.6 (s). ^{1}H NMR ($CDCl_3$), δ: 1.36 (s, 9H, CH_3, ^{t}Bu), 1.38 (s, 9H, CH_3, ^{t}Bu), 1.57 (b, 18H, CH_3, ^{t}Bu), 1.71 (b, 4H, CH_2, cod), 2.33 (m, 3H, CH_2, cod), 2.54 (b, 1H, CH_2, cod), 3.74 (m, 1H, CH=, cod), 4.12 (m, 2H, CH_2-OP), 4.21 (m, 2H, CH_2), 4.24 (b, 1H, CH= cod), 4.66 (m, 1H, CH), 4.84 (b, 1H, CH= cod), 5.45 (b, 1H, CH= cod), 7.1 – 8.5 (m, 21H, aromatics). ^{13}C NMR ($CDCl_3$), δ: 24.8 (b, CH_2, cod), 28.8 (b, CH_2, cod), 31.3 (CH_3, ^{t}Bu), 31.4 (CH_3, ^{t}Bu), 31.6 (b, CH_3, ^{t}Bu), 33.7 (b, CH_2, cod), 34.9 (C, *t*Bu), 35.1 (C, ^{t}Bu),

35.5 (C, ^{t}Bu), 36.0 (C, ^{t}Bu), 37.3 (b, CH_2, cod), 67.1 (CH=, cod), 68.7 (CH), 69.8 (b, CH_2-O and CH_2-OP), 70.2 (CH=, cod), 94.6 (d, CH=, cod, $J_{C\text{-}P}$= 22.2 Hz), 106.1 (d, CH=, cod, $J_{C\text{-}P}$= 12.2 Hz), 117.7 (b, CH=, BAr_F), 119-134 (aromatic carbons), 135.0 (b, CH=, BAr_F), 136-149 (aromatic carbons), 161.9 (q, C-B, BAr_F, $^{1}J_{C\text{-}B}$= 49.6 Hz), 171.5 (C=N). Anal. Calc (%) for $C_{78}H_{74}BF_{24}IrNO_4P$: C 52.65, H 4.19, N 0.79; found: C 52.62, H 4.22, N 0.83.

[Ir(cod)(L7a)]BAr$_F$. Yield: 118 mg (91%). ^{31}P NMR ($CDCl_3$), δ: 106.1 (s). ^{1}H NMR ($CDCl_3$), δ: 1.35 (s, 9H, CH_3, ^{t}Bu), 1.37 (s, 9H, CH_3, ^{t}Bu), 1.53 (s, 9H, CH_3, ^{t}Bu), 1.55 (b, 18H, CH_3, ^{t}Bu), 1.65 (b, 2H, CH_2, cod), 1.76 (b, 2H, CH_2, cod), 2.07 (m, 1H, CH_2, cod), 2.22 (m, 1H, CH_2, cod), 2.38 (m, 1H, CH_2, cod), 2.51 (m, 1H, CH_2, cod), 3.87 (m, 1H, CH=, cod), 4.08 (m, 3H, CH_2-OP and CH_2-O), 4.32 (b, 1H, CH), 4.48 (b, 1H, CH= cod), 4.73 (b, 2H, CH= cod and CH_2-O), 5.47 (b, 1H, CH= cod), 7.1 – 8.5 (m, 16H, aromatics). ^{13}C NMR ($CDCl_3$), δ: 24.4 (b, CH_2, cod), 28.4 (b, CH_2, cod), 29.2 (CH_3, ^{t}Bu), 31.2 (CH_3, ^{t}Bu), 31.4 (CH_3, ^{t}Bu), 31.5 (CH_3, ^{t}Bu), 31.6 (CH_3, ^{t}Bu), 34.5 (C, ^{t}Bu), 34.8 (b, CH_2, cod), 34.9 (C, *t* ^{t}Bu u), 35.0 (C, ^{t}Bu), 35.4 (C, ^{t}Bu), 36.0 (C, ^{t}Bu), 37.4 (b, CH_2, cod), 67.7 (b, CH=, cod), 69.2 (CH), 69.9 (CH_2-O), 70.0 (CH_2-OP), 70.6 (CH=, cod), 90.5 (d, CH=, cod, $J_{C\text{-}P}$= 26.2 Hz), 103.2 (d, CH=, cod, $J_{C\text{-}P}$= 10.5 Hz), 117.7 (b, CH=, BAr_F), 119-134 (aromatic carbons), 135.0 (b, CH=, BAr_F), 136-149 (aromatic carbons), 161.9 (q, C-B, BAr_F, $^{1}J_{C\text{-}B}$= 49.5 Hz), 182.8 (C=N). Anal. Calc (%) for $C_{76}H_{78}BF_{24}IrNO_4P$: C 51.88, H 4.47, N 0.80; found: C 51.93, H 4.52, N 0.77.

[Ir(cod)(L8a)]BAr$_F$. Yield 120 mg (91 %). ^{31}P NMR ($CDCl_3$), δ: 103.3 (s). ^{1}H NMR ($CDCl_3$), δ: 1.36 (s, 9H, CH_3, ^{t}Bu), 1.37 (s, 9H, CH_3, ^{t}Bu), 1.55 (s, 9H, CH_3, ^{t}Bu), 1.56 (s, 9H, CH_3, ^{t}Bu), 1.75 (b, 4H, CH_2, cod), 2.30 (m, 3H, CH_2, cod), 2.40 (m, 1H, cod), 2.52 (s, 3H, CH_3), 3.79 (m, 1H, CH=, cod), 4.10 (m, 1H, CH_2-OP), 4.20 (m, 2H, CH_2-OP and CH_2) 4.40 (b, 1H, CH=, cod), 4.63 (m, 1H, CH_2), 4.68 (b, 1H, CH=, cod), 4.81 (m, 1H, CH), 5.45 (b, 1H, CH=, cod) 7.1-8.6 (m, 20H, CH= aromatics). ^{13}C NMR ($CDCl_3$), δ: 24.8 (b, CH_2, cod), 28.8 (b, CH_2, cod), 31.2 (s, CH_3, ^{t}Bu), 31.4 (s, CH_3, ^{t}Bu), 31.5 (s, CH_3, ^{t}Bu), 31.6 (s, CH_3, ^{t}Bu), 33.7 (b, CH_2, cod), 34.9 (s, C, ^{t}Bu), 35.0 (s, C, ^{t}Bu), 35.4 (s, C, ^{t}Bu), 36.0 (s, CH_3), 37.2 (d, CH_2, cod, $J_{C\text{-}P}$ = 6.9 Hz), 66.9 (s, CH), 68.5 (s, CH=, cod), 69.5 (s, CH_2), 69.6 (s, CH=, cod), 70.2 (s, CH_2-OP), 94.2 (d, CH=, cod, $J_{C\text{-}P}$ = 22 Hz), 106.5 (d, CH=, cod, $J_{C\text{-}P}$ = 12.1 Hz), 117.7 (b, CH=, BAr_F), 119-132 (aromatic carbons), 135.0 (b, CH=, BAr_F), 138-150 (aromatic carbons), 161.9 (q, C-B, BAr_F, $^{1}J_{C\text{-}B}$ = 49.3 Hz), 171.3 (s, C=N). Anal. calc (%) for $C_{79}H_{76}BF_{24}IrNO_4P$: C 52.91, H 4.27, N 0.78; found: C 53.07, H 4.32, N 0.82.

[Ir(cod)(L9a)]BAr$_F$. Yield: 122 mg (92%). ^{31}P NMR ($CDCl_3$), δ: 102.0 (s). ^{1}H NMR ($CDCl_3$), δ: 1.37 (s, 9H, CH_3, ^{t}Bu), 1.38 (s, 9H, CH_3, ^{t}Bu), 1.55 (s, 9H, CH_3, ^{t}Bu), 1,61 (b, 4H, CH_2, cod) 1.72 (s, 9H, CH_3, ^{t}Bu), 2.17 (m, 3H, CH_2, cod), 2.33 (b, 1H, CH_2, cod), 2.36 (s, 3H, CH_3-Ph), 3.47 (m, 1H, CH=, cod), 4.26 (b, 5H, CH-N, CH_2-O, CH_2-OP and CH= cod), 4.83 (b, 2H, CH_2-O and CH= cod), 5.27 (b, 1H, CH= cod), 7.1 – 8.3 (m, 20H, aromatics). ^{13}C NMR ($CDCl_3$), δ: 25.6 (b, CH_2, cod), 29.3 (b, CH_2, cod), 31.3 (CH_3, ^{t}Bu), 31.5 (CH_3, ^{t}Bu), 31.6 (b, CH_3, ^{t}Bu), 32.4 (b, CH_2, cod), 34.9 (C, ^{t}Bu), 35.0 (C, ^{t}Bu), 35.5 (b, CH_2, cod), 36.0 (C, ^{t}Bu), 36.1 (CH_3-Ph), 36.2 (C, ^{t}Bu), 65.1 (CH), 66.0 (CH=, cod), 69.0 (CH_2-O), 72.2 (CH=, cod), 70.7 (CH_2-OP), 99.0 (d, CH=, cod, $J_{C\text{-}P}$= 20.2 Hz), 106.8 (d, CH=, cod, $J_{C\text{-}P}$= 13.7 Hz), 117.7 (b, CH=, BAr_F), 119-134 (aromatic carbons), 135.0 (b, CH=, BAr_F), 136-149 (aromatic carbons), 161.9 (q, C-B, BAr_F, $^{1}J_{C\text{-}B}$= 49.5 Hz), 174.4 (C=N). Anal. Calc (%) for $C_{79}H_{76}BF_{24}IrNO_4P$: C 52.91, H 4.27, N 0.78; found: C 52.33, H 4.20, N 0.75.

[Ir(cod)(L10d)]BAr$_F$. Yield: 109 mg (93%). ^{31}P NMR ($CDCl_3$), δ: 102.4 (s). ^{1}H NMR ($CDCl_3$), δ: 1.29 (s, 3H, CH_3), 1.36 (s, 3H, CH_3), 1.67 (m, 3H, CH_2, cod), 2.22 (m, 2H, CH_2, cod), 2.40 (m, 3H, CH_2, cod), 3.58 (m, 1H, CH=, cod), 3.94 (b, 1H, CH=, cod), 4.58 (dd, 1H, CH_2, $^2J_{H-H}$= 10.2 Hz, $^3J_{H-H}$= 3 Hz), 4.73 (t, 1H, CH_2, $^2J_{H-H}$= 9 Hz), 4.90 (dd, 1H, CH, $^3J_{H-H}$= 8.7 Hz, $^3J_{H-H}$= 2.4 Hz), 5.00 (b, 1H, CH= cod), 5.42 (b, 1H, CH= cod), 7.1 – 7.8 (m, 25H, aromatics). ^{13}C NMR ($CDCl_3$), δ: 20.9 (CH_3), 25.4 (b, CH_2, cod), 27.0 (CH_3), 29.3 (b, CH_2, cod), 32.1 (b, CH_2, cod), 36.9 (b, CH_2, cod), 66.1 (CH=, cod), 68.0 (CH=, cod), 70.6 (CH_2), 73.6 (CH), 86.0 (d, CMe_2, J_{C-P}= 6.5 Hz), 100.4 (d, CH=, cod, J_{C-P}= 18.7 Hz), 108.8 (d, CH=, cod, J_{C-P}= 14.0 Hz), 117.7 (b, CH=, BAr$_F$), 119-132 (aromatic carbons), 135.0 (b, CH=, BAr$_F$), 136-150 (aromatic carbons), 161.9 (q, C-B, BAr$_F$, $^1J_{C-B}$= 49.5 Hz), 172.6 (C=N). Anal. Calc (%) for $C_{64}H_{46}BF_{24}IrNO_4P$: C 48.56, H 2.93, N 0.88; found: C 48.63, H 2.98, N 0.90.

[Ir(cod)(L10a)]BAr$_F$. Yield 123 mg (92 %). ^{31}P NMR ($CDCl_3$), δ: 97.8 (s). ^{1}H NMR ($CDCl_3$), δ: 1.06 (s, 3H, CH_3), 1.29 (s, 3H, CH_3), 1.35 (s, 9H, CH_3, ^{t}Bu), 1.38 (s, 9H, CH_3, ^{t}Bu), 1.55 (s, 9H, CH_3, ^{t}Bu), 1.61 (s, 9H, CH_3, ^{t}Bu), 1.69 (m, 4H, CH_2, cod), 2.32 (m, 3H, CH_2, cod), 2.52 (m, 1H, CH_2, cod), 3.62 (b, 1H, CH= cod), 4.39 (m, 2H, CH= cod and CH_2), 4.58 (b, 2H, CH= cod and CH_2), 4.67 (dd, 1H, CH, $^3J_{H-H}$= 10. 0 Hz, $^3J_{H-H}$= 3.2 Hz), 5.32 (b, 1H, CH=, cod), 7.1-8.5 (m, 21H, CH= aromatics). ^{13}C NMR ($CDCl_3$), δ: 21.3 (s,CH_3), 24.8 (b, CH_2, cod), 26.5 (m, CH_3), 28.09 (b, CH_2, cod), 31.2 (s, CH_3, ^{t}Bu), 31.4 (s, CH_3, ^{t}Bu), 31.6 (s, CH_3, ^{t}Bu), 33.2 (b, CH_2, cod), 34.8 (s, C, ^{t}Bu), 34.9 (s, C, ^{t}Bu), 35.2 (s, C, ^{t}Bu), 37.3 (b, CH_2, cod), 66.3 (s, CH=, cod), 69.8 (s, CH=, cod), 70.0 (s, CH_2), 71.2 (s, CH), 84.9 (d, CMe_2, J_{C-P}= 5.2 Hz), 93.5 (d, CH=, cod, J_{C-P} = 21.1 Hz), 106.3 (d, CH=, cod, J_{C-P} = 6.2 Hz), 117.7 (b, CH=, BAr$_F$), 119-132 (aromatic carbons), 135.0 (b, CH=, BAr$_F$), 135.5-150 (aromatic carbons), 161.9 (q, C-B, BAr$_F$, $^1J_{C-B}$ = 48.6 Hz), 173.7 (s, C=N). Anal. calc (%) for $C_{80}H_{78}BF_{24}IrNO_4P$: C 53.16, H 4.35, N 0.77; found: C 53.63, H 4.41, N 0.74.

[Ir(cod)(L10b)]BAr$_F$. Yield 115mg (89 %). ^{31}P NMR ($CDCl_3$), δ: 99.0 (s). ^{1}H NMR ($CDCl_3$), δ: 1.19 (s, 3H, CH_3), 1.34 (s, 3H, CH_3), 1.54 (s, 9H, CH_3, ^{t}Bu), 1.61 (s, 9H, CH_3, ^{t}Bu), 1.67 (m, 4H, CH_2, cod), 2.18 (m, 1H, CH_2, cod), 2.25 (m 1H, CH_2, cod), 2.37 (m, 1H, CH_2, cod), 2.55 (dd, 1H, cod, $^2J_{H-H}$ = 15.2 Hz, $^3J_{H-H}$ = 6.4 Hz), 3.65 (m, 1H, CH=, cod), 3.84 (s, 3H, CH_3-O), 3.86 (s, 3H, CH_3-O), 4.40 (b, 1H, CH=, cod), 4.45 (dd, 1H, CH_2, $^2J_{H-H}$ = 10 Hz, $^3J_{H-H}$ = 3.6 Hz), 4.57 (b, 1H, CH=, cod), 4.63 (m, 1H, CH_2), 4.72 (dd, 1H, CH, $^3J_{H-H}$ = 9.2 Hz, $^3J_{H-H}$ = 2.8 Hz), 5.37 (b, 1H, CH=, cod) 6.6-8.5 (m, 21H, CH= aromatic). ^{13}C NMR ($CDCl_3$), δ: 21.5 (s, CH_3), 24.7 (b, CH_2, cod), 26.6 (d, CH_3, J_{C-P} = 6.9 Hz), 28.8 (b, CH_2, cod), 31.2 (s, CH_3, ^{t}Bu), 31.3 (s, CH_3, ^{t}Bu), 33.6 (b, CH_2, cod), 35.4 (s, C, ^{t}Bu), 35.7 (s, C, ^{t}Bu), 37.2 (d, CH_2, cod, J_{C-P} = 6.9 Hz), 55.8 (s, CH_3-O), 68.3 (s, CH=, cod), 69.8 (s, CH_2), 70.6 (s, CH=, cod), 74.0 (s, CH), 84.9 (d, CMe_2, J_{C-P} = 5.3 Hz), 94.6 (d, CH=, cod, J_{C-P} = 22 Hz), 106.2 (d, CH=, cod, J_{C-P} = 12.1 Hz), 113-115 (aromatic carbons), 117.7 (b, CH=, BAr$_F$), 120-132 (aromatic carbons), 135.0 (b, CH=, BAr$_F$), 138-150 (aromatic carbons), 161.9 (q, C-B, BAr$_F$, $^1J_{C-B}$ = 49.3 Hz), 172.4 (s, C=N). Anal. calc (%) for $C_{74}H_{66}BF_{24}IrNO_6P$: C 50.64, H 3.79, N 0.80; found: C 50.82, H 4.09, N 0.75.

[Ir(cod)(L10c)]BAr$_F$. Yield 110 mg (86 %). ^{31}P NMR ($CDCl_3$), δ: 95.5 (s). ^{1}H NMR ($CDCl_3$), δ: 0.49 (s, 9H, $SiMe_3$), 0.54 (s, 9H, $SiMe_3$) 1.02 (s, 3H, CH_3), 1.29 (s, 3H, CH_3), 1.67 (m, 4H, CH_2, cod), 2.24 (b, 2H, CH_2, cod), 2.45 (m, 2H, cod), 3.81 (m, 1H, CH=, cod), 3.38 (b, 1H, CH=, cod), 4.43 (dd, 1H, CH_2, $^2J_{H-H}$ = 10.4 Hz, $^3J_{H-H}$ = 3.6 Hz), 4.66 (b, 2H, CH= cod and CH_2), 4.79 (dd, 1H, CH, $^3J_{H-H}$ = 9.6 Hz, $^3J_{H-H}$ = 2.8 Hz), 5.44 (b, 1H, CH=, cod) 7.1-8.6 (m, 23H, CH= aromatics). ^{13}C NMR ($CDCl_3$), δ: 0.2 (s, $SiMe_3$), 0.4 (s, $SiMe_3$), 21.2 (s, CH_3), 25.0 (b, CH_2, cod), 26.5 (d, CH_3, J_{C-P}

= 7.6 Hz), 29.1 (b, CH_2, cod), 32.8 (b, CH_2, cod), 36.8 (d, CH_2, cod, J_{C-P} = 7.6 Hz), 67.5 (s, CH=, cod), 68.7 (s, CH=, cod), 69.9 (s, CH_2), 73.5 (s, CH), 84.7 (d, CMe_2, J_{C-P} = 5.3 Hz), 96.8 (d, CH=, cod, J_{C-P} = 21.2 Hz), 107.4 (d, CH=, cod, J_{C-P} = 13.7 Hz), 117.7 (b, CH=, BAr_F), 120-134 (aromatic carbons), 135.0 (b, CH=, BAr_F), 135.5-155 (aromatic carbons), 161.9 (q, C-B, BAr_F, $^1J_{C-B}$ = 49.3 Hz), 172.7 (s, C=N). Anal. calc (%) for $C_{70}H_{62}BF_{24}IrNO_4PSi_2$: C 48.67, H 3.62, N 0.81; found: C 48.74, H 3.71, N 0.84.

[Ir(cod)(L10h)]BAr_F. Yield 113 mg (91 %). ^{31}P NMR ($CDCl_3$), δ: 100.9 (s). ^{1}H NMR ($CDCl_3$), δ: 1.39 (s, 3H, CH_3), 1.48 (s, 3H, CH_3), 1.57 (b, 2H, CH_2, cod), 1.75 (m, 2H, CH_2, cod), 2.20 (b, 3H, cod), 2.36 (b, 1H, CH_2, cod), 3.85 (m, 1H, CH=, cod), 4.06 (b, 1H, CH=, cod), 4.13 (b, 1H, CH=, cod), 4.56 (dd, 1H, CH_2, $^2J_{H-H}$ = 10.4 Hz, $^3J_{H-H}$ = 2.8 Hz), 4.69 (m, 1H, CH_2), 4.87 (dd, 1H, CH, $^3J_{H-H}$ = 8.8 Hz, $^3J_{H-H}$ = 2.8 Hz), 5.29 (b, 1H, CH=, cod) 7.1-8.4 (m, 29H, CH= aromatics). ^{13}C NMR ($CDCl_3$), δ: 22.8 (s, CH_3), 25.8 (b, CH_2, cod), 27.5 (d, CH_3, J_{C-P} = 6.2 Hz), 30.5 (s, CH_2, cod), 31.7 (b, CH_2, cod), 36.0 (s, CH_2, cod, J_{C-P} = 5.3 Hz), 64.8 (s, CH=, cod), 66.1 (s, CH=, cod), 70.8 (s, CH_2), 72.5 (d, CH, J_{C-P}= 4.6 Hz), 86.0 (d, CMe_2, J_{C-P}= 4.9 Hz), 99.0 (d, CH=, cod, J_{C-P} = 20.5 Hz), 107.3 (s, CH=, cod, J_{C-P} = 13.7 Hz), 117.7 (b, CH=, BAr_F), 120-132 (aromatic carbons), 135.0 (b, CH=, BAr_F), 136-152 (aromatic carbons), 161.9 (q, C-B BAr_F, $^1J_{C-B}$ = 49.3 Hz), 173.2 (s, C=N). Anal. calc (%) for $C_{72}H_{50}BF_{24}IrNO_4P$: C 51.38, H 2.99, N 0.83; found: C 51.54, H 3.03. N 0.89.

[Ir(cod)(L10i)]BAr_F. Yield 111 g (89 %). ^{31}P NMR ($CDCl_3$), δ: 103.5 (s). ^{1}H NMR ($CDCl_3$), δ: 1.32 (s, 3H, CH_3), 1.40 (s, 3H, CH_3), 1.61 (b, 4H, CH_2, cod), 2.15 (m, 1H, CH_2, cod), 2.40 (m, 3H, cod), 3.12 (m, 1H, CH=, cod), 3.88 (b, 1H, CH=, cod), 3.99 (m, 1H, CH=, cod), 4.55 (dd, 1H, CH_2, $^2J_{H-H}$ = 10.4 Hz, $^3J_{H-H}$ = 2.8 Hz), 4.7 (m, 1H, CH_2), 4.89 (dd, 1H, CH, $^3J_{H-H}$ = 9.2 Hz, $^3J_{H-H}$ = 2.8 Hz), 5.40 (b, 1H, CH=, cod) 7.1-8.6 (m, 29H, CH= aromatics). ^{13}C NMR ($CDCl_3$), δ: 20.9 (s, CH_3), 25.9 (s, CH_2, cod), 26.9 (s, CH_3) 29.2 (s, CH_2, cod), 32.0 (b, CH_2, cod), 36.9 (s, CH_2, cod), 66.1 (s, CH=, cod), 68.2 (s, CH=, cod), 70.6 (s, CH_2), 73.6 (s, CH), 86.1 (d, CMe_2, J_{C-P}= 5.4 Hz), 100.5 (s, CH=, cod), 109.1 (s, CH=,cod), 117.7 (b, CH=, BAr_F), 120-132 (aromatic carbons), 135.0 (b, CH=, BAr_F), 138-150 (aromatic carbons), 161.9 (q, C-B BAr_F, $^1J_{C-B}$ = 49.3 Hz), 180.9 (s, C=N). Anal. calc (%) for $C_{72}H_{50}BF_{24}IrNO_4P$: C 51.38, H 2.99, N 0.83; found: C 51.29, H 2.93, N 0.78.

[Ir(cod)(L11a)]BAr_F. Yield 124 mg (92 %). ^{31}P NMR ($CDCl_3$), δ: 97.4 (s). ^{1}H NMR ($CDCl_3$), δ: 1.06 (s, 3H, CH_3), 1.27 (s, 3H, CH_3), 1.36 (s, 9H, CH_3, ^{t}Bu), 1.37 (s, 9H, CH_3, ^{t}Bu), 1.56 (s, 9H, CH_3, ^{t}Bu), 1.62 (s, 9H, CH_3, ^{t}Bu), 1.67 (b, 4H, CH_2, cod), 2.18 (b, 1H, CH_2, cod), 2.36 (m, 2H, CH_2, cod), 2.53 (m, 4H, CH_2 cod and CH_3), 3.73 (m, 1H, CH=, cod), 4.37 (m, 2H, CH_2 and CH= cod), 4.55 (m, 2H, CH_2 and CH= cod), 4.66 (dd, 1H, CH, $^3J_{H-H}$ = 8.8 Hz, $^3J_{H-H}$ = 2.8 Hz), 5.34 (b, 1H, CH=, cod) 7.1-8.4 (m, 20H, CH= aromatics). ^{13}C NMR ($CDCl_3$), δ: 21.4 (s, CH_3), 24.8 (b, CH_2, cod), 26.4 (s, CH_3), 28.9 (b, CH_2, cod), 31.3 (s, CH_3, ^{t}Bu), 31.4 (s, CH_3, ^{t}Bu), 31.5 (s, CH_3, ^{t}Bu), 31.6 (s, CH_3, ^{t}Bu), 33.7 (b, CH_2, cod), 34.9 (s, C, ^{t}Bu), 35.0 (s, C, ^{t}Bu), 35.4 (s, C, ^{t}Bu), 35.8 (s, CH_3), 37.1 (b, CH_2, cod), 67.9 (s, CH=, cod), 69.6 (s, CH_2), 70.0 (s, CH=, cod), 73.7 (s, CH), 84.8 (d, CMe_2, J_{C-P} = 5.2 Hz), 92.6 (m, CH=, cod), 106.4 (m, CH=, cod), 117.7 (b, CH=, BAr_F), 119-132 (aromatic carbons), 135.0 (b, CH=, BAr_F), 138-150 (aromatic carbons), 161.9 (q, C-B, BAr_F, $^1J_{C-B}$ = 48.6 Hz), 174.8 (s, C=N). Anal. calc (%) for $C_{81}H_{80}BF_{24}IrNO_4P$: C 53.41, H 4.43, N 0.77; found: C 53.53, H 4.52, N 0.79.

[Ir(cod)(L12a)]BAr_F. Yield 120 mg (87 %). ^{31}P NMR ($CDCl_3$), δ: 97.9 (s). ^{1}H NMR ($CDCl_3$), δ: 1.05 (s, 3H, CH_3), 1.25 (s, 3H, CH_3), 1.32 (s, 9H, CH_3, ^{t}Bu), 1.34 (s, 9H, CH_3, ^{t}Bu), 1.52 (s, 9H, CH_3, ^{t}Bu), 1.59 (s, 9H, CH_3, ^{t}Bu), 1.64 (m, 3H, CH_2, cod), 1.92 (m, 1H, CH_2, cod), 2.27 (b, 3H,

CH_2, cod), 2.57 (m, 1H, cod, $^2J_{H-H}$ = 15.6 Hz, $^3J_{H-H}$ = 9.6 Hz), 3.54 (m, 1H, CH=, cod), 4.38 (dd, 1H, CH_2, $^2J_{H-H}$ = 10 Hz, $^3J_{H-H}$ = 3.2 Hz), 4.43 (b, 1H, CH=, cod), 4.57 (m, 1H, CH_2), 4.61 (b, 1H, CH=, cod), 4.71 (dd, 1H, CH, $^3J_{H-H}$ = 9.2 Hz, $^3J_{H-H}$ = 3.2 Hz), 5.31 (b, 1H, CH=, cod) 7.1-8.6 (m, 20H, CH= aromatics). ^{13}C NMR ($CDCl_3$), δ: 21.3 (s, CH_3), 24.8 (b, CH_2, cod), 26.4 (d, CH_3, J_{C-P} = 6.8 Hz), 28.7 (b, CH_2, cod), 31.3 (s, CH_3, ^{t}Bu), 31.4 (s, CH_3, ^{t}Bu), 31.5 (s, CH_3, ^{t}Bu), 33.4 (b, CH_2, cod), 34.9 (s, C, ^{t}Bu), 35.0 (s, C, ^{t}Bu), 35.4 (s, C, ^{t}Bu), 35.7 (s, C, ^{t}Bu), 37.3 (d, CH_2, cod, J_{C-P} = 6.9 Hz), 69.1 (s, CH=, cod), 70.2 (s, CH_2), 71.0 (s, CH=, cod), 74.5 (s, CH), 84.5 (d, CMe_2, J_{C-P} = 5.3 Hz), 94.7 (d, CH=, cod, J_{C-P} = 21.9 Hz), 106.5 (d, CH=, cod, J_{C-P} = 12.2 Hz), 117.7 (b, CH=, BAr_F), 120-132 (aromatic carbons), 135.0 (b, CH=, BAr_F), 136.6 (q, CF_3, $^1J_{C-F}$ = 33.3 Hz), 138-150 (aromatic carbons), 161.9 (q, C-B, BAr_F, $^1J_{C-B}$ = 49.3 Hz), 171.0 (s, C=N). Anal. calc (%) for $C_{81}H_{77}BF_{27}IrNO_4P$: C 51.87, H 4.14, N 0.75; found: C 51.93, H 4.17, N 0.79.

[Ir(cod)(L13a)]BAr$_F$. Yield: 129 mg (96%). ^{31}P NMR ($CDCl_3$), δ: 96.2 (s). ^{1}H NMR ($CDCl_3$), δ: 1.08 (s, 3H, CH_3), 1.27 (s, 3H, CH_3), 1.36 (s, 9H, CH_3, ^{t}Bu), 1.38 (s, 9H, CH_3, ^{t}Bu), 1.54 (s, 9H, CH_3, ^{t}Bu), 1.72 (s, 9H, CH_3, ^{t}Bu), 1.62 (b, 4H, CH_2, cod), 2.11 (m, 2H, CH_2, cod), 2.24 (b, 2H, CH_2, cod), 2.36 (s, 3H, CH_3-Ph), 3.42 (m, 1H, CH=, cod), 4.19 (b, 1H, CH= cod), 4.33 (b, 1H, CH= cod), 4.48 (dd, 1H, CH_2, $^2J_{H-H}$= 9.3 Hz, $^3J_{H-H}$= 2.7 Hz), 4.70 (m, 2H, CH and CH_2), 5.19 (b, 1H, CH= cod), 7.1 – 8.4 (m, 20H, aromatics). ^{13}C NMR ($CDCl_3$), δ: 20.6 (CH_3), 21.6 (b, CH_2, cod), 25.4 (CH_3), 26.9 (b, CH_2, cod), 29.2 (b, CH_2, cod), 31.2 (CH_3-Ph), 31.3 (CH_3, ^{t}Bu), 31.4 (CH_3, ^{t}Bu), 31.6 (b, CH_3, ^{t}Bu), 34.9 (C, ^{t}Bu), 35.0 (C, ^{t}Bu), 35.4 (b, CH_2, cod), 35.8 (C, ^{t}Bu), 36.0 (C, ^{t}Bu), 65.0 (CH=, cod), 69.5 (CH=, cod), 70.6 (CH_2), 72.7 (CH), 84.6 (b, C, CMe_2), 98.5 (d, CH=, cod, J_{C-P}= 19.9 Hz), 106.8 (b, CH=, cod), 117.7 (b, CH=, BAr_F), 119-134 (aromatic carbons), 135.0 (b, CH=, BAr_F), 136-149 (aromatic carbons), 161.9 (q, C-B, BAr_F, $^1J_{C-B}$= 49.5 Hz), 175.1 (C=N). Anal. Calc (%) for $C_{81}H_{80}BF_{24}IrNO_4P$: C 53.41, H 4.43, N 0.77; found: C 53.48, H 4.39, N 0.83.

[Ir(cod)(L14a)]BAr$_F$. Yield: 124 mg (91%). ^{31}P NMR ($CDCl_3$), δ: 94.1 (s). ^{1}H NMR ($CDCl_3$), δ: 1.12 (s, 3H, CH_3), 1.30 (s, 3H, CH_3), 1.35 (s, 9H, CH_3, ^{t}Bu), 1.37 (s, 9H, CH_3, ^{t}Bu), 1.58 (s, 9H, CH_3, ^{t}Bu), 1.59 (s, 9H, CH_3, ^{t}Bu), 1.72 (b, 4H, CH_2, cod), 2.02 (m, 2H, CH_2, cod), 2.15 (b, 2H, CH_2, cod), 2.26 (s, 3H, CH_3-Ph), 2.80 (s, 3H, CH_3-Ph), 3.70 (m, 1H, CH=, cod), 4.01 (b, 2H, CH= cod), 4.42 (dd, 1H, CH_2, $^2J_{H-H}$= 10.2 Hz, $^3J_{H-H}$= 5.1 Hz), 4.27 (t, 1H, CH_2, $^2J_{H-H}$= 10.5 Hz), 4.51 (dd, 1H, CH, $^2J_{H-H}$ = 10.8 Hz, $^3J_{H-H}$= 5.1 Hz), 5.19 (b, 1H, CH= cod), 7.1 – 7.9 (m. 19H, aromatics). ^{13}C NMR ($CDCl_3$), δ: 20.5 (CH_3), 22.6 (b, CH_2, cod), 23.3 (CH_3), 27.7 (b, CH_2, cod), 29.7 (b, CH_2, cod), 31.2 (CH_3-Ph), 31.4 (CH_3, ^{t}Bu), 31.6 (b, CH_3, ^{t}Bu), 34.9 (C, ^{t}Bu), 35.0 (b, CH_2, cod), 35.2 (C, ^{t}Bu), 35.4 (b, C, ^{t}Bu), 35.8 (CH_3-Ph), 63.9 (CH=, cod), 66.0 (CH=, cod), 69.3 (CH_2), 74.0 (CH), 83.5 (b, C, CMe_2), 103.4 (d, CH=, cod, J_{C-P}= 18.0 Hz), 106.0 (d, CH=, cod, J_{C-P}= 10.5 Hz), 117.7 (b, CH=, BAr_F), 119-134 (aromatic carbons), 135.0 (b, CH=, BAr_F), 136-149 (aromatic carbons), 161.9 (q, C-B, BAr_F, $^1J_{C-B}$= 49.8 Hz), 176.6 (C=N). Anal. Calc (%) for $C_{82}H_{82}BF_{24}IrNO_4P$: C 53.66, H 4.50, N 0.76; found: C 53.69, H 4.47, N 0.73.

[Ir(cod)(L15a)]BAr$_F$. Yield: 119 mg (90%). ^{31}P NMR ($CDCl_3$), δ: 102.5 (s). ^{1}H NMR ($CDCl_3$), δ: 1.16 (s, 3H, CH_3), 1.27 (s, 3H, CH_3), 1.34 (s, 9H, CH_3, ^{t}Bu), 1.37 (s, 9H, CH_3, ^{t}Bu), 1.54 (s, 9H, CH_3, ^{t}Bu), 1.55 (s, 18H, CH_3, ^{t}Bu and *t*Bu-C=N), 1.71 (m, 4H, CH_2, cod), 2.07 (m, 1H, CH_2, cod), 2.20 (m, 1H, CH_2, cod), 2.37 (m, 1H, CH_2, cod), 2.55 (m, 1H, CH_2, cod), 4.09 (m, 1H, CH=, cod), 4.16 (dd, 1H, CH_2, $^2J_{H-H}$= 10.5 Hz, $^3J_{H-H}$= 3 Hz), 4.25 (t, 1H, CH_2, $^2J_{H-H}$= 10.5), 4.51 (b, 2H, CH and CH=, cod), 4.76 (b, 1H, CH=, cod), 5.36 (b, 1H, CH=, cod), 7.1 – 7.8 (m. 16H, aromatics). ^{13}C NMR ($CDCl_3$), δ: 21.1 (CH_3), 24.5 (b, CH_2, cod), 26.4 (CH_3), 28.3 (b, CH_2, cod), 29.4 (CH_3, ^{t}Bu),

31.2 (CH_3, ^{t}Bu), 31.3 (CH_3, ^{t}Bu), 31.5 (CH_3, ^{t}Bu), 31.6 (CH_3, ^{t}Bu), 34.5 (C, ^{t}Bu), 34.7 (b, CH_2, cod), 34.9 (C, ^{t}Bu), 35.3 (C, ^{t}Bu), 35.8 (C, ^{t}Bu), 37.6 (b, CH_2, cod), 69.1 (CH=, cod), 69.5 (CH=, cod), 69.6 (CH_2), 74.8 (CH), 83.8 (d, CMe_2, J_{C-P}= 5.7 Hz), 89.6 (d, CH=, cod, J_{C-P}= 26.2 Hz), 103.1 (d, CH=, cod, J_{C-P}= 10.5 Hz), 117.7 (b, CH=, BAr_F), 119-131 (aromatic carbons), 135.0 (b, CH=, BAr_F), 136-150 (aromatic carbons), 161.9 (q, C-B, BAr_F, $^1J_{C-B}$= 49.8 Hz), 183.9 (C=N). Anal. Calc (%) for $C_{78}H_{82}BF_{24}IrNO_4P$: C 52.41, H 4.62, N 0.78; found: C 52.38, H 4.60, N 0.75.

[Ir(cod)(L16a)]BAr$_F$. Yield:125 mg (88%). ^{31}P NMR ($CDCl_3$), δ: 98.3 (s). ^{1}H NMR ($CDCl_3$), δ: 1.16 (b, 3H, CH_3), 1.28 (b, 3H, CH_3), 1.39 (b, 18H, CH_3, ^{t}Bu), 1.55 (b, 18H, CH_3, ^{t}Bu), 1.69 (b, 3H, CH_2, cod), 2.27 (b, 3H, CH_2, cod), 2.46 (b, 2H, CH_2, cod), 4.01 (b, 1H, CH=, cod), 4.30 (b, 9H, CH=, Cp), 4.50 (b, 2H, CH=, cod), 4.70 (b, 2H, CH_2), 4.90 (b, 1H, CH), 5.23 (b, 1H, CH= cod), 5.42 (b, 1H, CH= cod), 7.1 – 7.8 (m. 16H, aromatics). ^{13}C NMR ($CDCl_3$), δ: 22.0 (b, CH_2, cod), 28.8 (b, CH_2, cod), 31.5 (CH_3, *t*Bu), 31.6 (CH_3, ^{t}Bu), 31.9 (CH_3, ^{t}Bu), 32.1 (CH_3, ^{t}Bu), 33.7 (b, CH_2, cod), 34.9 (C, ^{t}Bu), 35.0 (C, ^{t}Bu), 35.4 (C, ^{t}Bu), 35.9 (C, ^{t}Bu), 37.0 (b, CH_2, cod), 67.5 (CH=, cod), 70.4 (CH=, cod), 71.0 (b, CH=, Cp), 71.9 (CH_2), 73.8 (CH), 84.9 (b, CMe_2), 95.0 (CH=, cod), 100.9 (CH=, cod), 117.7 (b, CH=, BAr_F), 119-131 (aromatic carbons), 135.0 (b, CH=, BAr_F), 136-150 (aromatic carbons), 161.9 (q, C-B, BAr_F, $^1J_{C-B}$= 49.8 Hz), 176.9 (C=N). Anal. Calc (%) for $C_{84}H_{82}BF_{24}FeIrNO_4P$: C 52.67, H 4.32, N 0.73; found: C 52.78, H 4.34, N 0.74.

[Ir(cod)(L17a)]BAr$_F$. Yield 123 mg (92 %). ^{31}P NMR ($CDCl_3$), δ: 97.8 (s). 1H NMR ($CDCl_3$), δ: 1.06 (s, 3H, CH_3), 1.29 (s, 3H, CH_3), 1.35 (s, 9H, CH_3, ^{t}Bu), 1.38 (s, 9H, CH_3, ^{t}Bu), 1.54 (s, 9H, CH_3, ^{t}Bu), 1.61 (s, 9H, CH_3, ^{t}Bu), 1.70 (m, 4H, CH_2, cod), 2.32 (m, 3H, CH_2, cod), 2.51 (m, 1H, CH_2, cod), 3.60 (b, 1H, CH= cod), 4.41 (m, 2H, CH= cod and CH_2), 4.58 (b, 2H, CH= cod and CH_2), 4.67 (dd, 1H, CH, $^3J_{H-H}$= 10. 0 Hz, $^3J_{H-H}$= 3.2 Hz), 5.32 (b, 1H, CH=, cod), 7.1-8.5 (m, 21H, CH= aromatics). ^{13}C NMR ($CDCl_3$), δ: 21.3 (CH_3), 24.8 (b, CH_2, cod), 26.5 (m, CH_3), 28.09 (b, CH_2, cod), 31.2 (CH_3, *t*Bu), 31.4 (CH_3, ^{t}Bu), 31.6 (CH_3, ^{t}Bu), 33.2 (b, CH_2, cod), 34.8 (C, ^{t}Bu), 34.9 (C, ^{t}Bu), 35.2 (C, ^{t}Bu), 37.3 (b, CH_2, cod), 66.3 (CH=, cod), 69.8 (CH=, cod), 70.0 (CH_2), 71.2 (CH), 84.9 (d, CMe_2, J_{C-P}= 5.2 Hz), 93.5 (d, CH=, cod, J_{C-P} = 21.1 Hz), 106.3 (d, CH=, cod, J_{C-P} = 6.2 Hz), 117.7 (b, CH=, BArF), 119-132 (aromatic carbons), 135.0 (b, CH=, BArF), 135.5-150 (aromatic carbons), 161.9 (q, C-B, BArF, $^1J_{C-B}$ = 48.6 Hz), 173.7 (C=N). Anal. calc (%) for $C_{80}H_{78}BF_{24}IrNO_4P$: C 53.16, H 4.35, N 0.77; found: C 53.22, H 4.40, N 0.76.

[Ir(cod)(L18a)]BAr$_F$. Yield 117 mg (87 %). ^{31}P NMR ($CDCl_3$), δ: 95.0 (s). ^{1}H NMR ($CDCl_3$), δ: 1.09 (s, 3H, CH_3), 1.34 (s, 9H, CH_3, ^{t}Bu), 1.35 (s, 9H, CH_3, ^{t}Bu), 1.49 (s, 9H, CH_3, ^{t}Bu), 1.52 (s, 3H, CH_3),1.56 (s, 3H, $\underline{CH_3}$-CH), 1.57 (s, 9H, CH_3, ^{t}Bu), 1.64 (m, 4H, CH_2, cod), 2.27 (b, 3H, CH_2, cod), 2.55 (dd, 1H, cod, $^2J_{H-H}$ = 16.4 Hz, $^3J_{H-H}$ = 7.6 Hz), 3.63 (m, 1H, CH=, cod), 4.37 (b, 1H, CH=, cod), 4.39 (d, 1H, CH-N, $^3J_{H-H}$ = 8.4 Hz), 4.60 (b, 1H, CH=, cod), 5.06 (m, 1H, CH), 5.26 (b, 1H, CH=, cod) 7.1-8.6 (m, 21H, CH= aromatics). ^{13}C NMR ($CDCl_3$), δ: 23.6 (s, CH_3), 25.0 (b, CH_2, cod), 27.7 (d, CH_3, J_{C-P} = 6.8 Hz), 29.1 (b, CH_2, cod), 31.1 (s, CH_3, ^{t}Bu), 31.3 (s, CH_3 ^{t}Bu), 31.5 (s, CH_3, ^{t}Bu), 31.6 (s, CH_3, ^{t}Bu), 33.1 (b, CH_2, cod), 34.9 (s, C, ^{t}Bu), 35.0 (s, C, ^{t}Bu), 35.3 (s, C, ^{t}Bu), 35.8 (s, $\underline{CH_3}$-CH), 36.9 (d, CH_2, cod, J_{C-P} = 6.1 Hz), 67.7 (s, CH=, cod), 69.7 (s, CH=, cod), 76.0 (s, CH-N), 81.1 (s, CH-O), 84.5 (d, CMe_2, J_{C-P} = 6.9Hz), 95.7 (d, CH=, cod, J_{C-P} = 22 Hz), 106.6 (d, CH=, cod, J_{C-P} = 12.9 Hz), 117.7 (b, CH=, BAr_F), 120-132 (aromatic carbons), 135.0 (b, CH=, BAr_F),138-150 (aromatic carbons), 161.9 (q, C-B, BAr_F, $^1J_{C-B}$ = 49.3 Hz), 172.5 (s, C=N). Anal. calc (%) for $C_{81}H_{80}BF_{24}IrNO_4P$: C 53.41, H 4.43, N 0.77; found: C 53.74, H 4.56, N 0.81.

[Ir(cod)(L19a)]BAr$_F$. Yield: 124 mg (92%). ^{31}P NMR ($CDCl_3$), δ: 99.1 (s). ^{1}H NMR ($CDCl_3$), δ: 1.12 (s, 3H, CH_3), 1.31 (s, 3H, CH_3), 1.37 (b, 18H, CH_3, ^{t}Bu), 1.57 (s, 9H, CH_3, ^{t}Bu), 1.63 (s, 9H, CH_3, ^{t}Bu), 1.70 (b, 4H, CH_2, cod), 2.15 (s, 3H, CH_3), 2.33 (b, 3H, CH_2, cod), 2.55 (b, 1H, CH_2, cod), 3.65 (b, 1H, CH=, cod), 3.65 (b, 1H, CH=, cod), 4.22 (b, 1H, CH-N), 4.41 (b, 1H, CH=, cod), 4.41 (b, 1H, CH=, cod), 4.61 (b, 1H, CH=, cod), 4.74 (b, 1H, CH-O), 5.25 (b, 1H, CH=, cod), 7.1 – 8.4 (m, 21H, aromatics). ^{13}C NMR ($CDCl_3$), δ: 21.0 (CH_3), 21.8 (CH_3), 24.9 (b, CH_2, cod), 26.2 (b, CH_2, cod), 28.9 (b, CH_2, cod), 31.3 (CH_3, ^{t}Bu), 31.4 (CH_3, ^{t}Bu), 31.6 (b, CH_3, ^{t}Bu), 33.6 (CH_3), 35.0 (C, ^{t}Bu), 35.1 (C, ^{t}Bu), 35.4 (b, C, ^{t}Bu), 35.8 (C, ^{t}Bu), 37.2 (b, CH_2, cod), 68.4 (CH=, cod), 70.2 (CH=, cod), 79.1 (CH-O), 80.3 (CH-N), 84.5 (d, C, CMe_2, $J_{C\text{-}P}$= 5.4Hz), 94.7 (d, CH=, cod, $J_{C\text{-}P}$= 22.2 Hz), 105.7 (d, CH=, cod, $J_{C\text{-}P}$= 12.5 Hz), 117.7 (b, CH=, BAr$_F$), 119-134 (aromatic carbons), 135.0 (b, CH=, BAr$_F$), 136-149 (aromatic carbons), 161.9 (q, C-B, BAr$_F$, $^1J_{C\text{-}B}$= 49.5 Hz), 171.5 (C=N). Anal. Calc (%) for $C_{81}H_{80}BF_{24}IrNO_4P$: C 53.41, H 4.42, N 0.77; found: C 53.49, H 4.40, N 0.78.

[Ir(cod)(L20a)]BAr$_F$. Yield: 133 mg (93%). ^{31}P NMR ($CDCl_3$), δ: 92.7 (s). ^{1}H NMR ($CDCl_3$), δ: 1.37 (s, 9H, CH_3, ^{t}Bu), 1.39 (s, 9H, CH_3, ^{t}Bu), 1.57 (s, 9H, CH_3, ^{t}Bu), 1.58 (s, 9H, CH_3, ^{t}Bu), 1.67 (m, 2H, CH_2, cod), 1.80 (m, 2H, CH_2, cod), 2.30 (m, 1H, CH_2, cod), 2.39 (m, 2H, CH_2, cod), 3.68 (m, 1H, CH=, cod), 4.40 (b, 2H, CH=, cod and CH_2-O), 4.59 (b, 2H, CH=, cod and CH_2-O), 4.69 (dd, 1H, CH, $^2J_{H\text{-}H}$= 12.8 Hz, $^3J_{H\text{-}H}$= 3.2 Hz), 5.35 (b, 1H, CH= cod), 7.1 – 7.8 (m. 31H, aromatics). ^{13}C NMR ($CDCl_3$), δ: 22.9 (b, CH_2, cod), 28.9 (b, CH_2, cod), 31.4 (CH_3, ^{t}Bu), 31.5 (CH_3, ^{t}Bu), 31.6 (CH_3, ^{t}Bu), 31.7 (CH_3, ^{t}Bu), 33.4 (b, CH_2, cod), 35.0 (C, ^{t}Bu), 35.1 (C, ^{t}Bu), 35.4 (C, ^{t}Bu), 35.8 (C, ^{t}Bu), 37.1 (b, CH_2, cod), 68.1 (CH_2), 69.9 (CH), 70.2 (CH=, cod), 73.9 (CH=, cod), 84.8 (b, CPh_2), 95.1 (d, CH=, cod, $J_{C\text{-}P}$= 22 Hz), 106.4 (b, CH=, cod), 117.7 (b, CH=, BAr$_F$), 119-131 (aromatic carbons), 135.0 (b, CH=, BAr$_F$), 136-150 (aromatic carbons), 161.9 (q, C-B, BAr$_F$, $^1J_{C\text{-}B}$= 49.3 Hz), 172.1 (C=N). Anal. Calc (%) for $C_{90}H_{82}BF_{24}IrNO_4P$: C 55.96, H 4.28, N 0.73; found: C 55.93, H 4.26, N 0.70.

[Ir(cod)(L20h)]BAr$_F$. Yield: 123 mg (92%). ^{31}P NMR ($CDCl_3$), δ: 113.2 (s). ^{1}H NMR ($CDCl_3$), δ: 1.48 (m, 1H, CH_2, cod), 1.70 (m, 2H, CH_2, cod), 1.78 (m, 3H, CH_2, cod), 2.00 (m, 1H, CH_2, cod), 2.10 (m, 1H, CH_2, cod), 3.41 (m, 1H, CH=, cod), 3.94 (m, 1H, CH=, cod), 4.35 (m, 1H, CH_2), 4.47 (b, 2H, CH and CH=, cod), 5.28 (b, 1H, CH=, cod), 6.00 (m, 1H, CH_2), 6.9 – 8.5 (m. 39H, aromatics). ^{13}C NMR ($CDCl_3$), δ: 22.7 (b, CH_2, cod), 27.0 (b, CH_2, cod), 33.5 (b, CH_2, cod), 38.1 (b, CH_2, cod), 61.2 (CH), 64.6 (CH_2), 70.4 (CH=, cod), 71.8 (CH=, cod), 87.8 (b, CPh_2), 102.1 (d, CH=, cod, $J_{C\text{-}P}$= 17 Hz), 103.0 (b, CH=, cod, $J_{C\text{-}P}$= 17 Hz), 117.7 (b, CH=, BAr$_F$), 119-131 (aromatic carbons), 135.0 (b, CH=, BAr$_F$), 136-150 (aromatic carbons), 161.9 (q, C-B, BAr$_F$, $^1J_{C\text{-}B}$= 49.3 Hz), 173.5 (C=N). Anal. Calc (%) for $C_{90}H_{82}BF_{24}IrNO_4P$: C 54.50, H 3.01, N 0.78; found: C 54.43, H 3.09, N 0.79.

[Ir(cod)(L21a)]BAr$_F$. Yield 136 mg (92 %). ^{31}P NMR ($CDCl_3$), δ: 92.8 (s). ^{1}H NMR ($CDCl_3$), δ: 1.08 (s, 9H, CH_3, ^{t}Bu), 1.35 (s, 9H, CH_3, ^{t}Bu), 1.39 (s, 9H, CH_3, ^{t}Bu), 1.81 (m, 4H, CH_2, cod), 1.87 (s, 9H, CH_3, ^{t}Bu), 2.33 (m, 3H, CH_2, cod), 2.55 (m, 1H, CH_2, cod), 3.93 (m, 1H, CH=, cod), 4.51 (b, 1H, CH=, cod), 4.63 (b, 1H, CH=, cod), 4.68 (dd, 1H, CH_2, $^2J_{H\text{-}H}$ = 10 Hz, $^3J_{H\text{-}H}$ = 3.2 Hz), 4.87 (m, 1H, CH_2), 5.27 (b, 1H, CH=, cod), 5.78 (dd, 1H, CH, $^3J_{H\text{-}H}$ = 8.4 Hz, $^3J_{H\text{-}H}$ = 2.8 Hz), 6.5-8.6 (m, 30H, CH= aromatics). ^{13}C NMR ($CDCl_3$), δ: 25.9 (b, CH_2, cod), 29.9 (b, CH_2, cod), 30.5 (s, CH_3, ^{t}Bu), 31.2 (b, CH_2, cod), 31.5 (s, CH_3, ^{t}Bu), 31.6 (s, CH_3, ^{t}Bu), 31.7, (s, CH_3, ^{t}Bu), 34.9 (s, C, ^{t}Bu), 35.0 (s, C, ^{t}Bu), 35.4 (s, C, ^{t}Bu), 35.7 (s, C, ^{t}Bu), 36.0 (b, CH_2, cod), 67.7 (s, CH=, cod), 71.2 (s,

CH_2), 71.3 (s, CH=, cod), 71.4 (s, CH), 92.7 (s, CPh_2), 99.0 (d, CH=, cod, J_{C-P} = 19.7 Hz), 108.1 (d, CH=, cod, J_{C-P} = 13.6 Hz), 117.7 (b, CH=, BAr_F), 120-132 (aromatic carbons), 135.0 (b, CH=, BAr_F), 136.1 (m, CF_3), 138-150 (aromatic carbons), 161.9 (q, C-B, BAr_F, $^1J_{C-B}$ = 49.3 Hz), 172.3 (s, C=N). Anal. calc (%) for $C_{91}H_{81}BF_{27}IrNO_4P$: C 54.66, H 4.08, N 0.70; found: C 54.78, H 4.11, N 0.73.

3.3.5.3 Typical procedure for the hydrogenation of olefins

The alkene (1 mmol) and Ir complex (0.2 mol%) were dissolved in CH_2Cl_2 (2 mL) in a high-pressure autoclave. The autoclave was purged four times with hydrogen. Then, it was pressurized at the desired pressure. After the desired reaction time, the autoclave was depressurised and the solvent evaporated off. The residue was dissolved in Et_2O (1.5 ml) and filtered through a short celite plug. The enantiomeric excess was determined by chiral GC or chiral HPLC and conversions were determined by ^{1}H NMR. The enantiomeric excess was determined by chiral GC or chiral HPLC and conversions were determined by 1H NMR. The enantiomeric excesses of hydrogenated products were determined using the conditions previously described.[6b-c]

3.3.6. Acknowledgements

We thank the Spanish (Consolider Ingenio CSD2006-0003, CTQ2007-62288/BQU, 2008PGIR/07 to O.P. and 2008PGIR/08 to M.D.) and Catalan (2005SGR007777) Governments, COST D40, Vetenskapsrådet (VR), and Astra Zeneca for support. A. Börner and B. Schäffner acknowledge financial supported by the Graduate School 1213 of Deutsche Forschungsgemeinschaft. We thank Dr. Jordi Benet and Eduardo Escudero (ICIQ) for the analysis of the single-crystal X-ray structure.

3.3.7. References

[1] a) *Catalytic Asymmetric Synthesis*, 2nd, ed.; Ojima, I., Ed.; Wiley-VCH: New York, 2000. b) *Asymmetric Catalysis in Organic Synthesis*; Noyori, R., Ed.; Wiley: New York:, 1994. c) *Asymmetric Catalysis in Industrial Scale: Challenges, Approaches and Solutions*; Blaser, H. U., Schmidt, E., Eds.; Wiley: Weinheim, 2003. d) Brown, J. M. in *Comprehensive Asymmetric Catalysis*; Jacobsen, E. N., Pfaltz, A., Yamamoto, H., Eds.; Springer-Verlag: Berlin, 1999, Vol.1.

[2] For recent reviews, see: a) Källström, K.; Munslow, I.; Andersson, P. G. *Chem. Eur. J.* **2006**, *12*, 3194. b) Roseblade, S. J.; Pfaltz, A. *Acc. Chem. Res.* **2007**, *40*, 1402. c) Church, T. L.; Andersson, P. G. *Coord. Chem. Rev*. **2008**, *252*, 513. d) Cui, X.; Burgess, K. *Chem. Rev.* **2005**, *105*, 3272.

[3] See for instance: a) Tang, W.; Wang, W.; Zhang, X. *Angew. Chem. Int. Ed.* **2003**, *42*, 943. b) Hou, D.-R.; Reibenspies, J.; Colacot, T. J.; Burgess, K. *Chem. Eur. J.* **2001**, *7*, 5391. c) Cozzi, P. G.; Menges, F.; Kaiser, S. *Synlett* **2003**, 833. d) Lighfoot, A.; Schnider, P.; Pfaltz, A. *Angew. Chem. Int. Ed.* **1998**, *37*, 3897. e) Menges, F.; Neuburger, M.; Pfaltz, A. *Org. Lett.* **2002**, *4*, 4713. f) Liu, D.; Tang, W.; Zhang, X. *Org. Lett*. **2004**, *6*, 513. g) Drury III, W. J.; Zimmermann, N.; Keenan, M.; Hayashi, M.; Kaiser, S.; Goddard, R.; Pfaltz, A. *Angew. Chem. Int. Ed.* **2004**, *43*, 70.

[4] a) Perry, M. C.; Cui, X.; Powell, M. T.; Hou, D.-R.; Reibenspies, J. H.; Burgess, K. *J. Am. Chem. Soc.* **2003**, *125*, 5391. b) Blankestein, J.; Pfaltz, A. *Angew. Chem. Int. Ed.* **2001**, *40*, 4445. c)

Kaiser, S. ; Smidt, S: P.; Pfaltz, A. *Angew. Chem. Int. Ed.* **2006**, *45*, 5194. d) Källström, K.; Hedberg, C. Brandt, P.; Bayer, P.; Andersson, P. G. *J. Am. Chem. Soc.* **2004**, *126*, 14308. e) Engman, M.; Diesen, J. S.; Paptchikhine, A.; Andersson, P. G. *J. Am. Chem. Soc.* **2007**, *129*, 4536. f) Trifonova, A.; Diesen, J. S.; Andersson, P. G. *Chem. Eur. J.* **2006**, *12*, 2318. g) Menges, F. Pflatz, A. *Adv. Synth. Catal.* **2002**, *334*, 4044. h) Co, T. T.; Kim, T.-J. *Chem. Commun.* **2006**, 3537.

[5] For some representative examples see: a) Claver, C.; Diéguez, M.; Pàmies, O.; Castillón, S. in *Catalytic Carbonylation Reactions*; Beller, M., Ed.; Springer-Verlag: Berlin, 2006, pp 35-64. b) Diéguez, M.; Pàmies, O.; Ruiz, A.; Claver, C. in *Methodologies in Asymmetric Catalysis*; Malhotra, S. V., Ed.; ACS: Washington:, 2004, pp 161-174. c) Yan, M.; Zhou, Z.-Y.; Chan, A. S. C. *Chem. Commun*. **2000**, 115. d) Pàmies, O.; Diéguez, M.; Claver, C. *J. Am. Chem. Soc.* **2005**, *127*, 3646. e) Mata, Y.; Pàmies, O.; Diéguez, M. *Chem. Eur. J.* **2007**, *13*, 3296

[6] a) Hilgraf, R.; Pfaltz, A. *Adv. Synth. Catal.* **2005**, *347*, 61. b) Diéguez, M.; Mazuela, J.; Pàmies, O.; Verendel, J. J.; Andersson, P. G. *J. Am. Chem. Soc.* **2008**, *130*, 7208. c) Mazuela, J.; Norrby, P.-O.; Andersson, P. G.; Pàmies, O.; Diéguez, M. *J. Am. Chem Soc.* **2011**, *133,* 13634.

[7] Crystals of [Ir(cod)(**L6a**)]BArF could be obtained by slow evaporation of a solution of the compound in ethanol.

[8] The rapid ring inversions (tropoisomerization) in the biaryl phosphite moiety is usually stopped upon coordination to the metal center. See for example: a) Buisman, G. J. H.; van der Veen, L. A.; Klootwijk, A.; de Lange, W. G. J.; Kamer, P. C. J.; van Leeuwen, P. W. N. M.; Vogt, D. *Organometallics* **1997**, *16*, 2929. b) Diéguez, M.; Pàmies, O.; Ruiz, A.; Claver, C.; Castillón, S. *Chem. Eur. J.* **2001**, *7*, 3086. c) Pàmies, O.; Diéguez, M.; Net, G.; Ruiz, A.; Claver, C. *J. Org. Chem.* **2001**, *66*, 8364. d) Diéguez, M.; Pàmies, O.; Ruiz, A.; Claver, C. *New J. Chem*. **2002**, *26*, 827. e) Pàmies, O.; Diéguez, M. *Chem. Eur. J.* **2008**, *14*, 944.

[9] The related phosphinite-oxazoline ligands **2** afforded >99% ee for **S3**, 92% ee for **S4**, 85% ee for **S5**, 94% ee for **S6** and 92% for **S7** at 1 mol% Ir-catalyst. See: a) ref. 4g. b) Smidt, S. P.; Menges, F.; Pflatz, A. *Org. Lett.* **2004**, *6*, 2023. There is no data reported for substrates **S2** and **S8**.

[10] Forman, G. S.; Ohkuma, T.; Hems, W. P.; Noyori, R. *Tetrahedron Lett.* **2000**, *41*, 9471.

[11] Similar behavior has been observed using related Ir-phosphinite-oxazoline ligands. See: Bayardon, J.; Holz, J.; Schäffner, B.; Andrushko, V.; Verevkin, S.; Preetz, A.; Börner, A. *Angew. Chem. Int. Ed.* **2007**, *46*, 5971.

[12] Pfaltz and coworkers have successfully hydrogenated trisubstituted aryl alkenes with one aromatic heterocyclic substituent. See: Pfaltz, A.; Blankenstein, J.; Hilgraf, R.; Hormann, E.; McIntyre, S.; Menges, F.; Schonleber, M.; Smidt, S. P.; Wustenberg, B.; Zimmermann, N. *Adv. Synth. Catal.* **2003**, *345*, 33.

[13] a) Fessard, T. C.; Andrews, S. P.; Motoyohsi, H.; Carreira, E. *Angew. Chem. Int. Ed.* **2007**, *46*, 9331. b) Prat, L.; Dupas, G.; Duflos, J.; Quéguiner, G.; Bourguignon, J.; Levacher, V. *Tetrahedron Lett.* **2001**, *42*, 4515. c) Wilkinson, J. A.; Rossington, S. B.; Ducki, S.; Leonard, J.; Hussain, N. *Tetrahedron* **2006**, *62*, 1833.

[14] a) Okamoto, K.; Nishibayashi, Y.; Uemura, S.; Toshimitsu, A. *Angew. Chem. Int. Ed.* **2005**, *44*, 3588. b) Hatanaka, Y.; Hiyama, T. *J. Am. Chem. Soc.* **1990**, *112*, 7793.

[15] In this context, Noyori and coworkers have found moderate enantioselectivities in the Ru-catalyzed asymmetric transfer hydrogenation of differently para-substituted benzophenone derivatives. See: Fujii, A.; Hashiguchi, S.; Uematsu, N.; Ikariya, T.; Noyori, R. *J. Am. Chem. Soc.* **1996**, *118*, 2521.

[16] See for instance: a) Abate, A.; Brenna, E. Fuganti, C.; Gatti, G. G.; Givenzana, T.; Malpezzi, L.; Serra, S. *J. Org. Chem.* **2005**, *70*, 1281. b) Drescher, K.; Haupt, A.; Unger, L.; Rutner, S. C.; Braje, W:; Grandel, R.; Henry, C.; Backfisch, G:; Beyerbach, A.; Bisch, W. *WO Patent* 2006/040182 A1.
[17] Wipf, P.; Ribe, S. *Org. Lett.* **2000**, *2*, 1713.
[18] See for instance: a) Fleming, I.; Barbero, A.; Walter, D. *Chem. Rev.* **1997**, *97*, 2063. b) Jones, G. R.; Landais, Y. *Tetrahedron* **1996**, *52*, 7599. c) Bains, W.; Tacke, R. *Curr. Opin. Drug Discv. Dev.* **2003**, *6*, 526.
[19] See for instance: s) Schlosser, M. *Angew. Chem. Int. Ed.* **1998**, *37*, 1496. b) Smart, B. E. *J. Fluorine Chem.* **2001**, *109*, 3. c) *Asymmetric Fluoroorganic Chemistry: Synthesis, Application and Future Directions;* Ramachandran, P. V., Ed.; American Chemical Society: Washington DC, 2000. d) A special issue has been devoted to "Fluorine in the Life Sciences" *Chem BioChem* **2004**, *5*, 559.
[20] Diéguez, M.; Pàmies, O. *Chem. Eur. J.* **2008**, *14*, 3653.

3.3.8 Supporting Information

Table 3.3.8. Crystal data and structure refinement for [Ir(cod)(**L11a**)]BArF Ir-catalyzed asymmetric hydrogenation of trisubstituted olefins.

Identification code	[Ir(cod)(**L11a**)]BArF
Empirical formula	C81 H80 B F24 Ir N O4 P
Formula weight	1821.44
Temperature	100(2) K
Wavelength	0.71073 Å
Crystal system	Monoclinic
Space group	P2(1)
Unit cell dimensions	a = 10.2560(12) Å a= 90.00 °.
	b = 41.907(5) Å b = 97.396(3) °.
	c = 18.538(2) Å g = 90.00 °.
Volume	7901.5(16) $Å^3$
Z	4
Density (calculated)	1.531 Mg/m^3
Absorption coefficient	1.817 mm^{-1}
F(000)	3672
Crystal size	0.20 x 0.20 x 0.03 mm^3
Theta range for data collection	2.60 to 39.53 °.
Index ranges	-18 <=h<=18 ,-74 <=k<=39 ,-33 <=l<=32
Reflections collected	73138
Independent reflections	61684 [R(int) = 0.0677]
Completeness to theta =39.53 °	0.966 %
Absorption correction	Empirical
Max. and min. transmission	0.9475 and 0.7127
Refinement method	Full-matrix least-squares on F^2
Data / restraints / parameters	73138 / 163 / 2096
Goodness-of-fit on F^2	1.017
Final R indices [I>2sigma(I)]	R1 = 0.0525 , wR2 = 0.1289
R indices (all data)	R1 = 0.0648 , wR2 = 0.1342
Largest diff. peak and hole	8.414 and -2.461 $e.Å^{-3}$

For bond lengths [Å] and angles [°] see: http://pubs.acs.org/doi/suppl/10.1021/ja904152r

3.4 Expanded scope of the asymmetric Ir-catalyzed hydrogenation of minimally functionalized olefins using phosphite-thiazoline ligands

Javier Mazuela, Oscar Pàmies and Montserrat Diéguez in manuscript to be submitted.

3.4.1. Abstract

We have extended the ligand design of one of the most successful phosphite-oxazoline ligands (**L6**-**L21**, Chapter 3.3) in the Ir-catalyzed hydrogenation of minimally functionalized olefins by replacing the oxazoline group with a thiazoline moiety. A small but structurally important library of Ir-phosphite-thiazoline precatalysts (Ir-**L27**-**L28a**-**g**) have been developed by changing the substituents/configurations at the biaryl phosphite group. We have found that replacing the oxazoline with a thiazoline moiety in the ligand design has been beneficial in terms of substrate scope.

3.4.2. Introduction

The synthetic challenges arising from the high degree of enantiopurity required in life-science products have stimulated the development and industrial application of asymmetric catalysis.[1] Asymmetric hydrogenation is a fundamental technique in the modern organic chemist's repertoire of reliable catalytic methods for constructing optically active compounds. High enantioselectivity, low catalyst loadings, essentially quantitative yields, perfect atom economy, and mild conditions are attractive features of this transformation as is evident in the ever growing list of publications using these methods.[1] Whereas the reduction of olefins containing an adjacent polar group (i.e. dehydroamino acids) by Rh- and Ru- catalyst precursors modified with phosphorus ligands has a long history, the asymmetric hydrogenation of minimally functionalized olefins is less developed because these substrates have no adjacent polar group to direct the reaction.[2] A breakthrough in the hydrogenation of this type of substrate was made when Pfaltz and coworkers used Ir-complexes [Ir(PHOX)(cod)]BAr_F modified with phosphine-oxazoline PHOX ligands as chiral analogues of Crabtree's catalyst ([Ir(py)(PCy_3)(cod)]PF_6).[3] Since then the composition of ligands has been extended by introducing P-donor groups (or carbene analogues) other than phosphines and N-donor groups other than oxazolines, and varying the chiral backbone.[4] However, most of the chiral catalysts developed are still highly substrate-dependent and the development of efficient chiral ligands that tolerate a broader range of substrates remain a challenge.[2]

Some years ago we discovered that the presence of biaryl-phosphite moieties in ligand design is highly advantageous in this process.[5] Ir/phosphite-oxazoline catalytic systems provided greater substrate versatility than previous Ir/phosphinite-oxazoline systems, and high activities and enantioselectivities for several largely unfunctionalized *E*- and *Z*-trisubstituted and 1,1-disubstituted olefins. In this context, in 2008 we successfully used an amino acid-derived phosphite-oxazoline ligand library (Figure 3.4.1) to reduce minimally functionalized olefins,[5b-c] one of the two phosphite-containing ligand families with the broadest substrate scope.[5a-c,e] Although this phosphite-oxazoline ligand library proved to be highly efficient in the hydrogenation of

unfunctionalized aryl-alkyl *E*-trisubstituted and 1,1-disubstituted olefins, some substrates (such as *Z*-trisubstituted olefins, α,β-unsaturated ketones and trifluoromethyl olefins) still need to improve their enantioselectivities.

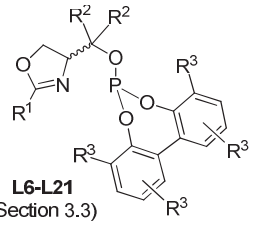

Figure 3.4.1. Basic structure of the amino acid-derived phosphite-oxazoline ligand library.

To address this point, in this chapter we used the amino acid derived-phosphite-oxazoline ligand library structure to design a new family of ligands in which the oxazoline group is replaced by a thiazoline moiety (ligands **L27**-**L28a**-**g**, Figure 3.4.2). We expected the subtle variation in the basicity of the N-donor group (the thiazoline group is more basic than the oxazoline) and the steric properties caused by the substituent at the N-heteroatom ring replacing the identity of the non-coordinating heteroatom to allow the catalysts to be fine-tuned for the most challenging substrates. We therefore report here the application of a small but structurally relevant library of Ir-phosphite-thiazoline precatalysts (Ir-**L27**-**L28a**-**g**) in the asymmetric hydrogenation of a wide range of *E*- and *Z*-trisubstituted and 1,1'-disubstituted terminal olefins, including examples with neighboring polar groups. The reactivity and selectivity of these new Ir-phosphite-thiazoline catalysts are excellent and similar to those of the phosphite-oxazoline analogues for most of the substrates and they performed better for the more challenging substrates.

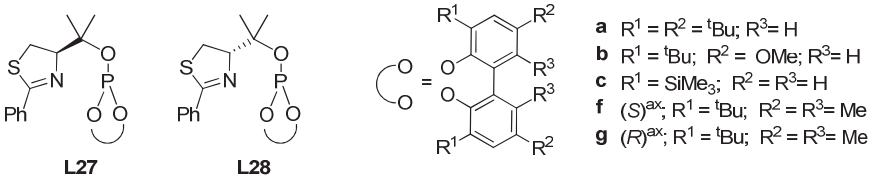

Figure 3.4.2. Phosphite-thiazoline ligands **L27**-**L28a**-**g**.

3.4.3. Results and discussions

3.4.3.1. Synthesis of ligands

Scheme 3.4.1 illustrates the sequence of ligand synthesis. Ligands **L27**-**L28a**-**g** were synthesized efficiently from the corresponding easily accessible (*R*)-cysteine methyl ester hydrochloride (**1**, Scheme 3.4.1). In the first step of the ligand synthesis, compound **1** was coupled with ethyl benzimidate hydrochloride in the presence of triethylamine to produce the corresponding thiazoline ester **2** in 61% enantiomeric excess (Scheme 3.4.1, step (a)).[6] Subsequent reduction of the ester group with MeMgBr afforded hydroxyl thiazoline **3** in 40% ee (Scheme 3.4.1, step (b)). Further enantiomer resolution using semipreparative chiral HPLC gave access to both enantiomers of hydroxyl-thiazoline compound **3**. In the last step of the ligand

synthesis, several phosphoric acid biaryl esters (**a**-**g**) were attached to this basic framework. Therefore, treatment of hydroxyl-thiazoline **3** with 1 equivalent of the appropriate *in situ* formed phosphorochloridite ($ClP(OR)_2$; $(OR)_2$ = **a**-**g**) in the presence of pyridine provided the desired phosphite-thiazoline ligands **L27-L28a**-**g** (Scheme 3.4.1, step (c)).

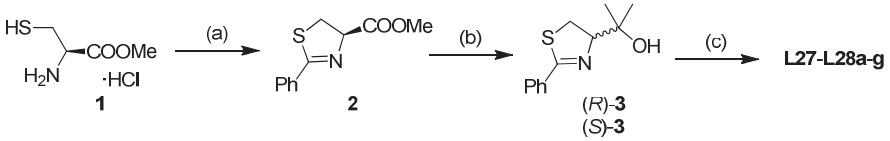

Scheme 3.4.1. Synthesis of new phosphite-thiazoline ligands **L27**-**L28a**-**g**. (a) Ref 6; (b) MeMgBr/THF/Et_2O; (c) $ClP(OR)_2$; $(OR)_2$ = **a**-**g** / Py / toluene.

All the ligands were stable during purification on neutral alumina under an atmosphere of argon and they were isolated in moderate-to-good yields as white solids. They were stable at room temperature and very stable to hydrolysis. Elemental analyses were in agreement with the structure assigned. The ^{1}H, ^{31}P and ^{13}C NMR spectra were as expected for these C_1 ligands. Rapid ring inversions (tropoisomerization) in the biphenyl-phosphorus moieties (**a**-**c**) occurred on the NMR time scale since the expected diastereoisomers were not detected by low-temperature phosphorus NMR.[7]

3.4.3.2. Synthesis of the Ir-catalyst precursors

Ir-complexation and subsequent chloride abstraction with sodium tetrakis[3,5-bis(trifluoromethyl)phenyl]borate ($NaBAr_F$) were performed in a one-pot process using previously literature procedure[5] affording $[Ir(cod)(L)]BAr_F$ (L = **L27**-**L28a**-**g**) complexes in almost quantitative yields as air-stable orange solids (Scheme 3.4.2).

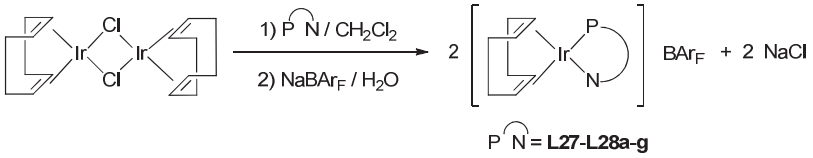

Scheme 3.4.2. Synthesis of catalyst precursors $[Ir(cod)(P\text{-}N)]BAr_F$ (P-N = **L27**-**L28a**-**g**).

The complexes were characterized by elemental analysis and ^{1}H, ^{13}C, and ^{31}P NMR spectroscopy. The spectral assignments were based on information from ^{1}H–^{1}H and ^{13}C–^{1}H correlation measurements and were as expected for these C_1 iridium complexes. The VT-NMR spectra indicate that only one isomer is present in solution. One singlet in the ^{31}P-{^{1}H} NMR spectra was obtained in all cases.[8]

3.4.3.3. Asymmetric hydrogenation of trisubstituted olefins

Asymmetric hydrogenation of minimally functionalized E- and Z-trisubstituted olefins

In order to evaluate the potential of phosphite-thiazoline ligands **L27**-**L28a**-**g** in the Ir-catalyzed hydrogenation of *E*-trisubstituted olefins a comparative study using substrates **S1**-**S4** was carried out. The results are shown in Table 3.4.1. Excellent activities and enantioselectivities (up to 99%) were obtained. We found that enantioselectivity is slightly affected by the substituents at the biaryl phosphite-moiety (Table 3.4.1, entries 1 and 2 *vs* 3). The best enantioselectivities were obtained with ligand **L27c** containing bulky trimethylsilyl groups at the *ortho* position of the biphenyl phosphite moiety (Table 3.4.1, entry 3). We also found that the configuration at the biaryl phosphite moiety does not affect enantioselectivity (Table 3.4.1, entries 4 and 5). This contrasts with the positive effect on enantioselectivity observed in related phosphite-oxazoline ligands when enantiopure *S*-configurated biaryl phosphite moieties were used.[5b]

Table 3.4.1. Ir-catalyzed asymmetric hydrogenation of several *E*-trisubstituted substrates **S1**-**S4** using phosphite-thiazoline ligands **L27**-**L28a**-**g**[a]

		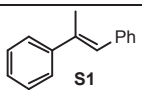 **S1**	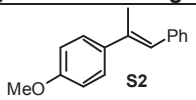 **S2**	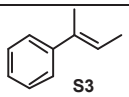 **S3**	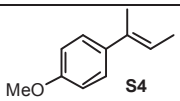 **S4**
Entry	Ligand	% ee[b]	% ee[b]	% ee[b]	% ee[b]
1	**L27a**	97 (*R*)	96 (*R*)	96 (*R*)	96 (*R*)
2	**L27b**	98 (*R*)	97 (*R*)	96 (*R*)	96 (*R*)
3	**L27c**	99 (*R*)	99 (*R*)	98 (*R*)	98 (*R*)
4	**L27f**	97 (*R*)	96 (*R*)	97 (*R*)	95 (*R*)
5	**L27g**	97 (*R*)	96 (*R*)	96 (*R*)	95 (*R*)
6	**L28a**	97 (*S*)	96 (*S*)	95 (*S*)	96 (*S*)

[a] Reactions carried out at room temperature by using 0.5 mmol of substrate and 0.25 mol% of Ir-catalyst precursor at 50 bar of H_2 using dichloromethane (2 mL) as solvent. Full conversions were obtained in all cases after 2 h. [b] Enantiomeric excess determined by HPLC (substrates **S1** and **S2**) or GC (substrates **S3** and **S4**).

Finally, when we compared the results obtained with ligands **L27a** and **L28a** we found that the different configuration of the alkyl backbone chain controls the sense of the enantioselectivity (Table 3.4.1, entries 1 *vs* 6). Both enantiomers of the reduced products are therefore accessible in high enantioselectivities. Overall, catalyst Ir-**L27c** offers the best enantioselectivity and compares well with the analogous phosphite-oxazoline catalyst.[5b]

In order to further assess the scope of phosphite–thiazoline ligands **L27**-**L28a**-**g**, we then moved on to investigate the asymmetric hydrogenation of more demanding *Z*-isomers (**S5**-**S7**), which are usually hydrogenated less enantioselectively than the corresponding *E*-isomers. By carefully selecting the ligand parameters we were able to obtain both enantiomers of the hydrogenated products in high enantioselectivities (ee's up to 96%) using Ir-**L27a** and Ir-**L28a** catalytic systems. The results, which are shown in Table 3.4.2, followed a different trend than for *E*-substrates. Enantioselectivities were therefore affected by both the substituents and the configuration of the biaryl phosphite moiety. Unlike the hydrogenation of *E*-substrates, enantioselectivities improved by introducing bulky substituents at the *para* positions of the biaryl

phosphite moiety (i.e. ^{t}Bu> OMe > H; Table 3.4.2, entries 1-3). We also found a cooperative effect between the configurations of the biaryl phosphite moiety and the ligand backbone that leads to a matched combination for ligand **L27g**, with an *R*-biaryl configuration (Table 3.4.2, entries 4 and 5). However, enantioselectivities were best with tropoisomeric biphenyl-containing ligand **L27a** containing *tert*-butyl groups at both *ortho* and *para* positions. This confirms that although the configuration of the biaryl phosphite moiety affects enantioselectivity, the presence of a *tert*-butyl group at the *para* position of the biaryl phosphite moiety is crucial if enantioselectivities are to be high.

Table 3.4.2. Ir-catalyzed asymmetric hydrogenation of several *Z*-trisubstituted substrates **S5**-**S7** using phosphite-thiazoline ligands **L27**-**L28a**-**g**[a]

		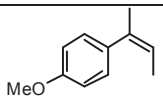 **S5**	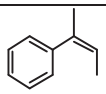 **S6**	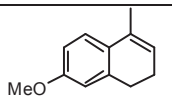 **S7**
Entry	Ligand	% ee[b]	% ee[b]	% ee[b]
1	**L27a**	95 (*S*)	94 (*S*)	96 (*S*)
2	**L27b**	83 (*S*)	84 (*S*)	83 (*S*)
3	**L27c**	79 (*S*)	79 (*S*)	80 (*S*)
4	**L27f**	58 (*S*)	61 (*S*)	72 (*S*)
5	**L27g**	74 (*S*)	73 (*S*)	81 (*S*)
6	**L28a**	94 (*R*)	94 (*R*)	95 (*R*)

[a] Reactions carried out at room temperature by using 0.5 mmol of substrate and 0.25 mol% of Ir-catalyst precursor at 50 bar of H_2 using dichloromethane (2 mL) as solvent. Full conversions were obtained in all cases after 2 h. [b] Enantiomeric excess determined by GC.

Interestingly, when the results of reducing *E*- and *Z*-trisubstituted olefins are compared with the enantioselectivities obtained with their corresponding Ir-phosphite-oxazoline systems, we can conclude that introducing a thiazoline moiety into the ligand design is advantageous. Therefore, while for *E*-trisubstituted olefins comparable excellent enantioselectivities were obtained, for *Z*-trisubstituted olefins enantioselectivities improved using phosphite-thiazoline ligands. In summary, by appropriately tuning the thiazoline-based ligands excellent enantioselectivities were achieved in the hydrogenation of both *E*- and *Z*-trisubstituted olefins.

Asymmetric hydrogenation of trisubstituted olefins containing a neighboring polar group

Substrates bearing a neighboring polar group need to be reduced because they are important intermediates in the synthesis of high-value chemicals and they allow for further functionalization. We therefore decided to further study the potential of our phosphite–thiazoline ligands **L27**-**L28a**-**g** in the reduction of a wide range of trisubstituted alkenes containing several types of polar groups. The results are summarized in Scheme 3.4.3. Again, excellent enantioselectivities were obtained in both enantiomers of the reduction products (ee values up to 99%) for a range of substrates under mild reaction conditions by suitable tuning of the ligand parameters.

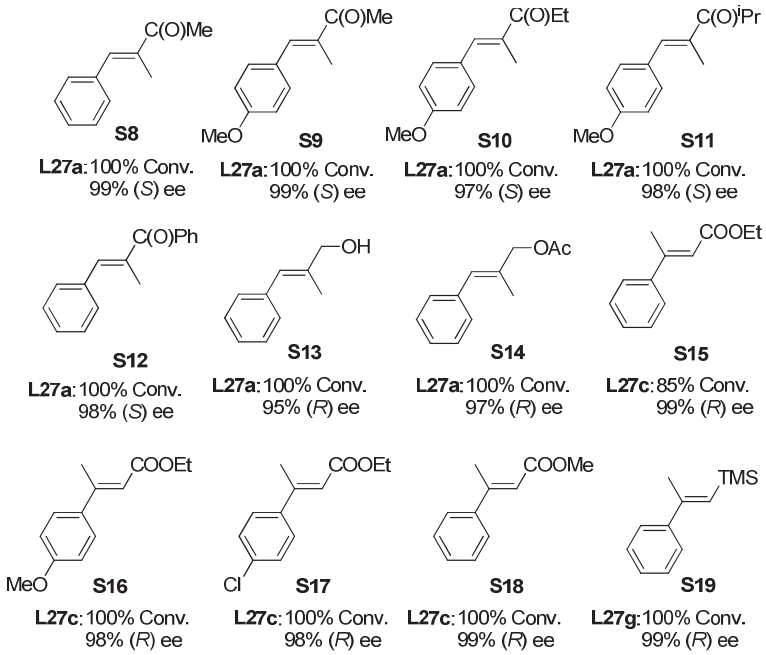

Scheme 3.4.3. Selected hydrogenation results of trisubstituted olefins bearing a neighboring polar group using [Ir(cod)(**L27**-**L28a**-**e**)]BAr_F catalyst precursors. Reaction conditions: 0.5 mol % catalyst precursor, CH_2Cl_2 as solvent, 50 bar H_2, rt, 2 h.

We first studied the hydrogenation of several α,β–unsaturated ketones (**S8**-**S12**) and obtained enantioselectivities up to 99% in both enantiomers of the hydrogenated product using Ir-**L27a** and Ir-**L28a** catalytic systems. It should be noted that ee's are highly independent of the electronic nature of the substrate phenyl ring and the substituent in the ketone functionality. Ir-**L27a** and Ir-**L28a** also provided excellent enantioselectivities in the reduction of allylic alcohol (**S13**) and allylic acetate (**S14**). If we compare all these results with those achieved using related Ir-phosphite-oxazoline catalysts, again the introduction of a thiazoline group was beneficial for enantioselectivity (i.e. for substrate **S8**, ee's improved from 93% when the related phosphite-oxazoline ligand was used[9] to 99%). We then went on to study the hydrogenation of several α,β-unsaturated esters (**S15**-**S18**). We were pleased to find that excellent enantioselectivities can also be achieved with the Ir-**L27c** catalytic system (ee's up to >99%). As for α,β-unsaturated ketones, enantioselectivites are highly independent of the electronic nature of the substrate phenyl ring and the substituent in the ester function, which allows the successful asymmetric reduction of a wide range of α,β-unsaturated esters. High enantioselectivities (up to 99% ee) were also obtained in the hydrogenation of vinylsilane **S19** using the Ir-**L27g** catalytic system. This is therefore one of the few catalytic systems that can hydrogenate a wide range of trisubstituted olefins, including those with a neighboring polar group, in high activities and enantioselectivities.[2]

3.4.3.4. Asymmetric hydrogenation of 1,1-disubstituted terminal olefins

To further study the potential of phosphite-thiazoline ligands **L27**-**L28a**-**g**, we tested them in the asymmetric hydrogenation of more demanding terminal olefins.[10] The enantioselectivity

obtained with 1,1-disubstituted terminal olefins is lower than with trisubtituted olefins largely because of the isomerization of the terminal double bond to the more stable internal alkene, which usually leads to the predominant formation of the opposite enantiomer of the hydrogenated product, and/or to difficulty in controlling face selectivity.[2d-e] Few known catalytic systems provide high enantioselectivities for these substrates, and those that do usually have limited substrate scope.[2d-e,9a-b,11] Related phosphite-oxazoline ligands (**L6**-**L21**, Figure 3.4.1) are one of the two most versatile ligand families for the hydrogenation of this substrate class.[5c]

In an initial set of experiments we used the Ir-catalyzed asymmetric hydrogenation of 2-(4-methoxyphenyl)but-1-ene **S20**. The results in optimized conditions are shown in Table 3.4.3. We were again able to fine-tune the ligand parameters to produce high activities and enantioselectivities (ee's up to 99%) in the hydrogenation of this substrate using ligand **L27g** at low catalyst loadings (0.25 mol%) and hydrogen pressures (1 bar). Again, both enantiomers of the hydrogenated product can be obtained by simply changing the configuration of the alkyl backbone chain (i.e., Table 3.4.3, entries 1 *vs* 6). In contrast to the reduction of *E*-trisubstituted substrates, enantioselectivity is mainly affected by the configuration at the biaryl phosphite moiety (Table 3.4.3, entries 4 and 5). This behavior is similar to that observed in the hydrogenation of *Z*-trisubstitued olefins. However, for disubstituted substrate **S20**, the presence of an enantiopure bulky (*R*)-biaryl phosphite moiety is crucial if the enantioselectivities of the ligand series ar to be highest. This finding contrasts with positive effect on enantioselectivity observed when an *S*-biaryl phosphite moiety was used in related phosphite-oxazoline ligands.[5c]

Table 3.4.3. Ir-catalyzed hydrogenation of **S20** using ligands **L27-L28a-g**[a]

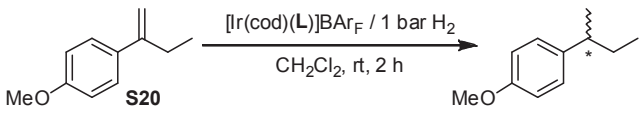

Entry	Ligand	% Conv[b]	% ee[c]
1	**L27a**	100	94 (*S*)
2	**L27b**	100	92 (*S*)
3	**L27c**	100	95 (*S*)
4	**L27f**	100	78 (*S*)
5	**L27g**	100	99 (*S*)
6	**L28a**	100	94 (*R*)

[a] Reactions carried out using 0.5 mmol of **S20** and 0.25 mol% of Ir-catalyst precursor at 1 bar of H_2.[b] Conversion measured by GC after 2 hours. [c] Enantiomeric excesses determined by chiral GC.

Next, we evaluated the phosphite-thiazoline ligands **L27**-**L28a**-**g** in the asymmetric hydrogenation of other 1,1-disubstituted substrates, including those containing an heteroaromatic ring and a neighboring polar group. The most noteworthy results are shown in Table 3.4.4. The results followed the same trend as for the hydrogenation of model substrate **S20**. Again, the catalyst precursor containing the phosphite-thiazoline ligand **L27g** provided the best enantioselectivities.

Our results with several 1,1-disubstituted aryl-alkyl substrates (**S20**-**S28**) indicated that enantioselectivity is relatively insensitive to the electronic effects in the aryl ring and to the steric properties of the alkyl substituent. Therefore, several *para*-substituted 2-phenylbut-2-enes (**S20**-**S22**; Table 3.4.3, entry 5 and Table 3.4.4, entries 1 and 2) and several α-alkylstyrenes (**S23**-**S28**; Table 3.4.4, entries 3-8) were hydrogenated an excellent levels of enantioselectivity were achieved (ee's ranging from 91-99%). Although these results are comparable to those obtained with related phosphite-oxazoline ligands, it should be noted that for substrates **S23**-**S25** the presence of a thiazoline group led to higher enantioselectivities (i.e. for substrate **S23**, ee's increased from 94% to 98%).

Table 3.4.4. Selected results for the Ir-catalyzed hydrogenation of minimally functionalized 1,1-disubstituted terminal olefins using ligands **L27**-**L28a-g**[a]

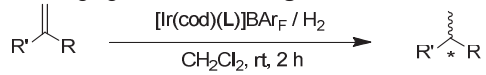

R' = aryl, 2-pyridine, 2-thiophene
R = alkyl, CH_2OH, CH_2OAc, CH_2TMS, CF_3

Entry	Substrate	Ligand	% ee[b]	Entry	Substrate	Ligand	% ee[b]
1	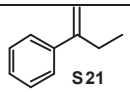 S21	**L27g**	99 (*S*)	9	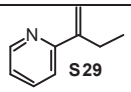 S29	**L27g**	98 (+)
2	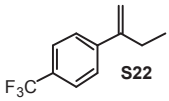 S22	**L27g**	98 (*S*)	10	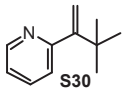 S30	**L27g**	99 (+)
3	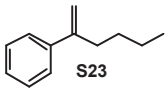 S23	**L27g**	98 (*S*)	11	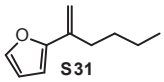 S31	**L27g**	95 (-)
4	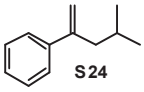 S24	**L27g**	97 (*S*)	12[c]	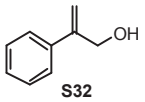 S32	**L27g**	94 (*R*)
5	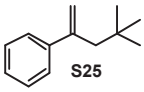 S25	**L27g**	93 (*S*)	13[c]	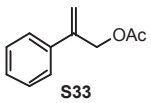 S33	**L27g**	91 (*R*)
6	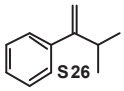 S26	**L27g**	91 (*S*)	14[c]	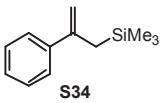 S34	**L27g**	93 (*S*)
7	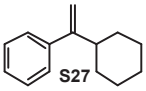 S27	**L27g**	94 (*S*)	15	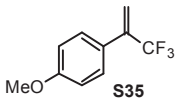 S35	**L27g**	99 (-)
8	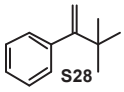 S28	**L27g**	99 (*S*)				

[a] Reactions carried out using 0.5 mmol of substrate and 0.25 mol% of Ir-catalyst precursor at 1 bar of H_2. Full conversion were achieved after 2 h. [b] Enantiomeric excesses determined by chiral GC (except for entries 11-13 that were measured by HPLC). [c] Reaction carried out at 50 bar of H_2.

Because heterocycles are of interest to industry and the heterocyclic part can be further modified posthydrogenation, we then moved on to investigate whether phosphite-thiazoline ligands can also be used in the hydrogenation of 1,1-heteroaromatic terminal olefins (Table 3.4.4, entries 9-11). We were pleased to find that several pyridine- and thiophene-containing substrates (**S29**-**S31**) were also readily hydrogenated in high enantioselectivities using the Ir-**L27g** catalytic system (ee's up to 99%).

Finally, we also examined the hydrogenation of several 1,1-disubstitued terminal olefins containing a neighboring polar group, which give rise to important intermediates for the synthesis of high-value products (i.e. derivatives of the hydrogenated product 2-phenylpropanol are frequently used in the fragrance industry)[12]. Allylic alcohol **S32**, allylic acetate **S33** and allylic silane **S34** were hydrogenated with similar high efficiencies (ee's ranging from 91-94%; Table 3.4.4, entries 12-14). Catalyst Ir-**L27g** clearly outperforms related phosphite-oxazoline ligands in the asymmetric hydrogenation of trifluoromethyl-olefin **S35** (99% ee using Ir-**L27g** *vs* 75% ee using related phosphite-oxazoline catalysts). This result compares favorably with the best reported in the literature and opens up the possibility of using Ir-hydrogenation catalysts for developing chiral organofluorine drug intermediates.[13]

3.4.4. Conclusions

We have extended the ligand design of one of the most successful phosphite-oxazoline ligands (**L6**-**L21**, Chapter 3.3) in the Ir-catalyzed hydrogenation of minimally functionalized olefins by replacing the oxazoline group with a thiazoline moiety. A small but structurally important library of Ir-phosphite-thiazoline precatalysts (Ir-**L27**-**L28a**-**g**) have been developed by changing the substituents/configurations at the biaryl phosphite group. By appropriate tuning of these ligand parameters we achieved excellent enantioselectivities in the hydrogenation of a wide range of *E*- and *Z*-trisubstituted and 1,1'-disubstituted terminal olefins, including examples with neighboring polar groups. We have found that replacing the oxazoline with a thiazoline moiety in the ligand design has been beneficial in terms of substrate scope. Thus, the range of substrates that can be hydrogenated with excellent enantioselectivities with the new Ir-phosphite-thiazoline catalysts has been extended because more challenging *Z*-trisubstituted olefins, α,β-unsaturated ketones and trifluoromethyl olefins have been included. These results open up a new class of ligands for the highly enantioselective Ir-catalyzed hydrogenation of a wide range of substrates, which compares favorably with the best reported in the literature.

3.4.5. Experimental section

3.4.5.1. General considerations

All reactions were carried out using standard Schlenk techniques under an argon atmosphere. Solvents were purified and dried by standard procedures. Phosphorochloridites are easily prepared in one step from the corresponding biaryls.[14] ^{1}H, $^{13}C\{^{1}H\}$, and $^{31}P\{^{1}H\}$ NMR spectra were recorded using a 400 MHz spectrometer. Chemical shifts are relative to that of $SiMe_4$ (^{1}H and ^{13}C) as internal standard or H_3PO_4 (^{31}P) as external standard. ^{1}H, ^{13}C and ^{31}P assignments were made

on the basis of ^{1}H-^{1}H gCOSY, ^{1}H-^{13}C gHSQC and ^{1}H-^{31}P gHMBC experiments. All catalytic experiments were performed three times.

3.4.5.2. General procedure for the preparation of the phosphite-thiazoline ligands

The corresponding phosphorochloridite (3.0 mmol) produced *in situ* was dissolved in toluene (12.5 mL) and pyridine (1.14 mL, 14 mmol) was added. The corresponding hydroxyl-thiazoline compound (2.8 mmol) was azeotropically dried with toluene (3 x 2 mL) and then dissolved in toluene (12.5 mL) to which pyridine (1.14 mL, 14 mmol) was added. The oxazoline solution was transferred slowly at 0 ºC to the solution of phosphorochloridite. The reaction mixture was stirred overnight at 80 ºC, and the pyridine salts were removed by filtration. Evaporation of the solvent gave a white foam, which was purified by flash chromatography in alumina to produce the corresponding ligand as a white solid.

L27a. Yield: 455 mg (69 %). ^{31}P NMR ($CDCl_3$), δ: 148.5 (s). ^{1}H NMR (C_6D_6), δ: 1.54 (s, 9H, CH_3, ^{t}Bu), 1.60 (s, 3H, CH_3), 1.63 (s, 9H, CH_3, ^{t}Bu), 1.74 (s, 9H, CH_3, ^{t}Bu), 1.77 (s, 9H, CH_3, ^{t}Bu), 1.94 (s, 3H, CH_3), 2.52 (dd, 1H, $^{2}J_{H\text{-}H}$= 11.6 Hz, $^{3}J_{H\text{-}H}$= 9.6 Hz, CH_2-S), 2.79 (dd, 1H, $^{2}J_{H\text{-}H}$= 11.6 Hz, $^{3}J_{H\text{-}H}$= 10 Hz, CH_2-S), 4.56 (m, 1H, CH-N), 7.2-8.2 (m, 9H, CH=). ^{13}C NMR (C_6D_6), δ: 23.3 (CH_3), 27.2 (d, CH_3, $J_{C\text{-}P}$= 11.8 Hz), 31.3 (CH_3, ^{t}Bu), 31.5 (CH_3, ^{t}Bu), 31.6 (CH_3, ^{t}Bu), 33.5 (CH_2-S), 34.9 (C, ^{t}Bu), 35.1 (C, ^{t}Bu), 35.2 (C, ^{t}Bu), 35.4 (C, ^{t}Bu), 81.8 (C), 86.3 (CH-N), 124.3 (CH=), 124.7 (CH=), 125.2 (C), 126.8 (CH=), 126.9 (CH=), 127.1 (CH=), 128.3 (CH=), 128.5 (CH=), 128.6 (CH=), 128.7 (CH=), 128.9 (CH=), 127.4 (C), 128.4 (CH=), 130.4 (CH=), 131.2 (CH=), 133.3 (C), 137.8 (C), 140.2 (C), 145.1 (C), 146.1 (CH=), 167.9 (C=N). Anal. calcd (%) for $C_{40}H_{54}NO_3PS$: C 72.80, H 8.25, N 2.12, S 4.96; found: C 72.85, H 8.28, N 2.09, S 4.90.

L27b. Yield: 353 mg (58 %). ^{31}P NMR ($CDCl_3$), δ: 149.3 (s). ^{1}H NMR (C_6D_6), δ: 1.47 (s, 9H, CH_3, ^{t}Bu), 1.60 (s, 3H, CH_3), 1.62 (s, 9H, CH_3, ^{t}Bu), 1.84 (s, 3H, CH_3), 2.67 (dd, 1H, $^{2}J_{H\text{-}H}$= 12.4 Hz, $^{3}J_{H\text{-}H}$= 8.8 Hz, CH_2-S), 2.87 (dd, 1H, $^{2}J_{H\text{-}H}$= 12.4 Hz, $^{3}J_{H\text{-}H}$= 10 Hz, CH_2-S), 3.26 (s, 3H, CH_3-O), 3.28 (s, 3H, CH_3-O), 4.39 (m, 1H, CH-N), 6.6-8.2 (m, 9H, CH=). ^{13}C NMR (C_6D_6), δ: 23.5 (d, CH_3, $J_{C\text{-}P}$= 4.3 Hz), 28.4 (d, CH_3, $J_{C\text{-}P}$= 11.8 Hz), 31.0 (CH_3, ^{t}Bu), 31.2 (CH_3, ^{t}Bu), 32.9 (CH_2-S), 34.9 (C, ^{t}Bu), 35.1 (C, ^{t}Bu), 55.3 (CH_3-O), 81.3 (C), 87.2 (CH-N), 113.2 (CH=), 113.5 (CH=), 114.7 (CH=), 114.9 (CH=), 126.5 (CH=), 128.3 (CH=), 128.5 (CH=), 128.9 (CH=), 130.9 (C), 134.5 (CH=), 134.7 (CH=), 137.3 (C), 142.7 (C), 142.9 (C), 155.9 (C), 165.7 (C=N). Anal. calcd (%) for $C_{34}H_{42}NO_5PS$: C 67.19, H 6.97, N 2.30, S 5.28; found: C 67.29, H 7.01, N 2.26, S 5.22.

L27c: Yield: 377 mg, 66 %. ^{31}P NMR ($CDCl_3$), δ: 154.2 (s). ^{1}H NMR (C_6D_6), δ: 0.34 (s, 9H, CH_3-$SiMe_3$), 0.43 (s, 9H, CH_3-$SiMe_3$), 1.54 (s, 3H, CH_3), 1.92 (s, 3H, CH_3), 2.62 (dd, 1H, $^{2}J_{H\text{-}H}$= 12.0 Hz, $^{3}J_{H\text{-}H}$= 9.2 Hz, CH_2-S), 2.81 (dd, 1H, $^{2}J_{H\text{-}H}$= 12.0 Hz, $^{3}J_{H\text{-}H}$= 10.4 Hz, CH_2-S), 4.42 (m, 1H, CH-N), 6.9-8.2 (m, 11H, CH=). ^{13}C NMR (C_6D_6), δ: 0.0 (d, CH_3-Si, $J_{C\text{-}P}$= 4.3 Hz), 0.4 (CH_3-Si), 23.8 (CH_3), 28.4 (d, CH_3, $J_{C\text{-}P}$= 9.4 Hz), 33.5 (CH_2-S), 82.4 (C), 86.8 (CH-N), 124.7 (CH=), 124.8 (CH=), 128.9 (CH=), 129.4 (CH=), 130.1 (C), 131.4 (CH=), 131.8 (C), 132.0 (C), 132.5 (CH=), 133.1 (CH=), 135.1 (CH=), 137.3 (C), 155.2 (C), 155.6 (C), 165.2 (C=N). Anal. calcd (%) for $C_{30}H_{38}NO_3PSSi_2$: C 62.14, H 6.61, N 2.42, S 5.53; found: C 62.19, H 6.64, N 2.38, S 5.49.

L27f: Yield: 428 mg, 71 %. ^{31}P NMR (400 MHz, C_6D_6) δ: 150.6 (s). ^{1}H NMR (C_6D_6), δ: 1.48 (s, 9H, CH_3, ^{t}Bu), 1.55 (s, 9H, CH_3, ^{t}Bu), 1.60 (s, 3H, CH_3), 1.62 (s, 3H, CH_3), 1.73 (s, 3H, CH_3), 1.80 (s, 3H, CH_3), 2.01 (s, 3H, CH_3), 2.07 (s, 3H, CH_3), 2.57 (dd, 1H, $^{2}J_{H\text{-}H}$= 12.0 Hz, $^{3}J_{H\text{-}H}$= 8.8 Hz, CH_2-S), 2.83 (dd, 1H, $^{2}J_{H\text{-}H}$= 12.0 Hz, $^{3}J_{H\text{-}H}$= 10 Hz, CH_2-S), 4.53 (m, 1H, CH-N), 6.7-8.2 (m, 7H,

CH=). ^{13}C NMR (C_6D_6), δ: 16.9 (CH_3-Ar), 17.1 (CH_3-Ar), 19.2 (CH_3-Ar), 20.1 (CH_3-Ar), 23.6 (CH_3), 28.1 (d, CH_3, J_{C-P}= 7.8 Hz), 31.4 (CH_3, ^{t}Bu), 32.1 (CH_3, ^{t}Bu), 33.7 (CH_2-S), 82.1 (C), 87.3 (CH-N), 123.8 (CH=), 128.3 (CH=), 127.0 (C), 127.3 (C), 128.9 (CH=), 132.2 (CH=), 132.7 (CH=), 133.0 (C), 137.3 (C), 144.9 (C), 146.1 (C), 146.7 (C), 148.8 (C), 149.1, 167.4 (C=N). Anal. calcd (%) for $C_{36}H_{46}NO_3PS$: C 71.61, H 7.68, N 2.32, S 5.31; found: C 71.67, H 7.70, N 2.29, S 5.27.

L27g: Yield: 380 mg, 63 %. ^{31}P NMR (400 MHz, C_6D_6) δ: 152.1 (s). ^{1}H NMR (C_6D_6), δ: 1.46 (s, 9H, CH_3, ^{t}Bu), 1.54 (s, 9H, CH_3, ^{t}Bu), 1.58 (s, 3H, CH_3), 1.64 (s, 3H, CH_3), 1.75 (s, 3H, CH_3), 1.89 (s, 3H, CH_3), 2.01 (s, 3H, CH_3), 2.05 (s, 3H, CH_3), 2.61 (dd, 1H, $^2J_{H-H}$= 12.0 Hz, $^3J_{H-H}$= 7.2 Hz, CH_2-S), 2.81 (dd, 1H, $^2J_{H-H}$= 12.0 Hz, $^3J_{H-H}$= 10 Hz, CH_2-S), 4.58 (m, 1H, CH-N), 6.7-8.2 (m, 7H, CH=). ^{13}C NMR (C_6D_6), δ: 16.8 (CH_3-Ar), 17.1 (CH_3-Ar), 19.8 (CH_3-Ar), 20.0 (CH_3-Ar), 23.5 (CH_3), 28.2 (d, CH_3, J_{C-P}= 7.8 Hz), 31.5 (CH_3, ^{t}Bu), 31.7 (CH_3, ^{t}Bu), 33.4 (CH_2-S), 82.0 (C), 87.3 (CH-N), 123.9 (CH=), 128.5 (CH=), 126.8 (C), 127.0 (C), 128.5 (CH=), 129.7 (CH=), 132.1 (CH=), 132.8 (CH=), 133.1 (C), 136.8 (C), 145.1 (C), 146.4 (C), 146.6 (C), 148.9 (C), 149.1, 167.2 (C=N). Anal. calcd (%) for $C_{36}H_{46}NO_3PS$: C 71.61, H 7.68, N 2.32, S 5.31; found: C 71.64, H 7.70, N 2.30, S 5.29.

L28a: Yield: 369 mg, 69 %. ^{31}P NMR ($CDCl_3$), δ: 149.1 (s). ^{1}H NMR (C_6D_6), δ: 1.55 (s, 9H, CH_3, ^{t}Bu), 1.62 (s, 3H, CH_3), 1.66 (s, 9H, CH_3, ^{t}Bu), 1.70 (s, 9H, CH_3, ^{t}Bu), 1.74 (s, 9H, CH_3, ^{t}Bu), 1.92 (s, 3H, CH_3), 2.51 (dd, 1H, $^2J_{H-H}$= 12.0 Hz, $^3J_{H-H}$= 9.2 Hz, CH_2-S), 2.76 (dd, 1H, $^2J_{H-H}$= 12.0 Hz, $^3J_{H-H}$= 10 Hz, CH_2-S), 4.52 (m, 1H, CH-N), 7.2-8.2 (m, 9H, CH=). ^{13}C NMR (C_6D_6), δ: 23.2 (CH_3), 27.1 (d, CH_3, J_{C-P}= 10.2 Hz), 31.5 (CH_3, ^{t}Bu), 31.6 (CH_3, ^{t}Bu), 31.7 (CH_3, ^{t}Bu), 33.1 (CH_2-S), 34.8 (C, ^{t}Bu), 35.2 (C, ^{t}Bu), 35.4 (C, ^{t}Bu), 35.8 (C, ^{t}Bu), 81.5 (C), 86.3 (CH-N), 124.2 (CH=), 124.9 (CH=), 125.1 (C), 126.7 (CH=), 126.9 (CH=), 127.0 (CH=), 128.3 (CH=), 128.4 (CH=), 128.6 (CH=), 128.9 (CH=), 130.3 (CH=), 127.2 (C), 128.4 (CH=), 130.4 (CH=), 131.2 (CH=), 133.5 (C), 137.9 (C), 140.2 (C), 145.1 (C), 146.1 (CH=), 168.1 (C=N). Anal. calcd (%) for $C_{40}H_{54}NO_3PS$: C 72.80, H 8.25, N 2.12, S 4.96; found: C 72.83, H 8.26, N 2.11, S 4.93.

3.4.5.3. Typical procedure for the preparation of [Ir(cod)(L)]BAr$_F$

The corresponding ligand (0.074 mmol) was dissolved in CH_2Cl_2 (2 mL) and [Ir(μ-Cl)cod]$_2$ (25 mg, 0.037 mmol) was added. The reaction was refluxed at 50 °C for 1 hour. After 5 min at room temperature, NaBAr$_F$ (77.1 mg, 0.082 mmol) and water (2 mL) were added and the reaction mixture was stirred vigorously for 30 min at room temperature. The phases were separated and the aqueous phase was extracted twice with CH_2Cl_2. The combined organic phases were filtered through a celite plug, dried with $MgSO_4$ and the solvent was evaporated to give the product as an orange solid.

[Ir(cod)(L27a)]BAr$_F$. Yield 124 mg (92 %). ^{31}P NMR ($CDCl_3$), δ: 99.7 (s). ^{1}H NMR (C_6D_6), δ: 1.11 (s, 3H, CH_3), 1.34 (s, 3H, CH_3), 1.46 (s, 9H, CH_3, ^{t}Bu), 1.56 (s, 9H, CH_3, ^{t}Bu), 1.64 (s, 9H, CH_3, ^{t}Bu), 1.72 (s, 9H, CH_3, ^{t}Bu), 2.1-2.3 (b, 5H, CH_2, cod), 2.32 (b, 1H, CH_2, cod), 2.39 (b, 2H, CH_2, cod), 3.25 (m, 1H, CH_2-S), 3.72 (m, 1H, CH_2-S), 4.32 (m, 1H, CH= cod), 4.54 (m, 1H, CH= cod), 5.09 (m, 1H, CH= cod), 5.13 (m, 1H, CH-N), 6.6-8.4 (m, 21H, CH=). ^{13}C NMR (C_6D_6), δ: 24.5 (CH_3), 27.5 (CH_2 cod), 27.7 (CH_2 cod), 28.4 (CH_3), 30.4 (CH_3), 30.6 (CH_3, ^{t}Bu), 30.8 (CH_3, ^{t}Bu), 31.0 (CH_2 cod), 32.2 (CH_3, ^{t}Bu), 33.3 (CH_2-S), 35.1 (C, ^{t}Bu), 35.3 (C, ^{t}Bu), 35.5 (C, ^{t}Bu), 35.7 (C, ^{t}Bu), 67.5 (CH= cod), 69.9 (CH= cod), 84.2 (CH-N), 85.5 (d, C, J_{C-P}= 4.2 Hz), 96.7 (d, CH= cod, J_{C-P}= 16.4 Hz), 104.6 (d, CH= cod, J_{C-P}= 12.0 Hz), 117.4 (b, CH=, BAr$_F$), 120-132 (aromatic

carbons), 134.7 (b, CH=, BAr_F), 135.8-157 (aromatic carbons), 161.9 (q, C-B, BAr_F, $^1J_{C-B}$ = 49 Hz), 179.9 (s, C=N). Anal. calc (%) for $C_{80}H_{78}BF_{24}IrNO_3PS$: C 52.69, H 4.31, N 0.77, S 1.76; found: C 52.73, H 4.33, N 0.75, S 1.72.

[Ir(cod)(L27b)]BAr_F. Yield 122 mg (93 %). ^{31}P NMR ($CDCl_3$), δ: 96.3 (s). ^{1}H NMR (C_6D_6), δ: 1.11 (s, 3H, CH_3), 1.34 (s, 3H, CH_3), 1.46 (s, 9H, CH_3, ^{t}Bu), 1.56 (s, 9H, CH_3, ^{t}Bu), 2.1-2.3 (b, 5H, CH_2, cod), 2.29 (b, 1H, CH_2, cod), 2.39 (b, 2H, CH_2, cod), 3.23 (m, 1H, CH_2-S), 3.68 (m, 2H, CH_2-S and CH= cod), 3.76 (s, 3H, CH_3-O), 3.77 (s, 3H, CH_3-O), 4.29 (m, 1H, CH= cod), 4.51 (m, 1H, CH= cod), 5.17 (m, 1H, CH= cod), 5.22 (m, 1H, CH-N), 6.6-8.4 (m, 21H, CH=). ^{13}C NMR (C_6D_6), δ: 24.5 (CH_3), 27.5 (CH_2 cod), 27.7 (CH_2 cod), 28.4 (CH_3), 30.4 (CH_2 cod), 30.6 (CH_3, ^{t}Bu), 30.8 (CH_3, ^{t}Bu), 31.0 (CH_2 cod), 33.1 (CH_2-S), 35.1 (C, ^{t}Bu), 35.5 (C, ^{t}Bu), 55.6 (CH_3-O), 67.2 (CH= cod), 69.8 (CH= cod), 83.6 (CH-N), 85.7 (d, C, J_{C-P}= 5.4 Hz), 95.8 (d, CH= cod, J_{C-P}= 18.7 Hz), 105.8 (d, CH= cod, J_{C-P}= 12.2 Hz), 113.2 (CH=), 114.5 (CH=), 114.8 (CH=), 117.4 (b, CH=, BAr_F), 120-132 (aromatic carbons), 134.7 (b, CH=, BAr_F), 135.8-157 (aromatic carbons), 161.9 (q, C-B, BAr_F, $^1J_{C-B}$ = 49 Hz), 182.9 (s, C=N). Anal. calc (%) for $C_{74}H_6BF_{24}IrNO_5PS$: C 50.18, H 3.58, N 0.79, S 1.81; found: C 50.24, H 3.61, N .0.76, S 1.78.

[Ir(cod)(L27c)]BAr_F. Yield 116 mg (90 %). ^{31}P NMR ($CDCl_3$), δ: 96.3 (s). ^{1}H NMR (C_6D_6), δ: 0.36 (s, 9H, CH_3-Si), 0.84 (s, 9H, CH_3-Si), 1.26 (s, 3H, CH_3), 1.42 (s, 3H, CH_3), 2.0-2.4 (b, 6H, CH_2, cod), 2.44 (b, 2H, CH_2, cod), 3.22 (m, 1H, CH_2-S), 3.59 (m, 2H, CH_2-S and CH= cod), 4.11 (m, 1H, CH= cod), 4.34 (m, 1H, CH= cod), 5.01 (m, 1H, CH= cod), 5.14 (m, 1H, CH-N), 6.6-8.4 (m, 23H, CH=). ^{13}C NMR (C_6D_6), δ: 0.2 (d, CH_3-Si, J_{C-P}= 6.2 Hz), 1.2 (CH_3-Si), 24.2 (CH_3), 27.7 (CH_2 cod), 27.9 (CH_3), 28.2 (CH_2 cod), 30.3 (CH_2 cod), 33.7 (CH_2-S), 68.3 (CH= cod), 70.3 (CH= cod), 83.7 (CH-N), 85.1 (C), 97.2 (d, CH= cod, J_{C-P}= 12.6 Hz), 104.2 (d, CH= cod, J_{C-P}= 12.6 Hz), 117.4 (b, CH=, BAr_F), 120-132 (aromatic carbons), 134.7 (b, CH=, BAr_F), 135.8-157 (aromatic carbons), 161.9 (q, C-B, BAr_F, $^1J_{C-B}$ = 49 Hz), 181.1 (s, C=N). Anal. calc (%) for $C_{70}H_{62}BF_{24}IrNO_3PSSi_2$: C 48.22, H 3.58, N 0.80, S 1.84; found: C 48.26, H 3.61, N 0.79, S 1.81.

[Ir(cod)(L27f)]BAr_F. Yield: 124 mg (95%). ^{31}P NMR ($CDCl_3$), δ: 99.1 (s). ^{1}H NMR (C_6D_6), δ: 1.19 (s, 3H, CH_3), 1.28 (s, 3H, CH_3), 1.43 (s, 9H, CH_3, ^{t}Bu), 1.49 (s, 9H, CH_3, ^{t}Bu), 1.85 (s, 3H, CH_3), 1.92 (s, 3H, CH_3), 2.04 (s, 3H, CH_3), 2.12 (s, 3H, CH_3-Si), 2.1-2.5 (b, 8H, CH_2, cod), 3.19 (m, 1H, CH_2-S), 3.57 (m, 1H, CH= cod), 3.62 (m, 1H, CH_2-S), 3.99 (m, 1H, CH= cod), 4.39 (m, 1H, CH= cod), 5.04 (m, 1H, CH= cod), 5.26 (m, 1H, CH-N), 6.6-8.4 (m, 19H, CH=). ^{13}C NMR (C_6D_6), δ: 16.4 (CH_3-Ar), 16.9 (CH_3-Ar), 19.9 (CH_3-Ar), 20.4 (CH_3-Ar), 24.1 (CH_3), 27.2 (CH_2 cod), 27.4 (CH_2 cod), 27.9 (CH_3), 30.4 (CH_2 cod), 31.2 (CH_3, ^{t}Bu), 31.4 (CH_3, ^{t}Bu), 31.5 (CH_2 cod), 33.7 (CH_2-S), 35.1 (C, ^{t}Bu), 35.3 (C, ^{t}Bu), 71.1 (CH= cod), 73.2 (CH= cod), 82.9 (CH-N), 84.9 (d, C, J_{C-P}= 4.8 Hz), 97.1 (d, CH= cod, J_{C-P}= 19.2 Hz), 103.9 (d, CH= cod, J_{C-P}= 11.4 Hz), 117.4 (b, CH=, BAr_F), 120-132 (aromatic carbons), 134.7 (b, CH=, BAr_F), 135.8-157 (aromatic carbons), 161.9 (q, C-B, BAr_F, $^1J_{C-B}$ = 49 Hz), 182.4 (s, C=N). Anal. calc (%) for $C_{76}H_{70}BF_{24}IrNO_3PS$: C 51.65, H 3.99, N 0.79, S 1.81; found: C 51.71, H 4.03, N 0.76, S 1.79.

[Ir(cod)(L27g)]BAr_F. Yield 119 mg (91 %). ^{31}P NMR ($CDCl_3$), δ: 98.4 (s). ^{1}H NMR (C_6D_6), δ: 1.22 (s, 3H, CH_3), 1.27 (s, 3H, CH_3), 1.47 (s, 9H, CH_3, ^{t}Bu), 1.63 (s, 9H, CH_3, ^{t}Bu), 1.85 (s, 3H, CH_3), 1.97 (s, 3H, CH_3), 2.01 (s, 3H, CH_3), 2.05 (s, 3H, CH_3-Si), 2.1-2.5 (b, 8H, CH_2, cod), 3.21 (m, 1H, CH_2-S), 3.49 (m, 1H, CH= cod), 3.53 (m, 1H, CH_2-S), 4.03 (m, 1H, CH= cod), 4.78 (m, 1H, CH= cod), 5.01 (m, 1H, CH= cod), 5.14 (m, 1H, CH-N), 6.6-8.4 (m, 19H, CH=). ^{13}C NMR (C_6D_6), δ: 16.5 (CH_3-Ar), 17.1 (CH_3-Ar), 20.1 (CH_3-Ar), 20.3 (CH_3-Ar), 24.4 (CH_3), 27.2 (CH_2 cod), 27.4 (CH_2

cod), 28.1 (CH_3), 30.0 (CH_2 cod), 31.4 (CH_3, ^{t}Bu), 31.7 (CH_3, ^{t}Bu), 32.3 (CH_2 cod), 33.2 (CH_2-S), 35.1 (C, ^{t}Bu), 35.3 (C, ^{t}Bu), 72.9 (CH= cod), 75.8 (CH= cod), 83.9 (CH-N), 84.2 (d, C, $J_{C\text{-}P}$= 2.4 Hz), 97.9 (d, CH= cod, $J_{C\text{-}P}$= 20.4 Hz), 105.2 (d, CH= cod, $J_{C\text{-}P}$= 10.4 Hz), 117.4 (b, CH=, BAr_F), 120-132 (aromatic carbons), 134.7 (b, CH=, BAr_F), 135.8-157 (aromatic carbons), 161.9 (q, C-B, BAr_F, $^1J_{C\text{-}B}$ = 49 Hz), 182.3 (s, C=N). Anal. calc (%) for $C_{76}H_{70}BF_{24}IrNO_3PS$: C 51.65, H 3.99, N 0.79, S 1.81; found: C 51.68, H 4.02, N 0.76, S 1.79.

[Ir(cod)(L28a)]BAr$_F$. Yield 124 mg (92 %). ^{31}P NMR ($CDCl_3$), δ: 99.7 (s). ^{1}H NMR (C_6D_6), δ: 1.17 (s, 3H, CH_3), 1.32 (s, 3H, CH_3), 1.49 (s, 9H, CH_3, ^{t}Bu), 1.54 (s, 9H, CH_3, ^{t}Bu), 1.69 (s, 9H, CH_3, ^{t}Bu), 1.71 (s, 9H, CH_3, ^{t}Bu), 2.1-2.3 (b, 5H, CH_2, cod), 2.34 (b, 1H, CH_2, cod), 2.43 (b, 2H, CH_2, cod), 3.21 (m, 1H, CH_2-S), 3.79 (m, 1H, CH_2-S), 4.39 (m, 1H, CH= cod), 4.63 (m, 1H, CH= cod), 5.12 (m, 1H, CH= cod), 5.24 (m, 1H, CH-N), 6.6-8.4 (m, 21H, CH=). ^{13}C NMR (C_6D_6), δ: 24.7 (CH_3), 27.6 (CH_2 cod), 27.7 (CH_2 cod), 28.9 (CH_3), 30.3 (CH_3), 30.9 (CH_3, ^{t}Bu), 31.2 (CH_3, ^{t}Bu), 31.6 (CH_2 cod), 32.2 (CH_3, ^{t}Bu), 32.5 (CH_3, ^{t}Bu), 33.3 (CH_2-S), 35.1 (C, ^{t}Bu), 35.3 (C, ^{t}Bu), 35.5 (C, ^{t}Bu), 35.7 (C, ^{t}Bu), 68.9 (CH= cod), 71.3 (CH= cod), 84.1 (CH-N), 85.2 (d, C, $J_{C\text{-}P}$= 4.2 Hz), 96.9 (d, CH= cod, $J_{C\text{-}P}$= 14.4 Hz), 105.1 (d, CH= cod, $J_{C\text{-}P}$= 9.6 Hz), 117.4 (b, CH=, BAr_F), 120-132 (aromatic carbons), 134.7 (b, CH=, BAr_F), 135.8-157 (aromatic carbons), 161.9 (q, C-B, BAr_F, $^1J_{C\text{-}B}$ = 49 Hz), 179.9 (s, C=N). Anal. calc (%) for $C_{80}H_{78}BF_{24}IrNO_3PS$: C 52.69, H 4.31, N 0.77, S 1.76; found: C 52.71, H 4.32, N 0.75, S 1.73.

3.4.5.4. Typical procedure for the hydrogenation of olefins

The alkene (1 mmol) and Ir complex (0.2 mol%) were dissolved in CH_2Cl_2 (2 mL) in a high-pressure autoclave, which was purged four times with hydrogen. Then, it was pressurized at the desired pressure. After the desired reaction time, the autoclave was depressurized and the solvent evaporated off. The residue was dissolved in Et_2O (1.5 ml) and filtered through a short celite plug. The enantiomeric excess was determined by chiral GC or chiral HPLC and conversions were determined by ^{1}H NMR. The enantiomeric excesses of hydrogenated products were determined using the conditions previously described.[4d-q,5c]

3.4.6. Acknowledgements

We would like to thank the Spanish Government for providing grant CTQ2010-15835, the Catalan Government for grant 2009SGR116, and the ICREA Foundation for providing M. Diéguez and O. Pàmies with financial support through the ICREA Academia awards.

3.4.7. References

[1] a) *Catalytic Asymmetric Synthesis*, 2nd, ed.; Ojima, I., Ed.; Wiley-VCH: New York, 2000. b) *Asymmetric Catalysis in Organic Synthesis*; Noyori, R., Ed.; Wiley: New York, 1994. c) *Asymmetric Catalysis on Industrial Scale*; Blaser, H.-U., Schmidt, E., Eds.; Wiley: New York, 2004. d) Brown, J. M. in *Comprehensive Asymmetric Catalysis*; Jacobsen, E. N., Pfaltz, A., Yamamoto, H., Eds.; Springer-Verlag: Berlin, 1999, Vol.1.

[2] For recent reviews, see: a) Källström, K.; Munslow, I.; Andersson, P. G. *Chem. Eur. J.* **2006**, *12*, 3194. b) Roseblade, S. J.; Pfaltz, A. *Acc. Chem. Res.* **2007**, *40*, 1402. c) Church, T. L.; Andersson, P.

G. *Coord. Chem. Rev*. **2008**, *252*, 513. d) Cui, X.; Burgess, K. *Chem. Rev.* **2005**, *105*, 3272. e) Pàmies, O.; Andersson, P. G.; Diéguez, M. *Chem. Eur. J.* **2010**, *16*, 14232. f) Woodmansee, D. H.; Pfaltz, A. *Chem. Commun.* **2011**, *47*, 7912.

[3] Lighfoot, A.; Schnider, P.; Pfaltz, A. *Angew. Chem. Int. Ed.* **1998**, *37*, 3897.

[4] See for instance: a) Perry, M. C.; Cui, X.; Powell, M. T.; Hou, D. –R.; Reibenspies, J. H.; Burgess, K. *J. Am. Chem. Soc.* **2003**, *125*, 5391. b) Blankestein, J.; Pfaltz, A. *Angew. Chem. Int. Ed.* **2001**, *40*, 4445. c) Kaiser, S.; Smidt, S.P.; Pfaltz, A. *Angew. Chem. Int. Ed.* **2006**, *45*, 5194. d) Källström, K.; Hedberg, C.; Brandt, P.; Bayer, P.; Andersson, P. G. *J. Am. Chem. Soc.* **2004**, *126*, 14308. e) Engman, M.; Diesen, J. S.; Paptchikhine, A.; Andersson, P. G. *J. Am. Chem. Soc.* **2007**, *129*, 4536. f) Trifonova, A.; Diesen, J. S.; Andersson, P. G. *Chem. Eur. J.* **2006**, *12*, 2318. g) Menges, G.; Pfaltz, A. *Adv. Synth. Catal.* **2002**, *334*, 4044. h) Drury III, W. J.; Zimmermann, N.; Keenan, M.; Hayashi, M.; Kaiser, S.; Goddard, R.; Pfaltz, A. *Angew. Chem. Int. Ed.* **2004**, *43*, 70. i) Hedberg, C.; Källström, K.; Brandt, P.; Hansen, L. K.; Andersson, P. G. *J. Am. Chem. Soc.* **2006**, *128*, 2995. j) Franzke, A.; Pfaltz A. *Chem. Eur. J.* **2011**, *17*, 4131. k) Tang, W.; Wang, W.; Zhang, X. *Angew. Chem. Int. Ed.* **2003**, *42*, 943. l) Hou, D. –R.; Reibenspies, J.; Colacot, T. J.; Burgess, K. *Chem. Eur. J.* **2001**, *7*, 5391. m) Cozzi, P. G.; Menges, F.; Kaiser, S. *Synlett* **2003**, 833. n) Lightfoot, A.; Schnider, P.; Pfaltz, A. *Angew. Chem. Int. Ed.* **1998**, *37*, 2897. o) Menges, F.; Neuburger, M.; Pfaltz, A. *Org. Lett.* **2002**, *4*, 4713. p) Liu, D.; Tang, W.; Zhang, X. *Org. Lett.* **2004**, *6*, 513. q) Lu, S.-M; Bolm, C. *Angew. Chem. Int. Ed.* **2008**, *47*, 8920. r) Lu, W.-J.; Chen, Y.-W.; Hou, X.-L. *Adv. Synth. Catal.* **2010**, *352*, 103. s) Paptchikhine, A.; Cheruku, P.; Engman, M.; Andersson, P. G. *Chem. Commun.* **2009**, 5996.

[5] a) Diéguez, M.; Mazuela, J.; Pàmies, O.; Verendel, J. J.; Andersson, P. G. *J. Am. Chem. Soc.* **2008**, *130*, 7208. b) Diéguez, M.; Mazuela, J.; Pàmies, O.; Verendel, J. J.; Andersson, P. G. *Chem. Commun.* **2008**, 3888. c) Mazuela, J.; Verendel, J. J.; Coll, M.; Schäffner, B.; Börner, A.; Andersson, P. G.; Pàmies, O.; Diéguez, M. *J. Am. Chem. Soc.* **2009**, *131*, 12344. d) Mazuela, J.; Paptchikhine, A.; Pàmies, O.; Andersson, P. G.; Diéguez, M. *Chem. Eur. J.* **2010**, *16*, 4567. e) Mazuela, J. Norrby, P.-O.; Andersson, P. G.; Pàmies, O.; Diéguez, M. *J. Am. Chem Soc.* **2011***, 133,* 13634. f) Diéguez M.; Andersson, P.G.; Pàmies, O. in *Innovative Catalysis in Organic Synthesis*; Andersson, P. G., Ed.; Wiley-VCH, 2011, pp. 153-166.

[6] Emtenäs, H.; Alderin, L.; Almqvist, F. *J. Org. Chem.* **2001**, *66*, 6756.

[7] Pàmies, O.; Diéguez, M.; Net, G.; Ruiz, A.; Claver, C. *Organometallics* **2000,** *19,* 1488.

[8] The rapid ring inversions (tropoisomerization) in the biaryl phosphite moiety is usually stopped upon coordination to the metal center. See for example: a) Buisman, G. J. H.; van der Veen, L. A.; Klootwijk, A.; de Lange, W. G. J.; Kamer, P. C. J.; van Leeuwen, P. W. N. M.; Vogt, D. *Organometallics* **1997**, *16*, 2929. b) Diéguez, M.; Pàmies, O.; Ruiz, A.; Claver, C.; Castillón, S. *Chem. Eur. J.* **2001**, *7*, 3086. c) Pàmies, O.; Diéguez, M.; Net, G.; Ruiz, A.; Claver, C. *Organometallics* **2000**, *19*, 1488. d) Pàmies, O.; Diéguez, M.; Net, G.; Ruiz, A.; Claver, C. *J. Org. Chem.* **2001**, *66*, 8364. e) Pàmies, O.; Diéguez, M. *Chem. Eur. J.* **2008**, *14*, 944.

[9] Unpublished results, the hydrogenation of **S8** using the corresponding phosphite-oxazoline ligand afforded 100% conversion and 93% ee at 50 bar of H_2 using 0.5 mol% of Ir-catalysts.

[10] In contrast to the hydrogenation of trisubstituted olefins, the enantioselectivity in the reduction of terminal alkenes is highly pressure dependent. Therefore, hydrogenation at an atmospheric pressure of H_2 gave, in general, significantly higher ee values than at higher pressures. See: a) McIntyre, S.; Hörmann, E.; Menges, F.; Smidt, S. P.; Pfaltz, A. *Adv. Synth. Catal.* **2005**, *347*, 282. b) ref 4b.

[11] For successful applications of Sm-, Ru- and Rh-complexes, see: a) Conticello, V. P.; Brard, L.; Giardello, M. A.; Tsuji, Y.; Sabat, M.; Stern, C. L.; Marks, T. J. *J. Am. Chem. Soc.* **1992**, *114*, 2761. b) Giardello, M. A.; Conticello, V. P.; Brard, L.; Gagné, M. R.; Marks, T. J. *J. Am. Chem. Soc.* **1994**, *116*, 10241. c) Co, T. T.; Kim, T. J. *Chem. Commun.* **2006**, 3537. d) Forman, G. S.; Ohkuma, T.; Hems, W. P.; Noyori, R. *Tetrahedron Lett.* **2000**, *41*, 9471.

[12] See for instance: a) Abate, A.; Brenna, E. Fuganti, C.; Gatti, G. G.; Givenzana, T.; Malpezzi, L.; Serra, S. *J. Org. Chem.* **2005**, *70*, 1281. b) Drescher, K.; Haupt, A.; Unger, L.; Rutner, S. C.; Braje, W:; Grandel, R.; Henry, C.; Backfisch, G:; Beyerbach, A.; Bisch, W. *WO Patent* 2006/040182 A1.

[13] See for instance: a) Schlosser, M. *Angew. Chem. Int. Ed.* **1998**, *37*, 1496. b) Smart, B. E. *J. Fluorine Chem.* **2001**, *109*, 3. c) *Asymmetric Fluoroorganic Chemistry: Synthesis, Application and Future Directions*; Ramachandran, P. V., Ed.; American Chemical Society: Washington DC, 2000. d) A special issue has been devoted to "Fluorine in the Life Sciences" *ChemBioChem* **2004**, *5*, 559.

[14] Buisman, G. J. H.; Kamer, P. C. J.; van Leeuwen, P. W. N. M. *Tetrahedron: Asymmetry* **1993**, *4*, 1625.

3.4.8. Supporting Information

Table 3.4.5. Ir-catalyzed hydrogenation of trisubstituted olefins containing a neighboring polar group using ligands **L27**-**L28a**-**g**

Entry	Ligand	Substrate	% Conv[b]	% ee[c]	Entry	Ligand	Substrate	% Conv[b]	% ee[c]
1	**L27b**	**S8**	100	97 (*S*)	11	**L27a**	**S15**	100	96 (*R*)
2	**L27c**	**S8**	100	96 (*S*)	12	**L27b**	**S15**	100	95 (*R*)
3	**L27f**	**S8**	100	93 (*S*)	13	**L27f**	**S15**	100	92 (*R*)
4	**L27g**	**S8**	100	95 (*S*)	14	**L27g**	**S15**	100	94 (*R*)
5	**L28a**	**S8**	100	98.5 (*R*)	15	**L28a**	**S15**	100	96 (*S*)
6	**L27b**	**S13**	100	93 (*R*)	16	**L27a**	**S19**	100	94 (*R*)
7	**L27c**	**S13**	100	92 (*R*)	17	**L27b**	**S19**	100	95 (*R*)
8	**L27f**	**S13**	100	88 (*R*)	18	**L27f**	**S19**	100	90 (*R*)
9	**L27g**	**S13**	100	92 (*R*)	19	**L27g**	**S19**	100	93 (*R*)
10	**L28a**	**S13**	100	94 (*S*)	20	**L28a**	**S19**	100	98 (*S*)

[a] Reactions carried out by using 1 mmol of substrate and 1 mol% of Ir-catalyst precursor at 50 bar of H_2 using dichloromethane (2 mL) as solvent. [b] Conversion measured by ^{1}H-NMR after 2 h. [c] Enantiomeric excess determined by GC.

Table 3.4.6. Ir-catalyzed hydrogenation of disubstituted olefins using ligands **L27**-**L28a**-**g**

Entry	Ligand	Substrate	% Conv[b]	% ee[c]	Entry	Ligand	Substrate	% Conv[b]	% ee[c]
1	**L27a**	**S23**	100	92 (*S*)	16	**L27a**	**S30**	100	93 (+)
2	**L27b**	**S23**	100	91 (*S*)	17	**L27b**	**S30**	100	93 (+)
3	**L27c**	**S23**	100	94 (*S*)	18	**L27c**	**S30**	100	95 (+)
4	**L27f**	**S23**	100	87 (*S*)	19	**L27f**	**S30**	100	81 (+)
5	**L28a**	**S23**	100	92 (*R*)	20	**L28a**	**S30**	100	93 (-)
6	**L27a**	**S25**	100	91 (*S*)	21	**L27a**	**S32**	100	93 (*R*)
7	**L27b**	**S25**	100	92 (*S*)	22	**L27b**	**S32**	100	92 (*R*)
8	**L27c**	**S25**	100	92 (*S*)	23	**L27c**	**S32**	100	92 (*R*)
9	**L27f**	**S25**	100	82 (*S*)	24	**L27f**	**S32**	100	81 (*R*)
10	**L28a**	**S25**	100	91 (*R*)	25	**L28a**	**S32**	100	93 (*S*)
11	**L27a**	**S28**	100	93 (*S*)	26	**L27a**	**S34**	100	92 (*S*)
12	**L27b**	**S28**	100	93 (*S*)	27	**L27b**	**S34**	100	91 (*S*)
13	**L27c**	**S28**	100	95 (*S*)	28	**L27c**	**S34**	100	89 (*S*)
14	**L27f**	**S28**	100	81 (*S*)	29	**L27f**	**S34**	100	83 (*S*)
15	**L28a**	**S28**	100	93 (*R*)	30	**L28a**	**S34**	100	92 (*R*)

[a] Reactions carried out by using 1 mmol of substrate and 1 mol% of Ir-catalyst precursor at 50 bar of H_2 using dichloromethane (2 mL) as solvent. [b] Conversion measured by ^{1}H-NMR after 2 h. [c] Enantiomeric excess determined by GC.

3.5 Adaptative biaryl phosphite-oxazole and phosphite-thiazole ligands for asymmetric Ir-catalyzed hydrogenation of alkenes

Javier Mazuela, Alexander Paptchikhine, Oscar Pàmies, Pher G. Andersson and Montserrat Diéguez in *Chem. Eur. J.* **2010**, *16*, 4567.

3.5.1. Abstract

A library of readily available phosphite-oxazole/thiazole ligands (**L29**-**L36a-g**) was applied in the Ir-catalyzed asymmetric hydrogenation of several largely unfunctionalized *E*- and *Z*-trisubstituted and 1,1-disubstituted terminal alkenes. The ability of the catalysts to transfer chiral information to the product could be tuned by choosing suitable ligand components (bridge length, the substituents in the heterocyclic ring and the alkyl backbone chain, the configuration of the ligand backbone, and the substituents/configurations in the biaryl phosphite moiety), so that enantioselectivities could be maximized for each substrate as required. Enantioselectivities were therefore excellent (ee's up to >99%) in a wide range of *E*- and *Z*-trisubstituted and 1,1-disubstituted terminal alkenes. The biaryl-phosphite moiety was a very advantageous ligand component in terms of substrate versatility.

3.5.2. Introduction

The preparation of enantiomerically enriched compounds currently plays a key role in such important areas as pharmaceuticals, agrochemicals, fine chemicals and natural product chemistry.[1] As a consequence of its high efficiency, atom economy and operational simplicity, asymmetric hydrogenation of properly selected prochiral starting materials is one of the most powerful synthetic tools for preparing these compounds.[1] Whereas the rhodium and ruthenium-catalyzed asymmetric hydrogenations of chelating olefins have a long history, the asymmetric hydrogenations of unfunctionalized olefins are less developed because these substrates lack an adjacent polar group to direct the reaction.[1] In recent years, iridium complexes with chiral P,N ligands have become established as efficient catalysts for the hydrogenation of unfunctionalized olefins, and their scope is complementary to those of Rh- and Ru-diphosphine complexes.[1,2] The first chiral ligands developed for this process were the phosphine-oxazolines, which are chiral mimics of Crabtree's catalyst. These ligands were successfully used for the asymmetric hydrogenation of a limited range of alkenes.[3] Since then, the composition of the ligands has been extended by the discovery of new mixed P,N ligands that have considerably broadened the scope of Ir-catalyzed hydrogenation.[4] Of them all, the most successful ligands contain a phosphine or phosphinite moiety as P-donor group and either an oxazoline,[4b,g] oxazole,[4d] thiazole[4i] or pyridine[4c] as N-donor group (Figure 3.5.1). However, the iridium-catalyzed asymmetric hydrogenation of unfunctionalized olefins is still highly substrate-dependent and the development of efficient chiral ligands that tolerate a broader range of substrates remains a challenge.

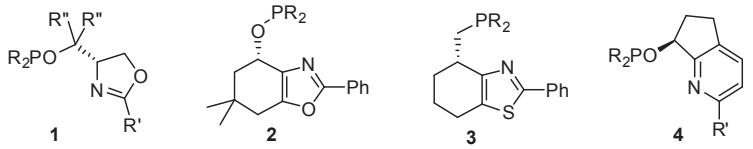

Figure 3.5.1. Privileged P,N-ligands for Ir-catalyzed hydrogenation of alkenes.

In this context, we have recently discovered that the presence of biaryl-phosphite moieties in ligand design is highly advantageous.[5] Ir/phosphite-oxazoline catalytic systems provided greater substrate versatility than previous Ir/phosphinite-oxazoline systems (Figure 3.5.1), and high activities and enantioselectivities for several largely unfunctionalized *E*- and *Z*-trisubstituted and 1,1-disubstituted olefins.[5a,c] Despite this success, little attention has been paid to this new class of highly efficient phosphite-containing ligands for this process[5a,c] and their potential as new ligands still needs to be systematically studied. To fully investigate this potential, we therefore decided to go one step further and study whether biaryl phosphite moiety maintains its effectiveness in combination with N-donor groups other than oxazolines. For this purpose, we took two of the most successful ligand families used in this process (**2** and **3**, Figure 3.4.1) and replaced their phosphinite or phosphine moieties with biaryl-phosphite groups to give ligands **L29**-**L36a**-**g** (Figure 3.5.2).

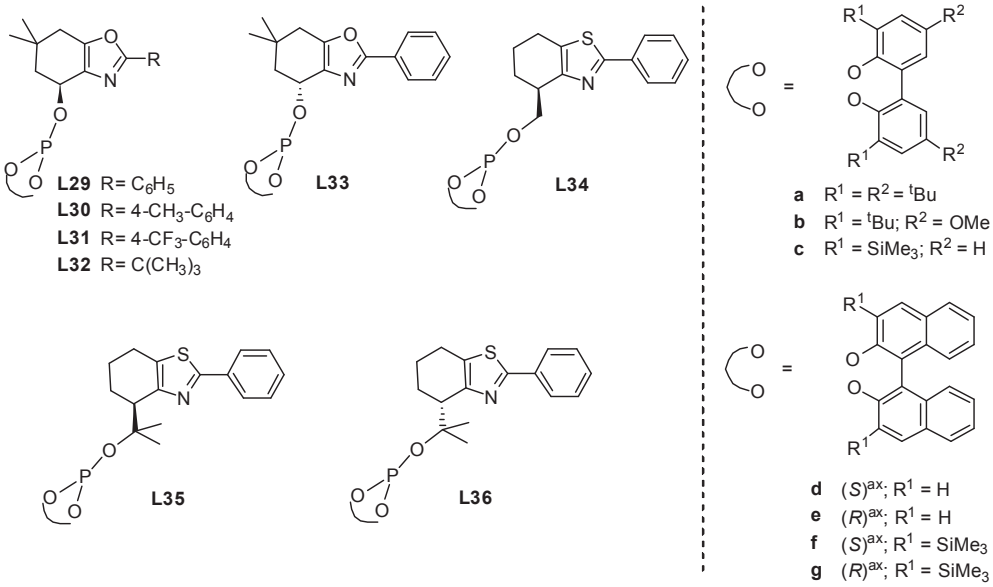

Figure 3.5.2. Phosphite-oxazole and phosphite-thiazole ligand library **L29**-**L36a-g**.

Ligands **2** and **3** proved to be highly efficient in the hydrogenation of unfunctionalized aryl-alkyl *E*-trisubstituted olefins (including those containing weakly coordinating groups),[4d,i] but they provided low-to-moderate enantioselectivities for the *Z*-analogues[6] and enol phosphinates[7]. Moreover, although ligand **2** provided high enantioselectivities for the terminal substrate 2-(4-methoxyphenyl)-1-butene, only moderate enantioselectivities were achieved for other terminal 2-arylbut-1-enes.[8] Therefore, with this new biaryl phosphite-oxazole and phosphite-thiazole design

(Figure 3.5.2) we expect to increase substrate versatility in the hydrogenation of largely unfunctionalized olefins. Interestingly, these ligands combine a priori the advantages of the oxazole/thiazole moieties with those of the phosphite moiety. So they are more stable than their oxazoline counterparts,[9] less sensitive to air and other oxidizing agents than phosphines and phosphinites and easy to synthesize from readily available alcohols.[10] As well as having biaryl phosphite moieties in their design, these ligands have a flexible ligand scaffold that enables several parameters to be tuned. Thus, the effect of ligand structure on catalytic performance can be explored. We systematically varied the bridge length (ligands **L29** and **L34**), the substituent in the heterocyclic ring (ligands **L29**-**L32**) and the alkyl backbone chain (ligands **L34** and **L35**), the configuration of the alkyl backbone chain (ligands **L35** vs **L36**), and the substituents and configurations in the biaryl phosphite moiety (**a**-**g**) in these ligands and examined their effects on asymmetric hydrogenation. By selecting the best ligand elements, we achieved high enantioselectivities and activities in the reduction of a wide range of *E*- and *Z*-trisubstituted and 1,1-disubstituted olefins.

3.5.3. Results and discussion

3.5.3.1. Synthesis of ligands

Scheme 3.5.1 illustrates the sequence of ligand synthesis. Ligands **L29**-**L36a**-**g** were synthesized very efficiently from the corresponding easily accessible ketone-oxazole or thiazole-ester derivatives (**6**-**9** and **17**, Scheme 3.5.1). Compounds **6**-**9** and **17** are easily made in two steps from the corresponding dimedone **5** and ketoester **16**, respectively.[4d,i] Ketone-oxazoles **6**-**9** were then reduced using (*R*)-Me-CBS or $NaBH_4$ (Scheme 3.5.1, step (b)). Enantioselective reduction of **6** using (*R*)-Me-CBS followed by single recrystallization afforded hydroxyl-oxazole **10** in >99% ee.[4d] The same procedure applied to ketones **7** and **8** afforded hydroxyl-oxazoles **12** and **13** but in <80% ee's. Thus, further enantiomer resolution was achieved using preparative chiral HPLC. For compounds **11** and **14**, the corresponding ketone-oxazoles **6** and **9** were reduced using $NaBH_4$ followed by enantiomer resolution using preparative HPLC. Reduction of **17** using $LiAlH_4$ (Scheme 3.5.1, step (d))[4i] or MeMgCl (Scheme 3.5.1, step (e)) gave good yields of the corresponding racemic alcohols **18** and **19**, respectively. This was followed by the resolution of racemates into their enantiomers by preparative chiral HPLC.

The last step of the ligand synthesis is common for all of them (Scheme 3.5.1, step (f)). Therefore, treating the corresponding hydroxyl-oxazole (**10**-**15**) or hydroxyl-thiazole (**18** and **19**) with 1 equiv of the corresponding in situ formed biaryl phosphorochloridite ($ClP(OR)_2$; $(OR)_2$ = **a**-**g**) in the presence of pyridine, in a parallel manner, provided easy access to the desired ligands **L29**-**L36a**-**g**. All of the ligands were stable during purification on neutral alumina under an atmosphere of argon and isolated in moderate-to-good yields as white solids. They were stable at room temperature and very stable to hydrolysis. The elemental analyses were in agreement with the assigned structure. The ^{1}H, ^{13}C and ^{31}P NMR spectra were as expected for these C_1 ligands. One singlet for each compound was observed in the ^{31}P NMR spectrum. Rapid ring inversions (tropoisomerization) in the biphenyl-phosphorus moieties (**a**-**c**) occurred on the NMR time scale because the expected diastereoisomers were not detected by low-temperature phosphorus NMR.[11]

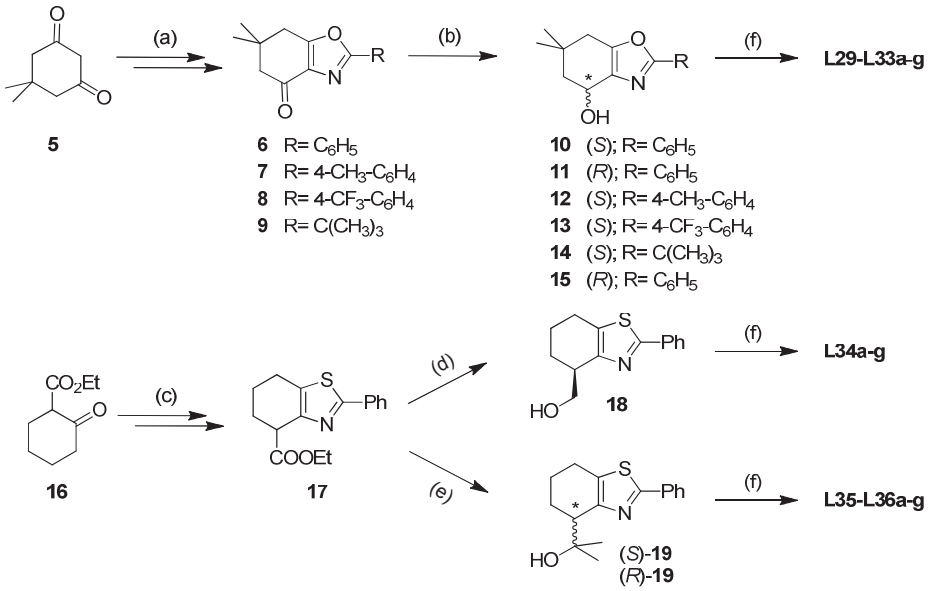

Scheme 3.5.1. Synthesis of a new phosphite-nitrogen ligand library **L29**-**L36a**-**g**. (a) and (b) see ref 8a and experimental section; (c) and (d) see ref 8b; (e) CH_3MgCl / THF / $CeCl_3$ (Yield: 71%); (f) $ClP(OR)_2$; $(OR)_2$ = **a**-**g** / Py / toluene (Yields: 42-76%).

3.5.3.2. Synthesis of the Ir-catalyst precursors

The catalyst precursors were made by refluxing a dichloromethane solution of the appropriate ligand (**L29**-**L36a**-**g**) in the presence of 0.5 equivalent of $[Ir(\mu\text{-}Cl)cod]_2$ for 2 h and then exchanging the counterion with sodium tetrakis[3,5-bis(trifluoromethyl)phenyl]borate ($NaBAr_F$) (1 equiv), in the presence of water (Scheme 3.5.2). All complexes were isolated as air-stable orange solids and were used without further purification.

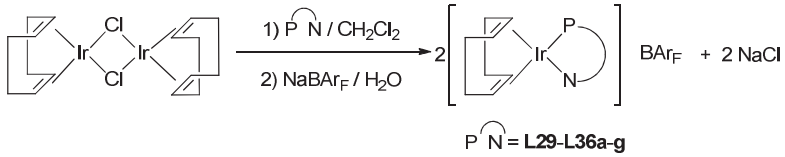

Scheme 3.5.2. Synthesis of catalyst precursors [Ir(cod)(P-N)]BArF (P-N = **L29**-**L36a-g**).

The complexes were characterized by elemental analysis and ^1H, ^{13}C, and ^{31}P NMR spectroscopy. The spectral assignments (see experimental section) were based on information from ^1H–^1H and ^{13}C–^1H correlation measurements and were as expected for these C_1 iridium complexes. The VT-NMR spectra indicate that only one isomer is present in solution. One singlet in the ^{31}P-{^1H} NMR spectra was obtained in all cases.

3.5.3.3. Asymmetric hydrogenation of trisubstituted olefins

Asymmetric hydrogenation of unfunctionalized trisubstituted olefins

In a first set of experiments, we used the Ir-catalyzed hydrogenation of *trans*-α-methylstilbene **S1** to study the potential of ligands **L29**-**L36a**-**g**. **S1** was chosen as the substrate because it has been hydrogenated by a wide range of catalysts, which enabled the efficiency of the various ligand systems to be compared directly. The results are summarized in Table 3.5.1. We found that enantioselectivities were highly affected by the bridge length, the substituents in the heterocyclic ring and the substituents and configurations in the biaryl phosphite moiety (**a**-**g**), but not by the substituents in the alkyl backbone chain.

The influence of the bridge length indicates that ligands **L34**-**L36**, which form a seven-membered chelate ring, provided higher enantioselectivity than ligands **L29**-**L32**, which form a six-membered chelate ring (Table 3.5.1, entries 1, 8-10 vs 11, 16-17).

In the heterocyclic ring, electron-withdrawing substituents had a negative effect on enantioselectivity (Table 3.5.1, entries 9 vs 1 and 8), and bulky substituents at this position decreased activity (Table 3.5.1, entries 10 vs 1).

Table 3.5.1. Selected results for the Ir-catalyzed hydrogenation of **S1** using the ligand library **L29**-**L36a**-**g**[a]

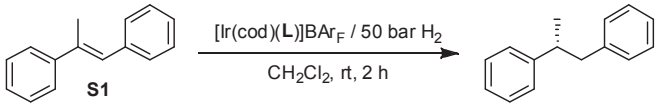

Entry	Ligand	% Conv[b]	% ee[c]	Entry	Ligand	% Conv[b]	% ee[c]
1	**L29a**	100	90 (*S*)	10	**L32a**	42	83 (*S*)
2	**L29b**	100	90 (*S*)	11	**L34a**	100	98 (*S*)
3	**L29c**	100	85 (*S*)	12	**L34b**	100	97 (*S*)
4	**L29d**	8	50 (*S*)	13	**L34c**	100	95 (*S*)
5	**L29e**	8	12 (*S*)	14	**L34h**	100	85 (*S*)
6	**L29f**	100	84 (*S*)	15	**L34i**	100	90 (*S*)
7	**L29g**	100	37 (*S*)	16	**L35a**	100	98 (*S*)
8	**L30a**	100	89 (*S*)	17	**L36a**	100	98 (*R*)
9	**L31a**	100	82 (*S*)				

[a] Reactions carried out using 1 mmol of **S1** and 0.2 mol% of Ir-catalyst precursor at 50 bar of H_2.[b] Conversion measured by ^{1}H-NMR after 2 hours. [c] Enantiomeric excesses determined by chiral GC.

Bulky *ortho* substituents in the biaryl phosphite moiety were highly advantageous for both activity and enantioselectivity (Table 3.5.1, entry 1-3 and 6-7 vs 4 and 5). However, substituents in the *para* positions also play a small but crucial role. Therefore, if enantioselectivities have to be high the *para*-position needs to be substituted (Table 3.5.1, entries 1 and 2 vs 3). For phosphite-oxazole ligands **L29**, we also found a cooperative effect between the configuration of the biaryl moiety and the configuration of the ligand backbone on enantioselectivity. This led to a matched combination for ligand **L29f**, which contains an *S*-binaphthyl moiety (Table 3.5.1, entries 6 and 7). This effect was less pronounced for phosphite-thiazole ligands **L34** (Table 3.5.1, entries 14 and 15). In addition, a comparison of the absolute stereochemistry obtained using ligand **L29c** with

those obtained using the related binaphthyl ligands **L29f** and **L29g** (Table 3.5.1, entries 3, 6 and 7) shows that the tropoisomeric biphenyl moiety in ligands **L29a-c** adopts an *S*-configuration upon complexating to iridium.[12]

In summary, activities and enantioselectivities (ee's up to 98%) were high with ligands **L34-L36a** (Table 3.5.1, entries 11, 16 and 17), which contain the optimal combination of ligand parameters (bridge length, the substituents in the heterocyclic ring and the substituents and configurations in the biaryl phosphite moiety). In addition, both enantiomers of the hydrogenated product can be accessed in high enantioselectivity simply by changing the configuration of the ligand backbone (Table 3.5.1, entries 16 and 17). These findings clearly show the efficiency of highly modular scaffolds in ligand design.

We then studied the asymmetric hydrogenation of other *E*- and *Z*-trisubstituted olefins (**S2-S6**) using the phosphite-oxazole/thiazole ligand library **L29-L36a-g**. The most noteworthy results are shown in Table 3.5.2.

Table 3.5.2. Selected results for the Ir-catalyzed hydrogenation of largely unfunctionalized *E*- and *Z*-trisubstituted olefins using the ligand library **L29-L36a-g**[a]

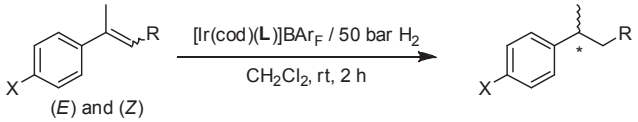

(*E*) and (*Z*)

Entry	Substrate	Ligand	% Conv[b]	% ee[c]
1	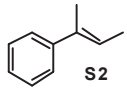 **S2**	**L34a**	100	99 (*S*)
2		**L35a**	100	99 (*S*)
3		**L36a**	100	98 (*R*)
4	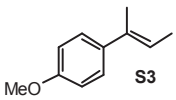 MeO **S3**	**L34a**	100	99 (*S*)
5		**L35a**	100	99 (*S*)
6		**L36a**	100	99 (*R*)
7	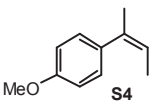 MeO **S4**	**L34g**	100	90 (*R*)
8	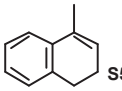 **S5**	**L34a**	100	78 (*R*)
9		**L35a**	100	93 (*R*)
10		**L36a**	100	93 (*S*)
11	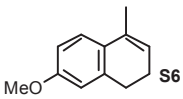 MeO **S6**	**L34a**	100	99 (*R*)

[a] Reactions carried out using 1 mmol of substrate and 0.2 mol% of Ir-catalyst precursor at 50 bar of H_2. [b] Conversion measured by ^{1}H-NMR or GC after 2 hours. [c] Enantiomeric excesses determined by chiral GC.

The enantioselectivities are among the best observed for these substrates. In general, the hydrogenation of *E*-trisubstituted olefins (**S2-S3**) followed the same trends as the hydrogenation of

S1. Again, the catalyst precursors containing ligands **L34**-**L36a** provided the best enantioselectivities (ee's up to 99%; Table 3.5.2, entries 1-6). It should be noted that if ligands are appropriately tuned, high enantioselectivities (ee's up to 99%) could also be obtained for the more demanding *Z*-trisubstituted olefins (**S4**-**S6**), which are usually hydrogenated less enantioselectively than the corresponding *E*-isomers (Table 3.5.2, entries 7-11). Interestingly when these excellent results are compared with the moderate enantioselectivity obtained for *Z*-trisubsituted olefins with the related ligands **2** and **3**,[6] we can conclude that the introduction of a biaryl phosphite moiety has been highly advantageous.

Asymmetric hydrogenation of trisubstituted olefins containing a neighboring polar group

We then applied the phosphite-oxazole/thiazole ligand library **L29**-**L36a-g** in the asymmetric hydrogenation of several trisubstituted olefins containing a neighboring polar group. These substrates are interesting because they allow for further functionalization. The results are summarized in Table 3.5.3.

Table 3.5.3. Selected results for the Ir-catalyzed hydrogenation of trisubstituted weakly coordinating functionalized olefins using the ligand library **L29-L36a-g**[a]

Entry	Substrate	Ligand	% Conv[b]	% ee[c]
1	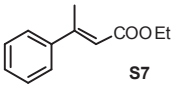 **S7**	**L29a**	65	99 (*S*)
2		**L34a**	100	99 (*S*)
3		**L35a**	100	98 (*S*)
4		**L36a**	100	98 (*R*)
5	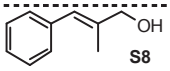 **S8**	**L29a**	100	84 (*S*)
6		**L34a**	100	96 (*S*)
7		**L35a**	100	96 (*S*)
8		**L36a**	100	96 (*R*)
9	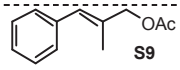 **S9**	**L34a**	100	95 (*S*)
10		**L35a**	100	94 (*S*)
11		**L36a**	100	94 (*R*)
12	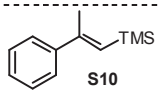 **S10**	**L34a**	100	98 (*S*)
13		**L35a**	100	97 (*S*)
14		**L36a**	100	97 (*R*)
15[d]	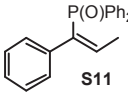 **S11**	**L29a**	100	91 (*S*)
16[d]		**L34a**	100	20 (*R*)
17[e]	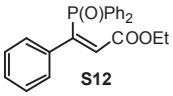 **S12**	**L29a**	45	92 (*S*)

[a] Reactions carried out using 1 mmol of substrate, dichloromethane as solvent and 0.2 mol% of Ir-catalyst precursor at 50 bar of H_2 and room temperature. [b] Conversion measured by ^{1}H-NMR or GC after 2 hours. [c] Enantiomeric excesses determined by chiral GC or HPLC. [d] t = 12 h. [e] 100 bar of H_2, t = 12 h.

Again, enantioselectivities in both enantiomers of the hydrogenation product were excellent (ee's up to 99%) under mild reaction conditions. Hydrogenation of α,β-unsaturated ester **S7**, allylic alcohol **S8**, allylic acetate **S9** and vinylsilane **S10** followed the same trends as those observed for

the previous *E*-trisubstituted substrates **S1**-**S3**. Therefore, enantioselectivities were best with ligands **L34-L36a** (Table 3.5.3, entries 2-4 and 5-14). However, for trisubsituted enol phosphinates **S11**-**S12** the enantioselectivity was best with ligand **L29a** (Table 3.5.3, entries 15 and 17). Once again, these results clearly show the efficiency of using modular scaffolds in ligand design and are among the best that have been reported for this type of substrates.[2] They also show that the introduction of a biaryl phosphite moiety in the ligand design is highly advantageous because it overcomes a substrate limitation of the related ligands **2** and **3** by hydrogenating enol phosphinates.[7]

3.5.3.4. Asymmetric hydrogenation of 1,1-disubstituted terminal olefins

Asymmetric hydrogenation of unfunctionalized 1,1-disubstituted terminal olefins

To further study the potential of the phosphite-oxazole/thiazole ligand library **L29**-**L36a-g**, we also screened it in the Ir-catalyzed hydrogenation of more demanding substrates: terminal olefins. As discussed in previous sections, enantioselectivity is more difficult to control in these substrates than in trisubstituted olefins. There are two main reasons for this.[2d] The first one is that the two substituents in the substrate can easily exchange positions in the chiral environment formed by the catalysts, thus reversing the face selectivity. The second reason is that the terminal double bond can isomerize to form the more stable internal alkene, which usually leads to the predominant formation of the opposite enantiomer of the hydrogenated product. Few known catalytic systems provide high enantioselectivities for these substrates, and those that do are usually limited in substrate scope.[13,14]

In a first set of experiments, we examined the Ir-catalyzed asymmetric hydrogenation of 2-phenylbut-1-ene **S13**. Table 3.5.4 shows the results obtained using the ligand library **L29**-**L36a-g** under optimized conditions. We were again able to fine-tune ligand parameters to produce high activities and enantioselectivities (ee's up to 94%) in the hydrogenation of this substrate. In contrast to the hydrogenation of *E*-trisubstituted olefins (**S1**-**S3** and **S7**-**S10**), among the other ligand parameters, activities and enantioselectivities were also affected by the substituents in the alkyl backbone chain. Therefore, ligand **L34** provided better enantioselectivities than ligands **L35** and **L36** that contain methyl substituents at the alkyl backbone chain (Table 3.5.4, entries 5 vs 10 and 11). Interestingly, the effect of bridge length was more pronounced in this reaction than in the reduction of *E*-trisubstituted olefins. The ligands that formed seven-membered chelate rings (**L34**) provided much higher enantioselectivities than the one that formed a six-membered chelate ring (**L29**). The effect of the substituents in the biaryl phosphite moiety followed the same trend as those observed for *E*-trisubstituted olefins. However, using ligands **L34f** and **L34g**, we found an important cooperative effect between the configuration of the biaryl moiety and the configuration of the ligand backbone on enantioselectivity. Ligand **L34f**, which contains an *S*-binaphthyl moiety, performed better than **L34g** (Table 3.5.4, entries 8 and 9). In addition, a comparison of the results obtained using ligand **L34c** with those from the related binaphthyl ligands **L34f** and **L34g** (Table 3.5.4, entries 7-9) shows that the tropoisomeric biphenyl moieties in ligands **L34a**-**c** adopt an *S*-configuration upon coordination to iridium.[12]

Table 3.5.4. Selected results for the Ir-catalyzed hydrogenation of **S13** using the ligands **L29**-**L36a-g**[a]

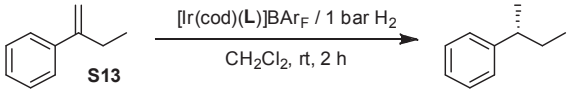

Entry	Ligand	% Conv[b]	% ee[c]
1	**L29a**	100	53 (*R*)
2	**L30a**	100	50 (*R*)
3	**L31a**	100	43 (*R*)
4	**L32a**	100	5 (*R*)
5	**L34a**	100	94 (*R*)
6	**L34b**	100	94 (*R*)
7	**L34c**	100	90 (*R*)
8	**L34f**	100	89 (*R*)
9	**L34g**	100	3 (*R*)
10	**L35a**	100	90 (*R*)
11	**L36a**	100	90 (*S*)

[a] Reactions carried out using 1 mmol of **S13** and 0.2 mol% of Ir-catalyst precursor at 1 bar of H_2. [b] Conversion measured by GC after 2 hours. [c] Enantiomeric excesses determined by chiral GC.

In summary, enantioselectivities were best when phosphite-thiazole ligands **L34a** and **L34b** were used. Once again, it was possible to access both enantiomers of the hydrogenation product. These results, which again clearly show the efficiency of using modular scaffolds in ligand design, are among the best that have been reported for this demanding substrate class.[13,14]

We then studied the asymmetric hydrogenation of other 1,1-disubstituted aryl-alkyl substrates (**S14**-**S20**) and 1,1-disubstituted heteroaryl-alkyl olefins (**S21**-**S23**) using the phosphite-oxazole/thiazole ligand library **L29**-**L36a-g**. The most noteworthy results are shown in Table 3.5.5. They follow the same trends as the hydrogenation of **S13**. Again, the catalyst precursor containing the phosphite-thiazole ligands **L34a** and **L34b** provided the best enantioselectivities (ee's up to 99%).

The hydrogenations of 1,1-disubstituted aryl-alkyl substrates bearing increasingly bulky alkyl substituents (**S14**-**S18**) all gave similar high activities and enantioselectivities (full conversion, ee's up to 95%; Table 3.5.5, entries 1-5). Our results with several *para*-substituted 2-phenylbut-2-enes (**S13**, **S19**-**S20**) indicated that enantioselectivity (ee's up to 97%) is relatively insensitive to the electronic nature of the substrate phenyl ring (Table 3.5.4, entry 5 and Table 3.5.5, entries 6 and 7). This is therefore one of the few catalytic systems able to hydrogenate a wide range of α-alkylstyrenes in high enantioselectivities.[5c,d]

We then decided to apply this ligand library in the asymmetric hydrogenation of 1,1-heteroaromatic alkenes (**S21**-**S23**) because heterocycles are used in industry and because the heterocyclic part can be modified post-hydrogenation. Under standard conditions, our catalytic systems were also able to hydrogenate several 1,1-heteroaromatic alkenes in high activities and enantioselectivities (ee's up to 99%; Table 3.5.5, entries 8-10).

Table 3.5.5. Selected results for the Ir-catalyzed hydrogenation of largely unfunctionalized 1,1-disubstituted terminal olefins using ligand **L34a**[a]

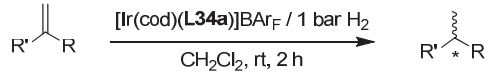

Entry	Substrate	% Conv[b]	% ee[c]	Entry	Substrate	% Conv[b]	% ee[c]
1	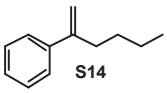 S14	100	95 (*R*)	6	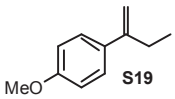 S19	100	97 (*R*)
2	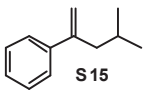 S15	100	94 (*R*)	7	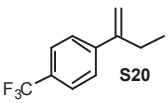 S20	100	94 (*R*)
3	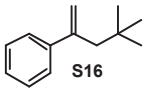 S16	100	85 (*R*)	8	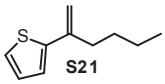 S21	100	90 (+)
4	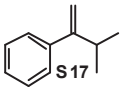 S17	100	95 (*R*)	9	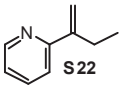 S22	100	99 (-)
5	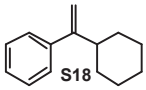 S18	100	94 (*R*)	10	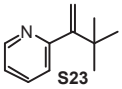 S23	100	96 (-)

[a] Reactions carried out using 1 mmol of substrate and 0.2 mol% of Ir-catalyst precursor at 1 bar of H_2. [b] Conversion measured by ^{1}H-NMR or GC. [c] Enantiomeric excesses determined by chiral GC.

Asymmetric hydrogenation of 1,1-disubstituted terminal olefins containing a neighboring polar group

Encouraged by the excellent results obtained up to this point, we examined the asymmetric hydrogenation of 1,1-disubstituted terminal olefins containing a polar neighboring group (**S24**-**S27**). The results are summarized in Table 3.5.6.

We initially tested the ligand library in the hydrogenation of the allylic alcohol **S24**. Derivatives of the hydrogenation product 2-phenylpropanol are frequently used as components of fragrance mixtures (i.e. commercial odorants Muguesia and Pamplefleur) and also as intermediates for the synthesis of natural products and drugs (i.e. modulators of dopamine D3 receptors).[15] Iridium complexes containing ligands **L34**-**L36a** proved to be the most selective catalysts, giving 90% ee at room temperature in both enantiomers of the hydrogenation product (Table 3.5.6, entry 1-3). Similarly, the hydrogenation of the allylic acetate **S25** also proceeds with high activity and enantioselectivity with the catalyst systems containing ligands **L34**-**L36a** (Table 3.5.6, entry 4-6). These results are among the best that have been reported for these substrate types.[5c-d,13a]

We next screened ligands **L29**-**L36a**-**g** in the asymmetric hydrogenation of the enol phosphinate **S26** and the allylic silane **S27**. The hydrogenation of these compounds gave rise to important chiral organic intermediates and a number of innovative new organosilicon[16] drugs are

being developed. As previously observed for the trisubstituted enol phosphinates, if ee's have to be high for substrate **S26** phosphite-oxazole ligand types (**L29**) need to be used. Enantioselectivities (ee's up to 82%) were best with catalyst precursor Ir-**L29g** (Table 3.5.6, entry 7). However, for the hydrogenation of **S27**, the best result (ee's up to 93%) was obtained with the Ir-**L34a** catalyst precursor (Table 3.5.6, entry 8). This is therefore one of the few catalytic systems able to hydrogenate allylic silane **S27** in high enantioselectivities.[5c-d] It is also noteworthy that phosphite-oxazole ligands **L29** provide better conversions and enantioselectivities than those obtained with related phosphinite-oxazole ligands **2** in the hydrogenation of enol phosphinate **S26**.[7] This shows once again the benefits of incorporating a biaryl phosphite-moiety into the ligand design for the hydrogenation of enol phosphinates.

Table 3.5.6. Selected results for the Ir-catalyzed hydrogenation of 1,1-disubstituted terminal olefins containing a neighboring polar group using the ligand library **L29-L36a-g**[a]

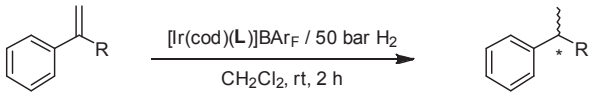

Entry	Substrate	Ligand	% Conv[b]	% ee[c]
1	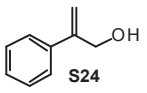	**L34a**	100	87 (*S*)
2		**L35a**	100	90 (*S*)
3		**L36a**	100	90 (*R*)
4	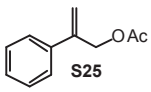	**L34a**	100	83 (*S*)
5		**L35a**	100	87 (*S*)
6		**L36a**	100	87 (*R*)
7[d]	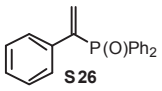	**L29g**	100	82 (*R*)
8	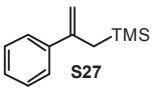	**L34a**	100	93 (*R*)

[a] Reactions carried out using 1 mmol of substrate and 0.5 mol% of Ir-catalyst precursor at 50 bar of H_2. [b] Conversion measured by ^{1}H-NMR measured after 2 h. [c] Enantiomeric excesses determined by chiral GC or HPLC. [d] t= 12 h.

3.5.4. Conclusions

A library of readily available phosphite-oxazole/thiazole ligands (**L29**-**L36a-g**) was applied in the Ir-catalyzed asymmetric hydrogenation of several largely unfunctionalized *E*- and *Z*-trisubstituted and 1,1-disubstituted terminal alkenes. This ligand library combines the advantages of the oxazole/thiazole moieties with those of the phosphite moiety. They are more stable than their oxazoline counterparts, less sensitive to air and other oxidizing agents than phosphines and phosphinites and easy to synthesize from readily available alcohols. Moreover, the highly modular nature of the ligand library enables the bridge length, the substituents in the heterocyclic ring and

the alkyl backbone chain, the configuration of the ligand backbone, and the substituents/configurations in the biaryl phosphite moiety to be easily and systematically varied. We found that the effectiveness at transferring the chiral information in the product can be tuned by choosing suitable ligand components, so that enantioselectivities can be maximized for each substrate as required. Enantioselectivities were therefore excellent (ee's up to >99%) in a wide range of *E*- and *Z*-trisubstituted and 1,1-disubstituted terminal alkenes. It should be noted that these catalytic systems also have high tolerance to the presence of a neighboring polar group and therefore tri- and disubstituted allylic alcohols, acetates, esters, silanes and enol phosphinates can be hydrogenated in high enantioselectivities (ee's up to 99%). We also demonstrated that the introduction of a biaryl-phosphite moiety into the ligand design is highly advantageous in terms of substrate versatility. Therefore, these Ir-phosphite-oxazole/thiazole catalytic systems provided higher enantioselectivities for a wider range of *E*- and *Z*-trisubstituted and 1,1-disubstituted substrates than their related phosphinite-oxazole (**2**) and phosphine-thiazole (**3**) counterparts. These results show that these catalytic systems are among the few alternatives that provide high substrate versatility for *E*- and *Z*-trisubstituted and 1,1-disubstituted terminal alkenes.

3.5.5. Experimental Section

3.5.5.1. General considerations

All reactions were carried out using standard Schlenk techniques under an atmosphere of argon. Solvents were purified and dried by standard procedures. ^{1}H, ^{13}C-{^{1}H}, and ^{31}P-{^{1}H} NMR spectra were recorded using a 400 MHz spectrometer. Chemical shifts are relative to that of $SiMe_4$ (^{1}H and ^{13}C) as internal standard or H_3PO_4 (^{31}P) as external standard. ^{1}H and ^{13}C assignments were made on the basis of ^{1}H-^{1}H gCOSY and ^{1}H-^{13}C gHSQC experiments.

3.5.5.2. Preparation of hydroxyl-oxazoles 12-14 and hydroxyl-thiazole 19

3.5.5.2.1. General procedure for the preparation of hydroxyl-oxazoles 12 and 13

Diazodimedone (2.00 g, 12 mmol) and the corresponding *para* substituted benzonitrile (60 mmol for 4-methylbenzonitrile and 14 mmol for 4-(trifluoromethyl)benzonitrile) were heated in oil bath at 60°C and $Rh(OAc)_2$ (10 mg, 0.045 mmol) was added. Reaction was stirred for 1.5 hours, and if starting material remained, another portion of $Rh(OAc)_2$ (10 mg, 0.045 mmol) was added. After additional 1.5 h reaction was cooled to room temperature and purified by chromatography on silica (pentane:ethyl acetate 75:25 to 25:75) to give the oxazole-ketones as white solids. **7** (2.02 g, 66% yield). ^{1}H NMR ($CDCl_3$), δ: 1.21 (s, 6H, 2 x CH_3), 2.41 (s, 3H, CH_3), 2.50 (s, 2H, CH_2), 2.90 (s, 2H, CH_2), 7.24-7.29 (m, 2H, Ar), 7.97-8.02 (m, 2H, Ar). **8** (1.53 g , 51% yield). ^{1}H NMR ($CDCl_3$), δ: 1.22 (s, 6H, 2 x CH_3), 2.52 (s, 2H, CH_2), 2.93 (s, 2H, CH_2), 7.71-7.75 (m, 2H, Ar), 8.20-8.25 (m, 2H, Ar).

For the reduction of the oxazole-ketones, $BH_3{\cdot}SMe_2$ (2.1 eq) and (*R*)-Me-CBS (0.1 eq) were dissolved in THF (5 mL for 4 mmol $BH_3{\cdot}SMe_2$) at 0°C and stirred for 1 hour. Temperature was raised to ambient and a solution of ketone (1 eq) in THF:toluene (4:1 mL for 2 mmol ketone) was added over 2 hours using a syringe pump. Reaction was stirred for additional 1 hour, cooled to 0°C and quenched with methanol. Solvent was evaporated and resulting oil was purified by

chromatography on silica (pentane:ethyl acetate 25:75) to afford hydroxyl-alcohols **12** and **13** as white solids (72% ee for **12** and 78% ee for **13**). Enantiomeric excess could not be increased by recrystallisation. The enantiomers were separated by chiral chromatography on semipreparative HPLC using (250x20 mm) Chiralcel OD column (hexane:isopropanol 95:5, 5 mL/min) to give ee >99%. Hydroxyl-oxazole **12**. ^{1}H NMR ($CDCl_3$), δ: 1.03 (s, 3H, CH_3), 1.19 (s, 3H, CH_3), 1.67 (dd, 1H, *J* = 13.2 and 8.0 Hz, CH_2), 1.99 (ddd, 1H, *J* = 13.4, 6.0 and 1.5 Hz, CH_2), 2.38 (s, 3H, CH_3-Ph), 2.45 (m, 1H, CH_2), 2.59 (dd, 1H, *J* = 16.4 and 2.2 Hz, CH_2), 3.66 (bs, 1H, OH), 4.85 (m, 1H, CH), 7.18-7.28 (m, 2H, CH=), 7.87-7.95 (m, 2H, CH=). ^{13}C NMR ($CDCl_3$), δ: 24.5, 26.9, 30.6, 33.0, 35.6, 45.5, 62.9, 124.9, 126.1, 129.4, 136.0, 140.3, 147.3, 161.3. Anal. Calc (%) for $C_{16}H_{19}NO_2$: C 74.68, H 7.44, N 5.44; found: C 74.47, H 7.50, N 5.43. Hydroxyl-oxazole **13**. ^{1}H NMR ($CDCl_3$), δ: 1.05 (s, 3H, CH_3), 1.21 (s, 3H, CH_3), 1.68 (dd, 1H, *J* = 13.3 and 8.1 Hz, CH_2), 2.02 (dd, 1H, *J* = 13.3 and 6.0 Hz, CH_2), 2.50 (d, 1H, *J* = 16.8 Hz, CH_2), 2.63 (d, 1H, *J* = 16.8 Hz, CH_2), 3.27 (bs, 1H, OH), 4.87 (m, 1H, CH), 7.63-7.74 (m, 2H, CH=), 8.07-8.18 (m, 2H, CH=). ^{13}C NMR ($CDCl_3$), δ: 27.2, 30.8, 33.3, 35.9, 45.7, 63.2, 126.0, 126.1, 126.6, 131.0, 137.0, 149.0, 160.0. Anal. Calc (%) for $C_{16}H_{16}F_3NO_2$: C 61.73, H 5.18, N 4.50; found: C 61.79, H 5.23, N 4.52.

3.5.5.2.2. Preparation of hydroxyl-oxazole 14

Diazodimedone (5.00 g, 30.1 mmol), pivalonitrile (12.5 g, 150 mmol) and $Rh(OAc)_2$ (27 mg, 0.12 mmol) were heated in oil bath at 60°C. Reaction was stirred for 1 hour and cooled to room temperature and purified by chromatography on silica (pentane:ethyl acetate 75:25 to 25:75) to give oxazole-ketone **9** as a white solid (4.23 g, 68% yield). ^{1}H NMR ($CDCl_3$), δ: 1.16 (s, 6H, 2 x CH_3), 1.39 (s, 9H, 3 x CH_3), 2.41 (s, 2H, CH_2), 2.78 (s, 2H, CH_2)

For the reduction of the oxazole-ketone, ketone (2.22 g, 10 mmol) was dissolved in 95% ethanol (125 mL) and $NaBH_4$ (1.14 g, 30 mmol) was added. Reaction was stirred and followed by TLC. Reaction was quenched with 1 M HCl and extracted with dichloromethane (2 x 25 mL). Organic phase was dried over $MgSO_4$, filtered and concentrated to give racemic hydroxyl-oxazole **14** as a white solid (1.94 g, 87% yield). The enantiomers were separated by chiral chromatography on semipreparative HPLC using (250x20 mm) Chiralcel OD column (hexane:isopropanol 98:2, 5 mL/min) to give ee >99%. ^{1}H NMR ($CDCl_3$), δ: 0.96 (s, 3H, CH_3), 1.11 (s, 3H, CH_3), 1.32 (s, 9H, CH_3, ^{t}Bu), 1.57 (dd, 1H, *J* = 3.2 and 8.0 Hz, CH_2), 1.86 (ddd, 1H, *J* = 13.2, 5.9 and 1.4 Hz, CH_2), 2.30 (dt, 1H, *J* = 16.2 and 1.6 Hz, CH_2), 2.45 (dd, 1H, *J* = 16.2 and 2.1 Hz, CH_2), 4.52 (bs, 1H, OH), 4.74 (m, 1H, CH). ^{13}C NMR ($CDCl_3$), δ: 26.8, 28.5, 30.5, 30.6, 32.9, 33.7, 35.4, 45.5, 62.0, 62.2, 134.2, 146.4, 170.4. Anal. Calc (%) for $C_{13}H_{21}NO_2$: C 69.92, H 9.48, N 6.27; found: C 69.89, H 9.52, N 6.22.

3.5.5.2.3. Preparation of hydroxyl-thiazole 19

$CeCl_3 \cdot 7H_2O$ (3.15 g) was dried in vacuum oven at 120°C over night. Flask with dry $CeCl_3$ (2.00 g, 8.10 mmol) was cooled under nitrogen in ice bath, THF was added (30 mL) and suspension was stirred at room temperature overnight. After cooling in ice bath, a 3 M solution of MeMgCl (4 mL, 12.0 mmol) was added. Suspension was stirred for 2 hours and a solution of thiazole-ester[8b] (0.65 g, 2.26 mmol) was added in THF (10 mL). After stirring overnight, reaction was cooled in ice bath and quenched by addition of saturated NH_4Cl solution (50 mL), stirred for 1 hour. Water (50

mL) was added, THF was evaporated and product was extracted with diethyl ether (2 times). After drying the organic phase over $MgSO_4$, filtering and evaporation of solvent, crude material was purified by chromatoraphy on silica (pentane:ethyl acetate 100:0 to 95:5) to give hydroxyl-thiazole **19** as a white solid (0.44 g, 71% yield). Resolution of enantiomers was achieved on semipreparative HPLC using (250x20 mm) Chiralcel OD column (hexane:isopropanol 95:5, 5 mL/min) to give both enantiomers with ee >99%. ^{1}H NMR ($CDCl_3$), δ: 1.01 (s, 3H, CH_3), 1.32 (s, 3H, CH_3), 1.39 (m, 1H, CH_2), 1.74 (m, 1H, CH_2), 2.02-2.15 (m, 2H, CH_2), 2.73 (m, 1H, CH_2), 2.85 (m, 1H, CH_2), 2.99 (m, 1H, CH_2), 6.48 (bs, 1H, OH), 7.33-7.46 (m, 2H, CH=), 7.80-7.92 (m, 2H, CH=). ^{13}C NMR ($CDCl_3$), δ: 23.1, 23.8, 24.2, 26.2, 27.7, 48.4, 73.5, 126.1, 128.8, 129.8, 131.1, 133.1, 152.4, 164.2. Anal. Calc (%) for $C_{16}H_{19}NOS$: C 70.29, H 7.00, N 5.12; found: C 70.35, H 7.02, N 5.11.

3.5.5.3. General procedure for the preparation of phosphite-nitrogen ligands L29-L36a-g.

Phosphorochloridite (2.2 mmol) produced *in situ* was dissolved in toluene (5 mL) and pyridine (0.36 mL, 4.6 mmol) was added. Hydroxyl-oxazole or hydroxyl-thiazole (2 mmol) was azeotropically dried with toluene (3 x 1 mL) and then dissolved in toluene (10 mL), to which pyridine (0.36 mL, 4.6 mmol) was added. The alcohol solution was transferred slowly at 0 ºC to the solution of phosphorochloridite. The reaction mixture was warmed up to 80 ºC and stirred overnight, and the pyridine salts were removed by filtration. Evaporation of the solvent gave a white foam, which was purified by flash chromatography (toluene/hexane/NEt_3) to produce the corresponding ligand as white powder.

L29a. Yield: 826 mg (60%). ^{31}P NMR (C_6D_6), δ: 148.7. ^{1}H NMR (C_6D_6), δ: 0.57 (s, 3H, CH_3), 0.77 (s, 3H, CH_3), 1.23 (s, 9H, CH_3, ^{t}Bu), 1.25 (s, 9H, CH_3, ^{t}Bu), 1.57 (m, 1H, CH_2), 1.61 (s, 9H, CH_3, ^{t}Bu), 1.69 (s, 9H, CH_3, ^{t}Bu), 1.73 (m, 1H, CH_2), 1.92 (m, 1H, CH_2-C=), 2.08 (m, 1H, CH_2-C=), 5.53 (m, 1H, CH-O), 7.1-8.2 (m, 9H, CH=). ^{13}C NMR (C_6D_6), δ: 27.7 (CH_3), 29.9 (CH_3), 31.9 (CH_3, ^{t}Bu), 33.1 (C, ^{t}Bu), 35.0 (CH_2-C=), 36.2 (CMe_2), 45.1 (CH_2), 67.8 (d, CH-O, $J_{C\text{-}P}$= 12.2 Hz), 124-165 (aromatic carbons). Anal. Calc (%) for $C_{43}H_{56}NO_4P$: C 75.74, H 8.28, N 2.05; found: C 75.82, H 8.11, N 2.11.

L29b. Yield: 725 mg (58%). ^{31}P NMR (C_6D_6), δ: 148.6. ^{1}H NMR (C_6D_6), δ: 0.60 (s, 3H, CH_3), 0.82 (s, 3H, CH_3), 1.55 (s, 9H, CH_3, ^{t}Bu), 1.62 (s, 9H, CH_3, ^{t}Bu), 1.77 (m, 1H, CH_2), 1.80 (m, 1H, CH_2), 1.97 (m, 1H, CH_2-C=), 2.12 (m, 1H, CH_2-C=), 3.28 (s, 3H, CH_3-O), 3.29 (s, 3H, CH_3-O), 5.52 (m, 1H, CH-O), 6.7-8.2 (m, 9H, CH=). ^{13}C NMR (C_6D_6), δ: 27.8 (CH_3), 29.2 (CH_3), 30.0 (CMe_2), 31.6 (CH_3, ^{t}Bu), 31.8 (CH_3, ^{t}Bu), 33.0 (C, ^{t}Bu), 35.6 (CH_2-C=), 45.1 (CH_2), 55.4 (CH_3-O), 55.5 (CH_3-O), 67.9 (d, CH-O, $J_{C\text{-}P}$= 13 Hz), 126-156 (aromatic carbons). Anal. Calc (%) for $C_{37}H_{44}NO_6P$: C 70.57, H 7.04, N 2.22; found: C 70.52, H 7.09, N 2.31.

L29c. Yield: 722 mg (59%). ^{31}P NMR (C_6D_6), δ: 147.8. ^{1}H NMR (C_6D_6), δ: 0.44 (s, 9H, CH_3-Si), 0.55 (s, 9H, CH_3-Si), 0.59 (s, 3H, CH_3), 0.81 (s, 3H, CH_3), 1.58 (m, 1H, CH_2), 1.76 (m, 1H, CH_2), 1.96 (m, 1H, CH_2-C=), 2.13 (m, 1H, CH_2-C=), 5.50 (m, 1H, CH-O), 6.9-8.3 (m, 11H, CH=). ^{13}C NMR (C_6D_6), δ: 0.8 (CH_3-Si), 0.9 (CH_3-Si), 27.9 (CH_3), 30.2 (CH_3), 33.2 (CMe_2), 35.9 (CH_2-C=), 45.3 (CH_2), 67.8 (d, CH-O, $J_{C\text{-}P}$= 8.4 Hz), 123-150 (aromatic carbons). Anal. Calc (%) for $C_{33}H_{40}NO_4PSi_2$: C 65.86, H 6.70, N 2.33; found: C 65.92, H 6.72, N 2.31.

L29f. Yield: 698 mg (49%). ^{31}P NMR (C_6D_6), δ: 146.3. ^{1}H NMR (C_6D_6), δ: 0.45 (s, 3H, CH_3), 0.54 (s, 9H, CH_3-Si), 0.73 (s, 9H, CH_3-Si), 0.82 (s, 3H, CH_3), 1.57 (m, 1H, CH_2), 1.88 (m, 1H,

CH_2), 2.11 (m, 2H, CH_2-C=), 5.02 (m, 1H, CH-O), 6.9-8.3 (m, 15H, CH=). ^{13}C NMR (C_6D_6), δ: 0.5 (CH_3-Si), 1.0 (CH_3-Si), 27.9 (CH_3), 29.7 (CH_3), 32.8 (CMe_2), 35.6 (CH_2-C=), 45.5 (CH_2), 70.2 (CH-O), 123-161 (aromatic carbons). Anal. Calc (%) for $C_{41}H_{44}NO_4PSi_2$: C 70.15, H 6.32, N 2.00; found: C 70.22, H 6.35, N 2.01.

L29g. Yield: 536 mg (39%). ^{31}P NMR (C_6D_6), δ: 147.4. ^{1}H NMR (C_6D_6), δ: 0.33 (s, 3H, CH_3), 0.55 (s, 9H, CH_3-Si), 0.65 (s, 3H, CH_3), 0.68 (s, 9H, CH_3-Si), 1.34 (m, 1H, CH_2), 1.61 (m, 1H, CH_2), 1.89 (m, 1H, CH_2-C=), 2.06 (m, 1H, CH_2-C=), 5.49 (m, 1H, CH-O), 6.9-8.3 (m, 15H, CH=). ^{13}C NMR (C_6D_6), δ: 0.3 (CH_3-Si), 0.4 (CH_3-Si), 26.5 (CH_3), 29.6 (CH_3), 32.4 (CMe_2), 35.1 (CH_2-C=), 44.3 (CH_2), 66.8 (d, CH-O, $J_{C\text{-}P}$= 7.2 Hz), 123-160 (aromatic carbons). Anal. Calc (%) for $C_{41}H_{44}NO_4PSi_2$: C 70.15, H 6.32, N 2.00; found: C 70.19, H 6.29, N 1.97.

L29d. Yield: 712 mg (64%). ^{31}P NMR (C_6D_6), δ: 138.7. ^{1}H NMR (C_6D_6), δ: 0.42 (s, 3H, CH_3), 0.78 (s, 3H, CH_3), 1.48 (dd, 1H, CH_2, $^{2}J_{H\text{-}H}$= 14 Hz, $^{3}J_{H\text{-}H}$= 5.6 Hz), 1.71 (dd, 1H, CH_2, $^{2}J_{H\text{-}H}$= 14 Hz, $^{3}J_{H\text{-}H}$= 5.6 Hz), 1.84 (m, 1H, CH_2-C=, $^{2}J_{H\text{-}H}$= 16 Hz), 2.06 (d, 1H, CH_2-C=, $^{2}J_{H\text{-}H}$= 16 Hz), 5.34 (m, 1H, CH-O), 6.9-8.3 (m, 17H, CH=). ^{13}C NMR (C_6D_6), δ: 28.0 (CH_3), 29.4 (CH_3), 32.7 (CH_2-C=), 35.7 (CMe_2), 45.2 (CH_2), 68.5 (d, CH-O, $J_{C\text{-}P}$= 4.7 Hz), 122-162 (aromatic carbons). Anal. Calc (%) for $C_{35}H_{28}NO_4P$: C 75.39, H 5.06, N 2.51; found: C 75.42, H 5.11, N 2.50.

L29e. Yield: 849 mg (76%). ^{31}P NMR (C_6D_6), δ: 153.1. ^{1}H NMR (C_6D_6), δ: 0.51 (s, 3H, CH_3), 0.72 (s, 3H, CH_3), 1.50 (dd, 1H, CH_2, $^{2}J_{H\text{-}H}$= 12.4 Hz, $^{3}J_{H\text{-}H}$= 5.6 Hz), 1.59 (dd, 1H, CH_2, $^{2}J_{H\text{-}H}$= 12.4 Hz, $^{3}J_{H\text{-}H}$= 7.2 Hz), 1.92 (m, 1H, CH_2-C=, $^{2}J_{H\text{-}H}$= 16.4 Hz), 2.01 (d, 1H, CH_2-C=, $^{2}J_{H\text{-}H}$= 16.4 Hz), 5.43 (m, 1H, CH-O), 6.8- 8.3 (m, 17H, CH=). ^{13}C NMR (C_6D_6), δ: 28.1 (CH_3), 29.7 (CH_3), 32.8 (CH_2-C=), 35.6 (CMe_2), 45.0 (d, CH_2, $J_{C\text{-}P}$= 3.1 Hz), 67.8 (d, CH-O, $J_{C\text{-}P}$= 20.1 Hz), 122-162 (aromatic carbons). Anal. Calc (%) for $C_{35}H_{28}NO_4P$: C 75.39, H 5.06, N 2.51; found: C 75.35, H 5.13, N 2.48.

L30a. Yield: 587 mg (42%). ^{31}P NMR (C_6D_6), δ: 148.0. ^{1}H NMR (C_6D_6), δ: 0.78 (s, 3H, CH_3), 0.98 (s, 3H, CH_3), 1.44 (s, 9H, CH_3, ^{t}Bu), 1.46 (s, 9H, CH_3, ^{t}Bu), 1.79 (m, 1H, CH_2), 1.83 (s, 9H, CH_3, ^{t}Bu), 1.91 (s, 9H, CH_3, ^{t}Bu), 1.95 (m, 1H, CH_2), 2.19 (m, 2H, CH_2-C=), 2.28 (m, 3H, CH_3-Ph), 5.75 (m, 1H, CH-O), 7.1-8.4 (m, 8H, CH=). ^{13}C NMR (C_6D_6), δ: 21.7 (CH_3-Ph), 27.8 (CH_3), 30.0 (CH_3), 31.9 (CH_3, ^{t}Bu), 32.0 (CH_3, ^{t}Bu), 33.1 (C, ^{t}Bu), 36.2 (CH_2-C=), 36.7 (CMe_2), 45.1 (CH_2), 67.9 (d, CH-O, $J_{C\text{-}P}$= 17 Hz), 124-164 (aromatic carbons). Anal. Calc (%) for $C_{44}H_{58}NO_4P$: C 75.94, H 8.40, N 2.01; found: C 75.89, H 8.41, N 2.0.5.

L30f. Yield: 698 mg (49%). ^{31}P NMR (C_6D_6), δ: 146.3. ^{1}H NMR (C_6D_6), δ: 0.43 (s, 3H, CH_3), 0.51 (s, 9H, CH_3-Si), 0.70 (s, 9H, CH_3-Si), 0.80 (s, 3H, CH_3), 1.52 (m, 1H, CH_2), 1.72 (m, 1H, CH_2), 2.18 (m, 2H, CH_2-C=), 2.23 (m, 3H, CH_3-Ph), 5.11 (m, 1H, CH-O), 6.9-8.3 (m, 15H, CH=). ^{13}C NMR (C_6D_6), δ: 0.4 (CH_3-Si), 0.6 (CH_3-Si), 20.9 (CH_3-Ph), 27.8 (CH_3), 29.2 (CH_3), 33.8 (CMe_2), 35.8 (CH_2-C=), 45.6 (CH_2), 69.8 (CH-O), 123-161 (aromatic carbons). Anal. Calc (%) for $C_{42}H_{46}NO_4PSi_2$: C 70.46, H 6.48, N 1.96; found: C 70.52, H 6.49, N 2.00.

L30g. Yield: 623 mg (44%). ^{31}P NMR (C_6D_6), δ: 146.9. ^{1}H NMR (C_6D_6), δ: 0.49 (s, 3H, CH_3), 0.510 (s, 9H, CH_3-Si), 0.66 (s, 9H, CH_3-Si), 0.76 (s, 3H, CH_3), 1.69 (m, 2H, CH_2), 2.21 (m, 2H, CH_2-C=), 2.25 (m, 3H, CH_3-Ph), 5.16 (m, 1H, CH-O), 6.9-8.3 (m, 15H, CH=). ^{13}C NMR (C_6D_6), δ: -0.2 (CH_3-Si), 0.1 (CH_3-Si), 21.1 (CH_3-Ph), 27.9 (CH_3), 29.5 (CH_3), 33.9 (CMe_2), 36.2 (CH_2-C=), 45.3 (CH_2), 70.1 (CH-O), 123-161 (aromatic carbons). Anal. Calc (%) for $C_{42}H_{46}NO_4PSi_2$: C 70.46, H 6.48, N 1.96; found: C 70.49, H 6.51, N 1.99

L31a. Yield: 674 mg (45%). ^{31}P NMR (C_6D_6), δ: 147.8. ^{1}H NMR (C_6D_6), δ: 0.61 (s, 3H, CH_3), 0.81 (s, 3H, CH_3), 1.28 (s, 9H, CH_3, ^{t}Bu), 1.29 (s, 9H, CH_3, ^{t}Bu), 1.60 (m, 1H, CH_2), 1.65 (s, 9H, CH_3, ^{t}Bu), 1.74 (s, 9H, CH_3, ^{t}Bu), 1.77 (m, 1H, CH_2), 1.97 (m, 1H, CH_2-C=), 2.12 (m, 1H, CH_2-C=), 5.55 (m, 1H, CH-O), 7.0-8.1 (m, 8H, CH=). ^{13}C NMR (C_6D_6), δ: 27.6 (CH_3), 30.0 (CH_3), 31.9 (CH_3, ^{t}Bu), 32.0 (CH_3, ^{t}Bu), 33.1 (CMe_2), 35.0 (C, ^{t}Bu), 35.7 (C, ^{t}Bu), 36.2 (CH_2-C=), 45.0 (CH_2), 67.5 (d, CH-O, $J_{C\text{-}P}$= 11.5 Hz), 124-160 (aromatic carbons). Anal. Calc (%) for $C_{44}H_{55}F_3NO_4P$: C 70.47, H 7.39, N 1.87; found: C 70.57, H 7.42, N 1.89.

L31c. Yield: 593 mg (44%). ^{31}P NMR (C_6D_6), δ: 146.8. ^{1}H NMR (C_6D_6), δ: 0.39 (s, 9H, CH_3-Si), 0.49 (s, 9H, CH_3-Si), 0.53 (s, 3H, CH_3), 0.77 (s, 3H, CH_3), 1.52 (m, 1H, CH_2), 1.69 (m, 1H, CH_2), 1.95 (m, 1H, CH_2-C=), 2.12 (m, 1H, CH_2-C=), 5.42 (m, 1H, CH-O), 6.9-8.1 (m, 10H, CH=). ^{13}C NMR (C_6D_6), δ: 0.9 (CH_3-Si), 1.0 (CH_3-Si), 27.7 (CH_3), 30.3 (CH_3), 33.2 (CMe_2), 35.9 (CH_2-C=), 45.0 (CH_2), 67.5 (d, CH-O, $J_{C\text{-}P}$= 6.1 Hz), 124-160 (aromatic carbons). Anal. Calc (%) for $C_{34}H_{39}F_3NO_4PSi_2$: C 60.97, H 5.87, N 2.09; found: C 60.99, H 5.89, N 2.07.

L31g. Yield: 676 mg (43%). ^{31}P NMR (C_6D_6), δ: 146.3. ^{1}H NMR (C_6D_6), δ: 0.43 (s, 3H, CH_3), 0.51 (s, 9H, CH_3-Si), 0.62 (s, 3H, CH_3), 0.65 (s, 9H, CH_3-Si), 1.34 (m, 1H, CH_2), 1.56 (m, 1H, CH_2), 1.84 (m, 1H, CH_2-C=), 2.02 (m, 1H, CH_2-C=), 5.42 (m, 1H, CH-O), 6.8-8.1 (m, 14H, CH=). ^{13}C NMR (C_6D_6), δ: 1.0 (CH_3-Si), 1.1 (CH_3-Si), 27.0 (CH_3), 30.3 (CH_3), 33.2 (CMe_2), 35.8 (CH_2-C=), 45.0 (CH_2), 67.2 (d, CH-O, $J_{C\text{-}P}$= 5.3 Hz), 123-160 (aromatic carbons). Anal. Calc (%) for $C_{42}H_{43}F_3NO_4PSi_2$: C 65.52, H 5.63, N 1.82; found: C 65.34, H 5.59, N 1.86.

L32a. Yield: 652 mg (49%). ^{31}P NMR (C_6D_6), δ: 148.0. ^{1}H NMR (C_6D_6), δ: 0.59 (s, 3H, CH_3), 0.80 (s, 3H, CH_3), 1.28 (s, 9H, CH_3, ^{t}Bu), 1.29 (s, 9H, CH_3, ^{t}Bu), 1.40 (s, 9H, CH_3, ^{t}Bu), 1.56 (m, 1H, CH_2), 1.66 (s, 9H, CH_3, ^{t}Bu), 1.71 (s, 9H, CH_3, ^{t}Bu), 1.75 (m, 1H, CH_2), 1.98 (m, 1H, CH_2-C=), 2.14 (m, 1H, CH_2-C=), 5.52 (m, 1H, CH-O), 7.0-7.7 (m, 4H, CH=). ^{13}C NMR (C_6D_6), δ: 27.8 (CH_3), 29.2 (CH_3), 29.9 (CH_3, ^{t}Bu), 32.0 (CH_3, ^{t}Bu), 32.2 (CH_3, ^{t}Bu), 33.1 (CMe_2), 34.4 (C, ^{t}Bu), 35.0 (C, ^{t}Bu), 36.1 (CH_2-C=), 36.2 (C, ^{t}Bu), 45.3 (CH_2), 68.1 (d, CH-O, $J_{C\text{-}P}$= 12 Hz), 124-170 (aromatic carbons). Anal. Calc (%) for $C_{41}H_{60}NO_4P$: C 74.40, H 9.14, N 2.12; found: C 74.45, H 9.18, N 2.08.

L32c. Yield: 709 mg (61%). ^{31}P NMR (C_6D_6), δ: 148.2. ^{1}H NMR (C_6D_6), δ: 0.49 (s, 9H, CH_3-Si), 0.54 (s, 9H, CH_3-Si), 0.57 (s, 3H, CH_3), 0.78 (s, 3H, CH_3), 1.21 (s, 9H, CH_3, ^{t}Bu), 1.45 (m, 1H, CH_2), 1.69 (m, 1H, CH_2), 1.96 (m, 1H, CH_2-C=), 2.19 (m, 1H, CH_2-C=), 5.48 (m, 1H, CH-O), 6.9-7.8 (m, 6H, CH=). ^{13}C NMR (C_6D_6), δ: 0.2 (CH_3-Si), 0.4 (CH_3-Si), 27.9 (CH_3), 29.8 (CH_3), 30.2 (CH_3, ^{t}Bu), 33.2 (CMe_2), 36.3 (CH_2-C=), 45.5 (CH_2), 68.3 (d, CH-O, $J_{C\text{-}P}$= 10 Hz), 123-155 (aromatic carbons). Anal. Calc (%) for $C_{31}H_{44}NO_4PSi_2$: C 63.99, H 7.62, N 2.41; found: C 64.03, H 7.65, N 2.39.

L33a. Yield: 843 mg (62%). ^{31}P NMR (C_6D_6), δ: 148.7. ^{1}H NMR (C_6D_6), δ: 0.57 (s, 3H, CH_3), 0.77 (s, 3H, CH_3), 1.23 (s, 9H, CH_3, ^{t}Bu), 1.25 (s, 9H, CH_3, ^{t}Bu), 1.57 (m, 1H, CH_2), 1.61 (s, 9H, CH_3, ^{t}Bu), 1.69 (s, 9H, CH_3, ^{t}Bu), 1.73 (m, 1H, CH_2), 1.92 (m, 1H, CH_2-C=), 2.08 (m, 1H, CH_2-C=), 5.53 (m, 1H, CH-O), 7.1-8.2 (m, 9H, CH=). ^{13}C NMR (C_6D_6), δ: 27.7 (CH_3), 29.9 (CH_3), 31.9 (CH_3, ^{t}Bu), 33.1 (C, ^{t}Bu), 35.0 (CH_2-C=), 36.2 (CMe_2), 45.1 (CH_2), 67.8 (d, CH-O, $J_{C\text{-}P}$= 12.2 Hz), 124-165 (aromatic carbons). Anal. Calc (%) for $C_{43}H_{56}NO_4P$: C 75.74, H 8.28, N 2.05; found: C 75.72, H 8.31, N 2.01.

L34a. Yield: 738 mg (54%). ^{31}P NMR (C_6D_6), δ: 137.9. ^{1}H NMR (C_6D_6), δ: 1.43 (s, 9H, CH_3, ^{t}Bu), 1.48 (s, 9H, CH_3, ^{t}Bu), 1.76 (m, 2H, CH_2), 1.82 (s, 9H, CH_3, ^{t}Bu), 1.87 (s, 9H, CH_3, ^{t}Bu), 2.00

(m, 2H, CH_2-CH), 2.46 (m, 2H, CH_2-C=), 3.36 (m, 1H, CH), 4.48 (m, 1H, CH_2-O), 4.83 (m, 1H, CH_2-O), 7.2-8.2 (m, 9H, CH=). ^{13}C NMR (C_6D_6), δ: 21.4 (CH_2), 23.9 (CH_2-C=), 26.1 (CH_2-CH), 31.8 (CH_3, ^{t}Bu), 35.0 (C, ^{t}Bu), 36.1 (C, ^{t}Bu), 39.1 (CH), 67.3 (CH_2-O), 125-165 (aromatic carbons). Anal. Calc (%) for $C_{42}H_{54}NO_3PS$: C 73.76, H 7.96, N 2.05; found: C 73.86, H 7.99, N 2.08.

L34b. Yield: 598 mg (48%). ^{31}P NMR (C_6D_6), δ: 137.5. ^{1}H NMR (C_6D_6), δ: 1.33 (m, 2H, CH_2), 1.54 (s, 9H, CH_3, ^{t}Bu), 1.59 (s, 9H, CH_3, ^{t}Bu), 1.82 (m, 2H, CH_2-CH), 2.27 (m, 2H, CH_2-C=), 3.15 (m, 1H, CH), 3.29 (s, 3H, CH_3-O), 3.33 (s, 3H, CH_3-O), 4.33 (m, 1H, CH_2-O), 4.71 (m, 1H, CH_2-O), 6.7-8.1 (m, 9H, CH=). ^{13}C NMR (C_6D_6), δ: 21.7 (CH_2), 23.9 (CH_2-C=), 26.3 (CH_2-CH), 31.3 (CH_3, ^{t}Bu), 31.4 (CH_3, ^{t}Bu), 35.9 (C, ^{t}Bu), 36.0 (C, ^{t}Bu), 39.2 (CH), 55.4 (CH_3-O), 67.7 (CH_2-O), 112-165 (aromatic carbons). Anal. Calc (%) for $C_{36}H_{42}NO_5PS$: C 68.44, H 6.70, N 2.22; found: C 68.48, H 6.72, N 2.20.

L34c. Yield: 640 mg (53%). ^{31}P NMR (C_6D_6), δ: 136.5. ^{1}H NMR (C_6D_6), δ: 0.44 (s, 9H, CH_3-Si), 0.52 (s, 9H, CH_3-Si), 1.36 (m, 1H, CH_2), 1.56 (m, 1H, CH_2), 1.79 (m, 2H, CH_2-CH), 2.27 (m, 2H, CH_2-C=), 3.15 (m, 1H, CH), 4.15 (m, 1H, CH_2-O), 4.68 (m, 1H, CH_2-O), 6.9-8.2 (m, 11H, CH=). ^{13}C NMR (C_6D_6), δ: 0.7 (CH_3-Si), 0.8 (CH_3-Si), 21.8 (CH_2), 24.2 (CH_2-C=), 26.5 (CH_2-CH), 39.3 (CH), 67.8 (CH_2-O), 125-165 (aromatic carbons). Anal. Calc (%) for $C_{32}H_{38}NO_3PSSi_2$: C 63.65, H 6.34, N 2.32; found: C 63.68, H 6.36, N 2.35.

L34f. Yield: 647 mg (47%). ^{31}P NMR (C_6D_6), δ: 136.2. ^{1}H NMR (C_6D_6), δ: 0.58 (s, 9H, CH_3-Si), 0.59 (s, 9H, CH_3-Si), 1.36 (m, 2H, CH_2), 1.72 (m, 2H, CH_2-CH), 2.32 (m, 2H, CH_2-C=), 2.94 (m, 1H, CH), 3.96 (m, 1H, CH_2-O), 4.76 (m, 1H, CH_2-O), 6.9-8.3 (m, 15H, CH=). ^{13}C NMR (C_6D_6), δ: -0.3 (CH_3-Si), -0.1 (CH_3-Si), 21.3 (CH_2), 23.2 (CH_2-C=), 25.8 (CH_2-CH), 38.4 (d, CH, $J_{C\text{-}P}$= 3.2 Hz), 67.1 (CH_2-O), 122-164 (aromatic carbons). Anal. Calc (%) for $C_{40}H_{42}NO_3PSSi_2$: C 68.24, H 6.01, N 1.99; found: C 68.21, H 5.98, N 1.97.

L34g. Yield: 605 mg (43%). ^{31}P NMR (C_6D_6), δ: 136.3. ^{1}H NMR (C_6D_6), δ: 0.61 (s, 9H, CH_3-Si), 0.73 (s, 9H, CH_3-Si), 1.31 (m, 1H, CH_2), 1.45 (m, 1H, CH_2), 1.63 (m, 1H, CH_2-CH), 1.88 (m, 1H, CH_2-CH), 2.16 (m, 2H, CH_2-C=), 3.21 (m, 1H, CH), 4.16 (m, 1H, CH_2-O), 4.43 (m, 1H, CH_2-O), 6.8-8.4 (m, 15H, CH=). ^{13}C NMR (C_6D_6), δ: -0.2 (CH_3-Si), -0.1 (CH_3-Si), 20.6 (CH_2), 23.0 (CH_2-C=), 25.6 (CH_2-CH), 38.1 (d, CH, $J_{C\text{-}P}$= 4.0 Hz), 67.1 (CH_2-O), 122-164 (aromatic carbons). Anal. Calc (%) for $C_{40}H_{42}NO_3PSSi_2$: C 68.24, H 6.01, N 1.99; found: C 68.27, H 6.03, N 2.02.

L35a. Yield: 598 mg (42%). ^{31}P NMR (C_6D_6), δ: 151.4. ^{1}H NMR (C_6D_6), δ: 1.19 (s, 3H, CH_3), 1.24 (s, 9H, CH_3, ^{t}Bu), 1.26 (s, 9H, CH_3, ^{t}Bu), 1.50 (s, 9H, CH_3, ^{t}Bu), 1.53 (s, 3H, CH_3), 1.62 (s, 9H, CH_3, ^{t}Bu), 1.89 (m, 2H, CH_2), 2.12 (m, 2H, CH_2-CH), 2.28 (m, 2H, CH_2-C=), 3.16 (m, 1H, CH), 7.0-8.0 (m, 9H, CH=). ^{13}C NMR (C_6D_6), δ: 22.4 (CH_2), 24.3 (CH_2-C=), 26.4 (CH_2-CH), 27.9 (CH_3), 30.4 (CH_3), 31.4 (CH_3, ^{t}Bu), 31.6 (CH_3, ^{t}Bu), 31.8 (CH_3, ^{t}Bu), 35.1 (C, ^{t}Bu), 36.3 (C, ^{t}Bu), 36.4 (C, ^{t}Bu), 40.3 (CH), 71.0 (CMe_2), 124-166 (aromatic carbons). Anal. Calc (%) for $C_{44}H_{58}NO_3PS$: C 74.23, H 8.21, N 1.97; found: C 74.31, H 8.24, N 1.93.

L35f. Yield: 638 mg (42%). ^{31}P NMR (C_6D_6), δ: 143.2. ^{1}H NMR (C_6D_6), δ: 0.53 (s, 9H, CH_3-Si), 0.56 (s, 9H, CH_3-Si), 1.14 (s, 3H, CH_3), 1.50 (s, 3H, CH_3), 1.77 (m, 2H, CH_2), 2.09 (m, 2H, CH_2-CH), 2.25 (m, 2H, CH_2-C=), 3.17 (m, 1H, CH), 7.0-8.0 (m, 15H, CH=). ^{13}C NMR (C_6D_6), δ: -0.3 (CH_3-Si), -0.1 (CH_3-Si), 22.1 (CH_2), 23.8 (CH_2-C=), 25.9 (CH_2-CH), 27.8 (CH_3), 29.9 (CH_3), 39.9 (CH), 70.3 (CH_2-O), 122-166 (aromatic carbons). Anal. Calc (%) for $C_{44}H_{50}NO_3PSSi_2$: C 69.53, H 6.63, N 1.84; found: C 69.55, H 6.64, N 1.80.

L36a. Yield: 798 mg (56%). ^{31}P NMR (C_6D_6), δ: 151.4. ^{1}H NMR (C_6D_6), δ: 1.24 (s, 9H, CH_3, ^{t}Bu), 1.26 (s, 9H, CH_3, ^{t}Bu), 1.50 (s, 9H, CH_3, ^{t}Bu), 1.53 (s, 3H, CH_3), 1.62 (s, 9H, CH_3, ^{t}Bu), 1.89 (m, 2H, CH_2), 2.12 (m, 2H, $\underline{CH_2}$-CH), 2.28 (m, 2H, CH_2-C=), 3.16 (m, 1H, CH), 7.0-8.0 (m, 9H, CH=). ^{13}C NMR (C_6D_6), δ: 22.4 (CH_2), 24.3 (CH_2-C=), 26.4 ($\underline{C}H_2$-CH), 27.9 (CH_3), 30.4 (CH_3), 31.4 (CH_3, ^{t}Bu), 31.6 (CH_3, ^{t}Bu), 31.8 (CH_3, ^{t}Bu), 35.1 (C, ^{t}Bu), 36.3 (C, ^{t}Bu), 36.4 (C, ^{t}Bu), 40.3 (CH), 71.0 (CMe_2), 124-166 (aromatic carbons). Anal. Calc (%) for $C_{44}H_{58}NO_3PS$: C 74.23, H 8.21, N 1.97; found: C 74.28, H 8.21, N 1.99.

L36f. Yield: 808 mg (50%). ^{31}P NMR (C_6D_6), δ: 143.1. ^{1}H NMR (C_6D_6), δ: 0.49 (s, 9H, CH_3-Si), 0.59 (s, 9H, CH_3-Si), 1.19 (s, 3H, CH_3), 1.53 (s, 3H, CH_3), 1.74 (m, 2H, CH_2), 2.04 (m, 2H, $\underline{CH_2}$-CH), 2.21 (m, 2H, CH_2-C=), 3.32 (m, 1H, CH), 7.0-8.0 (m, 15H, CH=). ^{13}C NMR (C_6D_6), δ: -0.1 (CH_3-Si), 0.1 (CH_3-Si), 21.9 (CH_2), 23.4 (CH_2-C=), 26.3 ($\underline{C}H_2$-CH), 27.9 (CH_3), 30.2 (CH_3), 39.3 (CH), 69.9 (CH_2-O), 122-166 (aromatic carbons). Anal. Calc (%) for $C_{44}H_{50}NO_3PSSi_2$: C 69.53, H 6.63, N 1.84; found: C 69.57, H 6.66, N 1.86.

3.5.5.4. Typical procedure for the preparation of [Ir(cod)(L)]BAr$_F$

The corresponding ligand (0.074 mmol) was dissolved in CH_2Cl_2 (2 mL) and $[Ir(COD)Cl]_2$ (25 mg, 0.037 mmol) was added. The reaction was refluxed at 50 °C for 1 hour. After 5 min at room temperature, $NaBAr_F$ (77.1 mg, 0.082 mmol) and water (2 mL) were added and the reaction mixture was stirred vigorously for 30 min at room temperature. The phases were separated and the aqueous phase was extracted twice with CH_2Cl_2. The combined organic phases were filtered through a celite plug, dried with $MgSO_4$ and the solvent was evaporated to give the product as an orange solid.

[Ir(cod)(L29a)]BAr$_F$. Yield: 127 mg (93%). ^{31}P NMR ($CDCl_3$), δ: 108.9. ^{1}H NMR ($CDCl_3$), δ: 1.08 (s, 3H, CH_3), 1.28 (s, 3H, CH_3), 1.37 (s, 9H, CH_3, ^{t}Bu), 1.39 (s, 9H, CH_3, ^{t}Bu), 1.51 (s, 9H, CH_3, ^{t}Bu), 1.59 (s, 9H, CH_3, ^{t}Bu), 1.68 (m, 4H, CH_2, cod), 1.81 (dd, 1H, CH_2, $^{2}J_{H-H}$= 18.1 Hz, $^{3}J_{H-H}$= 8.8 Hz), 2.04 (m, 1H, CH_2), 2.35 (m, 4H, CH_2, cod), 2.54 (d, 1H, CH_2-C=, $^{2}J_{H-H}$= 17.4 Hz), 2.68 (d, 1H, CH_2-C=, $^{2}J_{H-H}$= 17.1 Hz), 4.03 (m, 1H, CH=, cod), 4.39 (b, 2H, CH=, cod), 5.35 (b, 1H, CH=, cod), 5.61 (s, 1H, CH-O), 6.9-8.2 (m, 21H, CH=). ^{13}C NMR ($CDCl_3$), δ: 24.6 (CH_2, cod), 27.1 (CH_2, cod), 28.4 (CH_3), 29.2 (CH_3), 31.1 (CH_3, ^{t}Bu), 31.2 (CH_3, ^{t}Bu), 31.5 (CH_3, ^{t}Bu), 32.6 (CH_3, ^{t}Bu), 34.6 (CH_2, cod), 35.0 (CH_2-C=), 35.1 (b, C, ^{t}Bu), 35.6 (b, C, ^{t}Bu), 36.0 (CMe_2), 37.5 (b, CH_2, cod), 42.2 (b, CH_2), 69.5 (b, CH-O), 70.1 (CH=, cod), 70.9 (CH, cod), 91.7 (d, CH=, cod, J_{C-P}= 23.6 Hz), 105.5 (b, CH=, cod), 113-116 (aromatic carbons), 117.7 (b, CH=, BAr_F), 119-134 (aromatic carbons), 135.0 (b, CH= BAr_F), 136-157 (aromatic carbons), 161.9 (q, C-B, BAr_F, $^{1}J_{C-B}$= 49.5 Hz), 165.9 (C=N). Anal. Calc (%) for $C_{83}H_{80}BF_{24}IrNO_4P$: C 54.02, H 4.37, N 0.76; found: C 53.98, H 4.48, N 0.77.

[Ir(cod)(L29b)]BAr$_F$. Yield: 126 mg (95%). ^{31}P NMR ($CDCl_3$), δ: 111.6. ^{1}H NMR ($CDCl_3$), δ: 1.06 (s, 3H, CH_3), 1.08 (s, 3H, CH_3), 1.49 (s, 9H, CH_3, ^{t}Bu), 1.56 (s, 9H, CH_3, ^{t}Bu), 1.65 (m, 4H, CH_2, cod), 1.81 (dd, 1H, CH_2, $^{2}J_{H-H}$= 14.1 Hz, $^{3}J_{H-H}$= 6.6 Hz), 2,07 (dd, 1H, CH_2, $^{2}J_{H-H}$= 14.4 Hz, $^{3}J_{H-H}$= 6.6 Hz), 2.22 (m, 2H, CH_2, cod), 2.43 (m, 2H, CH_2, cod), 2.53 (d, 1H, CH_2-C=, $^{2}J_{H-H}$= 17.4 Hz), 2.67 (d, 1H, CH_2-C=, $^{2}J_{H-H}$= 17.1 Hz), 3.84 (s, 3H, CH_3-O), 3.86 (s, 3H, CH_3-O), 4.02 (m, 1H, CH=, cod), 4.44 (b, 1H, CH=, cod), 4.59 (b, 1H, CH=, cod), 5.34 (b, 1H, CH=, cod), 5.58 (s, 1H, CH-O), 6.6-8.2 (m, 21H, CH=). ^{13}C NMR ($CDCl_3$), δ: 24.5 (CH_2, cod), 27.1 (CH_2, cod), 28.4 (CH_3), 29.1 (CH_3), 31.1 (CH_3, ^{t}Bu), 32.2 (CH_3, ^{t}Bu), 34.7 (CH_2, cod), 35.0 (CH_2-C=), 35.6 (b, C, ^{t}Bu), 36.0

(CMe_2), 37.6 (CH_2, cod), 42.4 (b, CH_2), 55.8 (CH_3-O), 69.6 (b, CH-O), 70.5 (CH=, cod), 70.9 (CH=, cod), 91.2 (d, CH=, cod, J_{C-P}= 23.6 Hz), 105.5 (b, CH=, cod), 113-116 (aromatic carbons), 117.7 (b, CH=, BAr_F), 119-134 (aromatic carbons), 135.0 (b, CH= BAr_F), 136-157 (aromatic carbons), 161.9 (q, C-B, BAr_F, $^1J_{C-B}$= 49.5 Hz), 165.7 (C=N). Anal. Calc (%) for $C_{77}H_{68}BF_{24}IrNO_3PSSi_2$: C 51.57, H 3.82, N 0.78; found. C 51.62, H 3.85, N 0.75.

[Ir(cod)(L29c)]BAr_F. Yield: 120 mg (92%). ^{31}P NMR ($CDCl_3$), δ: 107.6. ^{1}H NMR ($CDCl_3$), δ: 0.28 (s, 9H, CH_3-Si), 0.50 (s, 9H, CH_3-Si), 1.06 (s, 3H, CH_3), 1.07 (s, 3H, CH_3), 1.61 (m, 4H, CH_2, cod), 1.81 (dd, 1H, CH_2, $^2J_{H-H}$= 14.1 Hz, $^3J_{H-H}$= 5.7 Hz), 2,07 (m, 2H, CH_2 and CH_2 cod), 2.16 (m, 1H, CH_2, cod), 2.43 (m, 2H, CH_2, cod), 2.53 (d, 1H, CH_2-C=, $^2J_{H-H}$= 17.4 Hz), 2.67 (d, 1H, CH_2-C=, $^2J_{H-H}$= 17.5 Hz), 4.07 (m, 1H, CH=, cod), 4.27 (b, 1H, CH=, cod), 4.41 (b, 1H, CH=, cod), 5.50 (b, 1H, CH=, cod), 5.64 (s, 1H, CH-O), 7.2-8.1 (m, 23H, CH=). ^{13}C NMR ($CDCl_3$), δ: 0.34 (CH_3-Si), 0.86 (CH_3-Si), 24.6 (CH_2, cod), 27.4 (CH_2, cod), 28.4 (CH_3), 28.8 (CH_3), 34.3 (CH_2, cod), 35.2 (CH_2-C=), 36.0 (CMe_2), 37.7 (d, CH_2, cod, J_{C-P}= 6.8 Hz), 42.4 (d, CH_2, J_{C-P}= 9.1 Hz), 65.6 (d, CH-O, J_{C-P}= 3.7 Hz), 70.3 (CH=, cod), 70.5 (CH=, cod), 93.4 (d, CH=, cod, J_{C-P}= 22.5 Hz), 107.1 (d, CH=, cod, J_{C-P}= 10.8 Hz), 117.7 (b, CH=, BAr_F), 119-134 (aromatic carbons), 135.0 (b, CH= BAr_F), 136-153 (aromatic carbons), 161.9 (q, C-B, BAr_F, $^1J_{C-B}$= 49.2 Hz), 165.9 (C=N). Anal. Calc (%) for $C_{73}H_{64}BF_{24}IrNO_3PSSi_2$: C 49.66, H 3.65, N 0.79; found. C 49.68, H 3.69, N 0.78.

[Ir(cod)(L29d)]BAr_F. Yield: 120 mg (94%). ^{31}P NMR ($CDCl_3$), δ: 104.2 (s). ^{1}H NMR ($CDCl_3$), δ: 0.92 (s, 3H, CH_3), 1.12 (s, 3H, CH_3), 1.52 (m, 4H, CH_2, cod), 1.62 (dd, 1H, CH_2, $^2J_{H-H}$= 14 Hz, $^3J_{H-H}$= 5.6 Hz), 1.92 (dd, 1H, CH_2, $^2J_{H-H}$= 14 Hz, $^3J_{H-H}$= 5.4 Hz), 2.09 (m,1H, CH_2 cod), 2.15 (m, 1H, CH_2, cod), 2.25 (m, 2H, CH_2, cod), 2.53 (m, 1H, CH_2-C=, $^2J_{H-H}$= 16 Hz), 2.61 (d, 1H, CH_2-C=, $^2J_{H-H}$= 16 Hz), 3.80 (m, 1H, CH=, cod), 4.20 (b, 2H, CH=, cod), 5.32 (b, 1H, CH=, cod), 5.59 (m, 1H, CH-O), 6.9-8.3 (m, 29H, CH=). ^{13}C NMR ($CDCl_3$), δ: 24.3 (CH_2, cod), 29.1 (CH_3), 29.9 (CH_2, cod), 30.4 (CH_3), 32.5 (CH_2, cod), 33.1 (CH_2-C=), 35.4 (CMe_2), 36.5 (CH_2), 43.1 (d, CH_2, J_{C-P}= 9.4 Hz), 61.9 (d, CH-O, J_{C-P}= 3.1 Hz), 69.9 (CH=, cod), 70.2 (CH=, cod), 97.3 (d, CH=, cod, J_{C-P}= 18.9 Hz), 107.8 (d, CH=, cod, J_{C-P}= 9.9 Hz), 117.6 (b, CH=, BAr_F), 119-134 (aromatic carbons), 135.0 (b, CH= BAr_F), 136-159 (aromatic carbons), 161.8 (q, C-B, BAr_F, $^1J_{C-B}$= 49.2 Hz), 167.4 (C=N). Anal. Calc (%) for $C_{75}H_{52}BF_{24}IrNO_4P$: C 52.34, H 3.05, N 0.81; found: C 52.36, H 3.07, N 0.79.

[Ir(cod)(L29e)]BAr_F. Yield: 118 mg (93%). ^{31}P NMR ($CDCl_3$), δ: 103.9 (s). ^{1}H NMR ($CDCl_3$), δ: 0.89 (s, 3H, CH_3), 1.11 (s, 3H, CH_3), 1.53 (m, 4H, CH_2, cod), 1.72 (dd, 1H, CH_2, $^2J_{H-H}$= 14.4 Hz, $^3J_{H-H}$= 6.0 Hz), 1.88 (dd, 1H, CH_2, $^2J_{H-H}$= 14.4 Hz, $^3J_{H-H}$= 5.6 Hz), 2.11 (m,1H, CH_2 cod), 2.14 (m, 1H, CH_2, cod), 2.23 (m, 2H, CH_2, cod), 2.48 (m, 1H, CH_2-C=, $^2J_{H-H}$= 16 Hz), 2.63 (d, 1H, CH_2-C=, $^2J_{H-H}$= 16 Hz), 3.81 (m, 1H, CH=, cod), 4.22 (b, 2H, CH=, cod), 5.28 (b, 1H, CH=, cod), 5.63 (m, 1H, CH-O), 6.9-8.3 (m, 29H, CH=). ^{13}C NMR ($CDCl_3$), δ: 24.1 (CH_2, cod), 28.9 (CH_2, cod), 29.7 (CH_3), 30.6 (CH_3), 32.4 (CH_2, cod), 33.0 (CH_2-C=), 35.6 (CMe_2), 36.8 (CH_2), 43.2 (d, CH_2, J_{C-P}= 8.4 Hz), 61.8 (d, CH-O, J_{C-P}= 2.8 Hz), 68.3 (CH=, cod), 70.1 (CH=, cod), 96.2 (d, CH=, cod, J_{C-P}= 16.5 Hz), 103.6 (d, CH=, cod, J_{C-P}= 10.2 Hz), 117.6 (b, CH=, BAr_F), 119-134 (aromatic carbons), 135.0 (b, CH=, BAr_F), 136-159 (aromatic carbons), 161.8 (q, C-B, BAr_F, $^1J_{C-B}$= 49.2 Hz), 167.7 (C=N). Anal. Calc (%) for $C_{75}H_{52}BF_{24}IrNO_4P$: C 52.34, H 3.05, N 0.81; found: C 52.32, H 3.08, N 0.80.

[Ir(cod)(L29f)]BAr_F. Yield: 130 mg (94%). ^{31}P NMR ($CDCl_3$), δ: 107.7. ^{1}H NMR ($CDCl_3$), δ: 0.21 (s, 9H, CH_3-Si), 0.54 (s, 9H, CH_3-Si), 1.04 (s, 3H, CH_3), 1.18 (s, 3H, CH_3), 1.49 (m, 2H, CH_2, cod), 1.53 (m, 2H, CH_2, cod), 1.78 (dd, 1H, CH_2, $^2J_{H-H}$= 14.2 Hz, $^3J_{H-H}$= 5.6 Hz), 2.09 (b, 2H, CH_2

and CH_2 cod), 2.14 (m, 1H, CH_2, cod), 2.25 (m, 2H, CH_2, cod), 2.56 (d, 1H, CH_2-C=, $^2J_{H-H}$= 17.2 Hz), 2.63 (d, 1H, CH_2-C=, $^2J_{H-H}$= 17.2 Hz), 3.81 (m, 1H, CH=, cod), 4.20 (b, 2H, CH=, cod), 5.41 (b, 1H, CH=, cod), 5.49 (s, 1H, CH-O), 7.2-8.1 (m, 27H, CH=). ^{13}C NMR ($CDCl_3$), δ: 0.3 (CH_3-Si), 1.2 (CH_3-Si), 25.4 (CH_2, cod), 29.7 (CH_2, cod), 30.0 (CH_3), 31.2 (CH_3), 32.3 (CH_2, cod), 33.6 (CH_2-C=), 35.4 (CMe_2), 36.2 (d, CH_2, cod, J_{C-P}= 7.2 Hz), 42.8 (d, CH_2, J_{C-P}= 8.4 Hz), 61.3 (d, CH-O, J_{C-P}= 4.2 Hz), 70.0 (CH=, cod), 70.4 (CH=, cod), 97.8 (d, CH=, cod, J_{C-P}= 20.4 Hz), 106.8 (d, CH=, cod, J_{C-P}= 9.6 Hz), 117.8 (b, CH=, BAr_F), 119-134 (aromatic carbons), 135.0 (b, CH= BAr_F), 136-153 (aromatic carbons), 161.9 (q, C-B, BAr_F, $^1J_{C-B}$= 49.2 Hz), 168.1 (C=N). Anal. Calc (%) for $C_{81}H_{68}BF_{24}IrNO_4PSi_2$: C 52.15, H 3.67, N 0.75; found: C 52.17, H 3.69, N 0.74.

[Ir(cod)(L29g)]BAr_F. Yield: 134 mg (97%). ^{31}P NMR ($CDCl_3$), δ: 108.0. ^{1}H NMR ($CDCl_3$), δ: 0.23 (s, 9H, CH_3-Si), 0.60 (s, 9H, CH_3-Si), 1.09 (s, 3H, CH_3), 1.20 (s, 3H, CH_3), 1.58 (m, 4H, CH_2, cod), 1.73 (dd, 1H, CH_2, $^2J_{H-H}$= 14.1 Hz, $^3J_{H-H}$= 5.7 Hz), 2.07 (m, 2H, CH_2 and CH_2 cod), 2.16 (m, 1H, CH_2, cod), 2.27 (m, 2H, CH_2, cod), 2.58 (d, 1H, CH_2-C=, $^2J_{H-H}$= 17.3 Hz), 2.67 (d, 1H, CH_2-C=, $^2J_{H-H}$= 17.5 Hz), 3.81 (m, 1H, CH=, cod), 4.22 (b, 2H, CH=, cod), 5.36 (b, 1H, CH=, cod), 5.51 (s, 1H, CH-O), 7.2-8.1 (m, 27H, CH=). ^{13}C NMR ($CDCl_3$), δ: 0.5 (CH_3-Si), 0.9 (CH_3-Si), 25.6 (CH_2, cod), 29.9 (CH_2, cod), 30.1 (CH_3), 30.8 (CH_3), 32.2 (CH_2, cod), 33.4 (CH_2-C=), 35.2 (CMe_2), 36.1 (d, CH_2, cod, J_{C-P}= 6.8 Hz), 42.9 (d, CH_2, J_{C-P}= 9.1 Hz), 61.4 (d, CH-O, J_{C-P}= 3.7 Hz), 69.5 (CH=, cod), 70.1 (CH=, cod), 97.1 (d, CH=, cod, J_{C-P}= 22.5 Hz), 107.3 (d, CH=, cod, J_{C-P}= 10.8 Hz), 117.7 (b, CH=, BAr_F), 119-134 (aromatic carbons), 135.0 (b, CH= BAr_F), 136-153 (aromatic carbons), 161.9 (q, C-B, BAr_F, $^1J_{C-B}$= 49.2 Hz), 167.9 (C=N). Anal. Calc (%) for $C_{81}H_{68}BF_{24}IrNO_4PSi_2$: C 52.15, H 3.67, N 0.75; found: C 52.13, H 3.70, N 0.73.

[Ir(cod)(L30a)]BAr_F. Yield: 132 mg (96%). ^{31}P NMR ($CDCl_3$), δ: 104.7 (s). ^{1}H NMR ($CDCl_3$), δ: 0.86 (s, 3H, CH_3), 0.99 (s, 3H, CH_3), 1.26 (s, 9H, CH_3, ^{t}Bu), 1.29 (s, 9H, CH_3, ^{t}Bu), 1.43 (s, 9H, CH_3, ^{t}Bu), 1.52 (s, 9H, CH_3, ^{t}Bu), 1.64 (m, 4H, CH_2, cod), 1.73 (dd, 1H, CH_2, $^2J_{H-H}$= 14.2 Hz, $^3J_{H-H}$= 6 Hz), 2.02 (dd, 1H, CH_2, $^2J_{H-H}$= 14.2 Hz, $^3J_{H-H}$= 6.4 Hz), 2.13 (m, 2H, CH_2, cod), 2.19 (m, 2H, CH_2, cod), 2.29 (s, 3H, CH_3-Ph), 2.43 (d, 1H, CH_2-C=, $^2J_{H-H}$= 19.2 Hz), 2.50 (d, 1H, CH_2-C=, $^2J_{H-H}$= 19.2 Hz), 3.85 (m, 1H, CH=, cod), 4.31 (b, 2H, CH=, cod), 5.11 (b, 1H, CH=, cod), 5.45 (m, 1H, CH-O), 7.1-8.2 (m, 20H, CH=). ^{13}C NMR ($CDCl_3$), δ: 21.9 (CH_3-Ph), 23.2 (CH_2, cod), 25.6 (CH_3), 27.3 (CH_2, cod), 27.9 (CH_3), 30.2 (CH_3, ^{t}Bu), 30.8 (b, CH_3, ^{t}Bu), 31.2 (CH_3, ^{t}Bu), 31.6 (C, ^{t}Bu), 31.8 (C, ^{t}Bu), 33.4 (C, ^{t}Bu), 33.9 (CH_2, cod), 34.5 (CH_2, cod), 34.9 (CMe_2), 36.7 (d, CH_2-C=, J_{C-P}= 8.0 Hz), 41.2 (d, CH_2, J_{C-P}= 9.2 Hz), 68.4 (CH-O), 69.8 (CH=, cod), 70.5 (CH=, cod), 89.7 (d, CH=, cod, J_{C-P}= 21.2 Hz), 103.9 (d, CH=, cod, J_{C-P}= 9.2 Hz), 117.7 (b, CH=, BAr_F), 119-134 (aromatic carbons), 135.0 (b, CH=, BAr_F), 136-153 (aromatic carbons), 161.9 (q, C-B, BAr_F, $^1J_{C-B}$= 49.2 Hz), 161.9 (C=N). Anal. Calc (%) for $C_{84}H_{82}BF_{24}IrNO_4P$: C 54.26, H 4.44, N 0.75; found: C 54.30, H 4.46, N 0.76.

[Ir(cod)(L31a)]BAr_F. Yield: 130 mg (92%). ^{31}P NMR ($CDCl_3$), δ: 108.8. ^{1}H NMR ($CDCl_3$), δ: 0.95 (s, 3H, CH_3), 0.97 (s, 3H, CH_3), 1.28 (s, 9H, CH_3, ^{t}Bu), 1.29 (s, 9H, CH_3, ^{t}Bu), 1.41 (s, 9H, CH_3, ^{t}Bu), 1.49 (s, 9H, CH_3, ^{t}Bu), 1.59 (m, 4H, CH_2, cod), 1.72 (dd, 1H, CH_2, $^2J_{H-H}$= 14.0 Hz, $^3J_{H-H}$= 6 Hz), 1.98 (dd, 1H, CH_2, $^2J_{H-H}$= 14.0 Hz, $^3J_{H-H}$= 6.4 Hz), 2.16 (m, 2H, CH_2, cod), 2.20 (m, 2H, CH_2, cod), 2.40 (d, 1H, CH_2-C=, $^2J_{H-H}$= 18.8 Hz), 2.54 (d, 1H, CH_2-C=, $^2J_{H-H}$= 16.8 Hz), 3.81 (m, 1H, CH=, cod), 4.33 (b, 2H, CH=, cod), 5.23 (b, 1H, CH=, cod), 5.51 (m, 1H, CH-O), 7.1-8.2 (m, 20H, CH=). ^{13}C NMR ($CDCl_3$), δ: 23.3 (CH_2, cod), 25.8 (CH_3), 27.1 (CH_2, cod), 27.8 (CH_3), 30.0 (CH_3, ^{t}Bu), 30.3 (b,CH_3, ^{t}Bu), 31.1 (CH_3, ^{t}Bu), 31.9 (b, C, ^{t}Bu), 33.4 (C, ^{t}Bu), 33.7 (b, C, ^{t}Bu and

CH_2, cod), 34.3 (CH_2, cod), 34.7 (CMe_2), 36.5 (d, CH_2-C=, J_{C-P}= 7.8 Hz), 40.9 (d, CH_2, J_{C-P}= 8.5 Hz), 68.1 (b, CH-O), 69.8 (CH=, cod), 70.5 (CH=, cod), 89.4 (d, CH=, cod, J_{C-P}= 23.3 Hz), 104.2 (d, CH=, cod, J_{C-P}= 10.8 Hz), 117.7 (b, CH=, BAr_F), 119-134 (aromatic carbons), 135.0 (b, CH= BAr_F), 136-153 (aromatic carbons), 161.9 (q, C-B, BAr_F, $^1J_{C-B}$= 49.2 Hz), 162.7 (C=N). Anal. Calc (%) for $C_{84}H_{79}BF_{27}IrNO_4P$: C 52.73, H 4.16, N 0.73; found. C 52.70, H 4.18, N 0.71.

[Ir(cod)(L32a)]BAr_F. Yield: 127 mg (94%). ^{31}P NMR ($CDCl_3$), δ: 115.8. ^{1}H NMR ($CDCl_3$), δ: 0.90 (s, 3H, CH_3), 1.03 (s, 3H, CH_3), 1.25 (s, 9H, CH_3, ^{t}Bu), 1.29 (s, 9H, CH_3, ^{t}Bu), 1.37 (s, 9H, CH_3, ^{t}Bu), 1.47 (s, 9H, CH_3, ^{t}Bu), 1.49 (m, 1H, CH_2), 1.54 (s, 9H, CH_3, ^{t}Bu), 1.62 (m, 2H, CH_2, cod), 1.82 (dd, 1H, CH_2, $^2J_{H-H}$= 14.4 Hz, $^3J_{H-H}$= 6 Hz), 1.99 (m, 3H, CH_2, cod and CH_2), 2.20 (m, 4H, CH_2, cod), 2.32 (d, 1H, CH_2-C=, $^2J_{H-H}$= 17.2 Hz), 2.43 (d, 1H, CH_2-C=, $^2J_{H-H}$= 16.8 Hz), 4.32 (b, 1H, CH=, cod), 4.46 (m, 1H, CH=, cod), 4.76 (b, 1H, CH=, cod), 5.32 (b, 1H, CH=, cod), 5.47 (m, 1H, CH-O), 6.9-8.3 (m, 16H, CH=). ^{13}C NMR ($CDCl_3$), δ: 21.7 (CH_3), 23.1 (CH_2, cod), 26.4 (CH_2, cod), 27.5 (CH_3), 29.3 (CH_3, ^{t}Bu), 29.7 (b, CH_3, ^{t}Bu), 30.3 (CH_3, ^{t}Bu), 30.7 (CH_3, ^{t}Bu), 31.6 (b, C, ^{t}Bu), 33.6 (C, ^{t}Bu), 33.7 (b, C, ^{t}Bu), 34.3 (CH_2, cod), 34.8 (CMe_2), 33.9 (s, CH_2-C=), 34.2 (C, ^{t}Bu), 34.7 (CH_2), 34.9 (C, ^{t}Bu), 36.5 (CH_2, cod), 40.7 (d, CH_2, cod, J_{C-P}= 9.3 Hz), 68.4 (b, CH-O and CH=, cod), 70.4 (CH=, cod), 85.7 (d, CH=, cod, J_{C-P}= 27.9 Hz), 101.2 (d, CH=, cod, J_{C-P}= 8.6 Hz), 117.7 (b, CH=, BAr_F), 119-134 (aromatic carbons), 135.0 (b, CH= BAr_F), 136-153 (aromatic carbons), 161.9 (q, C-B, BAr_F, $^1J_{C-B}$= 49.2 Hz), 174.4 (C=N). Anal. Calc (%) for $C_{81}H_{84}BF_{24}IrNO_4P$: C 53.29, H 4.64, N 0.77; found. C 53.26, H 4.65, N 0.78.

[Ir(cod)(L34a)]BAr_F. Yield: 128 mg (94%). ^{31}P NMR ($CDCl_3$), δ: 100.2 (s). ^{1}H NMR ($CDCl_3$), δ: 1.28 (s, 9H, CH_3, ^{t}Bu), 1.32 (s, 9H, CH_3, ^{t}Bu), 1.41 (s, 9H, CH_3, ^{t}Bu), 1.47 (m, 2H, CH_2, cod), 1.55 (m, 1H, $\underline{CH_2}$-CH), 1.60 (s, 9H, CH_3, ^{t}Bu), 1.76 (m, 1H, $\underline{CH_2}$-CH), 1.92 (m, 1H, CH_2), 1.99 (m, 1H, CH_2), 2.09 (m, 4H, CH_2, cod), 2.22 (m, 2H, CH_2, cod), 2.69 (m, 1H, CH_2-C=), 2.99 (dd, 1H, CH_2-C=, $^2J_{H-H}$= 17.7, $^3J_{H-H}$= 4.8), 3.41 (m, 1H, CH=, cod), 3.79 (b, 2H, CH, CH= and cod), 4.51 (m, 1H, CH_2-O), 4.56 (m, 1H, CH_2-O), 4.78 (b, 1H, CH=, cod), 5.19 (b, 1H, CH=, cod), 6.5-8.5 (m, 21H, CH=). ^{13}C NMR ($CDCl_3$), δ: 23.1 (CH_2-C=), 23.9 (CH_2), 24.7 (CH_2, cod), 29.2 (CH_2, cod), 30.2 ($\underline{CH_2}$-CH), 30.4 (CH_3, ^{t}Bu), 31.1 (CH_3, ^{t}Bu), 33.9 (CH_2, cod), 35.5 (C, ^{t}Bu), 36.1 (C, ^{t}Bu), 37.4 (CH_2, cod), 61.5 (CH=, cod), 70.2 (CH=, cod), 71.3 (b, CH and CH_2-O), 96.1 (d, CH=, cod, J_{C-P}= 22.0 Hz), 104.7 (d, CH=, cod, J_{C-P}= 11.2 Hz), 117.7 (b, CH=, BAr_F), 119-134 (aromatic carbons), 135.0 (b, CH= BAr_F), 136-158 (aromatic carbons), 161.9 (q, C-B, BAr_F, $^1J_{C-B}$= 49.5 Hz), 168.6 (s, C=N). Anal. Calc (%) for $C_{82}H_{78}BF_{24}IrNO_3PS$: C 53.31, H 4.26, N 0.76; found. C 53.28, H 4.28, N 0.75.

[Ir(cod)(L34b)]BAr_F. Yield: 128 mg (96%). ^{31}P NMR ($CDCl_3$), δ: 96.4 (s). ^{1}H NMR ($CDCl_3$), δ: 1.41 (s, 9H, CH_3, ^{t}Bu), 1.47 (m, 2H, CH_2, cod), 1.52 (m, 1H, $\underline{CH_2}$-CH), 1.63 (s, 9H, CH_3, ^{t}Bu), 1.81 (m, 1H, $\underline{CH_2}$-CH), 1.86 (m, 1H, CH_2), 1.96 (m, 1H, CH_2), 2.08 (m, 4H, CH_2, cod), 2.24 (m, 2H, CH_2, cod), 2.71 (m, 1H, CH_2-C=), 2.96 (dd, 1H, CH_2-C=, $^2J_{H-H}$= 17.7, $^3J_{H-H}$= 4.8), 3.46 (m, 1H, CH=, cod), 3.77 (b, 2H, CH, CH= and cod), 3.82 (s, 3H, CH_3-O), 3.87 (s, 3H, CH_3-O), 4.48 (m, 1H, CH_2-O), 4.59 (m, 1H, CH_2-O), 4.76 (b, 1H, CH=, cod), 5.19 (b, 1H, CH=, cod), 6.5-8.5 (m, 21H, CH=). ^{13}C NMR ($CDCl_3$), δ: 23.4 (CH_2-C=), 23.5 (CH_2), 24.8 (CH_2, cod), 29.1 (CH_2, cod), 30.0 ($\underline{CH_2}$-CH), 30.6 (CH_3, ^{t}Bu), 31.3 (CH_3, ^{t}Bu), 33.8 (CH_2, cod), 35.7 (C, ^{t}Bu), 36.0 (C, ^{t}Bu), 37.0 (CH_2, cod), 55.9 (CH_3-O), 61.3 (CH=, cod), 69.9 (CH=, cod), 71.6 (b, CH and CH_2-O), 96.0 (d, CH=, cod, J_{C-P}= 23.0 Hz), 105.1 (d, CH=, cod, J_{C-P}= 12.5 Hz), 117.7 (b, CH=, BAr_F), 119-134 (aromatic carbons), 135.0 (b, CH= BAr_F), 136-158 (aromatic carbons), 161.9 (q, C-B, BAr_F, $^1J_{C-B}$=

49.5 Hz), 169.6 (s, C=N). Anal. Calc (%) for $C_{76}H_{66}BF_{24}IrNO_5PS$: C 50.84, H 3.71, N 0.78; found. C 50.89, H 3.79, N 0.75.

[Ir(cod)(L34c)]BAr$_F$. Yield: 124 mg (95%). ^{31}P NMR ($CDCl_3$), δ: 98.6 (s). ^{1}H NMR ($CDCl_3$), δ: 0.06 (s, 9H, CH_3-Si), 0.52 (s, 9H, CH_3-Si), 1.30 (m, 2H, CH_2, cod), 1.44 (m, 1H, $\underline{CH_2}$-CH), 1.85 (m, 1H, $\underline{CH_2}$-CH), 1.89 (m, 1H, CH_2), 2.01 (m, 1H, CH_2), 2.19 (m, 4H, CH_2, cod), 2.39 (m, 2H, CH_2, cod), 2.73 (m, 1H, CH_2-C=), 2.99 (dd, 1H, CH_2-C=, $^2J_{H\text{-}H}$= 17.4, $^3J_{H\text{-}H}$= 5.5), 3.47 (m, 1H, CH=, cod), 3.93 (m, 1H, CH), 4.04 (b, 1H, CH=, cod), 4.42 (b, 1H, CH=, cod), 4.66 (m, 1H, CH_2-O), 4.76 (m, 1H, CH_2-O), 5.16 (b, 1H, CH=, cod), 7.2-8.5 (m, 23H, CH=). ^{13}C NMR ($CDCl_3$), δ: -0.33 (CH_3-Si), 0.74 (CH_3-Si), 23.4 ($\underline{CH_2}$-C=), 23.5 (CH_2), 24.7 (CH_2, cod), 29.1 (CH_2, cod), 29.9 ($\underline{CH_2}$-CH), 33.3 (CH_2, cod), 37.1 (CH_2, cod), 61.7 (CH=, cod), 67.2 (CH=, cod), 70.8 (b, CH and CH_2-O), 97.2 (d, CH=, cod, $J_{C\text{-}P}$= 21.9 Hz), 105.3 (d, CH=, cod, $J_{C\text{-}P}$= 12.5 Hz), 117.7 (b, CH=, BAr_F), 119-134 (aromatic carbons), 135.0 (b, CH= BAr_F), 136-154 (aromatic carbons), 161.9 (q, C-B, BAr_F, $^1J_{C\text{-}B}$= 49.5 Hz), 169.6 (s, C=N). Anal. Calc (%) for $C_{72}H_{62}BF_{24}IrNO_3PSSi_2$: C 48.93, H 3.54, N 0.79; found. C 48.95, H 3.56, N 0.78.

[Ir(cod)(L34f)]BAr$_F$. Yield: 133 mg (96%). ^{31}P NMR ($CDCl_3$), δ: 93.8 (s). ^{1}H NMR ($CDCl_3$), δ: 0.01 (s, 9H, CH_3-Si), 0.61 (s, 9H, CH_3-Si), 1.15 (m, 2H, CH_2, cod), 1.41 (m, 1H, $\underline{CH_2}$-CH), 1.73 (b, 2H, CH_2, cod), 1.85 (m, 1H, $\underline{CH_2}$-CH), 1.96 (m, 1H, CH_2), 2.06 (m, 1H, CH_2), 2.13 (m, 2H, CH_2, cod), 2.33 (m, 2H, CH_2, cod), 2.73 (m, 1H, CH_2-C=), 2.97 (dd, 1H, CH_2-C=, $^2J_{H\text{-}H}$= 18, $^3J_{H\text{-}H}$= 4.8), 3.15 (m, 1H, CH=, cod), 3.71 (b, 1H, CH=, cod), 4.16 (m, 1H, CH), 4.23 (b, 1H, CH=, cod), 4.62 (b, 1H, CH_2-O), 4.73 (m, 1H, CH_2-O), 4.94 (b, 1H, CH=, cod), 6.7-8.3 (m, 27H, CH=). ^{13}C NMR ($CDCl_3$), δ: -0.0 (CH_3-Si), 0.4 (CH_3-Si), 23.7 ($\underline{CH_2}$-C=), 24.4 (CH_2), 26.1 (CH_2, cod), 28.4 (CH_2, cod), 31.2 ($\underline{CH_2}$-CH), 34.3 (CH_2, cod), 36.6 (CH_2, cod), 68.1 (CH=, cod), 70.7 (CH and CH= cod), 71.9 (CH_2-O), 95.3 (d, CH=, cod, $J_{C\text{-}P}$= 22.7 Hz), 104.2 (b, CH=, cod), 117.7 (b, CH=, BAr_F), 119-134 (aromatic carbons), 135.0 (b, CH= BAr_F), 136-154 (aromatic carbons), 161.9 (q, C-B, BAr_F, $^1J_{C\text{-}B}$= 49.5 Hz), 169.3 (s, C=N). Anal. Calc (%) for $C_{80}H_{66}BF_{24}IrNO_3PSSi_2$: C 51.45, H 3.56, N 0.75; found. C 51.47, H 3.59, N 0.74.

[Ir(cod)(L34g)]BAr$_F$. Yield: 130 mg (94%). ^{31}P NMR ($CDCl_3$), δ: 103.8. ^{1}H NMR ($CDCl_3$), δ: 0.14 (s, 9H, CH_3-Si), 0.60 (s, 9H, CH_3-Si), 1.17 (m, 2H, CH_2, cod), 1.44 (m, 1H, $\underline{CH_2}$-CH), 1.86 (m, 1H, $\underline{CH_2}$-CH), 1.90 (m, 1H, CH_2), 1.99 (m, 1H, CH_2), 2.10 (m, 4H, CH_2, cod), 2.32 (m, 2H, CH_2, cod), 2.74 (m, 1H, CH_2-C=), 3.00 (dd, 1H, CH_2-C=, $^2J_{H\text{-}H}$= 23, $^3J_{H\text{-}H}$= 5.4), 3.49 (m, 1H, CH=, cod), 3.85 (m, 1H, CH), 3.97 (b, 1H, CH=, cod), 4.23 (b, 1H, CH=, cod), 4.72 (b, 2H, CH_2-O), 5.17 (b, 1H, CH=, cod), 6.6-8.3 (m, 27H, CH=). ^{13}C NMR ($CDCl_3$), δ: -0.4 (CH_3-Si), 0.9 (CH_3-Si), 23.4 (b, CH_2 and $\underline{CH_2}$-C=), 24.7 (CH_2, cod), 29.2 (CH_2, cod), 31.2 ($\underline{CH_2}$-CH), 33.3 (CH_2, cod), 37.1 (CH_2, cod), 61.6 (b, CH= cod and CH), 67.2 (CH=, cod), 71.1 (CH_2-O), 97.6 (d, CH=, cod, $J_{C\text{-}P}$= 21.6 Hz), 105.5 (b, CH=, cod), 117.7 (b, CH=, BAr_F), 119-134 (aromatic carbons), 135.0 (b, CH= BAr_F), 136-154 (aromatic carbons), 161.9 (q, C-B, BAr_F, $^1J_{C\text{-}B}$= 49.2 Hz), 169.6 (s, C=N). Anal. Calc (%) for $C_{80}H_{66}BF_{24}IrNO_3PSSi_2$: C 51.45, H 3.56, N 0.75; found. C 51.46, H 3.58, N 0.75.

[Ir(cod)(L35a)]BAr$_F$. Yield: 129 mg (93%). ^{31}P NMR ($CDCl_3$), δ: 92.1 (s). ^{1}H NMR ($CDCl_3$), δ: 0.94 (s, 3H, CH_3), 1.26 (s, 3H, CH_3), 1.34 (s, 9H, CH_3, ^{t}Bu), 1.35 (s, 9H, CH_3, ^{t}Bu), 1.37 (s, 9H, CH_3, ^{t}Bu), 1.46 (m, 2H, CH_2, cod), 1.52 (m, 1H, $\underline{CH_2}$-CH), 1.63 (s, 9H, CH_3, *tbu*), 1.73 (m, 1H, $\underline{CH_2}$-CH), 1.77 (m, 1H, CH_2), 1.94 (m, 1H, CH_2), 2.09 (m, 4H, CH_2, cod), 2.27 (m, 2H, CH_2, cod), 2.79 (m, 2H, CH_2-C=), 3.26 (m, 1H, CH=, cod), 3.82 (b, 1H, CH=, cod), 4.67 (b, 2H, CH and CH=, cod), 4.89 (b, 1H, CH=, cod), 6.5-8.5 (m, 21H, CH=). ^{13}C NMR ($CDCl_3$), δ: 19.8 (CH_3), 23.1 (CH_3),

24.6 ($\underline{CH_2}$-C=), 25.4 (CH_2), 26.7 (CH_2, cod), 28.9 (CH_2, cod), 29.9 ($\underline{CH_2}$-CH), 31.1 (CH_3, ^{t}Bu), 31.2 (CH_3, ^{t}Bu), 31.6 (CH_3, ^{t}Bu), 31.8 (CH_3, ^{t}Bu), 34.2 (b, C, ^{t}Bu and CH_2, cod), 34.9 (C, ^{t}Bu), 35.7 (C, ^{t}Bu), 36.1 (C, ^{t}Bu), 36.8 (CH_2, cod), 53.7 (CH), 60.9 (CH=, cod), 70.1 (CH=, cod), 93.4 (d, CH=, cod, $J_{C\text{-}P}$= 24.2 Hz), 94.1 (CMe_2), 103.5 (m, CH=, cod), 117.7 (b, CH=, BAr_F), 119-134 (aromatic carbons), 135.0 (b, CH= BAr_F), 136-158 (aromatic carbons), 161.9 (q, C-B, BAr_F, $^1J_{C\text{-}B}$= 49.5 Hz), 170.4 (s, C=N). Anal. Calc (%) for $C_{84}H_{80}BF_{24}IrNO_3PS$: C 53.79, H 4.41, N 0.75; found. C 53.78, H 4.43, N 0.74.

[Ir(cod)(L36a)]BAr$_F$. Yield: 133 mg (96%). ^{31}P NMR ($CDCl_3$), δ: 92.5 (s). ^{1}H NMR ($CDCl_3$), δ: 0.93 (s, 3H, CH_3), 1.26 (s, 3H, CH_3), 1.35 (s, 9H, CH_3, ^{t}Bu), 1.38 (s, 18H, CH_3, ^{t}Bu), 1.46 (m, 2H, CH_2, cod), 1.52 (m, 1H, $\underline{CH_2}$-CH), 1.63 (s, 9H, CH_3, ^{t}Bu), 1.73 (m, 1H, $\underline{CH_2}$-CH), 1.76 (m, 1H, CH_2), 1.94 (m, 1H, CH_2), 2.09 (m, 4H, CH_2, cod), 2.27 (m, 2H, CH_2, cod), 2.79 (m, 2H, CH_2-C=), 3.26 (m, 1H, CH=, cod), 3.82 (b, 1H, CH=, cod), 4.67 (b, 2H, CH and CH=, cod), 4.89 (b, 1H, CH=, cod), 6.5-8.5 (m, 21H, CH=). ^{13}C NMR ($CDCl_3$), δ: 19.9 (CH_3), 23.1 (CH_3), 24.6 ($\underline{CH_2}$-C=), 25.4 (CH_2), 26.7 (CH_2, cod), 28.9 (CH_2, cod), 30.1 ($\underline{CH_2}$-CH), 31.1 (CH_3, ^{t}Bu), 31.2 (CH_3, ^{t}Bu), 31.6 (CH_3, ^{t}Bu), 31.7 (CH_3, ^{t}Bu), 34.2 (b, C, ^{t}Bu and CH_2, cod), 34.9 (C, ^{t}Bu), 35.7 (C, ^{t}Bu), 36.1 (C, ^{t}Bu), 36.9 (CH_2, cod), 53.7 (CH), 60.9 (CH=, cod), 70.1 (CH=, cod), 93.4 (d, CH=, cod, $J_{C\text{-}P}$= 24.2 Hz), 94.2 (CMe_2), 103.5 (m, CH=, cod), 117.7 (b, CH=, BAr_F), 119-134 (aromatic carbons), 135.0 (b, CH= BAr_F), 136-158 (aromatic carbons), 161.9 (q, C-B, BAr_F, $^1J_{C\text{-}B}$= 49.5 Hz), 170.6 (s, C=N). Anal. Calc (%) for $C_{84}H_{80}BF_{24}IrNO_3PS$: C 53.79, H 4.41, N 0.75; found. C 53.71, H 4.43, N 0.76.

3.5.5.5. Typical procedure for the hydrogenation of olefins

The alkene (1 mmol) and Ir complex (0.2 mol%) were dissolved in CH_2CL_2 (2 mL) in a high-pressure autoclave. The autoclave was purged four times with hydrogen. Then, it was pressurized at the desired pressure. After the desired reaction time, the autoclave was depressurised and the solvent evaporated off. The residue was dissolved in Et_2O (1.5 ml) and filtered through a short celite plug. The enantiomeric excess was determined by chiral GC or chiral HPLC and conversions were determined by ^{1}H NMR. The enantiomeric excesses of hydrogenated products were determined using the conditions previously described.[4d,5c]

3.5.6. Acknowledgements

We thank the Spanish Government (Consolider-Ingenio CSD2006-0003, CTQ2007-62288/BQU, 2008PGIR/07 to O.P. and 2008PGIR/08 to M.D.) and the Catalan Government (2009SGR116), COST D40, Vetenskapsrådet (VR), and Astra Zeneca for support. Knut and Alice Wallenbergs Stiftelse are also greatfully acknowledged for generous financial support. We are grateful to Johan J. Verendel for providing us the terminal substrates.

3.5.7. References

[1] See for instance: a) *Catalytic Asymmetric Synthesis*, 2nd, ed.; Ojima, I., Ed.; Wiley-VCH: New York, 2000. b) *Applied Homogeneous Catalysis with Organometallic Compounds,* 2nd edition; Cornils, B.; Herrmann, W. A., Eds.; Wiley-VCH: Weinheim, 2002. c) *Asymmetric Catalysis on Industrial Scale*; Blaser, H.-U., Schmidt, E., Eds.; Wiley: New York, 2004. d) Brown, J. M. in *Comprehensive Asymmetric Catalysis*; Jacobsen, E. N., Pfaltz, A., Yamamoto, H., Eds.; Springer-

Verlag: Berlin, 1999, Vol.1. e) *Asymmetric Catalysis in Organic Synthesis*; Noyori, R., Ed.; Wiley: New York, 1994.

[2] For recent reviews, see: a) Källström, K.; Munslow, I.; Andersson, P. G. *Chem. Eur. J.* **2006**, *12*, 3194. b) Roseblade, S. J.; Pfaltz, A. *Acc. Chem. Res.* **2007**, *40*, 1402. c) Church, T. L.; Andersson, P. G. *Coord. Chem. Rev.* **2008**, *252*, 513. d) Cui, X.; Burgess, K. *Chem. Rev.* **2005**, *105*, 3272.

[3] See for instance: a) Tang, W.; Wang, W.; Zhang, X. *Angew. Chem. Int. Ed.* **2003**, *42*, 943. b) Hou, D.-R.; Reibenspies, J.; Colacot, T. J.; Burgess, K. *Chem. Eur. J.* **2001**, *7*, 5391. c) Cozzi, P. G.; Menges, F.; Kaiser, S. *Synlett* **2003**, 833. d) Lighfoot, A.; Schnider, P.; Pfaltz, A. *Angew. Chem. Int. Ed.* **1998**, *37*, 2897. e) Menges, F.; Neuburger, M.; Pfaltz, A. *Org. Lett.* **2002**, *4*, 4713. f) Liu, D.; Tang, W.; Zhang, X. *Org. Lett*. **2004**, *6*, 513.

[4] See for instance: a) Perry, M. C.; Cui, X.; Powell, M. T.; Hou, D.-R.; Reibenspies, J. H.; Burgess, K. *J. Am. Chem. Soc.* **2003**, *125*, 5391. b) Blankestein, J.; Pfaltz, A. *Angew. Chem. Int. Ed.* **2001**, *40*, 4445. c) Kaiser, S. ; Smidt, S: P.; Pfaltz, A. *Angew. Chem. Int. Ed.* **2006**, *45*, 5194. d) Källström, K.; Hedberg, C. Brandt, P.; Bayer, P.; Andersson, P. G. *J. Am. Chem. Soc.* **2004**, *126*, 14308. e) Engman, M.; Diesen, J. S.; Paptchikhine, A.; Andersson, P. G. *J. Am. Chem. Soc.* **2007**, *129*, 4536. f) Trifonova, A.; Diesen, J. S.; Andersson, P. G. *Chem. Eur. J.* **2006**, *12*, 2318. g) Menges, F. Pflatz, A. *Adv. Synth. Catal.* **2002**, *334*, 4044. h) Drury III, W. J.; Zimmermann, N.; Keenan, M.; Hayashi, M.; Kaiser, S.; Goddard, R.; Pfaltz, A. *Angew. Chem. Int. Ed.* **2004**, *43*, 70. i) Hedberg, C.; Källström, K.; Brandt, P.; Hansen, L. K.; Andersson, P. G. *J. Am. Chem. Soc.* **2006**, *128*, 2995.

[5] a) Diéguez, M.; Mazuela, J.; Pàmies, O.; Verendel, J. J.; Andersson, P. G. *J. Am. Chem. Soc.* **2008**, *130*, 7208. b) Diéguez, M.; Mazuela, J.; Pàmies, O.; Verendel, J. J.; Andersson, P. G. *Chem. Commun.* **2008**, 3888. c) Mazuela, J.; Verendel, J. J.; Coll, M.; Schäffner, B.; Börner, A.; Börner; Anderson, P. G.; Pàmies, O.; Diéguez, M. *J. Am. Chem. Soc.* **2009**, *131*, 12344. d) Mazuela, J.; Norrby, P.O.; Andersson, P. G.; Pàmies, O.; Diéguez, M. *J. Am. Chem. Soc.* **2011**, *133*, 13634.

[6] The only success in hydrogenating highly unfunctionalized Z-trisubstituted olefins using ligands **2** and **3** can be found with the less demanding 6-methoxy-1-methylene-1,2,3,4-tetrahydronaphthalene **S6**, see references 4d and 4i.

[7] Cheruku, P.; Gohil, S.; Andersson, P. G. *Org. Lett.* **2007**, *9*, 1659.

[8] Unpublished results (i.e. for substrate **S13**, ee's up to 41%)

[9] *Heterocyclic Chemistry*, 4th Ed; Joule, J. A.; Mills, K., Eds.; Blacwell Science Ltd: Oxford, 2000.

[10] For some representative examples see: a) Claver, C.; Pàmies, O.; Diéguez, M. *Chiral Diphosphinites, Diphosphonites, Diphosphites and Mixed PO-Ligands, in Phosphorous Ligands in Asymmetric Catalysis*; Börner, A., Ed.; Wiley-VCH: Weinheim, 2008, *Chapter 3*, vol. 2. b) Diéguez, M.; Pàmies, O. *Acc. Chem. Res.* ASAP doi:10.1021/ar9002152. c) Diéguez, M.; Ruiz A.; Claver, C. *J. Org. Chem.* **2002**, *67,* 3796. d) Reetz, M. T.; Mehler, G. *Angew. Chem., Int. Ed.* **2000**, *39*, 3889. e) Yan, M.; Zhou, Z. –Y.; Chan, A. S. C. *Chem. Commun.* **2000**, 115. f) Diéguez, M.; Ruiz, A.; Claver, C. *Tetrahedron: Asymmetry* **2001**, *12*, 2895. g) Pàmies, O.; Diéguez, M.; Claver, C. *J. Am. Chem. Soc.* **2005**, *127*, 3646. h) Diéguez, M.; Pàmies, O.; Claver, C. *Chem. Commun.* **2005**, 1221. i) Mata, Y.; Pàmies, O.; Diéguez, M. *Chem. Eur. J.* **2007**, *13*, 3296.

[11] Pàmies, O.; Diéguez, M.; Net, G.; Ruiz, A.; Claver, C. *Organometallics* **2000,** *19,* 1488.

[12] The rapid ring inversions (tropoisomerization) in the biaryl phosphite moiety is usually stopped upon coordination to the metal center. See for example: a) Buisman, G. J. H.; van der Veen, L. A.; Klootwijk, A.; de Lange, W. G. J.; Kamer, P. C. J.; van Leeuwen, P. W. N. M.; Vogt, D. *Organometallics* **1997**, *16*, 2929. b) Diéguez, M.; Pàmies, O.; Ruiz, A.; Claver, C.; Castillón, S. *Chem. Eur. J.* **2001**, *7*, 3086. c) Pàmies, O.; Diéguez, M.; Net, G.; Ruiz, A.; Claver, C. *J. Org. Chem.* **2001**, *66*, 8364. d) Diéguez, M.; Pàmies, O.; *Chem. Eur. J.* **2008**, *14*, 3653. e) Pàmies, O.; Diéguez, M. *Chem. Eur. J.* **2008**, *14*, 944.

[13] For successful applications of Ir-catalysts, see: a) McIntyre, S.; Hörmann, E.; Menges, F.; Smidt, S. P.; Pfaltz, A. *Adv. Synth. Catal.* **2005**, *347*, 282. b) ref. 4b. c) ref. 4d. d) ref. 5c.

[14] For successful applications of Sm-, Ru- and Rh-complexes, see: a) Conticello, V. P.; Brard, L.; Giardello, M. A.; Tsuji, Y.; Sabat, M.; Stern, C. L.; Marks, T. J. *J. Am. Chem. Soc.* **1992**, *114*, 2761. b) Giardello, M. A.; Conticello, V. P.; Brard, L.; Gagne, M. R.; Marks, T. J. *J. Am. Chem. Soc.* **1994**, *116*, 10241. c) Forman, G. S.; Ohkuma, T.; Hems, W. P.; Noyori, R. *Tetrahedron Lett.* **2000**, *41*, 9471. d) Co, T. T.; Kim, T. J. *Chem. Commun.* **2006**, 3537.

[15] See for instance: a) Abate, A.; Brenna, E. Fuganti, C.; Gatti, G. G.; Givenzana, T.; Malpezzi, L.; Serra, S. *J. Org. Chem.* **2005**, *70*, 1281. b) Drescher, K.; Haupt, A.; Unger, L.; Rutner, S. C.; Braje, W:; Grandel, R.; Henry, C.; Backfisch, G:; Beyerbach, A.; Bisch, W. *WO Patent* 2006/040182 A1.

[16] See for instance: a) Fleming, I.; Barbero, A.; Walter, D. *Chem. Rev.* **1997**, *97*, 2063. b) Jones, G. R.; Landais, Y. *Tetrahedron* **1996**, *52*, 7599. c) Bains, W.; Tacke, R. *Curr. Opin. Drug Discv. Dev.* **2003**, *6*, 526.

3.6. A phosphite-pyridine/iridium complex library as highly selective catalysts for the hydrogenation of minimally functionalized olefins

Javier Mazuela, Oscar Pàmies and Montserrat Diéguez in manuscript to be submitted.

3.6.1 Abstract

A modular library of readily available phosphite-pyridine ligands (**L38**-**L49a**-**g**) has been successfully applied for the first time in the Ir-catalyzed asymmetric hydrogenation of a broad range of minimally functionalized olefins. The modular ligand design has been shown to be crucial in finding highly selective catalytic systems for each substrate. Excellent enantioselectivities (ee's up to 99%) have therefore been obtained in a wide range of *E*- and *Z*-trisubstituted alkenes, including more demanding triarylsubstituted olefins, and dihydronaphthalenes. This good performance extends to the very challenging class of terminal disubstituted olefins, and to olefins containing neighboring polar groups (ee's up to 99%). Both enantiomers of the reduction product can be obtained in excellent enantioselectivities by simply changing the configuration of the carbon next to the phosphite moiety.

3.6.2 Introduction

The major progress in the field of asymmetric catalysis has been driven by the growing demand for enantiomerically pure pharmaceuticals, agrochemicals, flavors and other fine chemicals. Asymmetric hydrogenation utilizing molecular hydrogen to reduce prochiral olefins has become one of the most sustainable and reliable catalytic methods for the preparation of optically active compounds, mainly because of its high efficiency, atom economy, and operational simplicity.[1] Over many years the scope of this reaction has gradually extended in terms of reactant structure and catalyst efficiency. Today, an impressive range of chiral phosphorous ligands (mainly diphosphines) have been developed and successfully applied in Rh- and Ru-catalyzed hydrogenation. However, the range of olefins that can be hydrogenated with high enantiomeric excess is limited to substrates with a coordinating group next to the C=C bond, because substrate chelation to metal plays a pivotal role in stereodiscrimination.[1] With minimally functionalized olefins, these catalysts generally show low reactivity and unsatisfactory enantioselectivity.[1,2] In this context, Pfaltz introduced a new class of hydrogenation catalysts, iridium complexes with chiral P,N ligands, which mimic the Crabtree catalyst and overcome these limitations.[2,3,4] The first successful P,N ligands[5] contained a phosphine or phosphinite moiety as a P-donor group and either an oxazoline,[5b,g,j] oxazole,[5d] thiazole[5i] or pyridine[5c] as an N-donor group. Among these, the phosphorus/oxazoline ligands have played a dominant role. In recent years, research has focused on the design of ligands containing more robust N-donor groups than oxazolines. In this respect, the use of pyridine containing ligands as an alternative to oxazolines is of interest because of the robustness and the easy incorporation of the pyridine group. Soon after the successful application of phosphinite-oxazoline ligands, Pfaltz and coworkers developed the first generation of phosphinite-pyridine ligands (Figure 3.6.1),[5h,6] which was successfully used in a limited range of

alkenes. The performance was subsequently further improved by introducing a more rigid chiral bicyclic ligand backbone (2^{on} generation, Figure 3.6.1).[5c,7] Although the number of substrates that can be successfully reduced was increased, there is still a problem of substrate range limitation, since high enantioselectivities are mainly limited to trisubstituted substrates. More research is therefore needed to overcome this substrate range limitation.

Figure 3.6.1. Phosphinite-pyridine ligand libraries developed by Pfaltz and coworkers.

Some years ago, we discovered that the presence of biaryl phosphite moieties in ligand design is highly advantageous.[8] Ir/phosphite–oxazoline catalytic systems provide greater substrate versatility than previous Ir-systems based on phosphine/phosphinite–oxazoline ligands. However, the use of ligands that combine the phosphite moiety with other nitrogen donor groups rather than oxazoline has been limited.[8d] In this context, Ruffo's group, together with our group, developed a family of pyranoside phosphite-pyridine ligands for this process.[9] Nonetheless, the enantioselectivities and substrate versatility were only moderate. At this point it was unclear whether these unsatisfactory results were due to the large chelate ring size (nine-membered) formed by the pyranoside ligands or to the unsuccessful combination of a phosphite and pyridine moieties in the ligand. To address this point and in order to systematically study the possibilities of phosphite-pyridine ligands in this process, we decided to take the first generation of Pfaltz's phosphinite-pyridine ligands and replace the phosphinite moiety with a biaryl phosphite group to provide ligands **L38**-**L49a**-**g** (Figure 3.6.2).

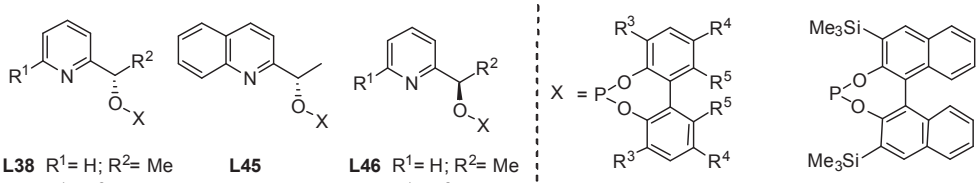

L38 R^1= H; R^2= Me
L39 R^1= R^2= Me
L40 R^1= Br; R^2= Me
L41 R^1= Ph; R^2= Me
L42 R^1= H; R^2= ^{t}Bu
L43 R^1= H; R^2= Ph
L44 R^1= Me; R^2= ^{t}Bu

L45

L46 R^1= H; R^2= Me
L47 R^1= R^2= Me
L48 R^1= H; R^2= ^{t}Bu
L49 R^1= H; R^2= Ph

a R^3 = R^4 = ^{t}Bu; R^5= H
b R^3 = ^{t}Bu; R^4 = OMe; R^5= H
c R^3 =$SiMe_3$; R^4 = R^5= H
d $(S)^{ax}$; R^3 = ^{t}Bu; R^4 = R^5= Me
e $(R)^{ax}$; R^3 = ^{t}Bu; R^4 = R^5= Me

f $(S)^{ax}$
g $(R)^{ax}$

Figure 3.6.2. Phosphite-pyridine ligand library **L38**-**L49a**-**g**.

These ligands a priori combine the advantages of both types of successful ligands for this process (phosphite and pyridine). They are therefore less sensitive to air and other oxidizing agents than phosphines and phosphinites, easy to synthesize from readily available alcohols, and more stable than their oxazoline counterparts.[10] The modular construction of these ligands allows sufficient flexibility to fine-tune the steric and electronic properties of both the ligand backbone and the biaryl moiety in order to explore how they affect catalytic performance (activity and selectivity).

We thereby studied the effect of systematically varying the substituents in the ligand backbone (R^1 and R^2, ligands **L38**-**L45**), the configuration of the ligand backbone (ligands **L38**-**L44** vs **L46**-**L49**), and the substituents and configurations in the biaryl phosphite moiety (**a**-**g**). As a result, the optimal combination for maximum activity and enantioselectivity for a wide range of *E*- and *Z*-trisubstituted and 1,1-disubstituted olefins were obtained.

3.6.3 Results and discussion

3.6.3.1 Synthesis of ligand library

Scheme 3.6.1 illustrates the sequence of ligand synthesis. Ligands **L38**-**L49a**-**g** were synthesized very efficiently from the corresponding easily accessible racemic hydroxyl-pyridine compounds ((*rac*)-**1**-**8**, Scheme 3.6.1). Racemic compounds **1**-**8** are easily made from the corresponding 6-bromopyridines or pyridyl-aldehydes.[11,12] Racemic hydroxyl-pyridine compounds **1**-**4** and **8**, bearing a methyl substituents at R^2, were resolved using CALB enzymatic kinetic resolution to yield the (*S*)-hydroxyl-pyridine compounds **1**-**4** and (*S*)-hydroxyl-quinoline compound **8** in excellent enantioselectivities (>99% ee; Scheme 3.6.1, step (a)) and the corresponding enantiopure (*R*)-acetates.[12] The (*R*)-hydroxyl-pyridine compounds **1**-**2** were prepared in high yields by basic-hydrolysis of the enantiopure acetates obtained from enzymatic kinetic resolution (Scheme 3.6.1, step (c)).[13] Resolution of racemic hydroxyl-pyridine compounds **5**-**7**, bearing bulky substituents at R^2, was achieved using preparative chiral HPLC (Scheme 3.6.1, step (b)).[14]

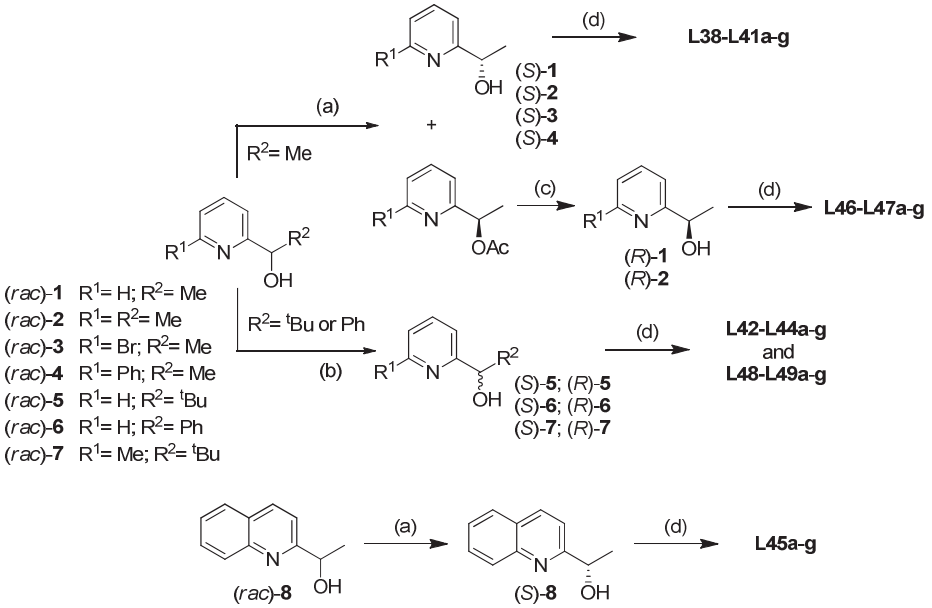

Scheme 3.6.1. Synthesis of a new phosphite-pyridine ligand library **L38**-**L49a**-**g**. (a) CALB/vinyl acetate;[12] (b) semipreparative HPLC;[5h] (c) K_2CO_3 / MeOH;[13] and (d) $ClP(OR)_2$; $(OR)_2$ = **a**-**g** / Py / toluene (Yields: 41-90%).

The last step in the ligand synthesis is common to them all (Scheme 3.6.1, step (d)). Therefore, treating the corresponding enantiopure hydroxyl-pyridines with 1 equiv of the

corresponding in-situ-formed biaryl phosphorochloridite ($ClP(OR)_2$; $(OR)_2$ = **a**-**g**) in the presence of pyridine, in a parallel manner, provided easy access to the desired ligands **L38**-**L49a**-**g**. All of the ligands were stable during purification on neutral alumina under an atmosphere of argon and isolated in moderate-to-good yields as white solids. They were stable at room temperature and very stable to hydrolysis. The elemental analyses were in agreement with the assigned structure. The ^{1}H, ^{13}C and ^{31}P NMR spectra were as expected for these C_1 ligands. One singlet for each compound was observed in the ^{31}P NMR spectrum. Rapid ring inversions (tropoisomerization) in the biphenyl-phosphorus moieties (**a**-**c**) occurred on the NMR time scale because the expected diastereoisomers were not detected by low-temperature phosphorus NMR.[15]

3.6.3.2 Synthesis of the Ir-catalyst precursors

The catalyst precursors were made by refluxing a dichloromethane solution of the appropriate ligand (**L38**-**L49a**-**g**) in the presence of 0.5 equivalent of $[Ir(\mu\text{-}Cl)cod]_2$ for 1 h. The Cl^-/BAr_F^- counterion exchange was then achieved by a reaction with sodium tetrakis[3,5-bis(trifluoromethyl)phenyl]borate ($NaBAr_F$) (1 equiv) in the presence of water (Scheme 3.6.2). All complexes were isolated as air-stable orange solids, and were used without further purification.

The complexes were characterized by elemental analysis and ^{1}H, ^{13}C, and ^{31}P NMR spectroscopy. The spectral assignments were based on information from ^{1}H–^{1}H and ^{13}C–^{1}H correlation measurements, and were as anticipated for these C_1 iridium complexes. The VT-NMR spectra indicate that only one isomer is present in solution. One singlet in the ^{31}P-{^{1}H} NMR spectra was obtained in all cases.[16]

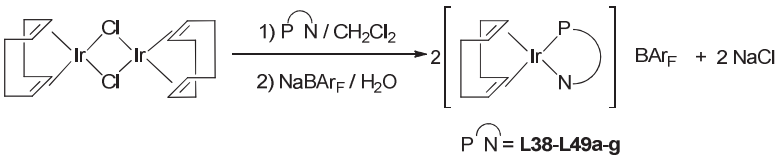

Scheme 3.6.2. Synthesis of catalyst precursors [Ir(cod)(P-N)]BArF (P-N = **L38**-**L49a-g**).

3.6.3.3 Asymmetric hydrogenation of trisubstituted olefins

Asymmetric hydrogenation of minimally functionalized trisubstituted olefins

In a first set of experiments, we used the Ir-catalyzed hydrogenation of substrates *E*-2-(4-methoxyphenyl)-2-butene **S1** and *Z*-2-(4-methoxyphenyl)-2-butene **S2** to study the potential of ligands **L38**-**L49a**-**g**. Substrate **S1** was chosen as a model for the hydrogenation of *E*-isomers because it has been reduced with a wide range of ligands, which enable the efficiency of the various ligand systems to be compared directly.[2] In order to assess the potential of the ligand library **L38**-**L49a**-**g** for the more demanding *Z*-isomers, which are usually hydrogenated less enantioselectively than the corresponding *E*-isomers, we chose substrate **S2** as a model. Excellent activities and enantioselectivities (up to 98% for **S1** and up to 91% for **S2**) were obtained. The results, which are summarized in Table 3.6.1, indicate that enantioselectivity is mainly affected by the substituents at the ligand backbone (R^1 and R^2) and by the substituents/configuration at the biaryl phosphite moiety. However, the effect of these ligand parameters on enantioselectivity

depends on the substrate type (*E*- or *Z*-isomers). While for the *E*-substrate **S1** the enantioselectivity was best with ligand **L39e** (98% ee (*S*)), enantioselectivities for the more demanding *Z*-substrate **S2** were therefore best with ligand **L43c** (91% ee (*R*)). Interestingly, for both types of substrates, the sense of enantioselectivity is controlled by the configuration of the stereogenic carbon next to the phosphite moiety. Ligands **L38**-**L45** therefore provide the opposite enantiomer to ligands **L46**-**L49** (i.e. Table 3.6.1; entry 10 vs 25, for substrate **S1**; and entry 17 vs 27 for substrate **S2**).

Table 3.6.1. Ir-catalyzed hydrogenation of **S1** and **S2** using ligands **L38**-**L49a-g**[a]

		4-OMe-C_6H_4 **S1**		4-OMe-C_6H_4 **S2**	
Entry	Ligand	% Conv[b]	% ee[c]	% Conv[b]	% ee[c]
1	**L38a**	100	61 (*S*)	100	75 (*R*)
2	**L38b**	100	48 (*S*)	100	84 (*R*)
3	**L38c**	100	50 (*S*)	100	88 (*R*)
4	**L38d**	100	27 (*S*)	100	73 (*R*)
5	**L38e**	100	64 (*S*)	100	25 (*R*)
6	**L38f**	100	38 (*S*)	100	74 (*R*)
7	**L38g**	100	58 (*S*)	100	30 (*R*)
8	**L39a**	100	90 (*S*)	100	72 (*R*)
9	**L39d**	100	87 (*S*)	100	59 (*R*)
10	**L39e**	100	98 (*S*)	100	45 (*R*)
11	**L40a**	100	58 (*S*)	100	72 (*R*)
12	**L41a**	100	63 (*S*)	100	68 (*R*)
13	**L42a**	100	89 (*S*)	100	72 (*R*)
14	**L42d**	100	45 (*S*)	100	52 (*R*)
15	**L42e**	100	90 (*S*)	100	58 (*R*)
16	**L43a**	100	80 (*S*)	100	84 (*R*)
17	**L43c**	100	74 (*S*)	100	91 (*R*)
18	**L43d**	100	55 (*S*)	100	85 (*R*)
19	**L43e**	100	90 (*S*)	100	48 (*R*)
20	**L44a**	100	62 (*S*)	100	11 (*R*)
21	**L45a**	100	70 (*S*)	100	75 (*R*)
22	**L46a**	100	60 (*R*)	100	77 (*S*)
23	**L46d**	100	36 (*R*)	100	64 (*S*)
24	**L46e**	100	66 (*R*)	100	6 (*S*)
25	**L47e**	100	97 (*R*)	100	38 (*S*)
26	**L48e**	100	88 (*R*)	100	38 (*S*)
27	**L49c**	100	72 (*R*)	100	90 (*S*)
28[d]	**L49e**	100	98 (*S*)	100	44 (*R*)
29[d]	**L43c**	100	74 (*S*)	100	91 (*R*)

[a] Reactions carried out at room temperature by using 0.5 mmol of substrate and 1 mol% of Ir-catalyst precursor at 50 bar of H_2 using dichloromethane (2 mL) as solvent. [b] Conversion measured by ^{1}H-NMR after 2 h. [c] Enantiomeric excess determined by GC. [d] Reaction carried out at 0.25 mol% of Ir-catalyst for 3 h.

The effect of the substituents of the ligand backbone (R^1 and R^2) was studied using ligands **L38**-**L45**. While for substrate **S1** the enantioselectivity is highly affected by the substituents at both R^1 and R^2 positions of the ligand backbone, for substrate **S2** the enantioselectivity is mainly affected by the substituent at R^2, and is relatively insensitive to the substituents at R^1. For substrate **S1**, although high enantioselectivities can be obtained by introducing either a methyl substituent at R^1 (ligands **L39**) or a *tert*-butyl substituent at R^2 (ligands **L42**), ligands **L39** provided somewhat higher enantioselectivities than **L42** (i.e. Table 3.6.1, entries 10 and 15). However, the introduction of both substituents simultaneously at R^1 and R^2 positions (ligands **L44**) led to lower enantioselectivities (Table 3.6.1, entry 20 vs 8 and 13). For substrate **S2**, the introduction of a phenyl substituent at R^2 position has a positive effect on enantioselectivities (Table 3.6.1, entry 16 vs 1).

The effect of the phosphite moieties was studied using ligands **L38a**-**g** (Table 3.6.1, entries 1-7). Once again, the effect of this moiety on enantioselectivity depends on the substrate type. Regarding the substituents in the tropoisomeric biphenyl phosphite moiety, for substrate **S1**, the presence of *tert*-butyl substituents at *para* positions of the biphenyl phosphite moiety provides higher enantioselectivities than when a methoxy group or hydrogen are present (i.e. **a**>**b**≈**c**; Table 3.6.1, entry 1 vs 2 and 3). However, the effect for substrate **S2** is opposite. The highest enantioselectivity is therefore obtained using non-*para* substituted biphenyl phosphite moiety (Table 3.6.1, entry 3 vs 2 and 1). Regarding the configuration of the biaryl phosphite, while for substrate **S1** the enantioselectivity is higher using enantiopure *R*-biaryl phosphite moiety, for substrate **S2** the presence of *S*-biaryl phosphite moiety provides higher enantioselectivities (Table 3.6.1, entries 4-7).

In summary, by the correct choice of the substituents at R^1 and R^2 of the ligand backbone, the configuration of the stereogenic carbon next to the phosphite moiety and the substituents/configuration at the biaryl phosphite moiety, we were able to obtain both enantiomers of the reduction product in high enantioselectivities for both *E*- and *Z*-trisubstituted model substrates (for substrate **S1**, ee's up to 98% were obtained using ligands **L39e** and **L47e**; and for substrate **S2**, ee's up to 91% were obtained using ligands **L43c** and **L49c**). In addition, the excellent enantioselectivities and activities were maintained at a low catalyst loading (0.25 mol%; Table 3.6.1, entries 28 and 29).

We then studied the asymmetric hydrogenation of other *E*- and *Z*-trisubstituted olefins (**S3**–**S12**) by using the phosphite–pyridine ligand library **L38**-**L49a**-**g**. The most noteworthy results are shown in Scheme 3.6.3 (see Supporting information for a complete set of results). The enantioselectivities are among the best observed for these substrates.[2,5] We first studied the hydrogenation of substrates **S3**-**S6**, related to **S1** and **S2** that differ in the substituents in both the aryl ring and the substituents *trans* to the aryl group. The results followed the same trends as those observed for substrates **S1** and **S2**. For *E*-substrates **S3**-**S5**, the enantioselectivities were therefore best with ligands **L39e** and **L47e**, while ligands **L43c** and **L49c** afforded the highest ee's for *Z*-substrate **S6**. We also found that enantioselectivity (ee values up to 99%) is relatively insensitive to the electronic nature of the substrate phenyl ring (i.e. substrates **S1**, **S2** and **S4** vs **S3**, **S6** and **S5**, respectively). It should be noted that if the ligands are appropriately tuned, high enantioselectivities can also be obtained for the more demanding dihydronaphthalenes (**S7**-**S10**) and triarylsubstituted substrates (**S11** and **S12**). For dihydronaphthalene substrates (**S7**-**S10**), high enantioselectivities (95%-98% ee) were obtained with Ir-**L39e** catalysts. Although the corresponding chiral tetraline

motif can be found in numerous natural products (i.e. natural antitumor agent (*R*)-(+)-7-demethyl-2-methoxycalamenene)[17], very few catalytic systems are able to hydrogenate this substrate class at high levels of enantioselectivities.[7b,17] Another important class of substrates that have also been scarcely studied is the triarylsubstituted group.[8e,18] This substrate class provides an easy entry point to diarylmethine chiral centers, which are present in several important drugs and natural products.[19] We were again pleased to find that this substrate class could also be reduced in high enantioselectivity using Ir-**L41a** catalytic system (Scheme 3.6.3, ee's ranging from 98% to >99%).

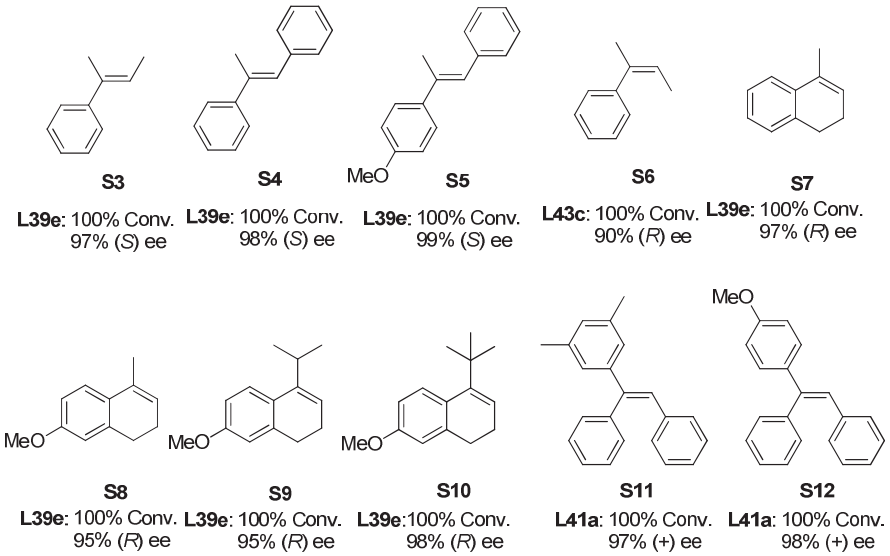

Scheme 3.6.3. Selected hydrogenation results of *E*- and *Z*-trisubstituted olefins using [Ir(cod)(**L38**-**L49a**-**g**)]BAr_F catalyst precursors. Reaction conditions: 1 mol % catalyst precursor, CH_2Cl_2 as solvent, 50 bar H_2, rt, 2 h.

Asymmetric hydrogenation of trisubstituted olefins containing a neighboring polar group

The reduction of substrates bearing a neighboring polar group is of great importance because they are important intermediates for the synthesis of high-value chemicals and they enable further functionalization. We therefore decided to study the potential of our phosphite–pyridine ligand library **L38**-**L49a**-**g** for the reduction of a wide range of trisubstituted alkenes containing several types of polar groups in greater depth. The results are summarized in Scheme 3.6.4. Once again, excellent enantioselectivities in both enantiomers of the reduction products (ee values up to 99%) for a range of substrates were obtained under mild reaction conditions by suitable tuning of the ligand parameters. The reduction of several α,β-unsaturated esters (**S13**-**S15**) followed different trends to those observed for the previous *E*-trisubstituted substrates. Enantioselectivities were therefore best using ligands **L42a**, **L42e**, **L48a** and **L48e** (ee's ranging from 96% to 99%). It should be noted that ee's are highly independent of the electronic nature of the substrate phenyl ring. We also found that the hydrogenation of allylic alcohol **S16** and allylic acetate **S17** followed the same trend. High enantioselectivities were therefore also obtained with catalyst systems containing the ligands **L42a**, **L42e**, **L48a** and **L48e** (ee's up to 98%). As observed for the *E*-trisubstituted substrate **S1**, the highest enantioselectivities in the hydrogenation of vinylsilane **S18**

were obtained using ligands **L39e** and **L47e** (ee's up to 78%). Ligand tuning was also essential to achieve the highest levels of enantioselectivity in the reduction of α,β-unsaturated ketone **S19** and several vinylboronates **S20**-**S22**. For substrate **S19**, enantioselectivities are therefore best when using Ir-**L39a** and Ir-**L47a** catalysts (ee's up to 99%), while for substrates **S20**-**S22**, Ir-**L38a** and Ir-**L46a** catalytic systems provided the highest enantioselectivities (ee's up to 99%). The hydrogenation of vinylboronates provides easy access to chiral borane compounds, which are useful building blocks in organic synthesis because the C-B bond can be readily converted to C-O, C-N and C-C bonds with retention of the chirality. For vinylboronates, our results show that ee's are again highly independent of the electronic properties of the phenyl substrate ring. This is therefore one of the few catalytic systems that can hydrogenate a wide range of trisubstituted olefins in high activities and enantioselectivities.[2,5]

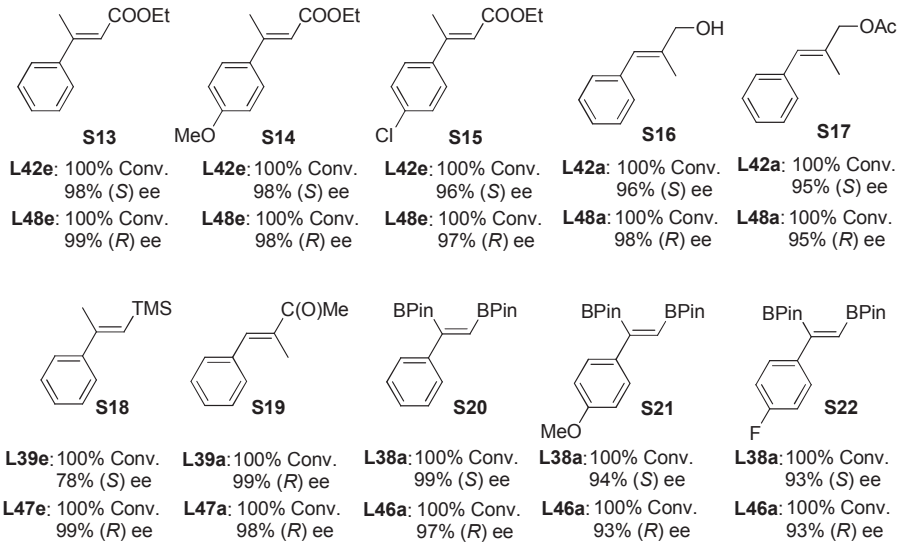

L42e: 100% Conv. 98% (*S*) ee	**L42e**: 100% Conv. 98% (*S*) ee	**L42e**: 100% Conv. 96% (*S*) ee	**L42a**: 100% Conv. 96% (*S*) ee	**L42a**: 100% Conv. 95% (*S*) ee
L48e: 100% Conv. 99% (*R*) ee	**L48e**: 100% Conv. 98% (*R*) ee	**L48e**: 100% Conv. 97% (*R*) ee	**L48a**: 100% Conv. 98% (*R*) ee	**L48a**: 100% Conv. 95% (*R*) ee
L39e: 100% Conv. 78% (*S*) ee	**L39a**: 100% Conv. 99% (*R*) ee	**L38a**: 100% Conv. 99% (*S*) ee	**L38a**: 100% Conv. 94% (*S*) ee	**L38a**: 100% Conv. 93% (*S*) ee
L47e: 100% Conv. 99% (*R*) ee	**L47a**: 100% Conv. 98% (*R*) ee	**L46a**: 100% Conv. 97% (*R*) ee	**L46a**: 100% Conv. 93% (*R*) ee	**L46a**: 100% Conv. 93% (*R*) ee

Scheme 3.6.4. Selected hydrogenation results of trisubstituted olefins bearing a neighboring polar group using [Ir(cod)(**L38**-**L49a**-**g**)]BAr_F catalyst precursors. Reaction conditions: 1 mol % catalyst precursor, CH_2Cl_2 as solvent, 50 bar H_2, rt, 2 h.

3.6.3.4 Asymmetric hydrogenation of 1,1-disubstituted terminal olefins

To further study the potential of these readily available ligands, we tested **L38**-**L49a**-**g** in the asymmetric hydrogenation of more demanding terminal olefins. The lower enantioselectivity obtained with 1,1-disubstituted terminal olefins compared with trisubstituted olefins is attributed to two main factors.[2d-e] The first is that the two substituents in the substrate can easily exchange positions in the chiral environment formed by the catalysts, thus reversing the face selectivity. The second reason is that the terminal double bond can isomerize to form the more stable internal alkene, which usually leads to the predominant formation of the opposite enantiomer of the hydrogenated product. Few known catalytic systems provide high enantioselectivities for these substrates, and those that do are usually limited in substrate scope.[2e,20,21] Unlike the hydrogenation of trisubstituted olefins, the enantioselectivity in the reduction of terminal alkenes is

highly pressure-dependent. Hydrogenation at an atmospheric pressure of H_2 therefore generally gave significantly higher ee values than at higher pressures.[20]

Asymmetric hydrogenation of minimally functionalized 1,1-disubstituted terminal olefins

In an initial set of experiments, we used the Ir-catalyzed asymmetric hydrogenation of 2-(4-methoxyphenyl)but-1-ene **S23**. The results obtained using the ligand library **L38**-**L49a**-**g** under optimized conditions are shown in Table 3.6.2. We were again able to fine-tune the ligand parameters to produce high activities and enantioselectivities (ee's up to 96%) in the hydrogenation of this substrate using ligands **L39e** and **L47e** at low catalyst loadings (0.25 mol%) and hydrogen pressures (1 bar). Once again, it was possible to obtain both enantiomers of the hydrogenated product by simply changing the configuration of the stereogenic carbon next to the phosphite moiety (see Table 3.6.2, entries 10 vs 24). Enantioselectivity is also affected by the substituents at the ligand backbone (R^1 and R^2) and by the substituents/configuration in the biaryl phosphite moiety. Regarding the effect of the substituents at the ligand backbone, we found that enantioselectivities are best with ligands that contain a methyl substituent at R^1 and a hydrogen substituent at R^2 positions (ligands **L39** and **L47**).

Table 3.6.2. Selected results for the Ir-catalyzed hydrogenation of **S23** using the ligands **L38-L49a-g**[a]

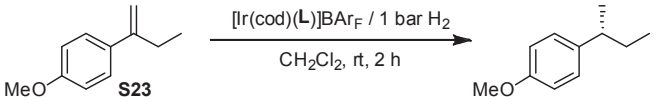

Entry	Ligand	% Conv[b]	% ee[c]	Entry	Ligand	% Conv[b]	% ee[c]
1	**L38a**	100	48 (*R*)	14	**L42d**	100	77 (*R*)
2	**L38b**	100	49 (*R*)	15	**L42e**	100	30 (*S*)
3	**L38c**	100	50 (*R*)	16	**L43a**	100	63 (*R*)
4	**L38d**	100	40 (*S*)	17	**L43d**	100	62 (*R*)
5	**L38e**	100	58 (*R*)	18	**L43e**	100	42 (*S*)
6	**L38f**	100	36 (*S*)	19	**L44a**	100	33 (*S*)
7	**L38g**	100	58 (*R*)	20	**L45a**	100	60 (*R*)
8	**L39a**	100	72 (*R*)	21	**L46a**	100	49 (*S*)
9	**L39d**	100	8 (*S*)	22	**L46d**	100	56 (*S*)
10	**L39e**	100	96 (*R*)	23	**L46e**	100	43 (*R*)
11	**L40a**	100	42 (*R*)	24	**L47e**	100	95 (*S*)
12	**L41a**	100	19 (*R*)	25[d]	**L39e**	100	96 (*R*)
13	**L42a**	100	64 (*R*)	26[d]	**L47e**	100	95 (*S*)

[a] Reactions carried out using 0.5 mmol of **S21** and 1 mol% of Ir-catalyst precursor at 1 bar of H_2.[b] Conversion measured by GC after 2 hours. [c] Enantiomeric excesses determined by chiral GC. [d] Reaction carried out at 0.25 mol% of Ir-catalyst for 3 h.

As far as the effect of the substituents/configuration of the phosphite moiety is concerned, enantioselectivity is mainly affected by the configuration of the biaryl phosphite moiety, and is relatively insensitive to the substituents at both *ortho* and *para* positions of the biaryl phosphite

groups. The best enantioselectivities are therefore obtained using ligands containing an enantiopure *R*-biaryl phosphite moiety (see Table 3.6.2, entry 10 vs 9).

We then studied the asymmetric hydrogenation of other 1,1-disubstituted aryl–alkyl substrates (**S24**-**S31**), 1,1-disubstituted pyridyl–alkyl olefins (**S32**-**S33**) and 1,1-diaryl terminal alkenes (**S34**-**S36**) using the phosphite–pyridine ligand library **L38**-**L49a**-**g**. The most noteworthy results are shown in Table 3.6.3. The results follow the same trends as the hydrogenation of **S23** for all substrates. The catalyst precursors containing the phosphite–pyridine ligands **L39e** and **L47e** therefore provided the best enantioselectivities in both enantiomers of the reduction product. These results are again among the best reported for these substrates.[2e]

Table 3.6.3. Selected results for the Ir-catalyzed hydrogenation of minimally functionalized 1,1-disubstituted terminal olefins using ligands **L38**-**L49a**-**g**[a]

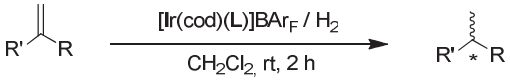

R' = aryl, 2-pyridine
R = alkyl, aryl

Entry	Substrate	Ligand	% ee[b]	Entry	Substrate	Ligand	% ee[b]
1	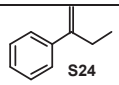	**L39e**	97 (*R*)	15	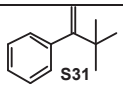	**L39e**	92 (*R*)
2	**S24**	**L47e**	97 (*S*)	16	**S31**	**L47e**	92 (*S*)
3	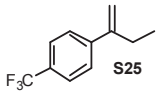	**L39e**	96 (*R*)	17	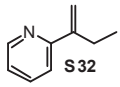	**L39e**	92 (-)
4	**S25**	**L47e**	96 (*S*)	18	**S32**	**L47e**	93 (+)
5	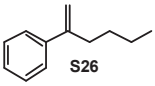	**L39e**	96 (*R*)	19	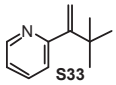	**L39e**	94 (-)
6	**S26**	**L47e**	96 (*S*)	20	**S33**	**L47e**	94 (+)
7	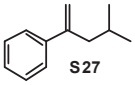	**L39e**	96 (*R*)				
8	**S27**	**L47e**	95 (*S*)	21[d]	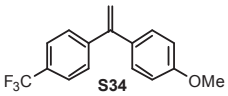	**L39e**	18 (-)
9	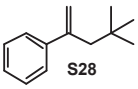	**L39e**	97 (*R*)	22[c]		**L39e**	80 (-)
10	**S28**	**L47e**	96 (*S*)	23[c]	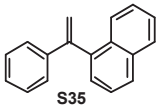	**L47e**	79 (+)
11	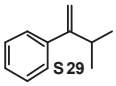	**L39e**	92 (*R*)		**S35**		
12	**S29**	**L47e**	91 (*S*)	24[c]	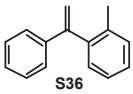	**L39e**	82 (-)
13	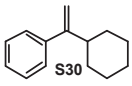	**L39e**	92 (*R*)		**S36**		
14	**S30**	**L47e**	92 (*S*)				

[a] Reactions carried out using 0.5 mmol of substrate and 0.25 mol% of Ir-catalyst precursor at 1 bar of H_2. Full conversions were achieved in all cases. [b] Enantiomeric excesses determined by chiral GC (except for entries 11-13 that were measured by HPLC). [c] Reaction carried out at 50 bar of H_2.

Our results with several 1,1-disubstituted aryl–alkyl substrates (**S24**-**S31**) indicated that enantioselectivity is not affected by the electronic nature of the substrate aryl ring (Table 3.6.2, entry 10; and Table 3.6.3, entries 1 and 3), but it is slightly affected by the nature of the alkyl chain

(ee's ranging from 92% to 97%; Table 3.6.3, entries 1, 5-16). Enantioselectivities therefore decrease from 97%-96% to 92% by increasing the steric bulk of the alkyl substituent. This can be attributed to the restrictions imposed by the Ir-catalysts themselves rather than to the presence of an isomerization process under hydrogenation conditions. This is supported by the fact that the hydrogenation of substrate **S31** bearing a *tert*-butyl group, for which isomerization cannot occur, provides the same enantioselectivity as those obtained using substrates **S29** and **S30**, which are more prone to isomerization and also contain bulky alkyl substituents (Table 3.6.3, entry 15 vs 11 and 13).

Due to the interest of heterocycles for industry and because the heterocyclic part can be modified post-hydrogenation, we decided to test the scope of our ligand library by performing the hydrogenation of pyridyl-alkyl substrates **S32** and **S33**. We were pleased to see that we also obtained high activities and enantioselectivities under mild reaction conditions (Table 3.6.3, entries 17-20).

Finally, we studied the hydrogenation of several diaryl terminal alkenes (**S34**-**S36**; Table 3.6.3, entries 21-24). Enantiopure diarylalkanes are important intermediates for the preparation of drugs and research materials.[22] They have traditionally been prepared using rather laborious approaches.[22,23] It has recently been shown that they can be prepared more efficiently using enantioselective hydrogenation.[5c] Substrates differing sterically (**S35** and **S36**) were also hydrogenated with high enantioselectivities (ee's up to 82%) using the Ir-**L39e** catalytic system. However, as anticipated, the control of enantioselectivity in substrate **S34**, which aryl groups only differs electronically, was less effective.

Asymmetric hydrogenation of 1,1-disubstituted terminal olefins containing a neighboring polar group

Encouraged by the excellent results obtained up to this point, we also decided to examine the asymmetric hydrogenation of 1,1-disubstituted terminal olefins containing a polar neighboring group (**S37**-**S40**). The results are summarized in Scheme 3.6.5. In all cases, both enantiomers of the hydrogenated product can be obtained in high enantioselectivities by simply changing the configuration of the carbon next to the phosphite moiety.

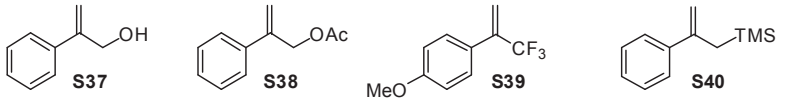

S37	**S38**	**S39**	**S40**
L42e: 100% Conv. 84% (*S*) ee	**L42e**: 100% Conv. 79% (*S*) ee	**L38c**: 100% Conv. 99% (+) ee	**L39e**: 100% Conv. 95% (*R*) ee
L48e: 100% Conv. 83% (*R* ee	**L48e**: 100% Conv. 79% (*R*) ee	**L46c**: 100% Conv. 99% (-) ee	**L47e**: 100% Conv. 94% (*S*) ee

Scheme 3.6.5. Selected hydrogenation results of 1,1-disubstituted terminal olefins containing a neighboring polar group using [Ir(cod)(**L38**-**L49a**-**g**)]BAr_F catalyst precursors. Reaction conditions: 0.5 mol % catalyst precursor, CH_2Cl_2 as solvent, 50 bar H_2, rt, 2 h.

We initially tested the ligand library in the hydrogenation of the allylic alcohol **S37** and allylic acetate **S38**. Derivatives of the hydrogenation of these products are important intermediates for the synthesis of high-value cosmetics, natural products and drugs.[24] Enantioselectivities followed

a different trend to that observed with previous 1,1,-disubstituted terminal olefins **S23**-**S36**, and the best enantioselectivities (up to 84%) were obtained using ligands **L42e** and **L48e**. We then turned our attention to the asymmetric reduction of the trifluoromethyl olefin **S39** and allylic silane **S40**. The hydrogenation of these compounds gave rise to important organic intermediates and a number of innovative new organofluorine[25] and organosilicon[26] drugs are now being developed. For substrate **S39**, an unprecedented high enantioselectivity (ee up to 99%) has been obtained with Ir/**L38c** and Ir/**L46c** catalytic systems. However, for substrate **S40**, we also obtained high enantioselectivities but with ligands **L39e** and **L47e**. Once again, these results clearly show the efficiency of using highly modular scaffolds in the ligand design.

3.6.4 Conclusions

We have reported the first successful application of phosphite-pyridine ligands in the Ir-catalyzed asymmetric hydrogenation of minimally functionalized olefins. These ligands combine the advantages of both types of successful ligands for this process (phosphite and pyridine). They are therefore more robust than their oxazoline and phosphine/phosphinite counterparts, and the incorporation of the desired diversity is easier to achieve in both the pyridine and the phosphite moieties. The modular ligand design has been shown to be crucial in finding highly selective catalytic systems for each substrate. By carefully selecting the ligand components, we obtained excellent enantioselectivities (ee's up to 99%) in a wide range of *E*- and *Z*-trisubstituted alkenes, including more demanding triarylsubstituted olefins, and dihydronaphthalenes. The good performance extends to the very challenging class of terminal disubstituted olefins (ee's up to 99%). These catalysts are also very tolerant to the presence of a neighboring polar group. A range of allylic alcohols, acetates, α,β–unsaturated esters and ketones, allylic silanes, vinylboronates and trifluoromethyl olefins were thus hydrogenated with high enantioselectivities. Note that both enantiomers of the reduction product can be obtained in excellent enantioselectivities by simply changing the configuration of the carbon next to the phosphite moiety. We also demonstrated that the introduction of a biaryl phosphite moiety into the ligand design is highly advantageous in terms of substrate versatility. The efficiency of this ligand design is therefore also corroborated by the fact that these Ir-phosphite-pyridine catalysts provided higher enantioselectivity and broader substrate versatility than their phosphinite-pyridine analogues. These results open up a new class of Ir catalysts for the highly enantioselective hydrogenation of minimally functionalized olefins, including those with a neighboring polar group, which is of great practical interest.

3.6.5 Experimental Section

3.6.5.1 General considerations

All reactions were carried out using standard Schlenk techniques under an atmosphere of argon. Solvents were purified and dried by standard procedures. Phosphorochloridites were easily prepared in one step from the corresponding biaryls.[27] Enantiopure hydroxyl-pyridine compounds **1**-**6** and **8** were prepared as previously described.[5h,12] ^{1}H, ^{13}C-{^{1}H}, and ^{31}P-{^{1}H} NMR spectra were recorded using a 400 MHz spectrometer. Chemical shifts are relative to that of $SiMe_4$ (^{1}H

and ^{13}C) as internal standard or H_3PO_4 (^{31}P) as external standard. ^{1}H and ^{13}C assignments were made on the basis of ^{1}H-^{1}H gCOSY and ^{1}H-^{13}C gHSQC experiments.

3.6.5.2. Preparation of hydroxyl-pyridine (*S*)-7

Compound **7** was synthesized by a modified previously reported methodology.[5h] 2-bromo-6-methylpyridine (4.27 ml, 37.5 mmol) was dissolved in ether (150 ml) and the mixture cooled to -78 °C. To this clear, colorless solution was added ^{n}BuLi (1.55 M in hexanes, 27 ml, 41.2 mmol). This causes the solution to turn yellow initially and then deep red. The solution was stirred at low temperature for 1 h and pivalaldehyde (4.89 ml, 45 mmol) was added, which immediately turned the solution a light shade of orange and deposited a solid mass. The mixture was allowed to stir and warm up slowly overnight. Next, the reaction was quenched with sat. NH_4Cl (aq.) (100 ml) and the biphasic mixture was stirred until all the solids had dissolved. The layers were separated and the organic phase further extracted with 3 x 50 ml ether. The organic extracts were combined, washed with brine, dried ($MgSO_4$) and concentrated to a crude oil. The resulting oil was purified by chromatography on silica (petroleum ether:ethyl acetate 70:30, R_f = 0.3) to afford the (*rac*)-**7** as a white solid. The racemate was separated into its enantiomers by chiral semi-preparative HPLC using a (250x20 mm) Chiracel OD column (1% isopropanol in hexanes, 4 ml/min, 31 min (*S*), 33 min (*R*)) to yield (*S*)-**7** in >99% ee. ^{1}H NMR ($CDCl_3$), δ: 0.9 (s, 9H, ^{t}Bu), 2.55 (s, 3H, CH_3), 4.32 (b, 1H, OH), 4.35 (s, 1H, CH-O), 7.0-7.6 (m, 3H, CH=).

3.6.5.3 General procedure for the preparation of phosphite-pyridine ligands L38-L49a-g

Phosphorochloridite (1.1 mmol) produced *in situ* was dissolved in toluene (5 mL) and pyridine (0.18 mL, 2.3 mmol) was added. Hydroxyl-pyridine (1 mmol) was azeotropically dried with toluene (3 x 1 mL) and then dissolved in toluene (5 mL), to which pyridine (0.18 mL, 2.3 mmol) was added. The alcohol solution was transferred slowly at 0 ºC to the solution of phosphorochloridite. The reaction mixture was warmed to 80 ºC and stirred for 2 hours, and the pyridine salts were removed by filtration. Evaporation of the solvent gave a white foam, which was purified by flash chromatography (toluene/hexane/NEt_3) to produce the corresponding ligand as white solid.

L38a. Yield: 426 mg (76%). ^{31}P NMR (C_6D_6), δ: 145.0 (s). ^{1}H NMR (C_6D_6), δ: 1.24 (s, 9H, CH_3, ^{t}Bu), 1.25 (s, 9H, CH_3, ^{t}Bu), 1.44 (s, 9H, CH_3, ^{t}Bu), 1.45 (s, 9H, CH_3, ^{t}Bu), 1.54 (d, 3H, CH_3, $^{3}J_{H\text{-}H}$= 6.4 Hz), 5.64 (m, 1H, CH-O), 6.5-8.4 (m, 8H, CH=). ^{13}C NMR (C_6D_6), δ: 23.9 (d, CH_3, $J_{C\text{-}P}$= 3.7 Hz), 31.2 (CH_3, ^{t}Bu), 31.5 (CH_3, ^{t}Bu), 34.6 (C, ^{t}Bu), 35.5 (C, ^{t}Bu), 75.8 (d, CH, $J_{C\text{-}P}$= 9.9 Hz), 120.4 (CH=), 122.1 (CH=), 124.2 (CH=), 124.3 (CH=), 125.5 (C), 126.9 (CH=), 128.4 (CH=), 129.2 (C), 133.4 (C), 133.8 (C), 136.2 (CH=), 137.7 (C), 140.4 (C), 140.5 (C), 146.4 (C), 146.9 (C), 148.8 (CH=), 162.7 (C). Anal. calcd (%) for $C_{35}H_{48}NO_3P$: C 74.84, H 8.61, N 2.49; found: C 74.89, H 8.62, N 2.47.

L38b. Yield: 265 mg (52%). ^{31}P NMR (C_6D_6), δ: 144.7 (s). ^{1}H NMR (C_6D_6), δ: 1.44 (s, 9H, CH_3, ^{t}Bu), 1.49 (s, 9H, CH_3, ^{t}Bu), 1.65 (d, 3H, CH_3, $^{3}J_{H\text{-}H}$= 6.8 Hz), 3.36 (s, 6H, O-CH_3), 5.75 (m, 1H, CH-O), 6.5-8.4 (m, 8H, CH=). ^{13}C NMR (C_6D_6), δ: 24.5 (d, CH_3, $J_{C\text{-}P}$= 4.6 Hz), 31.4 (CH_3, ^{t}Bu), 31.5 (CH_3, ^{t}Bu), 35.8 (C, ^{t}Bu), 55.4 (CH_3-O), 76.3 (d, CH, $J_{C\text{-}P}$= 10.6 Hz), 113.6 (C), 113.8 (C), 115.2 (CH=), 120.8 (CH=), 122.6 (CH=), 134.5 (C), 135.1 (C), 136.7 (CH=), 142.6 (C), 143.0 (C),

143.2 (C), 149.3 (CH=), 140.4 (C), 156.6 (C), 156.8 (C), 163.3 (C). Anal. calcd (%) for $C_{29}H_{36}NO_5P$: C 68.35, H 7.12, N 2.75; found: C 68.38, H 7.13, N 2.71.

L38c. Yield: 332 mg (69%). ^{31}P NMR (C_6D_6), δ: 144.4 (s). ^{1}H NMR (C_6D_6), δ: 0.23 (s, 9H, CH_3-Si), 0.29 (s, 9H, CH_3-Si), 1.52 (d, 3H, CH_3, $^{3}J_{H-H}$= 6.8 Hz), 5.59 (m, 1H, CH-O), 6.5-8.3 (m, 10H, CH=). ^{13}C NMR (C_6D_6), δ: 0.4 (CH_3-Si), 0.5 (CH_3-Si), 24.6 (d, CH_3, J_{C-P}= 3.0 Hz), 75.9 (d, CH, J_{C-P}= 4.6 Hz), 120.5 (CH), 121.9 (C), 122.6 (CH=), 125.2 (CH=), 125.5 (CH=), 131.8 (C), 132.1 (C), 132.2 (C), 135.7 (CH=), 135.8 (CH=), 136.5 (C), 136.7 (CH=), 149.3 (CH=), 155.0 (C), 155.5 (C), 163.0 (C). Anal. calcd (%) for $C_{25}H_{32}NO_3PSi_2$: C 62.34, H 6.70, N 2.91; found: C 62.39, H 6.69, N 2.88.

L38d. Yield: 358 mg (71%). ^{31}P NMR (C_6D_6), δ: 140.4 (s). ^{1}H NMR (C_6D_6), δ: 1.38 (s, 9H, CH_3, ^{t}Bu), 1.49 (s, 9H, CH_3, ^{t}Bu), 1.59 (d, 3H, CH_3, $^{3}J_{H-H}$= 6.4 Hz), 1.67 (s, 3H, CH_3-Ar), 1.71 (s, 3H, CH_3-Ar), 2.01 (s, 3H, CH_3-Ar), 2.05 (s, 3H, CH_3-Ar), 5.56 (m, 1H, CH-O), 6.55 (m, 1H, CH=), 6.9-7.2 (m, 4H, CH=), 8.32 (m, 1H, CH=). ^{13}C NMR (C_6D_6), δ: 16.9 (CH_3-Ar), 17.2 (CH_3-Ar), 20.8 (CH_3-Ar), 24.7 (d, CH_3, J_{C-P}= 4.6 Hz), 31.7 (d, CH_3, ^{t}Bu, J_{C-P}= 4.6 Hz), 32.2 (CH_3, ^{t}Bu), 35.1 (C, ^{t}Bu), 35.4 (C, ^{t}Bu), 76.2 (d, CH, J_{C-P}= 16.3 Hz), 121.1 (CH=), 122.5 (CH=), 126.0 (C), 128.4 (CH=), 128.8 (CH=), 129.6 (C), 131.6 (d, C, J_{C-P}= 2.9 Hz), 132.1 (C), 132.9 (C), 134.9 (CH=), 135.7 (C), 136.6 (C), 138.0 (C), 138.7 (d, C, J_{C-P}= 2.4 Hz), 146.2 (C), 146.3 (C), 149.1 (CH=), 163.2 (C). Anal. calcd (%) for $C_{31}H_{40}NO_3P$: C 73.64, H 6.24, N 2.41; found: C 73.67, H 6.26, N 2.38.

L38e. Yield: 338 mg (67%). ^{31}P NMR (C_6D_6), δ: 136.5 (s). ^{1}H NMR (C_6D_6), δ: 1.43 (s, 9H, CH_3, ^{t}Bu), 1.51 (d, 3H, CH_3, $^{3}J_{H-H}$= 6.4 Hz), 1.52 (s, 9H, CH_3, ^{t}Bu), 1.69 (s, 3H, CH_3-Ar), 1.76 (s, 3H, CH_3-Ar), 2.05 (s, 3H, CH_3-Ar), 2.09 (s, 3H, CH_3-Ar), 5.46 (m, 1H, CH-O), 6.59 (m, 1H, CH=), 6.9-7.2 (m, 4H, CH=), 8.33 (m, 1H, CH=). ^{13}C NMR (C_6D_6), δ: 16.9 (CH_3-Ar), 17.1 (CH_3-Ar), 20.8 (CH_3-Ar), 24.3 (d, CH_3, J_{C-P}= 3.4 Hz), 31.7 (d, CH_3, ^{t}Bu, J_{C-P}= 4.0 Hz), 32.1 (CH_3, ^{t}Bu), 35.0 (C, ^{t}Bu), 35.4 (C, ^{t}Bu), 76.2 (d, CH, J_{C-P}= 5.4 Hz), 120.4 (CH=), 122.5 (CH=), 126.0 (C), 128.3 (CH=), 128.9 (CH=), 129.6 (C), 131.8 (d, C, J_{C-P}= 3.3 Hz), 132.2 (C), 132.7 (d, C, J_{C-P}= 4.6 Hz), 132.8 (CH=), 135.2 (C), 135.7 (C), 136.6 (CH=), 138.1 (C), 138.6 (d, C, J_{C-P}= 2.7 Hz), 146.1 (C), 146.2 (C), 146.5 (C), 149.3 (CH=), 163.5 (d, C, J_{C-P}= 4.2 Hz). Anal. calcd (%) for $C_{31}H_{40}NO_3P$: C 73.64, H 6.24, N 2.41; found: C 73.66, H 6.23, N 2.40.

L38f. Yield: 419 mg (72%). ^{31}P NMR (C_6D_6), δ: 146.2 (s). ^{1}H NMR (C_6D_6), δ: 0.41 (s, 9H, CH_3-Si), 0.46 (s, 9H, CH_3-Si), 1.63 (d, 3H, CH_3, $^{3}J_{H-H}$= 6.4 Hz), 5.56 (m, 1H, CH-O), 6.49 (m, 1H, CH=), 6.77 (m, 1H, CH=), 6.89 (m, 3H, CH=), 7.12 (m, 1H, CH=), 7.33 (m, 2H, CH=), 7.73 (m, 2H, CH=), 8.01 (s, 1H, CH=), 8.14 (s, 1H, CH=), 8.31 (m, 1H, CH=). ^{13}C NMR (C_6D_6), δ: 0.0 (d, CH_3-Si, J_{C-P}= 4.6 Hz), 0.4 (CH_3-Si), 24.6 (d, CH_3, J_{C-P}= 3.9 Hz), 75.6 (d, CH, J_{C-P}= 7.8 Hz), 120.5 (CH=), 122.1 (CH=), 122.7 (d, C, J_{C-P}= 3.1 Hz), 123.6 (d, C, J_{C-P}= 4.4 Hz), 125.0 (CH=), 126.8 (CH=), 126.9 (CH=), 127.1 (CH=), 127.3 (CH=), 128.7 (CH=), 129.2 (C), 131.1 (C), 131.5 (C), 132.6 (C), 132.7 (C), 134.4 (d, C, J_{C-P}= 2.1 Hz), 134.8 (d, C, J_{C-P}= 1.5 Hz), 136.0 (CH=), 137.1 (C), 137.5 (C), 148.7 (CH=), 152.2 (d, C, J_{C-P}= 3.8 Hz), 152.9 (d, C, J_{C-P}= 5.2 Hz), 162.2 (d, C, J_{C-P}= 1.8 Hz). Anal. calcd (%) for $C_{33}H_{36}NO_3PSi_2$: C 68.13, H 6.24, N 2.41; found: C 68.19, H 6.26, N 2.36.

L38g. Yield: 389 mg (67%). ^{31}P NMR (C_6D_6), δ: 143.6 (s). ^{1}H NMR (C_6D_6), δ: 0.36 (s, 9H, CH_3-Si), 0.50 (s, 9H, CH_3-Si), 1.43 (d, 3H, CH_3, $^{3}J_{H-H}$= 6.4 Hz), 5.49 (m, 1H, CH-O), 6.53 (m, 1H, CH=), 6.87 (m, 3H, CH=), 7.01 (m, 1H, CH=), 7.16 (m, 2H, CH=), 7.35 (m, 2H, CH=), 7.71 (m, 2H, CH=), 8.07 (s, 1H, CH=), 8.18 (s, 1H, CH=), 8.30 (m, 1H, CH=). ^{13}C NMR (C_6D_6), δ: 0.2 (d, CH_3-Si, J_{C-P}= 3.5 Hz), 0.7 (CH_3-Si), 24.1 (d, CH_3, J_{C-P}= 2.8 Hz), 76.1 (CH), 120.2 (CH=), 122.5 (CH=),

123.4 (d, C, J_{C-P}= 3.0 Hz), 123.7 (d, C, J_{C-P}= 4.7 Hz), 125.3 (CH=), 125.5 (CH=), 126.0 (C), 127.3 (CH=), 127.4 (CH=), 127.5 (CH=), 127.6 (CH=), 128.8 (CH=), 128.9 (CH=), 129.0 (CH=), 129.6 (CH=), 131.5 (C), 131.9 (C), 133.0 (C), 133.2 (C), 134.9 (C), 135.1 (C), 136.6 (CH=), 137.3 (C), 137.8 (C), 149.4 (CH=), 153.0 (C). Anal. calcd (%) for $C_{33}H_{36}NO_3PSi_2$: C 68.13, H 6.24, N 2.41; found: C 68.15, H 6.25, N 2.37.

L39a. Yield: 373 mg (65%). ^{31}P NMR (C_6D_6), δ: 145.7 (s). ^{1}H NMR (C_6D_6), δ: 1.24 (s, 9H, CH_3, ^{t}Bu), 1.25 (s, 9H, CH_3, ^{t}Bu), 1.44 (s, 9H, CH_3, ^{t}Bu), 1.45 (s, 9H, CH_3, ^{t}Bu), 1.58 (d, 3H, CH_3, $^3J_{H-H}$= 7.0 Hz), 2.34 (s, 3H, CH_3), 5.69 (m, 1H, CH-O), 6.5-7.6 (m, 7H, CH=). ^{13}C NMR (C_6D_6), δ: 24.4 (d, CH_3, J_{C-P}= 3.8 Hz), 24.8 (CH_3-Py), 31.7 (CH_3, ^{t}Bu), 32.0 (CH_3, ^{t}Bu), 35.0 (C, ^{t}Bu), 36.0 (C, ^{t}Bu), 76.4 (d, CH, J_{C-P}= 10.6 Hz), 117.9 (CH=), 122.1 (CH=), 124.6 (CH=), 124.8 (C), 126.0 (C), 127.4 (CH=), 127.5 (CH=), 128.9 (C), 129.7 (C), 133.9 (C), 134.4 (C), 137.1 (CH=), 140.9 (C), 141.0 (C), 146.9 (C), 147.2 (C), 157.9 (C), 162.6 (C). Anal. calcd (%) for $C_{36}H_{50}NO_3P$: C 75.10, H 8.75, N 2.43; found: C 75.13, H 8.74, N 2.41.

L39b. Yield: 282 mg (54%). ^{31}P NMR (C_6D_6), δ: 145.1 (s). ^{1}H NMR (C_6D_6), δ: 1.52 (s, 9H, CH_3, ^{t}Bu), 1.55 (s, 9H, CH_3, ^{t}Bu), 1.74 (d, 3H, CH_3, $^3J_{H-H}$= 6.4 Hz), 2.44 (s, 3H, CH_3), 3.42 (s, 6H, O-CH_3), 5.82 (m, 1H, CH-O), 6.5-7.4 (m, 7H, CH=). ^{13}C NMR (C_6D_6), δ: 24.4 (d, CH_3, J_{C-P}= 4.6 Hz), 25.0 (CH_3-Py), 31.6 (CH_3, ^{t}Bu), 31.7 (CH_3, ^{t}Bu), 35.9 (C, ^{t}Bu), 56.2 (CH_3-O), 75.5 (d, CH, J_{C-P}= 10.1 Hz), 112.9 (CH=), 113.0 (CH=), 114.4 (CH=), 114.5 (CH=), 117.1 (CH=), 121.4 (CH=), 133.9 (C), 134.0 (C), 134.3 (C), 134.4 (C), 136.4 (CH=), 141.9 (C), 142.3 (C), 142.4 (C), 155.9 (C), 156.1 (C), 157.2 (C), 161.9 (C. Anal. calcd (%) for $C_{30}H_{38}NO_5P$: C 68.82, H 7.32, N 2.68; found: C 68.85, H 7.35, N 2.61.

L39c. Yield: 361 mg (73 %). ^{31}P NMR (C_6D_6), δ: 144.4 (s). ^{1}H NMR (C_6D_6), δ: 0.32 (s, 9H, CH_3-Si), 0.38 (s, 9H, CH_3-Si), 1.62 (d, 3H, CH_3, $^3J_{H-H}$= 6 Hz), 2.35 (s, CH_3), 5.66 (m, 1H, CH-O), 6.5-7.5 (m, 9H, CH=). ^{13}C NMR (C_6D_6), δ: 0.3 (CH_3-Si), 0.4 (CH_3-Si), 24.5 (d, CH_3, J_{C-P}= 3.7 Hz), 25.1 (CH_3-Py), 75.9 (d, CH, J_{C-P}= 10.4 Hz), 112.9 (CH=), 116.9 (CH=), 121.4 (CH=), 124.5 (CH=), 124.7 (CH=), 131.1 (C), 131.2 (C), 131.5 (C), 131.8 (C), 132.3 (CH=), 132.4 (CH=), 135.0 (CH=), 136.4 (CH=), 154.3 (C), 154.4 (C), 154.7 (C), 154.8 (C), 157.2 (C), 162.1 (C). Anal. calcd (%) for $C_{26}H_{34}NO_3PSi_2$: C 63.00, H 6.91, N 2.83; found: C 63.05, H 6.94, N 2.79.

L39d. Yield: 364 mg (70%). ^{31}P NMR (C_6D_6), δ: 140.9 (s). ^{1}H NMR (C_6D_6), δ: 1.42 (s, 9H, CH_3, ^{t}Bu), 1.54 (s, 9H, CH_3, ^{t}Bu), 1.65 (d, 3H, CH_3, $^3J_{H-H}$= 6.4 Hz), 1.71 (s, 3H, CH_3-Ar), 1.74 (s, 3H, CH_3-Ar), 2.05 (s, 3H, CH_3-Ar), 2.09 (s, 3H, CH_3-Ar), 2.35 (s, 3H CH_3-Py), 5.59 (m, 1H, CH-O), 6.55 (m, 1H, CH=), 6.9-7.2 (m, 4H, CH=). ^{13}C NMR (C_6D_6), δ: 16.9 (CH_3-Ar), 17.2 (CH_3-Ar), 20.7 (CH_3-Ar), 20.8 (CH_3-Ar), 24.6 (d, CH_3, J_{C-P}= 4.5 Hz), 24.8 (CH_3-Py), 31.7 (d, CH_3, ^{t}Bu, J_{C-P}= 5.3 Hz), 32.4 (CH_3, ^{t}Bu), 35.1 (C, ^{t}Bu), 35.4 (C, ^{t}Bu), 76.4 (d, CH, J_{C-P}= 16.8 Hz), 118.2 (CH=), 122.0 (CH=), 126.0 (C), 128.8 (CH=), 129.6 (CH=), 131.7 (d, C, J_{C-P}= 3.1 Hz), 132.0 (C), 132.9 (C), 133.1 (d, C, J_{C-P}= 7.3 Hz), 134.9 (C), 135.7 (C), 137.0 (CH=), 138.0 (C), 138.2 (C), 146.2 (C), 146.3 (C), 157.7 (C), 162.6 (C). Anal. calcd (%) for $C_{32}H_{42}NO_3P$: C 73.96, H 8.15, N 2.70; found: C 74.01, H 8.18, N 2.65.

L39e. Yield: 281 mg (54%). ^{31}P NMR (C_6D_6), δ: 136.8 (s). ^{1}H NMR (C_6D_6), δ: 1.44 (s, 9H, CH_3, ^{t}Bu), 1.54 (s, 9H, CH_3, ^{t}Bu), 1.55 (d, 3H, CH_3, $^3J_{H-H}$= 6.4 Hz), 1.69 (s, 3H, CH_3-Ar), 1.76 (s, 3H, CH_3-Ar), 2.05 (s, 3H, CH_3-Ar), 2.09 (s, 3H, CH_3-Ar), 2.32 (s, 3H CH_3-Py), 5.47 (m, 1H, CH-O), 6.55 (m, 1H, CH=), 6.9-7.2 (m, 4H, CH=). ^{13}C NMR (C_6D_6), δ: 16.9 (CH_3-Ar), 17.0 (CH_3-Ar), 20.7 (CH_3-Ar), 24.3 (d, CH_3, J_{C-P}= 3.8 Hz), 24.7 (CH_3-Py), 31.6 (d, CH_3, ^{t}Bu, J_{C-P}= 4.6 Hz), 32.24 (CH_3,

^{t}Bu), 35.0 (C, ^{t}Bu), 35.4 (C, ^{t}Bu), 76.3 (d, CH, J_{C-P}= 5.3 Hz), 117.4 (CH=), 121.9 (CH=), 126.0 (C), 128.8 (CH=), 129.6 (CH=), 131.9 (d, C, J_{C-P}= 1.8 Hz), 132.1 (C), 132.7 (C), 132.9 (C), 135.2 (C), 135.7 (C), 136.9 (CH=), 138.1 (C), 138.6 (C), 146.1 (d, C, J_{C-P}= 5.3 Hz), 146.5 (d, C, J_{C-P}= 2.3 Hz), 157.9 (C), 162.7 (d, C, J_{C-P}= 4.6 Hz). Anal. calcd (%) for $C_{32}H_{42}NO_3P$: C 73.96, H 8.15, N 2.70; found: C 74.02, H 8.17, N 2.68.

L39g. Yield: 375 mg (63%). ^{31}P NMR (C_6D_6), δ: 143.7 (s). ^{1}H NMR (C_6D_6), δ: 0.37 (s, 9H, CH_3-Si), 0.51 (s, 9H, CH_3-Si), 1.44 (d, 3H, CH_3, $^{3}J_{H-H}$= 6.4 Hz), 2.27 (s, 3H, CH_3-Py), 5.49 (m, 1H, CH-O), 6.53 (m, 1H, CH=), 6.87 (m, 2H, CH=), 7.01 (m, 2H, CH=), 7.16 (m, 2H, CH=), 7.31 (m, 2H, CH=), 7.73 (m, 2H, CH=), 8.07 (s, 1H, CH=), 8.18 (s, 1H, CH=). ^{13}C NMR (C_6D_6), δ: 0.0 (CH_3-Si), 0.7 (CH_3-Si), 23.8 (CH_3), 24.4 (CH_3-Py), 75.2 (CH), 117.0 (CH=), 121.8 (CH=), 123.1 (C), 123.9 (C), 125.0 (CH=), 125.2 (CH=), 125.7 (C), 127.0 (CH=), 127.2 (CH=), 127.4 (CH=), 128.7 (CH=), 128.8 (CH=), 129.3 (C), 131.2 (C), 131.6 (C), 132.7 (C), 132.9 (C), 134.7 (C), 136.7 (CH=), 137.0 (CH=), 137.6 (CH=), 152.8 (C), 157.8 (C), 162.2 (C). Anal. calcd (%) for $C_{34}H_{38}NO_3PSi_2$: C 68.54, H 6.43, N 2.35; found: C 68.57, H 6.45, N 2.31.

L40a. Yield: 365 mg (57%). ^{31}P NMR (C_6D_6), δ: 143.8 (s). ^{1}H NMR (C_6D_6), δ: 1.23 (s, 9H, CH_3, ^{t}Bu), 1.25 (s, 9H, CH_3, ^{t}Bu), 1.39 (d, 3H, CH_3, $^{3}J_{H-H}$= 6.0 Hz), 1.42 (s, 9H, CH_3, ^{t}Bu), 1.44 (s, 9H, CH_3, ^{t}Bu), 5.45 (m, 1H, CH-O), 6.5-7.6 (m, 7H, CH=). ^{13}C NMR (C_6D_6), δ: 24.1 (d, CH_3, J_{C-P}= 3.8 Hz), 31.6 (CH_3, ^{t}Bu), 31.9 (CH_3, ^{t}Bu), 35.1 (C, ^{t}Bu), 35.9 (C, ^{t}Bu), 75.2 (d, CH, J_{C-P}= 10.7 Hz), 119.7 (CH=), 124.7 (C), 124.9 (C), 126.0 (CH=), 127.5 (C), 129.7 (CH=), 133.7 (C), 134.3 (C), 138.1 (C), 139.2 (CH=), 140.8 (C), 140.9 (C), 141.7 (CH=), 146.7 (C), 146.8 (CH=), 147.1 (C), 147.4 (CH=), 164.5 (C). Anal. calcd (%) for $C_{35}H_{47}BrNO_3P$: C 65.62, H 7.39, N 2.19; found: C 65.66, H 7.41, N 2.16.

L40b. Yield: 299 mg (51%). ^{31}P NMR (C_6D_6), δ: 143.5 (s). ^{1}H NMR (C_6D_6), δ: 1.35 (s, 9H, CH_3, ^{t}Bu), 1.36 (s, 9H, CH_3, ^{t}Bu), 1.42 (d, 3H, CH_3, $^{3}J_{H-H}$= 6.8 Hz), 3.28 (s, 3H, CH_3-O), 3.31 (s, 3H, CH_3-O), 5.49 (m, 1H, CH-O), 6.5-7.2 (m, 7H, CH=). ^{13}C NMR (C_6D_6), δ: 23.5 (d, CH_3, J_{C-P}= 3.8 Hz), 30.7 (CH_3, ^{t}Bu), 30.8 (CH_3, ^{t}Bu), 35.1 (C, ^{t}Bu), 54.7 (CH_3-O), 74.5 (d, CH, J_{C-P}= 9.9 Hz), 112.8 (CH=), 113.1 (CH=), 114.5 (CH=), 119.0 (CH=), 125.3 (C), 126.4 (CH=), 128.1 (C), 128.9 (CH=), 133.8 (C), 134.2 (C), 137.5 (C), 138.6 (CH=), 141.1 (C), 142.3 (C), 142.4 (C), 156.0 (C), 156.2 (C), 163.9 (C). Anal. calcd (%) for $C_{29}H_{35}BrNO_5P$: C 59.19, H 5.99, N 2.38; found: C 59.24, H 6.03, N 2.33.

L40c. Yield: 257 mg (46%). ^{31}P NMR (C_6D_6), δ: 143.1 (s). ^{1}H NMR (C_6D_6), δ: 0.08 (s, 9H, CH_3-Si), 0.13 (s, 9H, CH_3-Si), 1.15 (d, 3H, CH_3, $^{3}J_{H-H}$= 6.4 Hz), 5.21 (m, 1H, CH-O), 6.5-7.2 (m, 9H, CH=). ^{13}C NMR (C_6D_6), δ: 0.1 (CH_3-Si), 0.3 (CH_3-Si), 23.5 (d, CH_3, J_{C-P}= 3 Hz), 74.1 (d, CH, J_{C-P}= 4 Hz), 118.7 (CH=), 124.8 (CH=), 124.9 (CH=), 126.4 (CH=), 128.2 (C), 128.9 (C), 130.9 (C), 131.0 (C), 131.4 (C), 131.8 (C), 132.3 (CH=), 132.4 (CH=), 135.0 (CH=), 135.2 (CH=), 138.5 (CH=), 141.1 (CH=), 154.2 (C), 154.5 (C), 163.6 (C). Anal. calcd (%) for $C_{28}H_{31}BrNO_3PSi_2$: C 53.56, H 5.57, N 2.50; found: C 53.60, H 5.61, N 2.43.

L41a. Yield: 523 mg (82%). ^{31}P NMR (C_6D_6), δ: 144.6 (s). ^{1}H NMR (C_6D_6), δ: 1.28 (s, 9H, CH_3, ^{t}Bu), 1.29 (s, 9H, CH_3, ^{t}Bu), 1.48 (s, 9H, CH_3, ^{t}Bu), 1.51 (s, 9H, CH_3, ^{t}Bu), 1.64 (d, 3H, CH_3, J_{H-H}= 6.8 Hz), 5.78 (m, 1H, CH-O), 7.0-8.1 (m, 12H, CH=). ^{13}C NMR (C_6D_6), δ: 24.4 (d, CH_3, J_{C-P}= 3.8 Hz), 31.6 (CH_3, ^{t}Bu), 31.9 (CH_3, ^{t}Bu), 35.8 (C, ^{t}Bu), 35.9 (C, ^{t}Bu), 76.4 (d, CH, J_{C-P}= 10.7 Hz), 119.1 (CH=), 119.4 (CH=), 124.6 (CH=), 124.7 (CH=), 125.8 (C), 127.4 (CH=), 127.5 (CH=), 127.7 (CH=), 127.8 (CH=), 128.8 (C), 129.1 (CH=), 129.2 (CH=), 129.4 (CH=), 130.1 (C), 133.8 (C),

134.2 (C), 137.7 (CH=), 139.9 (C), 140.9 (C), 141.0 (C), 146.8 (C), 147.1 (C), 156.7 (C), 162.9 (C). Anal. calcd (%) for $C_{41}H_{52}NO_3P$: C 77.21, H 8.22, N 2.20; found: C 77.29, H 8.24, N 2.15.

L41b. Yield: 526 mg (90%). ^{31}P NMR (C_6D_6), δ: 143.8 (s). ^{1}H NMR (C_6D_6), δ: 1.37 (s, 9H, CH_3, ^{t}Bu), 1.38 (s, 9H, CH_3, ^{t}Bu), 1.62 (d, 3H, CH_3, $^2J_{H-H}$= 6.4 Hz), 3.29 (s, 6H, CH_3-O), 5.74 (m, 1H, CH-O), 6.6-8.1 (m, 12H, CH=). ^{13}C NMR (C_6D_6), δ: 24.9 (d, CH_3, J_{C-P}= 3.8 Hz), 31.7 (CH_3, ^{t}Bu), 31.8 (CH_3, ^{t}Bu), 36.2 (C, ^{t}Bu), 55.8 (CH_3-O), 76.8 (d, CH, J_{C-P}= 9.2 Hz), 113.9 (CH=), 114.0 (CH=), 115.4 (CH=), 115.5 (CH=), 119.5 (CH=), 119.8 (CH=), 127.9 (CH=), 128.0 (CH=), 129.8 (CH=), 129.9 (CH=), 129.4 (CH=), 134.3 (C), 134.4 (C), 135.2 (C), 135.3 (C), 138.1 (CH=), 140.1 (C), 142.8 (C), 142.9 (C), 143.3 (C), 143.5 (C), 156.9 (C), 157.1 (C), 163.3 (C). Anal. calcd (%) for $C_{35}H_{40}NO_5P$: C 71.78, H 6.88, N 2.39; found: C 71.83, H 6.90, N 2.35.

L41c. Yield: 456 mg (82%). ^{31}P NMR (C_6D_6), δ: 143.6 (s). ^{1}H NMR (C_6D_6), δ: 0.22 (s, 9H, CH_3-Si), 0.30 (s, 9H, CH_3-Si), 1.57 (d, 3H, CH_3, $^3J_{H-H}$= 6 Hz), 5.67 (m, 1H, CH-O), 6.9-8.0 (m, 14H, CH=). ^{13}C NMR (C_6D_6), δ: 0.0 (CH_3-Si), 0.2 (CH_3-Si), 24.0 (d, CH_3, J_{C-P}= 3.1 Hz), 75.3 (d, CH, J_{C-P}= 3.8 Hz), 118.5 (CH=), 118.6 (CH=), 124.6 (CH=), 124.8 (CH=), 125.3 (C), 126.9 (CH=), 127.0 (CH=), 128.4 (CH=), 128.8 (CH=), 131.1 (C), 131.4 (C), 131.7 (C), 131.9 (C), 132.3 (CH=), 135.0 (CH=), 135.1 (CH=), 137.1 (CH=), 139.1 (CH=), 154.3 (C), 154.4 (C), 154.7 (C), 154.8 (C), 155.9 (C), 162.0 (C). Anal. calcd (%) for $C_{31}H_{36}NO_3PSi_2$: C 66.75, H 6.51, N 2.51; found: C 66.81, H 6.54, N 2.47.

L42a. Yield: 326 mg (54%). ^{31}P NMR (C_6D_6), δ: 148.3 (s). ^{1}H NMR (C_6D_6), δ: 1.05 (s, 9H, CH_3, ^{t}Bu), 1.24 (s, 9H, CH_3, ^{t}Bu), 1.27 (s, 9H, CH_3, ^{t}Bu), 1.43 (s, 9H, CH_3, ^{t}Bu), 1.68 (s, 9H, CH_3, ^{t}Bu), 5.44 (d, 1H, CH-O, J_{H-P}= 10 Hz), 6.56 (m, 1H, CH=), 6.98 (m, 2H, CH=), 7.31 (m, 2H, CH=), 7.54 (d, 1H, CH=, $^3J_{H-H}$= 6.4 Hz) , 7.62 (d, 1H, CH=, $^3J_{H-H}$= 6.4 Hz) , 8.37 (m, 1H, CH=). ^{13}C NMR (C_6D_6), δ: 26.9 (CH_3, ^{t}Bu), 31.3 (d, CH_3, ^{t}Bu, J_{C-P}= 4.6 Hz), 32.5 (CH_3, ^{t}Bu), 35.0 (C, ^{t}Bu), 35.5 (C, ^{t}Bu), 36.2 (C, ^{t}Bu), 85.8 (d, CH, J_{C-P}= 10.2 Hz), 120.4 (CH=), 122.1 (CH=), 123.6 (CH=), 126.0 (C), 128.4 (CH=), 128.8 (C), 129.6 (C), 131.7 (d, C, J_{C-P}= 2.9 Hz), 132.7 (C), 135.2 (CH=), 135.3 (C), 138.5 (C), 138.8 (C), 145.4 (d, C, J_{C-P}= 2.2 Hz), 146.6 (C), 147.8 (CH=), 160.3 (C). Anal. calcd (%) for $C_{38}H_{54}NO_3P$: C 75.59, H 9.01, N 2.32; found: C 75.63, H 8.99, N 2.39.

L42d. Yield: 334 mg (61%). ^{31}P NMR (C_6D_6), δ: 142.6 (s). ^{1}H NMR (C_6D_6), δ: 1.08 (s, 9H, CH_3, ^{t}Bu), 1.38 (s, 9H, CH_3, ^{t}Bu), 1.60 (s, 3H, CH_3-Ar), 1.66 (s, 3H, CH_3-Ar), 1.72 (s, 9H, CH_3, ^{t}Bu), 2.00 (s, 3H, CH_3-Ar), 2.09 (s, 3H, CH_3-Ar), 5.40 (d, 1H, CH-O, J_{H-P}= 10.4 Hz), 6.52 (m, 1H, CH=), 6.73 (m, 1H, CH=), 7.04 (m, 1H, CH=), 7.15 (m, 2H, CH=), 7.28 (s, 1H, CH=), 8.34 (m, 1H, CH=). ^{13}C NMR (C_6D_6), δ: 16.8 (CH_3-Ar), 17.0 (CH_3-Ar), 20.6 (CH_3-Ar), 20.8 (CH_3-Ar), 26.7 (CH_3, ^{t}Bu), 31.5 (d, CH_3, ^{t}Bu, J_{C-P}= 4.6 Hz), 32.3 (CH_3, ^{t}Bu), 35.0 (C, ^{t}Bu), 35.5 (C, ^{t}Bu), 36.7 (C, ^{t}Bu), 85.5 (d, CH, J_{C-P}= 10.7 Hz), 122.1 (CH=), 123.6 (CH=), 126.0 (C), 128.8 (C), 129.6 (C), 131.7 (d, C, J_{C-P}= 2.9 Hz), 132.7 (C), 135.0 (C), 135.2 (CH=), 135.6 (C), 138.1 (C), 138.7 (C), 145.9 (d, C, J_{C-P}= 2.3 Hz), 146.6 (d, C, J_{C-P}= 7.6 Hz), 147.8 (CH=), 160.4 (C). Anal. calcd (%) for $C_{34}H_{46}NO_3P$: C 74.56, H 8.47, N 2.56; found: C 74.62, H 8.49, N 2.52.

L43a. Yield: 393 mg (63%). ^{31}P NMR (C_6D_6), δ: 141.0 (s). ^{1}H NMR (C_6D_6), δ: 1.28 (s, 9H, CH_3, ^{t}Bu), 1.31 (s, 9H, CH_3, ^{t}Bu), 1.33 (s, 9H, CH_3, ^{t}Bu), 1.34 (s, 9H, CH_3, ^{t}Bu), 6.46 (m, 1H, CH=), 6.60 (d, 1H, CH-O, J_{H-P}= 10 Hz), 7.0-7.2 (m, 4H, CH=), 7.35 (m, 4H, CH=), 7.44 (d, 1H, CH=, $^3J_{H-H}$= 8.0 Hz) , 7.55 (m, 2H, CH=), 8.23 (m, 1H, CH=). ^{13}C NMR (C_6D_6), δ: 31.3 (d, CH_3, ^{t}Bu, J_{C-P}= 4.5 Hz), 32.7 (CH_3, ^{t}Bu), 35.0 (C, ^{t}Bu), 35.5 (C, ^{t}Bu), 85.4 (d, CH, J_{C-P}= 8.1 Hz), 120.4 (CH=), 120.3 (CH=), 122.1 (CH=), 123.6 (CH=), 125.4 (CH=), 126.0 (C), 128.8 (CH=), 129.6 (C), 129.6 (C),

131.7 (d, C, $J_{C\text{-}P}$= 2.9 Hz), 132.7 (C), 132.6 (C), 132.9 (CH=), 133.1 (CH=), 135.7 (CH=), 135.9 (CH=), 136.9 (CH=), 141.1 (C), 141.2 (C), 142.7 (C), 148.3 (CH=), 154.3 (C), 154.4 (C), 164.1 (C). Anal. calcd (%) for $C_{40}H_{50}NO_3P$: C 77.07, H 8.08, N 2.25; found: C 77.16, H 8.09, N 2.19.

L43c. Yield: 321 mg (59%). ^{31}P NMR (C_6D_6), δ: 141.5 (s). ^{1}H NMR (C_6D_6), δ: 0.16 (s, 9H, CH_3-Si), 0.17 (s, 9H, CH_3-Si), 6.46 (m, 1H, CH=), 6.53 (d, 1H, CH-O, $J_{H\text{-}P}$= 10 Hz), 6.9-7.4 (m, 13H, CH=), 8.23 (m, 1H, CH=). ^{13}C NMR (C_6D_6), δ: 0.2 (CH_3-Si), 81.4 (CH), 120.7 (CH=), 122.5 (CH=), 125.4 (CH=), 125.7 (C), 128.8 (CH=), 129.6 (C), 131.3 (d, C, $J_{C\text{-}P}$= 2.9 Hz), 132.0 (C), 132.6 (C), 132.9 (CH=), 133.1 (CH=), 135.7 (CH=), 135.9 (CH=), 136.7 (CH=), 141.5 (C), 141.6 (C), 141.7 (C), 149.5 (CH=), 154.3 (C), 154.3 (C), 154.5 (C), 162.3 (C). Anal. calcd (%) for $C_{30}H_{34}NO_3PSi_2$: C 66.27, H 6.30, N 2.58; found: C 66.32, H 6.33, N 2.56.

L43d. Yield: 295 mg (52%). ^{31}P NMR (C_6D_6), δ: 137.9 (s). ^{1}H NMR (C_6D_6), δ: 1.35 (s, 9H, CH_3, ^{t}Bu), 1.39 (s, 9H, CH_3, ^{t}Bu), 1.70 (s, 3H, CH_3-Ar), 1.81 (s, 3H, CH_3-Ar), 2.04 (s, 3H, CH_3-Ar), 2.13 (s, 3H, CH_3-Ar), 6.39 (d, 1H, CH-O, $J_{C\text{-}P}$= 7.2 Hz), 6.48 (m, 1H, CH=), 6.9-7.2 (m, 6H, CH=), 7.44 (m, 3H, CH=), 8.28 (m, 1H, CH=). ^{13}C NMR (C_6D_6), δ: 16.1 (CH_3-Ar), 16.4 (CH_3-Ar), 20.0 (CH_3-Ar), 20.1 (CH_3-Ar), 30.8 (d, CH_3, ^{t}Bu, $J_{C\text{-}P}$= 5.4 Hz), 31.9 (CH_3, ^{t}Bu), 34.2 (C, ^{t}Bu), 34.6 (C, ^{t}Bu), 81.1 (d, CH, $J_{C\text{-}P}$= 11.9 Hz), 120.7 (CH=), 121.7 (CH=), 125.2 (CH=), 127.4 (CH=), 128.1 (CH=), 128.9 (CH=), 130.9 (C), 131.5 (C), 132.1 (d, C, $J_{C\text{-}P}$= 5.4 Hz), 132.3 (C), 134.3 (C), 134.9 (C), 135.9 (CH=), 137.4 (C), 138.0 (C), 141.7 (d, C, $J_{C\text{-}P}$= 4.6 Hz), 145.4 (C), 145.6 (C), 148.6 (CH=), 161.5 (C). Anal. calcd (%) for $C_{36}H_{42}NO_3P$: C 76.16, H 7.46, N 2.47; found: C 76.21, H 7.43, N 2.49.

L43e. Yield: 392 mg (69%). ^{31}P NMR (C_6D_6), δ: 137.4 (s). ^{1}H NMR (C_6D_6), δ: 1.32 (s, 9H, CH_3, ^{t}Bu), 1.43 (s, 9H, CH_3, ^{t}Bu), 1.71 (s, 3H, CH_3-Ar), 1.81 (s, 3H, CH_3-Ar), 2.04 (s, 3H, CH_3-Ar), 2.09 (s, 3H, CH_3-Ar), 6.42 (d, 1H, CH-O, $J_{C\text{-}P}$= 8.0 Hz), 6.49 (m, 1H, CH=), 6.9-7.2 (m, 6H, CH=), 7.46 (m, 3H, CH=), 8.33 (m, 1H, CH=). ^{13}C NMR (C_6D_6), δ: 16.1 (CH_3-Ar), 16.6 (CH_3-Ar), 20.0 (CH_3-Ar), 30.9 (d, CH_3, ^{t}Bu, $J_{C\text{-}P}$= 4.2 Hz), 33.1(CH_3, ^{t}Bu), 34.9 (C, ^{t}Bu), 35.5(C, ^{t}Bu), 81.9 (d, CH, $J_{C\text{-}P}$= 7.6 Hz), 120.9 (CH=), 121.3 (CH=), 125.7 (CH=), 127.3(CH=), 128.8 (CH=), 128.9 (CH=), 130.1 (C), 131.8 (C), 132.2 (d, C, $J_{C\text{-}P}$= 3.1 Hz), 132.7 (C), 134.7 (C), 135.2 (C), 135.4 (CH=), 137.9 (C), 138.0 (C), 141.5 (C), 145.2 (C), 145.5 (C), 148.9 (CH=), 162.3 (C). Anal. calcd (%) for $C_{36}H_{42}NO_3P$: C 76.16, H 7.46, N 2.47; found: C 76.22, H 7.47, N 2.38.

L44a. Yield: 303 mg (49%). ^{31}P NMR (C_6D_6), δ: 148.6 (s). ^{1}H NMR (C_6D_6), δ: 1.07 (s, 9H, CH_3, ^{t}Bu), 1.24 (s, 9H, CH_3, ^{t}Bu), 1.27 (s, 9H, CH_3, ^{t}Bu), 1.44 (s, 9H, CH_3, ^{t}Bu), 1.67 (s, 9H, CH_3, ^{t}Bu), 2.38 (s, 3H, CH_3-Py), 5.41 (d, 1H, CH-O, $J_{H\text{-}P}$= 10 Hz), 6.53 (m, 1H, CH=), 6.9-7.2 (m, 2H, CH=), 7.30 (d, 1H, CH=, $^{3}J_{H\text{-}H}$= 2.4 Hz), 7.33 (d, 1H, CH=, $^{3}J_{H\text{-}H}$= 2.4 Hz), 7.54 (d, 1H, CH=, $^{3}J_{H\text{-}H}$= 2.4 Hz), 7.62 (d, 1H, CH=, $^{3}J_{H\text{-}H}$= 2.4 Hz). ^{13}C NMR (C_6D_6), δ: 24.0 (CH_3-Py), 26.0 (CH_3, ^{t}Bu), 30.7 (d, CH_3, ^{t}Bu, $J_{C\text{-}P}$= 4.6 Hz), 31.3 (CH_3, ^{t}Bu), 34.2 (C, ^{t}Bu), 35.1 (C, ^{t}Bu), 35.4 (C, ^{t}Bu), 85.5 (d, CH, $J_{C\text{-}P}$= 11.4 Hz), 119.9 (CH=), 121.2 (CH=), 123.8 (CH=), 125.3 (C), 126.6 (CH=), 127.0 (CH=), 128.1 (C), 128.9 (C), 131.3 (C), 133.7 (C), 135.3 (CH=), 140.1 (C), 140.4 (C), 145.8 (C), 146.3 (C), 155.9 (CH=), 158.9 (C). Anal. calcd (%) for $C_{39}H_{56}NO_3P$: C 75.82, H 9.14, N 2.27; found: C 75.86, H 9.16, N 2.24.

L44d. Yield: 354 mg (63%). ^{31}P NMR (C_6D_6), δ: 142.6 (s). ^{1}H NMR (C_6D_6), δ: 1.09 (s, 9H, CH_3, ^{t}Bu), 1.32 (s, 9H, CH_3, ^{t}Bu), 1.67 (s, 3H, CH_3-Ar), 1.69 (s, 3H, CH_3-Ar), 1.77 (s, 9H, CH_3, ^{t}Bu), 2.03 (s, 3H, CH_3-Ar), 2.15 (s, 3H, CH_3-Ar), 2.38 (s, 3H, CH_3-Py), 5.38 (d, 1H, CH-O, $J_{H\text{-}P}$= 10.4 Hz), 6.55 (m, 1H, CH=), 6.9-7.6 (m, 4H, CH=). ^{13}C NMR (C_6D_6), δ: 16.9 (CH_3-Ar), 17.2 (CH_3-

Ar), 20.2 (CH_3-Ar), 20.6 (CH_3-Ar), 26.7 (CH_3, ^{t}Bu), 31.5 (d, CH_3, ^{t}Bu, J_{C-P}= 4.6 Hz), 32.8 (CH_3, ^{t}Bu), 35.4 (C, ^{t}Bu), 35.7 (C, ^{t}Bu), 36.7 (C, ^{t}Bu), 85.2 (d, CH, J_{C-P}= 8.6 Hz), 122.0(CH=), 123.6 (CH=), 126.2 (C), 127.4 (CH=), 128.9 (C), 129.6 (C), 131.7 (d, C, J_{C-P}= 2.9 Hz), 132.7 (C), 135.0 (C), 135.2 (CH=), 135.6 (C), 138.2 (C), 138.7 (C), 145.9 (d, C, J_{C-P}= 2.8 Hz), 146.7 (d, C, J_{C-P}= 4.9 Hz), 147.5 (CH=), 160.2 (C). Anal. calcd (%) for $C_{35}H_{48}NO_3P$: C 74.84, H 8.61, N 2.49; found: C 74.87, H 8.62, N 2.44.

L45a. Yield: 250 mg (41%). ^{31}P NMR (C_6D_6), δ: 145.4 (s). ^{1}H NMR (C_6D_6), δ: 1.24 (s, 9H, CH_3, ^{t}Bu), 1.25 (s, 9H, CH_3, ^{t}Bu), 1.37 (s, 9H, CH_3, ^{t}Bu), 1.42 (s, 9H, CH_3, ^{t}Bu), 1.59 (d, 3H, CH_3, $^3J_{H-H}$= 6.4 Hz), 5.85 (m, 1H, CH-O), 6.9-8.2 (m, 10H, CH=). ^{13}C NMR (C_6D_6), δ: 24.0 (d, CH_3, J_{C-P}= 3.8 Hz), 31.3 (CH_3, ^{t}Bu), 31.5 (CH_3, ^{t}Bu), 34.5 (C, ^{t}Bu), 35.6 (C, ^{t}Bu), 76.0 (d, CH, J_{C-P}= 10.0 Hz), 113.4 (CH=), 113.5 (CH=), 114.3 (CH=), 118.3 (CH=), 125.7 (C), 126.1 (CH=), 127.9 (CH=), 128.9 (CH=), 129.5 (C), 129.7 (CH=), 130.2 (CH=), 132.8 (C), 133.4 (C), 133.2 (C), 134.1 (C), 136.9 (CH=), 142.9 (C), 142.7 (C), 148.8 (C), 163.4 (C). Anal. calcd (%) for $C_{39}H_{50}NO_3P$: C 76.56, H 8.24, N 2.29; found: C 76.61, H 8.26, N 2.21.

L45b. Yield: 285 mg (51%). ^{31}P NMR (C_6D_6), δ: 144.7 (s). ^{1}H NMR (C_6D_6), δ: 1.32 (s, 9H, CH_3, ^{t}Bu), 1.33 (s, 9H, CH_3, ^{t}Bu), 1.63 (d, 3H, CH_3, $^3J_{H-H}$= 6.4 Hz), 3.29 (s, 6H, CH_3-O), 5.87 (m, 1H, CH-O), 6.5-8.2 (m, 10H, CH=). ^{13}C NMR (C_6D_6), δ: 23.9 (d, CH_3, J_{C-P}= 3.8 Hz), 30.9 (CH_3, ^{t}Bu), 31.0 (CH_3, ^{t}Bu), 35.3 (C, ^{t}Bu), 55.0 (CH_3-O), 76.5 (d, CH, J_{C-P}= 9.9 Hz), 113.1 (CH=), 113.3 (CH=), 114.7 (CH=), 118.7 (CH=), 125.6 (C), 126.3 (CH=), 128.1 (CH=), 128.4 (CH=), 129.1 (C), 129.4 (CH=), 129.8 (CH=), 133.5 (C), 134.6 (C), 136.7 (CH=), 142.5 (C), 142.6 (C), 147.8 (C), 156.1 (C), 156.3 (C), 163.5 (C). Anal. calcd (%) for $C_{33}H_{38}NO_5P$: C 70.82, H 6.84, N 2.50; found: C 70.91, H 6.86, N 2.45.

L45c. Yield: 380 mg (72%). ^{31}P NMR (C_6D_6), δ: 144.4 (s). ^{1}H NMR (C_6D_6), δ: 0.18 (s, 9H, CH_3-Si), 0.27 (s, 9H, CH_3-Si), 1.58 (d, 3H, CH_3, $^3J_{H-H}$= 6.8 Hz), 5.79 (m, 1H, CH-O), 6.9-8.2 (m, 12H, CH=). ^{13}C NMR (C_6D_6), δ: 0.1 (CH_3-Si), 0.2 (CH_3-Si), 24.0 (CH_3), 76.1 (CH), 118.4 (CH=), 124.9 (CH=), 125.1 (CH=), 125.3 (C), 125.4 (C), 126.3 (CH=), 127.5 (CH=), 127.7 (CH=), 128.2 (CH=), 131.4 (C), 131.7 (CH=), 132.0 (C), 132.6 (C), 135.3 (CH=), 136.7 (CH=), 137.7 (C), 143.8 (C), 147.8 (C), 154.3 (C), 154.9 (C), 162.5 (C). Anal. calcd (%) for $C_{29}H_{34}NO_3PSi_2$: C 65.51, H 6.44, N 2.63; found: C 65.59, H 6.45, N 2.57.

L46a. Yield: 376 mg (67%). ^{31}P NMR (C_6D_6), δ: 144.6 (s). ^{1}H NMR (C_6D_6), δ: 1.22 (s, 9H, CH_3, ^{t}Bu), 1.26 (s, 9H, CH_3, ^{t}Bu), 1.42 (s, 9H, CH_3, ^{t}Bu), 1.49 (s, 9H, CH_3, ^{t}Bu), 1.52 (d, 3H, CH_3, $^3J_{H-H}$= 6.4 Hz), 5.63 (m, 1H, CH-O), 6.5-8.4 (m, 8H, CH=). ^{13}C NMR (C_6D_6), δ: 24.5 (d, CH_3, J_{C-P}= 4.2 Hz), 31.0 (CH_3, ^{t}Bu), 31.3 (CH_3, ^{t}Bu), 34.5 (C, ^{t}Bu), 35.3 (C, ^{t}Bu), 75.3 (d, CH, J_{C-P}= 9.9 Hz), 120.6 (CH=), 122.3 (CH=), 124.5 (CH=), 124.7 (CH=), 125.3 (C), 126.7 (CH=), 128.3 (CH=), 129.1 (C), 133.3 (C), 133.5 (C), 136.2 (CH=), 137.9 (C), 140.3 (C), 140.6 (C), 146.1 (C), 146.5 (C), 148.2 (CH=), 162.3 (C). Anal. calcd (%) for $C_{35}H_{48}NO_3P$: C 74.84, H 8.61, N 2.49; found: C 74.87, H 8.62, N 2.45.

L46d. Yield: 292 mg (58%). ^{31}P NMR (C_6D_6), δ: 140.2 (s). ^{1}H NMR (C_6D_6), δ: 1.36 (s, 9H, CH_3, ^{t}Bu), 1.52 (s, 9H, CH_3, ^{t}Bu), 1.57 (d, 3H, CH_3, $^3J_{H-H}$= 6.4 Hz), 1.64 (s, 3H, CH_3-Ar), 1.71 (s, 3H, CH_3-Ar), 2.01 (s, 3H, CH_3-Ar), 2.05 (s, 3H, CH_3-Ar), 5.54 (m, 1H, CH-O), 6.55 (m, 1H, CH=), 6.9-7.2 (m, 4H, CH=), 8.32 (m, 1H, CH=). ^{13}C NMR (C_6D_6), δ: 16.9 (CH_3-Ar), 17.1 (CH_3-Ar), 20.7 (CH_3-Ar), 24.8 (d, CH_3, J_{C-P}= 3.4 Hz), 31.9 (d, CH_3, ^{t}Bu, J_{C-P}= 4.0 Hz), 32.4 (CH_3, ^{t}Bu), 35.1 (C, ^{t}Bu), 35.4 (C, ^{t}Bu), 76.1 (d, CH, J_{C-P}= 7.3 Hz), 120.6 (CH=), 122.8 (CH=), 126.1 (C), 128.4 (CH=),

128.9 (CH=), 129.6 (C), 131.9 (d, C, J_{C-P}= 2.8 Hz), 132.6 (C), 132.8 (d, C, J_{C-P}= 4.6 Hz), 132.8 (CH=), 135.1 (C), 135.4 (C), 136.6 (CH=), 138.1 (C), 138.9 (d, C, J_{C-P}= 2.4 Hz), 146.0 (C), 146.2 (C), 146.5 (C), 149.6 (CH=), 161.9 (d, C, J_{C-P}= 4.0 Hz). Anal. calcd (%) for $C_{31}H_{40}NO_3P$: C 73.64, H 6.24, N 2.41; found: C 73.69, H 6.25, N 2.38.

L46e. Yield: 318 mg (63%). ^{31}P NMR (C_6D_6), δ: 136.9 (s). ^{1}H NMR (C_6D_6), δ: 1.39 (s, 9H, CH_3, ^{t}Bu), 1.49 (d, 3H, CH_3, $^3J_{H-H}$= 6.4 Hz), 1.53 (s, 9H, CH_3, ^{t}Bu), 1.69 (s, 3H, CH_3-Ar), 1.76 (s, 3H, CH_3-Ar), 2.03 (s, 3H, CH_3-Ar), 2.15 (s, 3H, CH_3-Ar), 5.49 (m, 1H, CH-O), 6.54 (m, 1H, CH=), 6.9-7.2 (m, 4H, CH=), 8.31 (m, 1H, CH=). ^{13}C NMR (C_6D_6), δ: 16.9 (CH_3-Ar), 17.3(CH_3-Ar), 20.3 (CH_3-Ar), 20.5 (CH_3-Ar), 24.7 (d, CH_3, J_{C-P}= 6.1 Hz), 31.9 (d, CH_3, ^{t}Bu, J_{C-P}= 4.3 Hz), 32.6 (CH_3, ^{t}Bu), 35.4 (C, ^{t}Bu), 35.6 (C, ^{t}Bu), 76.0 (d, CH, J_{C-P}= 16.3 Hz), 120.8 (CH=), 122.2 (CH=), 126.3 (C), 128.5 (CH=), 128.6 (CH=), 129.2 (C), 133.2 (d, C, J_{C-P}= 3.6 Hz), 133.7 (C), 133.9 (C), 134.2 (CH=), 135.5 (C), 136.8 (C), 138.2 (C), 138.9 (C), 146.8 (C), 146.9 (C), 149.2 (CH=), 162.8 (C). Anal. calcd (%) for $C_{31}H_{40}NO_3P$: C 73.64, H 6.24, N 2.41; found: C 73.71, H 6.26, N 2.34.

L46f. Yield: 320 mg (55%). ^{31}P NMR (C_6D_6), δ: 143.6 (s). ^{1}H NMR (C_6D_6), δ: 0.37 (s, 9H, CH_3-Si), 0.50 (s, 9H, CH_3-Si), 1.41 (d, 3H, CH_3, $^3J_{H-H}$= 6.4 Hz), 4.96 (m, 1H, CH-O), 6.54 (m, 1H, CH=), 6.86 (m, 2H, CH=), 7.01 (m, 1H, CH=), 7.12 (m, 3H, CH=), 7.28 (m, 2H, CH=), 7.73 (m, 2H, CH=), 8.07 (s, 1H, CH=), 8.17 (s, 1H, CH=), 8.29 (m, 1H, CH=). ^{13}C NMR (C_6D_6), δ: 0.2 (d, CH_3-Si, J_{C-P}= 5.4 Hz), 0.7 (CH_3-Si), 24.1 (d, CH_3, J_{C-P}= 3.0 Hz), 76.1 (CH), 120.2 (CH=), 122.5 (CH=), 122.7 (d, C, J_{C-P}= 2.3 Hz), 123.8 (d, C, J_{C-P}= 5.1 Hz), 125.3 (CH=), 125.6 (CH=), 126.0 (CH=), 127.3 (CH=), 127.4 (CH=), 127.5.7 (CH=), 128.8 (CH=), 128.9 (CH=), 129.0 (CH=), 129.6 (CH=), 131.5 (C), 131.9 (C), 132.9 (C), 133.1 (C), 134.9 (C), 135.1 (C), 136.6 (CH=), 137.3 (C), 137.8 (CH=), 138.2 (C), 149.4 (CH=), 153.0 (d, C, J_{C-P}= 4.6 Hz), 163.0 (d, C, J_{C-P}= 3.8 Hz). Anal. calcd (%) for $C_{33}H_{36}NO_3PSi_2$: C 68.13, H 6.24, N 2.41; found: C 68.19, H 6.25, N 2.35.

L46g. Yield: 285 mg (49%). ^{31}P NMR (C_6D_6), δ: 146.2 (s). ^{1}H NMR (C_6D_6), δ: 0.41 (s, 9H, CH_3-Si), 0.45 (s, 9H, CH_3-Si), 1.63 (d, 3H, CH_3, $^3J_{H-H}$= 6.4 Hz), 5.56 (m, 1H, CH-O), 6.49 (m, 1H, CH=), 6.74 (m, 1H, CH=), 6.9-7.2 (m, 5H, CH=), 7.33 (m, 2H, CH=), 7.75 (m, 2H, CH=), 8.13 (s, 1H, CH=), 8.16 (s, 1H, CH=), 8.32 (m, 1H, CH=). ^{13}C NMR (C_6D_6), δ: 0.0 (d, CH_3-Si, J_{C-P}= 4.6 Hz), 0.4 (CH_3-Si), 24.6 (d, CH_3, J_{C-P}= 3.8 Hz), 75.5 (d, CH, J_{C-P}= 7.8 Hz), 120.9 (CH=), 122.5 (CH=), 123.1 (d, C, J_{C-P}= 3.0 Hz), 124.0 (d, C, J_{C-P}= 4.8 Hz), 125.4 (CH=), 125.5 (CH=), 126.0 (C), 127.2 (CH=), 127.3 (CH=), 127.5 (CH=), 127.6 (CH=), 128.8 (CH=), 128.9 (CH=), 129.1 (CH=), 129.6 (CH=), 131.5 (C), 131.9 (C), 133.0 (d, C, J_{C-P}= 2.1 Hz), 133.2 (C), 134.8 (C), 135.1 (C), 136.4 (CH=), 137.5 (C), 137.8 (CH=), 138.1 (C), 149.1 (CH=), 152.6 (C), 153.2 (C), 162.6 (C). Anal. calcd (%) for $C_{33}H_{36}NO_3PSi_2$: C 68.13, H 6.24, N 2.41; found: C 68.21, H 6.27, N 2.34.

L47a. Yield: 403 mg (70%). ^{31}P NMR (C_6D_6), δ: 145.3 (s). ^{1}H NMR (C_6D_6), δ: 1.22 (s, 9H, CH_3, ^{t}Bu), 1.26 (s, 9H, CH_3, ^{t}Bu), 1.41 (s, 9H, CH_3, ^{t}Bu), 1.45 (s, 9H, CH_3, ^{t}Bu), 1.54 (d, 3H, CH_3, $^3J_{H-H}$= 7.0 Hz), 2.32 (s, 3H, CH_3), 5.67 (m, 1H, CH-O), 6.5-7.6 (m, 7H, CH=). ^{13}C NMR (C_6D_6), δ: 24.3 (d, CH_3, J_{C-P}= 3.8 Hz), 24.8 (CH_3-Py), 31.9 (CH_3, ^{t}Bu), 32.2 (CH_3, ^{t}Bu), 35.1 (C, ^{t}Bu), 35.7 (C, ^{t}Bu), 76.7 (d, CH, J_{C-P}= 10.2 Hz), 118.3 (CH=), 121.7 (CH=), 124.3 (CH=), 124.9 (C), 125.7 (C), 126.9 (CH=), 127.2 (CH=), 128.8 (C), 130.2 (C), 133.5 (C), 134.2 (C), 137.0 (CH=), 140.3 (C), 140.6 (C), 146.3 (C), 147.0 (C), 157.9 (C), 162.5(C). Anal. calcd (%) for $C_{36}H_{50}NO_3P$: C 75.10, H 8.75, N 2.43; found: C 75.18, H 8.78, N 2.38.

L47e. Yield: 354 mg (68%). ^{31}P NMR (C_6D_6), δ: 138.5 (s). ^{1}H NMR (C_6D_6), δ: 1.43 (s, 9H, CH_3, ^{t}Bu), 1.54 (s, 9H, CH_3, ^{t}Bu), 1.64 (d, 3H, CH_3, $^3J_{H-H}$= 6.4 Hz), 1.72 (s, 3H, CH_3-Ar), 1.75 (s,

3H, CH_3-Ar), 2.05 (s, 3H, CH_3-Ar), 2.09 (s, 3H, CH_3-Ar), 2.35 (s, 3H CH_3-Py), 5.61 (m, 1H, CH-O), 6.54 (m, 1H, CH=), 6.9-7.2 (m, 4H, CH=). ^{13}C NMR (C_6D_6), δ: 16.7 (CH_3-Ar), 17.0 (CH_3-Ar), 20.5 (CH_3-Ar), 20.6 (CH_3-Ar), 24.4 (d, CH_3, J_{C-P}= 4.0 Hz), 24.8 (CH_3-Py), 31.9 (d, CH_3, ^{t}Bu, J_{C-P}= 5.3 Hz), 32.3 (CH_3, ^{t}Bu), 35.4 (C, ^{t}Bu), 35.6 (C, ^{t}Bu), 76.2 (d, CH, J_{C-P}= 16.4 Hz), 118.0 (CH=), 122.1 (CH=), 125.8 (C), 128.9 (CH=), 129.2 (CH=), 131.3 (d, C, J_{C-P}= 3.0 Hz), 132.1 (C), 132.6 (C), 133.3 (d, C, J_{C-P}= 4.3 Hz), 134.6 (C), 135.6 (C), 137.2 (CH=), 137.8 (C), 138.1 (C), 146.1 (C), 146.5 (C), 157.6 (C), 162.4 (C). Anal. calcd (%) for $C_{32}H_{42}NO_3P$: C 73.96, H 8.15, N 2.70; found: C 74.04, H 8.17, N 2.63.

L47f. Yield: 306 mg (59%). ^{31}P NMR (C_6D_6), δ: 143.1 (s). ^{1}H NMR (C_6D_6), δ: 0.25 (s, 9H, CH_3-Si), 0.37 (s, 9H, CH_3-Si), 1.41 (d, 3H, CH_3, $^3J_{H-H}$= 6.4 Hz), 2.29 (s, 3H, CH_3-Py), 5.52 (m, 1H, CH-O), 6.54 (m, 1H, CH=), 6.98 (m, 2H, CH=), 7.03 (m, 2H, CH=), 7.19 (m, 2H, CH=), 7.36 (m, 2H, CH=), 7.68 (m, 2H, CH=), 8.11 (s, 1H, CH=), 8.21 (s, 1H, CH=). ^{13}C NMR (C_6D_6), δ: 0.1 (CH_3-Si), 0.4 (CH_3-Si), 23.4 (CH_3), 24.2 (CH_3-Py), 75.1 (CH), 117.3 (CH=), 121.9 (CH=), 123.4 (C), 124.3 (C), 125.3 (CH=), 125.2 (CH=), 125.9 (C), 127.1 (CH=), 127.2 (CH=), 127.6 (CH=), 128.2 (CH=), 128.7 (CH=), 129.2 (C), 131.2 (C), 131.4 (C), 132.7 (C), 132.9 (C), 134.8 (C), 137.8 (CH=), 137.9 (CH=), 138.4 (CH=), 152.7 (C), 157.1 (C), 162.0 (C). Anal. calcd (%) for $C_{34}H_{38}NO_3PSi_2$: C 68.54, H 6.43, N 2.35; found: C 68.59, H 6.44, N 2.28.

L48a. Yield: 368 mg (61%). ^{31}P NMR (C_6D_6), δ: 143.9 (s). ^{1}H NMR (C_6D_6), δ: 1.11 (s, 9H, CH_3, ^{t}Bu), 1.22 (s, 9H, CH_3, ^{t}Bu), 1.29 (s, 9H, CH_3, ^{t}Bu), 1.41 (s, 9H, CH_3, ^{t}Bu), 1.71 (s, 9H, CH_3, ^{t}Bu), 5.43 (d, 1H, CH-O, J_{H-P}= 10 Hz), 6.59 (m, 1H, CH=), 6.95 (m, 2H, CH=), 7.28 (m, 2H, CH=), 7.56 (d, 1H, CH=, $^3J_{H-H}$= 6.4 Hz) , 7.64 (d, 1H, CH=, $^3J_{H-H}$= 6.4 Hz) , 8.32 (m, 1H, CH=). ^{13}C NMR (C_6D_6), δ: 26.9 (CH_3, ^{t}Bu), 31.1 (d, CH_3, ^{t}Bu, J_{C-P}= 4.6 Hz), 32.4 (CH_3, ^{t}Bu), 35.1 (C, ^{t}Bu), 35.3 (C, ^{t}Bu), 36.1 (C, ^{t}Bu), 85.2 (d, CH, J_{C-P}= 10.7 Hz), 120.8 (CH=), 121.8 (CH=), 122.6 (CH=), 125.1 (C), 127.9 (CH=), 128.1 (C), 129.5 (C), 131.7 (d, C, J_{C-P}= 3.5 Hz), 132.4 (C), 135.1 (CH=), 135.8 (C), 138.2 (C), 138.6(C), 145.2(C), 145.4 (C), 147.2 (CH=), 161.9 (C). Anal. calcd (%) for $C_{38}H_{54}NO_3P$: C 75.59, H 9.01, N 2.32; found: C 75.61, H 9.00, N 2.31.

L48d. Yield: 317 mg (58%). ^{31}P NMR (C_6D_6), δ: 142.1 (s). ^{1}H NMR (C_6D_6), δ: 1.11 (s, 9H, CH_3, ^{t}Bu), 1.36 (s, 9H, CH_3, ^{t}Bu), 1.55 (s, 3H, CH_3-Ar), 1.63 (s, 3H, CH_3-Ar), 1.70 (s, 9H, CH_3, ^{t}Bu), 2.01 (s, 3H, CH_3-Ar), 2.14 (s, 3H, CH_3-Ar), 5.43 (d, 1H, CH-O, J_{H-P}= 10.0 Hz), 6.55 (m, 1H, CH=), 6.83 (m, 1H, CH=), 7.03 (m, 1H, CH=), 7.16 (m, 2H, CH=), 7.31 (s, 1H, CH=), 8.31 (m, 1H, CH=). ^{13}C NMR (C_6D_6), δ: 16.6 (CH_3-Ar), 16.7 (CH_3-Ar), 20.4 (CH_3-Ar), 20.6 (CH_3-Ar), 26.2 (CH_3, ^{t}Bu), 31.0 (CH_3, ^{t}Bu), 31.8 (CH_3, ^{t}Bu), 35.1(C, ^{t}Bu), 35.4 (C, ^{t}Bu), 36.1 (C, ^{t}Bu), 85.1 (d, CH, J_{C-P}= 8.4 Hz), 121.3 (CH=), 123.4 (CH=), 126.5 (C), 129.1 (C), 131.5 (C), 132.4 (C), 134.7 (C), 134.8 (CH=), 135.2 (C), 137.8 (C), 138.4 (C), 145.9 (C), 146.2 (C), 147.1 (CH=), 162.1 (C). Anal. calcd (%) for $C_{34}H_{46}NO_3P$: C 74.56, H 8.47, N 2.56; found: C 74.61, H 8.48, N 2.53.

L48e. Yield: 350 mg (64%). ^{31}P NMR (C_6D_6), δ: 142.6 (s). ^{1}H NMR (C_6D_6), δ: 1.08 (s, 9H, CH_3, ^{t}Bu), 1.38 (s, 9H, CH_3, ^{t}Bu), 1.60 (s, 3H, CH_3-Ar), 1.66 (s, 3H, CH_3-Ar), 1.72 (s, 9H, CH_3, ^{t}Bu), 2.00 (s, 3H, CH_3-Ar), 2.09 (s, 3H, CH_3-Ar), 5.38 (d, 1H, CH-O, J_{H-P}= 10.4 Hz), 6.52 (m, 1H, CH=), 6.78 (m, 1H, CH=), 7.01 (m, 1H, CH=), 7.12 (m, 2H, CH=), 7.28 (s, 1H, CH=), 8.33 (m, 1H, CH=). ^{13}C NMR (C_6D_6), δ: 16.5 (CH_3-Ar), 16.7 (CH_3-Ar), 20.2 (CH_3-Ar), 20.4 (CH_3-Ar), 26.4 (CH_3, ^{t}Bu), 31.2 (CH_3, ^{t}Bu), 31.9 (CH_3, ^{t}Bu), 34.6 (C, ^{t}Bu), 35.0 (C, ^{t}Bu), 36.3 (C, ^{t}Bu), 85.2 (d, CH, J_{C-P}= 10.1 Hz), 121.8 (CH=), 123.3 (CH=), 126.1 (C), 129.3 (C), 131.5 (C), 132.4 (C), 134.7 (C), 134.8

(CH=), 135.3 (C), 137.8 (C), 138.4 (C), 145.4 (C), 146.0 (C), 147.5 (CH=), 160.1 (C). Anal. calcd (%) for $C_{34}H_{46}NO_3P$: C 74.56, H 8.47, N 2.56; found: C 74.69, H 8.49, N 2.49.

L49d. Yield: 403 mg (71%). ^{31}P NMR (C_6D_6), δ: 135.6 (s). ^{1}H NMR (C_6D_6), δ: 1.30 (s, 9H, CH_3, ^{t}Bu), 1.35 (s, 9H, CH_3, ^{t}Bu), 1.69 (s, 3H, CH_3-Ar), 1.83 (s, 3H, CH_3-Ar), 2.04 (s, 3H, CH_3-Ar), 2.16 (s, 3H, CH_3-Ar), 6.3 (d, 1H, CH-O, J_{H-P}= 10.4 Hz), 6.46 (m, 1H, CH=), 6.9-7.4 (m, 9H, CH=), 8.25 (m, 1H, CH=). ^{13}C NMR (C_6D_6), δ: 16.8 (CH_3-Ar), 17.1 (CH_3-Ar), 20.7 (CH_3-Ar), 31.5 (d, CH_3, ^{t}Bu, J_{C-P}= 6.1 Hz), 31.8 (CH_3, ^{t}Bu), 34.9 (C, ^{t}Bu), 35.2 (C, ^{t}Bu), 81.8 (d, CH, J_{C-P}= 6.2 Hz), 126.0 (CH=), 128.2 (CH=), 128.7 (CH=), 128.8 (C), 128.9 (C), 129.6 (C), 131.8 (d, C, J_{C-P}= 3.1 Hz), 132.2 (C), 132.6 (d, C, J_{C-P}= 4.5 Hz), 132.9 (C), 135.3 (C), 135.6 (C), 136.6 (CH=), 138.2 (C), 138.7 (C), 141.9 (C), 146.2 (d, C, J_{C-P}= 4.6 Hz), 149.4 (CH=), 162.7 (d, C, J_{C-P}= 4.6 Hz). Anal. calcd (%) for $C_{36}H_{42}NO_3P$: C 76.16, H 7.46, N 2.47; found: C 76.24, H 7.44, N 2.41.

L49e. Yield: 278 mg (49%). ^{31}P NMR (C_6D_6), δ: 137.1 (s). ^{1}H NMR (C_6D_6), δ: 1.24 (s, 9H, CH_3, ^{t}Bu), 1.41 (s, 9H, CH_3, ^{t}Bu), 1.67 (s, 3H, CH_3-Ar), 1.77 (s, 3H, CH_3-Ar), 2.01 (s, 3H, CH_3-Ar), 2.11 (s, 3H, CH_3-Ar), 6.42 (d, 1H, CH-O, J_{C-P}= 8.0 Hz), 6.48 (m, 1H, CH=), 6.9-7.2 (m, 6H, CH=), 7.53 (m, 3H, CH=), 8.25 (m, 1H, CH=). ^{13}C NMR (C_6D_6), δ: 16.5 (CH_3-Ar), 16.7 (CH_3-Ar), 20.1 (CH_3-Ar), 30.6 (d, CH_3, ^{t}Bu, J_{C-P}= 4.1 Hz), 32.6 (CH_3, ^{t}Bu), 34.3 (C, ^{t}Bu), 35.2 (C, ^{t}Bu), 81.3 (d, CH, J_{C-P}= 9.5 Hz), 120.3 (CH=), 121.0 (CH=), 125.4 (CH=), 127.1 (CH=), 128.4 (CH=), 128.9 (CH=), 130.2 (C), 131.1 (C), 132.0 (d, C, J_{C-P}= 2.8 Hz), 132.4 (C), 134.1 (C), 135.8 (C), 135.9 (CH=), 137.4 (C), 138.5 (C), 141.5 (C), 145.2 (C), 145.5 (C), 148.4 (CH=), 162.0 (C). Anal. calcd (%) for $C_{36}H_{42}NO_3P$: C 76.16, H 7.46, N 2.47; found: C 76.23, H 7.47, N 2.40.

L49g Yield: 354 mg (55%). ^{31}P NMR (C_6D_6), δ: 145.3 (s). ^{1}H NMR (C_6D_6), δ: 0.31 (s, 9H, CH_3-Si), 0.33 (s, 9H, CH_3-Si), 6.43 (d, 1H, CH-O, J_{C-P}= 9.2 Hz), 6.48 (m, 1H, CH=), 6.9-7.2 (m, 8H, CH=), 7.29 (m, 3H, CH=), 7.38 (d, 1H, CH=, $^3J_{H-H}$= 8.4 Hz), 7.66 (d, 1H, CH=, $^3J_{H-H}$= 7.6 Hz), 7.76 (d, 1H, CH=, $^3J_{H-H}$= 7.6 Hz), 8.05 (s, 1H, CH=), 8.13 (s, 1H, CH=), 8.23 (m, 1H, CH=). ^{13}C NMR (C_6D_6), δ: 0.1 (d, CH_3-Si, J_{C-P}= 4.6 Hz), 0.5 (CH_3-Si), 81.5 (d, CH, J_{C-P}=4.6 Hz), 121.6 (CH=), 122.6 (CH=), 123.2 (C), 123.8 (C), 125.4 (CH=), 125.5 (CH=), 126.0 (C), 127.3 (CH=), 127.4 (CH=), 127.5 (CH=), 127.6 (CH=), 129.0 (CH=), 129.6 (CH=), 131.6 (C), 131.9 (C), 133.0 (C), 133.1 (C), 135.0 (d, C, J_{C-P}= 8.6 Hz), 136.5 (CH=), 137.5 (C), 137.8 (CH=), 142.1 (C), 142.2 (C), 139.4 (CH=), 152.8 (C), 153.1 (d, C, J_{C-P}= 4.6 Hz), 161.5 (C). Anal. calcd (%) for $C_{38}H_{38}NO_3PSi_2$: C 66.27, H 6.30, N 2.58; found: C 66.32, H 6.29, N 2.51.

3.6.5.4. Typical procedure for the preparation of [Ir(cod)(L)]BAr$_F$

The corresponding ligand (0.074 mmol) was dissolved in CH_2Cl_2 (2 mL) and $[Ir(COD)Cl]_2$ (25 mg, 0.037 mmol) was added. The reaction was refluxed at 50 °C for 1 hour. After 5 min at room temperature, $NaBAr_F$ (77.1 mg, 0.082 mmol) and water (2 mL) were added and the reaction mixture was stirred vigorously for 30 min at room temperature. The phases were separated and the aqueous phase was extracted twice with CH_2Cl_2. The combined organic phases were filtered through a celite plug, dried with $MgSO_4$ and the solvent was evaporated to give the product as an orange solid.

[Ir(cod)(L38a)]BAr$_F$. Yield: 118 mg (93%). ^{31}P NMR ($CDCl_3$), δ: 106.0 (s). ^{1}H NMR ($CDCl_3$), δ: 1.29 (s, 9H, CH_3, ^{t}Bu), 1.33 (s, 18H, CH_3, ^{t}Bu), 1.51 (s, 9H, CH_3, ^{t}Bu), 1.87 (b, 2H, CH_2, cod), 2.13 (b, 3H, CH_3), 2.18 (b, 4H, CH_2, cod), 2.36 (b, 2H, CH_2, cod), 3.94 (b, 1H, CH=, cod), 4.29 (b, 1H, CH=, cod), 4.71 (b, 1H, CH=, cod), 5.35 (b, 1H, CH=, cod), 6.12 (m, 1H, CH-O), 7.1-8.6 (m, 20H,

CH=). ^{13}C NMR ($CDCl_3$), δ: 25.3 (b, CH_2, cod), 29.0 (b, CH_2, cod), 30.9 (CH_3), 31.1 (CH_3, ^{t}Bu), 31.2 (CH_3, ^{t}Bu), 31.3 (CH_3, ^{t}Bu), 31.9 (CH_3, ^{t}Bu), 33.0 (b, CH_2, cod), 34.8 (C, ^{t}Bu), 35.4 (C, ^{t}Bu), 35.5 (C, ^{t}Bu), 36.3 (b, CH_2, cod), 65.8 (b, CH=, cod), 69.9 (b, CH=, cod), 77.2 (CH-O), 100.7 (d, CH=, cod, $J_{C\text{-}P}$= 20.9 Hz), 104.5 (d, CH=, cod, $J_{C\text{-}P}$= 12.5 Hz), 117.7 (b, CH=, BAr_F), 119-131 (aromatic carbons), 135.0 (b, CH=, BAr_F), 139-159 (aromatic carbons), 161.9 (q, C-B, BAr_F, ^1J= 49 Hz). Anal. calcd (%) for $C_{75}H_{72}BF_{24}IrNO_3P$: C 52.21, H 4.21, N 0.81; found: C 52.16, H 4.17, N 0.78.

[Ir(cod)(L38b)]BAr$_F$. Yield: 117 mg (95%). ^{31}P NMR ($CDCl_3$), δ: 109.0 (s). ^{1}H NMR ($CDCl_3$), δ: 1.21 (s, 9H, CH_3, ^{t}Bu), 1.41 (s, 9H, CH_3, ^{t}Bu), 1.76 (b, 2H, CH_2, cod), 2.02 (b, 3H, CH_3), 2.05 (b, 4H, CH_2, cod), 2.29 (b, 2H, CH_2, cod), 3.73 (s, 6H, CH_3, CH_3-O), 4.13 (b, 1H, CH=, cod), 4.30 (b, 1H, CH=, cod), 4.59 (b, 1H, CH=, cod), 5.22 (b, 1H, CH=, cod), 6.03 (m, 1H, CH-O), 6.5-8.5 (m, 20H, CH=). ^{13}C NMR ($CDCl_3$), δ: 25.5 (b, CH_2, cod), 29.1 (b, CH_2, cod), 31.0 (CH_3, ^{t}Bu), 31.2 (CH_3), 31.8 (CH_3, ^{t}Bu), 33.5 (b, CH_2, cod), 35.6 (C, ^{t}Bu), 35.7 (C, ^{t}Bu), 36.7 (b, CH_2, cod), 55.8 (CH_3, CH_3-O), 55.9 (CH_3, CH_3-O), 66.3 (b, CH=, cod), 70.2 (b, CH=, cod), 77.4 (CH-O), 100.4 (d, CH=, cod, $J_{C\text{-}P}$= 21.7 Hz), 104.7 (d, CH=, cod, $J_{C\text{-}P}$= 11.7 Hz), 113-116 (aromatic carbons), 117.7 (b, CH=, BAr_F), 120-133 (aromatic carbons), 135.0 (b, CH=, BAr_F), 139-159 (aromatic carbons), 161.9 (q, C-B, BAr_F, ^1J= 49 Hz). Anal. calcd (%) for $C_{69}H_{60}BF_{24}IrNO_5P$: C 49.53, H 3.61, N 0.84; found: C 49.46, H 3.57, N 0.79.

[Ir(cod)(L38c)]BAr$_F$. Yield: 112 mg (92%). ^{31}P NMR ($CDCl_3$), δ: 109.1 (s). ^{1}H NMR ($CDCl_3$), δ: 0.20 (s, 9H, CH_3, $SiMe_3$), 0.48 (s, 9H, CH_3, $SiMe_3$), 1.78 (b, 2H, CH_2, cod), 1.89 (b, 3H, CH_3), 2.19 (b, 4H, CH_2, cod), 2.40 (b, 2H, CH_2, cod), 4.13 (b, 1H, CH=, cod), 4.30 (b, 1H, CH=, cod), 4.73 (b, 1H, CH=, cod), 5.38 (b, 1H, CH=, cod), 6.19 (m, 1H, CH-O), 7.2-8.7 (m, 22H, CH=). ^{13}C NMR ($CDCl_3$), δ: 0.8 (CH_3, $SiMe_3$), 1.5 (CH_3, $SiMe_3$), 26.2 (b, CH_2, cod), 29.6 (b, CH_2, cod), 31.9 (CH_3), 34.4 (b, CH_2, cod), 37.5 (b, CH_2, cod), 67.9 (b, CH=, cod), 71.6 (b, CH=, cod), 78.2 (CH-O), 101.2 (d, CH=, cod, $J_{C\text{-}P}$= 21 Hz), 104.7 (d, CH=, cod, $J_{C\text{-}P}$= 11.6 Hz), 117.7 (b, CH=, BAr_F), 120-135 (aromatic carbons), 135.0 (b, CH=, BAr_F), 137-159 (aromatic carbons), 161.9 (q, C-B, BAr_F, ^1J= 49 Hz). Anal. calcd (%) for $C_{65}H_{56}BF_{24}IrNO_3PSi_2$: C 47.45, H 3.43, N 0.85; found: C 47.38, H 3.38, N 0.81.

[Ir(cod)(L38d)]BAr$_F$. Yield: 118 mg (96%). ^{31}P NMR ($CDCl_3$), δ: 103.0 (s). ^{1}H NMR ($CDCl_3$), δ: 1.28 (s, 9H, CH_3, ^{t}Bu), 1.50 (s, 9H, CH_3, ^{t}Bu), 1.77 (b, 6H, CH_3-Ar), 1.78 (b, 3H, CH_3), 2.15 (b, 2H, CH_2, cod), 2.26 (b, 6H, CH_3-Ar), 2.28 (b, 4H, CH_2, cod), 2.37 (b, 2H, CH_2, cod), 3.82 (b, 1H, CH=, cod), 4.43 (b, 1H, CH=, cod), 4.60 (b, 1H, CH=, cod), 5.23 (b, 1H, CH=, cod), 6.09 (m, 1H, CH-O), 7.2-8.6 (m, 18H, CH=). ^{13}C NMR ($CDCl_3$), δ: 16.6 (CH_3-Ar), 16.7 (CH_3-Ar), 17.4 (CH_3-Ar), 17.5 (CH_3-Ar), 20.4 (CH_3), 25.0 (b, CH_2, cod), 28.6 (b, CH_2, cod), 31.2 (CH_3, ^{t}Bu), 32.4 (CH_3, ^{t}Bu), 33.6 (b, CH_2, cod), 34.8 (C, ^{t}Bu), 34.9 (C, ^{t}Bu), 36.7 (b, CH_2, cod), 65.8 (b, CH=, cod), 70.7 (b, CH=, cod), 77.2 (CH-O), 99.6 (d, CH=, cod, J= 24.4 Hz), 104.0 (d, CH=, cod, J= 12.3 Hz), 117.7 (b, CH=, BAr_F), 120-134 (aromatic carbons), 135.0 (b, CH=, BAr_F), 136-159 (aromatic carbons), 161.9 (q, C-B, BAr_F, ^1J= 49 Hz). Anal. calcd (%) for $C_{71}H_{64}BF_{24}IrNO_3P$: C 51.09, H 3.86, N 0.84; found: C 51.04, H 3.84, N 0.81.

[Ir(cod)(L38e)]BAr$_F$. Yield: 120 mg (97%). ^{31}P NMR ($CDCl_3$), δ: 102.3 (s). ^{1}H NMR ($CDCl_3$), δ: 1.18 (s, 9H, CH_3, ^{t}Bu), 1.50 (s, 9H, CH_3, ^{t}Bu), 1.72 (b, 6H, CH_3-Ar), 1.79 (b, 3H, CH_3), 2.13 (b, 2H, CH_2, cod), 2.24 (s, 3H, CH_3-Ar), 2.25 (s, 3H CH_3-Ar), 2.27 (b, 4H, CH_2, cod), 2.43 (b, 2H, CH_2, cod), 3.49 (b, 1H, CH=, cod), 4.12 (b, 1H, CH=, cod), 4.77 (b, 1H, CH=, cod), 5.33 (b, 1H, CH=,

cod), 5.46 (m, 1H, CH-O), 7.2-8.6 (m, 18H, CH=). ^{13}C NMR ($CDCl_3$), δ: 16.5 (CH_3-Ar), 16.6 (CH_3-Ar), 20.3 (CH_3-Ar), 20.4 (CH_3-Ar), 24.8 (b, CH_2, cod), 25.2 (CH_3), 28.5 (b, CH_2, cod), 31.9 (CH_3, ^{t}Bu), 32.3 (CH_3, ^{t}Bu), 32.9 (b, CH_2, cod), 34.9 (C, ^{t}Bu), 35.0 (C, ^{t}Bu), 36.8 (b, CH_2, cod), 63.7 (b, CH=, cod), 67.6 (b, CH=, cod), 80.8 (CH-O), 102.5 (b, CH=, cod), 102.7 (b, CH=, cod), 117.7 (b, CH=, BAr_F), 120-134 (aromatic carbons), 135.0 (b, CH=, BAr_F), 136-158 (aromatic carbons), 161.9 (q, C-B, BAr_F, ^1J= 49 Hz). Anal. calcd (%) for $C_{71}H_{64}BF_{24}IrNO_3P$: C 51.09, H 3.86, N 0.84; found: C 51.02, H 3.83, N 0.82.

[Ir(cod)(L38f)]BAr$_F$. Yield: 119 mg (92%). ^{31}P NMR (C_6D_6), δ: 112.1 (s). ^{1}H NMR (C_6D_6), δ: 0.17 (s, 9H, CH_3, $SiMe_3$), 0.48 (s, 9H, CH_3, $SiMe_3$), 1.09 (b, 3H, CH_3), 1.29 (b, 2H, CH_2, cod), 1.67 (b, 2H, CH_2, cod), 1.82 (b, 2H, CH_2, cod), 1.93 (b, 2H, CH_2, cod), 3.64 (b, 1H, CH=, cod), 4.06 (b, 1H, CH=, cod), 4.12 (b, 1H, CH=, cod), 4.80 (b, 1H, CH=, cod), 5.76 (m, 1H, CH-O), 6.6-8.5 (m, 26H, CH=). ^{13}C NMR (C_6D_6), δ: 0.0 (CH_3, $SiMe_3$), 1.1 (CH_3, $SiMe_3$), 17.5 (d, CH_3, $J_{C\text{-}P}$= 10.9 Hz), 25.0 (b, CH_2, cod), 28.4 (b, CH_2, cod), 34.1 (b, CH_2, cod), 37.1 (b, CH_2, cod), 66.3 (b, CH=, cod), 71.2 (b, CH=, cod), 76.8 (d, CH, $J_{C\text{-}P}$= 7 Hz), 100.5 (d, CH=, cod, $J_{C\text{-}P}$= 22.5 Hz), 105.6 (d, CH=, cod, $J_{C\text{-}P}$= 11.6 Hz), 117.7 (b, CH=, BAr_F), 121-135 (aromatic carbons), 135.0 (b, CH=, BAr_F), 137-159 (aromatic carbons), 161.9 (q, C-B, BAr_F, ^1J= 49 Hz). Anal. calcd (%) for $C_{73}H_{60}BF_{24}IrNO_3PSi_2$: C 50.23, H 3.46, N 0.80; found: C 50.20, H 3.44, N 0.76.

[Ir(cod)(L38g)]BAr$_F$. Yield: 123 mg (95%). ^{31}P NMR (C_6D_6), δ: 107.6 (s). ^{1}H NMR (C_6D_6), δ: 0.05 (s, 9H, CH_3, $SiMe_3$), 0.48 (s, 9H, CH_3, $SiMe_3$), 0.99 (b, 2H, CH_2, cod), 1.40 (b, 2H, CH_2, cod), 1.71 (b, 2H, CH_2, cod), 1.85 (b, 2H, CH_2, cod), 1.9 (d, 3H, CH_3, $3J_{H\text{-}H}$= 6.8 Hz), 2.99 (b, 1H, CH=, cod), 3.70 (b, 1H, CH=, cod), 4.32 (b, 1H, CH=, cod), 4.61 (m, 1H, CH-O), 4.80 (b, 1H, CH=, cod), 6.1-8.4 (m, 26H, CH=). ^{13}C NMR (C_6D_6), δ: 0.9 (CH_3, $SiMe_3$), 1.1 (CH_3, $SiMe_3$), 24.9 (b, CH_2, cod), 25.9 (d, CH_3, $J_{C\text{-}P}$= 3.9 Hz), 28.3 (b, CH_2, cod), 33.0 (b, CH_2, cod), 37.1 (b, CH_2, cod), 65.1 (b, CH=, cod), 68.6 (b, CH=, cod), 81.0 (s, CH-O), 104.6 (s, CH=, cod), 104.8 (d, CH=, cod, $J_{C\text{-}P}$= 7 Hz), 117.7 (b, CH=, BAr_F), 121-135 (aromatic carbons), 135.0 (b, CH=, BAr_F), 137-159 (aromatic carbons), 161.9 (q, C-B, BAr_F, ^1J= 49 Hz). Anal. calcd (%) for $C_{73}H_{60}BF_{24}IrNO_3PSi_2$: C 50.23, H 3.46, N 0.80; found: C 50.18, H 3.42, N 0.76.

[Ir(cod)(L39a)]BAr$_F$. Yield: 124 mg (96%). ^{31}P NMR ($CDCl_3$), δ: 110.7 (s). ^{1}H NMR ($CDCl_3$), δ: 1.31 (s, 9H, CH_3, ^{t}Bu), 1.35 (s, 9H, CH_3, ^{t}Bu), 1.36 (s, 9H, CH_3, ^{t}Bu), 1.58 (s, 9H, CH_3, ^{t}Bu), 1.73 (b, 3H, CH_3), 1.98 (b, 2H, CH_2, cod), 2.41 (b, 2H, CH_2, cod), 2.53 (b, 2H, CH_2, cod), 3.16 (b, 3H, CH_3-Py), 3.95 (b, 1H, CH=, cod), 4.59 (b, 1H, CH=, cod), 5.05 (b, 1H, CH=, cod), 5.25 (b, 1H, CH=, cod), 6.24 (m, 1H, CH-O), 7.0-8.0 (m, 19H, CH=). ^{13}C NMR ($CDCl_3$), δ: 17.9 (b, CH_3), 23.9 (b, CH_2, cod), 27.8 (b, CH_2, cod), 29.1 (CH_3-Py), 30.4 (CH_3, ^{t}Bu), 30.9 (C, ^{t}Bu), 31.2 (C, ^{t}Bu), 31.3 (CH_3, ^{t}Bu), 31.4 (CH_3, ^{t}Bu), 34.7 (b, CH_2, cod), 35.2 (C, ^{t}Bu), 35.4 (C, ^{t}Bu), 37.5 (b, CH_2, cod), 70.4 (b, CH=, cod), 72.9 (b, CH=, cod), 75.4 (CH-O), 88.6 (d, CH=, cod, $J_{C\text{-}P}$= 26 Hz), 104.1 (b, CH=, cod), 117.7 (b, CH=, BAr_F), 120-131 (aromatic carbons), 135.0 (b, CH=, BAr_F), 139-158 (aromatic carbons), 161.9 (q, C-B, BAr_F, ^1J= 49 Hz). Anal. calcd (%) for $C_{76}H_{74}BF_{24}IrNO_3P$: C 52.48, H 4.29, N 0.80 found: C 52.43, H 4.26, N 0.77.

[Ir(cod)(L39d)]BAr$_F$. Yield: 118 mg (95%). ^{31}P NMR ($CDCl_3$), δ: 103.1 (s). ^{1}H NMR ($CDCl_3$), δ: 1.26 (s, 9H, CH_3, ^{t}Bu), 1.44 (s, 9H, CH_3, ^{t}Bu), 1.65 (s, 3H, CH_3-Ar), 1.68 (s, 3H, CH_3-Ar), 1.74 (b, 3H, CH_3), 2.15 (b, 2H, CH_2, cod), 2.19 (s, 3H, CH_3-Ar), 2.24 (s, 3H, CH_3-Ar), 2.28 (b, 4H, CH_2, cod), 2.37 (b, 2H, CH_2, cod), 3.04 (s, 3H, CH_3-Py), 3.80 (b, 1H, CH=, cod), 4.42 (b, 1H, CH=, cod), 4.57 (b, 1H, CH=, cod), 5.21 (b, 1H, CH=, cod), 6.06 (m, 1H, CH-O), 7.2-8.6 (m, 17H, CH=). ^{13}C

NMR ($CDCl_3$), δ: 16.5 (CH_3-Ar), 16.8 (CH_3-Ar), 17.1 (CH_3-Ar), 17.4 (CH_3-Ar), 20.2 (CH_3), 25.1 (b, CH_2, cod), 28.5 (b, CH_2, cod), 29.3 (CH_3-Py), 31.2 (CH_3, ^{t}Bu), 31.9 (CH_3, ^{t}Bu), 33.6 (b, CH_2, cod), 34.8 (C, ^{t}Bu), 34.9 (C, ^{t}Bu), 36.2 (b, CH_2, cod), 65.9 (b, CH=, cod), 70.3 (b, CH=, cod), 77.7 (CH-O), 99.8 (d, CH=, cod, *J*= 24.4 Hz), 103.6 (d, CH=, cod, *J*= 12.0 Hz), 117.7 (b, CH=, BAr_F), 120-134 (aromatic carbons), 135.0 (b, CH=, BAr_F), 136-159 (aromatic carbons), 161.9 (q, C-B, BAr_F, ^1J= 49 Hz). Anal. Calc (%) for $C_{72}H_{66}BF_{24}IrNO_3P$: C 51.37, H 3.95, N 0.83; found. C 51.33, H 3.92, N 0.79.

[Ir(cod)(L39e)]BAr$_F$. Yield: 114 mg (93%). ^{31}P NMR ($CDCl_3$), δ: 102.9 (s). ^{1}H NMR ($CDCl_3$), δ: 1.19 (s, 9H, CH_3, ^{t}Bu), 1.44 (s, 9H, CH_3, ^{t}Bu), 1.71 (b, 6H, CH_3-Ar), 1.76 (b, 3H, CH_3), 2.13 (b, 2H, CH_2, cod), 2.23 (s, 3H, CH_3-Ar), 2.85 (s, 3H, CH_3-Ar), 2.29 (b, 4H, CH_2, cod), 2.52 (b, 2H, CH_2, cod), 3.07 (s, 3H, CH_3-Py), 3.56 (b, 1H, CH=, cod), 4.09 (b, 1H, CH=, cod), 4.73 (b, 1H, CH=, cod), 5.31 (b, 1H, CH=, cod), 5.39 (m, 1H, CH-O), 7.2-8.6 (m, 17H, CH=). ^{13}C NMR ($CDCl_3$), δ: 16.8 (CH_3-Ar), 16.9 (CH_3-Ar), 20.5 (CH_3-Ar), 20.8 (CH_3-Ar), 24.8 (b, CH_2, cod), 25.1 (CH_3), 28.8 (b, CH_2, cod), 29.8 (CH_3-Py), 31.7 (CH_3, ^{t}Bu), 32.2 (CH_3, ^{t}Bu), 32.8 (b, CH_2, cod), 34.6 (C, ^{t}Bu), 34.8 (C, ^{t}Bu), 36.5 (b, CH_2, cod), 64.9 (b, CH=, cod), 69.3 (b, CH=, cod), 80.1 (CH-O), 102.3 (b, CH=, cod), 102.9 (b, CH=, cod), 117.7 (b, CH=, BAr_F), 120-134 (aromatic carbons), 135.0 (b, CH=, BAr_F), 136-158 (aromatic carbons), 161.9 (q, C-B, BAr_F, ^1J= 49 Hz). Anal. Calc (%) for $C_{72}H_{66}BF_{24}IrNO_3P$: C 51.37, H 3.95, N 0.83; found. C 51.35, H 3.93, N 0.80.

[Ir(cod)(L40a)]BAr$_F$. Yield: 128 mg (96%). ^{31}P NMR ($CDCl_3$), δ: 108.4 (s). ^{1}H NMR ($CDCl_3$), δ: 1.31 (s, 9H, CH_3, ^{t}Bu), 1.37 (s, 9H, CH_3, ^{t}Bu), 1.38 (s, 9H, CH_3, ^{t}Bu), 1.58 (s, 9H, CH_3, ^{t}Bu), 1.60 (b, 3H, CH_3), 1.79 (b, 2H, CH_2, cod), 2.29 (b, 4H, CH_2, cod), 2.53 (b, 2H, CH_2, cod), 4.31 (b, 1H, CH=, cod), 4.75 (b, 1H, CH=, cod), 5.16 (b, 1H, CH=, cod), 5.30 (b, 1H, CH=, cod), 6.11 (m, 1H, CH-O), 7.0-7.7 (m, 19H, CH=). ^{13}C NMR ($CDCl_3$), δ: 17.8 (b, CH_3), 23.8 (b, CH_2, cod), 28.0 (b, CH_2, cod), 30.7 (C, ^{t}Bu), 31.2 (C, ^{t}Bu), 31.5 (CH_3, ^{t}Bu), 31.7 (CH_3, ^{t}Bu), 34.9 (C, ^{t}Bu), 35.0 (C, ^{t}Bu), 35.4 (b, CH_2, cod), 37.6 (b, CH_2, cod), 72.3 (b, CH=, cod), 74.9 (b, CH=, cod), 75.0 (CH-O), 89.0 (d, CH=, cod, $J_{C\text{-}P}$= 26.7 Hz), 102.8 (d, CH=, cod, $J_{C\text{-}P}$= 8.4 Hz), 117.7 (b, CH=, BAr_F), 120-132 (aromatic carbons), 135.0 (b, CH=, BAr_F), 139-150 (aromatic carbons), 161.9 (q, C-B, BAr_F, ^1J= 49 Hz). Anal. calcd (%) for $C_{75}H_{71}BBrF_{24}IrNO_3P$: C 49.93, H 3.97, N 0.78; found: C 49.88, H 3.94, N 0.75.

[Ir(cod)(L41a)]BAr$_F$. Yield: 125 mg (94%). ^{31}P NMR ($CDCl_3$), δ: 98.2 (s). ^{1}H NMR ($CDCl_3$), δ: 1.33 (s, 9H, CH_3, ^{t}Bu), 1.34 (s, 9H, CH_3, ^{t}Bu), 1.38 (s, 9H, CH_3, ^{t}Bu), 1.54 (b, 3H, CH_3), 1.59 (s, 9H, CH_3, ^{t}Bu), 1.89 (b, 2H, CH_2, cod), 2.19 (b, 4H, CH_2, cod), 2.63 (b, 2H, CH_2, cod), 4.62 (b, 1H, CH=, cod), 4.68 (b, 1H, CH=, cod), 4.79 (b, 1H, CH=, cod), 5.29 (b, 1H, CH=, cod), 6.07 (m, 1H, CH-O), 7.1-8.2 (m, 24H, CH=). ^{13}C NMR ($CDCl_3$), δ: 17.2 (d, CH_3, $J_{C\text{-}P}$= 10.8), 23.2 (b, CH_2, cod), 28.4 (b, CH_2, cod), 30.2 (CH_3, ^{t}Bu), 30.5 (CH_3, ^{t}Bu), 30.9 (C, ^{t}Bu), 31.3 (CH_3, ^{t}Bu), 31.4 (CH_3, ^{t}Bu), 34.7 (b, CH_2, cod), 35.0 (C, ^{t}Bu), 35.3 (C, ^{t}Bu), 35.6 (C, ^{t}Bu), 35.7 (b, CH_2, cod), 70.6 (b, CH=, cod), 73.1 (b, CH=, cod), 74.6 (CH-O), 83.2 (d, CH=, cod, $J_{C\text{-}P}$ = 29.4 Hz), 97.6 (d, CH=, cod, $J_{C\text{-}P}$= 7 Hz), 117.7 (b, CH=, BAr_F), 120-133 (aromatic carbons), 135.0 (b, CH=, BAr_F), 137-159 (aromatic carbons), 161.9 (q, C-B, BAr_F, ^1J= 49 Hz). Anal. calcd (%) for $C_{81}H_{76}BF_{24}IrNO_3P$: C 54.00, H 4.25, N 0.78; found: C 53.96, H 4.22, N 0.76.

[Ir(cod)(L42a)]BAr$_F$. Yield: 123 mg (94%). ^{31}P NMR ($CDCl_3$), δ: 108.8 (s). ^{1}H NMR ($CDCl_3$), δ: 1.06 (s, 9H, CH_3, ^{t}Bu), 1.18 (s, 9H, CH_3, ^{t}Bu), 1.33 (s, 9H, CH_3, ^{t}Bu), 1.34 (s, 9H, CH_3, ^{t}Bu), 1.40 (s, 9H, CH_3, ^{t}Bu), 2.02 (b, 2H, CH_2, cod), 2.21 (b, 4H, CH_2, cod), 2.36 (b, 2H, CH_2, cod), 4.22 (b,

1H, CH=, cod), 4.36 (b, 1H, CH=, cod), 5.16 (b, 1H, CH=, cod), 5.17 (b, 1H, CH=, cod), 5.20 (m, 1H, CH-O), 7.1-8.7 (m, 20H, CH=). ^{13}C NMR ($CDCl_3$), δ: 24.9 (b, CH_2, cod), 26.9 (CH_3, ^{t}Bu), 29.8 (b, CH_2, cod), 30.6 (C, ^{t}Bu), 30.9 (CH_3, ^{t}Bu), 31.0 (CH_3, ^{t}Bu), 31.2 (CH_3, ^{t}Bu), 31.3 (CH_3, ^{t}Bu), 31.5 (C, ^{t}Bu), 34.7 (b, CH_2, cod), 34.8 (C, ^{t}Bu), 35.0 (C, ^{t}Bu), 35.4 (C, ^{t}Bu), 36.4 (b, CH_2, cod), 63.5 (b, CH=, cod), 65.9 (b, CH=, cod), 89.7 (CH-O), 101.1 (d, CH=, cod, $J_{C\text{-}P}$= 17.6 Hz), 104.3 (d, CH=, cod, $J_{C\text{-}P}$= 16.8 Hz), 117.7 (b, CH=, BAr_F), 120-131 (aromatic carbons), 135.0 (b, CH=, BAr_F), 138-155 (aromatic carbons), 161.9 (q, C-B, BAr_F, ^1J= 49 Hz). Anal. calcd (%) for $C_{78}H_{78}BF_{24}IrNO_3P$: C 53.01, H 4.45, N 0.79; found: C 52.99, H 4.43, N 0.77.

[Ir(cod)(L42d)]BAr$_F$. Yield: 122 mg (96%). ^{31}P NMR ($CDCl_3$), δ: 106.4 (s). ^{1}H NMR ($CDCl_3$), δ: 1.04 (s, 9H, CH_3, ^{t}Bu), 1.21 (s, 9H, CH_3, ^{t}Bu), 1.47 (s, 9H, CH_3, ^{t}Bu), 1.73 (s, 3H, CH_3-Ar), 1.79 (s, 3H, CH_3-Ar), 2.14 (b, 2H, CH_2, cod), 2.22 (s, 3H, CH_3-Ar), 2.27 (s, 3H, CH_3-Ar), 2.29 (b, 4H, CH_2, cod), 2.33 (b, 2H, CH_2, cod), 3.86 (b, 1H, CH=, cod), 4.41 (b, 1H, CH=, cod), 4.73 (b, 1H, CH=, cod), 5.19 (b, 1H, CH=, cod), 6.01 (m, 1H, CH-O), 7.2-8.6 (m, 18H, CH=). ^{13}C NMR ($CDCl_3$), δ: 16.2 (CH_3-Ar), 16.5 (CH_3-Ar), 17.2 (CH_3-Ar), 17.5 (CH_3-Ar), 25.0 (b, CH_2, cod), 27.8 (b, CH_2, cod), 30.5 (C, ^{t}Bu), 31.1 (CH_3, ^{t}Bu), 31.5 (CH_3, ^{t}Bu), 32.2 (CH_3, ^{t}Bu), 33.4 (b, CH_2, cod), 34.3 (C, ^{t}Bu), 34.6 (C, ^{t}Bu), 36.1 (b, CH_2, cod), 66.9 (b, CH=, cod), 70.9 (b, CH=, cod), 79.5 (CH-O), 99.1 (d, CH=, cod, J= 24.8 Hz), 103.4 (d, CH=, cod, J= 11.6 Hz), 117.7 (b, CH=, BAr_F), 120-134 (aromatic carbons), 135.0 (b, CH=, BAr_F), 136-159 (aromatic carbons), 161.9 (q, C-B, BAr_F, ^1J= 49 Hz). Anal. Calc (%) for $C_{74}H_{70}BF_{24}IrNO_3P$: C 51.94, H 4.12, N 0.82; found. C 51.91, H 4.10, N 0.81.

[Ir(cod)(L42e)]BAr$_F$. Yield: 119 mg (94%). ^{31}P NMR ($CDCl_3$), δ: 105.2 (s). ^{1}H NMR ($CDCl_3$), δ: 1.02 (s, 9H, CH_3, ^{t}Bu), 1.25 (s, 9H, CH_3, ^{t}Bu), 1.44 (s, 9H, CH_3, ^{t}Bu), 1.71 (s, 3H, CH_3-Ar), 1.76 (s, 3H, CH_3-Ar), 2.11 (b, 2H, CH_2, cod), 2.27 (s, 6H, CH_3-Ar), 2.29 (b, 4H, CH_2, cod), 2.37 (b, 2H, CH_2, cod), 3.63 (b, 1H, CH=, cod), 4.26 (b, 1H, CH=, cod), 4.83 (b, 1H, CH=, cod), 5.29 (b, 1H, CH=, cod), 5.51 (m, 1H, CH-O), 7.2-8.6 (m, 18H, CH=). ^{13}C NMR ($CDCl_3$), δ: 16.5 (CH_3-Ar), 16.6 (CH_3-Ar), 20.1 (CH_3-Ar), 20.4 (CH_3-Ar), 24.9 (b, CH_2, cod), 28.7 (b, CH_2, cod), 30.3 (C, ^{t}Bu), 31.1 (CH_3, ^{t}Bu), 32.3 (CH_3, ^{t}Bu), 32.7 (CH_3, ^{t}Bu), 32.6 (b, CH_2, cod), 33.9 (C, ^{t}Bu), 34.2 (C, ^{t}Bu), 35.9 (b, CH_2, cod), 64.2 (b, CH=, cod), 69.8 (b, CH=, cod), 81.2 (CH-O), 102.2 (b, CH=, cod), 104.2 (b, CH=, cod), 117.7 (b, CH=, BAr_F), 120-134 (aromatic carbons), 135.0 (b, CH=, BAr_F), 136-158 (aromatic carbons), 161.9 (q, C-B, BAr_F, ^1J= 49 Hz). Anal. Calc (%) for $C_{74}H_{70}BF_{24}IrNO_3P$: C 51.94, H 4.12, N 0.82; found. C 51.90, H 4.11, N 0.80.

[Ir(cod)(L43a)]BAr$_F$. Yield: 123 mg (93%). ^{31}P NMR ($CDCl_3$), δ: 103.6 (s). ^{1}H NMR ($CDCl_3$), δ: 1.13 (s, 9H, CH_3, ^{t}Bu), 1.15 (s, 9H, CH_3, ^{t}Bu), 1.20 (s, 9H, CH_3, ^{t}Bu), 1.23 (s, 9H, CH_3, ^{t}Bu), 1.43 (b, 2H, CH_2, cod), 1.62 (b, 2H, CH_2, cod), 1.96 (b, 2H, CH_2, cod), 2.39 (b, 2H, CH_2, cod), 3.70 (b, 1H, CH=, cod), 4.24 (b, 1H, CH=, cod), 4.74 (b, 1H, CH=, cod), 5.30 (b, 1H, CH=, cod), 6.91 (m, 1H, CH-O), 7.0-8.5 (m, 25H, CH=). ^{13}C NMR ($CDCl_3$), δ: 25.1 (b, CH_2, cod), 28.6 (b, CH_2, cod), 30.9 (CH_3, ^{t}Bu), 31.3 (CH_3, ^{t}Bu), 31.5 (CH_3, ^{t}Bu), 32.1 (CH_3, ^{t}Bu), 33.2 (b, CH_2, cod), 34.7 (C, ^{t}Bu), 34.8 (C, ^{t}Bu), 35.2 (C, ^{t}Bu), 35.6 (C, ^{t}Bu), 36.7 (b, CH_2, cod), 65.2 (b, CH=, cod), 70.6 (b, CH=, cod), 81.9 (d, CH, $J_{C\text{-}P}$= 10.1 Hz), 101.7 (d, CH=, cod, $J_{C\text{-}P}$= 21 Hz), 105.0 (d, CH=, cod, $J_{C\text{-}P}$= 12.4 Hz), 117.7 (b, CH=, BAr_F), 120-133 (aromatic carbons), 135.0 (b, CH=, BAr_F), 139-160 (aromatic carbons), 161.9 (q, C-B, BAr_F, ^1J= 49 Hz). Anal. calcd (%) for $C_{80}H_{74}BF_{24}IrNO_3P$: C 53.76, H 4.17, N 0.78; found: C 53.73, H 4.15, N 0.76.

[Ir(cod)(L43c)]BAr$_F$. Yield: 116 mg (92%). ^{31}P NMR ($CDCl_3$), δ: 103.2 (s). ^{1}H NMR ($CDCl_3$), δ: 0.20 (s, 9H, CH_3, $SiMe_3$), 0.24 (s, 9H, CH_3, $SiMe_3$), 1.75 (b, 2H, CH_2, cod), 1.91 (b, 2H, CH_2, cod),

2.19 (b, 2H, CH_2, cod), 2.53 (b, 2H, CH_2, cod), 4.18 (b, 1H, CH=, cod), 4.44 (b, 1H, CH=, cod), 4.80 (b, 1H, CH=, cod), 5.54 (b, 1H, CH=, cod), 7.03 (m, 1H, CH-O), 7.1-8.7 (m, 27H, CH=). ^{13}C NMR ($CDCl_3$), δ: 0.2 (CH_3, $SiMe_3$), 1.3 (CH_3, $SiMe_3$), 25.5 (b, CH_2, cod), 28.9 (b, CH_2, cod), 34.4 (b, CH_2, cod), 37.4 (d, CH_2, cod, J_{C-P}= 6.2 Hz), 67.3 (b, CH=, cod), 72.1 (b, CH=, cod), 82.7 (d, CH, J_{C-P}= 9.3 Hz), 101.4 (d, CH=, cod, J_{C-P}= 21.7 Hz), 106.0 (d, CH=, cod, J_{C-P}= 11.7 Hz), 117.7 (b, CH=, BAr_F), 120-134 (aromatic carbons), 135.0 (b, CH=, BAr_F), 136-160 (aromatic carbons), 161.9 (q, C-B, BAr_F, ^1J= 49 Hz). Anal. calcd (%) for $C_{70}H_{58}BF_{24}IrNO_3PSi_2$: C 49.24, H 3.42, N 0.82 found: C 49.21, H 3.40, N 0.79.

[Ir(cod)(L43d)]BAr_F. Yield: 116 mg (92%). ^{31}P NMR ($CDCl_3$), δ: 102.3 (s). ^{1}H NMR ($CDCl_3$), δ: 1.28 (s, 9H, CH_3, ^{t}Bu), 1.39 (s, 9H, CH_3, ^{t}Bu), 1.68 (s, 6H, CH_3-Ar), 1.73 (s, 6H, CH_3-Ar), 1.75 (s, 3H, CH_3), 2.12 (b, 2H, CH_2, cod), 2.13 (s, 3H, CH_3-Ar), 2.19 (s, 3H, CH_3-Ar), 2.28 (b, 4H, CH_2, cod), 2.34 (b, 2H, CH_2, cod), 3.92 (b, 1H, CH=, cod), 4.41 (b, 1H, CH=, cod), 4.54 (b, 1H, CH=, cod), 5.33 (b, 1H, CH=, cod), 6.02 (m, 1H, CH-O), 7.2-8.6 (m, 23H, CH=). ^{13}C NMR ($CDCl_3$), δ: 16.2 (CH_3-Ar), 16.4 (CH_3-Ar), 17.2 (CH_3-Ar), 17.5 (CH_3-Ar), 20.9 (CH_3), 25.1 (b, CH_2, cod), 27.9 (b, CH_2, cod), 31.9 (CH_3, ^{t}Bu), 32.2 (CH_3, ^{t}Bu), 34.2 (b, CH_2, cod), 34.9 (C, ^{t}Bu), 35.1 (C, ^{t}Bu), 36.7 (b, CH_2, cod), 68.2 (b, CH=, cod), 70.2 (b, CH=, cod), 77.2 (CH-O), 101.2 (d, CH=, cod, J= 23.8 Hz), 104.1 (d, CH=, cod, J= 16.0 Hz), 117.7 (b, CH=, BAr_F), 120-134 (aromatic carbons), 135.0 (b, CH=, BAr_F), 136-159 (aromatic carbons), 161.9 (q, C-B, BAr_F, ^1J= 49 Hz). Anal. Calc (%) for $C_{76}H_{66}BF_{24}IrNO_3P$: C 52.72, H 3.84, N 0.81; found. C 52.71, H 3.83, N 0.80.

[Ir(cod)(L43e)]BAr_F. Yield: 119 mg (93%). ^{31}P NMR ($CDCl_3$), δ: 102.1 (s). ^{1}H NMR ($CDCl_3$), δ: 1.21 (s, 9H, CH_3, ^{t}Bu), 1.44 (s, 9H, CH_3, ^{t}Bu), 1.63 (s, 6H, CH_3-Ar), 1.69 (s, 3H, CH_3-Ar), 1.72 (s, 3H, CH_3-Ar), 1.77 (s, 3H, CH_3), 2.11 (b, 2H, CH_2, cod), 2.17 (s, 3H, CH_3-Ar), 2.19 (s, 3H, CH_3-Ar), 2.24 (b, 4H, CH_2, cod), 2.31 (b, 2H, CH_2, cod), 3.98 (b, 1H, CH=, cod), 4.37 (b, 1H, CH=, cod), 4.47 (b, 1H, CH=, cod), 5.26 (b, 1H, CH=, cod), 6.06 (m, 1H, CH-O), 7.2-8.6 (m, 23H, CH=). ^{13}C NMR ($CDCl_3$), δ: 16.1 (CH_3-Ar), 16.2 (CH_3-Ar), 17.0 (CH_3-Ar), 17.3 (CH_3-Ar), 20.7 (CH_3), 25.1 (b, CH_2, cod), 27.9 (b, CH_2, cod), 31.9 (CH_3, ^{t}Bu), 32.2 (CH_3, ^{t}Bu), 34.2 (b, CH_2, cod), 34.8 (C, ^{t}Bu), 35.2 (C, ^{t}Bu), 36.3 (b, CH_2, cod), 71.1 (b, CH=, cod), 72.6 (b, CH=, cod), 79.2 (CH-O), 100.2 (d, CH=, cod, J= 24.8 Hz), 102.6 (d, CH=, cod, J= 12.0 Hz), 117.7 (b, CH=, BAr_F), 120-134 (aromatic carbons), 135.0 (b, CH=, BAr_F), 136-159 (aromatic carbons), 161.9 (q, C-B, BAr_F, ^1J= 49 Hz). Anal. Calc (%) for $C_{76}H_{66}BF_{24}IrNO_3P$: C 52.72, H 3.84, N 0.81; found. C 52.68, H 3.81, N 0.78.

[Ir(cod)(L44a)]BAr_F. Yield: 128 mg (97%). ^{31}P NMR ($CDCl_3$), δ: 105.1 (s). ^{1}H NMR ($CDCl_3$), δ: 1.01 (s, 9H, CH_3, ^{t}Bu), 1.13 (s, 9H, CH_3, ^{t}Bu), 1.28 (s, 9H, CH_3, ^{t}Bu), 1.38 (s, 9H, CH_3, ^{t}Bu), 1.53 (s, 9H, CH_3, ^{t}Bu), 2.04 (b, 2H, CH_2, cod), 2.12 (s, 3H, CH_3, MePy), 2.25 (b, 4H, CH_2, cod), 2.43 (b, 2H, CH_2, cod), 3.90 (b, 1H, CH=, cod), 4.38 (b, 1H, CH=, cod), 4.99 (b, 1H, CH=, cod), 5.38 (b, 1H, CH=, cod), 5.73 (d, 1H, CH-O, J_{C-P} = 6.4 Hz), 7.0-7.8 (m, 19H, CH=). ^{13}C NMR ($CDCl_3$), δ: 23.9 (b, CH_2, cod), 27.2 (b, CH_2, cod), 28.2 (C, ^{t}Bu), 30.0 (CH_3, ^{t}Bu), 30.1 (CH_3, MePy), 30.9 (CH_3, ^{t}Bu), 31.0 (CH_3, ^{t}Bu), 31.2 (CH_3, ^{t}Bu), 31.3 (CH_3, ^{t}Bu), 34.6 (C, ^{t}Bu), 34.8 (b, CH_2, cod), 34.9 (C, ^{t}Bu), 35.0 (C, ^{t}Bu), 35.4 (C, ^{t}Bu), 35.8 (b, CH_2, cod), 37.3 (b, CH_2, cod), 67.4 (b, CH=, cod), 73.8 (b, CH=, cod), 87.6 (s, CH-O), 87.9 (d, CH=, cod, J_{C-P}= 26.4 Hz), 103.8 (d, CH=, cod, J_{C-P}= 9.3 Hz), 117.7 (b, CH=, BAr_F), 120-131 (aromatic carbons), 135.0 (b, CH=, BAr_F), 138-157 (aromatic carbons), 161.9 (q, C-B, BAr_F, ^1J= 49 Hz). Anal. calcd (%) for $C_{79}H_{80}BF_{24}IrNO_3P$: C 53.26, H 4.53, N 0.79; found: C 53.23, H 4.51, N 0.76.

[Ir(cod)(L45a)]BAr$_F$. Yield: 126 mg (96%). ^{31}P NMR ($CDCl_3$), δ: 111.1 (s). ^{1}H NMR ($CDCl_3$), δ: 1.01 (s, 9H, CH_3, ^{t}Bu), 1.22 (s, 9H, CH_3, ^{t}Bu), 1.29 (s, 9H, CH_3, ^{t}Bu), 1.53 (s, 9H, CH_3, ^{t}Bu), 1.70 (b, 2H, CH_2, cod), 1.77 (d, 3H, CH_3, $^3J_{H-H}$= 6.8 Hz), 2.22 (b, 4H, CH_2, cod), 2.58 (b, 2H, CH_2, cod), 4.18 (b, 1H, CH=, cod), 4.57 (b, 1H, CH=, cod), 5.04 (b, 1H, CH=, cod), 5.16 (b, 1H, CH=, cod), 6.29 (m, 1H, CH-O), 6.9-9.0 (m, 22H, CH=). ^{13}C NMR ($CDCl_3$), δ: 18.3 (CH_3), 24.0 (b, CH_2, cod), 27.8 (b, CH_2, cod), 30.5 (CH_3, ^{t}Bu), 31.0 (CH_3, ^{t}Bu), 31.1 (CH_3, ^{t}Bu), 31.2 (CH_3, ^{t}Bu), 31.3 (C, ^{t}Bu), 34.7 (b, CH_2, cod), 35.0 (C, ^{t}Bu), 35.1 (C, ^{t}Bu), 35.3 (C, ^{t}Bu), 37.6 (b, CH_2, cod), 70.5 (b, CH=, cod), 72.0 (b, CH=, cod), 77.2 (CH-O), 91.0 (d, CH=, cod, J_{C-P}= 24 Hz), 104.5 (d, CH=, cod, J_{C-P}= 9.3 Hz), 117.7 (b, CH=, BAr$_F$), 119-132 (aromatic carbons), 135.0 (b, CH=, BAr$_F$), 138-161 (aromatic carbons), 161.9 (q, C-B, BAr$_F$, ^1J= 49 Hz). Anal. calcd (%) for $C_{79}H_{74}BF_{24}IrNO_3P$: C 53.44, H 4.20, N 0.79; found: C 53.41, H 4.17, N 0.76.

[Ir(cod)(L46a)]BAr$_F$. Yield: 116 mg (92%). ^{31}P NMR ($CDCl_3$), δ: 106.0 (s). ^{1}H NMR ($CDCl_3$), δ: 1.29 (s, 9H, CH_3, ^{t}Bu), 1.34 (s, 18H, CH_3, ^{t}Bu), 1.51 (s, 9H, CH_3, ^{t}Bu), 1.87 (b, 2H, CH_2, cod), 2.13 (b, 3H, CH_3), 2.21 (b, 4H, CH_2, cod), 2.36 (b, 2H, CH_2, cod), 3.94 (b, 1H, CH=, cod), 4.29 (b, 1H, CH=, cod), 4.71 (b, 1H, CH=, cod), 5.24 (b, 1H, CH=, cod), 6.12 (m, 1H, CH-O), 7.1-8.6 (m, 20H, CH=). ^{13}C NMR ($CDCl_3$), δ: 25.3 (b, CH_2, cod), 29.0 (b, CH_2, cod), 30.7 (C, ^{t}Bu), 30.9 (CH_3), 31.1 (CH_3, ^{t}Bu), 31.2 (CH_3, ^{t}Bu), 31.3 (CH_3, ^{t}Bu), 31.9 (CH_3, ^{t}Bu), 33.0 (b, CH_2, cod), 34.8 (C, ^{t}Bu), 35.4 (C, ^{t}Bu), 35.5 (C, ^{t}Bu), 36.3 (b, CH_2, cod), 65.8 (b, CH=, cod), 69.9 (b, CH=, cod), 77.2 (CH-O), 100.7 (d, CH=, cod, J_{C-P}= 20.9 Hz), 104.5 (d, CH=, cod, J_{C-P}= 12.5 Hz), 117.7 (b, CH=, BAr$_F$), 119-131 (aromatic carbons), 135.0 (b, CH=, BAr$_F$), 139-159 (aromatic carbons), 161.9 (q, C-B, BAr$_F$, ^1J= 49 Hz). Anal. calcd (%) for $C_{75}H_{72}BF_{24}IrNO_3P$: C 52.21, H 4.21, N 0.81; found: C 52.18, H 4.19, N 0.78.

[Ir(cod)(L46d)]BAr$_F$. Yield: 118 mg (96%). ^{31}P NMR ($CDCl_3$), δ: 102.9 (s). ^{1}H NMR ($CDCl_3$), δ: 1.19 (s, 9H, CH_3, ^{t}Bu), 1.42 (s, 9H, CH_3, ^{t}Bu), 1.69 (b, 6H, CH_3, Ar-Me), 1.73 (b, 3H, CH_3), 2.02 (b, 2H, CH_2, cod), 2.18 (b, 6H, CH_3, Ar-Me), 2.29 (b, 4H, CH_2, cod), 2.52 (b, 2H, CH_2, cod), 3.73 (b, 1H, CH=, cod), 4.27 (b, 1H, CH=, cod), 4.52 (b, 1H, CH=, cod), 5.15 (b, 1H, CH=, cod), 6.00 (m, 1H, CH-O), 7.1-8.5 (m, 18H, CH=). ^{13}C NMR ($CDCl_3$), δ: 16.6 (CH_3, Ar-Me), 16.7 (CH_3, Ar-Me), 17.3 (CH_3, Ar-Me), 17.4 (CH_3, Ar-Me), 20.3 (CH_3), 25.0 (b, CH_2, cod), 28.5 (b, CH_2, cod), 31.2 (CH_3, ^{t}Bu), 32.3 (CH_3, ^{t}Bu), 33.5 (b, CH_2, cod), 34.8 (C, ^{t}Bu), 34.9 (C, ^{t}Bu), 36.7 (b, CH_2, cod), 65.8 (b, CH=, cod), 70.7 (b, CH=, cod), 77.2 (s, CH-O), 99.6 (d, CH=, cod, J_{C-P}= 20.9 Hz), 104.0 (d, CH=, cod, J_{C-P}= 11.6 Hz), 117.7 (b, CH=, BAr$_F$), 120-135 (aromatic carbons), 135.0 (b, CH=, BAr$_F$), 136-159 (aromatic carbons), 161.9 (q, C-B, BAr$_F$, ^1J= 49 Hz). Anal. calcd (%) for $C_{71}H_{64}BF_{24}IrNO_3P$: C 51.09, H 3.86, N 0.84; found: C 51.06, H 3.84, N 0.81.

[Ir(cod)(L46e)]BAr$_F$. Yield: 113 mg (94%). ^{31}P NMR ($CDCl_3$), δ: 102.2 (s). ^{1}H NMR ($CDCl_3$), δ: 1.12 (s, 9H, CH_3, ^{t}Bu), 1.43 (s, 9H, CH_3, ^{t}Bu), 1.65 (b, 6H, CH_3, Ar-Me), 1.72 (b, 3H, CH_3), 2.05 (b, 2H, CH_2, cod), 2.17 (b, 6H, CH_3, Ar-Me), 2.19 (b, 4H, CH_2, cod), 2.36 (b, 2H, CH_2, cod), 3.42 (b, 1H, CH=, cod), 4.05 (b, 1H, CH=, cod), 4.70 (b, 1H, CH=, cod), 5.33 (b, 1H, CH=, cod), 5.41 (m, 1H, CH-O), 7.0-8.5 (m, 18H, CH=). ^{13}C NMR ($CDCl_3$), δ: 16.7 (CH_3, Ar-Me), 16.8 (CH_3, Ar-Me), 20.4 (CH_3, Ar-Me), 20.5 (CH_3, Ar-Me), 25.1 (b, CH_2, cod), 25.4 (CH_3), 28.7 (b, CH_2, cod), 32.2 (CH_3, ^{t}Bu), 32.5 (CH_3, ^{t}Bu), 33.1 (b, CH_2, cod), 35.2 (C, ^{t}Bu), 35.3 (C, ^{t}Bu), 37.1 (b, CH_2, cod), 64.0 (b, CH=, cod), 67.8 (b, CH=, cod), 81.1 (CH-O), 102.7 (b, CH=, cod), 102.9 (b, CH=, cod), 117.7 (b, CH=, BAr$_F$), 120-135 (aromatic carbons), 135.0 (b, CH=, BAr$_F$), 135-159 (aromatic

carbons), 161.9 (q, C-B, BAr_F, ^1J= 49 Hz). Anal. calcd (%) for $C_{71}H_{64}BF_{24}IrNO_3P$: C 51.09, H 3.86, N 0.84; found: C 51.02, H 3.81, N 0.80.

[Ir(cod)(L47a)]BAr_F. Yield: 124 mg (96%). ^{31}P NMR ($CDCl_3$), δ: 109.9 (s). ^{1}H NMR ($CDCl_3$), δ: 1.32 (s, 9H, CH_3, ^{t}Bu), 1.35 (s, 9H, CH_3, ^{t}Bu), 1.39 (s, 9H, CH_3, ^{t}Bu), 1.57 (s, 9H, CH_3, ^{t}Bu), 1.72 (b, 3H, CH_3), 1.97 (b, 2H, CH_2, cod), 2.40 (b, 2H, CH_2, cod), 2.53 (b, 2H, CH_2, cod), 3.19 (b, 3H, CH_3-Py), 3.98 (b, 1H, CH=, cod), 4.61 (b, 1H, CH=, cod), 5.03 (b, 1H, CH=, cod), 5.22 (b, 1H, CH=, cod), 6.21 (m, 1H, CH-O), 7.0-8.0 (m, 19H, CH=). ^{13}C NMR ($CDCl_3$), δ: 17.8 (b, CH_3), 23.8 (b, CH_2, cod), 27.8 (b, CH_2, cod), 29.1 (CH_3-Py), 30.4 (CH_3, ^{t}Bu), 30.9 (C, ^{t}Bu), 31.2 (C, ^{t}Bu), 31.3 (CH_3, ^{t}Bu), 31.4 (CH_3, ^{t}Bu), 34.6 (b, CH_2, cod), 35.2 (C, ^{t}Bu), 35.4 (C, ^{t}Bu), 37.7 (b, CH_2, cod), 70.3 (b, CH=, cod), 72.8 (b, CH=, cod), 75.4 (CH-O), 89.2 (d, CH=, cod, $J_{C\text{-}P}$= 22.4 Hz), 104.2 (b, CH=, cod), 117.7 (b, CH=, BAr_F), 120-131 (aromatic carbons), 135.0 (b, CH=, BAr_F), 139-158 (aromatic carbons), 161.9 (q, C-B, BAr_F, ^1J= 49 Hz). Anal. Calc (%) for $C_{76}H_{74}BF_{24}IrNO_3P$: C 52.48, H 4.29, N 0.81; found. C 52.42, H 4.25, N 0.78.

[Ir(cod)(L47e)]BAr_F. Yield: 116 mg (94%). ^{31}P NMR ($CDCl_3$), δ: 105.2 (s). ^{1}H NMR ($CDCl_3$), δ: 1.27 (s, 9H, CH_3, ^{t}Bu), 1.46 (s, 9H, CH_3, ^{t}Bu), 1.61 (b, 6H, CH_3, Ar-Me), 1.76 (b, 3H, CH_3), 1.95 (b, 2H, CH_2, cod), 2.07 (b, 2H, CH_2, cod), 2.16 (s, 3H, CH_3, Ar-Me), 2.19 (s, 3H, CH_3, Ar-Me), 2.28 (b, 2H, CH_2, cod), 2.37 (b, 2H, CH_2, cod), 3.04 (s, 3H, CH_3, MePy), 3.77 (b, 1H, CH=, cod), 4.50 (b, 1H, CH=, cod), 4.80 (b, 1H, CH=, cod), 5.10 (b, 1H, CH=, cod), 6.11 (m, 1H, CH-O), 7.0-7.7 (m, 17H, CH=). ^{13}C NMR ($CDCl_3$), δ: 16.5 (CH_3, Ar-Me), 16.7 (CH_3, Ar-Me), 20.3 (CH_3, Ar-Me), 20.4 (CH_3, Ar-Me), 23.8 (b, CH_2, cod), 27.7 (CH_3, MePy), 29.4 (CH_3), 29.7 (b, CH_2, cod), 30.7 (CH_3, ^{t}Bu), 31.9 (CH_3, ^{t}Bu), 34.6 (C, ^{t}Bu), 34.7 (C, ^{t}Bu), 35.5 (b, CH_2, cod), 37.4 (b, CH_2, cod), 71.4 (b, CH=, cod), 72.7 (b, CH=, cod), 75.0 (CH-O), 88.2.7 (d, CH=, cod, $J_{C\text{-}P}$= 27.1), 103.4 (d, CH=, cod, $J_{C\text{-}P}$= 8.6 Hz), 117.7 (b, CH=, BAr_F), 120-135 (aromatic carbons), 135.0 (b, CH=, BAr_F), 135-158 (aromatic carbons), 161.9 (q, C-B, BAr_F, ^1J= 49 Hz). Anal. calcd (%) for $C_{72}H_{66}BF_{24}IrNO_3P$: C 51.37, H 3.95, N 0.83; found: C 51.34, H 3.92, N 0.80.

[Ir(cod)(L48a)]BAr_F. Yield: 123 mg (94%). ^{31}P NMR ($CDCl_3$), δ: 108.4 (s). ^{1}H NMR ($CDCl_3$), δ: 1.08 (s, 9H, CH_3, ^{t}Bu), 1.16 (s, 9H, CH_3, ^{t}Bu), 1.32 (s, 9H, CH_3, ^{t}Bu), 1.37 (s, 9H, CH_3, ^{t}Bu), 1.41 (s, 9H, CH_3, ^{t}Bu), 2.01 (b, 2H, CH_2, cod), 2.21 (b, 4H, CH_2, cod), 2.36 (b, 2H, CH_2, cod), 4.24 (b, 1H, CH=, cod), 4.34 (b, 1H, CH=, cod), 5.19 (b, 1H, CH=, cod), 5.21 (b, 1H, CH=, cod), 5.27 (m, 1H, CH-O), 7.1-8.7 (m, 20H, CH=). ^{13}C NMR ($CDCl_3$), δ: 24.8 (b, CH_2, cod), 26.8 (CH_3, ^{t}Bu), 29.9 (b, CH_2, cod), 30.5 (C, ^{t}Bu), 30.7 (CH_3, ^{t}Bu), 31.1 (CH_3, ^{t}Bu), 31.1 (CH_3, ^{t}Bu), 31.2 (CH_3, ^{t}Bu), 31.4 (C, ^{t}Bu), 34.6 (b, CH_2, cod), 34.7 (C, ^{t}Bu), 35.0 (C, ^{t}Bu), 35.4 (C, ^{t}Bu), 36.4 (b, CH_2, cod), 63.5 (b, CH=, cod), 66.2 (b, CH=, cod), 89.5 (CH-O), 101.0 (d, CH=, cod, $J_{C\text{-}P}$= 16.4 Hz), 104.1 (d, CH=, cod, $J_{C\text{-}P}$= 18.2 Hz), 117.7 (b, CH=, BAr_F), 120-131 (aromatic carbons), 135.0 (b, CH=, BAr_F), 138-155 (aromatic carbons), 161.9 (q, C-B, BAr_F, ^1J= 49 Hz). Anal. Calc (%) for $C_{78}H_{78}BF_{24}IrNO_3P$: C 53.01, H 4.45, N 0.79; found. C 52.97, H 4.43, N 0.76.

[Ir(cod)(L48e)]BAr_F. Yield: 114 mg (92%). ^{31}P NMR ($CDCl_3$), δ: 106.5 (s). ^{1}H NMR ($CDCl_3$), δ: 1.05 (s, 9H, CH_3, ^{t}Bu), 1.09 (s, 9H, CH_3, ^{t}Bu), 1.37 (s, 9H, CH_3, ^{t}Bu), 1.55 (s, 3H, CH_3, Ar-Me), 1.74 (s, 3H, CH_3, Ar-Me), 1.95 (b, 2H, CH_2, cod), 2.05 (b, 4H, CH_2, cod), 2.33 (b, 2H, CH_2, cod), 2.60 (s, 3H, CH_3, Ar-Me), 2.62 (s, 3H, CH_3, Ar-Me), 4.31 (b, 1H, CH=, cod), 4.32 (b, 1H, CH=, cod), 4.40 (b, 1H, CH=, cod), 5.36 (b, 1H, CH=, cod), 5.38 (m, 1H, CH-O), 7.0-8.7 (m, 18H, CH=). ^{13}C NMR ($CDCl_3$), δ: 16.4 (CH_3, Ar-Me), 16.5 (CH_3, Ar-Me), 20.2 (CH_3, Ar-Me), 20.4 (CH_3, Ar-Me), 24.7 (b, CH_2, cod), 27.7 (CH_3, ^{t}Bu), 28.3 (b, CH_2, cod), 29.7 (C, ^{t}Bu), 31.5 (CH_3, ^{t}Bu), 31.6 (CH_3,

^{t}Bu), 34.4 (b, CH_2, cod), 34.5 (C, ^{t}Bu), 35.0 (C, ^{t}Bu), 36.9 (b, CH_2, cod), 67.6 (b, CH=, cod), 69.6 (b, CH=, cod), 88.2 (CH-O), 97.4 (d, CH=, cod, J_{C-P}= 23.2 Hz), 102.9 (d, CH=, cod, J_{C-P}= 11.7 Hz), 117.7 (b, CH=, BAr_F), 120-134 (aromatic carbons), 135.0 (b, CH=, BAr_F), 135-157 (aromatic carbons), 161.9 (q, C-B, BAr_F, ^1J= 49 Hz). Anal. calcd (%) for $C_{74}H_{70}BF_{24}IrNO_3P$: C 51.94, H 4.12, N 0.82; found: C 51.90, H 4.09, N 0.79.

[Ir(cod)(L49c)]BAr_F. Yield: 114 mg (91%). ^{31}P NMR ($CDCl_3$), δ: 103.2 (s). ^{1}H NMR ($CDCl_3$), δ: 0.21 (s, 9H, CH_3, $SiMe_3$), 0.24 (s, 9H, CH_3, $SiMe_3$), 1.74 (b, 2H, CH_2, cod), 1.90 (b, 2H, CH_2, cod), 2.17 (b, 2H, CH_2, cod), 2.49 (b, 2H, CH_2, cod), 4.17 (b, 1H, CH=, cod), 4.37 (b, 1H, CH=, cod), 4.77 (b, 1H, CH=, cod), 5.52 (b, 1H, CH=, cod), 7.02 (m, 1H, CH-O), 7.1-8.7 (m, 27H, CH=). ^{13}C NMR ($CDCl_3$), δ: 0.2 (CH_3, $SiMe_3$), 1.1 (CH_3, $SiMe_3$), 25.6 (b, CH_2, cod), 28.9 (b, CH_2, cod), 34.9 (b, CH_2, cod), 36.8 (d, CH_2, cod, J_{C-P}= 6.2 Hz), 67.6 (b, CH=, cod), 72.3 (b, CH=, cod), 82.3 (d, CH, J_{C-P}= 7.2 Hz), 101.2 (d, CH=, cod, J_{C-P}= 20.4 Hz), 105.4 (d, CH=, cod, J_{C-P}= 12.0 Hz), 117.7 (b, CH=, BAr_F), 120-134 (aromatic carbons), 135.0 (b, CH=, BAr_F), 136-160 (aromatic carbons), 161.9 (q, C-B, BAr_F, ^1J= 49 Hz). Anal. Calc (%) for $C_{70}H_{58}BF_{24}IrNO_3PSi_2$: C 49.24, H 3.24, N 0.82; found. C 49.21, H 3.22, N 0.80.

[Ir(cod)(L49e)]BAr_F. Yield: 122 mg (94%). ^{31}P NMR ($CDCl_3$), δ: 101.0 (s). ^{1}H NMR ($CDCl_3$), δ: 1.53 (s, 9H, CH_3, ^{t}Bu), 1.60 (s, 9H, CH_3, ^{t}Bu), 2.08 (s, 3H, CH_3, Ar-Me), 2.15 (s, 3H, CH_3, Ar-Me), 2.02 (b, 2H, CH_2, cod), 2.39 (b, 4H, CH_2, cod), 2.49 (b, 2H, CH_2, cod), 2.59 (s, 3H, CH_3, Ar-Me), 2.63 (s, 3H, CH_3, Ar-Me), 3.63 (b, 1H, CH=, cod), 4.29 (b, 1H, CH=, cod), 5.32 (b, 1H, CH=, cod), 5.48 (b, 1H, CH=, cod), 6.75 (m, 1H, CH-O), 7.5-8.9 (m, 23H, CH=). ^{13}C NMR ($CDCl_3$), δ: 16.7 (b, CH_3, Ar-Me), 20.4 (CH_3, Ar-Me), 20.5 (CH_3, Ar-Me), 25.2 (b, CH_2, cod), 28.9 (b, CH_2, cod), 31.3 (b, CH_2, cod), 31.7 (CH_3, ^{t}Bu), 32.5 (CH_3, ^{t}Bu), 35.0 (C, ^{t}Bu), 35.2 (C, ^{t}Bu), 36.9 (b, CH_2, cod), 62.8 (b, CH=, cod), 66.5 (b, CH=, cod), 85.8 (CH-O), 103.2 (d, CH=, cod, J_{C-P}= 14 Hz), 105.8 (d, CH=, cod, J_{C-P}= 18.6 Hz), 117.7 (b, CH=, BAr_F), 120-135 (aromatic carbons), 135.0 (b, CH=, BAr_F), 135-157 (aromatic carbons), 161.9 (q, C-B, BAr_F, ^1J= 49 Hz). Anal. calcd (%) for $C_{76}H_{66}BF_{24}IrNO_3P$: C 52.72, H 3.84, N 0.81; found: C 52.69, H 3.82, N 0.78.

3.6.5.5. Typical procedure for the hydrogenation of olefins

The alkene (1 mmol) and Ir complex (0.2 mol%) were dissolved in CH_2Cl_2 (2 mL) in a high-pressure autoclave. The autoclave was purged four times with hydrogen. Then, it was pressurized at the desired pressure. After the desired reaction time, the autoclave was depressurised and the solvent evaporated off. The residue was dissolved in Et_2O (1.5 ml) and filtered through a short celite plug. The enantiomeric excess was determined by chiral GC or chiral HPLC and conversions were determined by ^{1}H NMR. The enantiomeric excesses of hydrogenated products were determined using the conditions previously described.[5d-q,8c]

3.6.6. Acknowledgements

We would like to thank the Spanish Government for providing grant CTQ2010-15835, the Catalan Government for grant 2009SGR116, and the ICREA Foundation for providing M. Diéguez and O. Pàmies with financial support through the ICREA Academia awards.

3.6.7. References

[1] a) *Catalytic Asymmetric Synthesis*, 2nd, ed.; Ojima, I., Ed.; Wiley-VCH: New York, 2000. b) *Asymmetric Catalysis in Organic Synthesis*; Noyori, R., Ed.; Wiley: New York, 1994. c) *Asymmetric Catalysis on Industrial Scale*; Blaser, H.-U., Schmidt, E., Eds.; Wiley: New York, 2004. d) Brown, J. M. in *Comprehensive Asymmetric Catalysis*; Jacobsen, E. N., Pfaltz, A., Yamamoto, H., Eds.; Springer-Verlag: Berlin, 1999, Vol.1.

[2] For recent reviews, see: a) Källström, K.; Munslow, I.; Andersson, P. G. *Chem. Eur. J.* **2006**, *12*, 3194. b) Roseblade, S. J.; Pfaltz, A. *Acc. Chem. Res.* **2007**, *40*, 1402. c) Church, T. L.; Andersson, P. G. *Coord. Chem. Rev*. **2008**, *252*, 513. d) Cui, X.; Burgess, K. *Chem. Rev.* **2005**, *105*, 3272. e) Pàmies, O.; Andersson, P. G.; Diéguez, M. *Chem. Eur. J.* **2010**, *16*, 14232. f) Woodmansee, D. H.; Pfaltz, A. *Chem. Commun.* **2011**, *47*, 7912.

[3] Chelating oxazoline-carbene ligands, mainly developed by Burgess and coworkers, have also been successful used and also to a less extent chiral diphosphines. See for instance: (a) Perry, M. C.; Cui, X.; Powell, M. T.; Hou, D. R.; Reibenspies, J. H,.; Burgess, K. *J. Am. Chem. Soc.* **2003**, *125*, 113. (b) Cui, X.; Burgess, K. *J. Am. Chem. Soc.* **2003**, *125*, 14212. (c) Cui, X.; Ogle, J. W.; Burgess, K. *Chem. Commun.* **2005**, 672. (d) Zhao, J.; Burgess, K. *J. Am. Chem. Soc.* **2009**, *131*, 13236. (e) Co, T. T.; Kim, T. J. *Chem. Commun.* **2006**, 3537. (f) Forman, G. S.; Ohkuma, T.; Hems, W. P.; Noyori, R. *Tetrahedron Lett.* **2000**, *41*, 9471.

[4] Very recently, the ligand scope has been extended to the use of other non-nitrogen containing heterodonor ligands like P,O and P,S. See: a) Rageot, D.; Woodmansee, D. H.; Pugin, B.; Pfaltz, A. *Angew. Chem. Int. Ed.* **2011**, *50*, 9598. b) Coll, M.; Pàmies, O.; Diéguez, M. *Chem. Commun.* **2011**, *47*, 9215.

[5] See for instance: a) Perry, M. C.; Cui, X.; Powell, M. T.; Hou, D. –R.; Reibenspies, J. H.; Burgess, K. *J. Am. Chem. Soc.* **2003**, *125*, 5391. b) Blankestein, J.; Pfaltz, A. *Angew. Chem. Int. Ed.* **2001**, *40*, 4445. c) Kaiser, S.; Smidt, S.P.; Pfaltz, A. *Angew. Chem. Int. Ed.* **2006**, *45*, 5194. d) Källström, K.; Hedberg, C.; Brandt, P.; Bayer, P.; Andersson, P. G. *J. Am. Chem. Soc.* **2004**, *126*, 14308. e) Engman, M.; Diesen, J. S.; Paptchikhine, A.; Andersson, P. G. *J. Am. Chem. Soc.* **2007**, *129*, 4536. f) Trifonova, A.; Diesen, J. S.; Andersson, P. G. *Chem. Eur. J.* **2006**, *12*, 2318. g) Menges, G.; Pfaltz, A. *Adv. Synth. Catal.* **2002**, *334*, 4044. h) Drury III, W. J.; Zimmermann, N.; Keenan, M.; Hayashi, M.; Kaiser, S.; Goddard, R.; Pfaltz, A. *Angew. Chem. Int. Ed.* **2004**, *43*, 70. i) Hedberg, C.; Källström, K.; Brandt, P.; Hansen, L. K.; Andersson, P. G. *J. Am. Chem. Soc.* **2006**, *128*, 2995. j) Franzke, A.; Pfaltz A. *Chem. Eur. J.* **2011**, *17*, 4131. k) Tang, W.; Wang, W.; Zhang, X. *Angew. Chem. Int. Ed.* **2003**, *42*, 943. l) Hou, D. –R.; Reibenspies, J.; Colacot, T. J.; Burgess, K. *Chem. Eur. J.* **2001**, *7*, 5391. m) Cozzi, P. G.; Menges, F.; Kaiser, S. *Synlett* **2003**, 833. n) Lightfoot, A.; Schnider, P.; Pfaltz, A. *Angew. Chem. Int. Ed.* **1998**, *37*, 2897. o) Menges, F.; Neuburger, M.; Pfaltz, A. *Org. Lett.* **2002**, *4*, 4713. p) Liu, D.; Tang, W.; Zhang, X. *Org. Lett.* **2004**, *6*, 513. q) Lu, S.-M; Bolm, C. *Angew. Chem. Int. Ed.* **2008**, *47*, 8920. r) Lu, W.-J.; Chen, Y.-W.; Hou, X.-L. *Adv. Synth. Catal.* **2010**, *352*, 103. s) Paptchikhine, A.; Cheruku, P.; Engman, M.; Andersson, P. G. *Chem. Commun.* **2009**, 5996.

[6] Zalubovskis, R.; Hörmann, E.; Pfaltz, A.; Moberg, C. *ARKIVOK* **2008**, 58.

[7] a) Bell, S.; Wüstenberg, B.; Kaiser, S.; Menges, F.; Netscher, T.; Pflatz, A. *Science* **2006**, *311*, 642. b) Woodmansee, D. H.; Müller, M.-A.; Neuburger, M.; Pfaltz, A. *Chem. Sci.* **2010**, *1*, 72.

[8] a) Diéguez, M.; Mazuela, J.; Pàmies, O.; Verendel, J. J.; Andersson, P. G. *J. Am. Chem. Soc.* **2008**, *130*, 7208. b) Diéguez, M.; Mazuela, J.; Pàmies, O.; Verendel, J. J.; Andersson, P. G. *Chem. Commun.* **2008**, 3888. c) Mazuela, J.; Verendel, J. J.; Coll, M.; Schäffner, B.; Börner, A.; Andersson, P. G.; Pàmies, O.; Diéguez, M. M. *J. Am. Chem. Soc.* **2009**, *131*, 12344. d) Mazuela, J.;

Paptchikhine, A.; Pàmies, O.; Andersson, P. G.; Diéguez, M. *Chem. Eur. J.* **2010**, 16, 4567. e) Mazuela, J.; Norrby, P.-O.; Andersson, P. G.; Pàmies, O.; Diéguez, M. *J. Am. Chem. Soc.* **2011**, *133*, 13634.

[9] Margalef, J.; Lega, M.; Ruffo, F.; Pàmies, O.; Diéguez, M. *Tetrahedron: Asymmetry* **2012**, *23*, 945.

[10] See for instance: a) van Leeuwen, P. W. N. M.; Kamer, P. C. J.; Claver, C.; Pàmies, O.; Diéguez, M. *Chem. Rev.* **2011**, *111*, 2077. b) *Heterocyclic Chemistry*, 4th Edition; Joule, J. A.; Mills, K., Eds.; Blackwell Science Ltd.: Oxford, 2000.

[11] a) Uenishi, J.; Tanaka, T.; Nishiwaki, K.; Wakabayashi, S.; Oae, S.; Tsukube, H. *J. Org. Chem.* **1993**, *58*, 4382. b) Tsukube, H.; Uenishi, J.; Higaki, H.; Kikkawa, K.; Tanaka, T.; Wakabayashi, S.; Oae, S. *J. Org. Chem.* **1993**, *58*, 4389.

[12] Uenishi, J.; Hiraoka, T.; Hata, S.;Nishiwaki, K.; Yonemitsu, O. *J. Org. Chem*. **1998**, *63*, 2481.

[13] Horchler, C. L.; Murphy, M.; Steelman, G. B.; Empfield, J. R.; Forst, J. M.; Herzog, K. J.; Xiao, W.; Dyroff, M. C.; Lee, C-M. C.; Trivedi, S.; Neilson, K. L.; Keith, R. A. *Biorg. & Med. Chem. Lett.***2003**, *13*, 3553.

[14] Compounds **5** and **6** were prepared as in reference 5h.

[15] Pàmies, O.; Diéguez, M.; Net, G. ; Ruiz, A. ; Claver, C. *Organometallics* **2000,** *19,* 1488.

[16] The rapid ring inversions (tropoisomerization) in the biaryl phosphite moiety are usually stopped upon coordination to the metal center. See for example: a) Buisman, G. J. H.; van der Veen, L. A.; Klootwijk, A.; de Lange, W. G. J.; Kamer, P. C. J.; van Leeuwen, P. W. N. M.; Vogt, D. *Organometallics* **1997**, *16*, 2929. b) Diéguez, M.; Pàmies, O.; Ruiz, A.; Claver, C.; Castillón, S. *Chem. Eur. J.* **2001**, *7*, 3086. c) Pàmies, O.; Diéguez, M.; Net, G.; Ruiz, A.; Claver, C. *Organometallics* **2000**, *19*, 1488. d) Pàmies, O.; Diéguez, M.; Net, G.; Ruiz, A.; Claver, C. *J. Org. Chem.* **2001**, *66*, 8364. e) Pàmies, O.; Diéguez, M. *Chem. Eur. J.* **2008**, *14*, 944.

[17] Schrems, M. G.; Pfaltz, A. *Chem. Commun.* **2009**, 6210.

[18] Tolstoy, P.; Engman, M.; Paptchikhine, A.; Bergquist, J.; Church, T. L.; Leung, A. W. –M.; Andersson, P. G. *J. Am. Chem. Soc.* **2009**, *131*, 8855.

[19] a) Rovner, E. S.; Wein, A. *J. Eur. Urol.* **2002**, *41*, 6. b) Wefer, J.; Truss, M. C.; Jonas, U. *World J. Urol.* **2001**, *19*, 312. c) Hills, C. J.; Winter, S. A.; Balfour, J. A. *Drugs* **1998**, *55*, 813. (d) McRae, A. L.; Brady, K. T. *Expert Opin. Pharmacother.* **2001**, *2*, 883.

[20] For successful application of Ir-catalysts, see: a) McIntyre, S.; Hörmann, E.; Menges, F.; Smidt, S. P.; Pfaltz, A. *Adv. Synth. Catal.* **2005**, *347*, 282. b) ref. 4b.

[21] For successful applications of Sm-, Ru- and Rh-complexes, see: a) Conticello, V. P.; Brard, L.; Giardello, M. A.; Tsuji, Y.; Sabat, M.; Stern, C. L.; Marks, T. J. *J. Am. Chem. Soc.* **1992**, *114*, 2761. b) Giardello, M. A.; Conticello, V. P.; Brard, L.; Gagné, M. R.; Marks, T. J. *J. Am. Chem. Soc.* **1994**, *116*, 10241. c) Co, T. T.; Kim, T. J. *Chem. Commun.* **2006**, 3537. d) Forman, G. S.; Ohkuma, T.; Hems, W. P.; Noyori, R. *Tetrahedron Lett.* **2000**, *41*, 9471.

[22] a) Fessard, T. C.; Andrews, S. P.; Motoyohsi, H.; Carreira, E. *Angew. Chem. Int. Ed.* **2007**, *46*, 9331. b) Prat, L.; Dupas, G.; Duflos, J.; Quéguiner, G.; Bourguignon, J.; Levacher, V. *Tetrahedron Lett.* **2001**, *42*, 4515. c) Wilkinson, J. A.; Rossington, S. B.; Ducki, S.; Leonard, J.; Hussain, N. *Tetrahedron* **2006**, *62*, 1833.

[23] a) Okamoto, K.; Nishibayashi, Y.; Uemura, S.; Toshimitsu, A. *Angew. Chem. Int. Ed.* **2005**, *44*, 3588. b) Hatanaka, Y.; Hiyama, T. *J. Am. Chem. Soc.* **1990**, *112*, 7793.

[24] See for instance: a) Abate, A.; Brenna, E. Fuganti, C.; Gatti, G. G.; Givenzana, T.; Malpezzi, L.; Serra, S. *J. Org. Chem.* **2005**, *70*, 1281. b) Drescher, K.; Haupt, A.; Unger, L.; Rutner, S. C.; Braje, W:; Grandel, R.; Henry, C.; Backfisch, G:; Beyerbach, A.; Bisch, W. *WO Patent* 2006/040182 A1.

[25] See for instance: a) Schlosser, M. *Angew. Chem. Int. Ed.* **1998**, *37*, 1496. b) Smart, B. E. *J. Fluorine Chem.* **2001**, *109*, 3. c) *Asymmetric Fluoroorganic Chemistry: Synthesis, Application and Future Direction;* Ramachandran, P. V., Ed.; American Chemical Society: Washington DC, 2000. d) A special issue has been devoted to "Fluorine in the Life Sciences" *Chem BioChem* **2004**, *5*, 559.

[26] See for instance: a) Fleming, I.; Barbero, A.; Walter, D. *Chem. Rev.* **1997**, *97*, 2063. b) Jones, G. R.; Landais, Y. *Tetrahedron* **1996**, *52*, 7599. c) Bains, W.; Tacke, R. *Curr. Opin. Drug Discv. Dev.* **2003**, *6*, 526.

[27] Buisman, G. J. H.; Kamer, P. C. J.; van Leeuwen, P. W. N. M. *Tetrahedron: Asymmetry* **1993**, *4*, 1625.

3.6.8 Supporting Information

Table 3.6.4. Ir-catalyzed asymmetric hydrogenation of trisubstituted olefins using ligands **L38-L49a-g**[a]

Entry	Ligand	Substrate	% Conv[b]	% ee[c]	Entry	Ligand	Substrate	% Conv[b]	% ee[c]
1	**L38a**	**S3**	100	60 (*S*)	23	**L38a**	**S6**	100	74 (*R*)
2	**L38b**	**S3**	100	50 (*S*)	24	**L38b**	**S6**	100	79 (*R*)
3	**L38d**	**S3**	100	29 (*S*)	25	**L38d**	**S6**	100	75 (*R*)
4	**L38e**	**S3**	100	62 (*S*)	26	**L38e**	**S6**	100	31 (R)
5	**L39a**	**S3**	100	89 (*S*)	27	**L39a**	**S6**	100	73 (R)
6	**L39d**	**S3**	100	86 (*S*)	28	**L41a**	**S6**	100	67 (*R*)
7	**L41a**	**S3**	100	65 (*S*)	29	**L42a**	**S6**	100	71 (*R*)
8	**L42a**	**S3**	100	87 (*S*)	30	**L43a**	**S6**	100	84 (*R*)
9	**L43a**	**S3**	100	81 (*S*)	31	**L46a**	**S6**	100	76 (S)
10	**L46a**	**S3**	100	61 (*R*)	32	**L47a**	**S6**	64	73 (*S*)
11	**L47e**	**S3**	100	97 (*R*)	33	**L49c**	**S6**	100	90 (*S*)
12	**L38a**	**S4**	100	61 (*S*)	34	**L38a**	**S7**	100	89 (*R*)
13	**L38b**	**S4**	100	52 (*S*)	35	**L38d**	**S7**	100	7 (*R*)
14	**L38d**	**S4**	100	32 (*S*)	36	**L39e**	**S7**	100	80 (*R*)
15	**L38e**	**S4**	100	61 (*S*)	37	**L43a**	**S7**	100	54 (*R*)
16	**L39a**	**S4**	100	91 (*S*)	38	**L46e**	**S7**	100	96 (*S*)
17	**L39d**	**S4**	100	86 (*S*)	39	**L38a**	**S12**	100	67 (+)
18	**L41a**	**S4**	100	66 (*S*)	40	**L38d**	**S12**	100	67 (+)
19	**L42a**	**S4**	100	85 (*S*)	41	**L38e**	**S12**	100	26 (+)
20	**L43a**	**S4**	100	79 (*S*)	42	**L39d**	**S12**	100	7 (+)
21	**L46a**	**S4**	100	61 (*R*)	43	**L43d**	**S12**	100	94 (+)
22	**L47e**	**S4**	100	98 (*R*)	44	**L46a**	**S12**	100	66 (-)

[a] Reactions carried out by using 1 mmol of substrate and 1 mol% of Ir-catalyst precursor at 50 bar of H_2 using dichloromethane (2 mL) as solvent. [b] Conversion measured by ^{1}H-NMR after 2 h. [c] Enantiomeric excess determined by GC.

Table 3.6.5. Ir-catalyzed asymmetric hydrogenation of trisubstituted olefins bearing a neighboring polar group using ligands **L38**-**L49a**-**g**[a]

Entry	Ligand	Substrate	% Conv[b]	% ee[c]	Entry	Ligand	Substrate	% Conv[b]	% ee[c]
1	**L38a**	**S13**	100	88 (*S*)	26	**L38e**	**S17**	100	79 (*S*)
2	**L38b**	**S13**	100	86 (*S*)	27	**L39a**	**S17**	100	61 (*S*)
3	**L38d**	**S13**	100	79 (*S*)	28	**L41a**	**S17**	100	72 (*S*)
4	**L38e**	**S13**	100	89 (*S*)	29	**L42d**	**S17**	100	54 (*S*)
5	**L39a**	**S13**	100	41 (*S*)	30	**L42e**	**S17**	100	92 (*S*)
6	**L41a**	**S13**	100	25 (*S*)	31	**L43d**	**S17**	100	34 (*S*)
7	**L42a**	**S13**	100	96(*S*)	32	**L45a**	**S17**	100	70 (*S*)
8	**L42d**	**S13**	100	96 (*S*)	33	**L46a**	**S17**	100	76 (*R*)
9	**L43a**	**S13**	100	61 (*S*)	34	**L38a**	**S16**	100	5 (*S*)
10	**L45a**	**S13**	100	29 (*S*)	35	**L38b**	**S16**	100	5 (*S*)
11	**L46a**	**S13**	100	88 (*R*)	36	**L38d**	**S16**	100	48 (*S*)
12	**L38a**	**S16**	100	82 (*S*)	37	**L38e**	**S16**	100	30 (*S*)
13	**L38b**	**S16**	100	78 (*S*)	38	**L39a**	**S16**	100	77 (*S*)
14	**L38d**	**S16**	100	51 (*S*)	39	**L39d**	**S16**	100	75 (*S*)
15	**L38e**	**S16**	100	80 (*S*)	40	**L41a**	**S16**	100	8 (*S*)
16	**L39a**	**S16**	100	63 (*S*)	41	**L42a**	**S16**	100	13 (*S*)
17	**L41a**	**S16**	100	76 (*S*)	42	**L43a**	**S16**	100	73 (*S*)
18	**L42d**	**S16**	100	59 (*S*)	43	**L44a**	**S16**	100	44 (*S*)
19	**L42e**	**S16**	100	96 (*S*)	44	**L45a**	**S16**	100	61 (*S*)
20	**L43d**	**S16**	100	34 (*S*)	45	**L39a**	**S20**	100	14 (*S*)
21	**L45a**	**S16**	100	71 (*S*)	46	**L39d**	**S20**	100	69 (*S*)
22	**L46a**	**S16**	100	82 (*R*)	47	**L39e**	**S20**	100	70 (*S*)
23	**L38a**	**S17**	100	81 (*S*)	48	**L40a**	**S20**	100	16 (*S*)
24	**L38b**	**S17**	100	74 (*S*)	49	**L41a**	**S20**	100	52 (*S*)
25	**L38d**	**S17**	100	50 (*S*)	50	**L42d**	**S20**	100	70 (*S*)

[a] Reactions carried out by using 1 mmol of substrate and 1 mol% of Ir-catalyst precursor at 50 bar of H_2 using dichloromethane (2 mL) as solvent. [b] Conversion measured by ^{1}H-NMR after 2 h. [c] Enantiomeric excess determined by GC or HPLC.

Table 3.6.6. Ir-catalyzed asymmetric hydrogenation of 1,1-disubstituted olefins using ligands **L38**-**L49a**-**g**[a]

Entry	L	Substrate	% Conv[b]	% ee[c]	Entry	L	Substrate	% Conv[b]	% ee[c]
1	**L38a**	**S26**	100	47 (*R*)	27	**L38a**	**S31**	100	45 (*R*)
2	**L38c**	**S26**	100	49 (*R*)	28	**L38c**	**S31**	100	43 (*R*)
3	**L38d**	**S26**	100	42 (*S*)	29	**L38d**	**S31**	100	38 (*S*)
4	**L38e**	**S26**	100	57 (*R*)	30	**L38e**	**S31**	100	53 (*R*)
5	**L39a**	**S26**	100	70 (*R*)	31	**L39a**	**S31**	100	68 (*R*)
6	**L40a**	**S26**	100	41 (*R*)	32	**L40a**	**S31**	100	40 (*R*)
7	**L41a**	**S26**	100	21 (*R*)	33	**L41a**	**S31**	100	17 (*R*)
8	**L42a**	**S26**	100	62 (*R*)	34	**L42a**	**S31**	100	61 (*R*)
9	**L43a**	**S26**	100	64 (*R*)	35	**L43a**	**S31**	100	59 (*R*)
10	**L44a**	**S26**	100	32 (*R*)	36	**L44a**	**S31**	100	26 (*R*)
11	**L46a**	**S26**	100	47 (*S*)	37	**L46a**	**S31**	100	45 (*S*)
12	**L38a**	**S27**	100	45 (*R*)	38	**L38a**	**S33**	100	47 (-)
13	**L38c**	**S27**	100	46 (*R*)	39	**L39a**	**S33**	100	69 (-)
14	**L38d**	**S27**	100	40 (*S*)	40	**L41a**	**S33**	100	23 (-)
15	**L38e**	**S27**	100	59 (*R*)	41	**L42a**	**S33**	100	64 (-)
16	**L39a**	**S27**	100	72 (*R*)	42	**L46a**	**S33**	100	46 (+)
17	**L40a**	**S27**	100	42 (*R*)	43	**L38a**	**S37**	100	75 (*S*)
18	**L43a**	**S27**	100	61 (*R*)	44	**L39a**	**S37**	100	66 (*S*)
19	**L44a**	**S27**	100	33 (*R*)	45	**L42a**	**S37**	100	81 (*S*)
20	**L46a**	**S27**	100	46 (*S*)	46	**L42d**	**S37**	100	45 (*S*)
21	**L39a**	**S29**	100	46 (*R*)	47	**L46a**	**S37**	100	75 (*R*)
22	**L39a**	**S29**	100	70 (*R*)	48	**L38a**	**S40**	100	55 (*S*)
23	**L40a**	**S29**	100	41 (*R*)	49	**L39a**	**S40**	100	79 (*S*)
24	**L43a**	**S29**	100	59 (*R*)	50	**L39d**	**S40**	100	59 (*R*)
25	**L44a**	**S29**	100	30 (*R*)	51	**L42a**	**S40**	100	48 (*S*)
26	**L46a**	**S29**	100	46 (*S*)	52	**L46a**	**S40**	100	57 (*R*)

[a] Reactions carried out by using 1 mmol of substrate and 1 mol% of Ir-catalyst precursor at 50 bar of H_2 using dichloromethane (2 mL) as solvent. [b] Conversion measured by ^{1}H-NMR after 2 h. [c] Enantiomeric excess determined by GC.

Chapter 4

Asymmetric allylic substitution reactions

4. Asymmetric allylic substitution reactions

4.1 Background

As we discussed in the introduction most of the successful ligands reported to date for Pd-catalyzed allylic substitution reactions have been designed using two main strategies. The first one was to increase the ligand's bite angle in order to create a chiral cavity in which the allyl system is perfectly embedded. This idea paved the way for the successful application of ligands with large bite angles for the allylic substitution of sterically undemanding substrates. The second strategy was the use of heterodonor ligands that result in an electronic discrimination of the two allylic terminal carbon atoms due to the different *trans* influences of the donor groups. This made it possible to successfully use a wide range of heterodonor ligands (mainly P,N-ligands) in allylic substitution reactions. More recently, we found that the use of biaryl phosphite-containing heterodonor ligands is highly advantageous by overcoming the most common limitations of this process, such as low reaction rates and high substrate specificity. Introducing a biaryl phosphite in the ligand design was beneficial because of its larger π-acceptor ability, which increases reaction rates, and because of its flexibility that allows the catalyst chiral pocket to adapt to both hindered and unhindered substrates. In addition, the presence of a biaryl phosphite moiety was also beneficial in the allylic substitution of more challenging monosubstituted substrates. In this respect, in 2008 we reported the successful application of the phosphite-oxazoline ligand library **L6**-**L21**, previously synthesized in chapter 3, in the Pd-catalyzed allylic substitution of several substrates with different steric proprieties. However the enantioselectivity obtained in unhindered cyclic substrates was not completely satisfactory. One the other hand, the potential of phosphite-containing ligands is limited to the use of dimethyl malonate as nucleophile. The use of other types of carbon nucleophiles still required much attention. Although the substrate versatility has recently increased, there are still important substrate classes that give unsatisfactory results with known catalysts. For example, for trisubstituted substrates, which allow the formation of enantiomerically enriched acid derivatives and lactones, more active and enantioselective Pd-catalysts are needed. This encourages further research into phosphite-nitrogen ligands.

Most of the research has been focused on phosphorus-oxazoline ligands. In recent years the range of heterodonor-phosphorous-nitrogen ligands has been extended to include more robust N-donor groups than oxazolines, but with moderate success. In this respect, phosphine/phosphinite-pyridine compounds are an important class of ligands. However, only few of them have been successfully applied and these are limited in the substrate scope. More research is therefore needed to find more robust and versatile Pd-catalytic systems.

In this chapter, we therefore report the synthesis and screening of 3 large modular phosphite-nitrogen ligand libraries for asymmetric Pd-catalyzed allylic substitution reactions. More specifically, in section 4.2 we describe the application of the phosphite-thiazoline ligand library **L27**-**L28a**-**k**, previously synthesized in chapter 3, in the Pd-catalyzed allylic substitution of a wide range of mono-, di- and trisubstituted substrates using several carbon nucleophiles, including the less studied α-substituted malonates and β-diketones. These ligands are based on previous phosphite-oxazoline **L6**-**L21**, in which the oxazoline group is replaced by a thiazoline moiety. We thought that the introduction of a thiazoline moiety will create a smaller chiral pocket more suitable

for unhindered cyclic substrates, while maintaining the flexibility conferred by the biaryl phosphite group. For the purpose of comparison, we have also expanded our previous work on phosphite-oxazoline ligands **L6**-**L21** to the use of other carbon-nucleophiles and to the alkylation of challenging trisubstituted substrates. By the correct combination of substrate and ligand type (P-oxazoline or P-thiazoline), we have identified one of the few catalytic systems that provided high regio- and enantioselectivities in both enantiomers of the alkylation product for several hindered and unhindered mono-, di- and trisubstituted substrates using a wide range of carbon-nucleophiles. We also discuss the synthesis and characterization of the Pd-π-allyl intermediates in order to provide greater insight into the origin of enantioselectivity in these catalytic systems. In the next two sections, we focus our research in the synthesis and application of heterodonor-phosphite-nitrogen ligands that include more robust N-donor groups (such as oxazole, thiazole and pyridine) than oxaxolines. In this respect in section 4.3 we describe the application of the phosphite-oxazole/thiazole ligand library **L29**-**L36a**-**g**, previously synthesized in chapter 3, in the Pd-catalyzed allylic substitution of a wide range of mono-, di- and trisubstituted substrates. By carefully selecting the ligand components, high regio- and enantioselectivities (ee's up to 96%) and good activities were achieved. The NMR and DFT studies on the Pd-π-allyl intermediates provided a deeper understanding of the effect of ligand parameters on the origin of enantioselectivity. In next section 4.4, we describe the first successful application of the phosphite-pyridine ligand library **L38**-**L49a**-**g**, previously synthesized in chapter 3, in the Pd-catalyzed allylic substitution reactions of several di- and trisubstituted substrates using a wide range of C-, N- and O-nucleophiles. Of particular note were the high enantioselectivities (up to >99% ee) obtained for the trisubstituted substrates, which compare favorably with the best that have been reported in the literature. The new phosphite-pyridine ligand library also performs well in alternative environmentally friendly solvents such as propylene carbonate and ionic liquids. Ionic liquids allowed the palladium catalyst to be reused while maintaining the excellent enantioselectivities. The NMR studies on the Pd-π-allyl intermediates provided a deeper understanding of the effect of ligand parameters on the origin of enantioselectivity.

4.2. Phosphite-thiazoline versus phosphite-oxazoline for Pd-catalyzed allylic substitution reactions. A case for comparison

Javier Mazuela, Oscar Pàmies and Montserrat Diéguez in manuscript to be submitted.

4.2.1 Abstract

We have expanded the ligand design of one of the most successful phosphite-oxazoline ligands (**L6**-**L21**) in Pd-catalyzed allylic alkylation by replacing the oxazoline group with a thiazoline moiety. These phosphite-thiazoline ligands have been evaluated in the Pd-catalyzed allylic substitution of a wide range of mono-, di- and trisubstituted substrates using several carbon nucleophiles, including the less studied α-substituted malonates and β-diketones. For hindered substrates such as disubstituted **S1** and trisubstituted **S8** and **S9**, enantioselectivities (ee's up to >99%) are best using phosphite-oxazoline ligands, while for unhindered cyclic substrates (**S3**-**S5**) enantioselectivities (ee's up to 94%) improved considerably when phosphite-thiazoline ligands were used. In the case of monosubstituted substrates the regio- and enantioselectivities obtained using both ligand types were comparable and excellent (regio's up to 90% and ee's up to 95%). Therefore, by correctly combining substrate and ligand type (P-oxazoline or P-thiazoline), we have identified one of the few catalytic systems that provide high regio- and enantioselectivities in both enantiomers of the alkylation product for several hindered and unhindered mono-, di- and trisubstituted substrates using a wide range of carbon-nucleophiles. We also discuss the synthesis and characterization of the Pd-π-allyl intermediates in order to provide greater insight into the origin of enantioselectivity in these catalytic systems.

4.2.2. Introduction

The formation of chiral carbon-carbon bonds is the most fundamental process in the synthesis of complex molecules from simple ones. Of all the carbon-carbon bond forming strategies, asymmetric Pd-catalyzed allylic substitution is the one that has received most attention for decades, mainly because of the mild reaction conditions required, the high functional group tolerance and the versatility of the alkene functionality adjacent to the chiral center for stereoselective functionalization.[1] In general, new catalysts make use of either ligands with large bite-angles to create a chiral cavity in which the allyl system is embedded (i.e. Trost's ligands)[2] or ligands containing different donor atoms, which can electronically discriminate the two allylic terminal carbon atoms due to the different *trans* influences of the donor groups.[3] This latter strategy made it possible to successfully use a wide range of heterodonor ligands, mainly P,N-ligands, in allylic substitution reactions.[1] More recently, we have found that the use of biaryl phosphite-containing heterodonor ligands is highly advantageous because they overcome such common limitations of the process as low reaction rates and high substrate specificity. Introducing a biaryl phosphite into the ligand design was beneficial because its larger π-acceptor ability increased reaction rates and its flexibility allowed the catalyst chiral pocket to adapt to both hindered and unhindered substrates.[4] The presence of a biaryl phosphite moiety was also beneficial in the allylic substitution of more challenging monosubstituted substrates.

Regioselectivity towards the desired branched isomer in this substrate class increased thanks to the π-acceptor ability of the phosphite moiety, which decreased the electron density of the most substituted allylic terminal carbon atom via the *trans* influence, favoring the nucleophilic attack to this carbon atom.[4,5]

In this context, in 2008 we developed a highly modular phosphite-oxazoline ligand library (**L6**-**L21**) from readily available hydroxyl amino acid derivatives (Figure 4.2.1).[6] By carefully selecting the ligand components we were able to identify privileged ligand backbones (**L10** and **L12**) that provided high enantioselectivities in this process. We therefore found that the best combinations were either methyl or phenyl substituents at the alkyl backbone chain (R^2) and either a phenyl or a 4-CF_3-C_6H_4 group at the oxazoline substituent (R^1). We also found that selecting the appropriate substituents/configurations at the biaryl phosphite moiety is highly substrate dependent.

Despite this success, the enantioselectivity obtained in unhindered cyclic substrates was not completely satisfactory.[6] On the other hand, the potential of phosphite-containing ligands is limited to the use of dimethyl malonate as nucleophile.[4] The use of other types of nucleophiles, more suitable for the synthesis of more complex chiral organic molecules, still required much attention. Although the substrate versatility has recently increased, there are still important substrate classes that give unsatisfactory results with known catalysts. For example, for trisubstituted substrates, which allow enantiomerically-enriched acid derivatives and lactones to be formed, the Pd-catalysts need to be more active and enantioselective.[1]

To address all these points, we decided to take one of the privileged ligand backbones (**L10**) and expand the ligand design by replacing the oxazoline group with a thiazoline moiety (ligands **L27** and **L28**, Figure 4.2.1). The reason for this modification is that the introduction of a thiazoline moiety will create a smaller chiral pocket more suitable for unhindered cyclic substrates, while maintaining the flexibility conferred by the biaryl phosphite group. We therefore report here the application of new phosphite-thiazoline ligands **L27**-**L28a**-**k** in the Pd-catalyzed allylic substitution of a wide range of mono-, di- and trisubstituted substrates using several carbon nucleophiles, including the less studied α-substituted malonates and β-diketones. The potential application of the allylic substitution using functionalized malonates has been demonstrated by the practical synthesis of the carbocyclic compound dimethyl (*R*)-2-phenylcyclopent-3-ene-1,1-dicarboxylate in enantiopure form using a simple sequential allylic alkylation and ring-closing metathesis reactions. We also compare the effectiveness of these phosphite-thiazoline ligands (**L27**-**L28a**-**k**) and related privileged phosphite-oxazoline ligands (**L10** and **L12**). To do so, we have expanded our previous work on phosphite-oxazoline ligands (**L10** and **L12**)[6] to cover carbon-nucleophiles other than dimethyl malonate and the alkylation of challenging trisubstituted substrates. By carefully selecting the substrate and ligand type (P-oxazoline or P-thiazoline) we have identified one of the few catalytic systems that provide high regio- and enantioselectivities in several substrate types using a wide range of C-nucleophiles. In this paper, we also discuss the synthesis and characterization of Pd-π-allyl intermediates in order to provide greater insight into the origin of enantioselectivity in these catalytic systems.

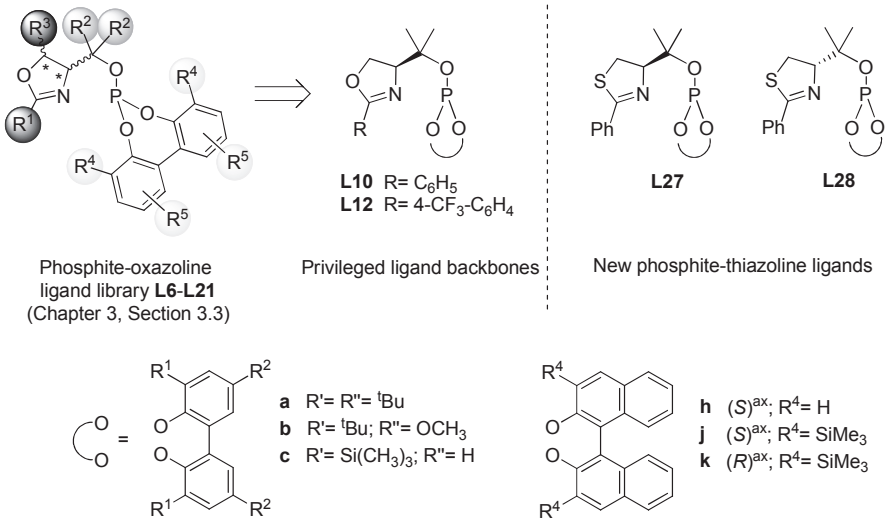

Figure 4.2.1. Phosphite-oxazoline/thiazoline ligands **L10**, **L12**, **L27** and **L28**.

4.2.3. Results and discussions

4.2.3.1. Synthesis of ligands

The new phosphite-thiazoline ligands **L27j-k** can be straightforwardly synthesized using the procedure previously described for ligands **L27**-**L28a**-**g** in Chapter 3, Section 3.4 (Scheme 4.2.1). They were therefore efficiently synthesized by reacting the corresponding thiazoline-alcohol **2** with 1 equiv of the appropriate *in situ* formed phosphorochloridite ($ClP(OR)_2$; $(OR)_2$= **j-k**) in the presence of pyridine. Thiazoline-alcohol **2** is prepared from easily accessible (*R*)-cysteine methyl ester hydrochloride (**1**) as shown in Scheme 4.2.1.

Ligands **L27j-k** were stable during purification on neutral alumina under an atmosphere of argon and isolated in good yields as white solids. They were stable at room temperature and very stable to hydrolysis. The elemental analysis was in agreement with the assigned structure. The ^1H, ^{13}C and ^{31}P NMR spectra were as expected for these C_1 ligands.

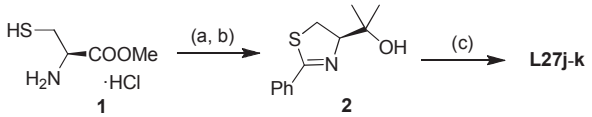

Scheme 4.2.1. Synthesis of new phosphite-thiazoline ligands **L27j-k**. (a) ethyl benzimidate hydrochloride [7]; (b) MeMgBr/THF/Et_2O; (c) $ClP(OR)_2$; $(OR)_2$ = **j-k** / Py / toluene.

4.2.3.2. Allylic substitution of symmetrical 1,3-disubstituted allylic substrates

In this section, we report the use of the new chiral phosphite-thiazoline ligands (**L27**-**L28a-k**) in the Pd-catalyzed allylic substitution of linear disubstituted substrates with different steric properties (Eq. 4.2.1a): *rac*-1,3-diphenyl-3-acetoxyprop-1-ene (**S1**) (widely used as a model

substrate) and *rac*-1,3-dimethyl-3-acetoxyprop-1-ene (**S2**); and cyclic substrates (Eq. 4.2.1b): *rac*-3-acetoxycyclohexene (**S3**) (widely used as a model substrate), *rac*-3-acetoxycyclopentene (**S4**) and *rac*-3-acetoxycycloheptene (**S5**). Several carbon-nucleophiles were tested, among which are the little studied α-substituted malonates and β-diketones. We also compared the effectiveness of these phosphite-thiazoline ligands with the results obtained using related phosphite-oxazoline ligands (**L10a**-**k**). To do so, we have also expanded our previous work on phosphite-oxazoline ligands (**L10** and **L12**) to cover carbon-nucleophiles other than dimethyl malonate. In all cases, the catalysts were generated *in situ* from the π-allyl-palladium chloride dimer $[PdCl(\eta^3\text{-}C_3H_5)]_2$ and the corresponding ligand.[1]

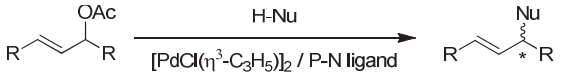

(4.2.1a)

S1 R= Ph
S2 R= Me

3 R= Ph; H-Nu= H-CH(COOMe)$_2$
4 R= Ph; H-Nu= H-CH(COOEt)$_2$
5 R= Ph; H-Nu= H-CH(COOBn)$_2$
6 R= Ph; H-Nu= H-CH(COMe)$_2$
7 R= Ph; H-Nu= H-CMe(COOMe)$_2$
8 R= Ph; H-Nu= H-CAllyl(COOMe)$_2$
9 R= Me; H-Nu= H-CH(COOMe)$_2$
10 R= Me; H-Nu= H-CH(COOBn)$_2$
11 R= Me; H-Nu= H-CH(COMe)$_2$
12 R= Me; H-Nu= H-CMe(COOMe)$_2$
13 R= Me; H-Nu= H-CAllyl(COOMe)$_2$

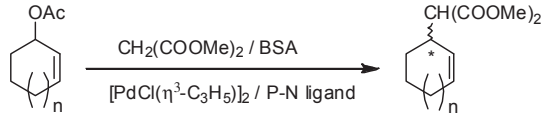

(4.2.1b)

S3 n=1
S4 n=0
S5 n=2

14 n=1; H-Nu= H-CH(COOMe)$_2$
15 n=1; H-Nu= H-CH(COOEt)$_2$
16 n=1; H-Nu= H-CH(COOBn)$_2$
17 n=1; H-Nu= H-CH(COMe)$_2$
18 n=1; H-Nu= H-CMe(COOMe)$_2$
19 n=1; H-Nu= H-CAllyl(COOEt)$_2$
20 n=0; H-Nu= H-CH(COOMe)$_2$
21 n=2; H-Nu= H-CH(COOMe)$_2$

Allylic substitution of symmetrical 1,3-disubstituted allylic substrates using dimethyl malonate as nucleophile

In the first set of experiments, we used the palladium-catalyzed asymmetric allylic substitution reactions of substrates **S1**-**S5**, with dimethyl malonate as nucleophile, to study the potential of the phosphite-thiazoline ligands (**L27**-**L28a**-**k**). For purposes of comparison, the reactions were conducted using the optimal reaction conditions found in our previous study of related phosphite-oxazoline ligands (**L10a**-**k**): that is, a ligand-to-palladium ratio of 1.1 and dichloromethane as solvent.[6] The results, which are shown in Table 4.2.1, indicated that substituents/configurations at the biaryl phosphite moiety had the same effect on catalytic performance (activity and enantioselectivity) as the related phosphite-oxazoline ligands (**L10a**-**k**) (i.e. Table 4.2.1, entries 1-6). Thus, while for linear substrates **S1** and **S2** enantioselectivities were best when an unsubstituted *S*-binol phosphite group was used (**h**; Table 4.2.1, entries 4 and 10), for the cyclic substrates, they were highest with the ligand bearing a trimethylsilyl *ortho*-disubstituted *S*-binol phosphite moiety (**j**; Table 4.2.1, entries 17, 19 and 20). As observed for phosphite-oxazoline ligands, the configuration of the alkylation product is governed by the configuration of the alkyl backbone chain. Both enantiomers of the alkylated product can therefore be obtained using

phosphite-thiazoline ligands **L27**-**L28a**-**k** (i.e. with the Pd/**L28a** catalytic system the opposite enantiomers of the alkylation products **3**, **9** and **14** were obtained in 65% (*R*), 37% (*S*) and 45% (*S*) ee, respectively).

Table 4.2.1. Selected results for the Pd-catalyzed allylic alkylation of **S1**-**S5** with dimethyl malonate[a]

			Phosphite-thiazoline (**L27**)		Phosphite-oxazoline (**L10**)	
Entry	Substrate	Ligand	% Conv (h)[b]	% ee[c]	% Conv (h)[b]	% ee[c]
1	**S1**	**a**	100 (0.25)[g]	66 (*S*)[d]	100 (0.25)	84 (*S*)
2	**S1**	**b**	100 (0.25)	67 (*S*)	100 (0.25)	85 (*S*)
3	**S1**	**c**	100 (0.25)	69 (*S*)	100 (0.25)	89 (*S*)
4	**S1**	**h**	100 (0.5)[g]	71 (*S*)	99 (0.5)	90 (*S*)
5	**S1**	**j**	100 (0.5)[g]	41 (*S*)	100 (0.5)	55 (*S*)
6	**S1**	**k**	100 (0.5)	67 (*S*)	100 (0.5)	88 (*S*)
7	**S2**	**a**	100 (1.5)[g]	36 (*R*)[e]	100 (1.5)	39 (*R*)
8	**S2**	**b**	100 (1.5)	21 (*R*)	100 (1.5)	25 (*R*)
9	**S2**	**c**	100 (1.5)	30 (*R*)	100 (1.5)	32 (*R*)
10	**S2**	**h**	100 (2)[g]	64 (*R*)	93 (2)	72 (*R*)
11	**S2**	**j**	100 (2)	52 (*R*)	100 (2)	58 (*R*)
12	**S2**	**k**	100 (2)	22 (*R*)	98 (2)	29 (*R*)
13	**S3**	**a**	100 (1.5)[g]	46 (*R*)[f]	88 (1.5)	42 (*R*)
14	**S3**	**b**	100 (2)	58 (*R*)	46 (2)	58 (*R*)
15	**S3**	**c**	100 (2)	32 (*R*)	50 (2)	60 (*R*)
16	**S3**	**h**	42 (2)	47 (*S*)	8 (2)	35 (*S*)
17	**S3**	**j**	100 (2)[g]	82 (*S*)	42 (2)	70 (*S*)
18	**S3**	**k**	100 (2)	75 (*R*)	58 (2)	58 (*R*)
19	**S4**	**j**	100 (12)[g]	71 (*S*)	100 (12)	56 (*S*)
20	**S5**	**j**	100 (12)[g]	90 (*S*)	76 (12)	75 (*S*)

[a] All reactions were run at 23 ºC. 0.5 mol% $[PdCl(\eta^3\text{-}C_3H_5)]_2$. Dichloromethane as solvent. 1 mol% ligand. [b] Conversion measured by ^{1}H-NMR. Reaction time shown in parentheses. [c] Enantiomeric excesses measured by HPLC. Absolute configuration shown in parentheses. [d] Pd/**L28a** afforded 65% (*R*). [e] Pd/**L28a** afforded 37% (*S*). [f] Pd/**L28a** afforded 45% (*S*). [g] Isolated yields of alkylation products **3**, **9**, **14**, **20** and **21** were > 92%.

Finally, the effect of introducing a thiazoline group on enantioselectivity depends on the bulkiness of the substrate type. For hindered linear substrate **S1** the introduction of a thiazoline group has a negative effect on enantioselectivity (Table 4.2.1, entries 1-6), but for the less sterically hindered linear substrate **S2** enantioselectivity is hardly affected (Table 4.2.1, entries 7-12) and for the more demanding unhindered cyclic substrates (**S3**-**S5**) enantioselectivities improved considerably (ee's up to 90%; Table 4.2.1, entries 13-20).[i] Our study of Pd-intermediates (see Section 4.2.3.4) shows that for cyclic substrates the presence of a thiazoline group favors the formation of the most reactive Pd-allyl intermediate and therefore gives higher enantioselectivities, while for hindered substrates the formation of the less reactive Pd-allyl intermediate is preferred. This behavior has been attributed to the formation of a more sterically congested chiral pocket when a thiazoline group is used in the ligand design.

[i] It should be noted that for cyclic substrates activities also improved when a thiazoline group was used.

Allylic substitution of symmetrical 1,3-disubstituted allylic substrates using other carbon nucleophiles

To further study the potential of phosphite-oxazoline/thiazoline ligands (**L10**, **L12**, **L27**-**L28**), we next applied them in the allylic substitution of symmetrical 1,3-disubstituted substrates **S1**-**S3** using several carbon nucleophiles. The most notable results are summarized in Figure 4.2.2. We were pleased to see that by using the complementary scope of the phosphite-oxazoline and phosphite-thiazoline ligands, we were again able to identify ligands that provide high enantioselectivities (ee's up to >99%) for each substrate type (**S1**-**S3**). Thus, the results follow the same trends as for the allylic alkylations when dimethyl malonate was used as nucleophile. So, for hindered substrate **S1**, enantioselectivities were best with phosphite-oxazoline ligands, while for cyclic substrate **S3** they were best with phosphite-thiazoline ligands. And for substrate **S2** enantioselectivities were similar with both types of ligand. It should be noted that for substrate **S1**, the enantioselectivity depends on the steric properties of the nucleophile. Excellent enantioselectivities, higher than those obtained using dimethyl malonate, were therefore obtained with dibenzyl malonate (ee's >99% in product **5**) and α-substituted malonates (ee's up to 94% and >99% in products **7** and **8**, respectively) as nucleophiles. The remaining nucleophiles (including acetylacetone) provided enantioselectivities that were as high as those observed when dimethyl malonate was added.

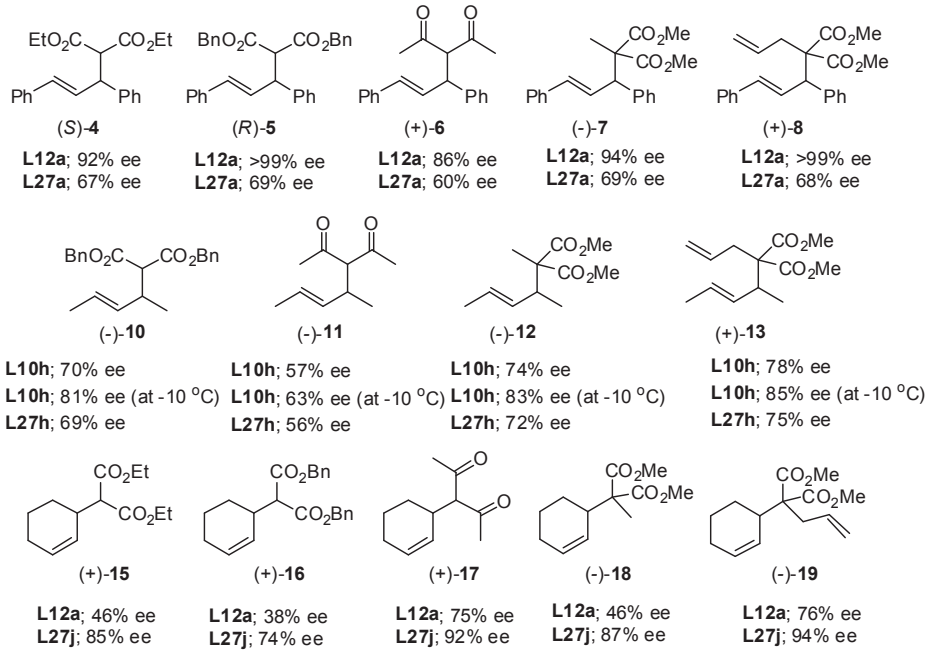

Figure 4.2.2. Selected results for the Pd-allylic substitution of **S1**-**S3** with several other carbon-nucleophiles using phosphite-oxazoline/thiazoline ligands.

However, for substrate **S2**, the enantioselectivity is relatively insensitive to the steric nature of the malonate nucleophiles. High enantioselectivities (ee's up to 85%) were therefore obtained with a variety of malonates (products **10**, **12** and **13**). On the other hand, the addition of acetylacetone

proceeds with less enantiocontrol (ee's up to 63% in product **11**). Various nucleophiles with cyclic substrate **S3** led to results that were different from those observed for linear substrates **S1** and **S2**. High-to-excellent enantioselectivities (ee's ranging from 85% to 94%) were achieved in all cases except when dibenzyl malonate was used as nucleophile (ee's up to 74% in product **16**).

A wide range of synthetic applications of the allylic substitution using nucleophiles other than dimethyl malonate can be envisaged. One example is the practical synthesis of the chiral carbocycle dimethyl (*R*)-2-phenylcyclopent-3-ene-1,1-dicarboxylate (*R*)-**22** by a simple sequential allylic alkylation of **S1**, with dimethyl allylmalonate using Pd/**L12a**, and ring-closing metathesis reactions (Scheme 4.2.2). Previous findings have shown that alkylated intermediate **8**, bearing a terminal alkene, can undergo clean ring-closing metathesis with no loss in enantiomeric excess, affording the desired (*R*)-**22**.[8]

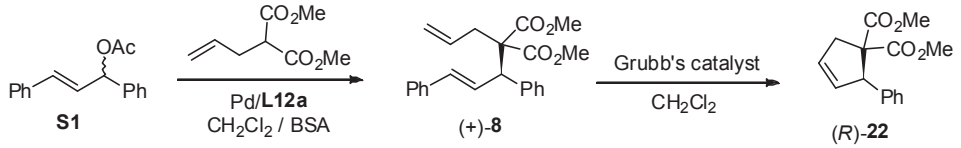

Scheme 4.2.2. Sequential allylic alkylation/ring-closing metathesis reactions for the preparation of carbocycle (*R*)-**22**.

To sum up, the replacement of the oxazoline moiety by a thiazoline group was crucial in overcoming the limitations of the allylic substitution of unhindered cyclic substrates using phosphite-oxazoline ligands. We have therefore been able to identify a phosphite-oxazoline/thiazoline ligand library **L10**, **L12** and **L27**-**L28**, which constitutes one of the few examples that can provide high activities and enantioselectivities in the allylic alkylation of both hindered and unhindered disubstituted substrates with a wide range of carbon-nucleophiles.

4.2.3.3. Allylic substitution of mono- and trisubstituted allylic substrates

In this section, we report the use of the chiral phosphite-oxazoline/thiazoline ligand library (**L10**, **L12**, **L27**-**L28**) in the Pd-catalyzed allylic substitution of more challenging unsymmetrical monosubstituted substrates (Eq. 4.2.2a): *rac*-1-(1-naphthyl)allyl acetate (**S6**) and *rac*-1-(1-naphthyl)-3-acetoxyprop-1-ene (**S7**); and unsymmetrical trisubstituted substrates (Eq. 4.2.2b): *rac*-1,1,-diphenyl-1-hepten-3-yl acetate (**S8**) and rac-1,3,3-triphenylprop-2-enyl acetate (**S9**).

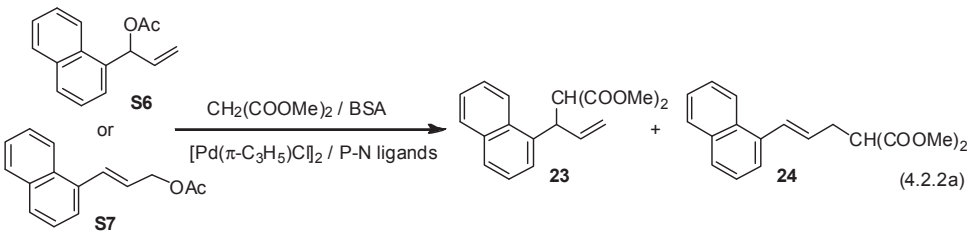

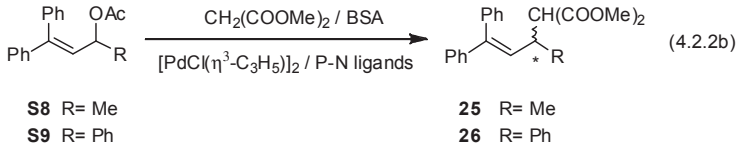

(4.2.2b)

S8 R= Me
S9 R= Ph

25 R= Me
26 R= Ph

Allylic substitution of unsymmetrical 1- and 3-monosubstituted allylic substrates

The allylic substitution of monosubstituted substrates is more challenging than that of disubstituted substrates because both the enantioselectivity and the regioselectivity of the process need to be controlled (the regioselectivity is often a problem since a mixture of regioisomers may be obtained). Most Pd-catalysts developed to date favor the formation of achiral linear product **24** rather than the desired branched isomer **23**.[1,9,10] Because of the π-acceptor capacity of the biaryl phosphite moiety, which decreases the electron density of the most substituted allylic terminal carbon atom via the *trans* influence, the use of heterodonor phosphite-containing ligands favors the formation of the desired branched isomer.[4]

In this section, we examine the regio- and stereoselective allylic alkylation of 1-(1-naphthyl)allyl acetate **S6** and 1-(1-naphthyl)-3-acetoxyprop-1-ene **S7** with dimethyl malonate (Eq. 4.2.2a) using the new phosphite-thiazoline ligands **L27**-**L28a**-**k**. The results, which are summarized in Table 4.2.2, indicate that activities and enantioselectivities were high (ee's up to 95%) and regioselectivities were up to 90% in favor of the branched product **23**, comparable to those obtained using phosphite-oxazoline ligands under standard reaction conditions.[6] We also found that the substituents/configurations at the biaryl phosphite moiety had the same effect on catalytic performance (activity and enantioselectivity) as the related phosphite-oxazoline ligands. Thus, both regio- and enantioselectivities are best with ligands that contain bulky trimethylsilyl-disubstituted *R*-binapthyl phosphite moieties (**L10k** and **L27k**, Table 4.2.2, entries 6, 9 and 11).

Table 4.2.2. Selected results for the Pd-catalyzed allylic alkylation of monosubstituted substrates **S6** and **S7** under standard conditions[a]

Entry	Ligand	Substrate	% Conv (min)[b]	**23**/**24**[c]	% ee[d]
1[e]	**L27a**	**S6**	100 (30)	85/15	83 (*S*)
2	**L27b**	**S6**	100 (30)	80/20	84 (*S*)
3	**L27c**	**S6**	100 (30)	85/15	89 (*S*)
4	**L27h**	**S6**	100 (30)	80/20	68 (*S*)
5	**L27j**	**S6**	100 (30)	85/15	83 (*S*)
6[e]	**L27k**	**S6**	100 (30)	90/10	95 (*S*)
7	**L28a**	**S6**	100 (30)	80/20	82 (*R*)
8	**L10a**	**S6**	100 (30)	85/15	76 (*S*)
9	**L10k**	**S6**	100 (30)	80/20	90 (*S*)
10	**L27a**	**S7**	100 (30)	85/15	82 (*S*)
11	**L27k**	**S7**	100 (30)	90/10	95 (*S*)

[a] All reactions were run at 23 °C. 1 mol% $[PdCl(\eta^3\text{-}C_3H_5)]_2$. Dichloromethane as solvent. 2 mol% ligand. Substrate (0.5 mmol). BSA (1.5 mmol). Dimethyl malonate (1.5 mmol). [b] Reaction time in minutes shown in parentheses. [c] Percentage of branched (**23**) and linear (**24**) isomers. [d] Enantiomeric excesses of **23** determined by HPLC. Absolute configuration shown in parentheses. [e] Isolated yield of **23** was > 72%.

As for the disubstituted substrates, both enantiomers of the alkylation product were obtained by simply changing the configuration of the alkyl backbone chain (Table 4.2.2, entry 1 vs 7). These results are among the best reported for this type of substrate.[10]

Allylic substitution of unsymmetrical 1,3,3-trisubstituted allylic substrates

To further study the potential of the phosphite-oxazoline/thiazoline ligands, we next examined them in the allylic substitution of *rac*-1,1-diphenyl-1-hepten-3-yl acetate (**S8**) and *rac*-1,3,3-triphenylprop-2-enyl acetate (**S9**) using dimethyl malonate as nucleophile (Eq. 4.2.2b). Trisubstituted substrates are more sterically demanding than the previously used hindered disubstituted substrate **S1**,[1] and it is therefore more difficult to achieve excellent enantioselectivities with them than with **S1**.[11] These substrates are of synthetic interest because the substitution products formed in this way can easily be transformed into enantiomerically enriched acid derivatives and lactones.[12]

The results, which are summarized in Table 4.2.3, indicate that enantioselectivities are best when phosphite-oxazoline ligands are used (i.e. Table 4.2.3, entry 1 vs 8). This behavior is in line with the favorable effect observed for the hindered disubstituted substrate **S1** of having an oxazoline moiety in the ligand rather than a thiazoline group. Interestingly, neither the substituents/configurations at the biaryl phosphite moiety nor the electronic properties of the oxazoline substituents have an important impact on the stereochemical outcome of the reaction. Unprecedented excellent enantioselectivities (ranging from 96% to >99% ee) were obtained using ligands **L10** and **L12** (Table 4.2.3, entries 1-7). It should be noted, though, that the enantioselectivities for both substrates (>99% ee for **S8** and 99% ee for **S9**) were highest using ligand **L10a**, which contains a phenyl oxazoline substituent and bulky *tert*-butyl groups at both *ortho* and *para* positions of the tropoisomeric biphenyl phosphite moiety (Table 4.2.3, entry 1). These results compare favorably with the best ones reported in the literature.[11]

Table 4.2.3. Selected results for the Pd-catalyzed allylic substitution of **S8** and **S9** using the phosphite-oxazoline/thiazoline ligands[a]

		S8		**S9**	
Entry	Ligand	% Conv (h)[b]	% ee[c]	% Conv (h)[b]	% ee[c]
1[d]	**L10a**	100 (24)[d]	>99 (*S*)	100 (24)	99 (*S*)
2	**L10b**	100 (24)	96 (*S*)	100 (24)	97 (*S*)
3[d]	**L10c**	100 (24)	97 (*S*)	97 (24)	97 (*S*)
4	**L10h**	43 (24)	97 (*S*)	56 (24)	96 (*S*)
5	**L10j**	100 (24)	96 (*S*)	100 (24)	95 (*S*)
6[d]	**L10k**	100 (24)	98 (*S*)	98 (24)	96 (*S*)
7	**L12a**	91 (24)	99 (*S*)	87 (24)	94 (*S*)
8[d]	**L27a**	100 (24)[d]	73 (*S*)	100 (24)[d]	67 (*S*)

[a] All reactions were run at 23 ºC. 1 mol% $[PdCl(\eta^3\text{-}C_3H_5)]_2$. Dichloromethane as solvent. 2 mol% ligand. [b] Conversion measured by ^{1}H-NMR. Reaction time shown in parentheses. [c] Enantiomeric excesses measured by HPLC. Absolute configuration shown in parentheses. [d] Isolated yields of **25** and **26** were > 88%.

4.2.3.4. Origin of enantioselectivity: study of the Pd-π-allyl intermediates

To study how replacing the oxazoline group by a thiazoline moiety affects catalytic performance, we prepared the Pd-π-allyl key intermediates **27**, **29** and **31** [Pd(η^3-allyl)(L)]BF_4 (L = **L27a**-**k**), and compared them with their related Pd-allyl complexes containing phosphite-oxazoline ligands (**L10a**-**k**).[6] For purposes of comparison in this paper we also report the preparation of Pd-complex **32**, which contains phosphite-oxazoline ligand **L10j**. The corresponding ionic palladium complexes **27**, **29**, **31** and **32**, which contain 1,3-diphenyl, 1,3-dimethyl or cyclohexenyl allyl groups, were made by stirring a dichloromethane solution of the appropriate ligand in the presence of 0.5 equivalent of [Pd(η^3-allyl)(μ-Cl)]$_2$ for 30 minutes and then exchanging the counterion with silver tetrafluoroborate (Scheme 4.2.3).[13] The complexes were characterized by elemental analysis and by ^{1}H, ^{13}C and ^{31}P NMR spectroscopy. The spectral assignments were based on information from ^{1}H-^{1}H, ^{31}P-^{1}H and ^{13}C-^{1}H correlation measurements in combination with ^{1}H-^{1}H NOESY experiments. Unfortunately, we were unable to obtain crystals of sufficient quality to perform X-ray diffraction measurements.

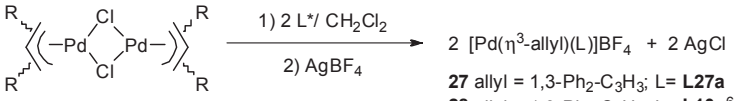

Scheme 4.2.3. Preparation of [Pd(η^3-allyl)(L)]BF_4 complexes **27**-**32**.

To understand why the enantioselectivity in the allylic alkylation of hindered substrate **S1** was lower using phosphite-thiazoline ligands than phosphite-oxazoline counterparts, we first investigated the Pd-1,3-diphenyl-allyl intermediate **27** containing the phosphite-thiazoline **L27a** and compared the results with the related Pd-allyl complex **28**[6] containing phosphite-oxazoline **L10a**. The VT-NMR study (30 ºC to -80 ºC) of the Pd-allyl intermediate **27**, which contains ligand **L27a**, had a mixture of two isomers in equilibrium at a ratio of 2:1. Both isomers were unambiguously assigned by NMR to the two *syn*/*syn endo* **A** and *exo* **B** isomers (Scheme 4.2.4). In both isomers, the NOE indicates interactions between both terminal protons of the allyl group, which clearly indicates a *syn*/*syn* disposition (Figure 4.2.3). Moreover, one of the terminal allyl protons of the major isomer **A** shows a NOE interaction with the *ortho* hydrogen of the phenyl-thiazoline substituent. In addition, one of the methyl substituents of the alkyl backbone chain shows a NOE interaction with the central allyl proton in isomer **A**, while in isomer **B** this interaction takes place with one of the terminal allyl protons. These interactions show that isomer **A** has a *syn*/*syn endo* disposition and isomer **B** a *syn*/*syn exo* disposition (Figure 4.2.3). This also explains why in isomer **A** the terminal allylic proton and carbon signals close to the thiazoline moiety shift to higher fields than the corresponding signals for isomer **B**. This is due to the shielding effect of the phenyl thiazoline ring.[14] For both isomers, the carbon NMR chemical shifts indicate that the most electrophilic allyl carbon terminus is *trans* to the phosphite moiety (Scheme 4.2.4). Assuming that the nucleophilic attack takes place at the most electrophilic allyl carbon terminus,[1] and taking into account the observed stereochemical outcome of the reaction (66% (*S*) in product **4**), and the fact

that the enantiomeric excess of alkylation product **4** is different from the diastereoisomeric excess (de 33% (*R*)) of the Pd-intermediates, the **B** isomer must react faster than the **A** isomer. To prove this we studied the reactivity of the Pd-intermediates with sodium malonate at low temperature by *in situ* NMR (Figure 4.2.4). Our results showed that minor isomer **B** reacts around 7.5 times faster than isomer **A**. If we take into account the relative reaction rates and the abundance of both isomers, the calculated ee should be 58% (*S*), which matches the ee obtained experimentally. We can therefore conclude that the nucleophilic attack takes place predominantly at the allyl terminus *trans* to the phosphite moiety of the minor **B** Pd-intermediate. This is also consistent with the fact that, for both isomers, the most electrophilic allylic terminal carbon atom is the one *trans* to the phosphite in minor isomer **B**. Finally, if we compare these results with the previously reported Pd/**L10a** complex **28**, for which the presence of two *syn*/*syn* isomers **A** and **B** was also observed (Scheme 4.2.4), we found that the only difference is the relative amount of the fast reacting isomer **B**, with respect to isomer **A**. Thus, the diasteroisomeric **B**/**A** ratio decreases by replacing the oxazoline moiety with a thiazoline group from 1/1.5 (for complex **28)** to 1/2 (for complex **27**). This fully explains why the enantioselectivities obtained with Pd-phosphite-thiazoline ligand **L27a** were lower than those obtained with the phosphite-oxazoline counterpart (**L10a**) in the allylic substitution of hindered substrate **S1**. The decrease in the diastereoisomeric ratio can be attributed to the fact that the presence of the thiazoline moiety bends the phenyl thiazoline substituent closer to the region in which the substrate is coordinated. This means that the steric interaction between the phenyl thiazoline substituent and one of the phenyl groups of the substrate in the **B** isomer of complex **27** is greater than in the Pd-phosphite-oxazoline complex, which leads to the preferential formation of isomer **A** in the phosphite-thiazoline complex.

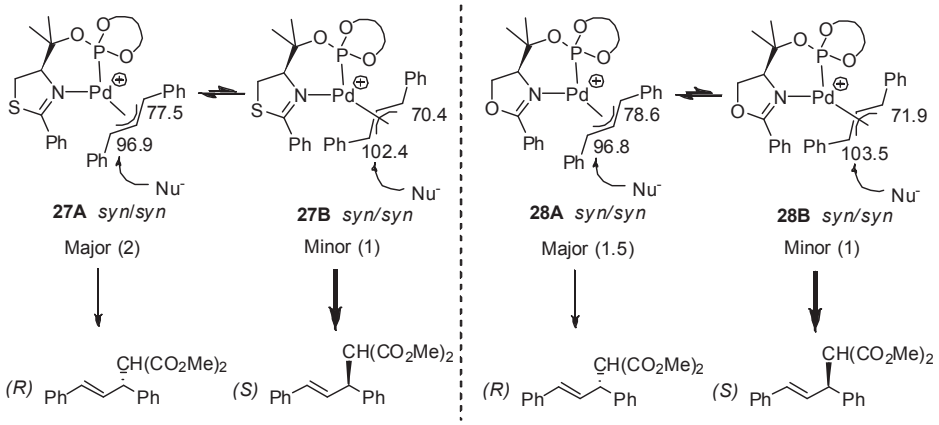

Scheme 4.2.4. Diastereoisomer Pd-allyl intermediates for **S1** with ligands **L27a** and **L10a**. The relative amounts of each isomer are shown in parentheses. The chemical shifts (in ppm) of the allylic terminal carbons are also shown.

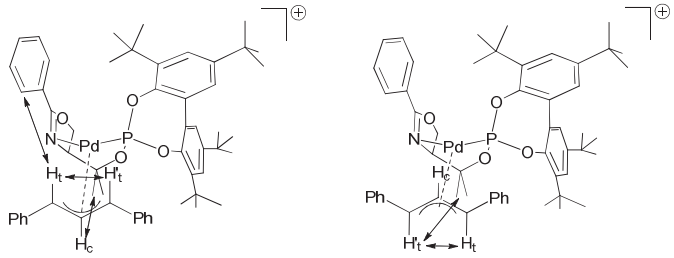

syn/*syn*-**27A** *syn*/*syn*-**27B**

Figure 4.2.3. Relevant NOE contacts from the NOESY experiment of [Pd(η^3-1,3-diphenylallyl)(**L27a**)]BF_4 (**27**) isomers.

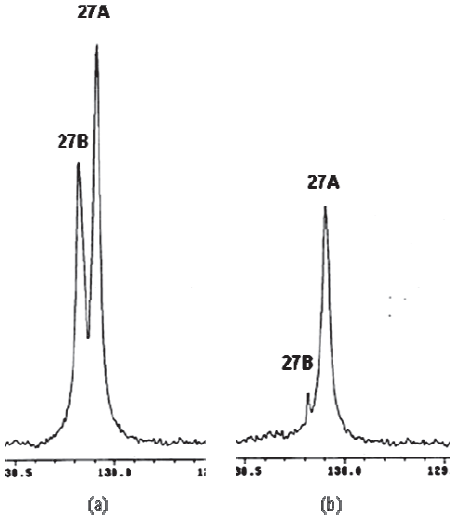

Figure 4.2.4. $^{31}P\{^1H\}$-NMR spectra of [Pd(η^3-1,3-diphenylallyl)(**L27a**)]BF_4 (**27**) in CD_2Cl_2 at –75 °C (a) before the addition of sodium malonate and (b) after the addition of sodium malonate.

We next studied the palladium 1,3-dimethyl-allyl intermediates using phosphite-thiazoline ligands that provide enantioselectivities that are similar to those provided by phosphite-oxazoline ligands. The VT-NMR study (30 ºC to -80 ºC) of Pd-allyl intermediate **29**, which contains ligand **L27a**, had a mixture of two isomers in equilibrium at a ratio of 1:1, which were assigned by NOE to the two *syn*/*syn endo* **A** and *exo* **B** isomers (Scheme 4.2.5). For both complexes, the NOE indicates interactions between both terminal protons of the allyl group and also between the central allyl proton with methyl protons of the allyl ligand, which clearly indicates a *syn*/*syn* disposition for all the isomers. Moreover, one of the methyl protons of the allyl ligand of the isomers **B** shows a NOE interaction with the *ortho* hydrogen of the phenyl-thiazoline substituent. These interactions can be explained by assuming a *syn*/*syn exo* disposition for isomer **B** (Figure 4.2.5). As for related Pd-intermediates using phosphite-oxazoline ligands,[6] the NMR data show that the most electrophilic allyl terminal carbon is *trans* to the phosphite moiety at the **B** isomer. In addition, the population and electronic properties at the allyl fragment in the Pd-phosphite-thiazoline isomers (**29A** and **29B**) are the same as those obtained for related palladium intermediates **30A** and **30B** containing phosphite-oxazoline ligand **L10a** (Scheme 4.2.5). This is in

agreement with the comparable enantioselectivities obtained experimentally using both ligand types in the allylic substitution of unhindered linear substrate **S2**.

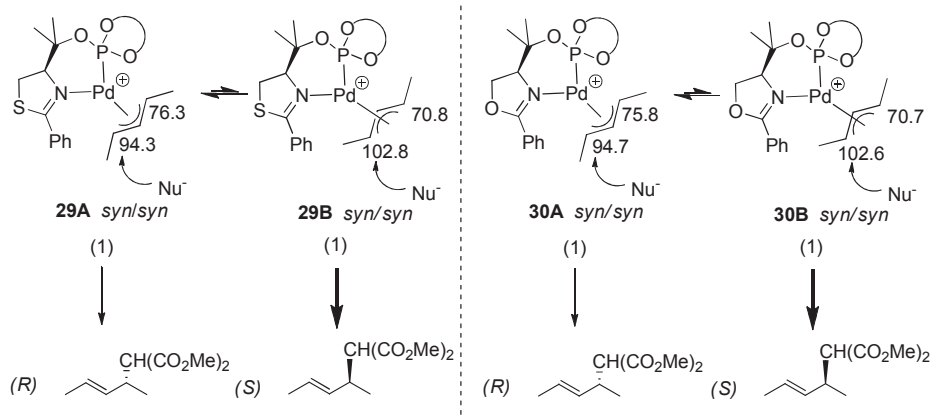

Scheme 4.2.5. Diastereoisomer Pd-allyl intermediates for **S2** with ligands **L27a** and **L10a**. The relative amounts of each isomer are shown in parentheses. The chemical shifts (in ppm) of the allylic terminal carbons are also shown.

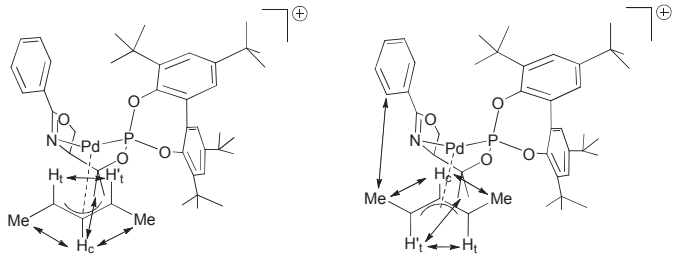

Figure 4.2.5. Relevant NOE contacts from the NOESY experiment of [Pd(η^3-1,3-dimethylallyl)(**L27a**)]BF_4 (**29**) isomers.

Finally, in an attempt to provide further information about the positive effect on enantioselectivity observed in the allylic substitution of the unhindered cyclic substrate **S3** when the oxazoline moiety is replaced with a thiazoline group, we also studied the Pd-1,3-cyclohexenyl-allyl intermediate **31,** which contains phosphite-thiazoline ligand **L27j**, and compared it with its related phosphite-oxazoline counterpart (Pd/**L10j**). The VT-NMR (35 °C to –80 °C) of Pd intermediates **31** and **32** showed a mixture of the two possible isomers at a ratio of 3:1 and 1.3:1, respectively (Scheme 4.2.6). All isomers were unambiguously assigned by NOE to isomers **A** and **B** (Figure 4.2.6). Therefore, for isomers **31A** and **32A**, the NOE indicates interactions between the central allyl proton and one of the methyl hydrogens in the alkyl backbone chain of the ligand and between the methylenic hydrogens of the allyl ligand and the *ortho* hydrogen of the phenyl-thiazoline/oxazoline substituent (Figure 4.2.6 (a)). However, for isomers **31B** and **32B**, the NOE indicates interactions between one of the terminal allyl protons and the *ortho* hydrogen of the phenyl-thiazoline/oxazoline substituent and also between the methylenic hydrogens in the allyl ligand and one of the methyl hydrogens in the alkyl backbone chain of the ligand (Figure 4.2.6 (b)). The carbon NMR chemical shifts indicated that the most electrophilic allylic terminus carbon

is *trans* to the phosphite moiety in the major isomers **31A** and **32A**. Assuming that the nucleophilic attack takes place at the most electrophilic allyl carbon terminus, and taking into account the observed stereochemical outcome of the reaction (82% (*S*) for complex **31** and 70% (*S*) for **32**), and the fact that the enantiomeric excesses of alkylation product **14** are different from the diastereoisomeric excesses of the Pd-intermediates (de = 50% (*S*) for **31** and de= 15% (*S*) for **32**), the **A** isomers must react faster than **B** isomers. This was confirmed by the reactivity of the Pd intermediates with sodium malonate at low temperature by *in situ* NMR spectroscopy. The higher enantioselectivities obtained with Pd-systems containing phosphite-thiazoline ligands than with related Pd/phosphite-oxazoline catalytic systems can therefore be attributed to the increase in the relative amount of fast reacting isomer **A** with respect to isomer **B** compared with the population of isomers (**A** and **B**) for complexes containing phosphite-oxazoline ligands.

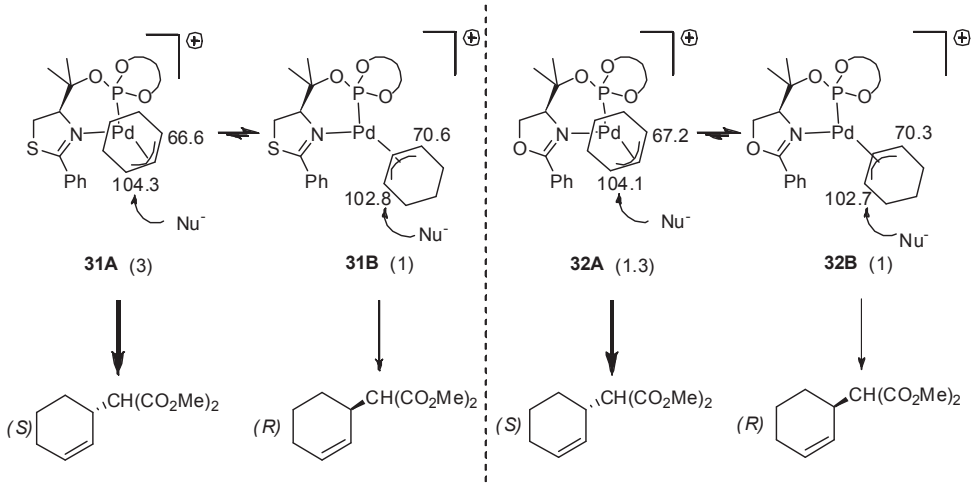

Scheme 4.2.6. Diastereoisomer Pd-allyl intermediates for **S3** with ligands **L27j** and **L10j**. The relative amounts of each isomer are shown in parentheses. The chemical shifts (in ppm) of the allylic terminal carbons are also shown.

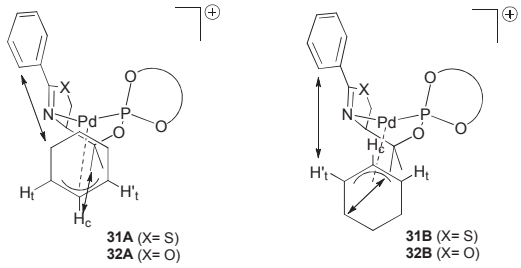

Figure 4.2.6. Relevant NOE contacts from the NOESY experiment of the [Pd(η^3-1,3-cyclohexenyl-allyl)(L)]BF_4 (L= **L27j** and **L10j**) isomers.

4.2.4. Conclusions

We have expanded the ligand design of one of the most successful phosphite-oxazoline ligands (**L6**-**L21**) in Pd-catalyzed allylic alkylation by replacing the oxazoline group with a

thiazoline moiety. These new phosphite-thiazoline ligands have been evaluated in the Pd-catalyzed allylic substitution of a wide range of mono-, di- and trisubstituted substrates using several carbon nucleophiles, including the less studied α-substituted malonates and β-diketones. For purposes of comparison, we have also extended our previous work on phosphite-oxazoline ligands to include carbon-nucleophiles other than dimethyl malonate and to the alkylation of challenging trisubstituted substrates. The results show that enantioselectivities depend not only on ligand parameters but also on the substrate structure. The general tendency is that for hindered substrates such as disubstituted **S1** and trisubstituted **S8** and **S9**, enantioselectivities (ee's up to >99%) are best using phosphite-oxazoline ligands, while for unhindered cyclic substrates (**S3**-**S5**) enantioselectivities (ee's up to 94%) improved considerably when phosphite-thiazoline ligands where used. In the case of monosubstituted substrates the regio- and enantioselectivities obtained using both ligand types were comparable and excellent (regio's up to 90% and ee's up to 95%). Therefore, by correctly combining substrate and ligand type (P-oxazoline or P-thiazoline), we have identified one of the few catalytic systems that provide high regio- and enantioselectivities in both enantiomers of the alkylation product for several hindered and unhindered mono- and disubstituted substrates using a wide range of carbon-nucleophiles. We even achieved unprecedented ee's (>99%) for the challenging class of trisubstituted olefins. The potential application of allylic substitution using functionalized malonates has been demonstrated by the practical synthesis of the carbocyclic compound dimethyl (*R*)-2-phenylcyclopent-3-ene-1,1-dicarboxylate in enantiopure form using a simple sequential allylic alkylation and ring-closing metathesis reactions.

By studying the Pd-1,3-diphenyl, 1,3-dimethyl and 1,3-cyclohexenyl allyl intermediates by means of NMR spectroscopy, we were able to better understand the observed catalytic behavior. We found that the nucleophilic attack takes place predominantly at the allylic terminal carbon atom located *trans* to the phosphite moiety. We also found that the changes in enantioselectivities observed by replacing the phosphite with a thiazoline could be explained by the variations in the relative amount of the species formed in solution. Thus, while for hindered substrates, the relative amount of the fastest reacting isomer increases when phosphite-oxazoline ligands are used, for cyclic substrates, it increases with phosphite-thiazoline ligands.

4.2.5. Experimental section

4.2.5.1. General considerations

All reactions were carried out using standard Schlenk techniques under an argon atmosphere. Solvents were purified and dried by standard procedures. Phosphorochloridites are easily prepared in one step from the corresponding biaryls.[15] The synthesis of ligands **L27**-**L28a**-**c** has been previously described in Chapter 3, Section 3.6. ^{1}H, $^{13}C\{^{1}H\}$, and $^{31}P\{^{1}H\}$ NMR spectra were recorded using a 400 MHz spectrometer. Chemical shifts are relative to that of $SiMe_4$ (^{1}H and ^{13}C) as internal standard or H_3PO_4 (^{31}P) as external standard. ^{1}H, ^{13}C and ^{31}P assignments were made on the basis of ^{1}H-^{1}H gCOSY, ^{1}H-^{13}C gHSQC and ^{1}H-^{31}P gHMBC experiments. All catalytic experiments were performed three times.

4.2.5.2. General procedure for the preparation of the phosphite-thiazoline ligands

The corresponding phosphorochloridite (1.1 mmol) produced *in situ* was dissolved in toluene (5 mL) and pyridine (0.19 mL, 2.3 mmol) was added. The corresponding hydroxyl-thiazoline compound (1 mmol) was azeotropically dried with toluene (3 x 2 mL) and then dissolved in toluene (5 mL) to which pyridine (0.19 mL, 2.3 mmol) was added. The oxazoline solution was transferred slowly at 0 ºC to the solution of phosphorochloridite. The reaction mixture was stirred overnight at 80 ºC, and the pyridine salts were removed by filtration. Evaporation of the solvent gave a white foam, which was purified by flash chromatography in alumina to produce the corresponding ligand as a white solid.

L27j. Yield: 328 mg (49 %). ^{31}P NMR ($CDCl_3$), δ: 156.5 (s). ^{1}H NMR (C_6D_6), δ: 0.42 (s, 9H, CH_3-Si), 0.49 (s, 9H, CH_3-Si), 1.45 (s, 3H, CH_3), 1.72 (s, 3H, CH_3), 2.58 (dd, 1H, $^{2}J_{H\text{-}H}$= 11.6 Hz, $^{3}J_{H\text{-}H}$= 9.6 Hz, CH_2-S), 2.84 (dd, 1H, $^{2}J_{H\text{-}H}$= 11.6 Hz, $^{3}J_{H\text{-}H}$= 10 Hz, CH_2-S), 4.51 (m, 1H, CH-N), 6.8-8.2 (m, 17H, CH=). ^{13}C NMR (C_6D_6), δ: 0.0 (d, CH_3-Si, $J_{C\text{-}P}$= 4.7 Hz), 0.5 (CH_3-Si), 25.6 (CH_3), 28.9 (d, CH_3, $J_{C\text{-}P}$= 12.4 Hz), 33.0 (CH_2-S), 82.4 (C), 87.3 (CH-N), 124.9 (CH=), 125.0 (CH=), 125.6 (C), 126.8 (CH=), 126.9 (CH=), 127.1 (CH=), 128.3 (CH=), 128.5 (CH=), 128.6 (CH=), 128.7 (CH=), 128.9 (CH=), 129.2 (CH=), 131.1 (CH=), 131.4 (C), 132.3 (C), 133.3 (C), 133.8 (C), 134.5 (C), 134.9 (C), 136.3 (CH=), 137.4 (CH=), 137.8 (C), 153.1 (C), 167.9 (C=N). Anal. calcd (%) for $C_{38}H_{42}NO_3PSSi_2$: C 67.12, H 6.23, N 2.06, S 4.72; found: C 67.18, H 6.26, N 2.03, S 4.67.

L27k. Yield: 380 mg (56 %). ^{31}P NMR ($CDCl_3$), δ: 153.6 (s). ^{1}H NMR (C_6D_6), δ: 0.52 (s, 9H, CH_3-Si), 0.54 (s, 9H, CH_3-Si), 1.41 (s, 3H, CH_3), 1.94 (s, 3H, CH_3), 2.78 (dd, 1H, $^{2}J_{H\text{-}H}$= 12.0 Hz, $^{3}J_{H\text{-}H}$= 10.8 Hz, CH_2-S), 3.01 (dd, 1H, $^{2}J_{H\text{-}H}$= 12.0 Hz, $^{3}J_{H\text{-}H}$= 11.2 Hz, CH_2-S), 4.77 (m, 1H, CH-N), 6.8-8.2 (m, 17H, CH=). ^{13}C NMR (C_6D_6), δ: 0.0 (d, CH_3-Si, $J_{C\text{-}P}$= 4.6 Hz), 0.8 (CH_3-Si), 24.7 (d, CH_3, $J_{C\text{-}P}$= 7.6 Hz), 28.9 (d, CH_3, $J_{C\text{-}P}$= 8.7 Hz), 33.7 (CH_2-S), 82.7 (C), 86.6 (CH-N), 126.9 (CH=), 127.0 (CH=), 127.2 (CH=), 127.3 (CH=), 128.0 (CH=), 128.4 (CH=), 128.5 (CH=), 128.7 (CH=), 128.8 (CH=), 129.3 (CH=), 132.3 (C), 133.0 (C), 134.5 (C), 134.9 (C), 135.0 (C), 136.5 (CH=), 137.5 (CH=), 152.6 (C), 152.9 (C), 168.6 (C=N). Anal. calcd (%) for $C_{38}H_{42}NO_3PSSi_2$: C 67.12, H 6.23, N 2.06, S 4.72; found: C 67.15, H 6.25, N 2.01, S 4.69.

4.2.5.3. General procedure for the preparation of [Pd(η^3-allyl)(L)]BF_4 complexes 27-32

The corresponding ligand (0.05 mmol) and the complex [Pd(μ-Cl)(η^3-1,3-allyl)]$_2$ (0.025 mmol) were dissolved in CD_2Cl_2 (1.5 mL) at room temperature under argon. $AgBF_4$ (9.8 mg, 0.05 mmol) was added after 30 minutes and the mixture was stirred for 30 minutes. The mixture was then filtered over celite under argon and the resulting solutions were analyzed by NMR. After the NMR analysis, the complexes were precipitated as pale yellow solids by adding hexane.

[Pd(η^3-1,3-diphenylallyl)(L27a)]BF_4 (27). Isomer **A** (66%): ^{31}P NMR (CD_2Cl_2), δ: 130.1 (s, 1P). ^{1}H NMR(CD_2Cl_2), δ: 1.21 (s, 9H, CH_3, ^{t}Bu), 1.24 (s, 9H, CH_3, ^{t}Bu), 1.29 (s, 3H, CH_3), 1.33 (s, 9H, CH_3, ^{t}Bu), 1.43 (s, 3H, CH_3), 1.74 (s, 9H, CH_3, ^{t}Bu), 3.42 (m, 1H, CH_2-S), 3.65 (m, 1H, CH_2-S), 4.51 (m, 1H, CH allyl *trans* to N), 4.89 (m, 1H, CH allyl *trans* to P), 5.09 (m, 1H, CH-N), 6.45 (dt, 1H, CH allyl central, $^{3}J_{H\text{-}H}$= 12.0 Hz, $J_{H\text{-}P}$= 2.0 Hz), 6.7-7.9 (m, 19H, CH=). ^{13}C NMR(CD_2Cl_2), δ: 23.0 (CH_3), 27.7 (CH_3), 30.5- 31.7 (CH_3, ^{t}Bu), 32.7 (CH_2-S), 34.7-35.8 (C, ^{t}Bu), 77.5 (b, CH allyl *trans* to N), 83.6 (CH-N), 88.5 (CMe_2), 96.8 (d, CH allyl *trans* to P, $J_{C\text{-}P}$= 36.6 Hz), 110.6 (d, CH allyl central, $J_{C\text{-}P}$= 8.2 Hz), 124-149 (aromatic carbons), 182.7 (C=N). Isomer **B** (33%): ^{31}P NMR

(CD_2Cl_2), δ: 130.5 (s, 1P). ^{1}H NMR(CD_2Cl_2), δ: 1.22 (s, 9H, CH_3, ^{t}Bu), 1.29 (s, 9H, CH_3, ^{t}Bu), 1.31 (s, 3H, CH_3), 1.33 (s, 9H, CH_3, ^{t}Bu), 1.39 (s, 3H, CH_3), 1.61 (s, 9H, CH_3, ^{t}Bu), 3.42 (m, 1H, CH_2-S), 4.03 (m, 1H, CH_2-S), 4.98 (m, 1H, CH allyl *trans* to N), 5.41 (m, 1H, CH-N), 6.05 (m, 1H, CH allyl *trans* to P), 6.25 (dt, 1H, CH allyl central, $^3J_{H-H}$= 13.6 Hz, J_{H-P}= 2.4 Hz), 6.7-7.9 (m, 19H, CH=). ^{13}C NMR(CD_2Cl_2), δ: 23.3 (CH_3), 27.3 (CH_3), 30.5- 31.7 (CH_3, ^{t}Bu), 32.3 (CH_2-S), 34.7-35.8 (C, ^{t}Bu), 70.4 (d, CH allyl *trans* to N, J_{C-P}= 7.2 Hz), 83.1 (s, CH-N), 88.5 (CMe_2), 102.4 (d, CH allyl *trans* to P, J_{C-P}= 36.3 Hz), 109.2 (d, CH allyl central, J_{C-P}= 8.4 Hz), 124-149 (aromatic carbons), 181.4 (C=N). Anal. calcd (%) for $C_{55}H_{67}BF_4NO_3PPdS$: C 63.13, H 6.45, N 1.34, S 3.06; found: C 63.22, H 6.51, N 1.31, S 3.02.

[Pd(η^3-1,3-dimethylallyl)(L27a)]BF_4 (29). Isomer **A** (50%): ^{31}P NMR (CD_2Cl_2), δ: 130.7 (s, 1P). ^{1}H NMR(CD_2Cl_2), δ: 0.78 (m, 3H, CH_3 *trans* to P), 0.90 (dd, 3H, CH_3 *trans* to N, *J*= 15.2 Hz, *J*= 4.0 Hz), 1.38 (s, 9H, CH_3, ^{t}Bu), 1.39 (s, 9H, CH_3, ^{t}Bu), 1.43 (s, 9H, CH_3, ^{t}Bu), 1.51 (s, 3H, CH_3), 1.62 (s, 3H, CH_3), 1.65 (s, 9H, CH_3, ^{t}Bu), 3.09 (m, 1H, CH allyl *trans* to N), 3.52 (m, 1H, CH_2-S), 3.59 (m, 1H, CH allyl *trans* to P), 4.11 (m, 1H, CH_2-S), 4.98 (m, 1H, CH allyl central), 5.42 (m, 1H, CH-N), 7.2-8.2 (m, 9H, CH=). ^{13}C NMR(CD_2Cl_2), δ: 16.9 (d, CH_3 *trans* to P, J_{C-P}= 7.2 Hz), 18.4 (b, CH_3 *trans* to N), 24.1 (CH_3), 28.4 (d, CH_3, J_{C-P}= 4.8 Hz), 31.6-32.0 (CH_3, ^{t}Bu), 34.0 (CH_2-S), 35.2-36.1 (C, ^{t}Bu), 76.3 (d, CH allyl *trans* to N, J_{C-P}= 7.4 Hz), 84.4 (CH-N), 89.2 (CMe_2), 94.3 (d, CH allyl *trans* to P, J_{C-P}= 40.2 Hz), 122.6 (dd, CH allyl central, J_{C-P}= 18.9 Hz), 125.0-150.0 (aromatic carbons), 182.8 (C=N). Isomer **B** (50%): ^{31}P NMR (CD_2Cl_2), δ: 130.3 (s, 1P). 1H NMR(CD_2Cl_2), δ: 0.44 (dd, 3H, CH_3 *trans* to P, *J*= 15.6 Hz, *J*= 4.0 Hz), 0.78 (m, 3H, CH_3 *trans* to N), 1.36 (s, 9H, CH_3, ^{t}Bu), 1.43 (s, 9H, CH_3, ^{t}Bu), 1.49 (s, 9H, CH_3, ^{t}Bu), 1.53 (s, 3H, CH_3), 1.68 (s, 9H, CH_3, ^{t}Bu), 1.71 (s, 3H, CH_3), 3.43 (m, 2H, CH allyl *trans* to N and CH_2-S), 3.65 (m, 1H, CH allyl trans to P), 4.03 (m, 1H, CH_2-S), 5.23 (m, 2H, CH allyl central and CH-N), 7.2-8.2 (m, 9H, CH=).^{13}C NMR(CD_2Cl_2), δ: 17.4 (d, CH_3 *trans* to P, J_{C-P}= 7.2 Hz), 19.1 (b, CH_3 *trans* to N), 24.1 (CH_3), 28.2 (d, CH_3, J_{C-P}= 4.4 Hz), 31.6-32.0 (CH_3, ^{t}Bu), 33.6 (CH_2-S), 35.2-36.1 (C, ^{t}Bu), 70.8 (d, CH allyl *trans* to N, J_{C-P}= 6.2 Hz), 84.4 (CH-N), 88.9 (CMe_2), 102.8 (d, CH allyl *trans* to P, J_{C-P}= 38.6 Hz), 122.9 (dd, CH allyl central, J_{C-P}= 18.3 Hz), 125.0-150.0 (aromatic carbons), 183.8 (C=N). Anal. calcd (%) for $C_{45}H_{63}BF_4NO_3PPdS$: C 58.60, H 6.89, N 1.52, S 3.48; found: C 58.59, H 6.87, N 1.47, S 3.45.

[Pd(η^3-1,3-cyclohexenylallyl)(L27j)]BF_4 (31). Isomer **A** (75%): ^{31}P NMR (CD_2Cl_2), δ: 133.2 (s, 1P). ^{1}H NMR(CD_2Cl_2), δ: 0.54 (s, 9H, CH_3-Si), 0.60 (s, 9H, CH_3-Si), 0.90 (m, 2H, CH_2), 1.22 (m, 2H, CH_2), 1.52 (m, 2H, CH_2), 1.58 (s, 3H, CH_3), 1.72 (s, 3H, CH_3), 3.55 (m, 1H, CH_2-S), 3.63 (m, 1H, CH allyl *trans* to N), 4.07 (m, 1H, CH_2-S), 4.99 (m, 1H, CH allyl *trans* to P), 5.04 (m, 1H, CH allyl central), 5.33 (m, 1H, CH-N), 6.9-8.3 (m, 15H, CH=). ^{13}C NMR(CD_2Cl_2), δ: 0.4 (CH_3-Si), 0.5 (CH_3-Si), 21.3 (CH_2), 23.0 (CH_3), 26.3 (CH_2), 27.2 (CH_2), 27.9 (CH_3), 34.2 (CH_2-S), 66.6 (d, CH allyl *trans* to N, J_{C-P}= 9.8 Hz), 83.5 (d, CH-N, J_{C-P}= 4.4 Hz), 89.4 (CMe_2), 104.3 (d, CH allyl *trans* to P, J_{C-P}= 32.6 Hz), 111.9 (d, CH allyl central, J_{C-P}= 11.4 Hz), 125.0-153.0 (aromatic carbons), 186.9 (C=N). Isomer **B** (25%): ^{31}P NMR (CD_2Cl_2), δ: 133.7 (s, 1P). ^{1}H NMR(CD_2Cl_2), δ: 0.53 (s, 9H, CH_3-Si), 0.63 (s, 9H, CH_3-Si), 0.90 (m, 2H, CH_2), 1.22 (m, 2H, CH_2), 1.52 (m, 2H, CH_2), 1.55 (s, 3H, CH_3), 1.76 (s, 3H, CH_3), 3.55 (m, 1H, CH_2-S), 4.07 (m, 1H, CH_2-S), 4.16 (m, 1H, CH allyl *trans* to N), 4.62 (m, 1H, CH allyl *trans* to P), 5.26 (m, 1H, CH allyl central), 5.51 (m, 1H, CH-N), 6.9-8.3 (m, 15H, CH=).^{13}C NMR(CD_2Cl_2), δ: 0.6 (CH_3-Si), 0.8 (CH_3-Si), 17.2 (CH_2), 22.8 (CH_3), 26.4 (CH_2), 27.7 (CH_2), 28.3 (CH_3), 34.2 (CH_2-S), 70.6 (d, CH allyl *trans* to N, J_{C-P}= 10.4 Hz), 82.9 (d,

CH-N, J_{C-P}= 4.8 Hz), 89.2 (CMe_2), 102.8 (d, CH allyl *trans* to P, J_{C-P}= 38.8 Hz), 112.4 (d, CH allyl central, J_{C-P}= 12.0 Hz), 125.0-153.0 (aromatic carbons), 186.9 (C=N). Anal. calcd (%) for $C_{44}H_{51}BF_4NO_3PPdSSi_2$: C 55.38, H 5.39, N 1.47, S 3.36; found: C 55.42, H 5.41, N 1.44, S 3.32.

[Pd(η^3-1,3-cyclohexenylallyl)(L10j)]BF_4 (32). Isomer **A** (57%): ^{31}P NMR (CD_2Cl_2), δ: 133.4 (s, 1P). ^{1}H NMR(CD_2Cl_2), δ: 0.51 (s, 9H, CH_3-Si), 0.62 (s, 9H, CH_3-Si), 0.90 (m, 2H, CH_2), 1.26 (m, 2H, CH_2), 1.44 (s, 3H, CH_3), 1.48 (m, 2H, CH_2), 1.52 (s, 3H, CH_3), 4.02 (m, 1H, CH allyl *trans* to N), 4.47 (m, 1H, CH_2-O), 4.96 (m, 1H, CH allyl *trans* to P), 5.04 (m, 1H, CH_2-O), 5.14 (m, 1H, CH allyl central), 5.24 (m, 1H, CH-N), 6.9-8.3 (m, 15H, CH=). ^{13}C NMR(CD_2Cl_2), δ: 0.3 (CH_3-Si), 0.5 (CH_3-Si), 21.1 (CH_2), 23.0 (CH_3), 26.4 (CH_2), 27.2 (CH_2), 27.8 (CH_3), 67.2 (d, CH allyl *trans* to N, J_{C-P}= 10.2 Hz), 72.8 (CH_2-O), 83.4 (b, CH-N), 89.6 (CMe_2), 104.1 (d, CH allyl *trans* to P, J_{C-P}= 36.2 Hz), 112.3 (d, CH allyl central, J_{C-P}= 7.8 Hz), 125.0-153.0 (aromatic carbons), 179.9 (C=N). Isomer **B** (43%): ^{31}P NMR (CD_2Cl_2), δ: 133.9 (s, 1P). ^{1}H NMR(CD_2Cl_2), δ: 0.48 (s, 9H, CH_3-Si), 0.62 (s, 9H, CH_3-Si), 0.90 (m, 2H, CH_2), 1.26 (m, 2H, CH_2), 1.48 (m, 2H, CH_2), 1.51 (s, 3H, CH_3), 1.62 (s, 3H, CH_3), 4.14 (m, 1H, CH allyl *trans* to N), 4.51 (m, 1H, CH_2-O), 4.82 (m, 1H, CH allyl *trans* to P), 5.14 (m, 1H, CH_2-O), 5.21 (m, 1H, CH allyl central), 5.57 (m, 1H, CH-N), 6.9-8.3 (m, 15H, CH=).^{13}C NMR(CD_2Cl_2), δ: 0.5 (CH_3-Si), 0.8 (CH_3-Si), 21.0 (CH_2), 23.2 (CH_3), 26.1 (CH_2), 27.6 (CH_2), 27.9 (CH_3), 70.3 (d, CH allyl *trans* to N, J_{C-P}= 9.2 Hz), 72.9 (CH_2-O), 83.1 (b, CH-N), 89.8 (CMe_2), 102.7 (d, CH allyl *trans* to P, J_{C-P}= 38.9 Hz), 112.5 (d, CH allyl central, J_{C-P}= 6.4 Hz), 125.0-153.0 (aromatic carbons), 179.6 (C=N). Anal. calcd (%) for $C_{44}H_{51}BF_4NO_4PPdSi_2$: C 56.33, H 5.48, N 1.49; found: C 56.37, H 5.51, N 1.45.

4.2.5.4. Study of the reactivity of the [Pd(η^3-allyl)(L))]BF_4 with sodium malonate by *in situ* NMR[16]

A solution of *in situ* prepared [Pd(η^3-allyl)(**L**)]BF_4 (L= phosphite-oxazoline/thiazoline, 0.05 mmol) in CD_2Cl_2 (1 mL) was cooled in the NMR at -80 °C. At this temperature, a solution of cooled sodium malonate (0.1 mmol) was added. The reaction was then followed by ^{31}P NMR. The relative reaction rates were calculated using a capillary containing a solution of triphenylphosphine in CD_2Cl_2 as external standard.

4.2.5.5. Typical procedure for the allylic alkylation of disubstituted linear (S1 and S2) and cyclic (S3-S5) substrates

A degassed solution of [PdCl(η^3-C_3H_5)]$_2$ (0.9 mg, 0.0025 mmol) and the corresponding phosphite-oxazoline/thiazoline (0.0055 mmol) in dichloromethane (0.5 mL) was stirred for 30 min. Subsequently, a solution of the corresponding substrate (0.5 mmol) in dichloromethane (1.5 mL), nucleophile (1.5 mmol), *N,O*-bis(trimethylsilyl)-acetamide (370 μL, 1.5 mmol) and a pinch of the corresponding base were added. The reaction mixture was stirred at room temperature. After the desired reaction time the reaction mixture was diluted with Et_2O (5 mL) and saturated NH_4Cl (aq) (25 mL) was added. The mixture was extracted with Et_2O (3 x 10 mL) and the extract dried over $MgSO_4$. For compound **3**, solvent was removed and conversion was measured by ^{1}H-NMR. To determine the ee by HPLC (Chiralcel OD, 0.5% 2-propanol/hexane, flow 0.5 mL/min), a sample was filtered over basic alumina using dichloromethane as the eluent.[17] For compounds **9**, **14** and

21, the conversion and enantiomeric excess were determined by GC.[18] For compound **20**, the conversion was measured by ^{1}H-NMR. To determine the ee by ^{1}H-NMR using [Eu(hfc)$_3$].[11b]

Diethyl 2-(1,3-diphenylallyl)malonate (4). Enantiomeric excess determined by HPLC using Chiralcel OJ-H column (87% hexane/2-propanol, flow 0.5 mL/min, λ= 254 nm). t_R 17.6 min (*S*); t_R 20.1 min (*R*).^{1}H NMR ($CDCl_3$), δ: 1.01 (t, 6H, CH_3,*J*=6.8 Hz), 3.92 (d, 1H, CH, *J*=11.2 Hz), 4.19 (q, 4H, CH_2, *J*=7.2 Hz), 4.23 (m, 1H, CH), 6.34 (dd, 1H, CH=,*J*=20 Hz, *J*=10 Hz), 6.41 (d, 1H, CH=,*J*=18 Hz), 7.1-7.4 (m, 10H, CH=).

Dibenzyl 2-(1,3-diphenylallyl)malonate (5). Enantiomeric excess determined by HPLC using Chiralcel OJ-H column (95% hexane/2-propanol, flow 1 mL/min, λ= 254 nm). t_R 94.0 min (*R*); t_R 107.4 min (*S*).^{1}H NMR ($CDCl_3$), δ: 4.03 (d, 1H, CH, *J*=9.6 Hz), 4.29 (t, 1H, CH, *J*=10 Hz), 4.92 (s, 2H, CH_2), 5.09 (s, 2H, CH_2), 6.28 (dd, 1H, CH=,*J*=24 Hz, *J*=8.4 Hz), 6.40 (d, 1H, CH=,*J*=17 Hz), 7.0-7.4 (m, 20H, CH=).

(1,3-diphenylallyl)pentane-2,4-dienone (6). Enantiomeric excess determined by HPLC using Chiralcel OJ-H column (98% hexane/2-propanol, flow 1 mL/min, λ= 254 nm). t_R 53.1 min (*S*); t_R 56.9 min (*R*).^{1}H NMR ($CDCl_3$), δ: 1.93 (s, 3H, CH_3), 2.25 (s, 3H, CH_3),4.34 (m, 2H, CH), 6.20 (dm, 1H, CH=, *J*=15.6 Hz), 6.44 (d, 1H, CH=, *J*=15.6 Hz), 7.1-7.4 (m, 10H, CH=).

Dimethyl 2-(1,3-diphenylallyl)-2-methylmalonate (7). Enantiomeric excess determined by HPLC using Chiralcel OD-H column (90% hexane/2-propanol, flow 1 mL/min, λ= 254 nm). t_R 9.9 min (*S*); t_R 12.5 min (*R*).^{1}H NMR ($CDCl_3$), δ: 1.48 (s, 3H, CH_3), 3.62 (s, 3H, CH_3), 3.71 (s, 3H, CH_3), 4.29 (d, 1H, CH, *J*=8.8 Hz), 6.46 (d, 1H, CH=, *J*=16Hz), 6.68 (dd, 1H, CH=, *J*=16 Hz, *J*=8.8 Hz), 7.1-7.4 (m, 10H, CH=).

Dimethyl 2-allyl-2-(1,3-diphenylallyl)malonate (8). Enantiomeric excess determined by HPLC using Chiralcel OJ-H column (87% hexane/2-propanol, flow 0.5 mL/min, λ= 254 nm). t_R 19.4 min (*R*); t_R 26.1 min (*S*). ^{1}H NMR ($CDCl_3$), δ: 2.48 (dd, 1H, CH_2,*J*=14Hz, *J*=8.8 Hz), 2.67 (dd, 1H, CH_2,*J*=14 Hz, *J*=8 Hz), 3.66 (s, 3H, CH_3), 3.75 (s, 3H, CH_3), 4.20(d, 1H, CH, *J*=8.8 Hz), 5.06 (m, 2H, CH_2=), 5.77 (m, 1H, CH=), 6.40 (d, 1H, CH=, *J*=15.6Hz), 6.77 (dd, 1H, CH=, *J*=16.4 Hz, *J*=8.4 Hz), 7.2-7.4 (m, 10H, CH=).

Dibenzyl 2-(1,3-dimethylallyl)malonate (10). Enantiomeric excess determined by HPLC using Chiralpak IA column (98% 2-propanol/hexane, flow 0.3 mL/min, λ= 226 nm). t_R 35.8 min (+); t_R 38.2 min (-). ^{1}H NMR ($CDCl_3$), δ: 1.02 (d, 3H, CH_3, *J*= 4.8 Hz), 1.53 (d, 3H, CH_3, *J*= 4 Hz), 2.91 (m, 1H, CH), 3.33 (d, 1H, CH, *J*=6.8 Hz), 5.10 (s, 2H, CH_2), 5.14 (s, 2H, CH_2), 5.31 (dd, 1H, CH=,*J*=15.6 Hz, *J*=8.4 Hz), 5.46 (m, 1H, CH=), 7.2-7.4 (m, 10H, CH=).

(1,3-dimethylallyl)pentane-2,4-dienone (11). Enantiomeric excess determined by GC using Chiradex B-DM column (100 kPa H_2, Isotherm at 60 ºC). t_R 37.2 min (-); t_R 38.0 min (+). ^{1}H NMR ($CDCl_3$), δ: 0.95 (d, 3H, CH_3, *J*= 6.4 Hz), 1.61 (d, 3H, CH_3, *J*= 5.2 Hz), 2.10 (s, 2H, CH_2), 2.19 (s, 2H, CH_2), 2.97 (m, 1H, CH), 3.54 (d, 1H, CH, *J*=10.4 Hz), 5.19 (dd, 1H, CH=,*J*=15.2 Hz, *J*=10.4 Hz), 5.48 (m, 1H, CH=).

Dimethyl 2-(1,3-dimethylallyl)-2-methylmalonate (12). Enantiomeric excess determined by GC using Chiralsil-Dex CB column (90 kPa H_2, Isotherm at 60 ºC). t_R 69.6 min (-); t_R 71.1 min (+). ^{1}H NMR ($CDCl_3$), δ: 1.01 (d, 3H, CH_3, *J*= 8 Hz), 1.32 (s, 3H, CH_3), 1.62 (d, 3H, CH_3, *J*= 8 Hz), 2.92 (m, 1H, CH), 3.67 (s, 3H, CH_3), 3.70 (s, 3H, CH_3), 5.31 (dd, 1H, CH=,*J*=16 Hz, *J*=8 Hz), 5.47 (m, 1H, CH=).

Dimethyl 2-allyl-2-(1,3-dimethylallyl)malonate (13). Enantiomeric excess determined by HPLC using Chiralcel OD-H column (99.5% 2-propanol/hexane, flow 0.5 mL/min). t_R 10.3 min (+); t_R 10.9 min (-). ^{1}H NMR ($CDCl_3$), δ: 1.06 (d, 3H, CH_3, *J*= 6.4 Hz), 1.64 (d, 3H, CH_3, *J*= 6.8 Hz), 2.59 (m, 2H, CH_2), 2.77 (m, 1H, CH), 3.68 (s, 3H, CH_3), 3.70 (s, 3H, CH_3), 5.03 (m, 2H, CH_2=), 5.33 (dd, 1H, CH=, *J*= 16.4 Hz, *J*= 8.8 Hz), 5.48 (m, 1H, CH=), 5.76 (m, 1H, CH=).

Diethyl 2-(1,3-cyclohexanylallyl)malonate (15). Enantiomeric excess determined by HPLC using Chiralpak IC column (98% 2-propanol/hexane, flow 0.5 mL/min, λ= 226 nm). t_R 22.4 min (+); t_R 23.5 min (-). ^{1}H NMR ($CDCl_3$), δ: 1.22 (t, 6H, CH_3, *J*= 7.2 Hz), 1.49 (m, 2H, CH_2), 1.67 (m, 2H, CH_2), 1.93 (m, 2H, CH_2), 2.86 (m, 1H, CH), 3.19 (d, 1H, CH, *J*= 9.6 Hz), 2.59 (m, 2H, CH_2), 4.14 (q, 4H, CH_2, *J*= 7.2 Hz), 5.50 (m, 1H, CH=), 5.72 (m, 1H, CH=).

Dibenzyl 2-(1,3-cyclohexanylallyl)malonate (16). Enantiomeric excess determined by HPLC using Chiralpak IA column (90% 2-propanol/hexane, flow 0.5 mL/min, λ= 226 nm). t_R 15.1 min (-); t_R 16.3 min (+). ^{1}H NMR ($CDCl_3$), δ: 1.41 (m, 2H, CH_2), 1.55 (m, 2H, CH_2), 1.95 (m, 2H, CH_2), 2.96 (m, 1H, CH), 3.40 (d, 1H, CH, *J*= 9.6 Hz), 5.15 (s, 4H, CH_2), 5.55 (m, 1H, CH=), 5.75 (m, 1H, CH=), 7.2-7.4 (m, 10H, CH=).

(1,3-cyclohexanylallyl)pentane-2,4-dienone (17). Enantiomeric excess determined by GC using Chiralsil-Dex CB column (77 kPa H_2, Isotherm at 100 ºC). t_R 21.6 min (-); t_R 22.4 min (+). ^{1}H NMR ($CDCl_3$), δ: 1.48 (m, 2H, CH_2), 1.62 (m, 2H, CH_2), 1.91 (m, 2H, CH_2),2.09 (s, 3H, CH_3),2.12 (s, 3H, CH_3), 2.94 (m, 1H, CH), 3.54 (d, 1H, CH, *J*= 10.8 Hz), 5.30 (m, 1H, CH=), 5.70 (m, 1H, CH=).

Dimethyl 2-(1,3-cyclohexanylallyl)-2-methylmalonate (18). Enantiomeric excess determined by HPLC using Chiralpak IC column (99.5% 2-propanol/hexane, flow 0.5 mL/min, λ= 226 nm). t_R 36.4 min (-); t_R 39.7 min (+).^{1}H NMR ($CDCl_3$), δ: 1.29 (s, 3H, CH_3), 1.51 (m, 2H, CH_2), 1.58 (m, 2H, CH_2), 1.92 (m, 2H, CH_2), 2.99 (m, 1H, CH), 3.68 (s, 6H, CH_3), 5.43 (m, 1H, CH=), 5.74 (m, 1H, CH=).

Dimethyl 2-allyl-2-(1,3-cyclohexanylallyl)malonate (19). Enantiomeric excess determined by HPLC using Chiralpak IC column (87% 2-propanol/hexane, flow 0.5 mL/min, λ= 226 nm). t_R 15.3 min (-); t_R 17.0 min (+).^{1}H NMR ($CDCl_3$), δ: 1.49 (m, 2H, CH_2), 1.77 (m, 2H, CH_2), 1.91 (m, 2H, CH_2), 2.65 (m, 2H, CH_2), 2.86 (m, 1H, CH), 3.65(s, 3H, CH_3), 3.68 (s, 3H, CH_3), 5.06 (m, 2H, CH_2=), 5.71 (m, 3H, CH=).

4.2.5.6. Typical procedure for the allylic alkylation of monosubstituted (S6 and S7) and 1,3,3-trisubstituted (S8 and S9) substrates

A degassed solution of $[PdCl(\eta^3\text{-}C_3H_5)]_2$ (1.8 mg, 0.005 mmol) and the corresponding phosphite-oxazoline/thiazoline (0.011 mmol) in dichloromethane (0.5 mL) was stirred for 30 min at room temperature. Subsequently, a solution of substrate (0.5 mmol) in dichloromethane (1.5 mL), dimethyl malonate (171 μL, 1.5 mmol), *N,O*-bis(trimethylsilyl)-acetamide (370 μL, 1.5 mmol) and a pinch of KOAc were added. After 2 hours at room temperature, the reaction mixture was diluted with Et_2O (5 mL) and saturated NH_4Cl (aq) (25 mL) was added. The mixture was extracted with Et_2O (3 x 10 mL) and the extract dried over $MgSO_4$. The solvent was removed and the conversion and regioselectivity were measured by ^{1}H-NMR. Enantiomeric excess was determined by HPLC (Chiralcel OJ, 13% 2-propanol/hexane, flow 0.5 mL/min). A sample was filtered over basic alumina using dichloromethane as the eluent.[6,18]

4.2.6. Acknowledgements

We would like to thank the Spanish Government for providing grant CTQ2010-15835, the Catalan Government for grant 2009SGR116, and the ICREA Foundation for providing M. Diéguez and O. Pàmies with financial support through the ICREA Academia awards.

4.2.7. References

[1] For reviews, see: (a) *Palladium Reagents and Catalysis, Innovations in Organic Synthesis*; Tsuji, J., Eds.; Wiley: New York, 1995. (b) Trost, B. M.; van Vranken, D. L. *Chem. Rev.* **1996**, *96*, 395. (c) Johannsen, M.; Jorgensen, K. A. *Chem. Rev.* **1998**, *98*, 1689. (d) Pfaltz, A.; Lautens, M. in *Comprehensive Asymmetric Catalysis*; Jacobsen, E. N., Pfaltz, A., Yamamoto, H., Eds.; Springer-Verlag: Berlin, 1999; Vol. 2, Chapter 24. (e) Helmchen, G.; Pfaltz, A. *Acc. Chem. Res.* **2000**, *33*, 336. (f) Masdeu-Bultó, A. M.; Diéguez, M.; Martín, E.; Gómez, M. *Coord. Chem. Rev.* **2003**, *242*, 159. (g) Trost, B. M.; Crawley, M. L. *Chem. Rev.* **2003**, *103*, 2921. (h) Martín, E.; Diéguez, M. *C. R. Chemie* **2007**, *10*, 188. (i) Lu, Z.; Ma, S. *Angew. Chem. Int. Ed.* **2008**, *47*, 258.
[2] See, for example: (a) Trost, B. M.; Bunt, R. C. *J. Am. Chem. Soc.* **1994**, *116*, 4089. (b) Trost, B. M.; Krueger, A. C.; Bunt, R. C.; Zambrano, J. *J. Am. Chem. Soc*. **1996**, *118*, 6520.
[3] See, for instance: (a) Dawson, G. J.; Frost, C. G.; Williams, J. M. J. *Tetrahedron Lett.* **1993**, *34*, 3149. (b) von Matt, P.; Pfaltz, A. *Angew. Chem. Int. Ed. Engl.* **1993**, *32*, 566. (c) Sennhenn, P.; Gabler, B.; Helmchen, G. *Tetrahedron Lett.* **1994**, *35*, 8595.
[4] See, for instance: a) Pàmies, O.; Diéguez, M. *Acc. Chem. Res.* **2010**, *43*, 212. b) van Leeuwen, P. W. N. M.; Kamer, P. C. J.; Claver, C.; Pàmies, O.; Diéguez, M. *Chem. Rev.* **2011**, *111*, 2077.
[5] Prétôt, R.; Pfaltz, A. *Angew. Chem. Int. Ed.* **1998**, *37*, 323.
[6] Diéguez, M.; Pàmies, O. *Chem. Eur. J*. **2008**, *14*, 3653.
[7] Emtenäs, H.; Alderin, L.; Almqvist, F. *J. Org. Chem.* **2001**, *66*, 6756.
[8] Dugal-Tessier, J.; Dake, G. R.; Gates, D. P. *Org. Lett*. **2010**, *12*, 4667.
[9] In contrast to Pd-catalytic systems, Ir-, Ru- and Mo-catalysts provide very high selectivity in order for the attack at the non-terminal carbon to give the chiral product. See, for instance: (a) Bruneau, C.; Renaud, J. L.; Demersemen, B. *Chem. Eur. J.* **2006**, *12*, 5178; (b) Malkov, A. V.; Gouriou, L.; Lloyd-Jones, G. C.; Starý, I.; Langer, V.; Spoor, P.; Vinader, V.; Kočovský, P. *Chem. Eur. J.* **2006**, *12*, 6910; (c) Trost, B. M.; Hildbrand, S.; Dogra, K. *J. Am. Chem. Soc.* **1999**, *121*, 10416; (d) Alexakis, A.; Polet, D. *Org. Let.* **2004**, *6*, 3529.
[10] For recent successful applications of Pd-catalysts, see: a) You, S.-L.; Zhu, X.-Z.; Luo, Y.-M.; Hou, X.-L.; Dai, L.-X. *J. Am. Chem. Soc.* **2001**, *123*, 7471; b) Hilgraf, R.; Pfaltz, A. *Synlett* **1999**, 1814. (c) Hilgraf, R.; Pfaltz, A. *Adv. Synth. Catal*. **2005**, *347*, 61. c) Pàmies, O.; Diéguez, M.; Claver, C. *J. Am. Chem. Soc.* **2005**, *127*, 3646. d) Mata, Y.; Pàmies, O.; Diéguez, M. *Adv. Synth. Catal.* **2009**, *352*, 3217. e) ref. 5. f) ref. 6.
[11] For successful applications, see: (a) Dawson, G. J.; Williams, J. M. J.; Coote, S. J. *Tetrahedron Lett.* **1995**, *36*, 461. (b) Evans, D. A.; Campos, K. R.; Tedrow, J. S.; Michael, F. E.; Gagné, M. R. *J. Am. Chem. Soc.* **2000**, *122*, 7905. (c) Popa, D.; Puigjaner, C.; Gómez, M.; Benet-Buchholz, J.; Vidal-Ferran, A.; Pericas, M. A. *Adv. Synth. Cat.* **2007**, *349*, 2265.
[12] See, for instance: (a) Sudo, A.; Saigo, K. *J. Org. Chem.* **1997**, 62, 5508. (b) Dawson, G. J.; Williams, J. M. J.; Coote, S. J. *Tetrahedron: Asymmetry* **1995**, 6, 2535. (c) Martin, C. J.; Rawson, D. J.; Williams, J. M. J. *Tetrahedron: Asymmetry* **1998**, 9, 3723.

[13] (a) Deerenberg, S.; Schrekker, H. S.; van Strijdonck, G. P. F.; Kamer, P. C. J.; van Leeuwen, P. W. N. M.; Fraanje, J.; Goubitz, K. *J. Org. Chem.* **2000**, *65*, 4810. (b) Fernández, F.; Gómez, M.; Jansat, S.; Muller, G.; Martín, E.; Flores Santos, L.; García, P. X.; Acosta, A.; Aghmiz, A.; Jiménez-Pedrós, M.; Masdeu-Bultó, A. M.; Diéguez, M.; Claver, C.; Maestro, M. A. *Organometallics* **2005**, *24*, 3946.
[14] Schaffner, S.; Müller, J. F. K.; Neuburger, M.; Zehner, M. *Helv. Chim. Acta* **1998**, *81*, 1223.
[15] Buisman, G. J. H.; Kamer, P. C. J.; van Leeuwen, P. W. N. M. *Tetrahedron: Asymmetry* **1993**, *4*, 1625.
[16] van Haaren, R. J.; Keeven, P. H.; van der Veen, L. A.; Goubitz, K.; van Strijdonck, G. P. F.; Oevering, H.; Reek, J. N. H.; Kamer, P. C. J.; van Leeuwen, P. W. N. M. *Inorg. Chim. Acta* **2002**, *327*, 108.
[17] Pàmies, O.; van Strijdonck, G. P. F.; Diéguez, M.; Deerenberg, S.; Net, G.; Ruiz, A.; Claver, C.; Kamer, P. C. J.; van Leeuwen, P. W. N. M. *J. Org. Chem.* **2001**, *66*, 8867.
[18] Pericàs, M. A.; Puigjaner, C.; Riera, A.; Vidal-Ferran, A.; Gómez, M.; Jiménez, F.; Muller, G.; Rocamora, M. *Chem. Eur. J.* **2002**, *8*, 4164.

4.3. A new class of modular P,N-ligand library for asymmetric Pd-catalyzed allylic substitution reactions. A study of the key Pd-π-allyl intermediates

Javier Mazuela, Alexander Paptchikhine, Päivi Tolstoy, Oscar Pàmies, Montserrat Diéguez and Pher G. Andersson in *Chem. Eur. J.* **2010**, *16*, 620.

4.3.1 Abstract

A new class of modular P,N-ligand library, **L29**-**L36a**-**g**, has been synthesized and screened in the Pd-catalyzed allylic substitution reactions of several substrate types. These series of ligands can be prepared efficiently from easily accessible hydroxyl-oxazole/thiazole derivatives. Their modular nature enables the bridge length, the substituents at the heterocyclic ring and in the alkyl backbone chain, the configuration of the ligand backbone, and the substituents/configurations in the biaryl phosphite moiety to be easily and systematically varied. By carefully selecting the ligand components, therefore, high regio- and enantioselectivities (ee's up to 96%) and good activities are achieved in a broad range of mono-, di- and trisubstituted linear hindered and unhindered substrates and cyclic substrates. The NMR and DFT studies on the Pd-π-allyl intermediates provide a deeper understanding of the effect of ligand parameters on the origin of enantioselectivity.

4.3.2. Introduction

The development of methods for enantioselective carbon-carbon and carbon-heteroatom bond formation is one of the key issues in organic synthesis. A versatile method for forming these bonds is palladium-catalyzed asymmetric allylic substitution.[1]

Most of the successful ligands reported to date for this process have been designed using two main strategies. The first one, developed by Trost and coworkers, was to increase the ligand's bite angle in order to create a chiral cavity in which the allyl system is embedded. This idea opened up the successful application of ligands with large bite angles for the allylic substitution of sterically undemanding substrates.[1,2] The second strategy, developed by groups led by Helmchen, Pfaltz and Williams, was the use of heterodonor ligands that result in an electronic discrimination of the two allylic terminal carbon atoms due to the different *trans* influences of the donor groups.[1,3] This made it possible to successfully use a wide range of heterodonor ligands (mainly P,N-ligands) in allylic substitution reactions.[1]

Nowadays, many chiral ligands (mainly P- and N-ligands), which possess either C_2 or C_1 symmetry, have been developed, and they provide high enantiomeric excesses for several types of disubstituted substrates.[1] Nevertheless, in general, there is still a problem of substrate specificity (for example, ee's are high in disubstituted linear hindered substrates and low in unhindered substrates, and vice versa) and reaction rates. Other types of substrates still require much attention. For example, for monosubstituted substrates, more active and more regio- and enantioselective Pd-catalysts are needed.[1] Another challenging class of substrates is that of

trisubstituted substrates. Although a few good enantioselective Pd-catalytic systems have been reported, their activities are still very low.[1] More research is needed on the development of new ligands that can overcome these limitations.

In this context, we recently demonstrated that the presence of biaryl-phosphite moieties in ligand design is highly advantageous because: (1) substrate specificity decreases because the chiral pocket created (i.e. the chiral cavity in which the allyl is embedded) is flexible enough to enable the perfect coordination of hindered and unhindered substrates,[4] (2) reaction rates increase thanks to the larger π-acceptor ability of these moieties,[5] and (3) regioselectivity towards the desired branched isomer in monosubstituted linear substrates increases thanks to the π-acceptor ability of the phosphite moiety that enhances the S_N1 character of the nucleophilic attack.[6]

Due to our interest in discovering faster and more versatile Pd-catalytic systems, we decided to go one step further in the design of a new ligand library for this process. Therefore, we developed a ligand library whose design incorporates the advantages of heterodonor and biaryl phosphite ligands and also allows extra control of the flexibility of the chiral pocket by changing the size of the chelate ring. To do this, we synthesized and screened a library of 56 potential new phosphite-oxazole/thiazole ligands (Figure 4.3.1).[7]

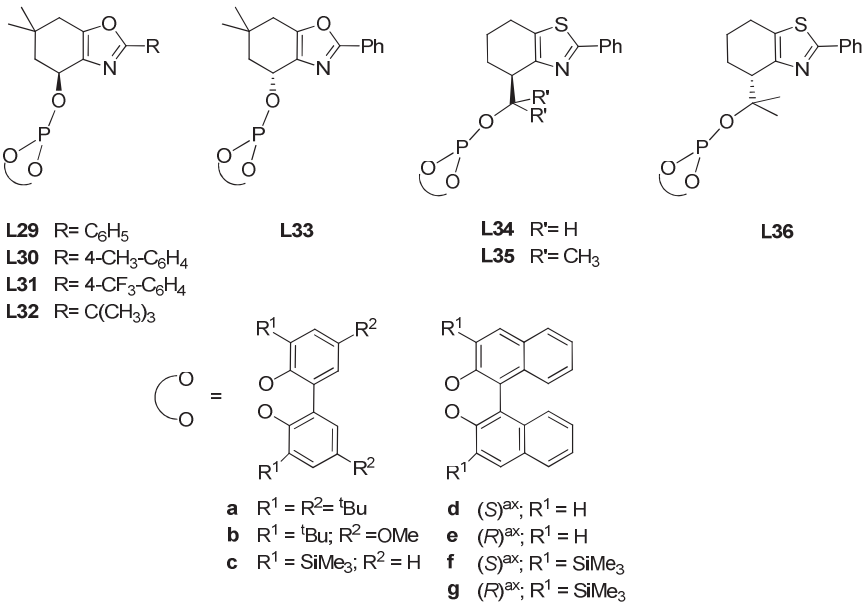

Figure 4.3.1. Library of phosphite-oxazole and phosphite-thiazole ligands (**L29-L36a-g**).

The highly modular construction of these ligands enabled a systematic study of the effect of bridge length (ligands **L29** and **L34**), the substituent at the heterocyclic ring (ligands **L29**-**L32**) and in the alkyl backbone chain (ligands **L34** and **L35**), the configuration of the ligand backbone (ligands **L29** vs. **L33** and **L35** vs. **L36**), and the substituents and configurations in the biaryl phosphite moiety (**a-g**). By carefully selecting these elements, we achieved high selectivities (regio- and enantioselectivities) and activities in a wide range of mono-, di- and trisubstituted substrates. In this paper, we also discuss the synthesis and characterization of the Pd-π-allyl

intermediates in order to provide greater insight into the origin of enantioselectivity in these catalytic systems.

4.3.3. Results and discussion

4.3.3.1. Allylic substitution of symmetrical 1,3-disubstituted allylic substrates

In this section, we report the use of the chiral phosphite-nitrogen ligand library (**L29**-**L36a**-**g**) in the Pd-catalyzed allylic substitution of linear disubstituted substrates with different steric properties (Eq 4.3.1a): *rac*-1,3-diphenyl-3-acetoxyprop-1-ene (**S1**) (widely used as a model substrate), *rac*-(*E*)-ethyl-2,5-dimethyl-3-hex-4-enylcarbonate (**S2**) and *rac*-1,3-dimethyl-3-acetoxyprop-1-ene (**S3**); and cyclic substrates (Eq 4.3.1b): *rac*-3-acetoxycyclohexene (**S4**) (widely used as a model substrate) and *rac*-3-acetoxycycloheptene (**S5**). Two nucleophiles were tested. In all cases, the catalysts were generated *in situ* from π-allyl-palladium chloride dimer $[PdCl(\eta^3\text{-}C_3H_5)]_2$ and the corresponding ligand.[1]

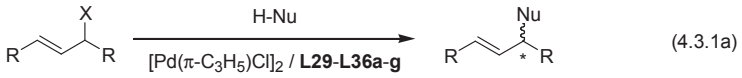

(4.3.1a)

S1 R= Ph; X= OAc
S2 R= ^{i}Pr; X= OCO_2Et
S3 R= Me; X= OAc

1 R= Ph; H-Nu= H-CH(COOMe)$_2$
2 R= Ph; H-Nu= H-NHCH$_2$Ph
3 R= ^{i}Pr; H-Nu= H-CH(COOMe)$_2$
4 R= Me; H-Nu= H-CH(COOMe)$_2$

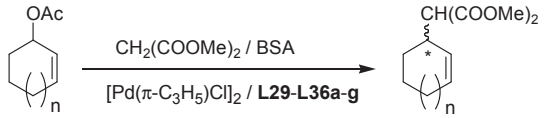

(4.3.1b)

S4 n=1
S5 n=2

5 n=1
6 n=2

*Allylic substitution of rac-1,3-diphenyl-3-acetoxyprop-1-ene **S1** using dimethyl malonate and benzylamine as nucleophiles*

In the first set of experiments, we used the palladium-catalyzed asymmetric substitution reactions of **S1** (Eq. 4.3.1a, R = Ph, X = OAc), with dimethyl malonate and benzylamine as nucleophiles, to study the potential of the phosphite-nitrogen ligand library **L29**-**L36a**-**g**. **S1** was chosen as a substrate because the reaction was performed with a wide range of ligands, which enabled the efficiency of the various ligand systems to be compared directly.[1]

First, we studied the effect of the reaction conditions by conducting a series of experiments with two ligands (**L29a** and **L34a**) using different solvents (tetrahydrofuran, toluene and dichloromethane) and ligand-to-palladium ratios (L/Pd = 0.75, L/Pd = 1 and L/Pd = 2). We found that the efficiency of the process was strongly dependent on the nature of the solvent and the ligand-to-palladium ratio (Table 4.3.1). Although toluene provided higher enantioselectivity than dichloromethane, its activity was much lower (entries 3 and 6 vs. 1 and 4). Tetrahydrofuran yielded the lowest enantioselectivities of all three solvents (entries 2 and 5). We also found that an

excess of ligand was not needed for enantioselectivities to be high (entries 1, 4 and 7-10). Interestingly, at higher ligand-to-palladium ratios, enantioselectivities were lower (entries 8 and 10 vs. 1 and 4). This is probably due to the fact that at a ligand-to-palladium ratio greater than 1 the phosphite-nitrogen ligands act as a monodentate ligand.[8]

Table 4.3.1. Selected results for the Pd-catalyzed allylic alkylation of **S1** using the ligand library **L29**-**L36a**-**g**. Effects of the solvent and the ligand-to-palladium ratio.[a]

Entry	Ligand	Solvent	L/Pd	% Conv (min)[b]	% ee[c]
1	**L29a**	CH_2Cl_2	1	100 (30)	82 (*S*)
2	**L29a**	THF	1	89 (60)	73 (*S*)
3	**L29a**	toluene	1	100 (1440)	92 (*S*)
4	**L34a**	CH_2Cl_2	1	100 (30)	21 (*S*)
5	**L34a**	THF	1	85 (180)	18 (*S*)
6	**L34a**	toluene	1	64 (600)	34 (*S*)
7	**L29a**	CH_2Cl_2	0.75	100 (60)	82 (*S*)
8	**L29a**	CH_2Cl_2	2	100 (30)	79 (*S*)
9	**L34a**	CH_2Cl_2	0.75	73 (30)	23 (*S*)
10	**L34a**	CH_2Cl_2	2	100 (30)	14 (*S*)

[a] All reactions were run at 23 ºC. 0.5 mol% $[PdCl(\eta^3\text{-}C_3H_5)]_2$. **S1** (0.5 mmol). BSA (1.5 mmol). Dimethyl malonate (1.5 mmol). [b] Conversion measured by ^{1}H-NMR. Reaction time shown in parentheses. [c] Enantiomeric excesses measured by HPLC. Absolute configuration shown in parentheses.

For comparison purposes, the rest of the ligands were tested using dichloromethane as a solvent and at a ligand-to-palladium ratio of 1. Table 4.3.2 shows the results obtained when dimethyl malonate and benzylamine were used as nucleophiles. We found that enantioselectivities were highly affected by the bridge length, the substituents at the heterocyclic ring and in the alkyl backbone chain, and the substituents and configurations in the biaryl phosphite moieties (**a-g**). High activities (TOF's up to 600 mol **S1** x (mol Pd x h)$^{-1}$) and enantioselectivities (ee's up to 92%) were obtained for both enantiomers of the substitution products **1** and **2** using ligands **L29a** and **L33a**. Catalytic performance in the Pd-catalyzed allylic amination of **S1** followed the same trend as for the allylic alkylation of **S1** (Table 4.3.2). As expected, however, the activity was lower than in the alkylation reaction of **S1**. The stereoselectivity of the amination was the same as for the alkylation reaction, though the CIP descriptor was inverted because the priority of the groups had changed.

The influence of the bridge length indicates that the use of ligands **L29** and **L33**, which form a six-membered chelate ring, provided higher enantioselectivity than the use of ligands **L34**-**L36**, which form a seven-membered chelate ring (Table 4.3.2, entries 1 and 11 vs 12-14). In line with this, increasing the rigidity of the ligand by replacing the hydrogen substituents in the alkyl backbone chain in ligand **L34a** with two methyl groups (ligand **L35a**) caused enantioselectivities to increase (Table 4.3.2, entries 12 vs 13).

The effect of the substituents at the heterocyclic ring indicated that the presence of either bulky or electron-donating substituents decreased both activities and enantioselectivities (Table 4.3.2, entries 1, 8-10). The fact that enantiomeric excesses decrease when a bulky *tert*-butyl is present is due to the formation of Pd-intermediate species with the phosphite-nitrogen ligand

acting as a monodentate ligand (see Section 4.3.3.5, "Origin of enantioselectivity: study of the Pd-π-allyl intermediates").

Table 4.3.2. Selected results for the Pd-catalyzed allylic substitution of **S1** using the ligand library **L29**-**L36a**-**g**[a]

		H-Nu = H-CH(COOMe)$_2$[a]		H-Nu = H-NHCH$_2$Ph[a]	
Entry	Ligand	% Conv (min)[b]	% ee[c]	% Conv (min)[b]	% ee[c]
1	**L29a**	100 (15)[d]	82 (*S*)	34 (360)	84 (*R*)
2	**L29b**	99 (20)	81 (*S*)	37 (360)	80 (*R*)
3	**L29c**	99 (15)	70 (*S*)	43 (360)	69 (*R*)
4	**L29f**	100 (30)[d]	69 (*S*)	28 (360)	71 (*R*)
5	**L29g**	100 (30)[d]	40 (*S*)	31 (360)	41 (*R*)
6	**L29d**	72 (30)	9 (*S*)	15 (360)	7 (*R*)
7	**L29e**	42 (30)	8 (*R*)	12 (360)	5 (*S*)
8	**L30a**	80 (30)	43 (*S*)	24 (360)	32 (*R*)
9	**L31a**	98 (30)[d]	79 (*S*)	36 (360)	82 (*R*)
10	**L32a**	78 (30)	22 (*S*)	19 (360)	25 (*R*)
11	**L33a**	100 (15)	81 (*R*)	32 (360)	84 (*S*)
12	**L34a**	100 (20)[d]	21 (*S*)	41 (360)	19 (*R*)
13	**L35a**	100 (30)[d]	52 (*S*)	38 (360)	49 (*R*)
14	**L36a**	100 (30)	51 (*R*)	33 (360)	50 (*S*)
15[e]	**L29a**	100 (360)	92 (*S*)	-	-

[a] All reactions were run at 23 ºC. 0.5 mol% [PdCl(η^3-C_3H_5)]$_2$. Dichloromethane as solvent. 1 mol% ligand. [b] Conversion measured by ^{1}H-NMR. Reaction time shown in parentheses. [c] Enantiomeric excesses measured by HPLC. Absolute configuration shown in parentheses. [d] Isolated yields of **1** were > 93%. [e] Toluene as solvent.

Regarding the effect of the substituents at the biphenyl phosphite moiety, we found that the presence of bulky *tert*-butyl substituents at both the *ortho* and *para* positions is highly adventitious in terms of activity and enantioselectivity (Table 4.3.2, entry 1). Therefore, the presence of methoxy groups in the *para* position of the biphenyl moieties has a negative effect on activity, while the presence of trimethylsilyl substituents at the *ortho* positions has a negative effect on enantioselectivity (Table 4.3.2, entries 2 and 3 vs 1). With ligands **L29f** and **L29g**, which contain different enantiomerically pure binaphthyl moieties, we found that there is a cooperative effect between the configuration of the biaryl moiety and the configuration of the ligand backbone on enantioselectivity. This led to a matched combination for ligand **L29f**, which contains an *S*-binaphthyl moiety (Table 4.3.2, entries 4 and 5). In addition, by comparing the results obtained using ligand **L29c** with those of the related binaphthyl ligands **L29f** and **L29g** (Table 4.3.2, entries 3-5), we can also conclude that the tropoisomeric biphenyl moiety in ligands **L29a**-**c** adopts an *S*-configuration when coordinated in the Pd-π-allyl intermediate species.

To sum up, the best result was obtained with ligands **L29a** and **L33a**, which contain the optimal combination of ligand parameters (Table 4.3.2, entries 1 and 11). These findings clearly show the efficiency of highly modular scaffolds in ligand design. Enantioselectivity can be further improved by controlling not only the structural but also the reaction parameters. As expected,

changing the solvent from dichloromethane to toluene increased enantioselectivity (ee's up to 92%, Table 4.3.2, entry 15).

*Allylic substitution of rac-(E)-ethyl-2,5-dimethyl-3-hex-4-enylcarbonate **S2** using dimethyl malonate as nucleophile*

We also screened the phosphite-nitrogen ligand library **L29**-**L36a**-**g** in the allylic alkylation process of **S2** using dimethyl malonate as nucleophile (Eq 4.3.1a, R = ^{i}Pr, X = OCO_2Et). This substrate is more sterically demanding than substrate **S1**, used previously.[1] If enantiomeric excesses are to be high, the ligand must create a slightly bigger chiral pocket (the chiral cavity in which the allyl is embedded) around the metal center in order to be able to accommodate the sterically demanding isopropyl substituents.[1] Due to the flexibility conferred by the biaryl phosphite moiety, we expected to obtain good enantioselectivities for this substrate, as well. Table 4.3.3 shows the most representative results.

In general, the trends were the same as for the allylic substitution of **S1**. Again, both enantiomers of the alkylation product **3** were accessible in high enantioselectivities (ee's up to 93%) when catalyst precursors containing ligands **L29a** and **L33a** were used (Table 4.3.3, entries 1, 9, 13 and 14). As expected, the activities were lower than in the alkylation reaction of **S1**.[1] The stereoselectivity of the alkylation of **S2** was the same as for the alkylation reaction of **S1**, though the CIP descriptor was inverted because of the change in the priority of the groups.

Table 4.3.3. Selected results for the Pd-catalyzed allylic substitution of **S2** using the ligand library **L29**-**L36a**-**g**[a]

Entry	Ligand	% Conv (h)[b]	% ee[c]
1[d]	**L29a**	100 (24)	84 (*R*)
2	**L29b**	95 (24)	82 (*R*)
3	**L29c**	100 (24)	73 (*R*)
4	**L29f**	78 (24)	67 (*R*)
5	**L29g**	82 (24)	39 (*R*)
6	**L30a**	75 (24)	47 (*R*)
7[d]	**L31a**	100 (24)	77 (*R*)
8	**L32a**	69 (24)	60 (*R*)
9	**L33a**	100 (24)	83 (*S*)
10[d]	**L34a**	100 (24)	12 (*R*)
11	**L35a**	100 (24)	24 (*R*)
12	**L36a**	100 (24)	23 (*S*)
13[e]	**L29a**	99 (48)	93 (*R*)
14[e]	**L33a**	94 (48)	92 (*S*)

[a] All reactions were run at 23 ºC. 1 mol% $[PdCl(\eta^3\text{-}C_3H_5)]_2$. Dichloromethane as solvent. 2 mol% ligand. [b] Conversion measured by ^{1}H-NMR. Reaction time shown in parentheses. [c] Enantiomeric excesses measured by ^{1}H NMR using $[Eu(hfc)_3]$. Absolute configuration shown in parentheses. [d] Isolated yields of **3** were > 92%. [e] Toluene as solvent.

*Allylic substitution of rac-1,3-dimethyl-3-acetoxyprop-1-ene **S3** using dimethyl malonate as nucleophile*

We also tested ligands **L29**-**L36a**-**g** in the allylic substitution of the linear substrate **S3** (Eq. 4.3.1a, R = Me, X = OAc). Substrate **S3** is less sterically demanding than substrates **S1** and **S2**, used previously. There are therefore fewer successful catalyst systems for the Pd-catalyzed allylic substitution of this substrate than for the allylic substitution of hindered substrates such as **S1** and **S2**.[2b,4,5e,8b,9] If enantiomeric excesses are to be high, the ligand must create a small chiral pocket around the metal center, mainly because of the presence of less sterically demanding methyl *syn* substituents.[1] Due to the flexibility conferred by the biaryl phosphite moiety in combination with the possibility of changing the size of the chelate ring in the ligand, we expected to adequately modulate the chiral pocket in order to obtain good enantioselectivities for this substrate, as well.

Preliminary investigations into the solvent and ligand-to-palladium ratio revealed a different trend in solvent effect than with the previously tested substrates **S1** and **S2**. Enantioselectivities and activities were both best when dichloromethane was used and the ligand-to-palladium ratio was 1 (see Section 4.3.8, "Supporting information"). Table 4.3.4 shows the results obtained using the ligand library **L29**-**L36a**-**g** in optimized conditions.

Table 4.3.4. Selected results for the Pd-catalyzed allylic substitution of **S3** using the ligand library **L29**-**L36a**-**g**[a]

Entry	Ligand	% Conv (h)[b]	% ee[c]
1[d]	**L29a**	100 (1)	59 (*S*)
2	**L29b**	100 (1)	67 (*S*)
3	**L29c**	100 (1)	54 (*S*)
4[d]	**L29f**	100 (2)	75 (*S*)
5[d]	**L29g**	100 (2)	51 (*S*)
6	**L29d**	82 (2)	30 (*S*)
7	**L29e**	63 (2)	21 (*S*)
8[d]	**L30a**	100 (2)	60 (*S*)
9[d]	**L30e**	100 (2)	74 (*S*)
10[d]	**L31a**	100 (2)	59 (*S*)
11[d]	**L31e**	100 (2)	75 (*S*)
12[d]	**L32a**	100 (2)	5 (*S*)
13	**L33a**	100 (1)	57 (*R*)
14	**L34a**	92 (2)	38 (*S*)
15	**L35a**	93 (3)	80 (*S*)
16	**L35f**	100 (4)	87 (*S*)
17	**L36f**	100 (4)	87 (*R*)
18[d,e]	**L29f**	100 (20)	84 (*S*)
19[e]	**L35f**	96 (24)	92 (*S*)

[a] All reactions were run at 23 ºC. 0.5 mol% $[PdCl(\eta^3\text{-}C_3H_5)]_2$. Dichloromethane as solvent. 1 mol% ligand. [b] Conversion measured by GC. Reaction time shown in parentheses. [c] Enantiomeric excesses measured by GC. Absolute configuration shown in parentheses. [d] Isolated yields of **4** were > 91%. [e] T = 0 ºC.

We were able to fine-tune the ligands in order to obtain high activities and enantioselectivities (ee's up to 92%) in the alkylation of this substrate. Again, activities and enantioselectivities were affected by the bridge length, the substituent at the nitrogen heterocycle, and the substituents and configurations in the biaryl phosphite moiety. However, the effect of these parameters was different from their effect on substitution of hindered substrates **S1** and **S2**. Enantioselectivities were best with ligands **L35j** and **L36j** (Table 4.3.4, entries 16, 17 and 19). Once again, it was possible to access both enantiomers of the substitution product **4**. These results, which again clearly show the efficiency of using modular scaffolds in ligand design, are among the best reported for this type of unhindered substrate.[2b,4,5e,8b,9]

Regarding the effect of ligand flexibility, in contrast to **S1** and **S2**, the highest enantioselectivities were obtained with ligands **L35** and **L36**, which form a seven-membered chelate ring and contain two methyl groups at the alkyl backbone chain. Concerning the effect of the substituents at the heterocyclic ring and the biaryl phosphite moiety, in contrast to **S1** and **S2**, the presence of aryl substituents in the heterocyclic moiety and a bulky *S*-binaphthyl phosphite moiety had a positive effect on enantioselectivities. In conclusion, our results indicate that both the size of the chelate ring and the flexibility of the biaryl phosphite moiety are the main ligand parameters that control the size of the chiral pocket in order to achieve high enantioselectivities.

*Allylic alkylation of cyclic substrates **S4** and **S5***

With the unhindered cyclic substrates **S4** and **S5**, enantioselectivity is difficult to control, mainly because of the presence of less sterically demanding *anti* substituents. These *anti* substituents are thought to play a crucial role in the enantioselection observed with cyclic substrates in the corresponding Pd-allyl intermediates.[1]

In this section, we show that the chiral ligand library **L29**-**L36a**-**g** applied previously to the Pd-catalyzed allylic substitution of 1,3-disubstituted linear substrates (**S1**-**S3**) can also be used for cyclic substrates (ee's up to 88%). We tested two cyclic substrates (Eq. 4.3.1b): *rac*-3-acetoxycyclohexene (**S4**) (which is widely used as a model substrate) and *rac*-3-acetoxycycloheptene (**S5**).

Preliminary investigations into the solvent effect and ligand-to-palladium ratio showed the same trends as with the previously tested unhindered linear substrate **S3**. The trade-off between enantioselectivities and reaction rates was therefore optimum with dichloromethane and a ligand-to-palladium ratio of 1 (see Section 4.3.8, "Supporting information"). Table 4.3.5 shows the results of using the ligand library **L29**-**L36a**-**g** under the optimized conditions. We also obtained high activities and enantioselectivities (up to 88%) in the allylic substitution of the cyclic substrates **S4** and **S5** using ligands **L29f**, **L29g** and **L31g**. The results indicate that the effect of the ligand parameters on the catalytic performance are different from those observed for the linear substrates **S1**-**S3**. In contrast to the alkylation of unhindered linear **S3**, ligands that form a six-membered chelate ring (**L29**) provided higher enantioselectivities than those which form a seven-membered chelate ring (**L34**-**L35**). The results also indicate that the presence of an enantiopure bulky binaphthyl phosphite moiety (**f** and **g**) is therefore required for enantioselectivity to be high (Table 4.3.5, entries 4, 5, 8, 14 and 15). Interestingly, the sense of enantioselectivity is also governed by the configuration of the biaryl phosphite moiety. Thus, both enantiomers of the

substitution products **5** and **6** can be accessed in high enantioselectivities by simply changing the configuration of the trimethylsilyl-substituted binaphthyl moiety (Table 4.3.5, entries 4 and 5).

Table 4.3.5. Selected results for the Pd-catalyzed allylic substitution of **S4** and **S5** using the ligand library **L29**-**L36a**-**g**[a]

Entry	Substrate	Ligand	% Conv (h)[b]	% ee[c]
1	**S4**	**L29a**	100 (6)	41 (*S*)
2	**S4**	**L29b**	100 (6)	59 (*S*)
3	**S4**	**L29c**	100 (6)	43 (*S*)
4[d]	**S4**	**L29f**	100 (6)	80 (*S*)
5[d]	**S4**	**L29g**	100 (6)	85 (*R*)
6	**S4**	**L30a**	100 (6)	41 (*S*)
7	**S4**	**L31a**	100 (6)	45 (*S*)
8[d]	**S4**	**L31e**	100 (6)	84 (*R*)
9[d]	**S4**	**L32a**	100 (6)	60 (*S*)
10	**S4**	**L33a**	100 (6)	39 (*R*)
11	**S4**	**L34a**	100 (6)	13 (*S*)
12	**S4**	**L35a**	100 (6)	29 (*S*)
13	**S4**	**L35f**	100 (6)	63 (*S*)
14	**S5**	**L29f**	100 (24)	83 (*S*)
15[d]	**S5**	**L29g**	100 (24)	88 (*R*)

[a] All reactions were run at 23 ºC. 0.5 mol% $[PdCl(\eta^3\text{-}C_3H_5)]_2$. Dichloromethane as solvent. 1 mol% ligand. [b] Conversion measured by GC. Reaction time shown in parentheses. [c] Enantiomeric excesses measured by GC. Absolute configuration shown in parentheses. [d] Isolated yields of **5** and **6** were > 91%.

In summary, the enantioselectivities obtained with ligands **L29f**, **L29g** and **L31f** are among the best reported for this type of 1,3-disubstituted cyclic substrate.[1e,2a,4a,8b,9a,10] Interestingly, compared with the hindered substrates **S1** and **S2** and in contrast to the unhindered linear substrate **S3**, the flexibility conferred by the biaryl phosphite moiety was enough to adequately control the size of the chiral pocket in order to achieve high enantioselectivities.

Allylic substitution of unsymmetrical 1,3,3-trisubstituted allylic substrates

We also screened the ligands **L29**-**L36a**-**g** in the allylic substitution of *rac*-1,3,3-triphenylprop-2-enyl acetate (**S6**) and *rac*-1,1,-diphenyl-1-hepten-3-yl acetate (**S7**) using dimethylmalonate as nucleophile (Eq.4.3.2, R = R' = R'' = Ph for **S6** and R = R' = Ph, R'' = Me for **S7**). These substrates are of synthetic interest because the so-formed substitution products can easily be transformed into enantiomerically enriched acid derivatives and lactones.[11] They are more sterically demanding than the previously used substrate **S1**,[1] and it is therefore more difficult to achieve excellent enantioselectivities with them than with **S1**.[12] Interestingly, with this P,N-ligand library, we obtained high enantiomeric excesses (ee's up to 96%) under standard reaction conditions. Although, as expected, the activities were lower than in the alkylation reaction of **S1**, they were much higher than those obtained with other successful ligands under similar reaction conditions.[12]

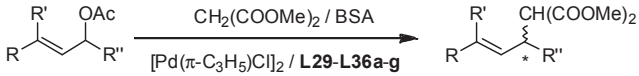

(4.3.2)

S6 R= R'= R''= Ph
S7 R= R'= Ph; R''= Me

7 R= R'= R'' = Ph
8 R= R'= Ph; R'' = Me

The results, summarized in Table 4.3.6, followed a trend similar to that of the more hindered substrates **S1** and **S2**. Thus, ligands **L29** and **L33**, which form a six-membered chelate ring and have a phenyl substituent at the nitrogen heterocycle, provided better enantioselectivities than ligands **L30**-**L32** and **L34**-**L36**. The presence of bulky substituents at the *ortho* positions of the biaryl phosphite moiety was necessary in order for enantioselectivities to be high. However, in contrast to **S1** and **S2**, enantioselectivities were less affected by the presence or lack of bulky substituents at the *para* positions of the biaryl phosphite moiety. Therefore, ligands **L29a**-**c** and **L33a**-**c** provided excellent enantiocontrol in the allylic substitution of the trisubstituted substrates **S6** and **S7**, and also gave access to both enantiomers of the alkylation products **7** and **8** (ee's up to 96%). These results are among the best reported for this class of substrate.[12]

Table 4.3.6. Selected results for the Pd-catalyzed allylic substitution of **S6** and **S7** using the ligand library **L29**-**L36a**-**g**[a]

		S6		**S7**	
Entry	Ligand	% Conv (h)[b]	% ee[c]	% Conv (h)[b]	% ee[c]
1[d]	**L29a**	92 (24)	88 (*R*)	100 (24)	95 (*R*)
2	**L29b**	88 (24)	95 (*R*)	100 (24)	94 (*R*)
3	**L29c**	79 (24)	96 (*R*)	100 (24)	95 (*R*)
4	**L29f**	46 (24)	42 (*R*)	53 (24)	32 (*R*)
5	**L29d**	33 (24)	18 (*R*)	48 (24)	21 (*R*)
6	**L30a**	90 (24)	81 (*R*)	100 (24)	78 (*R*)
7	**L31a**	88 (24)	90 (*R*)	100 (24)	85 (*R*)
8	**L32a**	45 (24)	23 (*R*)	85 (24)	38 (*R*)
9	**L33a**	88 (24)	90 (*S*)	100 (24)	95 (*S*)
10	**L34a**	67 (24)	40 (*R*)	73 (24)	57 (*R*)
11	**L35a**	29 (24)	30 (*R*)	46 (24)	44 (*R*)
12	**L36a**	27 (24)	30 (*S*)	42 (24)	42 (*S*)

[a] All reactions were run at 23 ºC. 1 mol% $[PdCl(\eta^3\text{-}C_3H_5)]_2$. Dichloromethane as solvent. 2 mol% ligand. [b] Conversion measured by ^{1}H-NMR. Reaction time shown in parentheses. [c] Enantiomeric excesses measured by ^{1}H-NMR. Absolute configuration shown in parentheses. [d] Isolated yields of **7** and **8** were > 88%.

Allylic substitution of unsymmetrical 1- or 3-monosubstituted allylic substrates

To further study the potential of these readily available ligands, we tested **L29**-**L36a**-**g** in the regio- and stereoselective allylic alkylation of 1-(1-naphthyl)allyl acetate (**S8**) and 1-(1-naphthyl)-3-acetoxyprop-1-ene (**S9**) with dimethyl malonate as nucleophile (Eq. 4.3.3). For these substrates, not only does the enantioselectivity of the process need to be controlled but regioselectivity is also a problem because a mixture of regioisomers can be obtained. Most Pd-catalysts developed to date favor the formation of achiral linear product **10** rather than the desired branched isomer **9**.[13]

The development of highly regio- and enantioselective Pd-catalysts is therefore still important.[4a,6,8b,14]

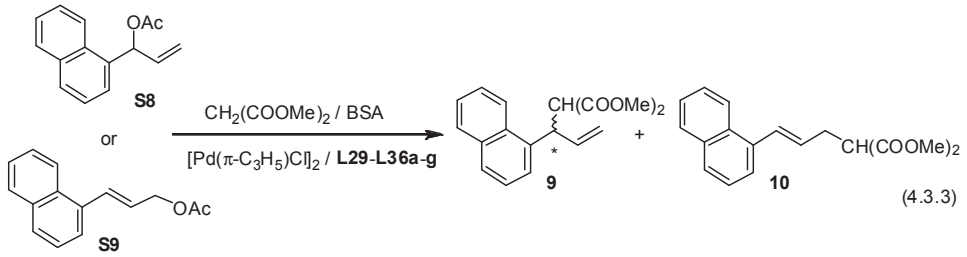

(4.3.3)

Table 4.3.7 summarizes the results obtained with the ligand library **L29**-**L36a**-**g**. High activities and enantioselectivities (of up to 92%) combined with regioselectivities of up to 80% in favor of the branched product **9** were obtained under standard reaction conditions.

Table 4.3.7. Selected results for the Pd-catalyzed allylic alkylation of monosubstituted substrates **S8** and **S9** using the ligand library **L29**-**L36a**-**g** under standard conditions.[a]

Entry	Ligand	Substrate	% Conv (min)[b]	**9**/**10**	% ee[d]
1	**L29a**	**S8**	100 (30)	70/30	20 (*R*)
2	**L29b**	**S8**	100 (30)	40/60	63 (*R*)
3	**L29c**	**S8**	100 (30)	55/45	70 (*R*)
4	**L29f**	**S8**	100 (30)	50/50	78 (*R*)
5	**L29g**	**S8**	100 (30)	55/45	34 (*R*)
6[e]	**L30a**	**S8**	100 (30)	80/20	45 (*R*)
7	**L30d**	**S8**	100 (30)	75/25	88 (*R*)
8	**L31a**	**S8**	100 (30)	75/25	19 (*R*)
9	**L31c**	**S8**	100 (30)	70/30	73 (*R*)
10	**L32a**	**S8**	100 (30)	75/25	25 (*R*)
11	**L34a**	**S8**	100 (30)	45/55	2 (*S*)
14	**L35a**	**S8**	100 (30)	80/20	92 (*R*)
15	**L35f**	**S8**	100 (30)	60/40	90 (*R*)
16	**L29f**	**S9**	100 (30)	50/50	79 (*R*)
17	**L31c**	**S9**	100 (30)	70/30	72 (*R*)
18	**L30f**	**S9**	100 (30)	75/25	87 (*R*)
19	**L35a**	**S9**	100 (30)	80/20	92 (*R*)

[a] All reactions were run at 23 °C. 1 mol% $[PdCl(\eta^3\text{-}C_3H_5)]_2$. Dichloromethane as solvent. 2 mol% ligand. Substrate (0.5 mmol). BSA (1.5 mmol). Dimethyl malonate (1.5 mmol). [b] Reaction time in minutes shown in parentheses. [c] Percentage of branched (**9**) and linear (**10**) isomers. [d] Enantiomeric excesses of **9** determined by HPLC. Absolute configuration shown in parentheses. [e] Isolated yield of **9** was > 72%.

The results indicate that the selectivity (regio- and enantioselectivity) is mainly affected by the ligand backbone, the substituent at the nitrogen heterocycle, and the substituents and configurations in the biaryl phosphite moiety. However, no general trend was seen. The trade-off between regio- and enantioselectivities was best for ligand **L35a**, which forms a seven-membered chelate ring and has methyl-substitutents at the alkyl-backbone chain and bulky *tert*-butyl groups

at the *ortho* and *para* positions of the biphenyl phosphite moiety (Table 4.3.7, entries 14 and 19). Again, these results are among the best reported for this type of substrate.[4a,6,8b,14]

4.3.3.2. Origin of enantioselectivity: study of the Pd-π-allyl intermediates

To provide further insight into how ligand parameters affect catalytic performance, we studied the Pd-π-allyl compounds **11**-**20** [Pd(η^3-allyl)(L)]BF_4 (L = **L29**-**L36a**-**g**), because they are key intermediates in the allylic substitution reactions studied.[1] These ionic palladium complexes, which contain 1,3-diphenyl, 1,3-dimethyl or cyclohexenyl allyl groups, were prepared using the previously reported method from the corresponding Pd-allyl dimer and the appropriate ligand in the presence of silver tetrafluoroborate (Scheme 4.3.1).[15] The complexes were characterized by elemental analysis and by ^{1}H, ^{13}C and ^{31}P NMR spectroscopy. The spectral assignments were based on information from ^{1}H-^{1}H, ^{31}P-^{1}H and ^{13}C-^{1}H correlation measurements in combination with ^{1}H-^{1}H NOESY experiments. Unfortunately, we were unable to obtain crystal of sufficient quality to perform X-ray diffraction measurements. For some of the key Pd-allyl complexes, we also performed a DFT study.

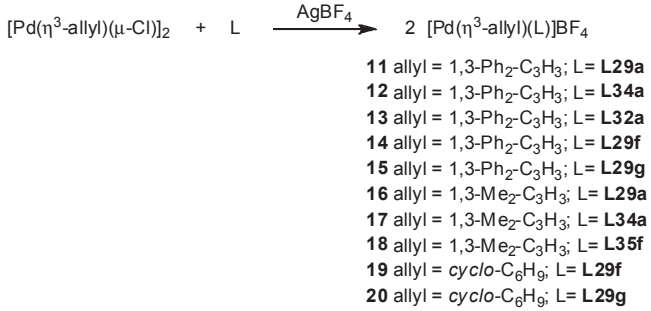

Scheme 4.3.1. Preparation of [Pd(η^3-allyl)(L)]BF_4 complexes **25**-**34**.

Palladium 1,3-diphenyl-allyl complexes

When the phosphite-nitrogen ligand library **L29**-**L36a**-**g** was used in the allylic substitution of substrate **S1**, the catalytic results showed that enantioselectivity is highly affected by the ligand parameters. A six-membered chelate ring, phenyl substituents in the nitrogen heterocyclic ring, and bulky substituents at the *ortho* position of the biaryl moiety are therefore required if enantioselectivity is to be high. To understand this catalytic behavior, we studied the Pd-π-allyl complexes **11**-**13**, which contain ligands **L29a, L34a** and **L32a**, respectively. Finally, with complexes **14** and **15**, which contain ligands **L29f** and **L29g**, we studied the cooperative effect seen between the configuration of the ligand backbone and the configuration of the biaryl phosphite moiety.

The VT-NMR (30 ºC to -80 ºC) study of the Pd-allyl intermediate **11**, which contains ligand **L29a**, had a mixture of two isomers in equilibrium at a ratio of 9:1.[16] Both isomers were unambiguously assigned by NMR (^{1}H, ^{31}P, ^{13}C, ^{1}H-^{1}H, ^{1}H-^{13}C and ^{1}H-^{31}P correlation and NOESY experiments) to the two *syn*/*syn endo* **A** and *exo* **B** isomers (Scheme 4.3.2). In both isomers, the NOE indicated interactions between the two terminal protons of the allyl group and also between the central allyl proton and *ortho* hydrogens of both phenyl groups of the allyl ligand, which clearly

indicates a *syn*/*syn* disposition (Figure 4.3.2). Moreover, the central allyl proton showed a NOE interaction with the hydrogen of the CH-O group of the ligand backbone of the major isomer **A**, while in isomer **B** this interaction appeared with the hydrogens of one *tert*-butyl group. These interactions can be explained by assuming a *syn*/*syn endo* disposition for isomer **A** and a *syn*/*syn exo* disposition for isomer **B** (Figure 4.3.2). We also carried out theoretical calculations at the DFT level for both isomers. Figure 4.3.2 shows these calculated structures and the relative values of the formation enthalpy, with isomer **A** being the most stable. The difference in the calculated formation enthalpy for the two isomers (ΔH = 1.8 Kcal/mol) is in agreement with the population observed by NMR of the different Pd-allyl intermediates formed in solution. For both isomers, the carbon NMR chemical shifts indicate that the more electrophilic allyl carbon terminus is *trans* to the phosphite moiety (Scheme 4.3.2). Assuming that the nucleophilic attack takes place at the more electrophilic allyl carbon terminus,[1] the matching between enantiomeric excesses (82% (*S*) in product **1**) and the diastereoisomeric Pd-ratio (de = 80% (*S*)) indicate that the two isomers react at a similar rate. This is in agreement with the fact that the electrophilicities of the allylic terminal carbon atom *trans* to the phosphite are rather similar in both complexes ($\Delta(\delta^{13}C)$ = 0.5 ppm). To prove this, we studied the reactivity of the Pd-intermediates with sodium malonate at low temperature by *in situ* NMR (see Section 4.3.8, "Supporting information"). Our results showed that the two isomers react at a similar rate. So, enantioselectivity is controlled by the diastereomeric excess of the Pd-intermediates present in solution.

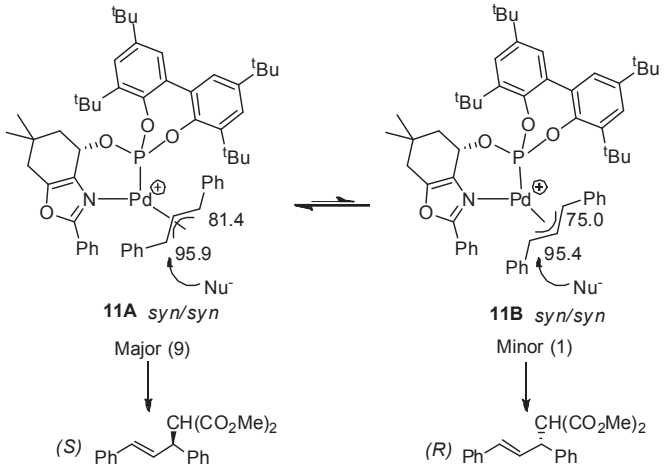

Scheme 4.3.2. Diastereoisomer Pd-allyl intermediates for **S1** with ligand **L29a**. The relative amounts of each isomer are shown in parentheses. The chemical shifts (in ppm) of the allylic terminal carbons are also shown.

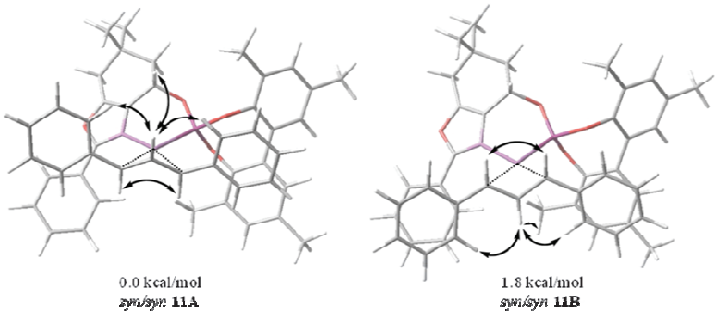

Figure 4.3.2. Calculated structures (DFT) for cationic species of complex [Pd(η^3-1,3-diphenylallyl)(**L29a**)]BF_4 (**11**) and their relative formation enthalpies. This figure also shows the relevant NOE contacts from the NOESY experiment.

The VT-NMR study of Pd-allyl intermediate **12** containing ligand **L34a**, which forms a seven-membered chelate ring and provides lower enantioselectivity than Pd-**L29a**, also had a mixture of two *syn*/*syn endo* (**A**) and *exo* (**B**) isomers, but at a ratio of 1.25:1. Also, the more electrophilic allyl carbon terminus was *trans* to the phosphite moiety (Scheme 4.3.3). In contrast to the Pd/**L29a** catalytic system, the diastereoisomeric excess (de = 11% (*S*)) of the Pd-intermediates differed from the enantiomeric excess (21% (*S*)) of alkylation product **1**. Therefore, isomer **A** reacted slightly faster than isomer **B**.[17] This was confirmed by an *in situ* NMR study of the reactivity of the Pd-intermediates with sodium malonate at low temperature.[18] However, the lower enantioselectivity with this system than with the previous Pd/**L29a** catalytic system can mainly be attributed to the decrease in the relative amount of isomer **A** with respect to isomer **B**, compared with the population of the isomers (**A** and **B**) for complex **11**.

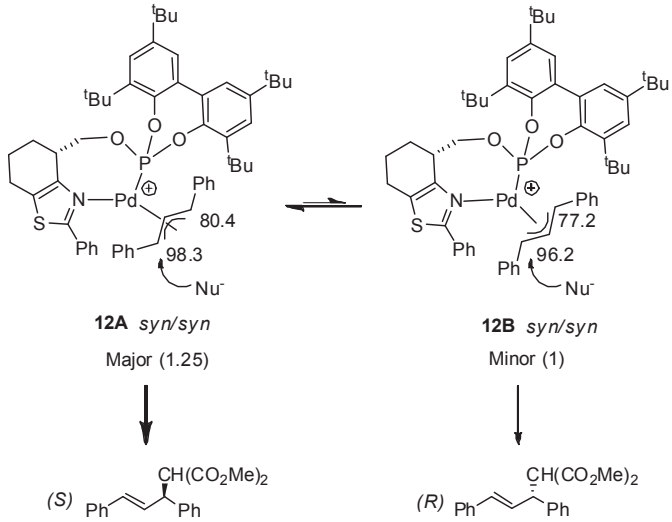

Scheme 4.3.3. Diastereoisomer Pd-allyl intermediates for **S1** with ligand **L34a**. The relative amounts of each isomer are shown in parentheses. The chemical shifts (in ppm) of the allylic terminal carbons are also shown.

Next, we studied the Pd-1,3-diphenyl allyl intermediate **13** containing ligand **L32a**, which differs from **L29a** due to the presence of a bulky *tert*-butyl group at the oxazole moiety instead of a phenyl substituent and provides much lower enantioselectivity than the Pd-**L29a** catalyst. The VT-NMR spectra indicated the presence of a mixture of two species at a ratio of 7:3. The major species were assigned by NOE to the *syn*/*syn endo* **A** isomer, while the minor species was attributed to compound **C**, which contains two ligands coordinated in a monodentated fashion (Scheme 4.3.4).[19] The formation of **C** is due to the fact that the replacement of the phenyl ozaxole substituents in ligand **L29a** by a bulky *tert*-butyl group caused greater steric interaction with one of the phenyl substitutents of substrate **S1** in the related *syn*/*syn exo* **B** isomer observed in Pd-**L29a** complex **11** (Scheme 4.3.4). The formation of compound **C** minimizes this new steric interaction and explains why the expected *syn*/*syn exo* **B** isomer in solution was not detected (Scheme 4.3.4). Therefore, the fact that enantioselectivity was lower when the Pd/**L32a** catalyst was used (ee's up to 22%) than when the Pd/**L29a** catalyst was used (ee's up to 82%) may be due to the presence of Pd-complex **C**. Complexes of this type are known to be faster and less enantioselective than their bidentate counterparts because they have more degrees of freedom.[8b,20]

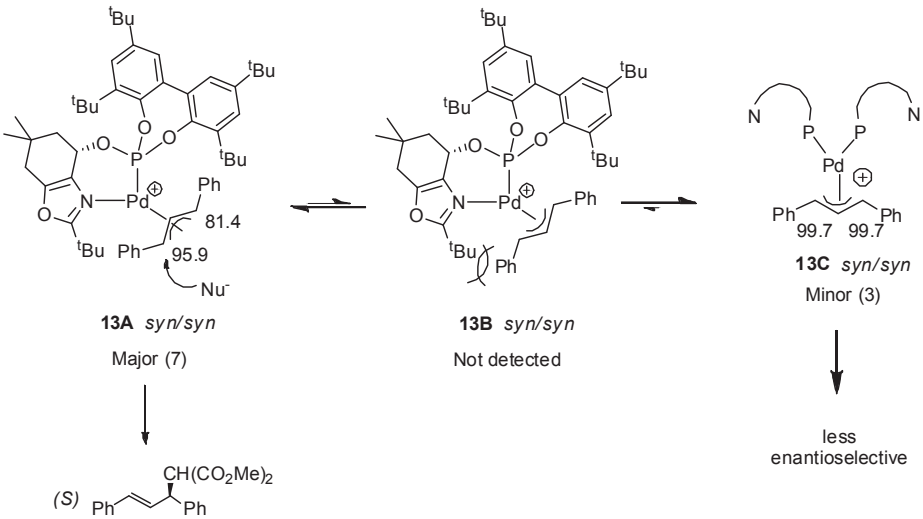

Scheme 4.3.4. Diastereoisomer Pd-allyl intermediates for **S1** with ligand **L32a**. The relative amounts of each isomer are shown in parentheses. The chemical shifts (in ppm) of the allylic terminal carbons are also shown.

Finally, we studied the cooperative effect observed between the configuration of the ligand backbone and the configuration of the biaryl phosphite moiety with complexes **14** and **15**, containing ligands **L29f** and **L29g**, respectively. The VT-NMR study indicated the presence of a mixture of two *syn*/*syn endo* (**A**) and *exo* (**B**) isomers in ratios of 5:1 and 1:2.5, respectively (Scheme 4.3.5). As for the 1,3-diphenylallyl intermediates discussed above, the NMR data showed that the more electrophilic allyl terminal carbon is *trans* to the phosphite moiety at the **A** isomers (**14A** and **15A**). For complex **14**, our results indicated that the stereochemical outcome of the reaction (ee = 69% (*S*)) was mainly due to the diastereoisomeric excess (de = 66% (*S*)) of the Pd-complexes in solution, as observed for Pd/**L29a**. However, for complex **15**, the

diastereoisomeric excess (de = 43% (*R*)) did not match the enantioselectivity obtained (ee = 40% (*S*)). Therefore, we conclude that isomer **15A** reacts faster than isomer **15B**. A clear indication of this fact can be found in the higher electrophilicity of the allylic terminal carbon *trans* to the phosphite in **15A** than in **15B** ($\Delta(\delta^{13}C)$ = 4.6 ppm). Although isomer **15A** has a faster reaction rate than isomer **14A**, this is not the reason why Pd/**L29g** causes lower enantioselectivity than Pd/**L29f**. Rather, Pd/**L29g**'s lower enantioselectivity is because the relative amount of isomer **A** respect to isomer **B** is much lower in Pd/**L29f** than in Pd/**L29g.** Therefore, as observed earlier, the presence of an *S*-configuration at the biaryl phosphite moiety is necessary for good enantioselectivity. In addition, these results provide further evidence that the flexible biphenyl phosphite moieties in ligands **L29a**-**c** adopt an *S*-configuration when coordinated to palladium.

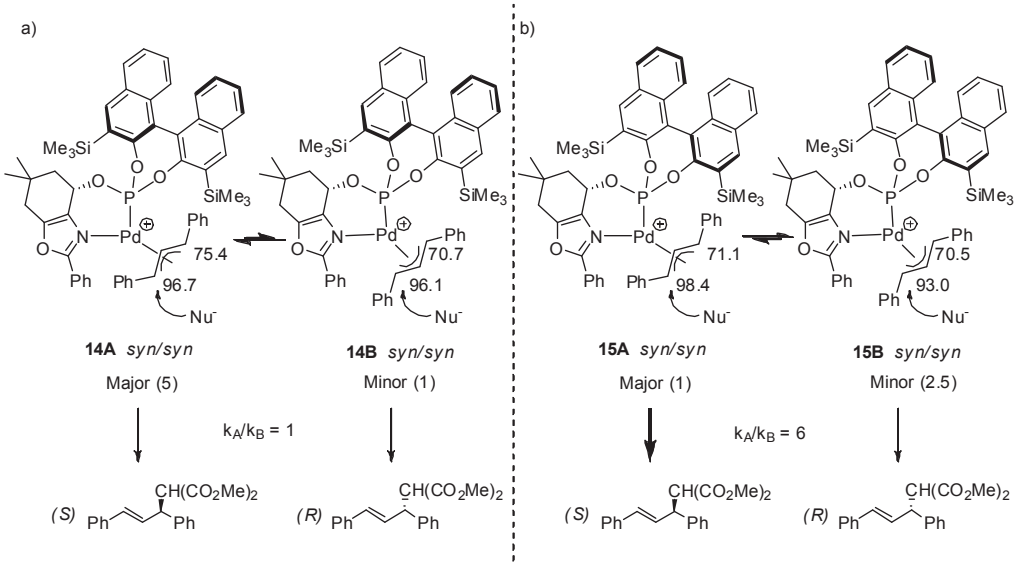

Scheme 4.3.5. Diastereoisomer Pd-allyl intermediates for **S1** with a) ligand **L29f** and b) ligand **L29g**. The relative amounts of each isomer are shown in parentheses. The chemical shifts (in ppm) of the allylic terminal carbons are also shown.

In summary, the study of the Pd-1,3-diphenylallyl intermediate showed that enantioselectivity is mainly controlled by the diastereoisomeric excess of the Pd-intermediates present in solution. So, for enantioselectivity to be high, the different ligand parameters need to be correctly combined in order to predominantly form one of the Pd-isomers and also to avoid the formation of species with ligands coordinated in a monodentated fashion.

Palladium 1,3-dimethyl-allyl complexes

When the phosphite-nitrogen ligand library **L29**-**L36a**-**g** was used in the allylic substitution of substrate **S3**, the catalytic results revealed a different trend with regard to the effect of the ligand parameters than with the hindered substrate **S1**. A seven-membered chelate ring, the presence of methyl substituents at the alkyl backbone chain, and a bulky *S*-binaphthyl phosphite moiety are necessary for high enantioselectivity. To understand this catalytic behavior, we studied Pd-π-allyl complexes **16**-**18**, which contain ligands **L29a**, **L35a** and **L35f**, respectively. With ligands **L29a**

and **L35a**, we studied the effect of the chelate ring size, whereas with ligand **L35f** we studied the configuration of the biaryl phosphite moiety.

The VT-NMR (30 ºC to -80 ºC) study of Pd-allyl intermediate **16**, which contains ligand **L29a**, had a mixture of three isomers in equilibrium at a ratio of 2.5:1:2. Isomers **A** and **B** were assigned by NOE to the two *syn*/*syn endo* **A** and *exo* **B** isomers, while isomer **D** was assigned to the *syn*/*anti* isomer (Scheme 4.3.6). For isomers **A** and **B**, the NOE indicated interactions between the two terminal protons of the allyl group, whereas for isomer **D** the central allyl proton showed a NOE interaction with the terminal allyl proton located *trans* to the oxazole group (Figure 4.3.3). Moreover, for isomers **A** and **D**, the central allyl proton showed a NOE interaction with the hydrogen of the CH-O group of the ligand, while in isomer **B** this interaction appeared with the hydrogens of the *tert*-butyl group. These interactions can be explained by assuming a *syn*/*syn endo* disposition for isomer **A**, a *syn*/*syn exo* disposition for isomer **B** and a *syn/anti* disposition for isomer **D** (Figure 4.3.3). The NOESY also indicated exchange between the allylic terminal protons located *trans* to the oxazole moiety of isomers **B** and **D** (Figure 4.3.3). This confirms the η^3-η^1-η^3 movement for the exchange between isomers **B** and **D**.[21] In addition, the fact that no other H_{anti}-H_{syn} exchange was observed indicates that the exchange took place by means of the selective opening of one of the terminal Pd-C bonds.

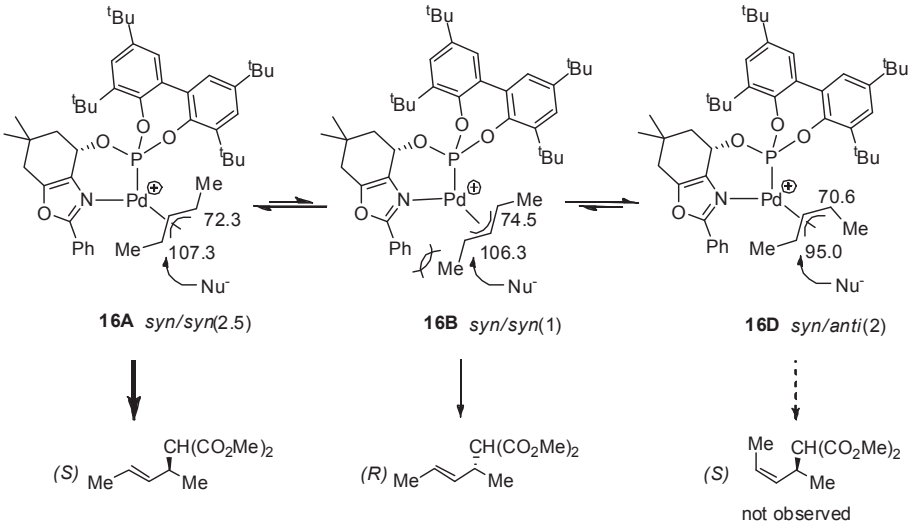

Scheme 4.3.6. Diastereoisomer Pd-allyl intermediates for **S3** with ligand **L29a**. The relative amounts of each isomer are shown in parentheses. The chemical shifts (in ppm) of the allylic terminal carbons are also shown.

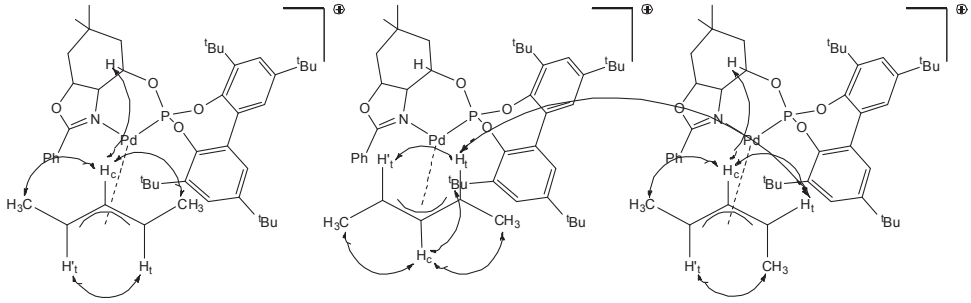

syn/*syn* **16A** *syn*/*syn* **16B** *syn*/*anti* **16D**

Figure 4.3.3. Relevant NOE contacts from the NOESY experiment of the [Pd(η^3-1,3-dimethylallyl)(**L29a**)]BF_4 (**16**) isomers.

The formation of isomer **D** is due to the fact that, in complex **B**, there was an increase in the steric interaction between the oxazole phenyl group and one of the methyl substitutents of **S3** due to the absence of the favorable π-stacking interaction observed in the related Pd-1,3-diphenylallyl complex **11**. The formation of isomer **D** minimized this steric interaction (Scheme 4.3.6). Therefore, the open Pd-C bond belongs to the most electrophilic carbon atom containing the substituent that undergoes the biggest steric hindrance with the phenyl oxazole fragment. The NMR data also indicated that the most electrophilic allyl carbon terminus is *trans* to the phosphite moiety in *syn*/*syn* isomer **A** and in *syn*/*syn* isomer **B**, and that the allylic terminus carbon in isomer **D** is far less electrophilic ($\Delta(\delta^{13}C)$ > 11 ppm). Assuming that the nucleophilic attack takes place at the most electrophilic allyl carbon terminus, on the basis of the observed stereochemical outcome of the reaction (59% (*S*) in product **4**), and since the ee of alkylation product **4** differs from the diastereoisomeric excess (de = 41% (*S*)) of the reacting Pd-intermediates **A** and **B**, we conclude that isomer **A** reacts faster than isomer **B**. This was confirmed by an *in situ* NMR study of the reactivity of the Pd-intermediates with sodium malonate at low temperature. This study indicated that isomer **16A** reacts approximately 1.5 times faster than isomer **16B**. This is also consistent with the fact that, for both isomers, the most electrophilic allylic terminal carbon atom is the one *trans* to the phosphite in the major **A** isomer.

The VT-NMR study of Pd-allyl intermediate **17**, which contains ligand **L35a**, which forms a seven-membered chelate ring and provides higher enantioselectivity than Pd-**L29a**, also had a mixture of three isomers at a ratio of 5:1:7. Isomers **A**, **B** and **D** were assigned by NOE to the *syn*/*syn endo, syn*/*syn exo* and *syn*/*anti* isomers, respectively (Scheme 4.3.7). Again, the most electrophilic allyl carbon terminus was *trans* to the phosphite moiety in *syn*/*syn* isomer **A** and *syn*/*syn* isomer **B**, and the allylic terminus carbon in isomer **D** was far less electrophilic ($\Delta(\delta^{13}C)$ > 11 ppm). As observed for complex Pd/**L29a** (**16**), isomer **A** reacts faster than isomer **B**. The higher enantioselectivity with this system than with the Pd/**L29a** catalytic system discussed above can be attributed to the decrease in the relative amount of isomer **B** with respect to isomer **A** compared with the population of the isomers (**A** and **B**) for complex **16**. The decrease in the population of isomer **B** is due to the formation of a smaller chiral pocket with ligand **L35a** than with ligand **L29a**. This smaller chiral pocket creates a greater steric interaction between the thiazole phenyl group and one of the methyl substitutents of **S3**, which results in the preferential formation of the less electrophilic *syn*/*anti* isomer **D**.

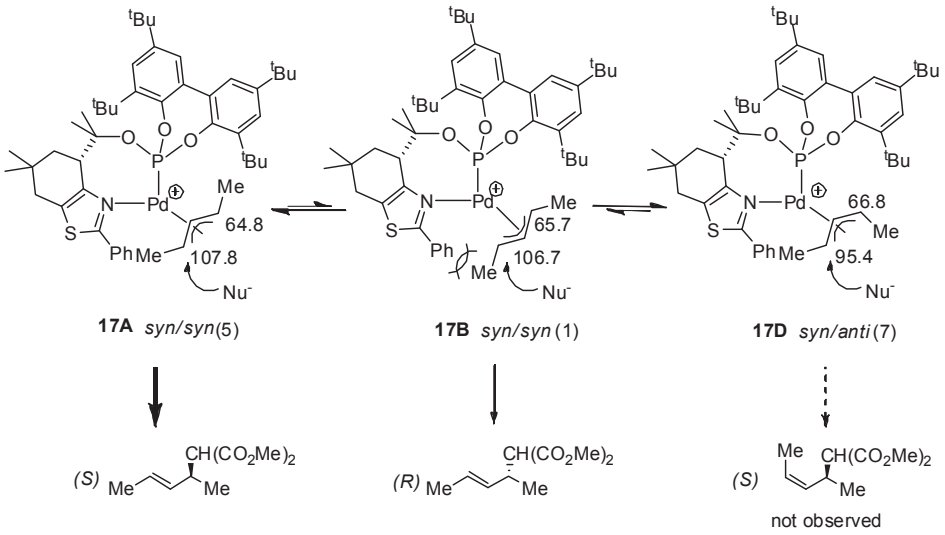

Scheme 4.3.7. Diastereoisomer Pd-allyl intermediates for **S3** with ligand **L35a**. The relative amounts of each isomer are shown in parentheses. The chemical shifts (in ppm) of the allylic terminal carbons are also shown.

Finally, the VT-NMR study of Pd-allyl intermediate **18**, which contains ligand **L35f**, had a mixture of three isomers in a ratio of 10:1:9 (see Section 4.3.5, "Experimental section"). Isomers **A**, **B** and **D** were assigned by NOE to the *syn*/*syn endo, syn*/*syn exo* and *syn*/*anti* isomers, respectively (Scheme 4.3.8).

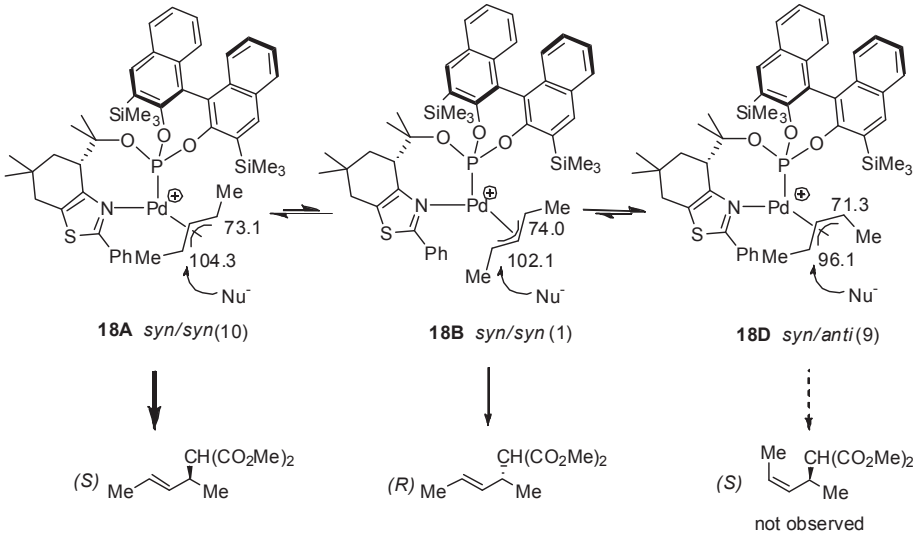

Scheme 4.3.8. Diastereoisomer Pd-allyl intermediates for **S3** with ligand **L35f**. The relative amounts of each isomer are shown in parentheses. The chemical shifts (in ppm) of the allylic terminal carbons are shown.

As for complexes **16** and **17**, the fastest-reacting isomer was the *syn*/*syn* isomer **A**, while isomer **D** was far less electrophilic and therefore did not play a direct role in the enantiodiscrimination process. The higher enantioselectivity obtained with Pd/**L35f** than with the Pd/**L35a** catalytic system is due to the larger amount of the most reactive isomer (isomer **A**) than in complex **17**.

In summary, for enantioselectivities to be high, the various ligand parameters need to be correctly combined in order to preferentially form the faster isomer **A**. The formation of this isomer is mainly governed by the size of the chelate ring and the configuration of the biaryl phosphite moiety.

Palladium 1,3-cyclohexenyl-allyl complexes

When the phosphite-nitrogen ligand library **L29**-**L36a**-**g** was used in the allylic substitution of cyclic substrates **S5** and **S6**, the catalytic results showed that the effect of the ligand parameters on enantioselectivity was different from the effect observed in the substitution of the linear substrates **S1** and **S2**. The best results were obtained with ligands **L29j** and **L29k**, which form a six-membered chelate ring, have phenyl substituents in the nitrogen heterocyclic ring, and have bulky enantiopure binaphthyl phosphite moieties. Interestingly, the sense of enantioselectivity was controlled by the configuration of the biaryl phosphite moiety. So, to understand this catalytic behavior, we studied Pd-π-allyl complexes **19** and **20**, which contain ligands **L29f** and **L29g**.

The VT NMR (35 °C to -80 °C) of Pd intermediate **19**, which contains ligand **L29f**, showed a mixture of the two possible isomers at a ratio of 1:6, respectively (see Scheme 4.3.9). All isomers were unambiguously assigned by NOE to the isomers **A** and **B** (Figure 4.3.4). Thus, for isomer **A**, the NOE indicated interactions between the hydrogen of the CH-O group and the central allyl proton, while for isomer **B** this interaction appeared with one of the methylenic hydrogens of the allyl ligand (Figure 4.3.4). The carbon NMR chemical shifts indicated that the most electrophilic allylic terminus carbon is *trans* to the phosphite moiety. The difference between the diastereoisomeric ratio and enantioselectivity observed in the alkylation of **S5** (de = 70% (*S*) vs. ee = 80% (*S*)) indicated that the nucleophile reacts faster with the major **B** isomer. This was confirmed by the reactivity of the Pd-intermediate with sodium malonate at low temperature by *in situ* NMR.[22] We also carried out theoretical calculations at the DFT level. Figure 4.3.5 shows these calculated structures and their relative formation enthalpy values, with isomer **B** being the most stable. The difference in the calculated formation enthalpies of the two isomers (ΔH = 1.5 Kcal/mol) is in agreement with the population observed by NMR.

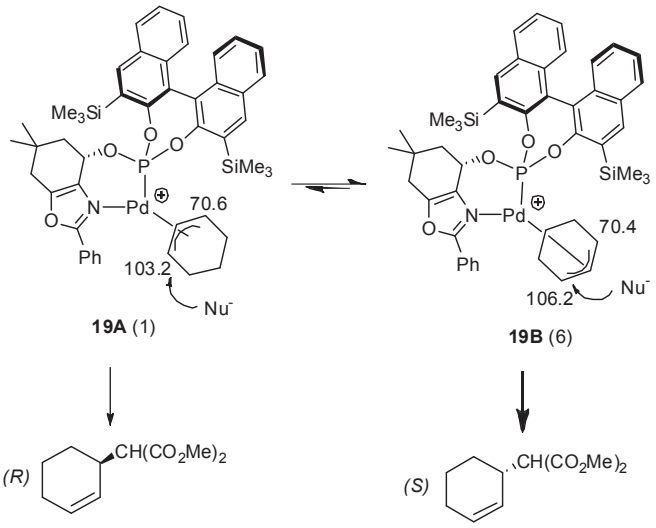

Scheme 4.3.9. Diastereoisomer Pd-allyl intermediates for **S5** with ligand **L29f**. The relative amounts of each isomer are shown in parentheses. The chemical shifts (in ppm) of the allylic terminal carbons are also shown.

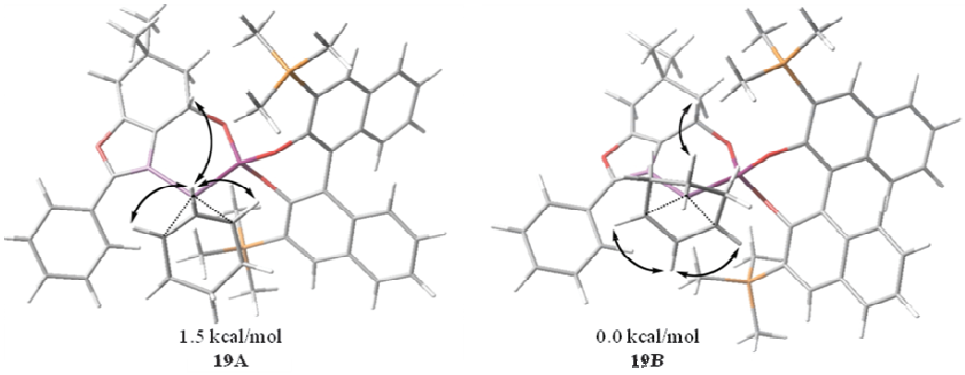

Figure 4.3.4. Calculated structures (DFT) for cationic species of complex [Pd(η^3-1,3-cyclohexenylallyl)(**L29a**)]BF_4 (**19**) and their relative formation enthalpies. This figure also shows the relevant NOE contacts from the NOESY experiment.

The VT NMR (35 °C to -80 °C) of Pd intermediate **20**, which contains ligand **L29g**, also showed a mixture of the two possible isomers (**A** and **B**), but at a ratio of 6.5:1, respectively (Scheme 4.3.10). The carbon NMR chemical shifts also indicated that the most electrophilic allylic terminus carbon is *trans* to the phosphite moiety. In contrast to Pd-intermediate **19**, the fastest-reacting isomer is **A**. This is in agreement with the fact that Pd/**L29g** provided a level of enantioselectivity similar to that of Pd/**L29f**, discussed above, but in the opposite enantiomer of the alkylation products **5** and **6**.

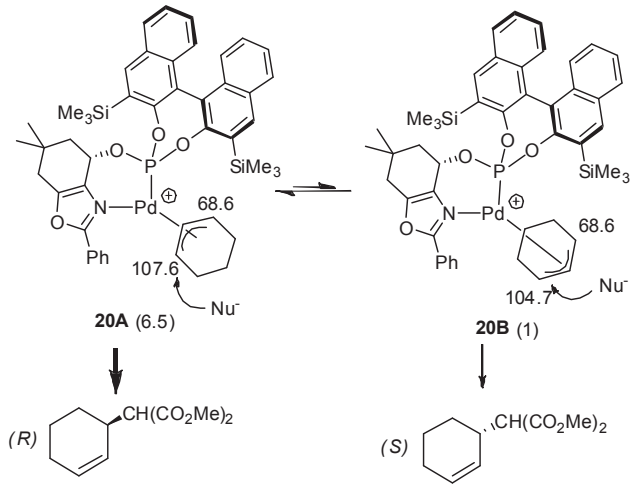

Scheme 4.3.10. Diastereoisomer Pd-allyl intermediates for **S5** with ligand **L29g**. The relative amounts of each isomer are shown in parentheses. The chemical shifts (in ppm) of the allylic terminal carbons are also shown.

4.3.4. Conclusions

A new P-N ligand library **L29**-**L36a**-**g** was synthesized for the Pd-catalyzed allylic substitution reactions of several substrates with different electronic and steric properties. These series of ligands have five main advantages: (1) they can be prepared efficiently from readily available hydroxyl-oxazole/thiazole derivatives; (2) the hydroxyl-oxazole/thiazole cores are much more robust than the usually used hydroxyl-oxazoline ones; (3) the flexibility and larger bite angle created by the biaryl phosphite moiety and the different bridge lengths increase versatility; (4) the π-acceptor character of the phosphite moiety increases reaction rates; and (5) their modular nature enables the bridge length, the substituents at the heterocyclic ring and in the alkyl backbone chain, the configuration of the ligand backbone, and the substituents/configurations in the biaryl phosphite moiety to be easily and systematically varied, so that activities and regio- and enantioselectivities can be maximized for each substrate as required. By carefully selecting the ligand components, therefore, high regio- and enantioselectivities (ee's up to 96%) and good activities were obtained in a broad range of mono-, di- and trisubstituted linear hindered and unhindered substrates and cyclic substrates. Of particular note were the high regio- and enantioselectivities (up to 96% ee) combined with high activities obtained for the mono- and trisubstituted substrates **S6**-**S9**. In addition, for all substrates, both enantiomers of the substitution products were obtained with high enantioselectivities.

By studying the Pd-1,3-diphenyl, 1,3-dimethyl and 1,3-cyclohexenyl allyl intermediates by means of NMR spectroscopy and DFT calculation, we were able to better understand the observed catalytic behavior. For enantioselectivities to be high, we conclude that ligand parameters need to be correctly combined in order to predominantly form the Pd-intermediate that has the fastest reaction with the nucleophile. We also found that the nucleophilic attack takes place predominantly at the allylic terminal carbon atom located *trans* to the phosphite moiety.

4.3.5. Experimental section

4.3.5.1. General considerations

All reactions were carried out using standard Schlenk techniques under an atmosphere of argon. Solvents were purified and dried by standard procedures. The synthesis of phosphite-oxazolie/thiazole ligands has been previously described in Chapter 3.5. Racemic substrates **S1**-**S9** were prepared as previously reported.[23,24,25,26,11b] $[Pd(\eta^3\text{-}1,3\text{-}Ph_2\text{-}C_3H_3)(\mu\text{-}Cl)]_2$,[27] $[Pd(\eta^3\text{-}1,3\text{-}Me_2\text{-}C_3H_3)(\mu\text{-}Cl)]_2$[28] and $[Pd(\eta^3\text{-cyclohexenyl})(\mu\text{-}Cl)]_2$[29] were prepared as previously described. ^1H, $^{13}C\{^1H\}$, and $^{31}P\{^1H\}$ NMR spectra were recorded using a 400 MHz spectrometer. Chemical shifts are relative to that of $SiMe_4$ (^1H and ^{13}C) as internal standard or H_3PO_4 (^{31}P) as external standard. ^1H, ^{13}C and ^{31}P assignments were done based on ^1H-^1H gCOSY, ^1H-^{13}C gHSQC and ^1H-^{31}P gHMBC experiments. Geometries of all substrates were optimized using the Jaguar program[30] by applying the B3LYP hybrid density functional[31] together with the LACVP** basis sets. Normal-mode analysis of stable structures revealed no imaginary frequencies, or a single imaginary frequency with negligibly low energy ($v < 100\ cm^{-1}$). LACVP in Jaguar defines a combination of the LANL30DZ basis set[32] for palladium and the 6-31G basis set for other atoms.

4.3.5.2. General procedure for the preparation of $[Pd(\eta^3\text{-allyl})(L)]BF_4$ complexes 11-20.

The corresponding ligand (0.05 mmol) and the complex $[Pd(\mu\text{-}Cl)(\eta^3\text{-}1,3\text{-allyl})]_2$ (0.025 mmol) were dissolved in CD_2Cl_2 (1.5 mL) at room temperature under argon. $AgBF_4$ (9.8 mg, 0.5 mmol) was added after 30 minutes and the mixture was stirred for 30 minutes. The mixture was then filtered over celite under argon and the resulting solutions were analyzed by NMR. After the NMR analysis, the complexes were precipitated adding hexane as pale yellow solids.

$[Pd(\eta^3\text{-}1,3\text{-diphenylallyl})(L29a)]BF_4$ (11). Isomer **A** (90%): ^{31}P NMR (CD_2Cl_2, 263 K), δ: 135.6 (s, 1P). ^1H NMR(CD_2Cl_2, 263 K), δ: 0.97 (s, 3H, CH_3), 1.05 (s, 3H, CH_3), 1.21 (s, 9H, CH_3, ^{t}Bu), 1.25 (s, 9H, CH_3, ^{t}Bu), 1.42 (s, 9H, CH_3, ^{t}Bu), 1.59 (s, 9H, CH_3, ^{t}Bu), 1.72 (m, 1H, CH_2), 1.84 (m, 1H, CH_2), 1.96 (m, 1H, CH_2-C=), 2.23 (m, 1H, CH_2-C=), 5.14 (m, 1H, CH allyl trans to N), 5.39 (m, 1H, CH-O), 5.99 (m, 1H, CH allyl trans to P), 6.55 (m, 1H, CH allyl central), 6.7-8.0 (m, 19H, CH=). ^{13}C NMR (CD_2Cl_2, 263 K), δ: 26.3 (CH_3), 29.8 (CH_3), 31.3 (CH_3, ^{t}Bu), 31.5 (CH_3, ^{t}Bu), 32.5 (C, ^{t}Bu), 34.8 (CH_2-C=), 35.6 (CMe_2), 42.5 (CH_2), 70.7 (b, CH-O), 81.4 (m, CH allyl *trans* to N), 95.9 (m, CH *trans* to P), 112.5 (m, CH allyl central), 125-164 (aromatic carbons). Isomer **B** (10%): ^{31}P NMR (CD_2Cl_2, 263 K), δ: 140.4 (s, 1P). ^1H NMR(CD_2Cl_2, 263 K), δ: 0.99 (s, 3H, CH_3), 1.03 (s, 3H, CH_3), 1.14 (s, 9H, CH_3, ^{t}Bu), 1.17 (s, 9H, CH_3, ^{t}Bu), 1.40 (s, 9H, CH_3, ^{t}Bu), 1.55 (s, 9H, CH_3, ^{t}Bu), 1.85 (m, 1H, CH_2), 1.92 (m, 1H, CH_2-C=), 2.10 (m, 1H, CH_2-C=), 4.84 (m, 1H, CH allyl *trans* to N), 5.34 (m, 1H, CH-O), 5.21 (m, 1H, CH allyl *trans* to P), 6.45 (m, 1H, CH allyl central), 6.7-8.0 (m, 19H, CH=). ^{13}C NMR (CD_2Cl_2, 263 K), δ: 26.8 (CH_3), 30.1 (CH_3), 31.4 (CH_3, ^{t}Bu), 31.6 (CH_3, ^{t}Bu), 32.0 (C, ^{t}Bu), 35.1 (CH_2-C=), 35.8 (CMe_2), 42.3 (CH_2), 69.7 (b, CH-O), 75.0 (m, CH allyl trans to N), 95.4 (m, CH trans to P), 112.7 (m, CH allyl central), 125-164 (aromatic carbons). Anal. calc (%) for $C_{58}H_{69}BF_4NO_4PPd$: C 65.20, H 6.51, N 1.31; found: C 65.43, H 6.61, N 1.35.

$[Pd(\eta^3\text{-}1,3\text{-diphenylallyl})(L34a)]BF_4$ (12). Isomer **A** (56%): ^{31}P NMR (CD_2Cl_2, 243 K), δ 132.5 (s, 1P). ^1H NMR (CD_2Cl_2, 243 K), δ: 1.45 (s, 9H, CH_3, ^{t}Bu), 1.49 (s, 9H, CH_3, ^{t}Bu), 1.65 (s, 9H, CH_3, ^{t}Bu), 1.69 (s, 9H, CH_3, ^{t}Bu), 1.82 (m, 2H, CH_2), 2.03 (m, 2H, $\underline{CH_2}$-CH), 2.56 (m, 2H, CH_2-C=),

3.43 (m, 1H, CH), 4.56 (m, 1H, CH_2-O), 4.93 (m, 1H, CH allyl *trans* to N), 4.98 (m, 1H, CH_2-O), 5.87 (m, 1H, CH allyl *trans* to P), 6.33 (m, 1H, CH allyl central), 7.0-8.4 (m, 19H, CH=). ^{13}C NMR (CD_2Cl_2, 243 K), δ: 22.1 (CH_2), 24.2 (CH_2-C=), 25.9 ($\underline{C}H_2$-CH), 31.8-32.9 (b, CH_3, ^{t}Bu), 35.0 (C, ^{t}Bu), 35.8 (C, ^{t}Bu), 39.3 (CH), 69.1 (CH_2-O), 80.4 (m, CH allyl *trans* to N), 98.3 (m, CH *trans* to P), 112.1 (m, CH allyl central), 125-165 (aromatic carbons). Isomer **B** (44%): ^{31}P NMR (CD_2Cl_2, 243 K), δ: 136.9 (s, 1P). ^{1}H NMR (CD_2Cl_2, 243 K), δ: 1.42 (s, 9H, CH_3, ^{t}Bu), 1.52 (s, 9H, CH_3, ^{t}Bu), 1.72 (s, 18H, CH_3, ^{t}Bu), 1.89 (m, 2H, CH_2), 2.12 (m, 2H, $\underline{CH_2}$-CH), 2.63 (m, 2H, CH_2-C=), 3.49 (m, 1H, CH), 4.53 (m, 1H, CH_2-O), 4.88 (m, 1H, CH allyl *trans* to N), 5.13 (m, 1H, CH_2-O), 5.45 (m, 1H, CH allyl *trans* to P), 6.28 (m, 1H, CH allyl central), 7.0-8.4 (m, 19H, CH=). ^{13}C NMR (CD_2Cl_2, 243 K), δ: 22.3 (CH_2), 24.5 (CH_2-C=), 26.1 ($\underline{C}H_2$-CH), 31.8-32.9 (b, CH_3, ^{t}Bu), 35.3 (C, ^{t}Bu), 35.5 (C, ^{t}Bu), 39.2 (CH), 70.0 (CH_2-O), 77.2 (m, CH allyl *trans* to N), 96.2 (m, CH *trans* to P), 112.0 (m, CH allyl central), 125-165 (aromatic carbons). Anal. calc (%) for $C_{57}H_{67}BF_4NO_3PPdS$: C 63.96, H 6.31, N 1.31; found: C 64.03, H 6.32, N 1.33.

[Pd(η^3-1,3-diphenylallyl)(L32a)]BF$_4$ (13). Isomer **A** (70%): ^{31}P NMR (CD_2Cl_2, 233 K), δ: 139.2 (s, 1P). ^{1}H NMR (CD_2Cl_2, 233 K), δ: 0.62 (s, 3H, CH_3), 0.89 (s, 3H, CH_3), 1.31 (s, 18H, CH_3, ^{t}Bu), 1.43 (s, 9H, CH_3, ^{t}Bu), 1.54 (s, 9H, CH_3, ^{t}Bu), 1.69 (m, 1H, CH_2), 1.74 (s, 9H, CH_3, ^{t}Bu), 1.86 (m, 1H, CH_2), 2.01 (m, 1H, CH_2-C=), 2.24 (m, 1H, CH_2-C=), 5.43 (m, 1H, CH allyl *trans* to N), 5.57 (m, 1H, CH-O), 6.02 (m, 1H, CH allyl *trans* to P), 6.21 (m, 1H, CH allyl central), 6.8-8.0 (m, 14H, CH=). ^{13}C NMR (CD_2Cl_2, 233 K), δ: 28.1 (CH_3), 29.4 (CH_3), 30.2-32.5 (CH_3, ^{t}Bu), 33.5 (CMe_2), 34.5 (C, *t*Bu), 34.7 (C, *t*Bu), 35.2 (C, ^{t}Bu), 36.2 (CH_2-C=), 36.4 (C, ^{t}Bu), 45.5 (CH_2), 68.4 (m, CH-O), 81.4 (m, CH allyl *trans* to N), 95.9 (m, CH *trans* to P), 112.3 (m, CH allyl central), 124-170 (aromatic carbons). Product **C** (30%): ^{31}P NMR (CD_2Cl_2, 233 K), δ: 143.1 (s, 1P). ^{1}H NMR (CD_2Cl_2, 233 K), δ: 0.59 (s, 6H, CH_3), 0.84 (s, 6H, CH_3), 1.29 (s, 18H, CH_3, ^{t}Bu), 1.33 (s, 18H, CH_3, ^{t}Bu), 1.59 (s, 36H, CH_3, ^{t}Bu), 1.64 (m, 2H, CH_2), 1.71 (s, 18H, CH_3, ^{t}Bu), 1.81 (m, 2H, CH_2), 2.06 (m, 2H, CH_2-C=), 2.18 (m, 2H, CH_2-C=), 5.32 (m, 1H, CH allyl), 5.52 (m, 2H, CH-O), 5.59 (m, 1H, CH allyl), 6.19 (m, 1H, CH allyl central), 6.8-8.0 (m, 18H, CH=). ^{13}C NMR (CD_2Cl_2, 233 K), δ: 28.2 (CH_3), 29.6 (CH_3), 30.2-32.5 (CH_3, ^{t}Bu), 33.7 (CMe_2), 34.3 (C, ^{t}Bu), 34.9 (C, ^{t}Bu), 35.0 (C, ^{t}Bu), 35.5 (C, ^{t}Bu), 36.3 (CH_2-C=), 45.3 (CH_2), 69.2 (m, CH-O), 99.7 (b, CH allyl), 112.5 (m, CH allyl central), 124-170 (aromatic carbons). Anal. calc (%) for 0.7 x $C_{56}H_{73}BF_4NO_4PPd$ + 0.3 x $C_{97}H_{133}BF_4N_2O_8P_2Pd$: C 65.79, H 7.36, N 0.87; found: C 65.87, H 7.42, N 0.92.

[Pd(η^3-1,3-diphenylallyl)(L29d)]BF$_4$ (14). Isomer **A** (83%): ^{31}P NMR (CD_2Cl_2, 273 K), δ: 138.1 (s, 1P). ^{1}H NMR (CD_2Cl_2, 273 K), δ: 0.22 (s, 9H, CH_3-Si), 0.75 (s, 9H, CH_3-Si), 1.04 (s, 3H, CH_3), 1.18 (s, 3H, CH_3), 1.92 (m, 1H, CH_2), 2.21 (m, 1H, CH_2), 2.53 (m, 2H, CH_2-C=), 4.97 (m, 1H, CH allyl trans to N), 5.38 (m, 1H, CH-O), 6.06 (m, 1H, CH allyl trans to P), 6.42 (m, 1H, CH allyl central), 6.6-8.3 (m, 25H, CH=). ^{13}C NMR (CD_2Cl_2, 273 K), δ: 0.7 (CH_3-Si), 1.0 (CH_3-Si), 28.2 (CH_3), 32.9 (CMe_2), 35.2 (CH_2-C=), 42.5 (d, CH_2, $J_{C\text{-}P}$= 1.2 Hz), 70.5 (d, CH-O, $J_{C\text{-}P}$= 7.2 Hz), 75.4 (m, CH allyl trans to N), 96.7 (m, CH allyl trans to P), 112.4 (m, CH allyl central), 121-165 (aromatic carbons). Isomer **B** (17%): ^{31}P NMR (CD_2Cl_2, 273 K), δ: 140.5 (s, 1P). ^{1}H NMR (CD_2Cl_2, 273 K), δ: 0.56 (s, 9H, CH_3-Si), 0.69 (s, 9H, CH_3-Si), 1.04 (s, 3H, CH_3), 1.07 (s, 3H, CH_3), 1.70 (m, 1H, CH_2), 1.98 (m, 1H, CH_2), 2.21 (m, 2H, CH_2-C=), 5.19 (m, 1H, CH allyl trans to N), 5.32 (m, 1H, CH allyl trans to P), 5.42 (m, 1H, CH-O), 6.49 (m, 1H, CH allyl central), 6.6-8.3 (m, 25H, CH=). ^{13}C NMR (CD_2Cl_2, 273 K), δ: 1.2 (CH_3-Si), 1.5 (CH_3-Si), 26.3 (CH_3), 29.5 (CH_3), 33.4 (CMe_2), 35.0 (CH_2-C=), 42.7 (d, CH_2, $J_{C\text{-}P}$= 3.2 Hz), 68.5 (d, CH-O, $J_{C\text{-}P}$= 7.2 Hz), 70.7 (m, CH allyl trans to N),

96.1 (m, CH allyl trans to P), 110.7 (m, CH allyl central), 121-165 (aromatic carbons). Anal. calc (%) for $C_{56}H_{57}BF_4NO_4PPdSi_2$: C 61.80, H 5.28, N 1.29; found: C 61.92, H 5.34, N 1.33.

[Pd(η^3-1,3-diphenylallyl)(L29e)]BF_4 (15). Isomer **A** (28%): ^{31}P NMR (CD_2Cl_2, 223 K), δ: 140.6 (s, 1P). ^{1}H NMR (CD_2Cl_2, 223 K), δ: 0.04 (s, 9H, CH_3-Si), 0.65 (s, 9H, CH_3-Si), 0.98 (s, 3H, CH_3), 1.20 (s, 3H, CH_3), 1.64 (m, 1H, CH_2), 2.03 (m, 1H, CH_2), 2.54 (m, 2H, CH_2-C=), 4.80 (m, 1H, CH allyl *trans* to N), 5.33 (m, 1H, CH-O), 5.77 (m, 1H, CH allyl *trans* to P), 6.17 (m, 1H, CH allyl central), 6.4-8.4 (m, 25H, CH=). ^{13}C NMR (CD_2Cl_2, 223 K), δ: -0.5 (CH_3-Si), 1.1 (CH_3-Si), 25.1 (CH_3), 30.2 (CH_3), 33.5 (CMe_2), 34.8 (CH_2-C=), 42.6 (d, CH_2, $J_{C\text{-}P}$= 10.2 Hz), 69.3 (CH-O), 71.1 (d, CH allyl *trans* to N, $J_{C\text{-}P}$= 8.0 Hz), 98.4 (m, CH allyl *trans* to P), 110.9 (m, CH allyl central), 120-165 (aromatic carbons). Isomer **B** (72%): ^{31}P NMR (CD_2Cl_2, 223 K), δ: 141.1 (s, 1P). ^{1}H NMR (CD_2Cl_2, 223 K), δ: 0.25 (s, 9H, CH_3-Si), 0.69 (s, 9H, CH_3-Si), 1.07 (s, 3H, CH_3), 1.14 (s, 3H, CH_3), 1.67 (m, 1H, CH_2), 2.18 (m, 1H, CH_2), 2.62 (m, 2H, CH_2-C=), 4.74 (m, 1H, CH allyl *trans* to N), 5.30 (m, 1H, CH allyl *trans* to P), 5.37 (m, 1H, CH-O), 6.21 (m, 1H, CH allyl central), 6.4-8.4 (m, 25H, CH=). ^{13}C NMR (CD_2Cl_2, 223 K), δ: 0.3 (CH_3-Si), 1.4 (CH_3-Si), 25.2 (CH_3), 30.8 (CH_3), 33.5 (CMe_2), 34.8 (CH_2-C=), 43.0 (d, CH_2, $J_{C\text{-}P}$= 9.4 Hz), 69.2 (CH-O), 70.5 (d, CH allyl *trans* to N, $J_{C\text{-}P}$= 9.6 Hz), 93.0 (d, CH allyl *trans* to P, $J_{C\text{-}P}$= 36.8 Hz), 111.2 (m, CH allyl central), 120-165 (aromatic carbons). Anal. calc (%) for $C_{56}H_{57}BF_4NO_4PPdSi_2$: C 61.80, H 5.28, N 1.29; found: C 61.91, H 5.37, N 1.34.

[Pd(η^3-1,3-dimethylallyl)(L29a)]BF_4 (16). Isomer **A** (46%): ^{31}P NMR (CD_2Cl_2, 295 K), δ: 134.3 (s, 1P). ^{1}H NMR(CD_2Cl_2, 295 K), δ: 0.84 (m, 3H, CH_3 allyl), 1.12 (m, 3H, CH_3 allyl), 1.15 (s, 3H, CH_3), 1.29 (s, 3H, CH_3), 1.35 (s, 9H, CH_3, ^{t}Bu), 1.39-1.42 (s, 18H, CH_3, ^{t}Bu), 1.59 (s, 9H, CH_3, ^{t}Bu), 1.95 (m, 1H, CH_2), 2.35 (m, 1H, CH_2), 2.69 (m, 1H, CH_2-C=), 2.73 (m, 1H, CH_2-C=), 4.12 (m, 1H, CH allyl *trans* to N), 5.03 (m, 1H, CH allyl *trans* to P), 5.36 (m, 1H, CH allyl central), 5.46 (m, 1H, CH-O), 7.1-8.1 (m, 9H, CH=). ^{13}C NMR (CD_2Cl_2, 295 K), δ: 16.3 (CH_3 allyl), 19.4 (CH_3 allyl), 26.8 (CH_3), 29.9 (CH_3), 31.4-32.1 (CH_3, ^{t}Bu), 32.5-33.6 (C, ^{t}Bu), 35.2 (CH_2-C=), 36.0 (CMe_2), 42.9 (b, CH_2), 70.6 (b, CH-O), 72.3 (m, CH allyl *trans* to N), 107.3 (m, CH *trans* to P), 115.3 (m, CH allyl central), 123-164 (aromatic carbons). Isomer **B** (18%): ^{31}P NMR (CD_2Cl_2, 295 K), δ: 135.2 (s, 1P). ^{1}H NMR(CD_2Cl_2, 295 K), δ: 0.90 (m, 3H, CH_3 allyl), 1.05 (m, 3H, CH_3 allyl), 1.18 (s, 3H, CH_3), 1.28 (s, 3H, CH_3), 1.39-1.42 (s, 18H, CH_3, ^{t}Bu), 1.49 (s, 9H, CH_3, ^{t}Bu), 1.53 (s, 9H, CH_3, ^{t}Bu), 1.98 (m, 1H, CH_2), 2.22 (m, 1H, CH_2), 2.73 (m, 1H, CH_2-C=), 2.78 (m, 1H, CH_2-C=), 4.50 (m, 1H, CH allyl *trans* to N), 4.73 (m, 1H, CH allyl *trans* to P), 5.42 (m, 1H, CH allyl central), 5.52 (m, 1H, CH-O), 7.1-8.1 (m, 9H, CH=). ^{13}C NMR (CD_2Cl_2, 295 K), δ: 16.2 (CH_3 allyl), 17.5 (CH_3 allyl), 27.3 (CH_3), 29.4 (CH_3), 31.4-32.1 (CH_3, ^{t}Bu), 32.5-33.6 (C, ^{t}Bu), 35.4 (CH_2-C=), 36.3 (CMe_2), 42.9 (b, CH_2), 70.2 (b, CH-O), 74.5 (m, CH allyl *trans* to N), 106.3 (m, CH *trans* to P), 116.8 (m, CH allyl central), 123-164 (aromatic carbons). Isomer **D** (36%): ^{31}P NMR (CD_2Cl_2, 295 K), δ: 134.7 (s, 1P). ^{1}H NMR(CD_2Cl_2, 295 K), δ: 0.54 (m, 3H, CH_3 allyl), 0.95 (m, 3H, CH_3 allyl), 1.20 (s, 3H, CH_3), 1.22 (s, 3H, CH_3), 1.39-1.42 (s, 9H, CH_3, ^{t}Bu), 1.45 (s, 9H, CH_3, ^{t}Bu), 1.54 (s, 9H, CH_3, ^{t}Bu), 1.60 (s, 9H, CH_3, ^{t}Bu), 1.98 (m, 1H, CH_2), 2.20 (m, 1H, CH_2), 2.78 (m, 1H, CH_2-C=), 2.82 (m, 1H, CH_2-C=), 3.61 (m, 1H, CH allyl *trans* to N), 3.87 (m, 1H, CH allyl *trans* to P), 5.23 (m, 1H, CH allyl central), 5.71 (m, 1H, CH-O), 7.1-8.1 (m, 9H, CH=). ^{13}C NMR (CD_2Cl_2, 295 K), δ: 17.5 (CH_3 allyl), 18.8 (CH_3 allyl), 27.5 (CH_3), 29.4 (CH_3), 31.4-32.1 (CH_3, ^{t}Bu), 32.5-33.6 (C, ^{t}Bu), 35.5 (CH_2-C=), 36.2 (CMe_2), 42.9 (b, CH_2), 69.8 (b, CH-O), 70.6 (m, CH allyl *trans* to N), 95.0 (m, CH *trans* to P), 118.6

(m, CH allyl central), 123-164 (aromatic carbons). Anal. calc (%) for $C_{48}H_{65}BF_4NO_4PPd$: C 61.06, H 6.94, N 1.48; found: C 61.11, H 6.96, N 1.49.

[Pd(η³-1,3-dimethylallyl)(L35a)]BF_4 (17). Isomer **A** (40%): ^{31}P NMR (CD_2Cl_2, 253 K), δ: 127.4 (s, 1P). ^{1}H NMR(CD_2Cl_2, 253 K), δ: 0.63 (m, 3H, CH_3 allyl), 0.85 (m, 3H, CH_3 allyl), 1.19 (s, 3H, CH_3), 1.26 (s, 3H, CH_3), 1.37 (s, 9H, CH_3, ^{t}Bu), 1.39 (s, 9H, CH_3, ^{t}Bu), 1.44 (s, 9H, CH_3, ^{t}Bu), 1.51 (s, 9H, CH_3, ^{t}Bu), 1.85 (m, 2H, CH_2), 2.06 (m, 2H, $\underline{CH_2}$-CH), 2.22 (m, 2H, CH_2-C=), 2.73 (m, 1H, CH_2-C=), 3.42 (m, 1H, CH allyl *trans* to N), 4.26 (m, 1H, CH-O), 4.56 (m, 1H, CH allyl *trans* to P), 4.91 (m, 1H, CH allyl central), 7.1-8.2 (m, 9H, CH=). ^{13}C NMR (CD_2Cl_2, 253 K), δ: 17.0 (CH_3 allyl), 18.1 (CH_3 allyl), 21.0 (CH_2), 23.8 (CH_2-C=), 26.0 ($\underline{C}H_2$-CH), 26.1 (CH_3), 29.5 (CH_3), 31.4-32.2 (CH_3, ^{t}Bu), 35.1-36.2 (C, ^{t}Bu), 46.5 (CH), 64.8 (m, CH allyl *trans* to N), 78.3(CMe_2), 107.8 (m, CH *trans* to P), 115.8 (m, CH allyl central), 125-170 (aromatic carbons). Isomer **B** (8%): ^{31}P NMR (CD_2Cl_2, 253 K), δ: 129.1 (s, 1P). ^{1}H NMR(CD_2Cl_2, 253 K), δ: 0.53 (m, 3H, CH_3 allyl), 0.74 (m, 3H, CH_3 allyl), 1.15 (s, 3H, CH_3), 1.31 (s, 3H, CH_3), 1.32 (s, 9H, CH_3, ^{t}Bu), 1.53 (s, 9H, CH_3, ^{t}Bu), 1.62 (s, 9H, CH_3, ^{t}Bu), 1.71 (s, 9H, CH_3, ^{t}Bu), 1.87 (m, 2H, CH_2), 2.06 (m, 2H, $\underline{CH_2}$-CH), 2.22 (m, 2H, CH_2-C=), 2.73 (m, 1H, CH_2-C=), 3.48 (m, 1H, CH allyl *trans* to N), 3.71 (m, 1H, CH allyl *trans* to P), 4.11 (m, 1H, CH-O), 5.07 (m, 1H, CH allyl central), 7.1-8.2 (m, 9H, CH=). ^{13}C NMR (CD_2Cl_2, 253 K), δ: 17.2 (CH_3 allyl), 18.6 (CH_3 allyl), 20.7 (CH_2), 23.8 (CH_2-C=), 25.7 ($\underline{C}H_2$-CH), 26.8 (CH_3), 29.1 (CH_3), 31.4-32.2 (CH_3, ^{t}Bu), 35.1-36.2 (C, ^{t}Bu), 46.7 (CH), 65.7 (m, CH allyl *trans* to N), 78.1 (CMe_2), 106.7 (m, CH *trans* to P), 115.9 (m, CH allyl central), 125-170 (aromatic carbons). Isomer **D** (52%): ^{31}P NMR (CD_2Cl_2, 253 K), δ: 128.0 (s, 1P). ^{1}H NMR(CD_2Cl_2, 253 K), δ: 0.59 (m, 3H, CH_3 allyl), 0.88(m, 3H, CH_3 allyl), 1.09 (s, 3H, CH_3), 1.21 (s, 3H, CH_3), 1.35 (s, 9H, CH_3, ^{t}Bu), 1.46 (s, 9H, CH_3, ^{t}Bu), 1.50 (s, 9H, CH_3, ^{t}Bu), 1.78 (s, 9H, CH_3, ^{t}Bu), 1.94 (m, 2H, CH_2), 2.06 (m, 2H, $\underline{CH_2}$-CH), 2.22 (m, 2H, CH_2-C=), 2.73 (m, 1H, CH_2-C=), 3.18 (m, 1H, CH allyl *trans* to N), 3.83 (m, 1H, CH allyl *trans* to P), 4.05 (m, 1H, CH-O), 4.89 (m, 1H, CH allyl central), 7.1-8.2 (m, 9H, CH=). ^{13}C NMR (CD_2Cl_2, 253 K), δ: 18.0 (CH_3 allyl), 18.3 (CH_3 allyl), 21.1 (CH_2), 23.8 (CH_2-C=), 25.9 ($\underline{C}H_2$-CH), 26.7 (CH_3), 30.2 (CH_3), 31.4-32.2 (CH_3, ^{t}Bu), 35.1-36.2 (C, ^{t}Bu), 46.5 (CH), 66.8 (m, CH allyl *trans* to N), 78.2 (CMe_2), 95.4 (m, CH *trans* to P), 115.7 (m, CH allyl central), 125-170 (aromatic carbons).Anal. calc (%) for $C_{49}H_{67}BF_4NO_3PPdS$: C 60.40, H 6.93, N 1.44; found: C 60.37, H 6.90, N 1.43.

[Pd(η³-1,3-dimethylallyl)(L35e)]BF_4 (18). Isomer **A** (45%): ^{31}P NMR (CD_2Cl_2, 253 K), δ: 132.2 (s, 1P). ^{1}H NMR(CD_2Cl_2, 253 K), δ: 0.42 (m, 9H, CH_3-Si), 0.60 (m, 9H, CH_3-Si), 0.68 (m, 3H, CH_3 allyl), 0.87 (m, 3H, CH_3 allyl), 1.21 (s, 3H, CH_3), 1.28 (s, 3H, CH_3), 1.84 (m, 2H, CH_2), 2.11 (m, 2H, $\underline{CH_2}$-CH), 2.24 (m, 2H, CH_2-C=), 2.69 (m, 1H, CH_2-C=), 3.89 (m, 1H, CH allyl *trans* to N), 4.13 (m, 1H, CH-O), 4.26 (m, 1H, CH allyl *trans* to P), 4.98 (m, 1H, CH allyl central), 7.0-8.4 (m, 15H, CH=). ^{13}C NMR (CD_2Cl_2, 253 K), δ: 0.8 (CH_3-Si), 1.4 (CH_3-Si), 16.5 (CH_3 allyl), 19.4 (CH_3 allyl), 21.5 (CH_2), 24.2 (CH_2-C=), 26.3 ($\underline{C}H_2$-CH), 26.6 (CH_3), 29.9 (CH_3), 45.8 (CH), 73.1 (m, CH allyl *trans* to N), 76.4 (CMe_2), 104.3 (m, CH *trans* to P), 115.3 (m, CH allyl central), 125-170 (aromatic carbons). Isomer **B** (5%): ^{31}P NMR (CD_2Cl_2, 253 K), δ: 136.3 (s, 1P). ^{1}H NMR(CD_2Cl_2, 253 K), δ: 0.39 (m, 9H, CH_3-Si), 0.57 (m, 9H, CH_3-Si), 0.74 (m, 3H, CH_3 allyl), 1.04 (m, 3H, CH_3 allyl), 1.24 (s, 3H, CH_3), 1.31 (s, 3H, CH_3), 1.86 (m, 2H, CH_2), 2.11 (m, 2H, $\underline{CH_2}$-CH), 2.24 (m, 2H, CH_2-C=), 2.69 (m, 1H, CH_2-C=), 3.90 (m, 1H, CH allyl *trans* to N), 4.10 (m, 1H, CH-O), 4.15 (m, 1H, CH allyl *trans* to P), 4.95 (m, 1H, CH allyl central), 7.0-8.4 (m, 15H, CH=). ^{13}C NMR (CD_2Cl_2, 253 K), δ: 0.5 (CH_3-Si), 1.2 (CH_3-Si), 16.2 (CH_3 allyl), 19.4 (CH_3 allyl), 21.6 (CH_2), 24.1 (CH_2-C=), 26.2 ($\underline{C}H_2$-

CH), 26.7 (CH_3), 30.1 (CH_3), 45.6 (CH), 74.0 (m, CH allyl *trans* to N), 76.3 (CMe_2), 102.1 (m, CH *trans* to P), 116.1 (m, CH allyl central), 125-170 (aromatic carbons). Isomer **D** (50%): ^{31}P NMR (CD_2Cl_2, 253 K), δ: 134.6 (s, 1P). ^{1}H NMR(CD_2Cl_2, 253 K), δ: 0.51 (m, 9H, CH_3-Si), 0.58 (m, 9H, CH_3-Si), 0.75 (m, 3H, CH_3 allyl), 0.82 (m, 3H, CH_3 allyl), 1.27 (s, 3H, CH_3), 1.41 (s, 3H, CH_3), 1.84 (m, 2H, CH_2), 2.11 (m, 2H, $\underline{CH_2}$-CH), 2.24 (m, 2H, CH_2-C=), 2.69 (m, 1H, CH_2-C=), 3.64 (m, 1H, CH allyl *trans* to N), 3.98 (m, 1H, CH allyl *trans* to P), 4.18 (m, 1H, CH-O), 4.79 (m, 1H, CH allyl central), 7.0-8.4 (m, 15H, CH=). ^{13}C NMR (CD_2Cl_2, 253 K), δ: 0.9 (CH_3-Si), 1.0 (CH_3-Si), 16.4 (CH_3 allyl), 19.2 (CH_3 allyl), 21.7 (CH_2), 24.0 (CH_2-C=), 26.1 ($\underline{CH_2}$-CH), 26.9 (CH_3), 30.2 (CH_3), 45.9 (CH), 71.3 (m, CH allyl *trans* to N), 76.3 (CMe_2), 96.1 (m, CH *trans* to P), 115.5 (m, CH allyl central), 125-170 (aromatic carbons). Anal. calc (%) for $C_{47}H_{55}BF_4NO_3PPdSSi_2$: C 56.77, H 5.58, N 1.41; found: C 56.73, H 5.55, N 1.38.

[Pd(η^3-1,3-cyclohexenylallyl)(L29d)]BF_4 (19). Isomer **A** (15%): ^{31}P NMR (CD_2Cl_2), δ: 139.1 (s, 1P). ^{1}H NMR(CD_2Cl_2), δ: 0.32 (s, 9H, CH_3-Si), 0.44 (s, 9H, CH_3-Si), 1.09 (s, 3H, CH_3), 1.16 (m, 3H, CH_3), 1.39 (m, 2H, CH_2, allyl), 1.49 (m, 2H, CH_2), 1.72 (m, 4H, CH_2 allyl), 1.92 (m, 1H, $\underline{CH_2}$-CH), 2.14 (m, 1H, $\underline{CH_2}$-CH), 2.72 (CH_2-C=), 4.94 (m, 1H, CH allyl *trans* to N), 5.49 (m, 1H, CH-O), 5.79 (m, 1H, CH allyl central), 5.98 (m, 1H, CH allyl *trans* to P), 6.8-8.4 (m, 15H, CH=). ^{13}C NMR(CD_2Cl_2), δ: 0.3 (CH_3-Si), 19.1 (CH_2 allyl), 26.3 (CH_2 allyl), 28.2 (CH_3), 28.7 (CH_3), 31.0 (CH_2 allyl), 33.0 (CMe_2), 35.5 (CH_2-C=), 42.2 (m, CH_2), 69.7 (CH-O), 70.6 (m, CH allyl *trans* to N), 103.2 (d, CH allyl *trans* to P, $J_{C\text{-}P}$= 38.2 Hz), 112.7 (m, CH allyl central), 121-167 (aromatic carbons). Isomer **B** (85%): ^{31}P NMR (CD_2Cl_2), δ: 138.7 (s, 1P). ^{1}H NMR(CD_2Cl_2), δ: 0.37 (s, 9H, CH_3-Si), 0.52 (s, 9H, CH_3-Si), 0.94 (m, 2H, CH_2, allyl), 1.14 (s, 3H, CH_3), 1.23 (s, 3H, CH_3), 1.42 (m, 4H, CH_2 and CH_2 allyl), 1.62 (m, 2H, CH_2 allyl), 2.03 (m, 1H, $\underline{CH_2}$-CH), 2.26 (m, 1H, $\underline{CH_2}$-CH), 2.75 (CH_2-C=), 3.72 (m, 1H, CH allyl *trans* to N), 5.30 (m, 1H, CH allyl central), 5.42 (m, 1H, CH allyl *trans* to P), 5.52 (m, 1H, CH-O), 6.8-8.4 (m, 15H, CH=). ^{13}C NMR(CD_2Cl_2), δ: 0.9 (CH_3-Si), 1.1 (CH_3-Si), 20.2 (CH_2 allyl), 25.5 (CH_2 allyl), 26.5 (CH_3), 29.1 (CH_3), 30.9 (CH_2 allyl), 33.6 (CMe_2), 35.5 (CH_2-C=), 43.7 (CH_2), 69.9 (m, CH-O), 70.4 (m, CH allyl *trans* to N), 106.2 (d, CH allyl *trans* to P, $J_{C\text{-}P}$= 38.2 Hz), 111.3 (m, CH allyl central), 121-167 (aromatic carbons). Anal. calc (%) for $C_{47}H_{53}BF_4NO_4PPdSi_2$: C 57.82, H 5.47, N 1.43; found: C 57.91, H 5.51, N 1.45.

[Pd(η^3-1,3-cyclohexenylallyl)(L29e)]BF_4 (20). Isomer **A** (87%): ^{31}P NMR (CD_2Cl_2), δ: 141.6 (s, 1P). ^{1}H NMR(CD_2Cl_2), δ: 0.53 (s, 9H, CH_3-Si), 0.56 (s, 9H, CH_3-Si), 0.89 (m, 2H, CH_2, allyl), 1.15 (s, 3H, CH_3), 1.21 (m, 2H, CH_2, allyl), 1.32 (s, 3H, CH_3), 1.36 (m, 2H, CH_2), 1.45 (m, 2H, CH_2 allyl), 1.96 (m, 1H, $\underline{CH_2}$-CH), 2.17 (m, 1H, $\underline{CH_2}$-CH), 2.72 (CH_2-C=), 3.87 (m, 1H, CH allyl *trans* to N), 5.21 (m, 1H, CH allyl central), 5.32 (m, 1H, CH-O), 5.36 (m, 1H, CH allyl *trans* to P), 6.8-8.4 (m, 15H, CH=). ^{13}C NMR(CD_2Cl_2), δ: 0.9 (CH_3-Si), 1.1 (CH_3-Si), 20.2 (CH_2 allyl), 25.5 (CH_2 allyl), 26.5 (CH_3), 29.1 (CH_3), 30.9 (CH_2 allyl), 33.6 (CMe_2), 35.5 (CH_2-C=), 43.7 (CH_2), 68.6 (m, CH allyl *trans* to N), 69.9 (m, CH-O), 107.6 (d, CH allyl *trans* to P, $J_{C\text{-}P}$= 38.2 Hz), 111.3 (m, CH allyl central), 121-167 (aromatic carbons). Isomer **B** (13%): ^{31}P NMR (CD_2Cl_2), δ: 140.3 (s, 1P). ^{1}H NMR(CD_2Cl_2), δ: 0.54 (s, 9H, CH_3-Si), 0.59 (s, 9H, CH_3-Si), 1.16 (s, 3H, CH_3), 1.24 (m, 4H, CH_3 and CH_2 allyl), 1.49 (m, 1H, CH_2 allyl), 1.67 (m, 1H, $\underline{CH_2}$-CH), 1.93 (m, 1H, CH_2 allyl), 2.08 (m, 1H, $\underline{CH_2}$-CH), 2.72 (CH_2-C=), 4.69 (m, 1H, CH allyl *trans* to N), 4.84 (m, 1H, CH-O), 5.18 (m, 1H, CH allyl *trans* to P), 5.41 (m, 1H, CH allyl central), 6.8-8.4 (m, 15H, CH=).^{13}C NMR(CD_2Cl_2), δ: 1.2 (CH_3-Si), 1.6 (CH_3-Si), 20.2 (CH_2 allyl), 25.5 (CH_2 allyl), 26.6 (CH_3), 29.2 (CH_3), 30.8 (CH_2 allyl), 33.4 (CMe_2), 35.5 (CH_2-C=), 45.6 (CH_2), 62.4 (m, CH-O), 68.6 (m, CH allyl *trans* to N), 104.7 (d,

CH allyl *trans* to P, $J_{C\text{-}P}$= 34.6 Hz), 112.4 (m, CH allyl central), 121-167 (aromatic carbons). Anal. calc (%) for $C_{47}H_{53}BF_4NO_4PPdSi_2$: C 57.82, H 5.47, N 1.43; found: C 57.87, H 5.49, N 1.44.

4.3.5.3. Study of the reactivity of the [Pd(η^3-allyl)(L))]BF_4 with sodium malonate by in situ NMR.[33]

A solution of *in situ* prepared [Pd(η^3-allyl)(**L**)]BF_4 (L= phosphite-nitrogen, 0.05 mmol) in CD_2Cl_2 (1 mL) was cooled in the NMR at -80 °C. At this temperature, a solution of cooled sodium malonate (0.1 mmol) was added. The reaction was then followed by ^{31}P NMR. The relative reaction rates were calculated using a capillary containing a solution of triphenylphosphine in CD_2Cl_2 as external standard.

4.3.5.4. Typical procedure for the Pd-catalyzed allylic substituition reaction of disubstituted linear (S1 and S3) and cyclic substrates (S4-S6)

A degassed solution of $[PdCl(\eta^3\text{-}C_3H_5)]_2$ (0.9 mg, 0.0025 mmol) and the corresponding phosphite-nitrogen (0.0055 mmol) in dichloromethane (0.5 mL) was stirred for 30 min. Subsequently, a solution of the corresponding substrate (0.5 mmol) in dichloromethane (1.5 mL), dimethyl malonate (171 µL, 1.5 mmol), *N,O*-bis(trimethylsilyl)-acetamide (370 µL, 1.5 mmol) and a pinch of the corresponding base were added. The reaction mixture was stirred at room temperature. After the desired reaction time the reaction mixture was diluted with Et_2O (5 mL) and saturated NH_4Cl (aq) (25 mL) was added. The mixture was extracted with Et_2O (3 x 10 mL) and the extract dried over $MgSO_4$. For substrate **S1**, solvent was removed and conversion was measured by ^{1}H-NMR. To determine the ee by HPLC (Chiralcel OD, 0.5% 2-propanol/hexane, flow 0.5 mL/min), a sample was filtered over basic alumina using dichloromethane as the eluent.[34] For substrates **S3**, **S4** and **S5**, conversion and enantiomeric excess was determined by GC.[35]

4.3.5.5. Typical procedure of allylic alkylation of disubstituted linear (S2), 1,3,3-trisubstituted (S6 and S7) and monosubstituted (S8 and S9) substrates.

A degassed solution of $[PdCl(\eta^3\text{-}C_3H_5)]_2$ (1.8 mg, 0.005 mmol) and the corresponding phosphite-nitrogen (0.011 mmol) in dichloromethane (0.5 mL) was stirred for 30 min at room temperature. Subsequently, a solution of substrate (0.5 mmol) in dichloromethane (1.5 mL), dimethyl malonate (171 µL, 1.5 mmol), *N,O*-bis(trimethylsilyl)-acetamide (370 µL, 1.5 mmol) and a pinch of KOAc were added. After 2 hours at room temperature, the reaction mixture was diluted with Et_2O (5 mL) and saturated NH_4Cl (aq) (25 mL) was added. The mixture was extracted with Et_2O (3 x 10 mL) and the extract dried over $MgSO_4$. Solvent was removed and conversion and regioselectivity were measured by ^{1}H-NMR. For substrate **S2**, enantiomeric excess was determined by ^{1}H-NMR using [Eu(hfc)$_3$] as resolving agent.[12b] For substrates **S6** and **S7**, to determine the ee by HPLC (Chiralcel OJ, 13% 2-propanol/hexane, flow 0.5 mL/min), a sample was filtered over basic alumina using dichloromethane as the eluent.[35] For substrates **S8** and **S9**, to determine the ee by HPLC (Chiralcel OJ, 13% 2-propanol/hexane, flow 0.7 mL/min), a sample was filtered over basic alumina using dichloromethane as the eluent.[36]

4.3.5.6. Typical procedure of allylic amination of disubstituted linear substrate S1.

A degassed solution of $[PdCl(\eta^3\text{-}C_3H_5)]_2$ (0.9 mg, 0.0025 mmol) and the corresponding phosphite-nitrogen (0.0055 mmol) in dichloromethane (0.5 mL) was stirred for 30 min. Subsequently, a solution of the corresponding substrate (0.5 mmol) in dichloromethane (1.5 mL) and benzylamine (131 µL, 1.5 mmol) were added. The reaction mixture was stirred at room temperature. After the desired reaction time, the reaction mixture was diluted with Et_2O (5 mL) and saturated NH_4Cl (aq) (25 mL) was added. The mixture was extracted with Et_2O (3 x 10 mL) and the extract dried over $MgSO_4$. Solvent was removed and conversion was measured by ^{1}H-NMR. To determine the ee by HPLC (Chiralcel OJ, 13% 2-propanol/hexane, flow 0.5 mL/min), a sample was filtered over silica using 10% Et_2O/hexane mixture as the eluent.[34]

4.3.6. Acknowledgements

We thank the Spanish Government (Consolider-Ingenio CSD2006-0003, CTQ2007-62288/BQU, 2008PGIR/07 to O.P. and 2008PGIR/08 to M.D.), the Catalan Government (2005SGR007777), COST D40, Vetenskapsrådet (VR) and Astra Zeneca for their support.

4.3.7. References

[1] For reviews, see: a) *Palladium Reagents and Catalysis, Innovations in Organic Synthesis*; Tsuji, J., Ed.; Wiley: New York, 1995. b) Trost, B. M.; van Vranken, D. L. *Chem. Rev.* **1996**, *96*, 395. c) Johannsen, M.; Jorgensen, K. A. *Chem. Rev.* **1998**, *98*, 1689. d) Pfaltz, A.; Lautens, M. in *Comprehensive Asymmetric Catalysis*; Jacobsen, E. N., Pfaltz, A., Yamamoto, H., Eds.; Springer-Verlag: Berlin, 1999; Vol. 2, Chapter 24. e) Helmchen, G.; Pfaltz, A. *Acc. Chem. Res.* **2000**, *33*, 336. f) Masdeu-Bultó, A. M.; Diéguez, M.; Martín, E.; Gómez, M. *Coord. Chem. Rev.* **2003**, *242*, 159. g) Trost, B. M.; Crawley, M. L. *Chem. Rev.* **2003**, *103*, 2921. h) Martín, E.; Diéguez, M. *C. R. Chemie* **2007**, *10*, 188. i) Lu, Z.; Ma, S. *Angew. Chem. Int. Ed.* **2008**, *47*, 258.
[2] See, for example: a) Trost, B. M.; Bunt, R. C. *J. Am. Chem. Soc.* **1994**, *116*, 4089. b) Trost, B. M.; Krueger, A. C.; Bunt, R. C.; Zambrano, J. *J. Am. Chem. Soc*. **1996**, *118*, 6520.
[3] See, for instance: a) Dawson, G. J.; Frost, C. G.; Williams, J. M. J. *Tetrahedron Lett.* **1993**, *34*, 3149. b) von Matt, P.; Pfaltz, A. *Angew. Chem. Int. Ed. Engl.* **1993**, *32*, 566. c) Sennhenn, P.; Gabler, B.; Helmchen, G. *Tetrahedron Lett.* **1994**, *35*, 8595.
[4] The flexibility that the biaryl moiety offers can be used to fine-tune the chiral pocket formed upon complexation. See, for example: a) Pàmies, O.; Diéguez, M.; Claver, C. *J. Am. Chem. Soc.* **2005**, *127*, 3646. b) Mata, Y.; Diéguez, M.; Pàmies, O.; Claver, C. *Adv. Synth. Catal.* **2005**, *347*, 1943.
[5] See, for instance: a) van Strijdonck, G. P. F.; Boele, M. D. K.; Kamer, P. C. J.; de Vries, J. G.; van Leeuwen, P. W. N. M. *Eur. J. Inorg. Chem.* **1999**, 1073. b) Diéguez, M.; Pàmies, O.; Claver, C. *Adv. Synth. Catal.* **2005**, *347*, 1257. c) Diéguez, M.; Pàmies, O.; Claver, C. *J. Org. Chem*. **2005**, *70*, 3363. d) Diéguez, M.; Pàmies, O.; Claver, C. *Adv. Synth. Catal*. **2007**, *349*, 836. e) Pàmies, O.; Diéguez, M. *Chem. Eur. J*. **2008**, *14*, 944. f) Raluy, E.; Pàmies, O.; Diéguez, M. *J. Org. Chem.* **2007**, *72*, 2842.
[6] Prétôt, R.; Pfaltz, A. *Angew. Chem. Int. Ed.* **1998**, *37*, 323.

[7] The choice of the oxazole and thiazole nitrogen donor units are based in the fact that they resemble to the successful oxazoline unit but they are much more robust.
[8] Similar behavior has been observed for other phosphite-nitrogen ligands. See, for example: a) ref. 4b. b) Diéguez, M.; Pàmies, O. *Chem. Eur. J*. **2008**, *14*, 3653..
[9] For more successful applications, see: a) Dierkes, P.; Randechul, S.; Barloy, L.; De Cian, A.; Fischer, J.; Kamer, P. C. J.; van Leeuwen, P. W. N. M.; Osborn, J. A. *Angew. Chem. Int. Ed*. **1998**, *37*, 3116. b) Wiene, B.; Helmchen, G. *Tetrahedron Lett.* **1998**, *39*, 5727.
[10] Helmchen, G.; Kudis, S.; Sennhenn, P.; Steinhagen, H. *Pure & Appl. Chem.* **1997**, *69*, 513.
[11] See, for instance: a) Sudo, A.; Saigo, K. *J. Org. Chem.* **1997**, 62, 5508. b) Dawson, G. J.; Williams, J. M. J.; Coote, S. J. *Tetrahedron: Asymmetry* **1995**, 6, 2535. c) Martin, C. J.; Rawson, D. J.; Williams, J. M. J. *Tetrahedron: Asymmetry* **1998**, 9, 3723
[12] For successful applications, see also: a) Dawson, G. J.; Williams, J. M. J.; Coote, S. J. *Tetrahedron Lett.* **1995**, *36*, 461. b) Evans, D. A.; Campos, K. R.; Tedrow, J. S.; Michael, F. E.; Gagné, M. R. *J. Am. Chem. Soc.* **2000**, *122*, 7905. c) Popa, D.; Puigjaner, C.; Gomez, M.; Benet-Buchholz, J.; Vidal-Ferran, A.; Pericas, M. A. *Adv. Synth. Cat.* **2007**, *349*, 2265.
[13] In contrast to Pd-catalytic systems, Ir-, Ru- and Mo-catalysts provide very high selectivity in order for the attack at the non-terminal carbon to give the chiral product. See, for instance: a) Bruneau, C.; Renaud, J. L.; Demersemen, B. *Chem. Eur. J.* **2006**, *12*, 5178; b) Malkov, A. V.; Gouriou, L.; Lloyd-Jones, G. C.; Starý, I.; Langer, V.; Spoor, P.; Vinader, V.; Kočovský, P. *Chem. Eur. J.* **2006**, *12*, 6910; c) Trost, B. M.; Hildbrand, S.; Dogra, K. *J. Am. Chem. Soc.* **1999**, *121*, 10416; d) Alexakis, A.; Polet, D. *Org. Let.* **2004**, *6*, 3529.
[14] For recent successful applications of Pd-catalysts, see: a) You, S.-L.; Zhu, X.-Z.; Luo, Y.-M.; Hou, X.-L.; Dai, L.-X. *J. Am. Chem. Soc.* **2001**, *123*, 7471; b) Hilgraf, R.; Pfaltz, A. *Synlett* **1999**, 1814. c) Hilgraf, R.; Pfaltz, A. *Adv. Synth. Catal*. **2005**, *347*, 61.
[15] a) Deerenberg, S.; Schrekker, H. S.; van Strijdonck, G. P. F.; Kamer, P. C. J.; van Leeuwen, P. W. N. M.; Fraanje, J.; Goubitz, K. *J. Org. Chem.* **2000**, *65*, 4810. b) Fernández, F.; Gómez, M.; Jansat, S.; Muller, G.; Martín, E.; Flores Santos, L.; García, P. X.; Acosta, A.; Aghmiz, A.; Jiménez-Pedrós, M.; Masdeu-Bultó, A. M.; Diéguez, M.; Claver, C.; Maestro, M. A. *Organometallics* **2005**, *24*, 3946.
[16] The equilibrium between the two diastereoisomers takes place via the so-called apparent μ-allyl rotation. This has been shown to occur via dissociation of one of the coordinated atoms of the bidentate ligand, which allows the ligand to rotate. See: Gogoll, A.; Örnebro, J.; Grennberg, H.; Bäckvall, J. E. *J. Am. Chem. Soc.* **1994**, *116*, 3631.
[17] This is also consistent with the fact that, for both isomers, the most electrophilic allylic terminal carbon atom is the one *trans* to the phosphite in the major isomer **A**.
[18] This study indicates that isomer **26A** reacts around 1.3 times faster than isomer **26B**.
[19] The formation of compound **C** was confirmed by adding an excess of ligand, which resulted in an increase in the amount of species **C** present in solution
[20] Porte, A. M.; Reibenspies, J.; Burgess, K. *J. Am. Chem. Soc.* **1998**, *120*, 9180.
[21] Pericàs, M. A.; Puigjaner, C.; Riera, A.; Vidal-Ferran, A.; Gómez, M.; Jiménez, F.; Muller, G.; Rocamora, M. *Chem. Eur. J.* **2002**, *8*, 4164.
[22] This study indicates that isomer **33B** reacts around 1.5 times faster than isomer **33A**.
[23] Auburn, P. R.; Mackenzie, P. B.; Bosnich B. *J. Am. Chem. Soc.* **1985**, *107*, 2033.
[24] Jia, C.; Müller, P.; Mimoun, H. *J. Mol. Cat. A: Chem*. **1995**, *101*, 127.
[25] Lehman, J.; Lloyd-Jones, G. C. *Tetrahedron* **1995**, *51*, 8863.

[26] Hayashi, T.; Yamamoto, A.; Ito, Y.; Nishioka, E.; Miura, H.; Yanagi, K. *J. Am. Chem. Soc.* **1989**, *111*, 6301.
[27] von Matt, P.; Lloyd-Jones, G. C.; Minidis, A. B. E.; Pfaltz, A.; Macko, L.; Neuburger, M.; Zehnder, M.; Ruegger, H.; Pregosin, P. S. *Helv. Chim. Acta* **1995**, *78*, 265.
[28] Kollmar, M.; Goldfuss, B.; Reggelin, M.; Rominger, F.; Helmchen, G. *Chem. Eur. J.* **2001**, *7*, 4913.
[29] Trost, B. M.; Strege, P. E.; Weber, L. *J. Am. Chem. Soc.* **1978**, *11*, 3407.
[30] Jaguar 4.2; Schrödinger, Inc. Portland, OR, 1991-2000.
[31] a) Becke, A. D. *J. Chem. Phys.* **1993**, *98*, 5648. b) Lee, C.; Yang, W.; Parr, R. G. *Phys. Rev. B* **1988**, *37*, 785.
[32] Hay, P. J.; Wadt, W. R. *J. Chem. Phys.* **1985**, *82*, 299.
[33] van Haaren, R. J.; Keeven, P. H.; van der Veen, L. A.; Goubitz, K.; van Strijdonck, G. P. F.; Oevering, H.; Reek, J. N. H.; Kamer, P. C. J.; van Leeuwen, P. W: N. M. *Inorg. Chim. Acta* **2002**, *327*, 108.
[34] Pàmies, O.; van Strijdonck, G. P. F.; Diéguez, M.; Deerenberg, S.; Net, G.; Ruiz, A.; Claver, C.; Kamer, P. C. J.; van Leeuwen, P. W. N. M. *J. Org. Chem.* **2001**, *66*, 8867.
[35] Pericàs, M. A.; Puigjaner, C.; Riera, A.; Vidal-Ferran, A.; Gómez, M.; Jiménez, F.; Muller, G.; Rocamora, M. *Chem. Eur. J.* **2002**, *8*, 4164.
[36] Janssen, J. P.; Helmchen, G. *Tetrahedron Lett.* **1997**, *38*, 8025.

4.3.8 Supporting information

Table 4.3.8. Selected results for the Pd-catalyzed allylic alkylation of **S3** using ligands **L29a** and **L34a**. Effect of the solvent and ligand-to-palladium ratio.[a]

Entry	Ligand	Solvent	L/Pd	% Conv (t/h)[b]	% ee[c]
1	**L29a**	CH_2Cl_2	1	100 (2)	59 (*S*)
2	**L29a**	THF	1	21 (2)	54 (*S*)
3	**L29a**	toluene	1	41 (24)	57(*S*)
4	**L34a**	CH_2Cl_2	1	92 (2)	38 (*S*)
5	**L34a**	THF	1	12 (2)	29 (*S*)
6	**L34a**	toluene	1	41 (24)	37 (*S*)
7	**L29a**	CH_2Cl_2	0.75	100 (2)	59 (*S*)
8	**L29a**	CH_2Cl_2	2	100 (2)	54 (*S*)
9	**L34a**	CH_2Cl_2	0.75	76 (2)	39 (*S*)
10	**L34a**	CH_2Cl_2	2	100 (2)	32 (*S*)

[a] All reactions were run at 23 ºC. 0.5 mol% $[PdCl(\eta^3\text{-}C_3H_5)]_2$. **S3** (0.5 mmol). BSA (1.5 mmol). Dimethyl malonate (1.5 mmol). [b] Conversion measured by GC. Reaction time shown in parentheses. [c] Enantiomeric excesses measured by GC. Absolute configuration shown in parentheses.

Table 4.3.9. Selected results for the Pd-catalyzed allylic alkylation of **S4** using ligands **L29a** and **L34a**. Effect of the solvent and ligand-to-palladium ratio.[a]

Entry	Ligand	Solvent	L/Pd	% Conv (t/h)[b]	% ee[c]
1	**L29a**	CH_2Cl_2	1	100 (6)	35 (*S*)
2	**L29a**	THF	1	35 (6)	33 (*S*)
3	**L29a**	toluene	1	52 (6)	36(*S*)
4	**L34a**	CH_2Cl_2	1	100 (6)	3 (*R*)
5	**L34a**	THF	1	21 (6)	2 (*R*)
6	**L34a**	toluene	1	33 (6)	3 (*R*)
7	**L29a**	CH_2Cl_2	0.75	100 (6)	36 (*S*)
8	**L29a**	CH_2Cl_2	2	100 (6)	32 (*S*)
9	**L34a**	CH_2Cl_2	0.75	100 (6)	3 (*R*)
10	**L34a**	CH_2Cl_2	2	100 (6)	2 (*R*)

[a] All reactions were run at 23 ºC. 0.5 mol% $[PdCl(\eta^3\text{-}C_3H_5)]_2$. **S4** (0.5 mmol). BSA (1.5 mmol). Dimethyl malonate (1.5 mmol). [b] Conversion measured by GC. Reaction time shown in parentheses. [c] Enantiomeric excesses measured by GC. Absolute configuration shown in parentheses.

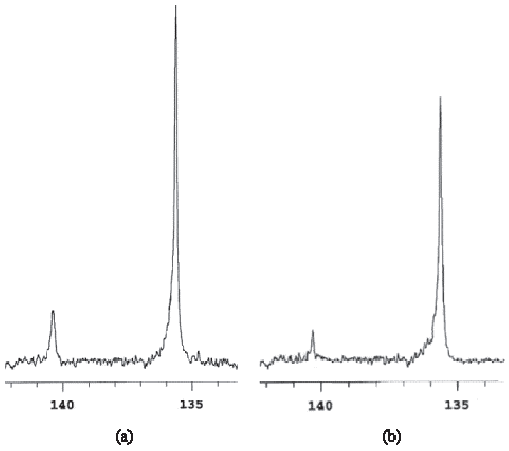

Figure 4.3.5. $^{31}P\{^{1}H\}$NMR spectra of [Pd(η^3-1,3-diphenylallyl)(**L29a**)]BF_4 (**25**) in CD_2Cl_2 at -70 ^{o}C (a) before the addition of sodium malonate and (b) after the addition of sodium malonate.

4.4. A new modular phosphite-pyridine ligand library for asymmetric Pd-catalyzed allylic substitution reactions. A study of the key Pd-π-allyl intermediates

Javier Mazuela, Oscar Pàmies and Montserrat Diéguez in manuscript to be submitted.

4.4.1. Abstract

A library of phosphite-pyridine ligands **L38**-**L49a**-**g** has been successfully applied for the first time in the Pd-catalyzed allylic substitution reactions of several di- and trisubstituted substrates using a wide range of C-, N- and O-nucleophiles, among which are the little studied α-substituted malonates, β-diketones and benzyl alcohol. The highly modular nature of this ligand library enables the substituents/configuration at the ligand backbone, and the substituents/configurations at the biaryl phosphite moiety to be easily and systematically varied. We found that the introduction of an enantiopure biaryl phosphite moiety played an essential role in increasing the versatility of the Pd-catalytic systems. Enantioselectivities were therefore high for several hindered and unhindered di- and trisubstituted substrates using a wide range of C-, N- and O-nucleophiles. Of particular note were the high enantioselectivities (up to >99% ee) and high activities obtained for the trisubstituted substrates **S6**-**S7**, which compare favorably with the best that have been reported in the literature. We have also extended the use of these new catalytic systems in alternative environmentally friendly solvents such as propylene carbonate and ionic liquids. Studies on the Pd-π-allyl intermediates provide a deeper understanding of the effect of ligand parameters on the origin of enantioselectivity.

4.4.2. Introduction

Fine chemicals and natural product chemistry rely on enantiomerically pure compounds. The discovery of synthetic routes for preparing these compounds is one of the most persistently pursued goals in chemistry. Asymmetric catalysis is one of the most attractive approaches, because it can provide very high reactivity and selectivity, and is environmentally friendly.[1] In this respect, the asymmetric Pd-catalyzed allylic substitution reaction, which forms C-C and C-heteroatom bonds, is a powerful and highly versatile procedure because it tolerates several functional groups.[2] Most of the successful ligands reported to date for this process have been designed using three main strategies. The first, developed by Hayashi and coworkers, involves a secondary interaction of the nucleophile with a side chain of the ligand to direct the approach of the nucleophile to one of the allylic terminal carbon atoms.[2,3] The second strategy, developed by Trost and coworkers, increases the ligand's bite angle to create a chiral cavity in which the allyl system is embedded.[2,4] This idea made it possible for ligands with large bite angles to be successfully applied to the allylic substitution of sterically undemanding substrates. The third strategy, developed by groups led by Helmchen, Pfaltz and Williams, uses heterodonor ligands to electronically discriminate between the two allylic terminal carbon atoms because of the different *trans* influences of the donor groups.[2,5] This made it possible to successfully use a wide range of heterodonor ligands (mainly P,N-ligands) in allylic substitution reactions. More recently, we have

shown that the introduction of biaryl-phosphite moieties into the ligand design is highly advantageous by overcoming the most common limitations of this process, such as low reaction rates and high substrate specificity.[6] These benefits has been attributed, on one hand, to the larger π-acceptor ability of the phosphite groups that increases reaction rates and, on the other hand, to the flexibility of the phosphite moieties that allows the catalyst chiral pocket (the chiral cavity in which the allyl is embedded) to adapt to both hindered and unhindered substrates[7]. Despite this success the potential of phosphite-containing ligands is limited to the use of dimethyl malonate as nucleophile.[6a] More effort has therefore to be made to enlarge the scope of nucleophiles increasing the possibilities for their use in the synthesis of more complex chiral organic molecules. Although the substrate versatility has recently increased, there are still important substrate classes that give unsatisfactory results with known catalysts. For example, for trisubstituted substrate, which allows the formation of enantiomerically enriched acid derivatives and lactones, more active and enantioselective Pd catalysts are needed.[2]

Mixed phosphorus-oxazoline ligands have played a dominant role among heterodonor ligands.[2] In recent years the range of heterodonor–phosphorous-nitrogen-ligands has been extended to include more robust N-donor groups (such as, amine,[8] imine,[9] thiazole,[10] etc.) than oxazolines with moderate success. In this context, the phosphine- and phosphinite-pyridine compounds are an important class of ligands.[11] However, only a few of them have been successfully applied and these are limited in substrate scope (enantioselectivities are only high in the allylic substitution of hindered standard substrate *rac*-1,3-diphenyl-3-acetoxyprop-1-ene).[11]

Because we are interested in discovering more robust and more versatile Pd-catalytic systems, we decided to take one further step in the design of a new ligand library for this process and incorporate the advantages of the heterodonor, the robustness of the pyridine moiety and the extra control provided by the flexibility of the chiral pocket through the presence of a biaryl phosphite group. To this end, we synthesized and screened a library of 84 potential new phosphite-pyridine ligands (Figure 4.4.1).

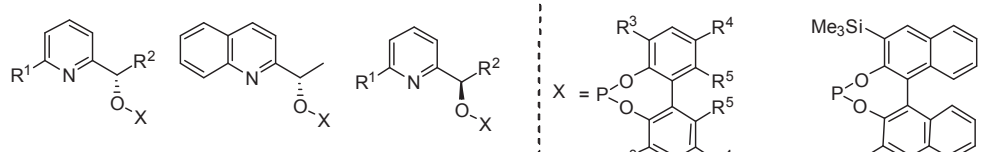

L38 R^1= H; R^2= Me
L39 R^1= R^2= Me
L40 R^1= Br; R^2= Me
L41 R^1= Ph; R^2= Me
L42 R^1= H; R^2= ^{t}Bu
L43 R^1= H; R^2= Ph
L44 R^1= Me; R^2= ^{t}Bu

L45

L46 R^1= H; R^2= Me
L47 R^1= R^2= Me
L48 R^1= H; R^2= ^{t}Bu
L49 R^1= H; R^2= Ph

a R^3 = R^4 = ^{t}Bu; R^5= H
b R^3 = ^{t}Bu; R^4 = OMe; R^5= H
c R^3 =$SiMe_3$; R^4 = R^5= H
d $(S)^{ax}$; R^3 = ^{t}Bu; R^4 = R^5= Me
e $(R)^{ax}$; R^3 = ^{t}Bu; R^4 = R^5= Me

f $(S)^{ax}$
g $(R)^{ax}$

Figure 4.4.1. Phosphite-pyridine ligand library **L38**-**L49a**-**g**.

Their highly modular construction enabled us to make a systematic study of the effect of the substituents at the ligand backbone (R^1 and R^2, ligands **L38**-**L45**), the configuration of the carbon next to the phosphite moiety (ligands **L38**-**L45** vs. **L46**-**L49**), and the substituents and configurations in the biaryl phosphite moiety (**a**-**g**). By carefully selecting these elements, we achieved high enantioselectivities and activities in several di- and trisubstituted substrates using a

wide range of C-, N- and O-nucleophiles, including the less studied α-substituted malonates, β-diketones and benzyl alcohol. We have also extended the use of these new catalytic systems in alternative environmentally friendly solvents such as propylene carbonate and ionic liquids. In this paper, we also discuss the synthesis and characterization of the Pd-π-allyl intermediates in order to provide greater insight into the origin of enantioselectivity in these catalytic systems.

4.4.3. Results and discussions

4.4.3.1. Allylic substitution of symmetrical 1,3-disubstituted allylic substrates

In this section, we report the use of the chiral phosphite-pyridine ligand library (**L38**-**L49a-g**) in the Pd-catalyzed allylic substitution of linear disubstituted substrates with different steric properties (Eq. 4.4.1a): *rac*-1,3-diphenyl-3-acetoxyprop-1-ene (**S1**) (widely used as a model substrate) and *rac*-1,3-dimethyl-3-acetoxyprop-1-ene (**S2**); and cyclic substrates (Eq. 4.4.1b): *rac*-3-acetoxycyclohexene (**S3**) (widely used as a model substrate), *rac*-3-acetoxycyclopentene (**S4**) and *rac*-3-acetoxycycloheptene (**S5**). Several nucleophiles were tested. In all cases, the catalysts were generated *in situ* from π-allyl-palladium chloride dimer $[PdCl(\eta^3\text{-}C_3H_5)]_2$ and the corresponding ligand.[2]

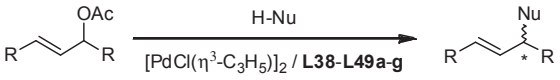

(4.4.1a)

S1 R= Ph
S2 R= Me

1 R= Ph; H-Nu= H-CH(COOMe)$_2$
2 R= Ph; H-Nu= H-CH(COOEt)$_2$
3 R= Ph; H-Nu= H-CH(COOBn)$_2$
4 R= Ph; H-Nu= H-CH(COMe)$_2$
5 R= Ph; H-Nu= H-CMe(COOMe)$_2$
6 R= Ph; H-Nu= H-CAllyl(COOMe)$_2$
7 R= Ph; H-Nu= H-NHCH$_2$Ph
8 R= Ph; H-Nu= H-OCH$_2$Ph
9 R= Me; H-Nu= H-CH(COOMe)$_2$
10 R= Me; H-Nu= H-CH(COOBn)$_2$
11 R= Me; H-Nu= H-CH(COMe)$_2$
12 R= Me; H-Nu= H-CMe(COOMe
13 R= Me; H-Nu= H-CAllyl(COOM
14 R= Me; H-Nu= H-NHCH$_2$Ph

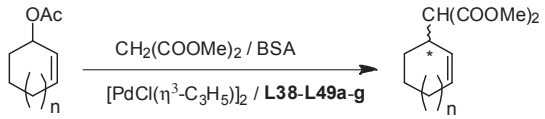

(4.4.1b)

S3 n=1
S4 n=0
S5 n=2

15 n=1; H-Nu= H-CH(COOMe)$_2$
16 n=1; H-Nu= H-CH(COOEt)$_2$
17 n=1; H-Nu= H-CH(COOBn)$_2$
19 n=1; H-Nu= H-CMe(COOMe)$_2$
20 n=1; H-Nu= H-CAllyl(COOEt)$_2$
21 n=0; H-Nu= H-CH(COOMe)$_2$

*Allylic substitution of rac-1,3-diphenyl-3-acetoxyprop-1-ene **S1** using several nucleophiles*

In the first set of experiments, we used the palladium-catalyzed asymmetric substitution reactions of **S1** (Eq. 4.4.1a, R = Ph), with dimethyl malonate as nucleophile, to study the potential of the phosphite-pyridine ligand library **L38-L49a-g**. **S1** was chosen as a substrate because the reaction was performed with a wide range of ligands, which enabled the efficiency of the various ligand systems to be compared directly.[2]

We first determined the optimal reaction conditions by conducting a series of experiments with two ligands (**L38a** and **L39a**) using different solvents (tetrahydrofuran, toluene and dichloromethane) and ligand-to-palladium ratios (L/Pd = 0.75, 1 and 2). We found that activities and enantioselectivities were best using dichloromethane as the solvent. We also found that an excess of ligand was not needed (see Supporting Information for details).

Under the optimized conditions (i.e. dichloromethane as solvent and a L/Pd ratio of 1) we tested the remaining ligands. The results, which are summarized in Table 4.4.1, indicate that enantioselectivity is mainly affected by the substituents at the ligand backbone (R^1 and R^2) and by the substituents/configuration at the biaryl phosphite moiety (**a**-**g**). Interestingly, the sense of the enantioselectivity is controlled by the configuration of the stereogenic carbon next to the phosphite moiety. High activities (TOF's up to 500 mol **S1** x (mol Pd x h)$^{-1}$)[12] and enantioselectivities (ee's up to 90%) were obtained for both enantiomers of the substitution product **1** using ligands **L38g** and **L46f**.

The effect of the substituents at the ligand backbone (R^1 and R^2) was studied using ligands **L38**-**L45a**. We found that enantioselectivity decreases when the steric hindrance is increased at both positions (Table 4.4.1, entries 1 *vs* 8, 12, 13 and 19 for substituent R^1; and entries 1 *vs* 14 and 15 for substituent R^2). Enantioselectivities were therefore best using ligands **L38** with a hydrogen and a methyl substituent at R^1 and R^2 positions, respectively.

Table 4.4.1. Selected results for the Pd-catalyzed allylic alkylation of **S1** with dimethyl malonate using the ligand library **L38-L49a-g**[a]

Entry	Ligand	% Conv (min)[b]	% ee[c]	Entry	Ligand	% Conv (min)[b]	% ee[c]
1	**L38a**	100 (30)[d]	32 (*S*)	14	**L42a**	100 (30)[d]	8 (*S*)
2	**L38b**	100 (30)	40 (*S*)	15	**L43a**	100 (30)[d]	21 (*S*)
3	**L38c**	100 (30)	45 (*S*)	16	**L43d**	100 (30)	3 (*S*)
4	**L38d**	100 (30)[d]	19 (*S*)	17	**L43e**	100 (30)	72 (*S*)
5	**L38e**	100 (30)[d]	59 (*S*)	18	**L44a**	100 (30)	12 (*S*)
6	**L38f**	100 (30)[d]	17 (S)	19	**L45a**	100 (30)	28 (*S*)
7	**L38g**	100 (30)[d]	90 (*S*)	20	**L46a**	100 (30)[d]	35 (*R*)
8	**L39a**	100 (30)	26 (*S*)	21	**L46d**	100 (30)	20 (*R*)
9	**L39d**	100 (30)	8 (*S*)	22	**L46e**	100 (30)	55 (*R*)
10	**L39e**	100 (30)	3 (*R*)	23	**L46f**	100 (30)[d]	89 (*R*)
11	**L39g**	100 (30)	50 (*S*)	24	**L46g**	100 (30)	10 (*R*)
12	**L40a**	100 (30)[d]	13 (*S*)	25	**L47a**	100 (30)	26 (*R*)
13	**L41a**	100 (30)	29 (*S*)	26	**L49g**	100 (30)	33 (*R*)

[a] All reactions were run at 23 ºC. 0.5 mol% $[PdCl(\eta^3\text{-}C_3H_5)]_2$. Dichloromethane as solvent. 1 mol% ligand. [b] Conversion measured by ^{1}H-NMR. Reaction time shown in parentheses. [c] Enantiomeric excesses measured by HPLC. Absolute configuration shown in parentheses. [d] Isolated yields of **1** were > 93%.

We then moved on to investigate the effect of the configuration of the stereogenic carbon next to the phosphite moiety using ligands **L46**-**L49a**-**g**. Interestingly, we found that this stereogenic carbon atom controls the sense of the enantioselectivity, which opens up the possibility of attaining both enantiomers of the alkylated product. Thus, ligands **L38**-**L45** with an *S*-configuration predominantly provided the *S*-**1**, while *R*-configured ligands **L46**-**L49** afforded the *R*-**1** (Table 4.4.1, entries 1-19 *vs* 20-26).

The effect of the phosphite moieties was studied using ligands **L38a**-**g** (Table 4.4.1, entries 1-7). Results indicate that the presence of trimethylsilyl groups at the *ortho* positions of the biaryl phosphite moiety has a positive effect on enantioselectivity (Table 4.4.1, entries 1 *vs* 3 and 5 *vs* 7). Moreover, when we compared ligands **L38f**-**g** and **L46f**-**g**, which have different configurations of the stereogenic carbon next to the phosphite moiety, we found a cooperative effect between the configuration of the biaryl phosphite moiety and the configuration of the stereogenic carbon next to the phosphite moiety. This leads to a matched combination for ligands **L38g** and **L46f** (Table 4.4.1, entries 7 and 23). In addition, when we compared the enantioselectivities obtained using ligands with bulky tropoisomeric biphenyl moieties (**L38a**-**c**; entries 1-3) with those obtained using the related enantiopure biaryl ligands **L38d**-**g** (entries 4-7), we found that the tropoisomerism in the biphenyl phosphite moieties (**a**-**c**) is not controlled once the ligand has coordinated to the palladium.[13] Enantiopure phosphite moieties are therefore needed if enantioselectivities are to be high.

To sum up, results were best with ligands **L38g** and **L46f**, which contain the optimal combination of ligand parameters (Table 4.4.1, entries 7 and 23). These findings clearly show the efficiency of highly modular scaffolds in ligand design.

We then went on to study the allylic substitution of **S1** using other nucleophiles. Figure 4.4.2 shows the most notable results of using several carbon nucleophiles and benzylamine as the nitrogen nucleophile. In general, Pd/**L38**-**L49a**-**g** catalysts followed the same trends as the allylic substitution of **S1** using dimethyl malonate. Again, the catalyst precursors containing ligands **L38g** and **L46f** provided the best enantioselectivities in both enantiomers of the substitution products (ee's up to 99%).

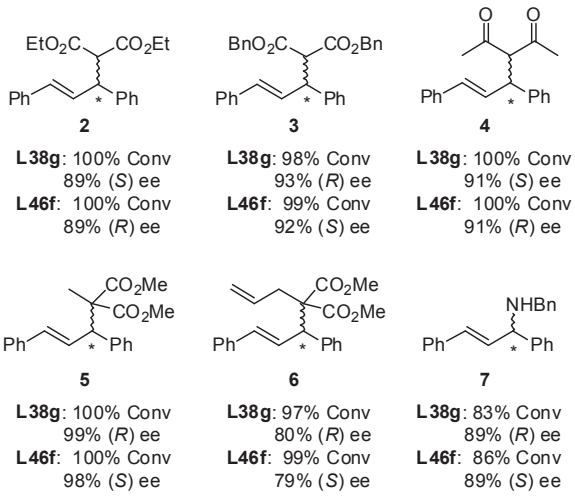

Figure 4.4.2. Selected results for the Pd-allylic substitution of **S1** with other several C- and N- nucleophiles using the ligand library **L38-L49a-g**. Reaction conditions: 1 mol % of Pd-catalyst precursor, CH_2Cl_2 as solvent, rt, 4 h.

It should be noted that enantioselectivity was relatively insensitive to the steric nature of the ester groups of the malonate nucleophiles and also to the replacement of the malonate by an acetylacetone and benzylamine. Thus, compounds **2**-**4** and **7** were obtained in high

enantioselectivities (ee's ranging from 89% to 93%). However, for α-substituted malonates, enantioselectivity depends on the nature of the substituent. Thus, while the presence of a methyl substitutent had an extremely positive effect on enantioselectivity (ee's up to 99%, compound **5**), the presence of an allyl substituent slightly decreased enantioselectivity (ee's up to 80%, compound **6**).

Finally, encouraged by these excellent results we decided to study the scope of ligands **L38**-**L49a**-**g** in the allylic substitution of a more challenging nucleophile: benzyl alcohol. The stereroselective construction of an ether linkage adjacent to a stererogenic carbon center is important for the synthesis of many biologically active targets.[14] Despite this, few examples on the Pd-catalyzed etherification of allylic substrates have been reported.[15,16] Most of them uses phenols as nucleophiles,[15a-g] being the aliphatic ethers much less studied[15e,h,i].

We were able to fine tune the ligands to obtain high enantioselectivities (ee's up to 87%) in the etherification of substrate **S1**. Although, as expected, the activities were lower than in the alkylation reaction of **S1**, they were similar to those obtained used other successful ligands under similar reaction conditions (Table 4.4.2, entry 20).[15h] The results, which are summarized in Table 4.4.2, indicated that enantioselectivity was again mainly affected by the substituents at the ligand backbone (R^1 and R^2) and by the substituents/configuration at the biaryl phosphite moiety (**a**-**g**). However, the effect of these parameters was different from their effect on the substitution of **S1** using C- and N-nucleophiles. Therefore, in contrast to the allylic substitution that used C- and N-nucleophiles and led to higher ee's with ligands containing small substituents at R^1 and R^2 of the ligand backbone, in the etherification of **S1** the presence of bulky substituents at either R^1 or R^2 had a positive effect on enantioselectivity (Table 4.4.2, entries 2 vs 6 and 10 for substituent R^1; and entries 2 vs 12 and 15 for substituent R^2). However, the simultaneous introduction of bulky substituents at both positions led to lower enantioselectivities (Table 4.4.2, entry 17).

Table 4.4.2. Selected results for the Pd-catalyzed allylic etherification of **S1** with benzyl alcohol using the ligand library **L38-L49a-g**[a]

Entry	Ligand	% Conv (h)[b]	% ee[c]	Entry	Ligand	% Conv (h)[b]	% ee[c]
1	**L38a**	100 (18)[d]	13 (*S*)	11	**L42a**	100 (18)	9 (*S*)
2	**L38d**	90 (18)	20 (*R*)	12	**L42d**	100 (18)	68 (*R*)
3	**L38e**	100 (18)[d]	51 (*S*)	13	**L42e**	100 (18)	74 (*S*)
4	**L38g**	100 (18)[d]	53 (*S*)	14	**L43a**	92 (18)	1 (*S*)
5	**L39a**	100 (18)	66 (*S*)	15	**L43d**	100 (18)[d]	71 (*R*)
6	**L39d**	94 (18)	25 (*R*)	16	**L43e**	100 (18)[d]	87 (*S*)
7	**L39g**	100 (18)	72 (S)	17	**L44e**	100 (18)	29 (*S*)
8	**L40a**	84 (18)	21 (*S*)	18	**L49d**	100 (18)[d]	85 (*R*)
9	**L41a**	85 (18)	64 (*S*)	19	**L49e**	98 (18)[d]	70 (*S*)
10	**L41d**	82 (18)	46 (*R*)	20	**L43e**	89 (6)	87 (*S*)

[a] All reactions were run at 23 ºC. 2 mol% $[PdCl(\eta^3\text{-}C_3H_5)]_2$. Dichloromethane as solvent. 4 mol% ligand. [b] Conversion measured by ^{1}H-NMR. Reaction time shown in parentheses. [c] Enantiomeric excesses measured by HPLC. Absolute configuration shown in parentheses. [d] Isolated yields of **8** were > 91%.

It should be noted that both enantiomers of the product can be obtained with high ee's simply by changing either the absolute configuration of the biaryl moieties (Table 4.4.2, entries 15 and 16) or the absolute configuration of the stereogenic carbon next to the phosphite moiety (Table 4.4.2,

entries 15 and 16 *vs* 18 and 19). Enantioselectivities were therefore best with ligands **L43d**-**e** and **L49d**-**e** (Table 4.4.2, entries 15-16 and 18-19). These results, which again clearly show the efficiency of using modular scaffolds in ligand design, are among the best reported for this type of more challenging nucleophile.[15h]

*Allylic substitution of rac-1,3-dimethyl-3-acetoxyprop-1-ene **S2** using several nucleophiles*

We also tested ligands **L38**-**L49a**-**g** in the allylic substitution of the linear substrate **S2** (Eq. 4.4.1a; R= Me). Substrate **S2** is less sterically demanding than substrate **S1** used previously. There are therefore fewer successful catalyst systems for the Pd-catalyzed allylic substitution of this substrate than for the allylic substitution of hindered substrates such as **S1**.[2] If enantiomeric excesses are to be high, the ligand must create a small chiral pocket around the metal center, mainly because of the presence of less sterically demanding methyl *syn* substituents. Due to flexibility conferred by the biaryl phosphite moiety in combination with the high modularity of this ligand library, we expected to be able to tune the chiral pocket to obtain good enantioselectivities for this substrate as well.

Table 4.4.3 summarizes the results of using the phosphite-pyridine ligand library **L38**-**L49a**-**g** with dimethyl malonate as nucleophile. In general, activities (TOF's up to > 250 mol **S2** x (mol Pd x h)$^{-1}$)[12] and enantioselectivities were also high (ee's up to 83%) in the alkylation of **S2**.

Table 4.4.3. Selected results for the Pd-catalyzed allylic alkylation of **S2** with dimethyl malonate using the ligand library **L38-L49a-g**[a]

Entry	Ligand	% Conv (h)[b]	% ee[c]
1[d]	**L38a**	100 (2)	37 (*S*)
2	**L38b**	100 (2)	38 (*S*)
3	**L38c**	100 (2)	40 (*S*)
4[d]	**L38d**	100 (2)	19 (*S*)
5[d]	**L38e**	100 (2)	46 (*S*)
6	**L38f**	100 (2)	3 (*S*)
7	**L38g**	100 (2)	72 (*S*)
8[d]	**L39a**	100 (2)	48 (*S*)
9[d]	**L39g**	100 (2)	79 (*S*)
10	**L40a**	100 (2)	19 (*S*)
11[d]	**L41a**	100 (2)	30 (*S*)
12[d]	**L42a**	100 (2)	36 (*S*)
13	**L43a**	100 (2)	32 (*R*)
14	**L46a**	100 (2)	31 (*R*)
15[d]	**L46f**	100 (2)	74 (*R*)
16	**L46g**	100 (2)	4 (*R*)
17[d]	**L47f**	100 (2)	83 (*R*)

[a] All reactions were run at 23 ºC. 0.5 mol% $[PdCl(\eta^3\text{-}C_3H_5)]_2$. Dichloromethane as solvent. 1 mol% ligand. [b] Conversion measured by GC. Reaction time shown in parentheses. [c] Enantiomeric excesses measured by GC. Absolute configuration shown in parentheses. [d] Isolated yields of **9** were > 91%.

Again, enantioselectivities were mainly affected by the substituents at the ligand backbone (R^1 and R^2) and by the substituents/configurations at the biaryl phosphite moiety (**a**-**g**). However, while the effect of the substituents/configurations of the biaryl moieties on enantioselectivity is similar to the effect in the alkylation of **S1**, the effect of the substituents at the ligand backbone (R^1 and R^2) is different: the presence of a methyl substituent at R^1 has a positive effect on enantioselectivity, while the substituents at R^2 have little effect. Again, both enantiomers of alkylation product **9** can be accessed in high enantioselectivities simply by changing the absolute configuration of the stereogenic carbon next to the phosphite moiety. Enantioselectivities (ee's up to 83%) were therefore best for ligands **L39g** and **L47f** (Table 4.4.3, entries 9 and 17).

Subsequently we studied the allylic substitution of **S2** using several carbon nucleophiles and benzylamine. The most notable results are shown in Figure 4.4.3. In general, they follow the same trends as for the allylic alkylation of **S2** using dimethyl malonate as nucleophile. Again, the catalyst precursors containing ligands **L39g** and **L47f** provided the best enantioselectivities for both enantiomers of the substitution products **10**-**14** (ee's up to 82%). In all cases, enantioselectivities (ee's up to 82%, compounds **10**, **12**-**14**) were similar to those obtained using dimethyl malonate, except when acetylacetone was used as nucleophile, which led to lower enantioselectivities (ee's up to 62%, compound **11**).

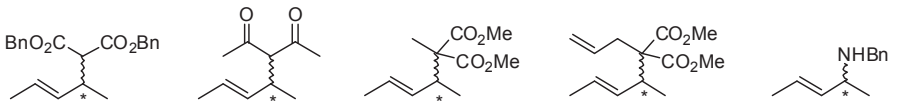

10	**11**	**12**	**13**	**14**
L39g: 100% Conv 75% (-) ee	**L39g**: 100% Conv 62% (-) ee	**L39g**: 100% Conv 73% (-) ee	**L39g**: 100% Conv 71% (+) ee	**L39g**: 54% Conv 82% (*S*) ee
L47f: 100% Conv 74% (+) ee	**L47f**: 100% Conv 62% (+) ee	**L47f**: 100% Conv 72% (+) ee	**L47f**: 100% Conv 72% (-) ee	**L47f**: 48% Conv 81% (*R*) ee

Figure 4.4.3. Selected results for the Pd-allylic substitution of **S2** with several other C- and N-nucleophiles using the ligand library **L38-L49a-g**. Reaction conditions: 1 mol % of Pd-catalyst precursor, CH_2Cl_2 as solvent, rt, 6 h.

*Allylic alkylation of cyclic substrates **S3**-**S5***

With the unhindered cyclic substrates **S3**-**S5**, enantioselectivity is difficult to control, mainly because of the presence of less sterically demanding *anti* substituents. These *anti* substituents are thought to play a crucial role in the enantioselection observed with cyclic substrates in the corresponding Pd-allyl intermediates.[2]

In this section, we show that the chiral ligand library **L38-L49a-g** applied previously to the Pd-catalyzed allylic substitution of 1,3-disubstituted linear substrates (**S1**-**S2**) can also be used for cyclic substrates (ee's up to 94%) using several nucleophiles. We tested three cyclic substrates (Eq. 4.4.1b): *rac*-3-acetoxycyclohexene (**S3**) (which is widely used as a model substrate), *rac*-3-acetoxycyclopentene (**S4**) and *rac*-3-acetoxycycloheptene (**S5**).

Table 4.4.4 shows the results of using the ligand library **L38-L49a-g** with dimethyl malonate as nucleophile. Enantioselectivities up to 93% were obtained in the allylic substitution of the cyclic substrates **S3**-**S5** using ligands **L38g** and **L46f**. The results indicate that the effect of the ligand parameters on the catalytic performance is different from the effect of the linear substrates **S1**-**S2**. However, although the substituents of the biaryl moieties have an effect on the enantioselectivity

that is similar to the effect in the alkylation of **S1** and **S2**, the effect of the substituents at the ligand backbone (R^1 and R^2) is different.

Unlike **S1** and **S2** the methyl substituent at R^2 has a positive effect on enantioselectivity (Table 4.4.4, entries 1 *vs* 12 and 13), while the substituents at R^1 have little effect (Table 4.4.4, entries 1 *vs* 8, 11 and 14). In addition, the cooperative effect between the configuration of the biaryl phosphite moiety and the configuration of the carbon atom next to the phosphite moiety is less pronounced for these cyclic substrates than for linear substrates. Thus, in the allylic alkylation of cyclic substrates, ligands containing enantiopure bulky *R*- and *S*-biaryl moieties (**f** and **g**) acted as *pseudo*-enantiomers (Table 4.4.4, entries 6 and 7). Therefore, both enantiomers of the alkylated products can be obtained with high ee's simply by changing either the absolute configuration of the biaryl moieties (Table 4.4.4, entries 6 and 7) or the absolute configuration of the stereogenic carbon next to the phosphite moiety (Table 4.4.4, entries 6 and 7 vs 18 and 19).

Table 4.4.4. Selected results for the Pd-catalyzed allylic substitution of **S3-S5** using the ligand library **L38-L49a-g**[a]

Entry	Substrate	Ligand	% Conv (h)[b]	% ee[c]
1	**S3**	**L38a**	100 (6)	18 (*S*)
2	**S3**	**L38b**	100 (6)	18 (*S*)
3	**S3**	**L38c**	100 (6)	20 (*S*)
4[d]	**S3**	**L38d**	100 (6)	42 (*S*)
5[d]	**S3**	**L38e**	100 (6)	64 (*R*)
6	**S3**	**L38f**	100 (6)	73 (*S*)
7	**S3**	**L38g**	100 (6)	87 (*R*)
8[d]	**S3**	**L39a**	100 (6)	24 (*S*)
9[d]	**S3**	**L39g**	100 (6)	80 (*R*)
10	**S3**	**L40a**	100 (6)	13 (*S*)
11	**S3**	**L41a**	100 (6)	17 (*S*)
12	**S3**	**L42a**	100 (6)	2 (*S*)
13	**S3**	**L43a**	100 (6)	3 (*R*)
14	**S3**	**L45a**	100 (6)	17 (*S*)
15	**S3**	**L46a**	100 (6)	11 (*S*)
16	**S3**	**L46d**	100 (6)	35 (*R*)
17	**S3**	**L46e**	100 (6)	73 (*S*)
18[d]	**S3**	**L46f**	100 (6)	91 (*S*)
19[d]	**S3**	**L46g**	100 (6)	75 (*R*)
20[d]	**S4**	**L38g**	100 (6)	65 (*R*)
21[d]	**S4**	**L46f**	100 (6)	67 (*S*)
22[d]	**S5**	**L38g**	100 (6)	87 (*R*)
23[d]	**S5**	**L46f**	100 (6)	93 (*S*)

[a] All reactions were run at 23 ºC. 0.5 mol% $[PdCl(\eta^3\text{-}C_3H_5)]_2$. Dichloromethane as solvent. 1 mol% ligand. [b] Conversion measured by GC. Reaction time shown in parentheses. [c] Enantiomeric excesses measured by GC (substrates **S3** and **S5**) and by ^{1}H-NMR using $[Eu(hfc)_3]$ (substrate **S4**). Absolute configuration shown in parentheses. [d] Isolated yields of **15**, **21** and **22** were > 89%.

We then moved on to study the allylic substitution of cyclic substrate **S3** using other carbon nucleophiles. The most notable results are shown in Figure 4.4.4. In general, they follow the same trends as for the allylic alkylation using dimethyl malonate. Again, the catalyst precursors containing ligands **L38g** and **L46f** provided the best enantioselectivities for both enantiomers of the alkylated products (ee's up to 94%). As observed for unhindered linear substrate **S2**, enantioselectivities were similar to those obtained using dimethyl malonate in all cases, except when acetylacetone was used as nucleophile, which led to lower enantioselectivities.

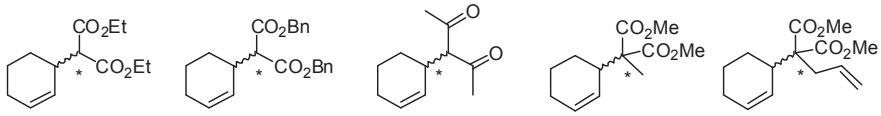

16	**17**	**18**	**19**	**20**
L38g: 100% Conv 86% (-) ee	**L38g**: 99% Conv 91% (+) ee	**L38g**: 100% Conv 62% (-) ee	**L38g**: 98% Conv 84% (+) ee	**L38g**: 97% Conv 94% (+) ee
L46f: 100% Conv 85% (+) ee	**L46f**: 100% Conv 90% (-) ee	**L46f**: 100% Conv 60% (+) ee	**L46f**: 100% Conv 83% (-) ee	**L46f**: 95% Conv 93% (-) ee

Figure 4.4.4. Selected results for the Pd-allylic substitution of **S3** with several other C-nucleophiles using the ligand library **L38-L49a-g**. Reaction conditions: 1 mol % of Pd-catalyst precursor, CH_2Cl_2 as solvent, rt,12 h.

4.4.3.2. Allylic substitution of unsymmetrical 1,3,3-trisubstituted allylic substrates

We also screened the ligands **L38**-**L49a**-**g** in the allylic substitution of *rac*-1,3,3-triphenylprop-2-enyl acetate (**S6**) and *rac*-1,1,-diphenyl-1-hepten-3-yl acetate (**S7**) using dimethyl malonate as nucleophile (Eq. 4.4.2, R= Ph for **S6** and R= Me for **S7**). These substrates are of synthetic interest because the so-formed substitution products can easily be transformed into enantiomerically enriched acid derivatives and lactones.[17] They are more sterically demanding than the previously used substrate **S1**, and it is therefore more difficult to achieve excellent enantioselectivities with them.[18] Interestingly, with this phosphite-pyridine ligand library, we obtained excellent enantiomeric excesses (ee's up to >99%) under standard reaction conditions. Although, as expected, the activities were lower than in the alkylation reaction of **S1**, they were higher than those obtained with few other successful ligands under similar reaction conditions.[18]

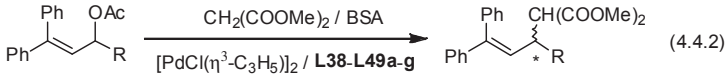

(4.4.2)

S6 R= Ph
S7 R= Me

23 R= Ph
24 R= Me

The results, summarized in Table 4.4.5, indicated that it is crucial to have a methyl substituent at the R^1 position if levels of enantioselectivity are to be excellent (ee's increased from 61% to 97% when the hydrogen (ligand **L38a**) was replaced by a methyl (ligand **L39a**) substituent at the R^1 position). Finally, by correctly tuning the substituents at both the biaryl phosphite and the R^2 position, enantioselectivities >99% can be achieved (Table 4.4.5, entry 9). In addition, both enantiomers of the alkylation products **23** and **24** can be obtained with excellent ee's simply by changing the absolute configuration of the stereogenic carbon next to the phosphite moiety (see

for example; Table 4.4.5, entry 8 *vs* 17). These results compare favorably with the best that have been reported for this class of substrate.[18]

Table 4.4.5. Selected results for the Pd-catalyzed allylic substitution of **S6** and **S7** using the ligand library **L38-L49a-g**[a]

		S6		S7	
Entry	Ligand	% Conv (h)[b]	% ee[c]	% Conv (h)[b]	% ee[c]
1	**L38a**	100 (24)[d]	61 (*R*)	100 (24)	58 (*R*)
2	**L38b**	100 (24)	60 (*R*)	100 (24)	60 (*R*)
3	**L38c**	100 (24)	63 (*R*)	100 (24)	62 (*R*)
4	**L38d**	100 (24)	63 (*R*)	100 (24)	67 (*R*)
5	**L38e**	100 (24)	78 (*S*)	100 (24)	77 (*S*)
6	**L38f**	100 (24)	66 (*R*)	100 (24)	64 (*R*)
7	**L38g**	100 (24)	68 (*S*)	100 (24)	62 (*S*)
8	**L39a**	100 (24)[d]	97 (*R*)	100 (24)[d]	96 (*R*)
9	**L39d**	100 (24)[d]	>99 (*R*)	100 (24)[d]	99 (*R*)
10	**L40a**	100 (24)	40 (*R*)	100 (24)	47 (*R*)
11	**L41a**	100 (24)	63 (*R*)	100 (24)	65 (*R*)
12	**L42a**	100 (24)	42 (*R*)	100 (24)	49 (*R*)
13	**L43a**	100 (24)	34 (*R*)	100 (24)	31 (*R*)
14	**L45a**	100 (24)	77 (*R*)	100 (24)	79 (*R*)
15	**L46f**	100 (24)	53 (*R*)	100 (24)	52 (*R*)
16	**L46g**	100 (24)	64 (*S*)	100 (24)	59 (*S*)
17	**L47a**	100 (24)[d]	95 (*S*)	100 (24)[d]	94 (*S*)

[a] All reactions were run at 23 ºC. 1 mol% $[PdCl(\eta^3\text{-}C_3H_5)]_2$. Dichloromethane as solvent. 2 mol% ligand. [b] Conversion measured by ^{1}H-NMR. Reaction time shown in parentheses. [c] Enantiomeric excesses measured by HPLC. Absolute configuration shown in parentheses. [d] Isolated yields of **23** and **24** were > 88%.

4.4.3.3. Allylic substitution using non-classical media

Encouraged by the excellent results obtained, we decided to go one step further and to study the Pd-catalyzed allylic substitution using environmentally friendly alternative solvents such as propylene carbonate (PC) and ionic liquids.

Recently, propylene carbonate (PC) has emerged as a sustainable "green" alternative to standard organic solvents because of its high boiling point, low toxicity and environmentally friendly synthesis.[19] To study whether the new Pd-phosphite-pyridine catalytic systems developed in this study can be used efficiently with PC, we performed the allylic substitution of substrates **S1**-**S7** using the ligands that provided the best enantioselectivities for each substrate type. The results can be found in Table 4.4.6. We were pleased to see that when the new catalyst library was used in PC, the enantioselectivities remained high for a wide range of nucleophiles. Unfortunately, the catalysts could not be efficiently recycled because of the high polarity of the alkylation and amination products considered.[20]

Table 4.4.6. Pd-catalyzed allylic substitution of **S1-S7** with the ligand library **L38-L49a-g** in PC as a solvent[a]

Entry	Substrate	Ligand	H-Nu	% Conv (h)[b]	% ee[c]
1[d]	**S1**	**L38g**	H-CH(COOMe)$_2$	100 (6)	89 (*S*)
2	**S1**	**L46f**	H-CH(COOMe)$_2$	100 (6)	88 (*R*)
3	**S1**	**L38g**	H-CMe(COOMe)$_2$	100 (12)	97 (*R*)
4	**S1**	**L38g**	H-NHCH$_2$Ph	96 (12)	87 (*R*)
5[d]	**S2**	**L39g**	H-CH(COOMe)$_2$	100 (10)	78 (*S*)
6	**S2**	**L47f**	H-CH(COOMe)$_2$	100 (10)	80 (*R*)
7	**S2**	**L39g**	H-CMe(COOMe)$_2$	100 (12)	72 (-)
8	**S2**	**L39g**	H-NHCH$_2$Ph	100 (24)	81 (*R*)
9[d]	**S3**	**L38g**	H-CH(COOMe)$_2$	100 (12)	78 (*R*)
10	**S3**	**L46f**	H-CH(COOMe)$_2$	100 (12)	89 (*S*)
11	**S4**	**L46f**	H-CH(COOMe)$_2$	100 (12)	66 (*S*)
12	**S5**	**L46f**	H-CH(COOMe)$_2$	100 (12)	92 (*S*)
13[e]	**S6**	**L39a**	H-CH(COOMe)$_2$	53 (24)	95 (*R*)
14[d,e]	**S6**	**L39d**	H-CH(COOMe)$_2$	67 (24)	99 (*R*)
15[e]	**S7**	**L39a**	H-CH(COOMe)$_2$	72 (24)	93 (*R*)

[a] All reactions were run at 23 ºC. 0.5 mol% [PdCl(η^3-C_3H_5)]$_2$. 1 mol% ligand. [b] Conversion measured by GC or ^{1}H-NMR. Reaction time shown in parentheses. [c] Enantiomeric excesses. Absolute configuration shown in parentheses. [d] Isolated yields were > 91% based on recovered starting material. [e] 1 mol% [PdCl(η^3-C_3H_5)]$_2$. 2 mol% ligand.

In practice, catalyst recycling is of fundamental importance because of the high price of the metal source. Recently, ionic liquids (ILs) have emerged as an alternative to standard organic solvents.[21] They enable catalysts to be repeatedly recycled by a simple two-phase extraction with an apolar solvent. However, they are little used in asymmetric Pd-allylic substitution and limited to the standard **S1** substrate.[22] To study whether our new phosphite-pyridine ligand library can be used efficiently with ILs, we studied the Pd-allylic substitution of substrates **S1**-**S7** using the ionic liquids 1-butyl-3-methyl imidazolium hexafluorophosphate (**IL1**) and *N*-butyl-*N*-methyl pyrrolidinium bis(trifluoromethylsulfonylamide (**IL2**) (Table 4.4.7). Again, we used the ligands that provided the best enantioselectivities for each substrate type. Two types of nucleophiles, dimethyl malonate and benzylamine, were tested. The results show that the nature of the IL has an important effect on catalytic performance. Thus, the imidazolium-based **IL1** led to significantly lower enantioselectivities in the allylic substitution of unhindered substrates **S2** and **S3** than dichloromethane (Table 4.4.7 entries 5, 7 and 9). **IL1** also decreases the catalytic activity in the amination reactions probably due to the formation of hydrogen bonds between the imidazolium cation and benzylamine, which decrease its nucleophilic behaviour.[23] Fortunately, when the reaction was carried out in the pyrrolidinium-based ionic liquid **IL2**, the activities and enantioselectivities were high and comparable to those obtained in dichloromethane (Table 4.4.7, entries 2, 4, 6, 8 and 10-14).

Table 4.4.7. Pd-catalyzed allylic substitution of **S1-S7** with the ligand library **L38-L49a-g** using ionic liquids (**IL1** and **IL2**) as solvents[a]

Entry	Solvent	Substrate	Ligand	H-Nu	% Conv (h)[b]	% ee[c]
1[d]	**IL1**	**S1**	**L38g**	H-CH(COOMe)$_2$	100 (0.5)	85 (*S*)
2	**IL2**	**S1**	**L38g**	H-CH(COOMe)$_2$	100 (0.5)	85 (*S*)
3	**IL1**	**S1**	**L38g**	H-NHCH$_2$Ph	41 (4)	85 (*R*)
4	**IL2**	**S1**	**L38g**	H-NHCH$_2$Ph	76 (4)	86 (*R*)
5[d]	**IL1**	**S2**	**L39g**	H-CH(COOMe)$_2$	100 (2)	44 (*S*)
6	**IL2**	**S2**	**L39g**	H-CH(COOMe)$_2$	100 (2)	71 (*S*)
7	**IL1**	**S2**	**L39g**	H-NHCH$_2$Ph	21 (6)	32 (*S*)
8	**IL2**	**S2**	**L39g**	H-NHCH$_2$Ph	51 (6)	78 (*S*)
9[d]	**IL1**	**S3**	**L38g**	H-CH(COOMe)$_2$	39 (6)	62 (*R*)
10	**IL2**	**S3**	**L38g**	H-CH(COOMe)$_2$	98 (6)	84 (*R*)
11	**IL2**	**S4**	**L38g**	H-CH(COOMe)$_2$	100 (6)	63 (*R*)
12[d]	**IL2**	**S5**	**L38g**	H-CH(COOMe)$_2$	97 (6)	88 (*R*)
13[e]	**IL2**	**S6**	**L39a**	H-CH(COOMe)$_2$	100 (24)	96 (*R*)
14[e]	**IL2**	**S7**	**L39a**	H-CH(COOMe)$_2$	96 (24)	96 (*R*)

[a] All reactions were run at 23 ºC. 0.5 mol% [PdCl(η^3-C_3H_5)]$_2$. 1 mol% ligand. [b] Conversion measured by GC or ^{1}H-NMR. Reaction time shown in parentheses. [c] Enantiomeric excesses measured by GC or HPLC. Absolute configuration shown in parentheses. [d] Isolated yields were > 87%. [e] 1 mol% [PdCl(η^3-C_3H_5)]$_2$. 2 mol% ligand.

It is interesting to note that for the allylic amination of substrates **S1** and **S2** using **IL2**, catalysts can be used up to five times with no significant loss in activity and the high enantioselectivities are preserved. Nevertheless, for the allylic alkylation with dimethyl malonate as nucleophile, the catalytic performance of the IL solutions was not fully recovered. In all cases, both the catalytic activity and the enantioselectivity decreased considerably after the first run.[24]

4.4.3.4. Origin of enantioselectivity: study of the Pd-π-allyl intermediates

To provide further insight into how ligand parameters affect catalytic performance, we studied the Pd-π-allyl compounds **25**-**32** [Pd(η^3-allyl)(L)]BF_4 (L = **L38**-**L49a**-**g**), because they are key intermediates in the allylic substitution reactions studied.[2] These ionic palladium complexes, which contain 1,3-diphenyl, 1,3-dimethyl or cyclohexenyl allyl groups, were prepared using the previously reported method from the corresponding Pd-allyl dimer and the appropriate ligand in the presence of silver tetrafluoroborate (Scheme 4.4.1).[25] The complexes were characterized by elemental analysis and by ^{1}H, ^{13}C and ^{31}P NMR spectroscopy. The spectral assignments were based on information from ^{1}H-^{1}H, ^{31}P-^{1}H and ^{13}C-^{1}H correlation measurements in combination with ^{1}H-^{1}H NOESY experiments. Unfortunately, we were unable to obtain crystal of sufficient quality to perform X-ray diffraction measurements.

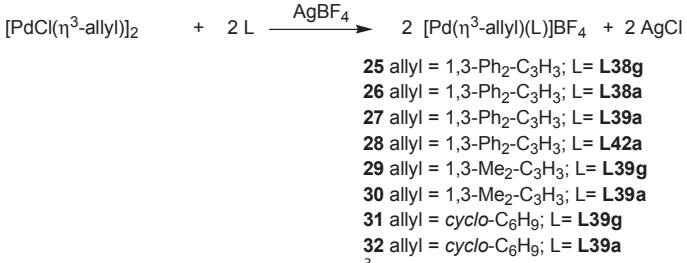

Scheme 4.4.1. Preparation of $[Pd(\eta^3\text{-allyl})(L)]BF_4$ complexes 25-32.

Palladium 1,3-diphenyl-allyl complexes

When the phosphite-pyridine ligand library **L38**-**L49a**-**g** was used in the allylic substitution of substrate **S1**, the catalytic results showed that enantioselectivity is highly affected by substituents at the ligand backbone (R^1 and R^2) and by the substituents/configurations at the biaryl phosphite moiety. A small hydrogen group at R^1 and a methyl substituent at R^2 in combination with an *R*-trimethylsilyl substituted binaphtyl phosphite moiety are therefore required if enantioselectivity is to be high. To understand this catalytic behavior, we studied the Pd-π-allyl complexes **25**-**28**, which contain ligands **L38g**, **L38a**, **L39a** and **L42a**, respectively. With complexes Pd/**L38g** and Pd/**L38a**, we studied the effect of the substituents/configuration of the biaryl phosphite moiety. These complexes have the same substituents at R^1 and R^2 and only differ in the phosphite moiety. Therefore, while ligand **L38g**, which contains an *R*-trimethylsilyl substituted binaphthyl phosphite, provided the highest enantioselectivity, ligand **L38a**, which has a *tert*-butyl substituted biphenyl phosphite moiety, was less enantioselective (ee's up to 32% (*S*)). By comparing the Pd-studies of complexes **26**-**28**, we studied how the substituents at R^1 and R^2 affect catalytic performance.

The VT-NMR study (30 ºC to -80 ºC) of the Pd-allyl intermediate **25**, which contains ligand **L38g**, had a mixture of two isomers in equilibrium at a ratio of 1.5:1.[26] Both isomers were unambiguously assigned by NMR (^{1}H, ^{31}P, ^{13}C, ^{1}H-^{1}H, ^{1}H-^{13}C and ^{1}H-^{31}P correlation and NOESY experiments) to the two *syn*/*syn endo* **A** and *exo* **B** isomers (Scheme 4.4.2). In both isomers, the NOE indicated interactions between the two terminal protons of the allyl group, which clearly indicates a *syn*/*syn* disposition (Figure 4.4.5). Moreover, the hydrogens of the methyl substituent at the R^2 position of the ligand backbone showed a NOE interaction with the central allyl proton of the minor isomer **B**, while in isomer **A** this interaction appeared with both terminal allyl protons. These interactions can be explained by assuming a *syn*/*syn endo* disposition for isomer **A** and a *syn*/*syn exo* disposition for isomer **B** (Figure 4.4.5). For both isomers, the carbon NMR chemical shifts indicate that the most electrophilic allyl carbon terminus is *trans* to the phosphite moiety (Scheme 4.4.2). Assuming that the nucleophilic attack takes place at the more electrophilic allyl carbon terminus,[2] and on the basis of the observed stereochemical outcome of the reaction (90% (*S*) in product **1**), and as the enantiomeric excess of alkylation product **1** differs from the diastereoisomeric excess (de 20% (*S*)) of the Pd-intermediates, the **A** isomer must react faster than the **B** isomer. To prove this we studied the reactivity of the Pd-intermediates with sodium malonate at low temperature by *in situ* NMR (Figure 4.4.6). Our results showed that the major isomer **A** reacts around nine times faster than isomer **B**. If we take into account the relative reaction rates and the abundance of both isomers, the calculated ee should be 86% (*S*), which

matches the ee obtained experimentally. We can therefore conclude that the nucleophilic attack takes place predominantly at the allyl terminus *trans* to the phosphite moiety of the major **A** Pd-intermediate. This is also consistent with the fact that, for both isomers, the most electrophilic allylic terminal carbon atom is the one *trans* to the phosphite in the major **A** isomer.

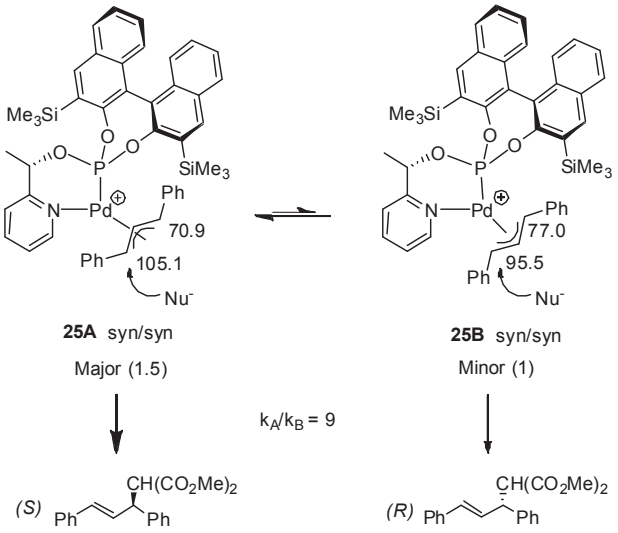

Scheme 4.4.2 Diastereoisomer Pd-allyl intermediates for **S1** with ligand **L38g**. The relative amounts of each isomer are shown in parentheses. The chemical shifts (in ppm) of the allylic terminal carbons are also shown.

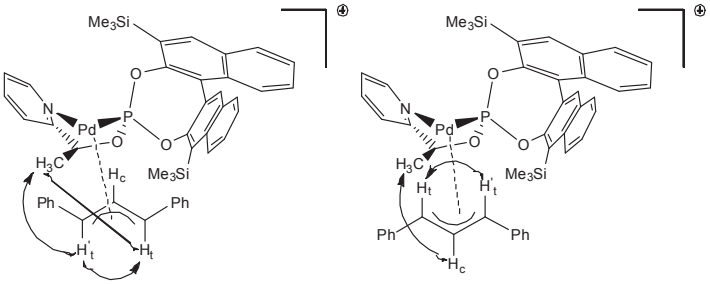

Figure 4.4.5. Main NOE contacts from the NOESY experiment of [Pd(η^3-1,3-diphenylallyl)(**L38g**)]BF_4 (**25**) isomers.

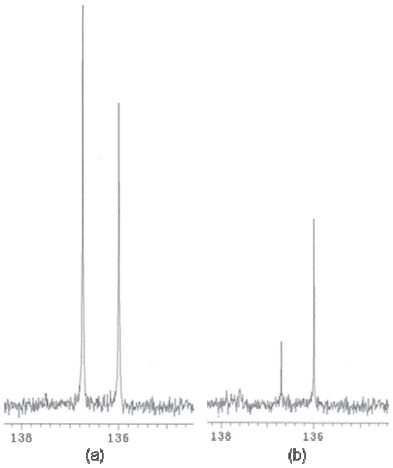

Figure 4.4.6. ^{31}P-{^{1}H}NMR spectra of [Pd(η^3-1,3-diphenylallyl)(**L38g**)]BF_4 (**25**) in CD_2Cl_2 at –80 ^{o}C (a) before the addition of sodium malonate and (b) after the addition of sodium malonate.

The VT-NMR study of Pd-allyl intermediate **26** containing ligand **L38a**, which has the same substituents at the ligand backbone and differs in the presence of a *tert*-butyl substituted biphenyl phosphite moiety, also had a mixture of two *syn*/*syn endo* (**A**) and *exo* (**B**) isomers, but at a ratio of 1.2:1. Also, the most electrophilic allyl carbon terminus was *trans* to the phosphite moiety in isomer **A** (Scheme 4.4.3). However, an important difference between complexes **25** and **26** is the lower electronic differentiation between the more electrophilic allylic terminus carbon atoms of both isomers (**A** and **B**) in complex **26** ($\Delta(\delta^{13}C) \approx 1.5$ ppm) than in complex **25** ($\Delta(\delta^{13}C) \approx 9.6$ ppm). This low electronic differentiation may explain the lower enantioselectivity obtained with Pd/**L38a** than with Pd/**L38g**. Accordingly, the reactivity of the Pd-intermediates with sodium malonate at low temperature by *in situ* NMR indicates that isomer **A** in complex **26** reacts only around 2.5 times faster than isomer **B**.

The VT-NMR study of Pd-allyl intermediates **27** and **28** containing ligands **L39a** and **L42a**, respectively, also had a mixture of two *syn*/*syn endo* (**A**) and *exo* (**B**) isomers, but at a ratio of 1:1 and 1.2:1, respectively (Scheme 4.4.3). By comparing complexes **25**-**28**, we found that the ratio of isomers **A** and **B** is affected by the substituent at R^1 position of the ligand backbone. The introduction of a bigger substituent at R^1 increases the relative amount of isomer **B**. The preferential formation of isomer **27B** can be attributed to the fact that the steric interaction between the methyl R^1 group and the phenyl groups of the substrate in isomer **27A** is greater than in complexes **26** and **28**, which contain a smaller hydrogen R^1 group. Again in complexes **27** and **28**, the most electrophilic allyl carbon terminus was *trans* to the phosphite moiety in isomer **A** (Scheme 4.4.3). Like complex **26**, the electronic differentiation between the more electrophilic allylic terminus carbon atoms of both isomers (**A** and **B**) is lower in these complexes than in complex **25** ($\Delta(\delta^{13}C) \approx 9.6$ ppm) which again explains the lower enantioselectivities obtained with respect to Pd/**L38g**. This behavior is more pronounced for complex **28,** which contains a *tert*-butyl group at the R^2 position, which agrees with its lower enantioselectivity. Finally, the trend of enantioselectivity observed between complexes Pd/**L38a** and Pd/**L39a** (32% (*S*) and 26% (*S*),

respectively) can therefore be mainly attributed to the increase in the amount of the less reactive isomer **B** caused by introducing bulkier substituent at the R^1 position.

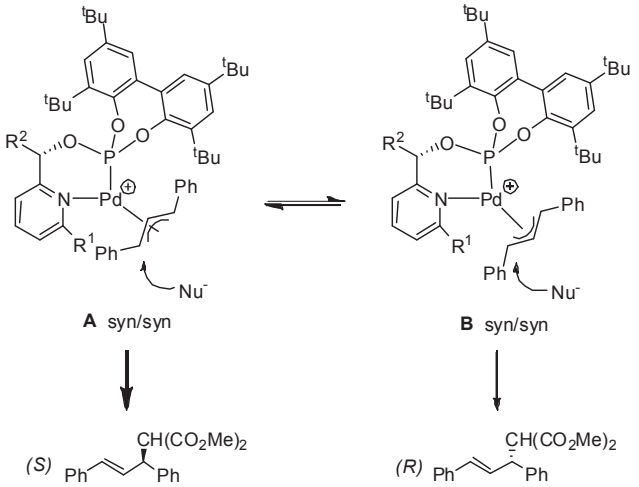

Complex	L	R^1	R^2	**A**/**B** ratio	$\Delta(\delta^{13}C)$ *trans* to P	k_A/k_B
26	**L38a**	H	Me	1.2/1	1.5	2.5
27	**L39a**	Me	Me	1/1	1.3	2
28	**L42a**	H	tBu	1.2/1	1.0	1

Scheme 4.4.3. Diastereoisomer Pd-allyl intermediates for **S1** with ligands **L38a**, **L39a** and **L42a**. The relative amounts of each isomer, the difference in chemical shifts of the most electrophilic allyl carbon atoms and the relative reaction rates are shown.

Palladium 1,3-dimethyl-allyl complexes

When the phosphite-pyridine ligand library **L38**-**L49a**-**g** was used in the allylic substitution of substrate **S2**, the catalytic results showed that there is an important effect of the substituents/configurations of the biaryl phosphite moiety. To understand this catalytic behavior, we studied Pd-π-allyl complexes **29** and **30**, which contain ligands **L39g** and **L39a** with different substituents/configuration at the biaryl phosphite moiety.

The VT-NMR (30 ºC to -80 ºC) study of Pd-allyl intermediate **29**, which contains ligand **L39g**, showed a mixture of two isomers in equilibrium at a ratio of 1:1.7. Isomers **A** and **B** were assigned by NOE to the two *syn*/*syn endo* **A** and *exo* **B** isomers (Scheme 4.4.4). In both isomers, the NOE indicated interactions between the two terminal protons of the allyl group, which clearly shows a *syn*/*syn* disposition (Figure 4.4.7). Moreover, the terminal allyl proton *trans* to the phosphite moiety showed a NOE interaction with the hydrogens of the methyl substituent at the R^2 position of the ligand backbone of the minor isomer **A**, while in isomer **B** this interaction appeared with the hydrogens of the methyl substituent at the R^1 position. These interactions can be explained by assuming a *syn*/*syn endo* disposition for isomer **A** and a *syn*/*syn exo* disposition for isomer **B** (Figure 4.4.7). The NMR data also indicated that the most electrophilic allyl carbon terminus is *trans* to the phosphite moiety in *syn*/*syn* isomer **A**. Assuming that the nucleophilic attack takes place at the most electrophilic allyl carbon terminus, on the basis of the observed stereochemical

outcome of the reaction (79% (*S*) in product **9**), and since the ee of alkylation product **9** differs from the diastereoisomeric excess (de = 25% (*R*)), we conclude that isomer **A** reacts faster than isomer **B**. This was confirmed by an *in situ* NMR study of the reactivity of the Pd-intermediates with sodium malonate at low temperature. This study indicated that isomer **29A** reacts approximately 10 times faster than isomer **29B**. This is also consistent with the fact that, for both isomers, the most electrophilic allylic terminal carbon atom is the one *trans* to the phosphite in the minor **A** isomer.

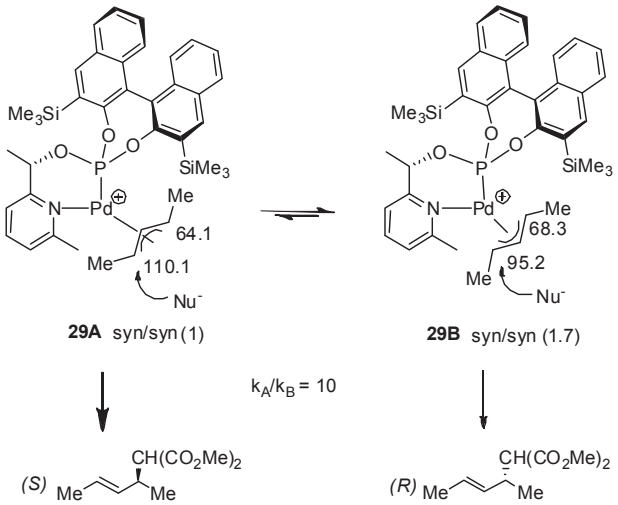

Scheme 4.4.4. Diastereoisomer Pd-allyl intermediates for **S2** with ligand **L39g**. The relative amounts of each isomer are shown in parentheses. The chemical shifts (in ppm) of the allylic terminal carbons are also shown.

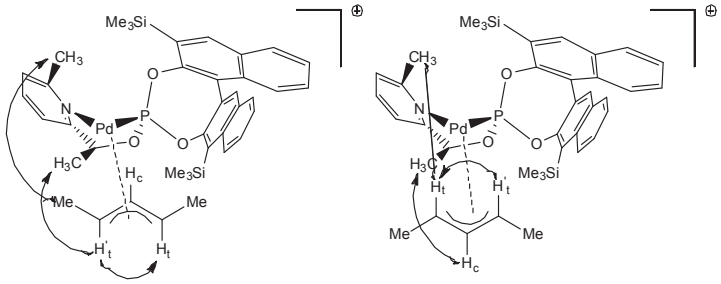

Figure 4.4.7. Main NOE contacts from the NOESY experiment of the [Pd(η^3-1,3-dimethylallyl)(**L39g**)]BF_4 (**29**) isomers.

The VT-NMR study of Pd-allyl intermediate **30**, which contains ligand **39a** with a *tert*-butyl substituted biphenyl phosphite group and provides lower enantioselectivity than Pd-**L39g**, had a mixture of three isomers at a ratio of 2.5:10:1. Isomers **A** and **B** were assigned by NOE to the two *syn/syn endo* **A** and *exo* **B** isomers, whereas isomer **C** was assigned to the *syn*/*anti* isomer (Scheme 4.4.5). For isomers **A** and **B**, the NOE indicated interactions between the two terminal protons of the allyl group, whereas for isomer **C** the central allyl proton showed a NOE interaction

with the terminal allyl proton located *trans* to the pyridine group (Figure 4.4.8). Moreover, for isomers **B** and **C**, the terminal allyl proton *trans* to the phosphite moiety showed a NOE interaction with the hydrogens of the methyl substituent at the R^1 position of the ligand backbone, whereas in isomer **A** this interaction appeared with the hydrogen atoms of the methyl substituent at the R^2 position. The NOESY also indicated an exchange between the allylic terminal protons located *trans* to the pyridine moiety of isomers **A** and **C** (Figure 4.4.8). This confirms the η^3-η^1-η^3 movement for the exchange between isomers **A** and **C**.[27] In addition, the fact that no other H_{anti}-H_{syn} exchange was observed indicates that the exchange took place by means of the selective opening of one of the terminal Pd-C bonds. Isomer **C** formed because, in complex **A**, the steric interaction increased between the pyridine methyl group and one of the methyl substituents of **S2**.

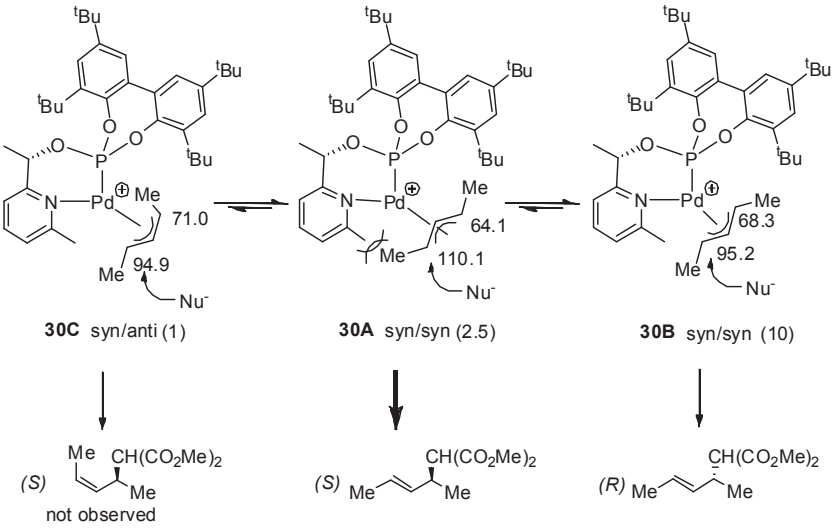

Scheme 4.4.5. Diastereoisomer Pd-allyl intermediates for **S2** with ligand **L39a**. The relative amounts of each isomer are shown in parentheses. The chemical shifts (in ppm) of the allylic terminal carbons are also shown.

The formation of isomer **C** minimized this steric interaction (Scheme 4.4.5). Therefore, the open Pd-C bond belongs to the most electrophilic carbon atom containing the substituent that undergoes the biggest steric hindrance with the methyl pyridine fragment. The NMR spectroscopic data also indicated that the most electrophilic allyl carbon terminus is *trans* to the phosphite moiety in *syn/syn* isomer **A** and in *syn/syn* isomer **B**, and that the allylic terminus carbon in isomer **C** is less electrophilic. Assuming that the nucleophilic attack takes place at the most electrophilic allyl carbon terminus, on the basis of the observed stereochemical outcome of the reaction (49% (*S*) in product **9**), and since the ee of alkylation product **9** differs from the diastereoisomeric excess (de=60% (*R*)) of the reacting Pd intermediates **A** and **B**, we conclude that isomer **A** reacts faster than isomer **B**.[28] The lower enantioselectivity with this system than with the Pd/**L39g** catalytic system discussed above can be attributed to the decrease in the relative amount of isomer **A** with respect to isomer **B** compared with the population of the isomers (**A** and **B**) for complex **29**.

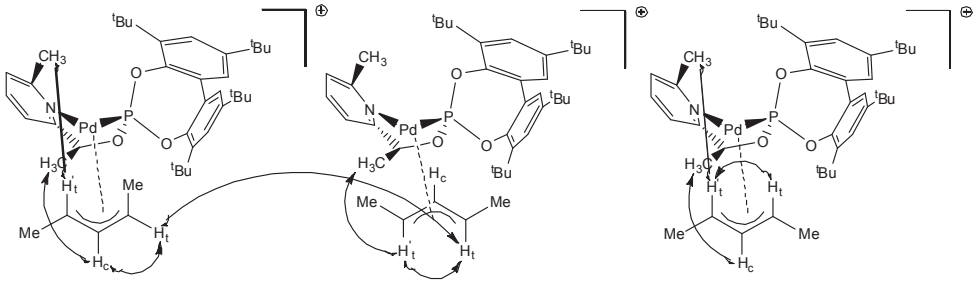

Figure 4.4.8. Main NOE contacts from the NOESY experiment of the [Pd(η^3-1,3-dimethylallyl)(**L39a**)]BF_4 (**30**) isomers.

Palladium 1,3-cyclohexenyl-allyl complexes

When the phosphite-pyridine ligand library **L38**-**L49a**-**g** was used in the allylic substitution of cyclic substrates **S3**-**S5**, the catalytic results showed that the substituents/configurations of the biaryl phosphite moiety have an important effect. To understand this catalytic behavior, we studied Pd-π-allyl complexes **31** and **32**. These complexes contain ligands **L39g** and **L39a,** which have different substituents/configuration at the biaryl phosphite moiety.

The VT NMR (35 °C to –80 °C) of Pd intermediate **31**, which contains ligand **L39g**, showed a mixture of the two possible isomers at a ratio of 10:1 (Scheme 4.4.6). All isomers were unambiguously assigned by NOE to isomers **A** and **B** (Figure 4.4.9). For isomer **A**, the NOE indicated interactions between the terminal allyl proton *trans* to the phosphite moiety and the hydrogens of the methyl substituent at the R^1 position of the ligand backbone. For isomer **B**, however, this interaction appeared with the hydrogens of the methyl substituent at the R^2 position of the ligand backbone (Figure 4.4.9). The carbon NMR chemical shifts indicated that the most electrophilic allylic terminus carbon is *trans* to the phosphite moiety. The matching between enantiomeric excesses (80% (*R*) in product **15**) and the diastereoisomeric Pd ratio (de=82% (*R*)) indicate that the two isomers react at a similar rate. This is in agreement with the fact that the electrophilicities of the allylic terminal carbon atom *trans* to the phosphite are rather similar in both complexes ($\Delta\delta^{13}C$= 0.3 ppm). To prove that the reaction rates really are similar, we studied the reactivity of the Pd intermediates with sodium malonate at low temperature by in situ NMR spectroscopy. Our results showed that the two isomers react at a similar rate.

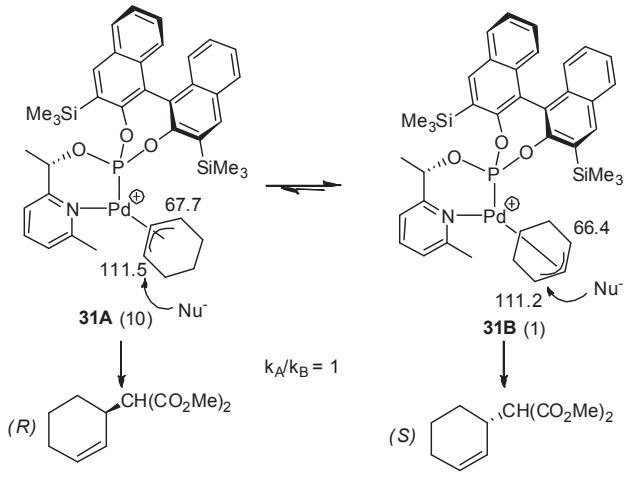

Scheme 4.4.6. Diastereoisomer Pd-allyl intermediates for **S3** with ligand **L39g**. The relative amounts of each isomer are shown in parentheses. The chemical shifts (in ppm) of the allylic terminal carbons are also shown.

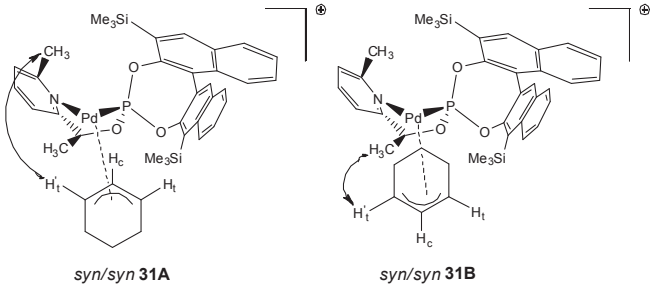

Figure 4.4.9. Main NOE contacts from the NOESY experiment of the [Pd(η^3-1,3-cyclohexenyl-allyl)(**L39g**)]BF_4 (**31**) isomers.

The VT NMR (35 °C to –80 °C) of Pd intermediate **32**, which contains ligand **L39a**, also showed a mixture of the two possible isomers (**A** and **B**), but at a ratio of 1:2.3, respectively (Scheme 4.4.7). The carbon NMR chemical shifts also indicated that the most electrophilic allylic terminus carbon is *trans* to the phosphite moiety. In contrast to Pd-intermediate **31**, the fact that the observed enantiomeric excess (24% (*S*) in product **15**) is lower than the diastereomeric excess (de= 40% (*S*)) indicates that isomer **A** should react slightly faster than isomer **B**. However, this catalytic system provides lower enantiosectivities than Pd/**L39g** (**31**) because of the lower population of isomer **A** in complex **32** than in complex **31**.

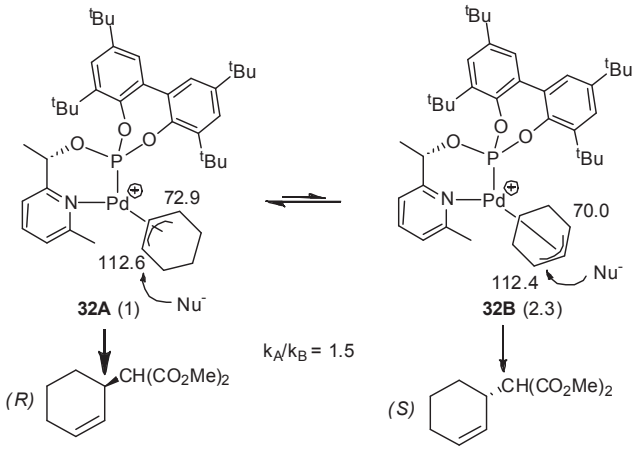

Scheme 4.4.7. Diastereoisomer Pd-allyl intermediates for **S3** with ligand **L39a**. The relative amounts of each isomer are shown in parentheses. The chemical shifts (in ppm) of the allylic terminal carbons are also shown.

4.4.4. Conclusions

A library of phosphite-pyridine ligands **L38**-**L39a**-**g** has been successfully applied for the first time in the Pd-catalyzed allylic substitution reactions of several di- and trisubstituted substrates using a wide range of C-, N- and O-nucleophiles, among which are the little studied α-substituted malonates, β-diketones and benzyl alcohol. This ligand library combines the advantages of the pyridine moiety with those of the phosphite group. The ligands are more stable than their oxazoline counterparts, less sensitive to air and other oxidizing agents than phosphines and phosphinites, and easy to synthesize from readily available feedstocks. Moreover, the highly modular nature of the ligand library enables the substituents/configuration at the ligand backbone, and the substituents/configurations at the biaryl phosphite moiety to be easily and systematically varied. We found that the extent to which the chiral information was transferred to the product can be tuned by correctly choosing the ligand components. The introduction of an enantiopure biaryl phosphite moiety played an essential role in increasing the versatility of the Pd-catalytic systems. Enantioselectivities were therefore high in a wide range of substrates using several C-, N- and O-nucleophiles. Of particular note were the high enantioselectivities (up to >99% ee) and high activities obtained for the trisubstituted substrates **S6**-**S7**, which compare favorably with the best that have been reported in the literature. The new phosphite-pyridine ligand library not only performs well in traditional organic solvents but also in alternative environmentally friendly solvents such as propylene carbonate and ionic liquids. Ionic liquids allowed the palladium catalyst to be reused while maintaining the excellent enantioselectivities. In addition, for all substrates, both enantiomers of the substitution products were obtained with high enantioselectivities. These results open up the asymmetric Pd-catalyzed allylic substitution of several substrates types with a wide range of nucleophiles to the potential effective use of readily available and highly modular phosphite-pyridine ligands.

By studying the Pd-1,3-diphenyl, 1,3-dimethyl and 1,3-cyclohexenyl allyl intermediates with NMR spectroscopy, we were able to better understand the observed catalytic behavior. Therefore,

for enantioselectivities to be high in the substitution of hindered substrate **S1**, the ligand parameters need to be correctly combined so that the electronic differentiation increases between the most electrophilic allylic terminus carbon atoms of the isomers formed and/or the isomer that reacts faster with the nucleophile is predominantly formed. Likewise, for unhindered substrates **S2** and **S3**, the ligand parameters need to be correctly combined so that the Pd-intermediate that has the fastest reaction with the nucleophile is predominantly formed, which leads to high enantioselectivities. We also found that the nucleophilic attack takes place predominantly at the allylic terminal carbon atom located *trans* to the phosphite moiety.

4.4.5. Experimental section

4.4.5.1. General considerations

All reactions were carried out using standard Schlenk techniques under an atmosphere of argon. Solvents were purified and dried by standard procedures. The synthesis of ligands **L38**-**L49a**-**g** has been previously described in Chapter 3.6. Racemic substrates **S1**-**S7** were prepared as previously reported.[29] $[Pd(\eta^3\text{-}1,3\text{-}Ph_2\text{-}C_3H_3)(\mu\text{-}Cl)]_2$,[30] $[Pd(\eta^3\text{-}1,3\text{-}Me_2\text{-}C_3H_3)(\mu\text{-}Cl)]_2$[31] and $[Pd(\eta^3\text{-cyclohexenyl})(\mu\text{-}Cl)]_2$[32] were prepared as previously described. ^1H, $^{13}C\{^1H\}$, and $^{31}P\{^1H\}$ NMR spectra were recorded using a 400 MHz spectrometer. Chemical shifts are relative to that of $SiMe_4$ (^1H and ^{13}C) as internal standard or H_3PO_4 (^{31}P) as external standard. ^1H, ^{13}C and ^{31}P assignments were made on the basis of ^1H-^1H gCOSY, ^1H-^{13}C gHSQC and ^1H-^{31}P gHMBC experiments.

4.4.5.2. General procedure for the preparation of $[Pd(\eta^3\text{-allyl})(L)]BF_4$ complexes 25-32

The corresponding ligand (0.05 mmol) and the complex $[Pd(\mu\text{-}Cl)(\eta^3\text{-}1,3\text{-allyl})]_2$ (0.025 mmol) were dissolved in CD_2Cl_2 (1.5 mL) at room temperature under argon. $AgBF_4$ (9.8 mg, 0.05 mmol) was added after 30 minutes and the mixture was stirred for 30 minutes. The mixture was then filtered over celite under argon and the resulting solutions were analyzed by NMR. After the NMR analysis, the complexes were precipitated as pale yellow solids by adding hexane.

$[Pd(\eta^3\text{-}1,3\text{-diphenylallyl})(L38g)]BF_4$ (25). Isomer **A** (60%): ^{31}P NMR (CD_2Cl_2, 298 K), δ: 136.7 (s, 1P). ^1H NMR(CD_2Cl_2, 298 K), δ: 0.00 (s, 9H, CH_3-Si), 0.58 (s, 9H, CH_3-Si), 1.70 (d, 3H, CH_3, $^3J_{H\text{-}H}$= 6.4 Hz), 4.66 (d, 1H, CH allyl trans to N, $^3J_{H\text{-}H}$= 10.8 Hz), 5.52 (m, 1H, CH-O), 6.01 (m, 1H, CH allyl central), 6.69 (m, 1H, CH allyl trans to P), 6.2-8.2 (m, 24H, CH=). ^{13}C NMR (C_6D_6, 298 K), δ: -0.4 (CH_3-Si), 1.0 (CH_3-Si), 18.4 (d, CH_3 allyl, $J_{C\text{-}P}$= 8.4 Hz), 70.9 (d, CH allyl trans to N, $J_{C\text{-}P}$= 9.9 Hz), 76.0 (d, CH-O, $J_{C\text{-}P}$= 6.1 Hz), 105.1 (d, CH allyl trans to P, $J_{C\text{-}P}$= 32.8 Hz), 113.3 (d, CH allyl central, $J_{C\text{-}P}$= 9.9 Hz), 121-158 (aromatic carbons). Isomer **B** (40%): ^{31}P NMR (CD_2Cl_2, 298 K), δ: 135.9 (s, 1P). ^1H NMR(CD_2Cl_2, 298 K), δ: 0.05 (s, 9H, CH_3-Si), 0.30 (s, 9H, CH_3-Si), 2.29 (d, 3H, CH_3, $^3J_{H\text{-}H}$= 6.4 Hz), 5.03 (d, 1H, CH allyl trans to N, $^3J_{H\text{-}H}$= 11.2 Hz), 5.56 (m, 1H, CH-O), 5.81 (m, 1H, CH allyl central), 6.49 (m, 1H, CH allyl trans to P), 6.2-8.2 (m, 24H, CH=). ^{13}C NMR (C_6D_6, 298 K), δ: -1.2 (CH_3-Si), 0.3 (CH_3-Si), 25.6 (d, CH_3, $J_{C\text{-}P}$= 7.6 Hz), 77.0 (d, CH allyl trans to N, $J_{C\text{-}P}$= 9.0 Hz), 80.1 (d, CH-O, $J_{C\text{-}P}$= 3.8 Hz), 95.5 (d, CH allyl trans to P, $J_{C\text{-}P}$= 34.3 Hz), 112.6 (d, CH allyl central, $J_{C\text{-}P}$= 11.5 Hz), 121-158 (aromatic carbons). Anal. calcd (%) for $C_{48}H_{49}BF_4NO_3PPdSi_2$: C 59.54, H 5.10, N 1.45; found: C 59.63, H 5.12, N 1.43.

[Pd(η^3-1,3-diphenylallyl)(L38a)]BF_4 (26). Isomer **A** (55%): ^{31}P NMR (CD_2Cl_2, 298 K), δ: 136.9 (s, 1P). ^{1}H NMR(CD_2Cl_2, 298 K), δ: 1.25 (s, 9H, CH_3, ^{t}Bu), 1.37 (s, 9H, CH_3, ^{t}Bu), 1.47 (s, 9H, CH_3, ^{t}Bu), 1.54 (s, 9H, CH_3, ^{t}Bu), 1.73 (d, 3H, CH_3, $^3J_{H\text{-}H}$= 6.4 Hz), 4.73 (d, 1H, CH allyl trans to N, $^3J_{H\text{-}H}$= 10.2 Hz), 5.48 (m, 1H, CH-O), 6.03 (m, 1H, CH allyl central), 6.53 (m, 1H, CH allyl trans to P), 6.6-8.0 (m, 18H, CH=). ^{13}C NMR (C_6D_6, 298 K), δ: 19.3 (d, CH_3 allyl, $J_{C\text{-}P}$= 8.4 Hz), 30.9-31.2 (CH_3, ^{t}Bu), 34.6-35.6 (C, ^{t}Bu), 69.7 (d, CH allyl trans to N, $J_{C\text{-}P}$= 10.3 Hz), 76.8 (d, CH-O, $J_{C\text{-}P}$= 5.3 Hz), 104.9 (d, CH allyl trans to P, $J_{C\text{-}P}$= 34.2 Hz), 113.5 (d, CH allyl central, $J_{C\text{-}P}$= 11.2 Hz), 121-162 (aromatic carbons). Isomer **B** (45%): ^{31}P NMR (CD_2Cl_2, 298 K), δ: 135.2 (s, 1P). ^{1}H NMR(CD_2Cl_2, 298 K), δ: 1.21 (s, 9H, CH_3, ^{t}Bu), 1.31 (s, 9H, CH_3, ^{t}Bu), 1.43 (s, 9H, CH_3, ^{t}Bu), 1.59 (s, 9H, CH_3, ^{t}Bu), 1.98 (d, 3H, CH_3, $^3J_{H\text{-}H}$= 6.4 Hz), 5.11 (d, 1H, CH allyl trans to N, $^3J_{H\text{-}H}$= 11.2 Hz), 5.54 (m, 1H, CH-O), 5.89 (m, 1H, CH allyl central), 6.31 (m, 1H, CH allyl trans to P), 6.2-8.2 (m, 18H, CH=). ^{13}C NMR (C_6D_6, 298 K), δ: 19.9 (d, CH_3 allyl, $J_{C\text{-}P}$= 8.4 Hz), 30.9-31.2 (CH_3, ^{t}Bu), 34.6-35.6 (C, ^{t}Bu), 77.6 (d, CH allyl trans to N, $J_{C\text{-}P}$= 10.2 Hz), 80.5 (d, CH-O, $J_{C\text{-}P}$= 4.4 Hz), 103.4 (d, CH allyl trans to P, $J_{C\text{-}P}$= 32.7 Hz), 112.9 (d, CH allyl central, $J_{C\text{-}P}$= 10.4 Hz), 121-162 (aromatic carbons). Anal. calcd (%) for $C_{50}H_{61}BF_4NO_3PPd$: C 63.33, H 6.48, N 1.48; found: C 63.51, H 6.52, N 1.35.

[Pd(η^3-1,3-diphenylallyl)(L39a)]BF_4 (27). Isomer **A** (50%): ^{31}P NMR (CD_2Cl_2, 298 K), δ: 136.4 (s, 1P). ^{1}H NMR(CD_2Cl_2, 298 K), δ: 1.17 (s, 9H, CH_3, ^{t}Bu), 1.33 (s, 9H, CH_3, ^{t}Bu), 1.35 (s, 9H, CH_3, ^{t}Bu), 1.65 (s, 9H, CH_3, ^{t}Bu), 1.92 (d, 3H, CH_3, $^3J_{H\text{-}H}$= 6.4 Hz), 2.32 (s, 3H, CH_3-Py), 4.99 (d, 1H, CH allyl trans to N, $^3J_{H\text{-}H}$= 9.2 Hz), 5.33 (m, 1H, CH-O), 6.43 (m, 1H, CH allyl central), 6.59 (m, 1H, CH allyl trans to P), 6.6-8.0 (m, 17H, CH=). ^{13}C NMR (C_6D_6, 298 K), δ: 19.6 (d, CH_3 allyl, $J_{C\text{-}P}$= 8.4 Hz), 27.9 (CH_3-Py), 32.7-33.3 (CH_3, ^{t}Bu), 36.4-37.4 (C, ^{t}Bu), 72.7 (d, CH allyl trans to N, $J_{C\text{-}P}$= 12.2 Hz), 79.3 (d, CH-O, $J_{C\text{-}P}$= 12.2 Hz), 107.5 (d, CH allyl trans to P, $J_{C\text{-}P}$= 38.4 Hz), 115.6 (d, CH allyl central, $J_{C\text{-}P}$= 6.2 Hz), 122-163 (aromatic carbons). Isomer **B** (50%): ^{31}P NMR (CD_2Cl_2, 298 K), δ: 135.8 (s, 1P). ^{1}H NMR(CD_2Cl_2, 298 K), δ: 1.21 (s, 9H, CH_3, ^{t}Bu), 1.33 (s, 9H, CH_3, ^{t}Bu), 1.39 (s, 9H, CH_3, ^{t}Bu), 1.59 (s, 9H, CH_3, ^{t}Bu), 1.95 (d, 3H, CH_3, $^3J_{H\text{-}H}$= 6.4 Hz), 2.26 (s, 3H, CH_3-Py), 5.06 (d, 1H, CH allyl trans to N, $^3J_{H\text{-}H}$= 11.2 Hz), 5.37 (m, 1H, CH-O), 6.32 (m, 1H, CH allyl central), 6.46 (m, 1H, CH allyl trans to P), 6.2-8.2 (m, 17H, CH=). ^{13}C NMR (C_6D_6, 298 K), δ: 21.3 (d, CH_3 allyl, $J_{C\text{-}P}$= 8.4 Hz), 27.3 (CH_3-Py), 32.7-33.3 (CH_3, ^{t}Bu), 36.4-37.4 (C, ^{t}Bu), 74.8 (d, CH allyl trans to N, $J_{C\text{-}P}$= 10.8 Hz), 79.1 (b, CH-O), 106.2 (d, CH allyl trans to P, $J_{C\text{-}P}$= 36.8 Hz), 115.9 (d, CH allyl central, $J_{C\text{-}P}$= 5.2 Hz), 122-163 (aromatic carbons). Anal. calcd (%) for $C_{51}H_{63}BF_4NO_3PPd$: C 63.66, H 6.60, N 1.46; found: C 63.71, H 6.64, N 1.42.

[Pd(η^3-1,3-diphenylallyl)(L42a)]BF_4 (28). Isomer **A** (55%): ^{31}P NMR (CD_2Cl_2, 298 K), δ: 137.3 (s, 1P). ^{1}H NMR(CD_2Cl_2, 298 K), δ: 1.11 (s, 9H, CH_3, ^{t}Bu), 1.26 (s, 9H, CH_3, ^{t}Bu), 1.33 (s, 9H, CH_3, ^{t}Bu), 1.48 (s, 9H, CH_3, ^{t}Bu), 1.63 (s, 9H, CH_3, ^{t}Bu), 4.67 (d, 1H, CH allyl trans to N, $^3J_{H\text{-}H}$= 9.8 Hz), 5.57 (d, 1H, CH-O, $J_{H\text{-}P}$= 10.2 Hz), 6.11 (m, 1H, CH allyl central), 6.49 (m, 1H, CH allyl trans to P), 6.6-8.0 (m, 18H, CH=). ^{13}C NMR (C_6D_6, 298 K), δ: 27.3 (CH_3, ^{t}Bu), 31.1-33.4 (CH_3, ^{t}Bu), 34.2-35.4 (C, ^{t}Bu), 73.5 (d, CH allyl trans to N, $J_{C\text{-}P}$= 10.2 Hz), 84.5 (d, CH-O, $J_{C\text{-}P}$= 6.2 Hz), 105.2 (d, CH allyl trans to P, $J_{C\text{-}P}$= 33.6 Hz), 112.9 (d, CH allyl central, $J_{C\text{-}P}$= 9.4 Hz), 121-162 (aromatic carbons). Isomer **B** (45%): ^{31}P NMR (CD_2Cl_2, 298 K), δ: 136.4 (s, 1P). ^{1}H NMR(CD_2Cl_2, 298 K), δ: 1.09 (s, 9H, CH_3, ^{t}Bu), 1.21 (s, 9H, CH_3, ^{t}Bu), 1.32 (s, 9H, CH_3, ^{t}Bu), 1.46 (s, 9H, CH_3, ^{t}Bu), 1.59 (s, 9H, CH_3, ^{t}Bu), 4.87 (d, 1H, CH allyl trans to N, $^3J_{H\text{-}H}$= 10.2 Hz), 5.61 (d, 1H, CH-O, $J_{H\text{-}P}$= 9.8 Hz), 6.12 (m, 1H, CH allyl central), 6.34 (m, 1H, CH allyl trans to P), 6.6-8.0 (m, 18H, CH=). ^{13}C

NMR (C_6D_6, 298 K), δ: 27.6 (CH_3, ^tBu), 31.1-33.4 (CH_3, ^tBu), 34.2-35.4 (C, ^tBu), 76.4 (d, CH allyl trans to N, J_{C-P}= 13.2 Hz), 85.2 (d, CH-O, J_{C-P}= 5.8 Hz), 104.2 (d, CH allyl trans to P, J_{C-P}= 34.8 Hz), 113.2 (d, CH allyl central, J_{C-P}= 9.1 Hz), 121-162 (aromatic carbons). Anal. calcd (%) for $C_{53}H_{67}BF_4NO_3PPd$: C 64.28, H 6.82, N 1.41; found: C 64.33, H 6.85, N 1.34.

[Pd(η^3-1,3-dimethylallyl)(L39g)]BF_4 (29). Isomer **A** (37%): ^{31}P NMR (CD_2Cl_2, 298 K), δ: 136.4 (s, 1P). ^{1}H NMR(CD_2Cl_2, 298 K), δ: -0.32 (s, 9H, CH_3-Si), -0.07 (dd, 3H, CH_3 allyl, $^3J_{H-H}$= 6.4 Hz, J_{H-P}= 13.6 Hz), 0.18 (s, 9H, CH_3-Si), 1.26 (dd, 3H, CH_3 allyl, $^3J_{H-H}$= 6.0 Hz, J_{H-P}= 18.0 Hz), 1.57 (d, 3H, CH_3, $^3J_{H-H}$= 6.4 Hz), 2.56 (s, 3H, CH_3-Py), 4.37 (m, 1H, CH allyl trans to N), 4.64 (m, 1H, CH allyl trans to P), 5.01 (m, 1H, CH allyl central), 5.52 (m, 1H, CH-O), 6.5-8.1 (m, 13H, CH=). ^{13}C NMR (C_6D_6, 298 K), δ: -0.2 (CH_3-Si), 1.5 (CH_3-Si), 14.4 (CH_3 allyl), 18.8 (b, CH_3), 19.4 (d, CH_3 allyl, J_{C-P}= 5.9 Hz), 26.2 (CH_3-Py), 64.1 (d, CH allyl trans to N, J_{C-P}= 7.8 Hz), 78.5 (b, CH-O), 110.1 (d, CH allyl trans to P, J_{C-P}= 39.8 Hz), 120.3 (d, CH allyl central, J_{C-P}= 10.4 Hz), 121-162 (aromatic carbons). Isomer **B** (67%): ^{31}P NMR (CD_2Cl_2, 298 K), δ: 139.5 (s, 1P). ^{1}H NMR(CD_2Cl_2, 298 K), δ: -0.30 (s, 9H, CH_3-Si), -0.06 (dd, 3H, CH_3 allyl, $^3J_{H-H}$= 6.0 Hz, J_{H-P}= 7.6 Hz), 0.23 (s, 9H, CH_3-Si), 1.37 (dd, 3H, CH_3 allyl, $^3J_{H-H}$= 6.4 Hz, J_{H-P}= 15.6 Hz), 1.59 (d, 3H, CH_3, $^3J_{H-H}$= 6.4 Hz), 2.42 (s, 3H, CH_3-Py), 3.40 (m, 1H, CH allyl trans to N), 4.92 (m, 1H, CH allyl trans to P), 5.15 (m, 1H, CH allyl central), 5.69 (m, 1H, CH-O), 6.5-8.1 (m, 13H, CH=). ^{13}C NMR (C_6D_6, 298 K), δ: -0.4 (CH_3-Si), 0.5 (CH_3-Si), 15.2 (CH_3 allyl), 17.9 (b, CH_3 allyl), 18.0 (b, CH_3), 28.6 (CH_3-Py), 68.3 (d, CH allyl trans to N, J_{C-P}= 9.0 Hz), 78.5 (b, CH-O), 95.2 (d, CH allyl trans to P, J_{C-P}= 43.2 Hz), 116.4 (d, CH allyl central, J_{C-P}= 12.0 Hz), 121-162 (aromatic carbons) Anal. calcd (%) for $C_{39}H_{47}BF_4NO_3PPdSi_2$: C 54.58, H 5.52, N 1.63; found: C 54.62, H 5.56, N 1.58.

[Pd(η^3-1,3-dimethylallyl)(L39a)]BF_4 (30). Isomer **A** (21%): ^{31}P NMR (CD_2Cl_2, 298 K), δ: 137.7 (s, 1P). ^{1}H NMR(CD_2Cl_2, 298 K), δ: 0.89 (m, 3H, CH_3 allyl), 1.21 (s, 9H, CH_3, ^tBu), 1.25 (m, 3H, CH_3 allyl), 1.32 (s, 9H, CH_3, ^tBu), 1.36 (s, 9H, CH_3, ^tBu), 1.61 (s, 9H, CH_3, ^tBu), 1.86 (d, 3H, CH_3, $^3J_{H-H}$= 6.4 Hz), 2.93 (s, 3H, CH_3-Py), 4.02 (m, 1H, CH allyl trans to N), 5.09 (m, 1H, CH allyl trans to P), 5.74 (m, 2H, CH allyl central and CH-O), 7.2-8.2 (m, 7H, CH=). ^{13}C NMR (C_6D_6, 298 K), δ: 15.4-18.2 (CH_3 allyl), 20.0 (b, CH_3), 27.9 (CH_3-Py), 30.9-31.2 (CH_3, ^tBu), 34.6-35.6 (C, ^tBu), 64.1 (b, CH allyl trans to N), 77.1 (d, CH-O, J_{C-P}= 10.9 Hz), 110.1 (d, CH allyl trans to P, J_{C-P}= 38.9 Hz), 118.0 (d, CH allyl central, J_{C-P}= 12.3 Hz), 121-162 (aromatic carbons). Isomer **B** (72%): ^{31}P NMR (CD_2Cl_2, 298 K), δ: 137.9 (s, 1P). ^{1}H NMR(CD_2Cl_2, 298 K), δ: 0.85 (dd, 3H, CH_3 allyl, $^3J_{H-H}$= 6.4 Hz, J_{C-P}= 13.2 Hz), 1.23 (s, 9H, CH_3, ^tBu), 1.25 (m, 3H, CH_3 allyl), 1.31 (s, 9H, CH_3, ^tBu), 1.38 (s, 9H, CH_3, ^tBu), 1.58 (s, 9H, CH_3, ^tBu), 1.90 (d, 3H, CH_3, $^3J_{H-H}$= 6.4 Hz), 2.80 (s, 3H, CH_3-Py), 3.84 (m, 1H, CH allyl trans to N), 5.20 (m, 1H, CH allyl trans to P), 5.63 (m, 1H, CH allyl central), 6.01 (m, 1H, CH-O), 7.2-8.2 (m, 7H, CH=). ^{13}C NMR (C_6D_6, 298 K), δ: 15.4-18.2 (CH_3 allyl), 19.4 (d, CH_3, J_{C-P}= 6.2 Hz), 26.6 (CH_3-Py), 30.9-31.2 (CH_3, ^tBu), 34.6-35.6 (C, ^tBu), 68.3 (d, CH allyl trans to N, J_{C-P}= 10.1 Hz), 77.7 (b, CH-O), 95.2 (d, CH allyl trans to P, J_{C-P}= 43.2 Hz), 117.1 (d, CH allyl central, J_{C-P}= 12.4 Hz), 121-162 (aromatic carbons). Isomer **C** (8%): ^{31}P NMR (CD_2Cl_2, 298 K), δ: 139.5 (s, 1P). ^{1}H NMR(CD_2Cl_2, 298 K), δ: 0.89 (m, 3H, CH_3 allyl), 1.19 (s, 9H, CH_3, ^tBu), 1.25 (m, 3H, CH_3 allyl), 1.34 (s, 18H, CH_3, ^tBu), 1.43 (s, 9H, CH_3, ^tBu), 1.82 (d, 3H, CH_3, $^3J_{H-H}$= 6.4 Hz), 2.76 (s, 3H, CH_3-Py), 4.31 (m, 1H, CH allyl trans to N), 4.82 (m, 1H, CH allyl trans to P), 5.59 (m, 1H, CH allyl central), 6.09 (m, 1H, CH-O), 7.2-8.2 (m, 7H, CH=). ^{13}C NMR (C_6D_6, 298 K), δ: 15.4-18.2 (CH_3 allyl), 19.8 (b, CH_3), 28.5 (CH_3-Py), 30.9-31.2 (CH_3, ^tBu), 34.6-35.6 (C, ^tBu), 71.0 (d, CH allyl trans to N, J_{C-P}= 8.1 Hz), 77.7 (b, CH-O), 94.9 (d, CH allyl trans to P, J_{C-P}= 36.2 Hz), 118.2 (d,

CH allyl central, J_{C-P}= 9.8 Hz), 121-162 (aromatic carbons). Anal. calcd (%) for $C_{41}H_{59}BF_4NO_3PPd$: C 58.76 H 7.10, N 1.67; found: C 58.81, H 7.09, N 1.65

[Pd(η³-1,3-cyclohexenylallyl)(L39g)]BF₄ (31). Isomer **A** (90%): ^{31}P NMR (CD_2Cl_2, 298 K), δ: 142.4 (s, 1P). ^{1}H NMR(CD_2Cl_2, 298 K), δ: 0.06 (s, 9H, CH_3-Si), 0.51 (s, 9H, CH_3-Si), 1.27 (m, 2H, CH_2, allyl), 1.72 (m, 2H, CH_2 allyl), 1.92 (d, 3H, CH_3, $^3J_{H-H}$= 6.4 Hz), 2.03 (m, 2H, CH_2 allyl), 2.85 (s, 3H, CH_3-Py), 4.96 (m, 1H, CH allyl trans to N), 5.61 (m, 1H, CH allyl central), 5.88 (m, 1H, CH-O), 6.41 (m, 1H, CH allyl trans to P), 6.8-8.4 (m, 13H, CH=). ^{13}C NMR (C_6D_6, 298 K), δ: 0.0 (CH_3-Si), 0.7 (CH_3-Si), 18.8 (d, CH_3, J_{C-P}= 10.6 Hz), 22.4 (CH_2 allyl), 27.6 (CH_3-Py), 29.2 (CH_2 allyl), 29.3 (CH_2 allyl), 67.7 (d, CH allyl trans to N, J_{C-P}= 12.2 Hz), 78.4 (d, CH-O, J_{C-P}= 10.4 Hz), 109.9 (d, CH allyl trans to P, J_{C-P}= 41.2 Hz), 111.5 (d, CH allyl central, J_{C-P}= 12.2 Hz), 121-164 (aromatic carbons). Isomer **B** (10%): ^{31}P NMR (CD_2Cl_2, 298 K), δ: 141.1 (s, 1P). ^{1}H NMR(CD_2Cl_2, 298 K), δ: 0.15 (s, 9H, CH_3-Si), 0.40 (s, 9H, CH_3-Si), 1.27 (m, 2H, CH_2, allyl), 1.72 (m, 2H, CH_2 allyl), 1.84 (d, 3H, CH_3, $^3J_{H-H}$= 6.4 Hz), 2.03 (m, 2H, CH_2 allyl), 2.73 (s, 3H, CH_3-Py), 5.42 (m, 1H, CH allyl trans to N), 5.73 (m, 1H, CH allyl central), 5.92 (m, 1H, CH-O), 6.62 (m, 1H, CH allyl trans to P), 6.8-8.4 (m, 13H, CH=). ^{13}C NMR (C_6D_6, 298 K), δ: 0.1 (CH_3-Si), 1.0 (CH_3-Si), 20.2 (d, CH_3, J_{C-P}= 9.5 Hz), 23.5 (CH_2 allyl), 27.4 (CH_3-Py), 30.2 (CH_2 allyl), 32.3 (CH_2 allyl), 66.4 (d, CH allyl trans to N, J_{C-P}= 8.5 Hz), 78.2 (d, CH-O, J_{C-P}= 9.4 Hz), 110.2 (d, CH allyl trans to P, J_{C-P}= 37.8 Hz), 111.2 (d, CH allyl central, J_{C-P}= 7.9 Hz), 121-164 (aromatic carbons). Anal. calcd (%) for $C_{40}H_{47}BF_4NO_3PPdSi_2$: C 55.21, H 5.44, N 1.61; found: C 55.28, H 5.47, N 1.56.

[Pd(η³-1,3-cyclohexenylallyl)(L39a)]BF₄ (32). Isomer **A** (30%): ^{31}P NMR (CD_2Cl_2, 298 K), δ: 140.0 (s, 1P). ^{1}H NMR(CD_2Cl_2, 298 K), δ: 1.19 (s, 9H, CH_3, ^{t}Bu), 1.35 (s, 9H, CH_3, ^{t}Bu), 1.39 (s, 9H, CH_3, ^{t}Bu), 1.55 (s, 9H, CH_3, ^{t}Bu), 1.93 (d, 3H, CH_3, $^3J_{H-H}$= 6.4 Hz), 2.05 (m, 4H, CH_2 allyl), 2.21 (m, 2H, CH_2 allyl), 2.79 (s, 3H, CH_3-Py), 5.15 (m, 1H, CH allyl trans to N), 5.77 (m, 1H, CH-O), 5.95 (m, 1H, CH allyl central), 6.34 (m, 1H, CH allyl trans to P), 7.2-8.2 (m, 7H, CH=). ^{13}C NMR (C_6D_6, 298 K), δ: 18.0 (d, CH_3, J_{C-P}= 10.1 Hz), 21.0 (CH_2 allyl), 27.3 (CH_3-Py), 28.3 (CH_2 allyl), 28.4 (CH_2 allyl), 28.5 (CH_2 allyl), 30.0-31.2 (CH_3, ^{t}Bu), 34.6-35.6 (C, ^{t}Bu), 72.9 (d, CH allyl trans to N, J_{C-P}= 10.7 Hz), 77.0 (d, CH-O, J_{C-P}= 11.4 Hz), 104.3 (d, CH allyl trans to P, J_{C-P}= 40.1 Hz), 112.7 (d, CH allyl central, J_{C-P}= 21.8 Hz), 120-164 (aromatic carbons). Isomer **B** (70%): ^{31}P NMR (CD_2Cl_2, 298 K), δ: 146.6 (s, 1P). ^{1}H NMR(CD_2Cl_2, 298 K), δ: 1.27 (s, 9H, CH_3, ^{t}Bu), 1.37 (s, 18H, CH_3, ^{t}Bu), 1.51 (s, 9H, CH_3, ^{t}Bu), 1.86 (d, 3H, CH_3, $^3J_{H-H}$= 6.4 Hz), 2.05 (m, 4H, CH_2 allyl), 2.21 (m, 2H, CH_2 allyl), 2.84 (s, 3H, CH_3-Py), 5.31 (m, 1H, CH allyl trans to N), 5.74 (m, 1H, CH allyl central), 5.95 (m, 1H, CH-O), 6.62 (m, 1H, CH allyl trans to P), 7.2-8.2 (m, 7H, CH=). ^{13}C NMR (C_6D_6, 298 K), δ: 18.2 (d, CH_3, J_{C-P}= 11.5 Hz), 28.6 (CH_3-Py), 29.1 (CH_2 allyl), 29.3 (CH_2 allyl), 29.4 (CH_2 allyl), 30.0-31.2 (CH_3, ^{t}Bu), 34.6-35.6 (C, ^{t}Bu), 70.0 (d, CH allyl trans to N, J_{C-P}= 9.9 Hz), 78.1 (d, CH-O, J_{C-P}= 12.9 Hz), 104.2 (d, CH allyl trans to P, J_{C-P}= 39.4 Hz), 112.4 (d, CH allyl central, J_{C-P}= 21.0 Hz), 120-164 (aromatic carbons). Anal. calcd (%) for $C_{42}H_{59}BF_4NO_3PPd$: C 59.34, H 7.00, N 1.65; found: C 59.37, H 7.03, N 1.59.

4.4.5.3. Study of the reactivity of the [Pd(η³-allyl)(L))]BF₄ with sodium malonate by in situ NMR[33]

A solution of *in situ* prepared [Pd(η³-allyl)(**L**)]BF_4 (L= phosphite-pyridine, 0.05 mmol) in CD_2Cl_2 (1 mL) was cooled in the NMR at -80 °C. At this temperature, a solution of cooled sodium

malonate (0.1 mmol) was added. The reaction was then followed by ^{31}P NMR. The relative reaction rates were calculated using a capillary containing a solution of triphenylphosphine in CD_2Cl_2 as external standard.

4.4.5.4. Typical procedure for the allylic alkylation of disubstituted linear (S1 and S2) and cyclic (S3-S5) substrates

A degassed solution of $[PdCl(\eta^3\text{-}C_3H_5)]_2$ (0.9 mg, 0.0025 mmol) and the corresponding phosphite-pyridine (0.0055 mmol) in dichloromethane (0.5 mL) was stirred for 30 min. Subsequently, a solution of the corresponding substrate (0.5 mmol) in dichloromethane (1.5 mL), nucleophile (1.5 mmol), *N*,*O*-bis(trimethylsilyl)-acetamide (370 μL, 1.5 mmol) and a pinch of the corresponding base were added. The reaction mixture was stirred at room temperature. After the desired reaction time the reaction mixture was diluted with Et_2O (5 mL) and saturated NH_4Cl (aq) (25 mL) was added. The mixture was extracted with Et_2O (3 x 10 mL) and the extract dried over $MgSO_4$. Conversion and enantiomeric excesses were measured as described in Chapter 4.2.

4.4.5.5. Typical procedure for the allylic alkylation of 1,3,3-trisubstituted substrates (S6 and S7)

A degassed solution of $[PdCl(\eta^3\text{-}C_3H_5)]_2$ (1.8 mg, 0.005 mmol) and the corresponding phosphite-pyridine (0.011 mmol) in dichloromethane (0.5 mL) was stirred for 30 min at room temperature. Subsequently, a solution of substrate (0.5 mmol) in dichloromethane (1.5 mL), dimethyl malonate (171 μL, 1.5 mmol), *N*,*O*-bis(trimethylsilyl)-acetamide (370 μL, 1.5 mmol) and a pinch of KOAc were added. After 2 hours at room temperature, the reaction mixture was diluted with Et_2O (5 mL) and saturated NH_4Cl (aq) (25 mL) was added. The mixture was extracted with Et_2O (3 x 10 mL) and the extract dried over $MgSO_4$. Conversion and enantiomeric excesses were measured as described in Chapter 4.2.

4.4.5.6. Typical procedure for the allylic amination of disubstituted linear substrates S1 and S2

A degassed solution of $[PdCl(\eta^3\text{-}C_3H_5)]_2$ (0.9 mg, 0.0025 mmol) and the corresponding phosphite-pyridine (0.0055 mmol) in dichloromethane (0.5 mL) was stirred for 30 min. Subsequently, a solution of the corresponding substrate (0.5 mmol) in dichloromethane (1.5 mL) and benzylamine (131 μL, 1.5 mmol) were added. The reaction mixture was stirred at room temperature. After the desired reaction time, the reaction mixture was diluted with Et_2O (5 mL) and saturated NH_4Cl (aq) (25 mL) was added. The mixture was extracted with Et_2O (3 x 10 mL) and the extract dried over $MgSO_4$. For substrate **S1**, conversion and enantiomeric excess was determined as described in Chapter 4.3. For substrate **S2**, conversion and enantiomeric excess was determined by GC.[34]

4.4.5.7. Typical procedure for the allylic etherification of disubstituted linear substrate S1

A degassed solution of $[PdCl(\eta^3\text{-}C_3H_5)]_2$ (0.9 mg, 0.0025 mmol) and the corresponding phosphite-pyridine (0.0055 mmol) in dichloromethane (0.5 mL) was stirred for 30 min.

Subsequently, a solution of the corresponding substrate (31.5 mg, 0.125 mmol) in dichloromethane (1.5 mL) was added. After 10 minutes, Cs_2CO_3 (122 mg, 0.375 mmol) and benzyl alcohol (40 μL, 0.375 mmol) were added. The reaction mixture was stirred at room temperature. After the desired reaction time, the reaction mixture was diluted with Et_2O (5 mL) and saturated NH_4Cl (aq) (25 mL) was added. The mixture was extracted with Et_2O (3 x 10 mL) and the extract dried over $MgSO_4$. Conversion was measured by ^{1}H-NMR. HPLC was used to determine the ee (Chiralcel OJ, 98% 2-propanol/hexane, flow 0.75 mL/min). A sample was filtered over silica using 10% Et_2O/hexane mixture as the eluent.[15i]

4.4.6. Acknowledgements

We would like to thank the Spanish Government for providing grant CTQ2010-15835, the Catalan Government for grant 2009SGR116, and the ICREA Foundation for providing M. Diéguez and O. Pàmies with financial support through the ICREA Academia awards.

4.4.7. References

[1] a) *Asymmetric Catalysis in Industrial Scale: Challenges, Approaches and Solutions*; Blaser, H. U, Schmidt, E., Eds.; Wiley: Weinheim, 2003. b) *Comprehensive Asymmetric Catalysis*; Jacobsen, E. N., Pfaltz, A., Yamamoto, H., Eds.; Springer-Verlag: Berlin, 1999. c) *Asymmetric Catalysis in Organic Synthesis*; Noyori, R., Ed.; Wiley: New York, 1994. d) *Applied Homogeneous Catalysis with Organometallics Compounds*, 2nd ed.; Cornils, B., Hermann, W. A., Eds.; Wiley-VCH: Wienhein, 2002. e) *Catalytic Asymmetric Synthesis;* Ojima, I., Ed.; Wiley: New Jersey:, 2010.

[2] For reviews, see: a) *Palladium Reagents and Catalysis, Innovations in Organic Synthesis*; Tsuji, J., Ed.; Wiley: New York, 1995. b) Trost, B. M.; van Vranken, D. L. *Chem. Rev.* **1996**, *96*, 395. c) Johannsen, M.; Jorgensen, K. A. *Chem. Rev.* **1998**, *98*, 1689. d) Pfaltz, A.; Lautens, M. in *Comprehensive Asymmetric Catalysis*; Jacobsen, E. N., Pfaltz, A., Yamamoto, H., Eds.; Springer-Verlag: Berlin, 1999; Vol. 2, Chapter 24. e) Helmchen, G.; Pfaltz, A. *Acc. Chem. Res.* **2000**, *33*, 336. f) Masdeu-Bultó, A. M.; Diéguez, M.; Martín, E.; Gómez, M. *Coord. Chem. Rev.* **2003**, *242*, 159. g) Trost, B. M.; Crawley, M. L. *Chem. Rev.* **2003**, *103*, 2921. h) Martín, E.; Diéguez, M. *C. R. Chemie* **2007**, *10*, 188. i) Lu, Z.; Ma, S. *Angew. Chem. Int. Ed.* **2008**, *47*, 258.

[3] a) Hayashi, T.; Yamamoto, A.; Hagihara, T.; Ito, Y. *Tetrahedron Lett.* **1986**, *27*, 191. b) Recently this concept has also been use to explain the chiral induction by the Trost ligand, see: Butts, C. P.; Filali, E.; Lloyd-Jones, G. C.; Norrby, P. O.; Sale, D. A.; Schramm, Y. *J. Am. Chem. Soc.* **2009**, *131*, 9945.

[4] See, for example: (a) Trost, B. M.; Bunt, R. C. *J. Am. Chem. Soc.* **1994**, *116*, 4089. (b) Trost, B. M.; Krueger, A. C.; Bunt, R. C.; Zambrano, J. *J. Am. Chem. Soc*. **1996**, *118*, 6520.

[5] See, for instance: (a) Dawson, G. J.; Frost, C. G.; Williams, J. M. J. *Tetrahedron Lett.* **1993**, *34*, 3149. (b) von Matt, P.; Pfaltz, A. *Angew. Chem. Int. Ed. Engl.* **1993**, *32*, 566. (c) Sennhenn, P.; Gabler, B.; Helmchen, G. *Tetrahedron Lett.* **1994**, *35*, 8595.

[6] See, for instance: a) Pàmies, O.; Diéguez, M. *Acc. Chem. Res.* **2010**, *43*, 212. b) van Leeuwen, P. W. N. M.; Kamer, P. C. J.; Claver, C.; Pàmies, O.; Diéguez, M. *Chem. Rev.* **2011**, *111*, 2077.

[7] The flexibility that the biaryl moiety offers can be used to fine-tune the chiral pocket formed upon complexation. See, for example: a) Pàmies, O.; Diéguez, M.; Claver, C. *J. Am. Chem. Soc.*

2005, *127*, 3646. b) Mata, Y.; Diéguez, M.; Pàmies, O.; Claver, C. *Adv. Synth. Catal.* **2005**, *347*, 1943.

[8] See for example: a) Jin, M. –J.; Jung, J. –A.; Kim, S. –H. *Tetrahedron Lett.* **1999**, *40*, 5197. b) Okuyama, Y.; Nakano, H.; Hongo, H. *Tetrahedron: Asymmetry* **2000**, *11*, 1193. c) Mino, T.; Tanaka, Y.; Akita, K.; Sakamoto, M.; Fujita, T. *Heterocycles* **2003**, *60*, 9. d) Mino, T.; Hata, S.; Ohtaka, K.; Salamoto, M.; Fujita, T. *Tetrahedron Lett*. **2001**, *42* 4837. e) Jin, M.-J.; Kim, S.-H.; Lee, S.-J.; Kim, Y.-M. *Tetrahedron Lett*. **2002**, *43*, 7409. f) Lee, E.-K.; Kim, S.-H.; Jung, B.-H.; Ahn, W.-S.; Kim, G.-J. *Tetrahedron Lett.* **2003**, *44*, 1971. g) Tanaka, Y.; Mino, T.; Akita, K.; Sakamoto, M.; Fujita, T. *J. Org. Chem.* **2004**, *69*, 6679. h) Kubota, H.; Koga, K. *Heterocycles* **1996**, *42*, 543. i) Widhalm, M.; Nettekoven, U.; Kalchhauser, H.; Mereiter, K.; Calhorda, M. J.; Félix, V. *Organometallics* **2002**, *21*, 315. j) Vasse, J.-L.; Stranne, R.; Zalubovskis, R.; Gayet, C.; Moberg, C. *J. Org. Chem*. **2003**, *68*, 3258. l) Chen, G.; Li, X.; Zhang, H.; Gong, L.; Mi, A.; Cui, X.; Jiang, Y.; Choi, M. C. K.; Chan, A. S. C. *Tetrahedron: Asymmetry* **2002**, *13*, 809. m) Braga, A. L.; Sehnem, J. A.; Lüdtke, D. S.; Zeni, G.; Silveira, C. C.; Marchi, M. I. *Synlett* **2005**, 1331. n) Sun, X.-M.; Koizumi, M.; Manabe, K.; Kobayashi, S. *Adv. Synth. Catal*. **2005**, *347*, 1893.

[9] See for example: a) Jang, H. –Y.; Seo, H.; Han, J. W.; Chung, Y. K. *Tetrahedron Lett* **2000**, *41*, 5083. b) Lee, J. H.; Son, S. U.; Chung, Y. K. *Tetrahedron: Asymmetry* **2003**, *14*, 2109. c) Hu, X.; Dai, H.; Hu, X.; Chen, H.; Wang, J.; Bai, C.; Zheng, Z. *Tetrahedron: Asymmetry* **2002**, *13*, 1687. d) Hu, X.; Dai, H.; Chen, H.; Wang, J.; Bai, C.; Zheng, Z. *Tetrahedron: Asymmetry* **2004**, *15*, 1065. e) Thiesen, K. E.; Maitra, K.; Olmstead, M. M.; Attar, S. *Organometallics* **2010**, *29*, 6334. f) Tsarev, V. N.; Lyubimov, S. E.; Bondarev, O. G.; Korlyukov, A.; Antipin, M. Y.; Pretovskii, P. V.; Davankov, V. A.; Shiryaev, A. A.; Benetsky, E. B.; Vologzhanin, P. A.; Gavrilov, K. N. *Eur. J. Org. Chem.* **2005**, 2097.

[10] Mazuela, J.; Paptchikhine, A.; Tolstoy, P.; Pàmies, O.; Diéguez, M.; Andersson, P. G. *Chem. Eur. J*. **2010**, *16*, 620.

[11] See for instance: a) Bunlaksananusorn, T.; Luna, A. P.; Bonin, M.; Micouin, L.; Knochel, P. *Synlett* **2003**, 2240. b) Ito, K.; Kashiwagi, R.; Iwsaki, K.; Katsuki, T. *Synlett* **1999**, 1563. c) Goldfuss, B.; Löschmann, T.; Rominger, F. *Chem. Eur. J.* **2004**, *10*, 5422. d) Liu, Q.-B.; Zhou, Y.-G. *Tetrahedron Lett.* **2007**, *48*, 2101. e) Meng, X.; Gao, Y.; Li, X.; Xu, D. *Cat. Commun.* **2009**, *10*, 950. f) Leca, F.; Fernández, F.; Muller, G.; Lescop, C.; Réau, R.; Gómez, M. *Eur. J. Inorg. Chem.* **2009**, 5583.

[12] Measured after 20% conversion approximately.

[13] The rapid ring inversions (tropoisomerization) in the biaryl phosphite moiety is usually stopped upon coordination to the metal center. See for example: a) Buisman, G. J. H.; van der Veen, L. A.; Klootwijk, A.; de Lange, W. G. J.; Kamer, P. C. J.; van Leeuwen, P. W. N. M.; Vogt, D. *Organometallics* **1997**, *16*, 2929. b) Diéguez, M.; Pàmies, O.; Ruiz, A.; Claver, C.; Castillón, S. *Chem. Eur. J.* **2001**, *7*, 3086. c) Pàmies, O.; Diéguez, M.; Net, G.; Ruiz, A.; Claver, C. *Organometallics* **2000**, *19*, 1488. d) Pàmies, O.; Diéguez, M.; Net, G.; Ruiz, A.; Claver, C. *J. Org. Chem.* **2001**, *66*, 8364. e) Pàmies, O.; Diéguez, M. *Chem. Eur. J.* **2008**, *14*, 944. f) Mazuela, J.; Norrby, P.-O.; Andersson, P. G.; Pàmies, O.; Diéguez, M. *J. Am. Chem. Soc.* **2011**, *133*, 13634.

[14] *Dictionary of Natural Products*; Buckingham, J., Ed.; Cambridge University Press.: Cambridge, 1994.

[15] For successful applications, see: a) Trost, B. M.; Shen, H. C.; Dong, L.; Surivet, J.-P. *J. Am. Chem. Soc.* **2003**, *125*, 9276. b) Trost, B. M.; Toste, F. D. *J. Am. Chem. Soc.* **1998**, *120*, 815; c) Trost, B. M.; Toste, F. D. *J. Am. Chem. Soc.* **1999**, *121*, 4545; d) Trost, B. M.; Toste, F. D. *J. Am. Chem. Soc.* **2000**, *122*, 11262; e) Haight, A. R.; Stoner, E. J.; Peterson, M. J.; Grover, V. K. *J. Org.*

Chem. **2003**, *68*, 8092; f) Uozumi, Y.; Kimura, M. *Tetrahedron: Asymmetry* **2006**, *17*, 161; g) Tietze, L. F.; Lohmann, J. K.; Stadler, C. *Synlett* **2004**, 1113; h) Iourtchenko, A.; Sinou, D. *J. Mol. Catal. A* **1997**, *122*, 91. i) Lam, F. L.; Au Yeung, T. T.-L.; Kwong, F. Y.; Zhou, Z.; Wong, K. Y.; Chan, A. S. C. *Angew. Chem. Int. Ed.* **2008**, *47*, 1280.

[16] For successful applications of Ir-catalysts with phenols, see: a) Shu, C.; Hartwig, J. F. *Angew. Chem. Int. Ed.* **2004**, *43*, 4794. b) Fischer, C.; Defieber, C.; Suzuki, T.; Carreira, E. M. *J. Am. Chem. Soc.* **2004**, *126*, 1628; c) Lopez, F.; Ohmura, T.; Hartwig, J. F. *J. Am. Chem. Soc.* **2003**, *125*, 3426. d) Lyothier, I.; Defieber, C.; Carreira, E. M. *Angew. Chem. Int. Ed.* **2006**, *45*, 6204. e) Welter, C.; Dahnz, A.; Brunner, B.; Streiff, S.; Dubon, P.; Helmchen, G. *Org. Lett.* **2005**, *7*, 1239. f) Kimura, M.; Uozumi, Y. *J. Org. Chem.* **2007**, *72*, 707.

[17] See, for instance: (a) Sudo, A.; Saigo, K. *J. Org. Chem.* **1997**, 62, 5508. (b) Dawson, G. J.; Williams, J. M. J.; Coote, S. J. *Tetrahedron: Asymmetry* **1995**, 6, 2535. (c) Martin, C. J.; Rawson, D. J.; Williams, J. M. J. *Tetrahedron: Asymmetry* **1998**, 9, 3723.

[18] For successful applications, see also: (a) Dawson, G. J.; Williams, J. M. J.; Coote, S. J. *Tetrahedron Lett.* **1995**, *36*, 461. (b) Evans, D. A.; Campos, K. R.; Tedrow, J. S.; Michael, F. E.; Gagné, M. R. *J. Am. Chem. Soc.* **2000**, *122*, 7905. (c) Popa, D.; Puigjaner, C.; Gomez, M.; Benet-Buchholz, J.; Vidal-Ferran, A.; Pericas, M. A. *Adv. Synth. Cat.* **2007**, *349*, 2265.

[19] Schäffner, B.; Schäffner, F.; Verevkin, S. P.; Börner, A. *Chem. Rev.* **2010**, *110*, 4554.

[20] Schäffner, B.; Holz, J.; Verevkin, S. P.; Börner, A. *ChemSusChem* **2008**, *1*, 249.

[21] *Ionic Liquids in Synthesis*; Wasserscheid, P., Welton, T., Eds.; Wiley-VCH: Weinheim, Germany, 2003.

[22] a) Benessere, V.; Lega, M.; Silipo, A.; Ruffo, F. *Tetrahedron* **2011**, *67*, 4826. b) Castillo, M. R.; Castillón, S.; Claver, C.; Fraile, J. M.; Gual, A.; Martín, M.; Mayoral, J. A.; Sola, E. *Tetrahedron* **2011**, *67*, 5402. c) Favier, I.; Castillo, A. B.; Godard, C.; Castillón, S.; Claver, C.; Gómez, M.; Teuma, E. *Chem. Commun.* **2011**, *47*, 7869.

[23] Ross, J.; Xiao, J. *Chem. Eur. J.* **2003**, *9*, 4900; b) Cammarata, L.; Kazarian, S. G.; Salter, P. A.; Welton, T. *Phys. Chem. Chem. Phys.* **2001**, *3*, 5192.

[24] This behavior has been previously observed using NPN ligands, see ref 22b.

[25] (a) Deerenberg, S.; Schrekker, H. S.; van Strijdonck, G. P. F.; Kamer, P. C. J.; van Leeuwen, P. W. N. M.; Fraanje, J.; Goubitz, K. *J. Org. Chem.* **2000**, *65*, 4810. (b) Fernández, F.; Gómez, M.; Jansat, S.; Muller, G.; Martín, E.; Flores Santos, L.; García, P. X.; Acosta, A.; Aghmiz, A.; Jiménez-Pedrós, M.; Masdeu-Bultó, A. M.; Diéguez, M.; Claver, C.; Maestro, M. A. *Organometallics* **2005**, *24*, 3946.

[26] The equilibrium between the two diastereoisomers takes place via the so-called apparent π-allyl rotation. This has been shown to occur via dissociation of one of the coordinated atoms of the bidentate ligand, which allows the ligand to rotate. See: Gogoll, A.; Örnebro, J.; Grennberg, H.; Bäckvall, J. E. *J. Am. Chem. Soc.* **1994**, *116*, 3631.

[27] Pericás, M. A.; Puigjaner, C.; Riera, A.; Vidal-Ferran, A.; Gómez, A.; Jiménez, F.; Muller, G.; Rocamora, M. *Chem. Eur. J.* **2002**, *8*, 4164.

[28] This was confirmed by an in situ NMR spectroscopic study of the reactivity of the Pd intermediates with sodium malonate at low temperature. This study indicated that isomer **30A** reacts approximately 10 times faster than isomer **30B**.

[29] a) Auburn, P. R.; Mackenzie, P. B.; Bosnich, B. *J. Am. Chem. Soc.* **1985**, *107*, 2033. b) Jia, C.; Müller, P.; Mimoun, H. *J. Mol. Cat. A: Chem.* **1995**, *101*, 127. c) Lehman, J.; Lloyd-Jones, G. C. *Tetrahedron* **1995**, *51*, 8863. d) Hayashi, T.; Yamamoto, A.; Ito, Y.; Nishioka, E.; Miura, H.; Yanagi, K. *J. Am. Chem. Soc.* **1989**, *111*, 6301.

[30] von Matt, P.; Lloyd-Jones, G. C.; Minidis, A. B. E.; Pfaltz, A.; Macko, L.; Neuburger, M.; Zehnder, M.; Ruegger, H.; Pregosin, P. S. *Helv. Chim. Acta* **1995**, *78*, 265.
[31] Kollmar, M.; Goldfuss, B.; Reggelin, M.; Rominger, F.; Helmchen, G. *Chem. Eur. J.* **2001**, *7*, 4913.
[32] Trost, B. M.; Strege, P. E.; Weber, L. *J. Am. Chem. Soc.* **1978**, *11*, 3407.
[33] van Haaren, R. J.; Keeven, P. H.; van der Veen, L. A.; Goubitz, K.; van Strijdonck, G. P. F.; Oevering, H.; Reek, J. N. H.; Kamer, P. C. J.; van Leeuwen, P. W: N. M. *Inorg. Chim. Acta* **2002**, *327*, 108.
[34] Evans, D. A.; Campos, K. R.; Tedrow, J. S.; Michael, F. E.; Gagné, M. R. *J. Am. Chem. Soc.* **2000**, *122*, 7905.

4.4.8. Supporting information

Table 4.4.8. Selected results for the Pd-catalyzed allylic substitution of **S1** with dimethyl malonate using ligands **L38a** and **L39a.** Effect of the solvent and ligand-to-palladium ratio[a]

Entry	Ligand	Solvent	L/Pd ratio	% Conv (t/h)[b]	% ee[c]
1	**L38a**	THF	1	100 (0.5)	23 (*S*)
2	**L38a**	CH_2Cl_2	1	100 (0.5)	32 (*S*)
3	**L38a**	Toluene	1	85 (0.5)	19 (*S*)
4	**L39a**	THF	1	100 (0.5)	21 (*S*)
5	**L39a**	CH_2Cl_2	1	100 (0.5)	26 (*S*)
6	**L39a**	Toluene	1	90 (0.5)	16 (*S*)
8	**L38a**	CH_2Cl_2	0.75	100 (0.5)	32 (*S*)
9	**L38a**	CH_2Cl_2	2	100 (0.5)	31 (*S*)
10	**L39a**	CH_2Cl_2	0.75	100 (0.5)	26 (*S*)
11	**L39a**	CH_2Cl_2	2	100 (0.5)	24 (*S*)

[a] All reactions were run at 23 ºC. 0.5 mol% $[PdCl(\eta^3\text{-}C_3H_5)]_2$. [b] Conversion measured by ^{1}H-NMR. Reaction time shown in parentheses. [c] Enantiomeric excesses measured by HPLC. Absolute configuration shown in parentheses.

Table 4.4.9. Results for the Pd-catalyzed allylic substitution of **S1** with several nucleophiles using the ligand library **L38-L49a-g**[a]

Entry	Ligand	Nucleophile	% ee[b]	Entry	Ligand	Nucleophile	% ee[b]
1	**L38a**	$CH_2(COOEt)_2$	31 (*S*)	24	**L46f**	$CH_2(COMe)_2$	91 (*R*)
2	**L38d**	$CH_2(COOEt)_2$	17 (*S*)	25	**L38a**	$CHMe(COOEt)_2$	34 (*R*)
3	**L38e**	$CH_2(COOEt)_2$	57 (*S*)	26	**L38g**	$CHMe(COOEt)_2$	99 (*R*)
4	**L38f**	$CH_2(COOEt)_2$	21 (*S*)	27	**L39a**	$CHMe(COOEt)_2$	27 (*R*)
5	**L38g**	$CH_2(COOEt)_2$	89 (*S*)	28	**L41a**	$CHMe(COOEt)_2$	19 (*R*)
6	**L39a**	$CH_2(COOEt)_2$	25 (*S*)	29	**L42a**	$CHMe(COOEt)_2$	2 (*S*)
7	**L41a**	$CH_2(COOEt)_2$	28 (*S*)	30	**L43a**	$CHMe(COOEt)_2$	14 (*R*)
8	**L42a**	$CH_2(COOEt)_2$	13 (*S*)	31	**L46f**	$CHMe(COOEt)_2$	98 (*S*)
9	**L43a**	$CH_2(COOEt)_2$	24 (*S*)	32	**L38a**	$CHallyl(COOEt)_2$	29 (*R*)
10	**L46f**	$CH_2(COOEt)_2$	89 (*R*)	33	**L38g**	$CHallyl(COOEt)_2$	80 (*R*)
11	**L38a**	$CH_2(COOBn)_2$	37 (*R*)	34	**L39a**	$CHallyl(COOEt)_2$	24 (*R*)
12	**L38g**	$CH_2(COOBn)_2$	93 (*R*)	35	**L41a**	$CHallyl(COOEt)_2$	23 (*R*)
13	**L39a**	$CH_2(COOBn)_2$	33 (*R*)	36	**L42a**	$CHallyl(COOEt)_2$	6 (*R*)
14	**L41a**	$CH_2(COOBn)_2$	29 (*R*)	37	**L43a**	$CHallyl(COOEt)_2$	21 (*R*)
15	**L42a**	$CH_2(COOBn)_2$	11 (*R*)	38	**L36f**	$CHallyl(COOEt)_2$	79 (*S*)
16	**L43a**	$CH_2(COOBn)_2$	26 (*R*)	39	**L38a**	$BnNH_2$	31 (*R*)
17	**L46f**	$CH_2(COOBn)_2$	92 (*S*)	40	**L38g**	$BnNH_2$	89 (*R*)
18	**L38a**	$CH_2(COMe)_2$	29 (*S*)	41	**L39a**	$BnNH_2$	23 (*R*)
19	**L38g**	$CH_2(COMe)_2$	91 (*S*)	42	**L41a**	$BnNH_2$	26 (*R*)
20	**L39a**	$CH_2(COMe)_2$	25 (*S*)	43	**L42a**	$BnNH_2$	16 (*R*)
21	**L41a**	$CH_2(COMe)_2$	19 (*S*)	44	**L43a**	$BnNH_2$	29 (*R*)
22	**L42a**	$CH_2(COMe)_2$	2 (*S*)	45	**L46f**	$BnNH_2$	89 (*S*)
23	**L43a**	$CH_2(COMe)_2$	18 (*S*)				

[a] All reactions were run at 23 ºC. Full conversions were measured in all cases. [b] Enantiomeric excesses measured by HPLC. Absolute configuration shown in parentheses.

Table 4.4.10. Results for the Pd-catalyzed allylic substitution of **S2** with several nucleophiles using the ligand library **L38-L49a-g**[a]

Entry	Ligand	Nucleophile	% ee[b]	Entry	Ligand	Nucleophile	% ee[b]
1	**L38a**	$CH_2(COOBn)_2$	38 (-)	16	**L41a**	$CHMe(COOEt)_2$	28 (-)
2	**L39a**	$CH_2(COOBn)_2$	44 (-)	17	**L43a**	$CHMe(COOEt)_2$	27 (-)
3	**L39g**	$CH_2(COOBn)_2$	75 (-)	18	**L47f**	$CHMe(COOEt)_2$	72 (+)
4	**L41a**	$CH_2(COOBn)_2$	29 (-)	19	**L38a**	$CHallyl(COOEt)_2$	32 (+)
5	**L43a**	$CH_2(COOBn)_2$	28 (-)	20	**L39a**	$CHallyl(COOEt)_2$	49 (+)
6	**L47f**	$CH_2(COOBn)_2$	74 (+)	21	**L39g**	$CHallyl(COOEt)_2$	71 (+)
7	**L38a**	$CH_2(COMe)_2$	32 (-)	22	**L41a**	$CHallyl(COOEt)_2$	25 (+)
8	**L39a**	$CH_2(COMe)_2$	42 (-)	23	**L43a**	$CHallyl(COOEt)_2$	28 (+)
9	**L39g**	$CH_2(COMe)_2$	62 (-)	24	**L47f**	$CHallyl(COOEt)_2$	72 (-)
10	**L41a**	$CH_2(COMe)_2$	31 (-)	25	**L38a**	$BnNH_2$	37 (*S*)
11	**L43a**	$CH_2(COMe)_2$	22 (-)	26	**L39a**	$BnNH_2$	45 (*S*)
12	**L47f**	$CH_2(COMe)_2$	62 (+)	27	**L39g**	$BnNH_2$	82 (*S*)
13	**L38a**	$CHMe(COOEt)_2$	34 (-)	28	**L41a**	$BnNH_2$	29 (*S*)
14	**L39a**	$CHMe(COOEt)_2$	51 (-)	29	**L43a**	$BnNH_2$	33 (*S*)
15	**L39g**	$CHMe(COOEt)_2$	73 (-)	30	**L47f**	$BnNH_2$	81(*R*)

[a] All reactions were run at 23 ºC. Full conversions were measured in all cases. [b] Enantiomeric excesses measured by HPLC or GC. Absolute configuration or optical rotation shown in parentheses.

Table 4.4.11. Results for the Pd-catalyzed allylic substitution of **S3** with several nucleophiles using the ligand library **L38-L49a-g**[a]

Entry	Ligand	Nucleophile	% ee[b]	Entry	Ligand	Nucleophile	% ee[b]
1	**L38a**	$CH_2(COOEt)_2$	21 (-)	16	**L41a**	$CH_2(COMe)_2$	17 (-)
2	**L38g**	$CH_2(COOEt)_2$	86 (-)	17	**L43a**	$CH_2(COMe)_2$	7 (-)
3	**L39a**	$CH_2(COOEt)_2$	25 (-)	18	**L46f**	$CH_2(COMe)_2$	60 (+)
4	**L41a**	$CH_2(COOEt)_2$	19 (-)	19	**L38a**	$CHMe(COOEt)_2$	17 (+)
5	**L43a**	$CH_2(COOEt)_2$	4 (+)	20	**L38g**	$CHMe(COOEt)_2$	84 (+)
6	**L46f**	$CH_2(COOEt)_2$	85 (+)	21	**L39a**	$CHMe(COOEt)_2$	14 (+)
7	**L38a**	$CH_2(COOBn)_2$	26 (+)	22	**L41a**	$CHMe(COOEt)_2$	22 (+)
8	**L38g**	$CH_2(COOBn)_2$	91 (+)	23	**L43a**	$CHMe(COOEt)_2$	2 (+)
9	**L39a**	$CH_2(COOBn)_2$	31 (+)	24	**L46f**	$CHMe(COOEt)_2$	83 (-)
10	**L41a**	$CH_2(COOBn)_2$	18 (+)	25	**L38a**	$CHallyl(COOEt)_2$	24 (+)
11	**L43a**	$CH_2(COOBn)_2$	2 (+)	26	**L38g**	$CHallyl(COOEt)_2$	94 (+)
12	**L46f**	$CH_2(COOBn)_2$	90 (-)	27	**L39a**	$CHallyl(COOEt)_2$	16 (+)
13	**L38a**	$CH_2(COMe)_2$	23 (-)	28	**L41a**	$CHallyl(COOEt)_2$	19 (+)
14	**L38g**	$CH_2(COMe)_2$	62 (-)	29	**L43a**	$CHallyl(COOEt)_2$	9 (+)
15	**L39a**	$CH_2(COMe)_2$	21 (-)	30	**L46f**	$CHallyl(COOEt)_2$	93 (-)

[a] All reactions were run at 23 ºC. Full conversions were measured in all cases. [b] Enantiomeric excesses measured by HPLC or GC. Absolute configuration or optical rotation shown in parentheses.

Chapter 5

Asymmetric Heck reaction

5. Asymmetric Heck reaction

5.1. Background

Phosphine-oxazoline ligands have emerged as suitable ligands for the intermolecular Heck reaction. Although some of them have provided high regio- and enantioselectivities, there is still a problem of low reaction rates and substrate versatility. We recently discovered that the pyranoside phosphite-oxazoline ligand library **L1**-**L5a**-**k**, previously synthesized in chapter 3, provided excellent activities and selectivities (regio- and enantioselectivities) in the Pd-catalyzed Heck coupling of several substrate types and triflate sources. Despite this success, the use of other phosphite-oxazoline ligands has not yet been reported and a systematic study of the possibilities offered by this ligand class for this process is still needed.

In this chapter, we therefore report the screening of two phosphite-nitrogen ligand libraries for asymmetric Pd-catalyzed intermolecular Heck reaction. More specifically, in section 5.2 we describe the application of a large modular library of readily available phosphite-oxazoline ligands in the Pd-catalyzed Heck reactions of several substrates and triflates under thermal and microwave conditions. This ligand library contains three main ligand structures that have been designed by systematic modifications of one of the most successful ligand family (PHOX) developed for this process. Both enantiomers of the Heck-coupling products were obtained in excellent activities (up to 100% conversion in 10 minutes), and regio- (up to >99%) and enantioselectivities (ee's up to >99%). In microwave irradiation conditions reaction times were considerably shorter (full conversion in a few minutes) and regio- and enantioselectivities were still excellent. These results compete favorably with the most successful ligands that have been developed for this reaction. Interestingly, the results were better than those obtained using pyranoside phosphite-oxazoline ligands **L1**-**L5a**-**k**. In next section 5.3, we report the first successful application of phosphite-oxazole/imidazole ligands in the intermolecular Pd-catalyzed Heck reactions under thermal and microwave conditions. These ligands are more stable than their oxazoline counterparts, less sensitive to air and other oxidizing agents than phosphines and phosphinites, and easy to synthesize from readily available alcohols. Excellent activities (up to 100% conversion in 30 minutes) and regio- (up to >99%) and enantioselectivities (up to 99% ee) were obtained using several triflate sources. The use of microwave irradiation conditions allowed considerably shorter reaction times maintaining excellent regio- and enantioselectivities. In addition, the efficiency of this ligand design is also corroborated by the fact that these Pd-phosphite-oxazole/imidazole catalysts provided higher enantioselectivity than their phosphinite analogues.

5.2. Biaryl phosphite-oxazolines from the chiral pool: Highly efficient modular ligands for the asymmetric Pd-catalyzed Heck reaction

Javier Mazuela, Oscar Pàmies and Montserrat Diéguez in *Chem. Eur. J*. **2010**, *16*, 3434.

5.2.1. Abstract

A highly modular library of readily available phosphite-oxazoline ligands (**L6**-**L26a**-**i**) was successfully applied in the asymmetric Pd-catalyzed Heck reactions of several substrates and triflates under thermal and microwave conditions. This ligand library contains three main ligand structures that have been designed by systematic modifications of one of the most successful ligand families developed for this process. As well as studying the effect of these three ligand structures on the catalytic performance, we also evaluated the effect of modifying several ligand parameters in these ligand structures. We found that their effectiveness at transferring the chiral information in the product can be tuned by correctly choosing the ligand components. Both enantiomers of the Heck-coupling products were obtained in excellent activities (up to 100% conversion in 10 minutes), and regio- (up to >99%) and enantioselectivities (ee's up to >99%). In microwave irradiation conditions reaction times were considerably shorter (full conversion in a few minutes) and regio- and enantioselectivities were still excellent.

5.2.2. Introduction

One of the main objectives in modern synthetic organic chemistry is the catalytic enantioselective formation of C-C bonds. In this respect, the asymmetric Pd-catalysed Heck reaction coupling of an aryl or alkenyl halide or triflate to an alkene is a powerful and highly versatile procedure since it tolerates several functional groups.[1] The bulk of the reported examples involve intramolecular reactions, which have the advantage that the alkene regiochemistry and geometry in the product can be easily controlled. In this respect, chiral bidentate phosphines have turned out to be excellent ligands for this process.[1] Fewer studies, however, have been conducted on the asymmetric intermolecular version. This is mainly because regioselectivity is often a problem. So, for example, in the intermolecular Heck reaction of 2,3-dihydrofuran **S1** with phenyl triflate, a mixture of two products is obtained - the expected product 2-phenyl-2,5-dihydrofuran **1** and 2-phenyl-2,3-dihydrofuran **2** (Scheme 5.2.1). The latter is formed due to an isomerization process.[1]

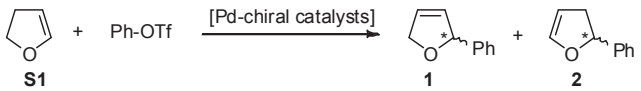

Scheme 5.2.1. Model Pd-catalyzed Heck reaction of 2,3-dihydrofurane **S1**.

In recent years, one class of heterodonor ligands - the phosphine-oxazolines - has emerged as being suitable for the intermolecular Heck reaction (Figure 5.2.1).[2,3] Although some of them have provided high regio- and enantioselectivities, there is still a problem of low reaction rates and

substrate versatility. Therefore, it is very important to develop ligands that induce higher rates and selectivities (regio- and enantioselectivities) on a basis of simple starting materials for several substrate types.

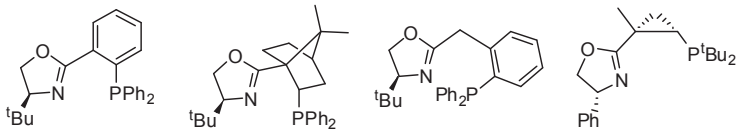

Figure 5.2.1. Privileged phosphine-oxazoline ligands for the Pd-catalyzed intermolecular Heck reaction.

In this context, the presence of biaryl-phosphite moieties in ligand design can be highly advantageous.[4] We recently discovered that a pyranoside phosphite-oxazoline ligand library provided excellent activities and selectivities (regio- and enantioselectivities) in the Pd-catalyzed Heck coupling of several substrate types and triflate sources.[4] Despite this success, the use of other phosphite-oxazoline ligands has not yet been reported and a systematic study of the possibilities offered by this ligand class for this process is still needed. To fully investigate these possibilities, in this paper we extend our previous study of 2007 to other phosphite-oxazoline ligands and to other substrate types. To do so, we synthesized and screened a library of 147 potential phosphite-oxazoline ligands (Figure 5.2.2), which is based on three main ligand structures.

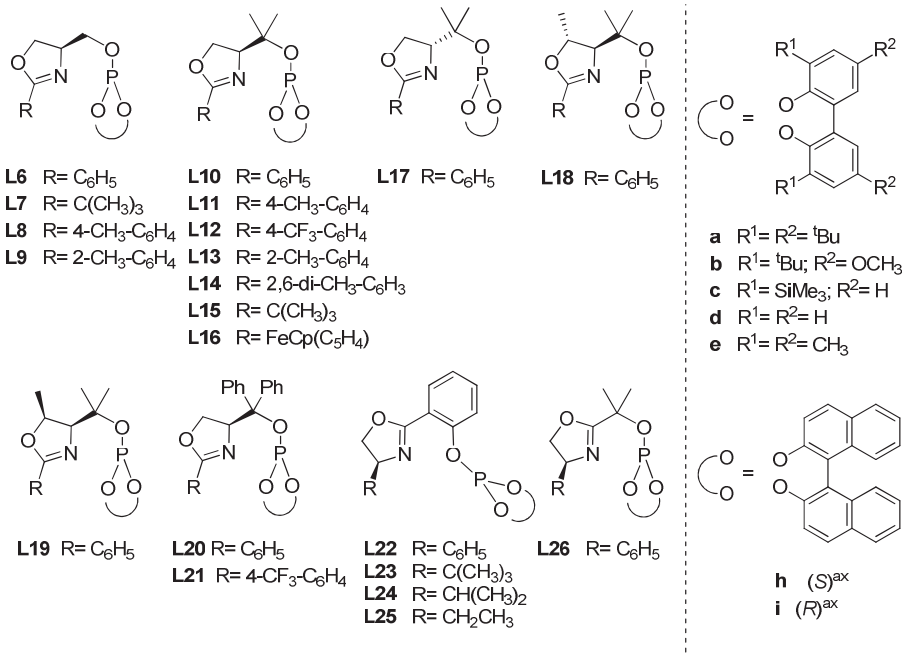

Figure 5.2.2. Phosphite-oxazoline ligand library **L6-L26a-i**.

The first one (ligands **L22**-**L25**)[5] is based on the phosphine-oxazoline PHOX ligands (Figure 5.2.1), in which the phosphine moiety has been replaced by a biaryl phosphite group. In the second one (ligand **L26**), the flat *ortho*-phenylene tether in the previous ligands **L22**-**L25** has been replaced by an alkyl chain. The third one (ligands **L6**-**L21**)[6] is similar to the second one but the alkyl chain is bonded to carbon 4 instead of carbon 2 of the oxazoline moiety, which shifts the chirality from the oxazoline substituent to the alkyl chain.

We also evaluated making systematic modifications to several ligand parameters in these prominent ligand structures, which are known to have an important effect on catalytic performance. Therefore, with this library we investigated the effect of systematically varying the substituents in the oxazoline (R) and the alkyl chain (Me, **L10**-**L16**, H, **L6**-**L9** and Ph, **L20**-**L21**). We also studied the configuration of the alkyl chain (ligands **L10** and **L17**), the presence of a second stereogenic centre in the oxazoline ring and its configuration (ligands **L18** and **L19**), and the substituents and configurations in the biaryl phosphite moiety (**a**-**i**). By carefully selecting these elements, we achieved excellent activities combined with high regio- and enantioselectivities in several substrate types and triflate sources.

5.2.3. Results and discussions

5.2.3.1. Asymmetric Heck reactions under thermal conditions

*Asymmetric Heck reaction of 2,3-dihydrofuran **S1** under thermal conditions*

In this section, we report the use of the chiral phosphite-oxazoline ligand library **L6**-**L26a-i** in the Pd-catalyzed asymmetric Heck reaction of 2,3-dihydrofuran **S1** (Scheme 5.2.1) using several triflates with different electronic and steric properties: phenyl triflate, 1-naphthyl triflate, *para*-toluyl triflate, *para*-nitrophenyl triflate and cyclohexenyl triflate. In all cases, the catalysts were generated *in situ* by mixing $[Pd_2(dba)_3]$·dba with the corresponding chiral ligand.

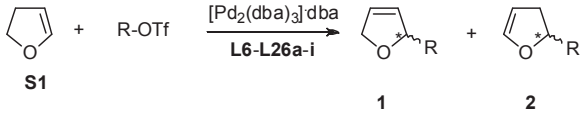

S1 **1** **2**

R= C_6H_5, 1-Naphthyl, *p*-CH_3-C_6H_4, *p*-NO_2-C_6H_4, C_6H_9

Scheme 5.2.2. Pd-catalyzed Heck reaction of 2,3-dihydrofurane **S1**.

In the first set of experiments, we used the palladium-catalyzed asymmetric phenylation of **S1** (Scheme 5.2.2, R= C_6H_5) to study the potential of the phosphite-oxazoline ligand library **L6-L26a-i**. Phenylation of **S1** was chosen because the reaction was performed with a wide range of ligands, which enabled the efficiency of the various ligand systems to be compared directly.[1]

First, we studied the effect of the reaction conditions by conducting a series of experiments with three ligands (**L22a, L26a** and **L10a**) and using different solvents, bases and temperature. We found that the efficiency of the process was strongly dependent on the nature of the solvent, base and temperature (see Supporting Information). The best activity and selectivity (regio- and enantioselectivity) was achieved with THF as solvent, and either diisopropylamine or proton sponge as base at 50 ºC. These optimal conditions were then used to test the catalytic performance of the complete series of ligands. The results are summarized in Table 5.2.1. They

indicate that catalytic performance (activities and selectivities) is affected by the ligand structure, the substituents at the oxazoline and the alkyl chain, the presence of a second stereogenic centre in the oxazoline ring and the substituents/configuration in the biaryl phosphite moiety. In general activities, regio- (up to >99%) and enantioselectivities (ee's up to >99%) were high in the phenylation of **S1**.

The effect of the ligand structure was studied with ligands **L10a**, **L22a** and **L26a**. We found that the regio- and enantioselectivities were best with ligands **L10**, which have a chiral alkyl chain bonded to carbon 4 of the oxazoline ring connecting it to the phosphite moiety (Table 5.2.1, entries 5 vs 23 and 27).

We found that the oxazoline substituents affected both activities and selectivities (Table 5.2.1, entries 5 and 12-17). In general, our results showed that the catalytic performance is highly influenced by the steric properties of the substituents in the oxazoline moiety, while the electronic properties have little effect. Bulky substituents in this position therefore decreased activities, regio- and enantioselectivities (i.e. Ph≈4-R-Ph≈Et>^{i}Pr>^{t}Bu). This contrasts with the oxazoline-substituent effect observed for the vast majority of successful phosphine-oxazoline ligands, whose enantioselectivites are higher when bulky *tert*-butyl groups are present.[2] Interestingly, the introduction of a ferrocenyl substituent has an extremely positive effect on regio- and enantioselectivities, and (*R*)-**1** is provided almost quantitatively in pure enantiomeric form (Table 5.2.1, entry 17).

We studied the effect of the substituents and the configuration of the alkyl chain using ligands **L6a**, **L10a**, **L17a** and **L20a** (Table 5.2.1, entries 1, 5, 18 and 21). Our results show that introducing methyl substituents in this position has an extremely positive effect on activity and enantioselectivity (entries 1 vs 5). Bulkier substituents such as phenyl, however, have an extremely negative effect on activities (entries 5 vs 21). They also show that the sense of the enantioselectivity is governed by the absolute configuration of the alkyl chain (Table 5.2.1, entries 5 vs 18). Both enantiomers of the phenylation product **1** can therefore be accessed in high regio- and enantioselectivity simply by changing the absolute configuration of the alkyl chain.

To study how a second stereogenic centre in the oxazoline and its configuration affect the catalytic performance, we also tested ligands **L18a** and **L19a** (Table 5.2.1, entries 19 and 20). The results show that the configuration of this second stereocentre and the configuration of the alkyl chain have a cooperative effect on enantioselectivity that results in a matched combination for ligand **L19a**, which contains an *S*-configuration at both the second stereocentre and the alkyl chain.

Finally, the effects of the biaryl phosphite moiety were studied using ligands **L10a**-**i** (Table 5.2.1, entries 5-11). These moieties mainly affected activity and regioselectivity while their effect on enantioselectivity was less important. Bulky substituents at the *ortho* positions of the biphenyl moiety therefore increased activities and regioselectivities (i.e. ^{t}Bu≈SiMe$_3$>Me>H) (Table 5.2.1, entries 5-11).

Table 5.2.1. Selected results for the Pd-catalysed enantioselective phenylation of 2,3-dihydrofuran **S1** by using phosphite–oxazoline ligand library **L6**-**L26a**-**i**[a]

Entry	Ligand	% conv (**1**:**2**)[b]	% ee **1**[c]	Entry	Ligand	% conv (**1**:**2**)[b]	% ee **1**[c]
1	**L6a**	61 (94:6)	93 (*R*)	15	**L14a**	100 (95:5)	99 (*R*)
2	**L7a**	6 (64:36)	35 (*R*)	16	**L15a**	13 (95:5)	92 (*R*)
3	**L8a**	36 (92:8)	96 (*R*)	17	**L16a**	99 (>99:<1)	>99 (*R*)
4	**L9a**	79 (88:12)	90 (*R*)	18	**L17a**	92 (96:4)	99 (*S*)
5	**L10a**	94 (96:4)	> 99 (*R*)	19	**L18a**	42 (90:10)	86 (*R*)
6	**L10b**	93 (97:3)	99 (*R*)	20	**L19a**	85 (96:4)	96 (*R*)
7	**L10c**	80 (96:4)	> 99 (*R*)	21	**L20a**	<5	nd[d]
8	**L10d**	12 (84:16)	98 (*R*)	22	**L21a**	<5	nd[d]
9	**L10e**	78 (94:6)	99 (*R*)	23	**L22a**	100 (91:9)	98 (*R*)
10	**L10h**	<5	nd[d]	24	**L23a**	21 (72:28)	72 (*R*)
11	**L10i**	6 (83:17)	86 (*R*)	25	**L24a**	36 (79:21)	80 (*R*)
12	**L11a**	81 (97:3)	99 (*R*)	26	**L25a**	100 (89:11)	96 (*R*)
13	**L12a**	74 (97:3)	98 (*R*)	27	**L26a**	100 (90:10)	92 (*R*)
14	**L13a**	75 (92:8)	97 (*R*)				

[a] $[Pd_2(dba)_3]$·dba (1.25 x 10^{-2} mmol), **S1** (2.0 mmol), phenyl triflate (0.5 mmol), ligand (2.8 x 10^{-2} mmol), THF (3 mL), $^{i}Pr_2NEt$ (1 mmol), T = 50 ºC, t = 24 h. [b] Conversion percentages determined by GC. [c] Enantiomeric excesses measured by GC. [d] not determined.

In summary, the best results were obtained with ligands **L10a**-**c**, **L16a**-**c** and **L17a**-**c** (Table 5.2.1, entries 5-7, 17 and 18; regio's up to >99% and ee's up to >99%), which contain the optimal combination of ligand parameters (ligand structure, substituents at the oxazoline and the alkyl chain, and substituents in the biaryl phosphite moiety). Moreover, both enantiomers of phenylation product **1** can be accessed in high activities, and high regio- and enantioselectivities simply by changing the absolute configuration of the alkyl chain. These results clearly show the efficiency of using highly modular scaffolds in the ligand design and compete favourably with the best that have been reported in the literature.[2a,b,e,k,l,4b]

*Heck reaction of 2,3-dihydrofuran **S1** using other triflate sources*

First we investigated the effects of the electronic and steric properties of the aryl triflate source on the product outcome. For this purpose, we tested ligands **L6**-**L26a**-**i** in the Pd-catalyzed Heck reaction of **S1** with several aryl triflates, in which these properties were systematically varied (Scheme 5.2.2, R= 1-naphthyl, *p*-CH_3-C_6H_4, *p*-NO_2-C_6H_4). The most noteworthy results are shown in Table 5.2.2 (entries 1-16). They followed the same trends as for the phenylation of **S1**. Again, both enantiomers of the arylated products **1** were accessible in high activities, and high regio- (up to >99%) and enantioselectivities (ee's up to >99%). The results indicate that both the steric and electronic parameters of the triflate mainly affected regioselectivity, while their effect on enantioselectivity was less important. Thus, regioselectivities are best for 1-naphthyl- and *para*-nitrophenyl triflate. Again, these results compete favourably with the best that have been reported in the literature.[2f,k,l,4b]

We next evaluate the ligand library in the Heck reaction of **S1** with cyclohexenyl triflate (Table 5.2.2, entries 17-21). Again the Pd-catalyst precursors containing ligands **L10a**, **L16a** and **L17a** provided access to both enantiomers of the alkenylated product **1** in high activity, and regio- (up to

>99%) and enantioselectivity (ee's up to 94%). These results are among the best reported so far.[2a,b,e,k,4b]

Table 5.2.2. Selected results for Pd-catalysed enantioselective arylation and cycloalkenylation of 2,3-dihydrofuran **S1** using ligands **L6**-**L26a**-**i**[a]

Entry	Ligand	R	% Conv (**1**:**2**)[b]	% ee **1**[c]
1	**L10a**	C_6H_5	94 (96:4)	> 99 (*R*)
2	**L10a**	4-CH_3-C_6H_4	80 (92:8)	99 (*R*)
3	**L10a**	4-NO_2-C_6H_4	86 (98:2)	99 (*R*)
4	**L10a**	1-Naphthyl	98 (99:1)	99 (*R*)
5	**L16a**	C_6H_5	99 (>99:<1)	>99 (*R*)
6	**L16a**	4-CH_3-C_6H_4	93 (97:3)	99 (*R*)
7	**L16a**	4-NO_2-C_6H_4	100 (>99:<1)	>99 (*R*)
8	**L16a**	1-Naphthyl	100 (>99:<1)	>99 (*R*)
9	**L17a**	C_6H_5	92 (96:4)	99 (*S*)
10	**L17a**	4-CH_3-C_6H_4	85 (93:7)	99 (*S*)
11	**L17a**	4-NO_2-C_6H_4	90 (98:2)	99 (*S*)
12	**L22a**	C_6H_5	100 (91:9)	98 (*R*)
13	**L22a**	4-NO_2-C_6H_4	100 (99:1)	99 (*R*)
14	**L22a**	1-Naphthyl	100 (93:7)	98 (*R*)
15	**L26a**	C_6H_5	100 (90:10)	92 (*R*)
16	**L26a**	4-NO_2-C_6H_4	100 (94:6)	99 (*R*)
17	**L10a**	C_6H_9	100 (>99:<1)	94 (*R*)
18	**L16a**	C_6H_9	100 (>99:<1)	94 (*R*)
19	**L17a**	C_6H_9	100 (99:1)	94 (*S*)
20	**L22a**	C_6H_9	100 (92:8)	90 (*R*)
21	**L26a**	C_6H_9	100 (89:11)	89 (*R*)

[a] $[Pd_2(dba)_3]$·dba (1.25 x 10^{-2} mmol), **S1** (2.0 mmol), triflate (0.5 mmol), ligand (2.8 x 10^{-2} mmol), THF (3 mL), $^{i}Pr_2NEt$ (1 mmol), T = 50 ºC, t = 24 h. [b] Conversion percentages determined by GC or ^{1}H-NMR. [c] Enantiomeric excesses measured by GC or HPLC.

*Asymmetric Heck reaction of N-carbomethoxy-2,3-dihydropyrrole **S2** under thermal conditions*

We then applied this ligand library in the arylation of *N*-carbomethoxy-2,3-dihydropyrrole **S2** (Scheme 5.2.3). Although, dihydropyrrole derivatives are suitable substrates and very useful in organic synthesis, their asymmetric Heck reactions have hardly been studied.[2b,c,k,7]

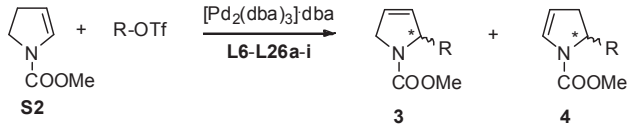

R= C_6H_5, *p*-CH_3-C_6H_4

Scheme 5.2.3. Pd-catalyzed Heck reaction of N-carbomethoxy-2,3-dihydropyrrole **S2**.

The results using the phosphite-oxazoline ligands **L6**-**L26a**-**i** are summarized in Table 5.2.3. They followed the same trend as for the arylation and alkenylation of **S1**. Again, both enantiomers

of the product **3** were accessible in high activities, regio- (up to >99%) and enantioselectivities (ee's up to 99%) using Pd/**L10a**-**c**, Pd/**L16a**-**c** and Pd/**L17a**-**c**. Although, as expected, the activities were lower than in the arylation reaction of **S1**, they were much higher than those obtained with other successful ligands under mild reaction conditions.[2b,c,k,7] Again, these results compete favourably with the best that have been reported in the literature.[2b,c,k,7]

Table 5.2.3. Selected results for the Pd-catalysed enantioselective arylation of **S2** using phosphite–oxazoline ligand library **L6**-**L26a**-**i**[a]

Entry	Ligand	R	% Conv (**3**:**4**)[b]	% ee **3**[c]
1	**L6a**	C_6H_5	69 (>99:<1)	73 (*R*)
2	**L10a**	C_6H_5	99 (>99:<1)	99 (*R*)
3	**L10b**	C_6H_5	99 (99: 1)	99 (*R*)
4	**L10c**	C_6H_5	100 (99: 1)	98 (*R*)
5	**L10e**	C_6H_5	11 (76:24)	96 (*R*)
6	**L11a**	C_6H_5	88 (>99:<1)	92 (*R*)
7	**L12a**	C_6H_5	92 (>99:<1)	88 (*R*)
8	**L16a**	C_6H_5	99 (>99:<1)	99 (*R*)
9	**L17a**	C_6H_5	97 (99:1)	99 (*S*)
10	**L22a**	C_6H_5	99 (>99:<1)	93 (*R*)
11	**L26a**	C_6H_5	95 (>99:<1)	88 (*R*)
12	**L10a**	4-CH_3-C_6H_4	99 (>99:<1)	99 (*R*)

[a] $[Pd_2(dba)_3]$·dba (1.5 x 10^{-2} mmol), **S2** (2.0 mmol), aryl triflate (0.5 mmol), ligand (3.5 x 10^{-2} mmol), THF (3 mL), $^{i}Pr_2NEt$ (1 mmol), T = 67 ºC, t = 72 h. [b] Conversion percentages determined by GC. [c] Enantiomeric excesses measured by HPLC.

*Asymmetric Heck reaction of 4,7-dihydro-1,3-dioxepin **S3** under thermal conditions*

To further study the potential of these readily available ligands, we also examined **L6**-**L26a**-**i** in the arylation of 4,7-dihydro-1,3-dioxepin **S3** (Scheme 5.2.4). This substrate is of great importance, since the resulting enol ethers **5** are easily converted to chiral β-aryl-γ-butyrolactones, which are useful synthetic intermediates.[8] Despite this interesting characteristic, there are only few reports that provided good enantioselectivities for this substrate and those that due usually proceed at low reaction rates (i.e. typically 5 to 7 days).[2a,b,e,h,4b] The most noteworthy results are shown in Table 5.2.4. In general, the effect of the ligand parameters on activity, regio- and enantioselectivity followed the same trends as for the arylation of **S1** and **S2**. Again, the catalysts precursors containing phosphite-oxazoline ligands **L10a**-**c**, **L16a**-**c** and **L17a**-**c** provided both enantiomers of the arylated products **5** in high enantioselectivities (ee's up to 98%). Again, these results compete favourably with the best that have been reported in the literature.[2a,b,e,h,4b]

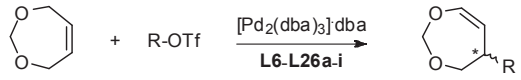

S3 **5**

R= C_6H_5, *p*-CH_3-C_6H_4

Scheme 5.2.4. Pd-catalyzed Heck reaction of 4.7-dihydro-1,3-dioxepin **S3**.

Table 5.2.4. Selected results for the Pd-catalysed enantioselective arylation of **S3** using phosphite–oxazoline ligand library **L6**-**L26a-i**[a]

Entry	Ligand	R	% Conv[b]	% ee **5**[c]
1	**L6a**	C_6H_5	72	82 (*R*)
2	**L10a**	C_6H_5	99	98 (*R*)
3	**L10b**	C_6H_5	100	98 (*R*)
4	**L10c**	C_6H_5	97	97 (*R*)
5	**L10e**	C_6H_5	<5	nd[d]
6	**L11a**	C_6H_5	92	95 (*R*)
7	**L12a**	C_6H_5	89	92 (*R*)
8	**L16a**	C_6H_5	99	98 (*R*)
9	**L17a**	C_6H_5	96	98 (*S*)
10	**L22a**	C_6H_5	100	95 (*R*)
11	**L26a**	C_6H_5	98	91 (*R*)
12	**L10a**	4-CH_3-C_6H_4	94	98 (*R*)

[a] $[Pd_2(dba)_3]$·dba (1.5 x 10^{-2} mmol), **S3** (2.0 mmol), aryl triflate (0.5 mmol), ligand (3.5 x 10^{-2} mmol), THF (3 mL), $^{i}Pr_2NEt$ (1 mmol), T = 67 ºC, t = 72 h. [b] Conversion percentages determined by GC. [c] Enantiomeric excesses measured by GC. [d] not determined.

*Asymmetric Heck reaction of cyclopentene **S4** under thermal conditions*

Encouraged by the excellent results obtained, we decided to go one step further and to study the arylation of cyclopentene **S4** (Scheme 5.2.5). Selectivity for **S4** is more difficult to control than for functionalized alkenes such as **S1** and **S2** due to extensive double bond migration.[1] Moreover, in addition to the desired product **6**, achiral regioisomers **7** and **8** can also be obtained. There are therefore fewer successful catalyst systems for the Pd-catalyzed arylation of this substrate than for the arylation of functionalized alkenes such as **S1**.[2a,b,4b]

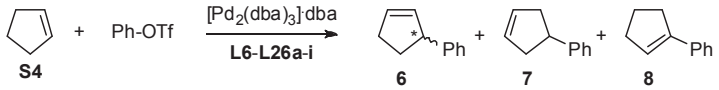

S4 **6** **7** **8**

Scheme 5.2.5. Pd-catalyzed Heck reaction of cyclopentene **S4**.

In this section, we report that the chiral phosphite-oxazoline ligands **L6**-**L26a-i** applied in the previous section to the Pd-catalyzed arylation and alkenylation of substrates **S1**-**S3** can also be used for unfunctionalised alkene substrate **S4**. The results, which are summarized in Table 5.2.5, follow the same trend as for the alkenylation of **S1**-**S3**. Both enantiomers of the phenylated product **6** were obtained in high activities and selectivities (regio's up to 94% and ee's up to 99%). Although, as expected, the activities were lower than in the alkenylation of **S1**, they were much higher than those obtained with the most successful phosphine-oxazoline ligands.[2a,b] Interestingly, the formation of achiral product **8** did not take place. Again, these results compete favourably with the best that have been reported in the literature.[2a,b,4b]

Table 5.2.5. Selected results for the Pd-catalysed enantioselective phenylation of cyclopentene **S4** using phosphite-oxazoline ligand library **L6**-**L26a-i**[a]

Entry	Ligand	% conv (**6**:**7**)[b]	% ee **6**[c]
1	**L6a**	73 (87:13)	91 (*R*)
2	**L10a**	100 (90:10)	99 (*R*)
3	**L10b**	100 (89:11)	99 (*R*)
4	**L10e**	9 (86:14)	95 (*R*)
5	**L11a**	99 (89:11)	98 (*R*)
6	**L15a**	15 (88:12)	87 (*R*)
7	**L16a**	100 (94:6)	99 (*R*)
8	**L17a**	100 (89:11)	99 (*S*)
9	**L22a**	100 (84:16)	94 (*R*)
10	**L26a**	100 (82:18)	90 (*R*)
11	**L20a**	<5	nd[d]

[a] $[Pd_2(dba)_3]\cdot dba$ (1.25 x 10^{-2} mmol), **S4** (2.0 mmol), phenyl triflate (0.5 mmol), ligand (2.8 x 10^{-2} mmol), THF (3 mL), $^{i}Pr_2NEt$ (1 mmol), T = 50 ºC, t = 48 h. [b] Conversion percentages determined by GC. [c] Enantiomeric excesses measured by GC. [d] not determined

5.2.3.2. Microwave-assisted asymmetric Heck reactions

Today it is known that by using controlled microwave dielectric heating, several C-C coupling reactions can be accelerated.[9] In 2002, Hallberg and coworkers demonstrated that the use of microwave irradiation for the enantioselective Heck reactions using PHOX Pfaltz's and BINAP ligands considerably shortened reaction times (from 4 days to 1 hour) but enantioselectivities were lower than those obtained under thermal conditions.[10] Recently, we[4b] and others[11] have also shown that, when microwaves are used as the source of heat, the reaction proceeds much faster and retains excellent enantioselectivity, allowing for a highly selective intermolecular Heck reaction. Therefore, we decided to use ligand library **L6**-**L26a-i** to take advantage of microwave irradiation in asymmetric Pd-catalyzed Heck reactions.

We first studied how temperature affected the Pd-catalyzed asymmetric Heck reaction of substrate **S1** using phenyl triflate with ligands **L22a** and **L10a** (Table 5.2.6). We found that the optimal temperature was 70 ºC. At lower temperatures, activities and enantioselectivities decreased (Table 5.2.6, entries 1 and 5 vs 2 and 6). Under these optimized conditions, we evaluated the complete ligand library. The most noteworthy results are shown in Table 5.2.6. It is interesting to note that under microwave irradiation, reaction times improve dramatically (from 24 hours to 10 minutes) and the excellent regio- (up to >99%) and enantioselectivities (ee's up to 99%) obtained under thermal conditions are maintained (Table 5.2.6, entries 2-4, 6-7). These observations are also true for other triflate sources (i.e aryl or cyclohexenyl triflates), so activities (full conversion in 10 min), and regio- (up to >99%) and enantioselectivities (up to 99% ee) are excellent (Table 5.2.6, entries 8-11).

Table 5.2.6. Selected results for the microwave-assisted Pd-catalysed enantioselective arylation and alkenylation of 2,3-dihydrofuran **S1** using ligands **L22a**, **L26a**, **L10a**, **L16a** and **L17a**[a]

Entry	L	R	T (ºC)	t (min)	% Conv (**1**:**2**)[b]	% ee **1**[c]
1	**L10a**	C_6H_5	50	15	96 (98:2)	95 (*R*)
2	**L10a**	C_6H_5	70	10	100 (97:3)	98 (*R*)
3	**L16a**	C_6H_5	70	10	100 (99:1)	99 (*R*)
4	**L17a**	C_6H_5	70	10	100 (97:3)	98 (*S*)
5	**L22a**	C_6H_5	50	20	98 (92:8)	96 (*R*)
6	**L22a**	C_6H_5	70	10	100 (93:7)	98 (*R*)
7	**L26a**	C_6H_5	70	10	100 (92:8)	92 (*R*)
8	**L10a**	4-NO_2-C_6H_4	70	10	100 (94:6)	98 (*R*)
9	**L10a**	4-CH_3-C_6H_4	70	10	100 (98:2)	99 (*R*)
10	**L10a**	1-Naphthyl	70	10	100 (>99:<1)	99 (*R*)
11	**L10a**	C_6H_9	70	10	100 (99:1)	94 (*R*)

[a] $[Pd_2(dba)_3]$·dba (1.25 x 10^{-2} mmol), **S1** (2.0 mmol), triflate (0.5 mmol), ligand (2.8 x 10^{-2} mmol), THF (3 mL), $^{i}Pr_2NEt$ (1 mmol). [b] Conversion percentages determined by GC or ^{1}H-NMR. [c] Enantiomeric excesses measured by GC or HPLC.

Encouraged by these excellent results, we also studied the arylation of *N*-carbomethoxy-2,3-dihydropyrrole **S2**, 4,7-dihydro-1,3-dioxepin **S3** and cyclopentene **S4**, which required longer reaction times under thermal conditions than substrate **S1** (Scheme 5.2.6). After the reaction parameters had been optimized, we found that the optimal temperature was 80 ºC for substrates **S2** and **S3** and 70 ºC for substrate **S4**. Again, the use of microwaves was highly advantageous: regio- and enantioselectivities were excellent and reaction times much shorter (6 hours versus 3 days for **S2** and **S3** and 45 minutes versus 2 days for **S4**). It should be noted that the use of microwave irradiation also improved regioselectivity for **S4**. Therefore, the reaction of **S4** and phenyltriflate at 70 ºC gave the coupling product **6** with 99% ee in 98% regioselectivity.

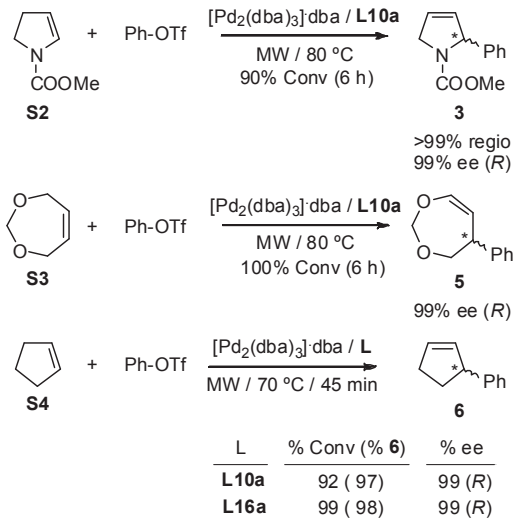

Scheme 5.2.6. Selected results for Pd-catalysed enantioselective arylation of *N*-carbomethoxy-2,3-dihydropyrrole **S2**, 4,7-dihydro-1,3-dioxepin **S3** and cyclopentene **S4** under microwave irradiation.

5.2.4. Conclusions

A highly modular library of readily available phosphite-oxazoline ligands has been applied in the Pd-catalyzed asymmetric Heck reactions of several substrates and triflates under thermal and microwave conditions. This ligand library contains three main ligand structures that have been designed by systematic modifications of one of the most successful ligand families developed for this process. As well as studying the effect of these three ligand structures on the catalytic performance, we also evaluated the effect of modifying several ligand parameters (i.e. substituents in the oxazoline and the alkyl chain, the configuration of the alkyl chain, the presence of a second stereogenic centre in the oxazoline ring and its configuration, and the substituents and configurations in the biaryl phosphite moiety). We found that the degree of isomerization and their effectiveness at transferring the chiral information in the product and the activity can be tuned by correctly choosing the ligand components (ligand structure and phosphite and oxazoline substituents). Excellent activities (up to 100% conversion in 10 minutes), and regio- (up to >99%) and enantioselectivities (ee's up to >99%) were obtained in both enantiomers of the Heck-coupling products using a wide range of substrates and triflate sources. These results compete favourably with the most successful ligands that have been developed for this reaction. Interestingly, the results were better than those obtained using pyranoside phosphite-oxazoline ligands[4b] which have recently emerged as a privileged ligand class for this process. Reaction times were considerably shorter in microwave irradiation conditions (full conversion in a few minutes) and regio- and enantioselectivities were maintained. These results open up a new class of ligands for the highly active and enantioselective Pd-catalysed Heck reaction, which will be of great practical interest.

5.2.5. Experimental section

5.2.5.1. General considerations

All syntheses were performed with standard Schlenk techniques under argon atmosphere. Solvents were purified by standard procedures. Ligands **L6**-**L21** and ligands **L22**-**L25** were synthesized as previously described.[5,6] Substrate **S2** was synthesized as previously reported and azeotropically dried using toluene prior to use.[12] All other reagents were used as commercially available. ^{1}H, $^{13}C\{^{1}H\}$ and $^{31}P\{^{1}H\}$ NMR spectra were recorded on a Varian Gemini 400 MHz spectrometer. The chemical shifts are referenced to tetramethylsilane (^{1}H and ^{13}C) as internal standard or H_3PO_4 (^{31}P) as external standard. The ^{1}H and ^{13}C NMR spectral assignments were determined by ^{1}H-^{1}H and ^{1}H-^{13}C correlation spectra. Microwave experiments were carried out using a CEM Explorer, in which the temperature is controlled by a non-contact infrared sensor that is located beneath the cavity floor and "looks" up to the bottom of the vessel.

5.2.5.2. Preparation of ligand L26a

(3,3',5,5'-Tetra-*tert*-butyl-1,1'-biphenyl-2,2'-diyl)phosphorochloridite (3.0 mmol) produced *in situ*[13] was dissolved in toluene (12.5 mL) and pyridine (1.14 mL, 14 mmol) was added. (*S*)-2-(1-Hydroxy-1-methylethyl)-4-phenyl-1,3-oxazoline[14] (2.8 mmol) was azeotropically dried with toluene (3 x 2 mL) and then dissolved in toluene (12.5 mL) to which pyridine (1.14 mL, 14 mmol) was

added. The oxazoline solution was transferred slowly at 0 ºC to the solution of phosphorochloridite. The reaction mixture was stirred overnight at 80 ºC, and the pyridine salts were removed by filtration. Evaporation of the solvent gave a white foam, which was purified by flash chromatography (toluene/NEt_3= 100/1) to produce the corresponding ligand as a white solid.

L26a: Yield: 0.63 g, 35 %. ^{31}P NMR (400 MHz, C_6D_6), δ: 148.3 (s). ^1H NMR (400 MHz, C_6D_6), δ: 0.97 (s, 18H, CH_3, ^{t}Bu), 1.36 (s, 9H, CH_3, ^{t}Bu), 1.38 (s, 9H, CH_3, ^{t}Bu), 1.42 (s, 3H, CH_3), 1.45 (s, 3H, CH_3), 3.54 (t, 1H, CH_2, *J* = 8.0 Hz), 3.87 (dd, 1H, CH_2, *J*= 10.0 Hz, *J*= 8.0 Hz), 4.66 (dd, 1H, CH, *J* = 10.0 Hz, *J* = 8.0 Hz), 6.7-7.4 (m, 9H, CH=). ^{13}C NMR (400 MHz, C_6D_6), δ: 28.7 (d, CH_3, J_{C-P} = 5.4 Hz), 28.8 (d, CH_3, J_{C-P} = 5.4 Hz), 31.9 (b, CH_3, ^{t}Bu), 34.9 (b, C, ^{t}Bu), 35.9 (C, ^{t}Bu), 36.0 (C, ^{t}Bu), 70.4 (CH), 75.6 (CH_2), 76.5 (d, C, J_{C-P} = 10.9 Hz), 124-151 (aromatic carbons), 169.8 (C=N). Anal. Calc (%) for $C_{40}H_{54}NO_4P$: C 74.62, H 8.45, N 2.18; found C 74.59, H 8.39, N 2.16.

5.2.5.3. General procedure for Pd-catalyzed enantioselective Heck reactions

A mixture of $[Pd_2(dba)_3]$dba (12 mg, 1.25 x 10^{-2} mmol for substrates **S1** and **S4**; and 15 mg, 1.5 x 10^{-2} mmol for substrates **S2** and **S3**) and the corresponding chiral ligand (2.3 equiv) in dry degassed solvent (3.0 mL) was stirred under argon at room temperature for 15 min. The corresponding olefin (2.0 mmol), triflate (0.50 mmol) and base (1.0 mmol) were added to the catalyst solution. The solution was stirred at the desired temperature under argon. After the desired reaction time, the mixture was diluted with additional diethyl ether and washed with water, dried over $MgSO_4$ and evaporated. For compounds 2-(1-naphthyl)-2,5-dihydrofuran, 2-(4-nitrophenyl)-2,5-dihydrofuran and 1-(methoxycarbony)-5-toluyl-3-pyrroline conversion was measured by ^1H-NMR and selectivity was measured by HPLC.[2b] For the rest of the compounds, conversion and selectivity were determined by GC.[2e]

5.2.6. Acknowledgements

We thank the Spanish Government (Consolider-Ingenio CSD2006-0003, CTQ2007-62288/BQU, 2008PGIR/07 to O.P. and 2008PGIR/08 to M.D.) and the Catalan Government (2005SGR007777) for financial support. We thank ICIQ (Institut Català d'Investigació Química) for technical support on the microwave experiments.

5.2.7. References

[1] For recent reviews, see: a) Tietze, L. T.; Ila, H.; Bell, H. P. *Chem Rev.* **2004**, *104*, 3453. b) Dai, L.X.; Tu, T.; You, S. L.; Deng, W. P.; Hou, X. L. *Acc. Chem. Res.* **2003**, *36*, 659. c) Bolm, C.; Hildebrand, J. P.; Muñiz, K.; Hermanns, N. *Angew. Chem., Int. Ed.* **2001**, *44*, 3284. d) Shibasaki, M.; Vogl E. M. *in Comprehensive Asymmetric Catalysis;* Jacobsen, E.N., Pfaltz, A., Yamamoto, H., Eds.; Springer: Heidelberg, 1999. e) Loiseleur, O.; Hayashi, M.; Keenan, M.; Schemees, N.; Pfaltz, A. *J. Organomet. Chem.* **1999**, ***576***, 16. f) Beller, M.; Riermeier, T. H.; Stark G. in *Transition Metals for Organic Synthesis*; Beller, M., Bolm, C., Eds.; Wiley-VCH: Weinheim, 1998.

[2] See for instance: a) Loiseleur, O.; Meier, P.; Pfaltz, A. *Angew. Chem., Int. Ed. Engl.* **1996**, *35*, 200. b) Loiseleur, O.; Hayashi, M.; Schmees, N.; Pfaltz, A. *Synthesis* **1997**, 1338. c) Tu, T.; Hou, X.L.; Dai, L.X. *Org. Lett.* **2003**, **5**, 3651. d) Gilbertson, S. R.; Xie, D.; Fu, Z. *J. Org. Chem.* **2001**, *66*, 7240. e) Gilbertson, S. R.; Fu,

Z. *Org. Lett.* **2001**, *3*, 161. f) Tu, T.; Deng, W.P.; Hou, X.L.; Dai, L.X.; Dong, X.C. *Chem. Eur. J*. **2003**, *9*, 3073. g) Gilbertson, S. R.; Genov, D. G.; Rheingold, A. L. *Org. Lett.* **2000**, *2*, 2885. h) Hashimoto, Y.; Horie, Y.; Hayashi, M.; Saigo, K. *Tetrahedron: Asymmetry* **2000**, *11*, 2205. i) Hou, X. L.; Dong, D. X.; Yuan, K. *Tetrahedron: Asymmetry* **2004**, *15*, 2189. j) Liu, D.; Dai, Q.; Zhang, X. *Tetrahedron* **2005**, *61*, 6460. k) Wu, W.-Q.; Peng, Q.; Dong, D.-X.; Hou, X.-L.; Wu, Y.-D. *J. Am. Chem. Soc.* **2008**, *130*, 9717. l) Rubina, M.; Sherrill, W. M.; Rubin, M. *Organometallics* **2008**, *27*, 6393.

[3] Few phosphinite-oxazoline ligands have also been successfully applied in this process, see: a) Yonehara, K.; Mori, K.; Hashizume, T.; Chung, K. G.; Ohe, K.; Uemura, S. *J. Organomet. Chem*. **2000**, *603*, 40. b) Drury III, W. J.; Zimmermann, N.; Keenan, M.; Hayashi, M.; Kaiser, S.; Goddard, R.; Pfaltz, A. *Angew. Chem. Int. Ed.* **2004**, *43*, 70. c) Henriksen, S. T.; Norrby, P. O.; Kaukoranta, P.; Andersson, P. G. *J. Am. Chem. Soc.* **2008**, *130*, 10414.

[4] a) Mata, Y.; Pàmies, O.; Diéguez, M. *Org. Lett.* **2005**, *7*, 5597. b) Mata, Y.; Pàmies, O.; Diéguez, M. *Chem. Eur. J.* **2007**, *13*, 3296.

[5] Ligands **L22**-**L25** have also been successfully applied in the Pd-catalyzed allylic subtitution reaction. See: Pàmies, O.; Diéguez, M.; Claver, C. *J. Am. Chem. Soc.* **2005**, *127*, 3646.

[6] Ligands **L6**-**L21** have also been successfully applied in the Pd-catalyzed allylic subtitution and Ir-catalyzed hydrogenation reactions. See: a) Pàmies, O.; Diéguez, M. *Chem. Eur. J.* **2008**, *14*, 3653. b) Diéguez, M.; Mazuela, J.; Pàmies, O.; Verendel, J. J.; Andersson, P. G. *Chem. Commun.* **2008**, 3888. c) Mazuela, J.; Verendel, J. J.; Coll, M.; Schäffner, B.; Börner, A.; Anderson, P. G.; Pàmies, O.; Diéguez, M. *J. Am. Chem. Soc.* **2009**, *131*, 12344.

[7] a) Ozawa, F.; Hayashi, T. *J. Organomet. Chem.* **1992**, *428*, 267. b) Tietze, L. F.; Thede, K. *Synlett* **2000**, 1470.

[8] Takano, S.; Dsmizu, K.; Ogasawara, K. *Synlett* **1993**, 393.

[9] See for instance: *Microwave Assisted Organic Synthesis;* Tierney, J. P., Lidström, P., Eds.; Blackwell Publishing Ltd.: Oxford, 2005 and references therein.

[10] Nilsson, P.; Gold, H.; Larhed, M.; Hallberg, A. *Synthesis* **2002**, 1611.

[11] Kaukoranta, P.; Källström, K.; Andersson, P. G. *Adv. Synth. Catal.* **2007**, *349*, 2595.

[12] Kraus, G. A.; Neuenschwander, K. *J. Org. Chem.* **1981**, *46*, 4791.

[13] Pàmies, O.; Diéguez, M.; Net, G.; Ruiz, A.; Claver, C. *Organometallics* **2000,** *19,* 1488.

[14] Allen, J. V.; Williams, J. M. J. *Tetrahedron: Asymmetry* **1994**, *5*, 277.

5.2.8. Supporting information

Table 5.2.7. Selected results for Pd-catalysed enantioselective phenylation of 2,3-dihydrofuran **S1** using ligands **L10a**, **L22a** and **L26a**. Effect of the base and temperature[a]

Entry	Ligand	T (ºC)	Base	% Conv (**1**:**2**)[b]	% ee **1**[c]
1	**L22a**	50	$^{i}Pr_2NEt$	100 (91:9)	98 (*R*)
2	**L22a**	70	$^{i}Pr_2NEt$	100 (88:12)	93 (*R*)
3	**L22a**	25	$^{i}Pr_2NEt$	14 (90:10)	98 (*R*)
4	**L22a**	50	PS	100 (90:10)	98 (*R*)
5	**L22a**	50	NEt_3	86 (87:13)	96 (*R*)
6	**L26a**	50	$^{i}Pr_2NEt$	100 (90:10)	92 (*R*)
7	**L26a**	70	$^{i}Pr_2NEt$	100 (88:12)	90 (*R*)
8	**L26a**	25	$^{i}Pr_2NEt$	9 (91:9)	91 (*R*)
9	**L26a**	50	PS	100 (91:9)	92 (*R*)
10	**L26a**	50	NEt_3	98 (85:15)	89 (*R*)
11	**L10a**	50	$^{i}Pr_2NEt$	94 (96:4)	>99 (*R*)
12	**L10a**	70	$^{i}Pr_2NEt$	100 (93:7)	95 (*R*)
13	**L10a**	25	$^{i}Pr_2NEt$	21 (96:4)	>99 (*R*)
14	**L10a**	50	PS	92 (96:4)	99 (*R*)
15	**L10a**	50	NEt_3	87 (92:8)	95 (*R*)
16	**L10a**	50	KOAc	54 (88:12)	>99 (*R*)
17	**L10a**	50	DBU	5 (65:35)	nd[d]

[a] $[Pd_2(dba)_3]$·dba (1.25 x 10^{-2} mmol), **S1** (2.0 mmol), phenyl triflate (0.5 mmol), Ligand (2.8 x 10^{-2} mmol), THF (3 mL), base (1 mmol), t = 24 h. [b] Conversion percentages determined by GC. [c] Enantiomeric excesses measured by GC. [d] Not determined.

2.- Examples of temperature, power and pressure vs time profiles for the microwaves experiments

Table 5.2.6, entry 1.

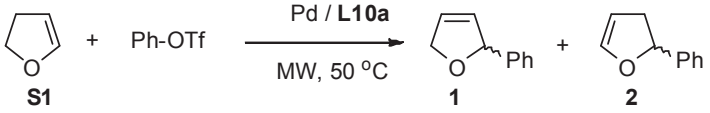

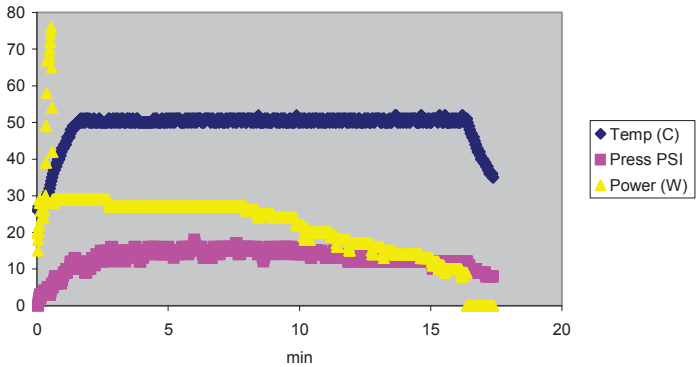

Table 5.2.6, entry 2.

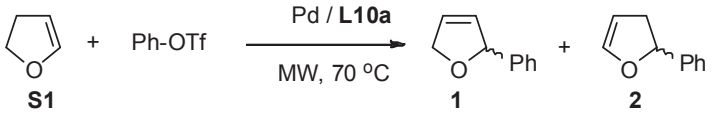

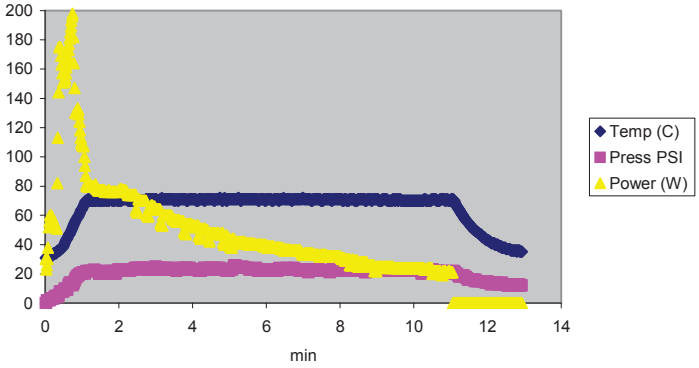

Scheme 5.2.6

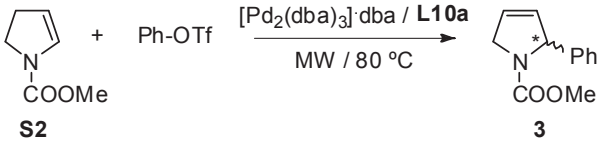

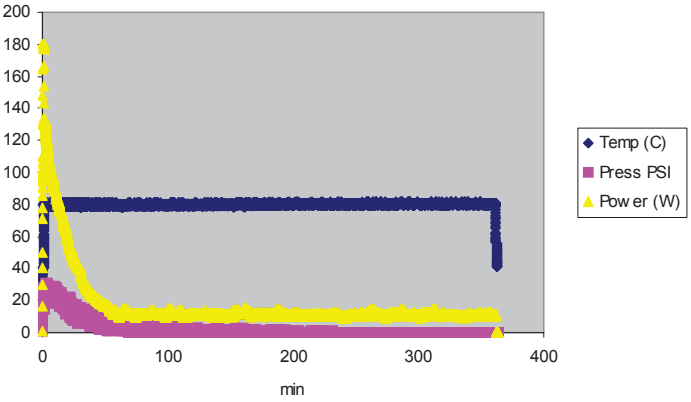

Scheme 5.2.6.

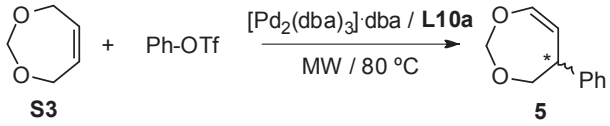

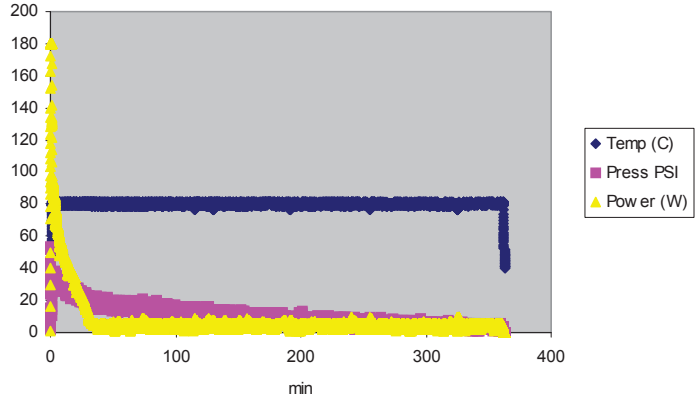

Scheme 5.2.6.

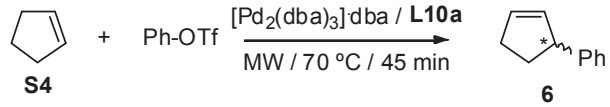

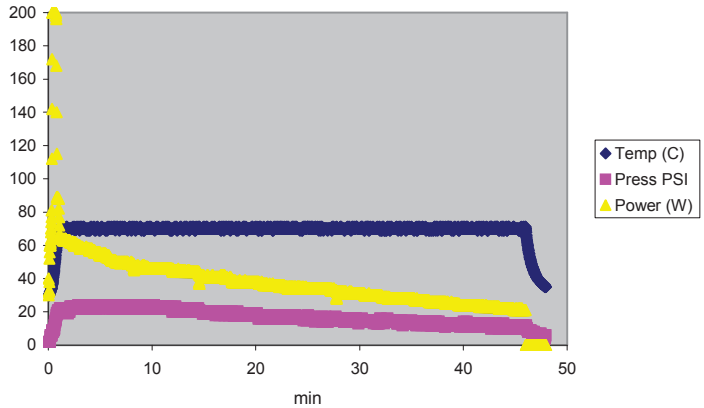

5.3. Phosphite-oxazole/imidazole ligands in asymmetric intermolecular Heck reaction.

Javier Mazuela, Paivi Tolstoy, Oscar Pàmies, Pher G. Andersson and Montserrat Diéguez in *Org. Biomol. Chem.* **2011**, *9*, 941.

5.3.1. Abstract

We described the application of a new class of ligands –the phosphite-oxazole/imidazole (**L29**-**L32** and **L37**)– in the asymmetric intermolecular Pd-catalyzed Heck reactions under thermal and microwave conditions. These ligands combine the advantages of the oxazole/imidazole moiety with those of the phosphite moiety: they are more stable than their oxazoline counterparts, less sensitive to air and other oxidizing agents than phosphines and phosphinites, and easy to synthesize from readily available alcohols. The results indicate that activities, regio- and enantioselectivities are highly influenced by the type of nitrogen donor group (oxazole or imidazole), the oxazole and biaryl-phosphite substituents and the axial chirality of the biaryl moiety of the ligand. By carefully selecting the ligand components, we achieved high activities, regio- (up to 99%) and enantioselectivities (up to 99%) using several triflate sources. Under microwave-irradiation conditions, reaction times were considerably shorter (from 24 hours to 30 minutes) and regio- and enantioselectivities were still excellent.

5.3.2. Introduction

The Heck reaction is one of the most versatile catalytic methods for C-C bond formation. In this process an aryl or alkenyl halide or triflate is coupled with an alkene. [1] Its applicability to highly functionalized substrates confers upon the reaction a very wide substrate scope, and it has been used in a number of syntheses of complex natural products.[1] During the past decade, research in the Heck reaction has focused on the possibility of controlling its enantioselectivity. The bulk of the reported examples involve intramolecular reactions, which have the advantage that the alkene regiochemistry and product geometry can be easily controlled.[1] Fewer studies, however, have been conducted on the asymmetric intermolecular version. This is mainly because regioselectivity is also often a problem.[1] Although diphosphines (such as BINAP) were used early on this process,[1,2] heterodonor phosphine-oxazolines have recently emerged as more suitable ligands for the intermolecular Heck reaction.[1a-b,3,4] Two drawbacks of these latter ligands are the long reaction times usually required to achieve full conversion and the substrate specificity.

In the last decade, a group of less electron-rich phosphorus compounds–phosphite-containing ligands–have demonstrated their huge potential utility in many transition-metal catalyzed reactions.[5] Their highly modular construction, facile synthesis from readily available chiral alcohols and greater resistance to oxidation than phosphines have proved to be highly advantageous.[6] Despite all these benefits, the use of phosphite-containing ligands for the Pd-catalyzed Heck reaction has not been reported until very recently. In this context, phosphite-oxazolines have emerged as extremely effective ligands for improving the activity and versatility of this process.[7]

Despite this success, little attention has been paid to phosphite-containing ligands for this process and their potential as new ligands still needs to be systematically studied.[7]

To further expand the range of ligands and encouraged by the success of biaryl phosphite-oxazoline ligands[7] in this process we report here the first application of a biaryl phosphite-oxazole/imidazole ligand library (**L29**-**L32a**-**h** and **L37a**-**h**) in the asymmetric intermolecular Pd-catalyzed Heck reaction (Figure 5.3.1). For comparative purposes, we also evaluated phosphinite-oxazole/imidazole analogues (ligands **L29h** and **L37h**, Figure 5.3.1). Phosphite-oxazole/imidazole ligands combine a priori the above mentioned advantages of introducing a phosphite moiety with those of the oxazole/imidazole moiety. So, ligands **L29**-**L32a**-**h** and **L37a**-**h** are more stable than their oxazoline counterparts.[8] With this library we fully investigated the effects of either an oxazole or imidazole group in the ligand backbone, the effect of systematically varying the electronic and steric properties of the oxazole substituents (**L29**-**L32**) and different substituents/configurations in the biaryl phosphite moiety (**a**-**g**). By carefully selecting these elements, we achieved high selectivities (regio- and enantioselectivities) and activities using several triflate sources.

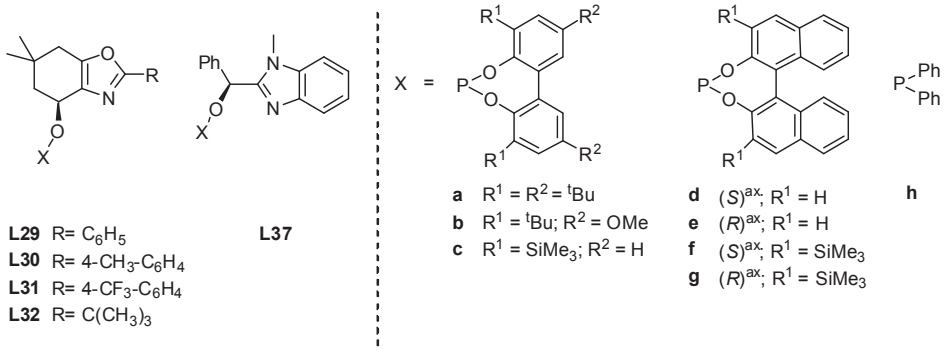

Figure 5.3.1. Phosphite-oxazole/imidazole ligand library **L29**-**L32a**-**g** and **L37a**-**g** and phosphinite-oxazole/imidazole ligands **L29h** and **L37h**.

5.3.3. Results and Discussion

5.3.3.1. Synthesis of ligands

Phosphite-oxazole ligands **L29**-**L32a**-**g** and phosphinite-oxazole ligand **L29h** have been synthesized from the corresponding easily accessible ketone-oxazole as previously described (see Section 3.5).[9,10] Scheme 5.3.1 illustrates the sequence of synthesis for the new phosphite-imidazole ligands **L37a**-**c** and phosphinite/imidazole ligand **L37h**. They were synthesized very efficiently from the easily accessible hydroxyl-imidazole **3**. This compound was prepared in a few steps from commercially available *N*-methyl benzimidazole **1**. In the first step of the synthesis, **1** was acetylated via a two step one pot procedure that involves deprotonation of **1** with LDA followed by reaction with methyl benzoate to produce ketone **2**.[11] Ketone **2** was then reduced by slow addition to a solution of (*R*)-Me-CBS catalyst (10 mol%, (*R*)-Me-CBS= α,α-diphenyl-D-prolinolmethylboronic acid cyclamide ester), employing $BH_3 \cdot SMe_2$ as stoichiometric reductant in THF.[12] Recrystalization from 95% ethanol of the obtained hydroxyl-imidazole yielded enantiomerically pure **3**. Treating alcohol **3** with 1 equivalent of either the appropriate *in situ*

formed phosphorochloridite ($ClP(OR)_2$; $(OR)_2$ = **a**-**c**) or clorodiphenylphosphine in the presence of pyridine provided easy access to the desired phosphite-imidazole (**L37a**-**c**) and phosphinite-imidazole (**L37h**) ligands, respectively. All the phosphite-imidazole ligands were stable during purification on neutral alumina under an atmosphere of argon and isolated in moderate-to-good yields as white solids. They were stable at room temperature and very stable to hydrolysis. The elemental analyses were in agreement with the assigned structure. The ^{1}H, ^{13}C and ^{31}P NMR spectra were as expected for these C_1 ligands. One singlet for each compound was observed in the ^{31}P NMR spectrum. Rapid ring inversions (tropoisomerization) in the biphenyl-phosphorus moieties (**a**-**c**) occurred on the NMR time scale because the expected diastereoisomers were not detected by low-temperature phosphorus NMR.[13]

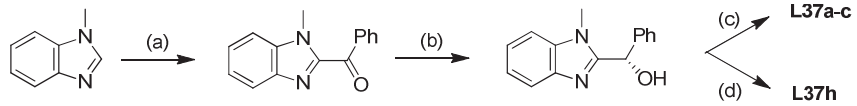

Scheme 5.3.1. Synthesis of new phosphite/phosphinite-imidazole ligands **L37a**-**c** and **L37h**. (a) LDA / THF then PhCOOEt (78% yield).[11] (b) (*R*)-Me-CBS / $BH_3{\cdot}SMe_2$ / THF (87% yield).[12] (c) $ClP(OR)_2$; $(OR)_2$ = **a**-**c** / Py / toluene (Yields: 54-71%). (d) $ClPPh_2$ / Py / DMAP / THF (68% yield).

5.3.3.2. Asymmetric phenylation of 2,3-dihydrofuran (S1) under thermal conditions

In a first set of experiments, we used the Pd-catalyzed phenylation of 2,3-dihydrofuran **S1** to study the potential of ligands **L29**-**L32a**-**h** and **L37a**-**h** (Scheme 5.3.2). **S1** was chosen as the substrate because the reaction was performed with a wide range of ligands, which enabled the efficiency of the various ligand systems to be compared directly.[1] In all cases, the catalysts were generated *in situ* by mixing $[Pd_2(dba)_3]{\cdot}dba$ with the corresponding chiral ligand.[7] The results are summarized in Table 5.3.1. We found that the catalytic performance was highly influenced by type of nitrogen donor group (oxazole or imidazole), the substituents at both oxazole and phosphite moieties and by the axial chirality of the biaryl phosphite group. In general, high activity, regio- (up to 97%) and enantioselectivity (up to 98%) were obtained in the phenylation of **S1**.

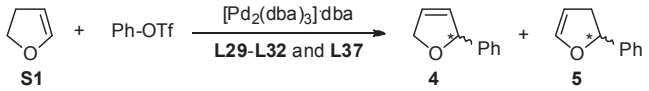

Scheme 5.3.2. Pd-catalyzed Heck reaction of 2,3-dihydrofurane **S1**.

Regarding the effect of the oxazole substituents, we found that these groups affected mainly activities (Table 5.3.1, entries 1 and 8-10). Bulky substituents at this position dramatically decreased activities (Table 5.3.1, entry 1 vs 10). This contrasts with the oxazoline-substituent effect observed for the vast majority of successful phosphine-oxazoline ligands, for which better results are obtained when bulky *tert*-butyl groups are present.[3] In addition, we also found that the presence of electron-withdrawing substituents has also a negative effect on activity, but almost no effect on the regio- and enantioselectivity of the process (Table 5.3.1, entries 1, 8 and 9).

Table 5.3.1. Selected results for the Pd-catalyzed enantioselective phenylation of 2,3-dihydrofuran **S1** using ligands **L29**-**L32a**-**h** and **L37a**-**h**[a]

Entry	Ligand	% Conv (**4**:**5**)[b]	% ee **4**[c]
1	**L29a**	77 (97:3)[e]	98 (*R*)
2	**L29b**	27 (97:3)	97 (*R*)
3	**L29c**	21 (94:6)	91 (*R*)
4	**L29d**	<5	nd[d]
5	**L29e**	<5	nd[d]
6	**L29f**	17 (96:4)	96 (*R*)
7	**L29g**	7 (92:8)	89 (*R*)
8	**L30a**	74 (97:3)	98 (*R*)
9	**L31a**	54 (96:4)	96 (*R*)
10	**L32a**	<5	nd[d]
11	**L37a**	24 (85:15)	75 (*R*)
12	**L37b**	7 (83:17)	73 (*R*)
13	**L37c**	8 (84:16)	64 (*R*)
14[f]	**L29h**	9 (81:19)	56 (*R*)
15[f]	**L37h**	6 (78:22)	21 (*R*)

[a] $[Pd_2(dba)_3]\cdot dba$ (1.25×10^{-2} mmol), **S1** (2.0 mmol), phenyl triflate (0.5 mmol), Ligand (2.8×10^{-2} mmol), THF (3 mL), $^{i}Pr_2NEt$ (1 mmol), T = 50 ºC, t = 24 h. [b] Conversion percentages determined by GC. [c] Enantiomeric excesses measured by GC. [d] Not determined. [e] 72% isolated yield of **4**. [f] t = 48 h.

Concerning the effect of the phosphite moiety on the catalytic performance, we found that bulky *tert*-butyl substituents at both the *ortho* and *para* positions are necessary for high activity and regio- and enantioselectivity (Table 5.3.1, entry 1 vs 2 and 3). To further investigate how enantioselectivity was influenced by the axial chirality of the biaryl moiety, ligands **L29f** and **L29g**, containing different enantiomerically pure trimethylsilyl-substituted binaphthyl moieties, were also tested (Table 5.3.1, entries 6 and 7). The results indicate that there is a cooperative effect between the configuration of the biaryl moiety and the configuration of the ligand backbone on enantioselectivity that results in a matched combination for ligand **L29f**, which contains an *S*-binaphthyl moiety (Table 5.3.1, entry 6). In addition, by comparing the results obtained using ligand **L29c** with those of the related binaphthyl ligands **L29f** and **L29g** (Table 5.3.1, entries 3, 6-7), we can conclude that: a) tropoisomerization in the biphenyl moiety can be controlled if substituents at the *para* position are present, and b) the biphenyl phosphite moieties in ligands **L29a** and **L29b** adopt *S*-configurations upon complexation to palladium.[14]

Finally, after comparing these results with those from phosphite-imidazole ligands **L37**, we found that the presence of an imidazole donor group has a negative effect on activity, regio- and enantioselectivity (Table 5.3.1, entries 11-13 vs 1-3).

To sum up, the best activities, regio- (up to 97%) and enantioselectivities (up to 98%) were obtained with ligand **L29a**, which contains the optimal combination of substituents in the oxazole and in the biaryl phosphite moiety. Interestingly, when this latter result is compared with the enantioselectivities obtained with their corresponding Pd-phosphinite-oxazole/imidazole (Pd-**L29h**/**L37h**) catalytic systems (Table 5.3.1, entries 14 and 15), we can conclude that introducing a phosphite moiety into the ligand design is advantageous. These results also clearly show the

efficiency of using highly modular scaffolds in the ligand design and are among the best that have been reported in the literature.[3a,b,e,k,l,7b,c]

5.3.3.3. Asymmetric Heck reaction of 2,3-dihydrofuran (S1) using other triflate sources under thermal conditions

To further study the potential of these readily available ligands, we also examined **L29**-**L32a**-**h** and **L37a**-**h** in the Pd-catalyzed Heck reaction of **S1** with several aryl triflates. Therefore the effects of the electronic and steric properties of the aryl triflate source on the product outcome were systematically evaluated (Scheme 5.3.3, R= *p*-CH_3-C_6H_4, *p*-NO_2-C_6H_4, 1-naphthyl).

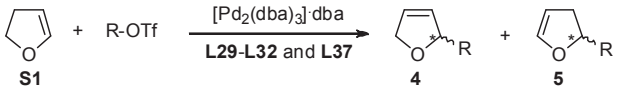

R= *p*-CH_3-C_6H_4, *p*-NO_2-C_6H_4, 1-Naphthyl, 1-Cyclohexenyl

Scheme 5.3.3. Pd-catalyzed Heck reaction of 2,3-dihydrofurane **S1**.

The most noteworthy results are shown in Table 5.3.2 (entries 1-13). They followed the same trends as for the phenylation of **S1**.

Table 5.3.2. Selected results for Pd-catalysed enantioselective arylation of 2,3-dihydrofuran **S1** using ligands **L29**-**L32a**-**h** and **L37a**-**h**[a]

Entry	L	R	% Conv (**4**:**5**)[b]	% Yield **4**	% ee **4**[c]
1	**L29a**	4-CH_3-C_6H_4	69 (92:8)	60	99 (*R*)
2	**L29b**	4-CH_3-C_6H_4	23 (92:8)	18	99 (*R*)
3	**L29c**	4-CH_3-C_6H_4	24 (90:10)	17	92 (*R*)
4	**L29f**	4-CH_3-C_6H_4	23 (92:8)	16	98 (*R*)
5	**L29g**	4-CH_3-C_6H_4	19 (89:11)	15	87 (*R*)
6	**L32a**	4-CH_3-C_6H_4	<5	nd[d]	nd[d]
7	**L37a**	4-CH_3-C_6H_4	21 (84:16)	15	73 (*R*)
8	**L29a**	4-NO_2-C_6H_4	99 (>99:<1)	97	99 (*R*)
9	**L29b**	4-NO_2-C_6H_4	37 (99:1)	34	99 (*R*)
10	**L29c**	4-NO_2-C_6H_4	31 (96:4)	28	97 (*R*)
11	**L32a**	4-NO_2-C_6H_4	<5	nd[d]	nd[d]
12	**L37a**	4-NO_2-C_6H_4	26 (88:12)	21	72 (*R*)
13	**L29a**	1-Naphthyl	98 (95:5)	93	>99 (*R*)
14	**L29a**	1-Cyclohexenyl	92 (99:1)	90	69 (*R*)
15	**L32a**	1-Cyclohexenyl	<5	nd[d]	nd[d]
16	**L37a**	1-Cyclohexenyl	15 (80:20)	9	54 (*R*)

[a] $[Pd_2(dba)_3]$·dba (2.5 x 10^{-2} mmol), **S1** (4.0 mmol), triflate (1 mmol), Ligand (5.6 x 10^{-2} mmol), THF (6 mL), $^iPr_2NEt$ (2 mmol), T = 50 ºC, t = 24 h. [b] Conversion percentages determined by GC or ^{1}H-NMR. [c] Enantiomeric excesses measured by GC or HPLC. [d] Not determined.

Again, the arylated products **4** were accessible in high activities, and high regio- (up to >99%) and enantioselectivities (ee's up to >99%) with Pd/**L29a** catalytic system. The results indicate that both the steric and electronic parameters of the triflate affected mainly regioselectivity, whereas

their effect on enantioselectivity was less important (Table 5.3.2, entries 1, 8 and 13). Thus, regioselectivities are best with the electron-deficient *para*-nitrophenyl triflate. Again, these results are among the best that have been reported in the literature.[3f,k,l,7b]

We next evaluated the ligand library in the Heck reaction of **S1** with cyclohexenyl triflate (eq 2, R= 1-cyclohexenyl; Table 5.3.2, entries 14-16). Although the Pd-catalyst precursors containing ligand **L29a** again provided the alkenylated product **4** in high activity and regioselectivity (up to 99%), enantioselectivity was only moderate (up to 69% ee).

5.3.3.4. Microwave-assisted asymmetric Heck reactions

The benefits of microwave irradiation, including reduction of reaction times and electricity costs, have already been reported in several C-C coupling reactions.[15] In this context we have recently shown that, when microwaves are used as the source of heat, the reaction proceeds much faster and retains excellent enantioselectivity, allowing for a highly selective intermolecular Heck reaction.[7b,16] Therefore, we decided to use ligands **L29**-**L32a**-**h** and **L37a**-**h** to take advantage of microwave irradiation in asymmetric Pd-catalyzed Heck reactions.

We first studied how temperature affected the Pd-catalyzed asymmetric Heck reaction of substrate **S1** using phenyl triflate with ligand **L29a** (Table 5.3.3). We found that the optimal temperature was 70 ºC. At a lower temperature, activities decreased considerably (Table 5.3.3, entries 1 vs 2 and 3). Under these optimized conditions, we evaluated the complete series of ligands. The most noteworthy results are shown in Table 5.3.3 (entries 3-8). Catalytic performance in the Pd-catalyzed phenylation of **S1** under microwave conditions followed the same trend as for the phenylation under thermal conditions. As expected, however, using controlled microwave dielectric heating considerably improved activities (from 24 hours to 30 minutes), while maintaining the excellent regio- (up to 98%) and enantioselectivities (up to 99% ee).

Table 5.3.3. Selected results for the microwave-assisted Pd-catalyzed enantioselective Heck reaction of 2,3-dihydrofuran **S1** using ligands **L29**-**L32a**-**h** and **L37a**-**h**[a]

Entry	L	R	T (ºC)	t (min)	% Conv (**4**:**5**)[b]	% ee **4**[c]
1	**L29a**	C_6H_5	50	30	<5	nd[d]
2	**L29a**	C_6H_5	70	10	48 (98:2)	99 (*R*)
3	**L29a**	C_6H_5	70	30	100 (98:2)	99 (*R*)
4	**L29c**	C_6H_5	70	30	32 (94:6)	92 (*R*)
5	**L30a**	C_6H_5	70	30	96 (98:2)	98 (*R*)
6	**L31a**	C_6H_5	70	30	85 (96:4)	96 (*R*)
7	**L32a**	C_6H_5	70	30	<5	nd[d]
8	**L37a**	C_6H_5	70	30	69 (89:11)	76 (*R*)
9	**L29a**	4-CH_3-C_6H_4	70	30	92 (99:1)	99 (*R*)
10	**L29a**	4-NO_2-C_6H_4	70	30	96 (98:2)	98 (*R*)
11	**L29a**	1-Naphthyl	70	30	92 (97:3)	99 (*R*)
12	**L29a**	1-Cyclohexenyl	80	360	89 (92:8)	89 (*R*)

[a] $[Pd_2(dba)_3]$·dba (1.25 x 10^{-2} mmol), **S1** (2.0 mmol), triflate (0.5 mmol), ligand (2.8 x 10^{-2} mmol), THF (3 mL), $^{i}Pr_2NEt$ (1 mmol). [b] Conversion percentages determined by GC or ^{1}H-NMR. [c] Enantiomeric excesses measured by GC or HPLC. [d] Not determined.

These observations are also true for other aryl triflate sources, so activities, and regio- (up to 99%) and enantioselectivities (up to 99% ee) are excellent (Table 5.3.3, entries 9-11).

Encouraged by these excellent results, we also studied the cyclohexenylation of **S1**, which provided moderate enantioselectivity under thermal conditions (Table 5.3.2, entry 12). After the reaction parameters had been optimized, we found that the optimal temperature was 80 ºC. By using microwave irradiation, enantioselectivity increased up to 89% with a regioselectivity of 92% (Table 5.3.3, entry 12).

5.3.4. Conclusions

We have described the first application of phosphite-oxazole/imidazole ligands in asymmetric intermolecular Pd-catalyzed Heck reactions under thermal and microwave conditions. These ligands are more stable than their oxazoline counterparts, less sensitive to air and other oxidizing agents than phosphines and phosphinites, and easy to synthesize from readily available alcohols. In addition, they can be easily tuned in the oxazole and biaryl phosphite moieties, so that their effect on catalytic performance can be explored. We found that regio- and enantioselectivities and activities are highly influenced by the ligand components. By carefully selecting them, excellent activities (up to 100% conversion in 30 minutes) and regio- (up to >99%) and enantioselectivities (up to 99% ee) were obtained using several triflate sources. The use of microwave irradiation conditions allowed considerably shorter reaction times maintaining excellent regio- and enantioselectivities. In addition, the efficiency of this ligand design is also corroborated by the fact that these Pd-phosphite-oxazole/imidazole catalysts provided higher enantioselectivity than their phosphinite analogues. These results open up a new class of robust phosphite-oxazole ligands for the highly active and enantioselective Pd-catalyzed Heck reaction, which will be of great practical interest.

5.3.5. Experimental section

5.3.5.1. General considerations

All syntheses were performed with standard Schlenk techniques under argon atmosphere. Solvents were purified by standard procedures. Ligands **L29**-**L32a**-**h** and **L29d** were synthesized as previously described.[9,10] All other reagents were used as commercially available. ^{1}H, $^{13}C\{^{1}H\}$ and $^{31}P\{^{1}H\}$ NMR spectra were recorded on a 400 MHz spectrometer. The chemical shifts are referenced to tetramethylsilane (^{1}H and ^{13}C) as internal standard or H_3PO_4 (^{31}P) as external standard. The ^{1}H and ^{13}C NMR spectral assignments were determined by ^{1}H-^{1}H and ^{1}H-^{13}C correlation spectra. Microwave experiments were carried out using a CEM Explorer, in which the temperature is controlled by a non-contact infrared sensor that is located beneath the cavity floor and "looks" up to the bottom of the vessel.

5.3.5.2. General procedure for the preparation of ligands L37a-c

The corresponding phosphorochloridite (1.5 mmol) produced *in situ* was dissolved in toluene (6 mL) and pyridine (0.57 mL, 12 mmol) was added. Hydroxyl-imidazole **3**[12] (333.6 mg, 1.4 mmol) was azeotropically dried with toluene (3 x 2 mL) and then dissolved in toluene (6 mL) to which

pyridine (0.57 mL, 12 mmol) was added. The imidazole solution was transferred slowly at 0 ºC to the solution of phosphorochloridite. The reaction mixture was stirred overnight at 80 ºC, and the pyridine salts were removed by filtration. Evaporation of the solvent gave a white foam, which was purified by flash chromatography in alumina (toluene/NEt_3= 100/1) to produce the corresponding ligand as a white solid.

L37a: Yield: 0.67 g, 71 %. ^{31}P NMR (400 MHz, C_6D_6), δ: 143.0 (s). ^{1}H NMR (400 MHz, C_6D_6), δ: 1.25 (br, 36H, CH_3, ^{t}Bu), 2.97 (s, 3H, CH_3-N), 6.86 (d, 1H, CH-O, *J*= 9.2 Hz), 6.76-7.92 (m, 13H, CH=). ^{13}C NMR (400 MHz, C_6D_6), δ: 30.7 (CH_3-N), 31.8 (CH_3, ^{t}Bu), 32.5 (CH_3, ^{t}Bu), 35.6 (C, ^{t}Bu), 36.3 (C, ^{t}Bu), 75.3 (d, C-O, $J_{C\text{-}P}$ = 8.4 Hz), 110-155 (aromatic carbons). Anal. Calc (%) for $C_{43}H_{53}N_2O_3P$: C 76.30, H 7.89, N 4.14; found C 76.35, H 7.92, N 4.11.

L37b: Yield: 0.47 g, 54 %. ^{31}P NMR (400 MHz, C_6D_6), δ: 143.1 (s). ^{1}H NMR (400 MHz, C_6D_6), δ: 1.23 (s, 9H, CH_3, ^{t}Bu), 1.25 (s, 9H, CH_3, ^{t}Bu), 3.09 (s, 3H, CH_3-N), 3.32 (s, 3H, CH_3-O), 3.34 (s, 3H, CH_3-O), 6.80 (d, 1H, CH-O, *J*= 7.2 Hz), 6.72-7.98 (m, 13H, CH=). ^{13}C NMR (400 MHz, C_6D_6), δ: 30.3 (CH_3-N), 31.1 (CH_3, ^{t}Bu), 35.7 (C, ^{t}Bu), 55.5 (CH_3-O), 74.9 (d, C-O, $J_{C\text{-}P}$ = 13 Hz), 110-155 (aromatic carbons). Anal. Calc (%) for $C_{37}H_{41}N_2O_5P$: C 71.14, H 6.62, N 4.48; found C 71.21, H 6.68, N 4.43.

L37c: Yield: 0.53 g, 63 %. ^{31}P NMR (400 MHz, C_6D_6), δ: 143.7 (s). ^{1}H NMR (400 MHz, C_6D_6), δ: 0.16 (s, 9H, CH_3-Si), 0.19 (s, 9H, CH_3-Si), 3.00 (s, 3H, CH_3-N), 6.89 (d, 1H, CH-O, *J*= 9.2 Hz), 6.84-8.00 (m, 15H, CH=). ^{13}C NMR (400 MHz, C_6D_6), δ: 0.0 (CH_3-Si), 0.1 (CH_3-Si), 30.1 (CH_3-N), 74.2 (d, C-O, $J_{C\text{-}P}$ = 3.8 Hz), 110-155 (aromatic carbons). Anal. Calc (%) for $C_{33}H_{37}N_2O_3PSi_2$: C 66.41, H 6.25, N 4.69; found C 66.38, H 6.21, N 4.71.

5.3.5.3. Procedure for the preparation of ligand L37h

A solution of chlorodiphenylphosphine (0.14 mL, 0.77 mmol) in THF (3 mL) was slowly added at 0 ^{o}C to a solution of **3** (166.8 mg, 0.7 mmol) and 18.3 mg (0.15 mmol) of DMAP in pyridine (1 mL). The reaction mixture was stirred overnight at room temperature. Ether ethylic was then added and the pyridine salts were removed by filtration. The residue was purified by flash chromatography (eluent: toluene/NEt_3 100/1, Rf. 0.9) to produce 0.10 g (34 %) of a colorless oil. ^{31}P NMR (400 MHz, C_6D_6), δ: 99.8 (s). ^{1}H NMR (400 MHz, C_6D_6), δ: 2.94 (s, 3H, CH_3-N), 6.43 (m, 1H, CH-O), 6.7-8.0 (m, 19H, CH=). ^{13}C NMR (400 MHz, C_6D_6), δ: 30.3 (CH_3-N), 69.8 (b, CH-O), 110-155 (aromatic carbons). Anal. Calc (%) for $C_{27}H_{23}N_2OP$: C 76.76, H 5.49, N 6.63; found C 76.75, H 5.51, N 6.61.

5.3.5.4. General procedure for Pd-catalyzed enantioselective Heck reactions

A mixture of $[Pd_2(dba)_3]dba$ (12 mg, 1.25 x 10^{-2} mmol) and the appropriate chiral ligand (2.8 x 10^{-2} mmol) in dry degassed THF (3.0 mL) was stirred under argon at room temperature for 15 min. The olefin (2.0 mmol), triflate (0.50 mmol) and base (1.0 mmol) were added to the catalyst solution. The solution was stirred at the desired temperature under argon. After the desired reaction time, the mixture was diluted with additional diethyl ether and washed with water, dried over $MgSO_4$, and evaporated. For compounds 2-(1-naphthyl)-2,5-dihydrofuran and 2-(4-nitrophenyl)-2,5-dihydrofuran, conversion and regioselectivity were measured by ^{1}H-NMR and

enantioselectivity was measured by HPLC.[3b] For the rest of the compounds, conversion and selectivity were determined by GC.[3e]

5.3.6. Acknowledgements

We thank the Spanish Government (Consolider-Ingenio CSD2006-0003, CTQ2010-15835/BQU, 2008PGIR/07 to O. Pàmies and 2008PGIR/08 to M. Diéguez and ICREA Academia award to M. Diéguez) and the Catalan Government (2009SGR116), COST D40, Vetenskapsrådet (VR), and Astra Zeneca for support. Knut and Alice Wallenbergs Stiftelse are also greatfully acknowledged for generous financial support.

5.3.7. References

[1] For recent reviews, see: a) Coeffard, V.; Guiry, P. J. *Current Organic Chemistry* **2010**, *14*, 212. b) *Mizoroki-Heck Reaction*; Oestreich, M., Ed.; Wiley-VCH: Weinheim, 2009. c) Tietze, L. T.; Ila, H.; Bell, H. P. *Chem Rev.* **2004**, *104*, 3453. d) Dai, L.X.; Tu, T.; You, S. L.; Deng, W. P.; Hou, X. L. *Acc. Chem. Res*. **2003**, *36*, 659. e) Bolm, C.; Hildebrand, J. P.; Muñiz, K.; Hermanns, N. *Angew. Chem., Int. Ed.* **2001**, *44*, 3284. f) Shibasaki, M.; Vogl E. M. *in Comprehensive Asymmetric Catalysis*; Jacobsen, E.N., Pfaltz, A., Yamamoto, H., Eds.; Springer: Heidelberg, 1999. g) Loiseleur, O.; Hayashi, M.; Keenan, M.; Schemees, N.; Pfaltz, A. *J. Organomet. Chem*. **1999**, *576*, 16. h) Beller, M.; Riermeier, T. H.; Stark G. in *Transition Metals for Organic Synthesis*; Beller, M., Bolm, C., Eds.; Wiley-VCH: Weinheim, 1998.

[2] For representative examples on the use of diphosphines in the intermolecular version, see: a) Ozawa, F.; Kubo, A.; Hayashi, T. *J. Am. Chem. Soc.* **1991**, *113*, 1417. b) Trabesinger, G.; Albinati, A.; Feiken, N.; Kunz, R. W.; Pregosin, P. S.; Tschoerner, M. *J. Am. Chem. Soc.* **1997**, *119*, 6315. c) Tschoerner, M.; Pregosin, P. S.; Albinati, A. *Organometallics* **1999**, *18*, 670. d) Tietze, L. F.; Thede, K.; Sannicolò, F. *Chem. Commun.* **1999**, 1811. e) Andersen, N. G.; Parvez, M.; Keay, B. A. *Org. Lett.* **2000**, *2*, 2817.

[3] For phosphine-oxazoline ligands, see for instance: a) Loiseleur, O.; Meier, P.; Pfaltz, A. *Angew. Chem., Int. Ed. Engl.* **1996**, *35*, 200. b) Loiseleur, O.; Hayashi, M.; Schmees, N.; Pfaltz, A. *Synthesis* **1997**, 1338. c) Tu, T.; Hou, X.L.; Dai, L.X. *Org. Lett.* **2003**, **5**, 3651. d) Gilbertson, S. R.; Xie, D.; Fu, Z. *J. Org. Chem.* **2001**, *66*, 7240. e) Gilbertson, S. R.; Fu, Z. *Org. Lett.* **2001**, *3*, 161. f) Tu, T.; Deng, W.P.; Hou, X.L.; Dai, L.X.; Dong, X.C. *Chem. Eur. J.* **2003**, *9*, 3073. g) Gilbertson, S. R.; Genov, D. G.; Rheingold, A. L. *Org. Lett.* **2000**, *2*, 2885. h) Hashimoto, Y.; Horie, Y.; Hayashi, M.; Saigo, K. *Tetrahedron: Asymmetry* **2000**, *11*, 2205. i) Hou, X. L.; Dong, D. X.; Yuan, K. *Tetrahedron: Asymmetry* **2004**, *15*, 2189. j) Liu, D.; Dai, Q.; Zhang, X. *Tetrahedron* **2005**, *61*, 6460. k) Wu, W.-Q.; Peng, Q.; Dong, D.-X.; Hou, X.-L.; Wu, Y.-D. *J. Am. Chem. Soc.* **2008**, *130*, 9717. l) Rubina, M.; Sherrill, W. M.; Rubin, M. *Organometallics* **2008**, *27*, 6393. m) Fitzpatrick, M. O.; Müller-Bunz, H.; Guiry, P. J. *Eur. J. Org. Chem.* **2009**, 1889. n) Kilroy, T. G.; Hennessy, A. J.; Connolly, D. J.; Malone, Y. M.; Farrell, A.; Guiry, P. J. *J. Mol. Catal. A.: Chem.* **2003**, *196*, 65. o) Ogasawara, M.; Yoshida, K.; Kamei, H.; Kato, K.; Uozumi, Y.; Hayashi, T. *Tetrahedron: Asymmetry* **1998**, *9*, 1779. p) Hennessy, A. J.; Malone, Y. M.; Guiry, P. J. *Tetrahedron Lett.* **1999**, *40*, 9163. q) Hennessy, A. J.; Connolly, D. J.; Malone, Y. M.; Guiry, P. J. *Tetrahedron Lett.* **2000**, *41*, 7757. r) Gilbertson, S. R.; Xie, D.; Fu, Z. *Tetrahedron Lett.* **2001**, *42*, 365. s) Kilroy, T. G.; Cozzi, P.-G.; End, N.; Guiry, P. J. *Synlett* **2004**, 106. t) Kilroy, T. G.; Cozzi, P.-G.; End, N.; Guiry, P. J. *Synthesis* **2004**, 1879.

[4] For other successful type of P,N-ligands such as phosphinite-oxazoline, phosphine-pyridine derivatives, phosphine-thiazole and phosphine-imidazole ligands, see: a) Yonehara, K.; Mori, K.; Hashizume, T.; Chung, K. G.; Ohe, K.; Uemura, S. *J. Organomet. Chem*. **2000**, *603*, 40. b) Drury III, W. J.; Zimmermann, N.; Keenan, M.; Hayashi, M.; Kaiser, S.; Goddard, R.; Pfaltz, A. *Angew. Chem. Int. Ed.* **2004**, *43*, 70. c) Henriksen, S. T.; Norrby, P. O.; Kaukoranta, P.; Andersson, P. G. *J. Am. Chem. Soc.* **2008**, *130*, 10414. d) Busacca, C. A.; Grossbach, D.; So, R. C.; O'Brien, E. M.; Spinelli, E. M. *Org. Lett.* **2003**, *5*, 595.

[5] For representative examples, see: Hydrogenation: a) Reetz, M. T.; Mehler, G. *Angew. Chem., Int. Ed.* **2000**, *39*, 3889. b) Ojima, I.; Takai, M.; Takahashi, T. PCT Int. Appl. WO 2004078766 A1, **2004**. c) Mazuela, J.; Verendel, J. J.; Coll, M.; Schäffner, B.; Börner, A.; Andersson, P. G.; Pàmies, O.; Diéguez, M. *J. Am. Chem. Soc.* **2009**, *131*, 12344. Hydroformylation: d) Diéguez, M.; Pàmies, O.; Ruiz, A.; Castillón, S.; Claver, C. *Chem. Eur. J.* **2001**, *7*, 3086. e) Buisman, G. J. H.; van der Veen, L. A.; Klootwijk, A.; de Lange, W. G. J.; Kamer, P. C. J.; van Leeuwen, P. W. N. M.; Vogt, D. *Organometallics* **1997**, *16*, 2929. f) Diéguez, M.; Pàmies, O.; Claver, C. *Chem. Commun.* **2005**, 1221. Conjugated addition: g) Yan, M.; Zhou, Z.-Y.; Chan, A. S. C. *Chem. Commun.* **2000**, 115. h) Diéguez, M.; Ruiz, A.; Claver, C. *Tetrahedron: Asymmetry* **2001**, *12*, 2895. i) Alexakis, A.; Benhaim, C.; Rosset, S.; Humam, M. *J. Am. Chem. Soc.* **2002**, *124*, 5262. Allylic substitution: j) Diéguez, M.; Pàmies, O. *Acc. Chem. Res.* **2010**, *43*, 312.

[6] For some representative reviews, see: a) Claver, C.; Pàmies, O.; Diéguez, M. Chiral *Diphosphinites, Diphosphonites, Diphosphites and Mixed PO-Ligands,* in *Phosphorous Ligands in Asymmetric Catalysis*; Börner, A., Eds.; Wiley-VCH: Weinheim, 2008, *Chapter 3*, vol. 2. b) Diéguez, M.; Pàmies, O.; Ruiz, A.; Claver, C. in *Methodologies in Asymmetric Catalysis*; Malhotra, S. V., Eds.; ACS: Washington, 2004, pp. 161.

[7] a) Mata, Y.; Pàmies, O.; Diéguez, M. *Org. Lett.* **2005**, *7*, 5597. b) Mata, Y.; Pàmies, O.; Diéguez, M. *Chem. Eur. J.* **2007**, *13*, 3296. c) Mazuela, J.; Pàmies, O.; Diéguez, M. *Chem. Eur. J.* **2010**, *16*, 3434.

[8] *Heterocyclic Chemistry*, Fourth Edition; Joule, J. A.; Mills, K., Eds.; Blackwell Science Ltd.: Oxford, 2000.

[9] Mazuela, J.; Paptchikhine, A.; Tolstoy, P.; Pàmies, O.; Diéguez, M.; Andersson, P. G. *Chem. Eur. J.* **2010**, *16*, 620.

[10] Källström, K.; Hedberg, C.; Brandt, P.; Bayer, A.; Andersson, P. G. *J. Am. Chem. Soc.* **2004**, *126*, 14308.

[11] Asakawa, K.; Dannenberg, J. J.; Fitch, K. J.; Hall, S. S.; Kadowaki, C.; Karady, S.; Kii, S.; Maeda, K.; Marcune, B. F.; Mase, T.; Miller, R. A.; Reamera, R. A.; Tschaen, D. M. *Tetrahedron Letters* **2005**, *46*, 5081.

[12] Torrens, A.; Castrillo, J. A.; Claparols, A.; Redondo, J. *Synlett* **1999**, 765.

[13] Pàmies, O.; Diéguez, M.; Net, G.; Ruiz, A.; Claver, C. *Organometallics* **2000,** *19,* 1488.

[14] The rapid ring inversion (tropoisomerization) in the biaryl phosphite moiety is usually stopped upon coordination to the metal center. See for example: a) Diéguez, M.; Pàmies, O. *Chem. Eur. J.* **2008**, *14*, 3653. b) Pàmies, O.; Diéguez, M. *Chem. Eur. J.* **2008**, *14*, 944.

[15] See for instance: *Microwave Assisted Organic Synthesis*; Tierney, J. P.; Lidström, P., Eds.; Blackwell Publishing Ltd.: Oxford, 2005 and references therein.

[16] Kaukoranta, P.; Källström, K.; Andersson, P. G. *Adv. Synth. Catal.* **2007**, *349*, 2595.

5.3.8. Supporting information

Examples of the temperature, power and pressure vs time profiles for the microwave experiments are included.

Table 5.3.3, entry 3

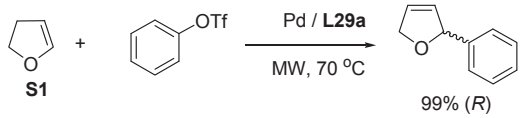

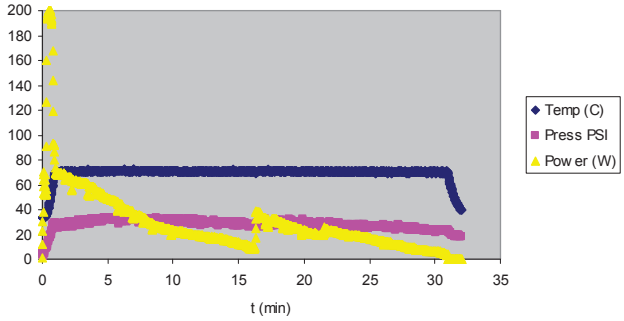

Table 5.3.3, entry 9

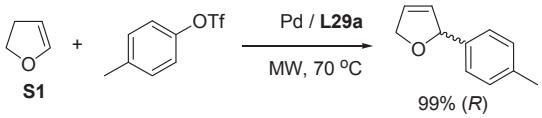

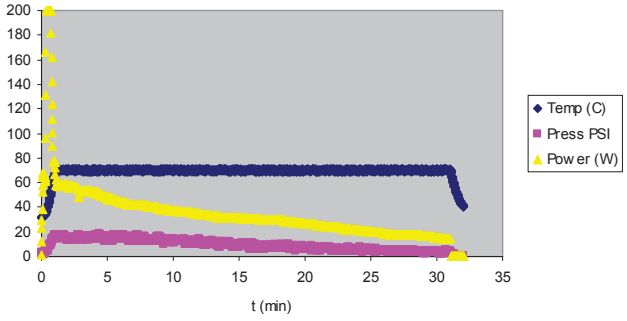

Table 5.3.3, entry 10

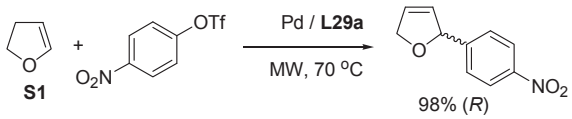

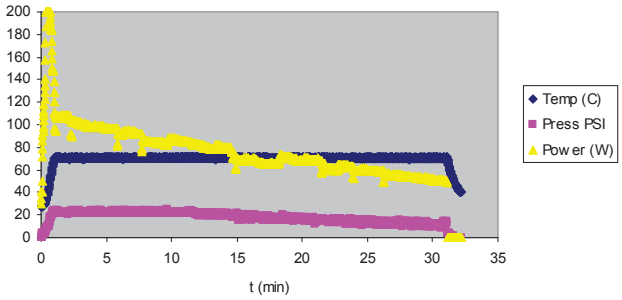

Table 5.3.3, entry 11

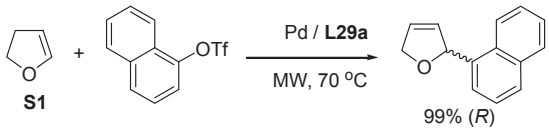

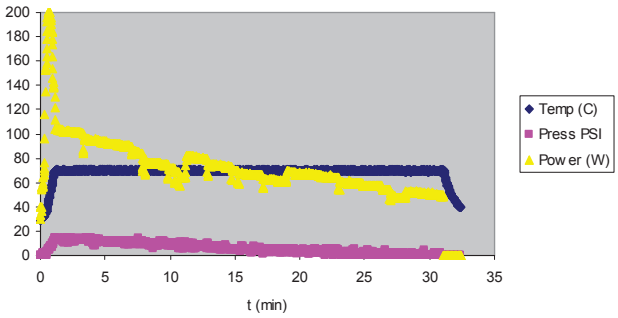

Table 5.3.3, entry 12

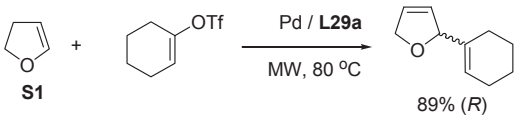

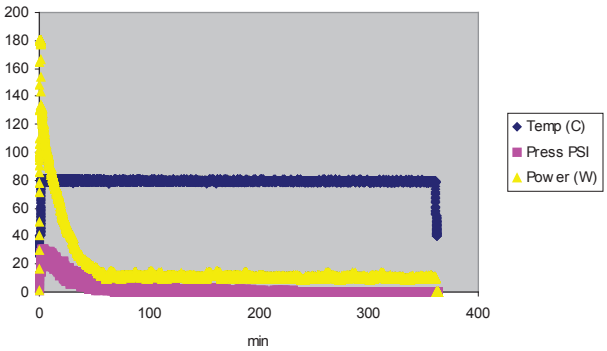

Chapter 6

Asymmetric hydroformylation

6. Asymmetric hydroformylation

6.1. Background

Asymmetric hydroformylation has attracted much attention as a potential tool for preparing enantiomerically pure aldehydes. Despite its importance, asymmetric hydroformylation is less developed than for example hydrogenation. Traditionally, vinylarenes have been the most studied substrates. Although Rh-diphosphites and Rh-BINAPHOS-type phosphine-phosphites have proved to be the most efficient catalytic systems, recently diphospholane, bis-(diazaphospholodine) and phosphine-phosphoroamidite have emerged as suitable alternatives. The use of these latter ligands has allowed the successful Rh-catalyzed hydroformylation of other type of substrates, like allyl cyanide, vinyl acetate and some byciclic olefins. However more research is still needed to expand the range of substrates to be studied. In this respect, few studies have been made on the asymmetric hydroformylation of heterocyclic olefins, which provide access to important building blocks for synthesizing natural products and pharmaceuticals. This is mainly because, for this kind of substrate, as well as having to control the enantioselectivity of the process, chemo- and regio-selectivity are often a problem. For a considerable time, only the phosphine-phosphite BINAPHOS ligand provided good regio- and enantiocontrol in the Rh-catalyzed asymmetric hydroformylation of heterocyclic compounds. In 2005, we reported the first successful application of a diphosphite ligand in the Rh-catalyzed asymmetric hydroformylation of 2,5- and 2,3-dihydrofurans. Despite this success, other diphosphite ligands have not yet been reported and the possibilities offered by diphosphites as new ligands for this process still need to be studied.

Most of the ligands reported to date for Rh-catalyzed hydroformylation have been designed with the advantages of bidentate ligands in mind. Although chiral monodentate ligands have recently proved to be highly efficient in several asymmetric catalytic transformations (i.e. hydrogenation, 1,2- and 1,4-additions, etc.), there have been rarely used in hydroformylation. In 2004, Ojima and coworkers reported the successful application of chiral biphenyl monophosphoroamidite ligands for the challenging Rh-catalyzed asymmetric hydroformylation of allyl cyanide. Despite this success, to our knowledge monophosphoroamidites have not been applied to other substrates and, therefore, the scope of catalyst systems containing monodentate P-ligands needs to be verified.

In this chapter, we therefore report the screening of diphosphite, monophosphoroamidite and N-phosphine ligands in the asymmetric Rh-catalyzed hydroformylation of heterocyclic olefins and styrene. We also present a preliminary study on the hydroformylation of 1,1'-disubstituted terminal enol esters. More specifically, in section 6.2 we screened a large series of diphosphite ligands to study the effect of the ligand backbone, the length of the bridge and the substituents of the biphenyl moieties and to determine the scope of this type of ligand in the Rh-catalyzed asymmetric hydroformylation of several heterocylic olefins. By carefully selecting the ligand components, we achieved high chemo-, regio- and enantioselectivities in different substrate types. Unprecedentedly high enantioselectivities for five-membered heterocyclic olefins were therefore obtained. For the seven-membered heterocyclic dioxepines, our results are among the best obtained. In next section 6.3, we screened a large biaryl-based monophosphoroamidite and

aminophosphine ligand library in the Rh-catalyzed asymmetric hydroformylation of several vinylarenes and heterocyclic olefins. Enantioselectivities were moderate in the hydroformylation of several vinylarenes and promising for the more challenging heterocyclic olefins. Finally, in section 6.4, we report our preliminary results on the Rh-catalyzed hydroformylation of isopropenyl acetate. The screening of several achiral ligands (phosphine and phosphite) and the study of several reaction conditions have permitted the formation of desired linear 3-acetoxybutanal as a major product, minimizing the byproducts formation from hydrogenation and decomposition.

6.2. Rh-catalyzed asymmetric hydroformylation of heterocyclic olefins using chiral diphosphite ligands. Scope and limitations

Javier Mazuela, Mercedes Coll, Oscar Pàmies and Montserrat Diéguez in *J.Org.Chem.* **2009**, *74*, 5440.

6.2.1. Abstract

We used a series of diphosphite ligands to study the effect of the ligand backbone, the length of the bridge and the substituents of the biphenyl moieties and determine the scope of this type of ligand in the Rh-catalyzed asymmetric hydroformylation of several hetereocylic olefins. By carefully selecting the ligand components, we achieved high chemo-, regio- and enantioselectivities in different substrate types. Unprecedentedly high enantioselectivities for five-membered heterocyclic olefins were therefore obtained. Note that both enantiomers of the hydroformylation products can be synthesized using the same ligand by simple substrate change. For the seven-membered heterocyclic dioxepines, our results are among the best obtained. Also, both enantiomers of the hydroformylation products can be obtained by using pseudoenantiomer ligands or by carefully tuning the ligand parameters.

6.2.2. Introduction

Asymmetric hydroformylation has attracted much attention as a potential tool for preparing enantiomerically pure aldehydes. [1] Despite its importance, asymmetric hydroformylation is underdeveloped compared to other processes such as hydrogenation. Traditionally, vinylarenes have been the most studied substrates. Although Rh-diphosphites and Rh-BINAPHOS-type phosphine-phosphites have proved to be the most efficient catalytic systems,[2] recently diphospholane[3], bis-(diazaphospholodine)[4] and phosphine-phosphoroamidite[5] have emerged as suitable alternatives. The use of these latter ligands has allowed the successful Rh-catalyzed hydroformylation of other type of substrates, like allyl cyanide, vinyl acetate and some byciclic olefins.[3,4,5] However more research is still needed to expand the range of substrates to be studied. In this respect, few studies have been made on the asymmetric hydroformylation of heterocyclic olefins, which provide access to important building blocks for synthesizing natural products and pharmaceuticals.[6] This is mainly because, for this kind of substrate, as well as having to control the enantioselectivity of the process, chemo- and regio-selectivity are often a problem.[6,7] For example, in the hydroformylation of 2,5-dihydrofuran **S1** the expected product is tetrahydrofuran-3-carbaldehyde **1** (Scheme 6.2.1). However, considerable amounts of 2,3-dihydrofuran **S2** and tetrahydrofuran-2-carbaldehyde **2** can also be formed due to an isomerization process that takes place simultaneously with the hydroformylation reaction. When the 2,5-dihydrofuran **S1** reacts with the rhodium hydride complex, the 3-alkyl intermediate is formed. This can evolve to 2,3-dihydrofuran **S2** via the β-hydride elimination reaction. Similarly, this new substrate can evolve to produce the 2-alkyl and 3-alkyl intermediates. Although the formation of the 3-alkyl intermediate is

thermodynamically favoured, the acylation occurs faster in the 2-alkyl intermediate.[6b] Regioselectivity is therefore dominated by the rate at which the acyl complex is formed.

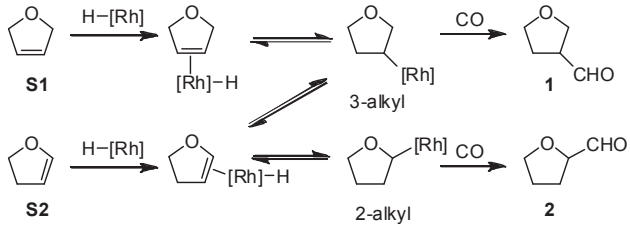

Scheme 6.2.1. Proposed mechanism for the isomerization process.

For a considerable time, only the phosphine-phosphite BINAPHOS ligand provided good regio- and enantiocontrol in the Rh-catalyzed asymmetric hydroformylation of heterocyclic compounds.[8] Several diphosphine,[6c] including some diphospholanes and the bis-(diazaphospholodine) ESPHOS ligand,[9] have been applied but with little success (ee's up to 32%). When diphosphites were used as ligands for the Rh-catalyzed hydroformylation of vinylarenes, activities and enantioselectivities were comparable to the best in the literature, obtained using the BINAPHOS ligand.[2] However, they have been used very little in the hydroformylation of heterocyclic substrates. This is mainly because extensive isomerization had been observed when phosphite ligands are used.[7]

In 2005, we reported the first successful application of a diphosphite ligand in the Rh-catalyzed asymmetric hydroformylation of 2,5- and 2,3-dihydrofurans.[10] Despite this success, other diphosphite ligands have not yet been reported and the possibilities offered by diphosphites as new ligands for this process still need to be studied. To fully investigate these possibilities, in this paper we extend our previous study (2005) to other diphosphite ligands (Figure 6.2.1) and other types of heterocyclic olefins.

To do so, we have synthesized and screened a library of 64 potential diphosphite ligands (Figure 6.2.1).[11] The ligands we have chosen are representative of the most successfully applied families of diphosphite ligands in hydroformylation (CHIRAPHITE **L52**, sugar-derivatives **L53** and **L56**, and KELLIPHITE **L66**). We have also evaluated systematic modifications of several ligand parameters in these prominent ligands, which are known to have an important effect on catalytic performance. Therefore, with this library, we have investigated how the ligand backbone, the length of the bridge and the substituents of the biphenyl moieties affected activities and selectivities (chemo-, regio- and enantioselectivity). By carefully selecting these elements, we have achieved high regio- and enantioselectivities and activities in different substrates.

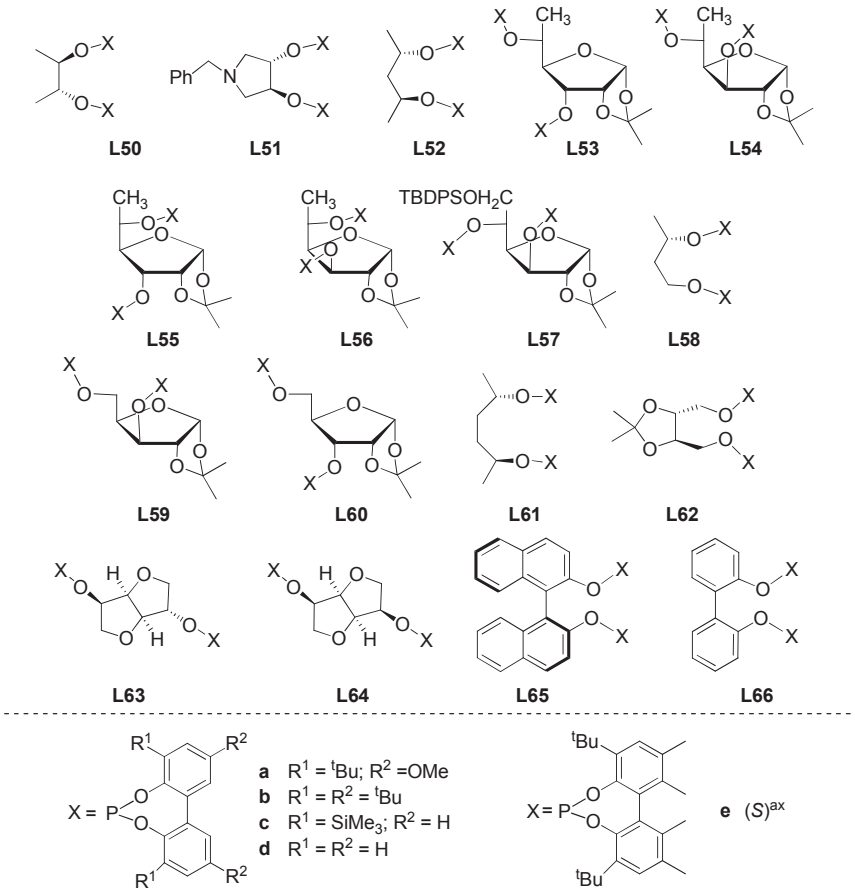

Figure 6.2.1. Disphosphite ligands **L50**-**L66a-e** used in the Rh-catalyzed asymmetric hydroformylation of heterocyclic olefins.

6.2.3. Results and Discussions

6.2.3.1. Asymmetric hydroformylation of five-membered heterocyclic olefins

Diphosphite ligands **L50**-**L66a**-**e** were first used in the Rh-catalyzed asymmetric hydroformylation of 2,5-dihydrofuran **S1**. The catalysts were prepared in situ by adding the corresponding diphosphite ligand to [Rh(acac)(CO)$_2$] as a catalyst precursor.

Initially, we determined the optimal reaction conditions by conducting a series of experiments with ligand **L59a** in which the ligand-to-rhodium ratio, CO/H$_2$ pressure ratio, temperature, reaction time and substrate-to-rhodium ratio were varied (Table 6.2.1).

Varying the ligand-to-rhodium ratio showed that the combination of chemo-, regio- and enantioselectivities was best when 2 equiv of ligand was used (Table 6.2.1, entries 1-3). A lower ligand-to-rhodium ratio decreased the regio- and enantioselectivities in aldehyde **1** (Table 6.2.1, entry 1), while a higher ligand-to-rhodium ratio negatively affected chemoselectivity and increased the formation of isomerized product **1** (Table 6.2.1, entry 3).

It is generally accepted that isomerization occurs as a result of competition between the β-hydride elimination process and CO insertion (Scheme 6.2.1). Since a high CO pressure is needed to suppress isomerization, we conducted experiments with increased CO partial pressure. This did not affect the rate of hydroformylation *vs* isomerization (Table 6.2.1, entries 2 *vs* 5), though decreasing the CO/H_2 pressure ratio negatively affected chemoselectivity, which increased the formation of isomerized product **1** (Table 6.2.1, entries 2 *vs* 6).

Table 6.2.1. Rh-catalyzed asymmetric hydroformylation of **S1** using ligand **L59a**. Optimization of the reaction conditions[a]

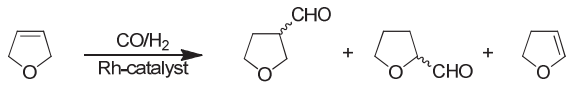

S1 **1** **2** **S2**

Entry	Ligand	**L**/Rh	CO/H_2	% Conv.[b]	% Ald. (**1**:**2**)[c]	% **S2**[d]	% ee of **1**[e]
1	**L59a**	1.1	1	100	82 (89:11)	18	31 (*S*)
2	**L59a**	2	1	100	88 (100:0)	12	53 (*S*)
3	**L59a**	4	1	100	75 (100:0)	25	53 (*S*)
4[f]	**L59a**	2	1	100	98 (95:5)	2	37 (*S*)
5	**L59a**	2	2	100	87 (100:0)	13	53 (*S*)
6	**L59a**	2	0.5	91	59 (100:0)	32	52 (*S*)
7[f,g]	**L59a**	2	1	100	100 (92:8)	0	34 (*S*)
8[h]	**L59a**	2	1	26	13 (100:0)	13	54 (*S*)
9[i]	**L59a**	2	1	100	94 (98:2)	6	51 (*S*)

[a] P= 18 bar. $[Rh(acac)(CO)_2]$ (0.012 mmol). **S1**/Rh= 400. Toluene (5 mL). T= 45 °C. t= 24 h. [b] Total conversion measured by ^{1}H NMR. [c] Conversion into aldehydes determined by ^{1}H NMR. [d] Isomerization measured by ^{1}H NMR. [e] Enantioselectivity of **1** measured by ^{1}H NMR using $Eu(hfc)_3$ on the corresponding methyl ester. [f] t= 48 h. [g] **S1**/Rh= 200. [h] T = 25 ºC. [i] T = 65 ºC.

A prolonged reaction time increased conversion into aldehydes (Table 6.2.1, entry 4) but decreased regio- and enantioselectivity in the desired product **1** (Table 6.2.1, entry 2 vs 4). To study whether the hydroformylation of the formed isomer 2,3-dihydrofuran **S2** accounts for this lost of selectivity, we performed the hydroformylation of **S2** under the same reaction conditions. After 48 hours, the hydroformylation of **S2** afforded a 78:22 mixture of (*R*)-**1** (48% ee) and **2** in 88% conversion (Table 6.2.3, entry 11). By comparing these results we concluded that the loss of regioselectivity with the prolonged reaction time was due to the hydroformylation of the 2,3-dihydrofuran **S2** formed under reaction conditions. This also caused a loss of enantioselectivity because the absolute configuration of the predominant enantiomer of **1** obtained from **S2** is *R*, which is opposite to that which is obtained from **S1**. These results show that the absence of isomerization of the substrate is important for achieving high enantioselectivity from the reaction of **S1**. Indeed, the ee of **1** dropped when the hydroformylation of **S2** (which is formed from the isomerization of **S1**) took place at a low ligand-to-rhodium ratio (Table 6.2.1, entry 1). Accordingly, a decrease in the substrate-to-rhodium ratio had a negative effect on regio- and enantioselectivity because of the hydroformylation of the isomerization product **S2** (Table 6.2.1, entry 7).

Varying the temperature strongly affects chemo- and regioselectivity (Table 6.2.1, entries 2, 8 and 9). Increasing the temperature negatively affected regioselectivity, whereas lowering the temperature to 25 ºC negatively affected activity and chemoselectivity. This is because at high

temperature hydroformylation of the isomerized 2,3-dihydrofuran **S2** takes place. The best trade-off between chemo- and regioselectivities was therefore achieved at 45 ºC.

For the purpose of comparison, the other ligands were tested under optimized conditions (i.e. ligand-to-rhodium ratio of 2, $P_{CO/H2}$= 1, 24 h reaction time at 45 °C). Our results indicate that selectivity is affected by the length of the bridge, the backbone of the ligand and the substituents of the biphenyl moieties (see Table 6.2.2). In no cases were hydrogenated or polymerized products of 2,5-dihydrofuran observed.

Table 6.2.2. Rh-catalyzed hydroformylation of **S1** using ligands **L50-L66a-e**[a]

Entry	Ligand	% Conv.[b]	% Ald. (**1**:**2**)[c]	% **S2**[d]	% ee of **1**[e]
1	**L50a**	100	100 (72:28)	0	< 5
2	**L51a**	100	70 (97:3)	30	6 (*S*)
3	**L52a**	100	99 (95:5)	1	23 (*R*)
4	**L53a**	100	92 (98:2)	8	47 (*R*)
5	**L54a**	100	99 (99:1)	1	74 (*S*)
6	**L54b**	98	86 (98:2)	12	43 (*S*)
7	**L54c**	100	98 (99:1)	2	63 (*S*)
8	**L54d**	76	64 (99:1)	8	< 5
9	**L55a**	90	75 (96:4)	15	27 (*R*)
10	**L56a**	100	94 (98:2)	6	25 (*R*)
11	**L57a**	100	92 (97:3)	8	61 (*S*)
12	**L58a**	100	100 (85:15)	0	14 (*R*)
13	**L59a**	100	88 (100:0)	12	53 (*S*)
14	**L59b**	73	66 (98:2)	7	15 (*S*)
15	**L59c**	100	89 (99:1)	11	34 (*S*)
16	**L59d**	61	55 (99:1)	6	< 5
17	**L60a**	100	91 (95:5)	9	24 (*R*)
18	**L60b**	100	100 (77:23)	0	5 (*S*)
19	**L61a**	100	100 (64:36)	0	< 5
20	**L62a**	100	100 (99:1)	0	< 5
21	**L63a**	100	100 (78:22)	0	7 (*S*)
22	**L64a**	100	100 (82:18)	0	<5
23	**L65a**	100	100 (96:4)	0	15 (*R*)
24	**L66e**	100	100 (100:0)	0	24 (*R*)
25[f]	**BINAPHOS**	100	100 (100:0)	0	64 (*R*)

[a] P= 18 bar. [Rh(acac)$(CO)_2$] (0.012 mmol). **S1**/Rh= 400. Toluene (5 mL). T= 45 °C. t= 24 h. [b] Total conversion measured by ^{1}H NMR. [c] Conversion into aldehydes determined by ^{1}H NMR. [d] Isomerization measured by ^{1}H NMR. [e] Enantioselectivity of **1** measured by ^{1}H NMR using Eu(hfc)$_3$ on the corresponding methyl ester. [f] P = 20 bar, [Rh(acac)$(CO)_2$] (0.012 mmol), **1**/Rh = 400, benzene (1.5 mL), Ligand/Rh = 4, T = 40 ºC, t = 24 h (see ref. 6b).

The influence of the bridge length indicates that the use of 1,3-diphosphites provided a better catalytic performance than 1,2- and 1,4-diphosphites. Ligands **L52**-**L60**, which have three carbon atoms in the bridge (Table 6.2.2, entries 3-18), therefore provided higher regio- and enantioselectivities than ligands **L50**-**L51** (Table 6.2.2, entries 1 and 2), which have two carbon

atoms in the bridge, and ligands **L61**-**L66** (Table 6.2.2, entries 19-24), which have four carbon atoms in the bridge.

The influence of the ligand backbone indicates that increasing the rigidity of the ligand is beneficial. Our results with ligands **L52a** and **L58a** are therefore worse than those with the corresponding ligands **L53a** and **L60a**, which have the same configuration of carbons adjacent to the phosphite groups but also a more rigid furanoside backbone (Table 6.2.2, entries 3 and 12 vs 4 and 18, respectively). We also found that both carbon atoms adjacent to the phosphite moieties must be substituted if regio-, chemo- and enantioselectivity need to be high. Accordingly, ligands **L52**-**L54**, substituted at both carbon atoms adjacent to the phosphite, provided higher selectivities than ligands **L58**-**L60**, which are substituted only at one carbon atom (Table 6.2.2, entries 3, 4 and 5 vs 12, 13 and 18).

For disubstituted ligands, we also found that the presence of a methyl substituent is more effective at transferring the chiral information than the presence of a *tert*-butyldimethylsilyl group (Table 6.2.2, entries 5 vs 11). Finally, our results with ligands **L53**-**L56** indicate that there is a cooperative effect between stereocentres C-3 and C-5 of the furanoside backbone that resulted in a matched combination for ligand **L54** (Table 6.2.2, entries 5 vs 4, 9 and 10).

We investigated the effect of the biphenyl substituents with ligands **L54, L59** and **L60** (Table 6.2.2, entries 5-8, 13-18) and found that these moieties affect catalytic performance. Bulky substituents in the *ortho* and *para* positions of the biphenyl moieties are needed for high enantioselectivity. Therefore, ligand **L54a** provided the highest enantioselectivity (Table 6.2.2, entry 5).

In summary, if chemo-, regio- and enantioselectivities are to be high, the length of the bridge and the rigidity of the ligand backbone need to be correctly combined and bulky *tert*-butyl groups in both the *ortho* and *para* positions of the biphenyl phosphite moieties need to be present. Accordingly, ligand **L54a** showed practically no isomerization with excellent regioselectivity (99 %) and unprecedently high enantioselectivity (ee's of 74 %). Ligand **L54a** therefore competes favourably with the BINAPHOS ligand, which so far has provided the best enantioselectivities for this substrate (Table 6.2.2, entry 5 vs 25).

Next we applied diphosphite ligands **L50**-**L66a**-**e** in the Rh-catalyzed asymmetric hydroformylation of 2,3-dihydrofuran **S2**. Our results are summarized in Table 6.2.3. In no cases were isomerized (product **S1**), hydrogenated or polymerized products of 2,3-dihydrofuran observed. Our results followed the same trend as for the hydroformylation of **S1**. The selectivities of the process were affected by the length of the bridge, the backbone of the ligand and the substituents of the biphenyl moieties. Accordingly, 1,3-diphosphites (Table 3, entries 2-11) were superior in terms of regio- and enantioselectivities to the 1,2- and 1,4-diphosphites (Table 6.2.3, entries 1 and 12-13, respectively). Again ligand **L54c**, with a methyl substituent at the C-5 position, provided unprecedented enantioselectivities in favour of the tetrahydrofuran-3-carbaldehyde **2** (Table 6.2.3, entry 4). Note, however, that the sense of the enantioselectivity was opposite to that in the hydroformylation of 2,5-dihydrofuran **S1** (Table 6.2.2, entry 5 vs Table 6.3.3, entry 4). Using the same ligand **L54a**, therefore, both enantiomers of tetrahydrofuran-3-carbaldehyde **1** can be accessed in high enantioselectivity by simple substrate change. Again, these results compete favourably with the best of those reported using the BINAPHOS ligand (Table 6.2.3, entry 4 vs 14).

Table 6.2.3. Selected results for the Rh-catalyzed asymmetric hydroformylation of **S2**.[a]

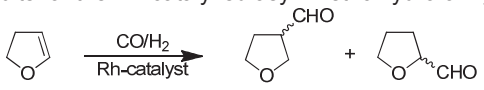

S2 **1** **2**

Entry	Ligand	% Conv.[b]	% Ald. (**1**:**2**)[c]	% ee of **1**[d]
1	**L50a**	100	100 (54:46)	< 5
2	**L52a**	100	100 (68:32)	43 (*S*)
3	**L53a**	100	100 (73:27)	48 (*S*)
4	**L54a**	100	100 (76:24)	75 (*R*)
5	**L54b**	100	100 (74:26)	49 (*R*)
6	**L54c**	100	100 (73:27)	61 (*R*)
7	**L54d**	80	80 (75:25)	< 5
8	**L55a**	100	97 (70:30)	29 (*S*)
9	**L56a**	100	92 (69:31)	21 (*S*)
10	**L57a**	100	100 (72:28)	58 (*R*)
11	**L59a**	88	88 (78:22)	48 (*R*)
12	**L61a**	100	100 (55:45)	< 5
13	**L62a**	100	100 (50:50)	< 5
14[e]	**BINAPHOS**	100	100 (50:50)	38 (*S*)

[a] P= 18 bar. [Rh(acac)(CO)$_2$] (0.012 mmol). **S2**/Rh= 400. Toluene (5 mL). T= 45 °C. t= 48 h. [b] Total conversion measured by ^{1}H NMR. [c] Conversion into aldehydes determined by ^{1}H NMR. [d] Enantioselectivity of **2** measured by ^{1}H NMR using Eu(hfc)$_3$ on the corresponding methyl ester. [e] P = 100 bar, [Rh(acac)(CO)$_2$] (0.012 mmol), **3**/Rh = 400, benzene (1.5 mL), Ligand/Rh = 4, T = 40 ºC, t = 24 h (see ref. 6b).

Encouraged by our excellent results in the Rh-catalyzed asymmetric hydroformylation of substrates **S1** and **S2**, we examined the hydroformylation of *N*-acetyl-3-pyrroline (**S3**). The results, which are summarized in Table 6.2.4, follow the same trend as in the hydroformylation of **S1** and **S2**. As expected, activities were lower than in the hydroformylation of **S1**.[6b] Again, using ligand **L54a** is highly advantageous as it provides the highest enantioselectivities obtained so far (Table 6.2.4, entry 3 vs 6).

Table 6.2.4. Selected results for the Rh-catalyzed asymmetric hydroformylation of **S3** using ligands **L50**-**L66a**-**e**[a]

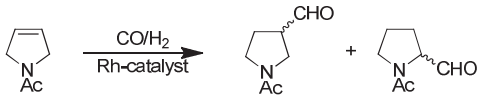

S3 **3** **4**

Entry	Ligand	% Conv.[b]	% Ald. (**3**:**4**)[c]	% ee of **3**[d]
1	**L50a**	100	100 (98:2)	< 5
2	**L52a**	100	100 (100:0)	19 (-)
3	**L54a**	100	100 (100:0)	71 (+)
4	**L59a**	100	100 (99:1)	49 (+)
5	**L61a**	100	100 (98:2)	< 5
6[e]	**BINAPHOS**	92	92 (100:0)	66 (-)

[a] P= 18 bar. [Rh(acac)(CO)$_2$] (0.012 mmol). **S3**/Rh= 400. Toluene (5 mL). T= 45 °C. t= 72 h. [b] Total conversion measured by ^{1}H NMR. [c] Conversion into aldehydes determined by ^{1}H NMR. [d] Enantioselectivity of **3**. [e] P = 100 bar, [Rh(acac)(CO)$_2$] (0.012 mmol), 1/Rh = 400, benzene (1.5 mL), Ligand/Rh = 4, T = 40 ºC, t = 24 h (see ref. 6b).

6.2.3.2. Asymmetric hydroformylation of seven-membered heterocyclic olefins

To further study the potential of these diphosphite ligands, we then tested them in the hydroformylation of *cis*-4,7-dihydro-1,3-dioxepin (**S4**) and *cis*-2,2-dimethyl-4,7-dihydro-1,3-dioxepin (**S5**). Our most important results are shown in Table 6.2.5.

Table 6.2.5. Selected results for the Rh-catalyzed asymmetric hydroformylation of **S4** and **S5** using ligands **L50-L66a-e**[a]

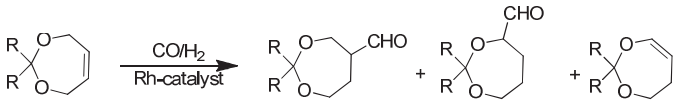

S4 R= H
S5 R= Me

5a R= H
b R= Me

7a R= H
b R= Me

6a R= H
b R= Me

Entry	Ligand	Substrate	% Conv.[b]	% Ald. (**5**:**7**)[c]	% **6**[d]	% ee of **5**[e]
1	**L50a**	**S4**	100	100 (100:0)	0	8 (-)
2[f]	**L50a**	**S4**	89	89 (100:0)	0	8 (-)
3[g]	**L50a**	**S4**	88	88 (100:0)	0	7 (-)
4	**L51a**	**S4**	88	88 (100:0)	0	9 (+)
5	**L52a**	**S4**	100	100 (100:0)	0	13 (-)
6	**L53a**	**S4**	79	79 (100:0)	0	37 (-)
7	**L54a**	**S4**	85	85 (100:0)	0	23 (+)
8	**L54b**	**S4**	75	75 (100:0)	0	18 (+)
9	**L54c**	**S4**	83	83 (100:0)	0	22 (+)
10	**L54d**	**S4**	54	54 (100:0)	0	< 5
11	**L55a**	**S4**	78	51 (100:0)	27	30 (+)
12	**L56a**	**S4**	90	90 (100:0)	0	35 (+)
13	**L57a**	**S4**	93	93 (100:0)	0	47 (+)
14	**L58a**	**S4**	91	91 (100:0)	0	8 (+)
15	**L59a**	**S4**	59	59 (100:0)	0	40 (+)
16	**L60a**	**S4**	74	48 (100:0)	26	30 (+)
17	**L62a**	**S4**	100	100 (100:0)	0	5 (-)
18	**L63a**	**S4**	96	96 (100:0)	0	15 (+)
19	**L64a**	**S4**	100	100 (100:0)	0	14 (+)
20	**L65a**	**S4**	56	56 (100:0)	0	56 (-)
21	**L66f**	**S4**	98	98 (99:1)	0	37 (+)
22[h]	**L65a**	**S4**	7	7 (100:0)	0	60 (-)
23[h]	**L59a**	**S4**	12	12 (100:0)	0	60 (+)
24[h]	**L57a**	**S4**	18	18 (100:0)	0	68 (+)
25[i]	**BINAPHOS**	**S4**	>99	>99 (100:0)	0	76 (-)
26[j]	**L57a**	**S5**	94	94 (100:0)	0	55 (*S*)
27[j]	**L59a**	**S5**	86	86 (100:0)	0	51 (*S*)
28[j]	**L65a**	**S5**	73	73 (100:0)	0	59 (*R*)
29[i]	**BINAPHOS**	**S5**	98	98 (100:0)	0	69 (*R*)

[a] P= 18 bar. CO/H_2= ½. $[Rh(acac)(CO)_2]$ (0.012 mmol). L/Rh= 2. Substrate/Rh= 400. Toluene (5 mL). T= 45 °C. t= 4 h. [b] Total conversion measured by ^1H NMR. [c] Conversion into aldehydes determined by ^1H NMR. [d] Isomerization measured by ^1H NMR. [e] Enantioselectivity of **5**. [f] CO/H_2= 1. [g] CO/H_2= 2. [h] T = 25 ºC. t= 24 h. [i] see ref. 6b. [j] t= 24 h.

Again, the selectivities of the process were affected by the length of the bridge, the backbone of the ligand and the substituents of the biphenyl moieties. However, the effect of these parameters was different from their effect on the hydroformylation of the previous substrates (**S1**-**S3**). In contrast to **S1**-**S3**, therefore, both 1,3- and 1,4-diphosphites can provide good regio- and enantioselectivities if the appropriate rigidity of the ligand's backbone is chosen. Accordingly, not only 1,3-diphosphite ligands **L57a** and **L59a** were shown to be effective, but the 1,4-diphosphite ligand **L65a** also provided good results. Also, and in contrast to the previous substrates, for disubstituted furanoside 1,3-diphosphites the presence of a *tert*-butyldimethylsilyl group is more effective than the presence of a methyl substituent (Table 5; entries 13 vs 7). Interestingly, both enantiomers of the hydroformylation products **5** can be obtained by using pseudoenantiomer ligands (i.e. ligands **L53** and **L56**; Table 5, entries 6 and 12) or by carefully tuning the ligand parameters (i.e. ligands **L57a** and **L59a** vs **L65a**; Table 5; entries 23 and 24 vs 22 for substrate **5a**, and entries 26 and 27 vs 28 for substrate **5b**).

We also observed an important effect of the temperature and this was more pronounced for the furanoside-based ligands **L57c** and **L59c**, therefore, lowering the temperature to 25 ºC substantially increased enantioselectivity (up to 68 %) and provided an excellent regioselectivity.

6.2.4. Conclusions

We have screened a library of modular diphosphite ligands **L50**-**L66a**-**e** in the Rh-catalyzed asymmetric hydroformylation of several hetereocylic olefins. Using this library we studied how the backbone of the ligand, the length of the bridge and the substituents of the biphenyl moieties affected the catalytic performance and determined the scope of diphosphite ligands. By carefully selecting the ligand components, we achieved high chemo-, regio- and enantioselectivities in different substrate types. Unprecedentedly high enantioselectivities for five-membered heterocyclic olefins were obtained using the furanoside diphosphite ligand **L54a**. Note that both enantiomers of the hydroformylation products can be synthesized using the same ligand by simple substrate change.[6b] For the seven-membered heterocyclic dioxepines, our results are among the best obtained. Also, both enantiomers of the hydroformylation products can be obtained by using pseudoenantiomer ligands or by carefully tuning the ligand parameters. These results open up the hydroformylation of heterocyclic compounds to the potentially effective use of readily available and highly modular diphosphite ligands.

6.2.5. Experimental Section

6.2.5.1. General Considerations

All experiments were carried out under argon atmosphere. All solvents were dried using standard methods and distilled prior to use. Ligands **L50**[12], **L51**[13], **L52**[12], **L53**-**L56**[14], **L57**[15], **L58**[12], **L59**[16], **L60**[17], **L61**[12], **L62**[13], **L63**[18] and **L64**-**L65**[13] were prepared by previously described methods. KELLIPHITE (**L66e**) and commercial substrates **S1**, **S2** and **S4** and were used without further purification. *N*-(acetyl)-2-pyrroline (**S3**)[6b] and *cis*-2,2-dimethyl-4,7-dihydro-1,3-dioxepin (**S5**)[19] were prepared according to the methods in the literature. The formation of **6a** was confirmed on the basis of the NMR assignments.[20] ^{1}H and ^{19}F NMR spectra were recorded on a 400 MHz

spectrometer. Hydroformylation reactions were carried out in a Parr series 4593 stainless steel autoclave.

6.2.5.2. Typical hydroformylation procedure.

The autoclave was purged three times with carbon monoxide. The solution of $[Rh(acac)(CO)_2]$ (3.1 mg, 0.012 mmol), diphosphite (0.024 mmol) and substrate (4.8 mmol) in toluene (5 mL) was transferred to the stainless-steel autoclave. After pressurizing to 18 bar of syngas and heating the autoclave to 45 ºC, the reaction was stirred for 24 h. Conversions and selectivities of the reaction were determined immediately by ^{1}H NMR analysis of the crude reaction without evaporation of the solvent. The determination of the enantiomeric excesses and absolute configurations was carried out using the procedures described in ref.[6b.]

6.2.6. Acknowledgements

We are indebted to Prof. C. Claver for her comments and suggestions. We thank the Spanish Government (Consolider Ingenio CSD2006-0003, CTQ2007-62288/BQU, 2008PGIR/07 to O.P. and 2008PGIR/08 to M.D.) and the Catalan Government (2005SGR007777 and Distinction to M.D.) for financial support.

6.2.7. References

[1] See for example: a) Claver, C.; Diéguez, M.; Pàmies, O.; Castillón, S. in *Topics in Organometallic Chemistry;* Beller, M., Ed.; Springer: Berlin, 2006, *Chapter 2*, 35. b) Claver, C.; Godard, C.; Ruiz, A.; Pàmies, O.; Diéguez, M. in *Modern Carbonylation Methods*; Kollár, L. Ed.; Wiley-VCH: Weinheim, 2008, *Chapter 3*. c) Nozaki, K. in *Comprehensive Asymmetric Catalysis*; Jacobsen, E.N., Pfaltz, A., Yamamoto, H., Eds.; Springer: Berlin, 1999**,** *Chapter 11*, 382.

[2] See for example: a) Diéguez, M.; Pàmies, O.; Claver, C. *Tetrahedron: Asymmetry* **2004**, *15*, 2113. b) Breit, B. *Top. Curr. Chem.* **2007**, *279*, 139. c) Klosin, J.; Landis, C. R. *Acc. Chem. Res.* **2007**, *40*, 1251. d) *Rhodium Catalysed Hydroformylation;* van Leeuwen, P.W.N.M.; Claver, C., Eds.; Kluwer Academic Press: Dordrecht, 2000. e) Claver, C.; Pàmies, O.; Diéguez, M. in *Phosphorous Ligands in Asymmetric Catalysis;* Börner, A. Ed.; Wiley-VCH: Weinheim, 2008, *Chapter 3*, vol. 2.

[3] See for example: a) Axtell, A. T.; Cobley, C. J.; Klosin, J.; Whiteker, G. T.; Zanotti-Gerosa, A.; Abboud, K. A. *Angew. Chem. Int. Ed.* **2005**, *44*, 5834. b) Huang, J.; Bunel, E.; Allgeier, A.; Tedrow, J.; Storz, T.; Preston, J.; Correll, T.; Manley, D.; Soukup, T.; Jensen, R.; Syed, R.; Moniz, G.; Larsen, R.; Martinelli, M.; Reider, P. J. *Tetrahedon Lett.* **2005**, *46*, 7831.

[4] See for instance: a) Clark, T. P.; Landis, C. R.; Freed, S. L.; Klosin, J.; Abboud, K. A. *J. Am. Chem. Soc.* **2005**, *127*, 5040. b) Thomas, P. J.; Axtell, A. T.; Klosin, J.; Peng, W.; Rand, C. L.; Clark, T. P.; Landis, C. R.; Abboud, K. A. *Org. Lett.* **2007**, *9*, 2665. c) Breeden, S.; Cole-Hamilton, D. J.; Foster, D. F.; Schwarz, G. F.; Wills, M. *Angew. Chem. Int. Ed.* **2000**, *39*, 4106. d) Peng, X.; Wang, Z.; Xia, C.; Ding, K. *Tetrahedron Lett.* **2008**, *49*, 4862.

[5] Yan, Y.; Zhang, X. *J. Am. Chem. Soc.* **2006**, *128*, 7198.

[6] a) Vietti, D. E. U.S. Patent 4376208, **1983**. b) Hoiuchi, T.; Ota, T.; Shirakawa, E.; Nozaki, K.; Takaya, H. *J. Org. Chem*. **1997**, *62*, 4285. c) del Rio, I.; van Leeuwen, P. W. N. M.; Claver, C. *Can. J. Chem.* **2001**, *79*, 560.

[7] a) Polo, A.; Real, J.; Claver, C.; Castillón, S.; Bayón, J. C. *J. Chem. Soc., Chem. Commun.* **1990**, 600. b) Polo, A.; Claver, C.; Castillón, S.; Ruiz, A.; Bayón, J. C.; Real, J.; Mealli, C.; Masi, D. *Organometallics* **1992**, *11*, 3525.

[8] Several modification on the BINAPHOS-type ligand have been studied. See ref. 5b.

[9] Unpublished results. For instance: (*R,R*)-Ph-BPE (22% ee), (*R,R*)-^{i}Pr-BPE (18% ee) and ESPHOS (32% ee).

[10] Diéguez, M.; Pàmies, O.; Claver, C. *Chem. Commun.* **2005**,1221.
[11] These ligands have the advantages of phosphite ligands: they are obtainable at low price from readily available alcohols, are highly resistant to oxidation and have facile modular constructions. See for instance: a) ref 2e. b) Diéguez, M.; Pàmies, O.; Ruiz, A.; Claver, C. in *Methodologies in Asymmetric Catalysis;* Malhotra, S. V., Ed.; American Chemical Society: Washington DC, 2004, *Chapter 11*.
[12] Buisman, G. J. H.; Vos, E. J.; Kamer, P. C. J.; van Leeuwen, P. W. N. M. *J. Chem. Soc., Dalton Trans.* **1995**, 409.
[13] Diéguez, M.; Pàmies, O.; Claver, C. *J. Org. Chem.* **2005**, *70*, 3363
[14] a) Diéguez, M.; Pàmies, O.; Castillón, S.; Ruiz, A.; Claver, C. *Chem. Eur. J.* **2001**, *7*, 3086. b) Diéguez, M.; Pàmies, O.; Ruiz, A.; Claver, C. *New J. Chem.* **2002**, *26*, 827
[15] Diéguez, M.; Pàmies, O.; Claver, C. *Adv. Synth. Catal.* **2005**, *347*, 1257
[16] Buisman, G. J. H.; Martin, M. E.; Vos, E. J.; Klootwijk, A.; Kamer, P. C. J.; van Leeuwen, P. W. N. M. *Tetrahedron: Asymmetry* **1995**, *8*, 719.
[17] Pàmies, O.; Net, G.; Ruiz, A.; Claver, C. *Tetrahedron: Asymmetry* **1999**, *11*, 1097.
[18] Reetz, M. T.; Neugebauer, T. *Angew. Chem. Int. Ed.* **1999**, *38*, 179.
[19] Elliott, W. J.; Fried, J. *J. Org. Chem.* **1976**, *41*, 2469.
[20] Taskinen, E.; Ihlainen, P. *Structural Chemistry* **1999**, *10*, 295.

6.3. Fine-tunable monodentate phosphoroamidite and aminophosphine ligands for Rh-catalyzed asymmetric hydroformylation

Javier Mazuela, Oscar Pàmies, Montserrat Diéguez, Laetitia Palais, Stephane Rosset and Alexandre Alexakis in *Tetrahedron: Asymmetry* **2010**, *21*, 2153

6.3.1. Abstract

A biaryl-based monophosphoroamidite (**L67**-**L70a**-**f**) and aminophosphine (**L71**-**L73a**-**f**) ligand library was screened in the Rh-catalyzed asymmetric hydroformylation of several vinylarenes and heterocyclic olefins. Our results indicated that selectivity strongly depended on the ligand parameters and on the substrate type. Enantioselectivities (up to 46%) were moderate in the hydroformylation of several vinylarenes **S1**-**S5** and promising (up to 58%) for the more challenging heterocyclic olefins **S6**-**S9**.

6.3.2. Introduction

Asymmetric hydroformylation has attracted much attention as a potential tool for preparing enantiomerically pure aldehydes.[1] Despite its importance, asymmetric hydroformylation is less developed than such other processes as hydrogenation. Traditionally, vinylarenes have been the most studied substrates. Although Rh-diphosphites and Rh-phosphine-phosphite (BINAPHOS) have proved to be the most efficient catalytic systems,[2] recently diphospholane,[3] bis-(diazaphospholodine)[4] and phosphine-phosphoroamidite[5] have emerged as suitable alternative ligands for this process. These latter ligands have led to the successful Rh-catalyzed hydroformylation of other types of substrate, such as allyl cyanide, vinyl acetate and some bicyclic olefins.[3,4,5] However further research is still needed if the range of substrates to be studied is to be extended. Most of the ligands reported to date for Rh-catalyzed hydroformylation have been designed with the advantages of bidentate ligands in mind. Although chiral monodentate ligands have recently proved to be highly efficient in several asymmetric catalytic transformations (i.e. hydrogenation,[6] 1,2-[7] and 1,4-additions,[8] etc.), there are rarely used in hydroformylation. In 2004, Ojima and coworkers reported the successful application of chiral biphenyl monophosphoroamidite ligands for the challenging Rh-catalyzed asymmetric hydroformylation of allyl cyanide (ee's up to 80%).[9,10] Despite this success, to our knowledge monophosphoroamidites have not been applied to other substrates and, therefore, the scope of catalyst systems containing monodentate P-ligands needs to be verified.

Encouraged by the success of monophosphoroamidite ligands in the hydroformylation of allyl cyanide, we report here the use of a biaryl-based monophosphoroamidite and aminophosphine ligand library **L67**-**L73a**-**f** (Figure 6.3.1) in the Rh-catalyzed asymmetric hydroformylation of vinylarenes and heterocyclic olefins. These ligands have the advantage of being readily accessible, highly diverse, air stable and inexpensive compared to most bidentate ligands.[11] In addition, they are amenable to parallel synthesis.[12] With this library, then, we fully investigate the effect of systematically varying the substituents and configuration at both the biaryl moiety (**L67**-

L70) and at the substituents attached to the nitrogen group (R= **a**-**f**) and the type of functional group (phosphoroamidite **L67**-**L70** or aminophosphine **L71**-**L73**).

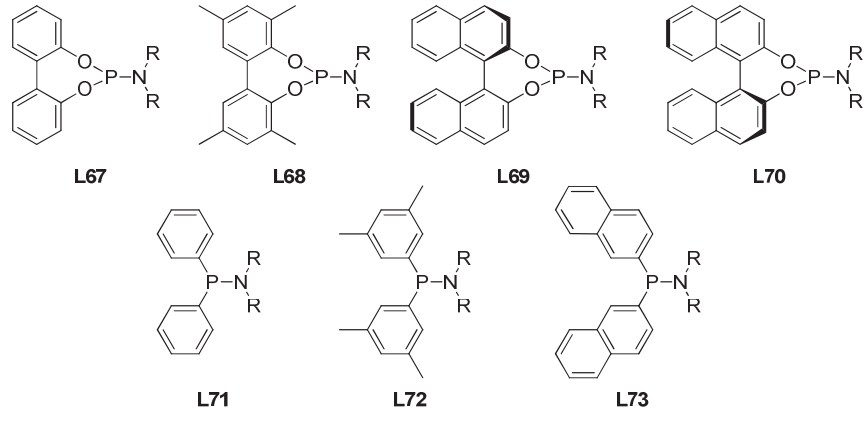

a R= (*S*)-CH(Ph)Me
b R= (*R*)-CH(Ph)Et
c R= (*R*)-CH(2-OMe-C_6H_4)Me
d R= (*R*)-CH(2-Napht)Me
e R= (*S*)-CH(2-Napht)Me
f R= Me

Figure 6.3.1. Monodentate phosphoroamidite and aminophosphine ligands (**L67**-**L73a**-**f**).

6.3.3. Results and Discussion

6.3.3.1. Asymmetric hydroformylation of vinylarenes

As have been mentioned above, vinylarenes, and especially styrene, have been the most popular substrates for asymmetric hydroformylation. This is largely because the hydroformylation of these substrates gives rise to important intermediates for the synthesis of chiral arylpropionic acids widely used as non-steroidal anti-inflammatory drugs.[1]

In the first set of experiments, we tested monodentated ligands **L67**-**L73a**-**f** in the rhodium-catalyzed hydroformylation of styrene **S1** (Scheme 6.3.1). The latter was chosen as a substrate because this reaction has been performed with a wide range of ligands with several donor groups, so the efficiency of the various ligand systems could be compared directly.[1] The catalytic system was generated *in situ* by adding the corresponding ligand to $[Rh(acac)(CO)_2]$ as a catalyst precursor. Hydrogenated or polymerized products of styrene were not observed.

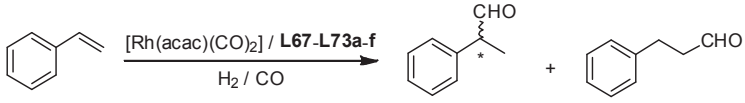

Scheme 6.3.1. Asymmetric Rh-catalyzed hydroformylation of styrene with ligands **L67**-**L73a**-**f**.

Initially, we determined the optimal reaction conditions by conducting a series of experiments with ligand **L67a** in which the ligand-to-rhodium ratio, temperature and CO/H_2 pressure ratio

were varied (Table 6.3.1). As expected, varying the ligand-to-rhodium ratio showed that the best trade-off between activities and selectivities was obtained using a ligand-to-rhodium ratio of 2 (Table 6.3.1, entries 1-3). A higher ligand-to-rhodium ratio negatively affected activity and regioselectivity. Varying the temperature had an important effect on regio- and enantioselectivity. Decreasing the temperature to 25 °C, then, had a positive effect on regio- and enantioselectivity, but decreased the activity (Table 6.3.1, entry 1 vs 4). After identical catalyst preparation, hydroformylation experiments were carried out under different CO and H_2 partial pressures (Table 6.3.1, entries 4-6). The results clearly show that higher partial pressures of H_2 lead to slightly higher initial turnover frequencies and, surprisingly, have an extremely positive effect on enantioselectivity (Table 6.3.1, entry 5).

Table 6.3.1. Rh-catalyzed asymmetric hydroformylation of **S1** using ligand **L67a**. Optimization of the reaction conditions[a]

Entry	L/Rh	T (°C)	% Conv (h) [b]	%-**1**[c]	%ee[d]
1	2	45	99 (1)	95	6 (*S*)
2	5	45	99 (1)	84	8 (*S*)
3	10	45	60 (1)	91	10 (*S*)
4	2	25	15 (2)	99	10 (*S*)
5[e]	2	25	19 (2)	99	40 (*S*)
6[f]	2	25	4 (2)	99	21 (*S*)

[a] P = 25 bar, P_{CO}/P_{H2} = 1, [Rh(acac)$(CO)_2$] (0.013 mmol), **S1**/Rh = 500, toluene (15 mL). Preactivation time 16 h. [b] Conversion into aldehydes measured by GC. Reaction time in hours shown in parentheses. [c] %-**1** measured by GC. [d] Enantioselectivity measured by GC. [e] P_{CO}/P_{H2} = ½. [f] P_{CO}/P_{H2} = 2.

For comparative purposes, the rest of the ligands were tested under the conditions that gave the optimum trade-off between enantioselectivities and reaction rates: that is to say, a ligand-to-rhodium ratio of 2, a temperature of 25 °C and a CO-to-H_2 ratio of 0.5. The results are summarized in Table 6.3.2. We found that regio- and enantioselectivities were highly affected by the type of functional group and the substitutents and configurations at both the biaryl moiety and the amine group. The trade-off between regio- (up to 99%) and enantioselectivities (ee's up to 40%) was best with ligand **L67a**, which combines a simple biphenyl group with a chiral bis[(*S*)-1-phenylethyl]amine moiety.

We first studied the effect of varying the steric properties at both the biphenyl group and the amino substituents with ligands **L67**-**L68a**-**d**. In general, we found that increasing the steric properties at both biphenyl group (ligands **L67** vs **L68**; Table 6.3.2, entries 1 vs 4) and at the amino substituents (**a** vs **b**-**d**, Table 6.3.2) decreased the regio- and enantioselectivities. Introducing small non-chiral methyl substitutents at the amine group (**f**) also decreased enantioselectivity (Table 6.3.2, entry 7).

We also used ligands **L69a** and **L70a**, which contain opposite enantiomerically pure binaphthyl moieties, to investigate the possibility of a cooperative effect on enantioselectivity of the configuration of the biaryl moiety and the amino group. The results indicated that there was a cooperative effect that led to a matched combination for ligand **L70a**, which contains an (*S*)-binaphthyl moiety. However, the enantioselectivity obtained using **L70a** is lower than that obtained with the biphenyl-based ligand **L67a** (Table 6.3.2, entries 6 and 8 vs 1).

Next, after comparing these results with those from the related aminophosphine ligands **L71**-**L73**, we found that replacing the biphenol or binaphthol moiety with simple aryl groups has a extremely positive effect on regioselectivity (up to >99.9%), although the enantioselectivities decreased (Table 6.3.2, entries 1-8 vs 9-12).

Table 6.3.2. Selected results for the Rh-catalyzed hydroformylation of **S1** using ligands **L67**-**L73a-f**[a]

Entry	Ligand	% Conv (h)[b]	%-**1**[c]	%ee[d]
1	**L67a**	16 (2)	99	40 (*S*)
2	**L67b**	20 (4)	95	8 (*R*)
3	**L67c**	30 (4)	95	0
4	**L68a**	20 (4)	94	3 (*R*)
5	**L68d**	8 (4)	96	7 (*S*)
6	**L69a**	25(4)	92	10 (*S*)
7	**L69f**	30 (4)	97	12 (*S*)
8	**L70a**	10(4)	94	20 (*R*)
9	**L71a**	12 (4)	>99.9	5 (*S*)
10	**L71e**	12 (4)	>99.9	5 (*S*)
11	**L72a**	10 (4)	>99.9	7 (*S*)
12	**L73a**	20 (4)	>99.9	12 (*S*)
13	**L67a/L67c**	18(4)	95	5 (*S*)
14	**L67a/L68a**	18(4)	93	15 (*S*)
15	**L67a/L69a**	20 (4)	95	23 (*S*)
16	**L67a/L70a**	21 (4)	95	4 (*R*)
17	**L67b/L67c**	16 (4)	96	4 (*S*)
18	**L67b/L69a**	13 (4)	93	2 (*S*)
19	**L67b/L70a**	18 (4)	94	22 (*R*)
20	**L68a/L68d**	12 (4)	96	5 (*S*)
21	**L68a/L69a**	17 (4)	92	4 (*S*)
22	**L68a/L70a**	19 (4)	93	13 (*R*)
23	**L69a/L70a**	21(4)	92	0
24	**L71a/L72a**	12 (4)	>99.9	8 (*S*)
25	**L71a/L73a**	14 (4)	>99.9	15 (*S*)
26	**L71e/L73a**	18 (4)	>99.9	15 (*S*)

[a] P = 25 bar, P_{CO}/P_{H2} = 1/2, [Rh(acac)$(CO)_2$] (0.0125 mmol), **S1**/Rh = 500, toluene (15 mL). Preactivation time 16 h. T= 25 °C. [b] Conversion into aldehydes measured by GC. Reaction time in hours shown in parentheses. [c] %-**1** measured by GC. [d] Enantioselectivity measured by GC.

Finally, following the pioneering work of Reetz and coworkers,[13] we studied combining mixtures of two different monodentate P-ligands. Unfortunately, none of the combinations led to any improvements in regio- or enantioselectivity (i.e. Table 6.3.2, entries 13-26).

We next applied ligand **L67a** in the Rh-catalyzed hydroformylation of other vinyl arenes (Table 6.3.3). The presence of a fluoro substituent in the *para* position of the substrate hardly affected conversion, or regio- or enantioselectivity (Table 6.3.3, entries 1 vs 2). However, the presence of

para-methoxy and naphthyl substituents in the substrate had a positive effect on enantioselectivity (Table 6.3.3, entries 1 vs 3-5).

Table 6.3.3. Rh-catalyzed hydroformylation of several vinylarenes using ligand **L67a**[a]

Entry	Substrate	% Conv (h)[b]	%-branched[c]	%ee[d]
1	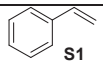 **S1**	99 (20)	99	40 (*S*)
2	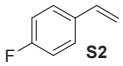 **S2**	100 (20)	98	39 (*S*)
3	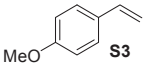 **S3**	84 (20)	99	45 (*S*)
4	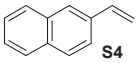 **S4**	78 (20)	99	46 (*S*)
5	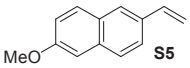 **S5**	66 (20)	99	49 (+)

[a] P = 25 bar, P_{CO}/P_{H2} = 1/2, [Rh(acac)$(CO)_2$] (0.0125 mmol), vinylarene/Rh = 500, toluene (15 mL). Preactivation time 16 h. T= 25 °C. [b] Conversion into aldehydes measured by GC. Reaction time in hours shown in parentheses. [c] %-branched measured by GC. [d] Enantioselectivity measured by GC.

6.3.3.2. Asymmetric hydroformylation of heterocyclic olefins

The asymmetric hydroformylation of heterocyclic olefins gives access to important building blocks for the synthesis of natural products and pharmaceuticals. Few studies had been made of this topic, however.[14] This is mainly because, for this kind of substrate, as well as having to control the enantioselectivity of the process, chemo- and regio-selectivity are often a problem.[13,15] For example, in the hydroformylation of 2,5-dihydrofuran **S6** the expected product is tetrahydrofuran-3-carbaldehyde **3** (Scheme 6.3.2). However, considerable amounts of 2,3-dihydrofuran **S7** and tetrahydrofuran-2-carbaldehyde **4** can also be formed due to an isomerization process. This isomerization takes place simultaneously with the hydroformylation reaction (Scheme 6.3.2).

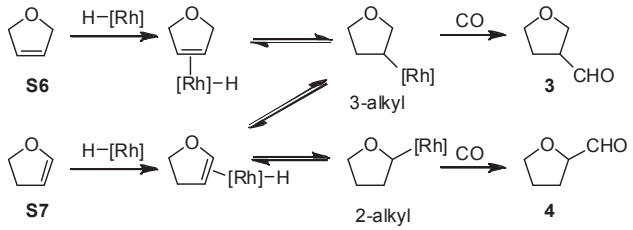

Scheme 6.3.2. Proposed mechanism for the isomerization process.

In an initial set of experiments, we tested monodentate ligands **L67**-**L73a-f** in the rhodium-catalyzed hydroformylation of 2,5-dihydrofuran **S6** (Scheme 6.3.3). In no cases were hydrogenated or polymerized products of 2,5-dihydrofuran observed.

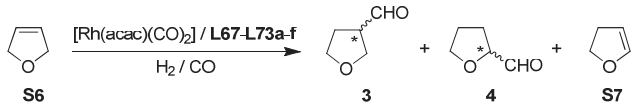

Scheme 6.3.3. Asymmetric Rh-catalyzed hydroformylation of styrene with ligands **L67**-**L73a**-**f**.

We first determined the optimal reaction conditions by conducting a series of experiments with ligand **L67a** in which the ligand-to-rhodium ratio, CO/H_2 pressure ratio, reaction time and temperature were varied (Table 6.3.4). Varying the ligand-to-rhodium ratio showed that the enantioselectivity was best when 2 equiv of ligand was used (Table 6.3.4, entries 1 and 2). A higher ligand-to-rhodium ratio negatively affected activity and enantioselectivity.

It is generally accepted that isomerization occurs as a result of competition between the β-hydride elimination process and CO insertion (Scheme 6.3.2). Since a high CO pressure is needed to suppress isomerization, we conducted experiments with increased CO partial pressure. This hardly affected the rate of hydroformylation *vs* isomerization (Table 6.3.4, entries 1 *vs* 4), though decreasing the CO/H_2 pressure ratio negatively affected chemoselectivity, which increased the formation of isomerized product **S7** (Table 6.3.4, entries 1 *vs* 3).

A prolonged reaction time increased conversion into aldehydes (Table 6.3.4, entry 5) but decreased regio- and enantioselectivity in the desired product **3** (Table 6.3.4, entry 1 vs 5). This decrease is due to the hydroformylation of the 2,3-dihydrofuran **S7** formed under reaction conditions. The hydroformylation of **S7** leads to the formation of the opposite enantiomer of **3** (see Scheme 6.3.4) and promotes the formation of undesired hydroformylation product **4**.[13d]

Lowering the temperature to 25 ºC negatively affected activity, but had a positive effect on chemo- and regioselectivity (Table 6.3.4, entry 6).

Table 6.3.4. Rh-catalyzed asymmetric hydroformylation of **S6** using ligand **L67a**. Optimization of the reaction conditions[a]

Entry	L/Rh	T (°C)	% Conv (h)[b]	% aldeh. (**3**:**4**)[c]	% **S7**[d]	%ee of **3**[e]
1	2	45	94 (6)	80 (95:5)	14	45 (*S*)
2	5	45	86 (6)	80 (98:2)	6	18 (*S*)
3[f]	2	45	82 (6)	39 (88:12)	43	n.d.
4[g]	2	45	91 (6)	81 (97:3)	10	42 (*S*)
5	2	45	100 (24)	100 (93:7)	0	28 (*S*)
6	2	25	11 (8)	10 (99:1)	1	44 (*S*)

[a] P = 25 bar, P_{CO}/P_{H2} = 1, $[Rh(acac)(CO)_2]$ (0.013 mmol), **S6**/Rh = 400, toluene (5 mL). Without preactivation of the catalyst. [b] Total conversion measured by ^{1}H-NMR. Reaction time in hours shown in parentheses. [c] Conversion into aldehydes determined by ^{1}H NMR. [d] Isomerization measured by ^{1}H NMR. [e] Enantioselectivity of **3** measured by ^{1}H NMR using $Eu(hfc)_3$ on the corresponding methyl ester. [f] P_{CO}/P_{H2} = 0.5 [g] P_{CO}/P_{H2} = 2.

We next applied the remaining ligands under the same reaction conditions. The results are summarized in Table 6.3.5. In general, enantioselectivities and activities followed the same trends as in the hydroformylation of styrene. The enantioselectivity was best, then, when ligand **L67a** was used (ee's up to 45%, Table 6.3.5, entry 1). However, in contrast to the hydroformylation of vinylarenes, regioselectivity in product **3** is positively affected by the presence of bulky substituents at either the biaryl moiety or the amino group (Table 6.3.5, entry 1 vs 2-5). Although the cooperative effect between the configuration of the biaryl moiety and the amino group on enantioselectivity was not very pronounced, it did have a strong effect on the chemo- and

regioselectivity of the process. So, while ligand **L69a**, with an *R*-binaphthyl group, provided good chemo- and regiocontrol, ligand **L70a**, with an *S*-binaphthyl group, provided the lowest chemo- and regioselectivity of all tested ligands. The 45% of enantiomeric excess obtained when the simple readily available Rh-**L67a** catalytic system was used is very promising for the hydroformylation of heterocyclic compounds because only three catalytic systems have provided better enantioselectivities for substrate **S6**.[13f,b,d]

Table 6.3.5. Selected results for the Rh-catalyzed hydroformylation of **S6** using ligands **L67**-**L73a**-**f**[a]

Entry	L	% Conv (h)[b]	% aldeh. (**3**:**4**)[c]	% **S7**[d]	%ee of **3**[e]
1	**L67a**	94 (6)	80 (93:7)	14	45 (*S*)
2	**L67b**	62 (4)	59 (99:1)	3	15 (*S*)
3	**L67c**	39 (4)	39 (100:0)	0	18 (*S*)
4	**L68a**	55 (4)	50 (100:0)	5	2 (*R*)
5	**L68d**	45 (4)	20 (100:0)	25	6 (*S*)
6	**L69a**	80 (4)	70 (100:0)	10	8 (*R*)
7	**L69f**	92 (4)	81 (96:4)	11	11 (*R*)
8	**L70a**	87 (4)	19 (70: 30)	68	14 (*R*)
9	**L71a**	63 (4)	58 (100:0)	5	2 (*R*)
10	**L72a**	34 (4)	34 (100:0)	0	6 (*R*)
11	**L73a**	42 (4)	42 (100:0)	0	8 (*R*)

[a] P = 25 bar, P_{CO}/P_{H2} = 1, [Rh(acac)$(CO)_2$] (0.0125 mmol), **S6**/Rh = 400, toluene (5 mL), L/Rh= 2. Without preactivation of the catalyst. T= 45 °C. [b] Total conversion measured by ^{1}H-NMR. Reaction time in hours shown in parentheses. [c] Conversion into aldehydes determined by ^{1}H NMR. [d] Isomerization measured by ^{1}H NMR. [e] Enantioselectivity of **3** measured by ^{1}H NMR using Eu(hfc)$_3$ on the corresponding ester.

Next we applied ligand **L67a**, which provided the best results in the Rh-catalyzed asymmetric hydroformylation of 2,3-dihydrofuran **S7** (Scheme 6.3.4). The hydroformylation of this substrate is slower and provides lower levels of regio- and enantioselectivity than for substrate **S6**.[13b,d-f] Low-to-moderate regio- and enantioselectivities were obtained. It should be pointed out that the hydroformylation of **S7** provided the opposite enantiomer on the desired aldehyde **3** that the hydroformylation of **S6**.

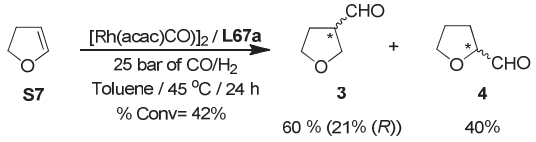

Scheme 6.3.4. Asymmetric hydroformylation of **S7** using the Rh-**L67a** catalytic system.

To further study the potential of ligands **L67**-**L73a**-**f**, we then tested them in the hydroformylation of *cis*-4,7-dihydro-1,3-dioxepin (**S8**) and *cis*-2,2-dimethyl-4,7-dihydro-1,3-dioxepin (**S9**) (Scheme 6.3.5). In all cases, these ligands exhibited high chemo- and regioselectivities to the desired aldehyde **5**. So, except for ligand **L73a** (Table 6.3.6, entry 10) neither aldehyde **6** nor isomerized product **7** were detected. Our most important results are shown in Table 6.3.6.

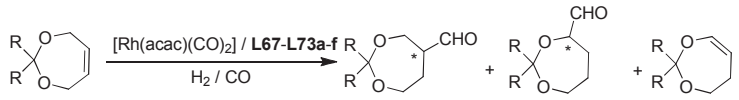

S8 R= H
S9 R= Me

5a R= H
b R= Me

6a R= H
b R= Me

7a R= H
b R= Me

Scheme 6.3.5. Asymmetric hydroformylation of **S8**-**S9** using the Rh-**L67**-**L73a**-**f** catalytic system.

Table 6.3.6. Selected results for the Rh-catalyzed hydroformylation of **S8** and **S9** using ligands **L67**-**L73a**-**f**[a]

Entry	L	Substrate	T (°C)	% Conv (h)[b]	% aldeh. (**5**:**6**)[c]	%ee of **5**[d]
1	**L67a**	**S8**	45	91 (2)	91 (100:0)	18 (+)
2	**L67b**	**S8**	45	100 (2)	100 (100:0)	36 (+)
3	**L67c**	**S8**	45	100 (2)	100 (100:0)	5 (+)
4	**L68a**	**S8**	45	83 (2)	83 (100:0)	0
5	**L68d**	**S8**	45	85 (2)	85 (100:0)	19 (+)
6	**L69a**	**S8**	45	72 (2)	72 (100:0)	2 (-)
7	**L69f**	**S8**	45	94 (2)	94 (100:0)	0
8	**L70a**	**S8**	45	96 (2)	96 (100:0)	16 (-)
9	**L71a**	**S8**	45	96 (2)	96 (100:0)	0
10	**L73a**	**S8**	45	93 (2)	78 (94:6)	0
11	**L67a/L67b**	**S8**	45	100 (2)	100 (100:0)	2 (+)
12	**L67a/L67c**	**S8**	45	100 (2)	100 (100:0)	4 (+)
13	**L67a/L68a**	**S8**	45	100 (2)	100 (100:0)	0
14	**L67a/ L69a**	**S8**	45	100 (2)	100 (100:0)	10 (+)
15	**L67a/ L70a**	**S8**	45	100 (2)	100 (100:0)	30 (-)
16	**L67b/L67c**	**S8**	45	100 (2)	100 (100:0)	27 (+)
17	**L69a/L70a**	**S8**	45	100 (2)	100 (100:0)	8 (-)
18	**L67b**	**S8**	25	96 (24)	96 (100:0)	58 (+)
19	**L67b**	**S9**	25	76 (24)	76 (100:0)	53 (*S*)

[a] P = 25 bar, P_{CO}/P_{H2} = 1/2, $[Rh(acac)(CO)_2]$ (0.0125 mmol), substrate/Rh = 100, toluene (5 mL), L/Rh= 2. Without preactivation of the catalyst. [b] Total conversion measured by ^{1}H-NMR. Reaction time in hours shown in parentheses. [c] Conversion into aldehydes determined by ^{1}H NMR. [d] Enantioselectivity of **5** measured by ^{1}H NMR using $Eu(hfc)_3$ on the crude reaction mixture.

Again, the selectivities of the process were affected by the type of functional group and the substituents and configurations at both the biaryl moiety and the amine group. However, the effect of these parameters was different from their effect on the hydroformylation of the previous substrates (**S1**-**S6**). Therefore, activities and selectivities were best with ligand **L67b** (Table 6.3.6, entry 2). As for substrates **S1**-**S6**, none of the ligand combinations improved the enantioselectivity (i.e. Table 6.3.6, entries 11-17).

We also observed that temperature had an important effect. A decrease from 45 ºC to 25 ºC substantially increased enantioselectivity (by as much as 58 % and 53% for **S8** and **S9**, respectively) while maintaining the excellent chemo- and regioselectivity. It should be noted that the enantioselectivity obtained using the Rh-**L67b** catalytic system is very promising and not so far from the best ee's obtained in the literature.[16]

6.3.4. Conclusions

A biaryl-based monophosphoroamidite (**L67**-**L70a**-**f**) and aminophosphine (**L71**-**L73a**-**f**) ligand library was tested to determine its effects on the asymmetric Rh-catalyzed hydroformylation of several vinylarenes and heterocyclic olefins. Our results indicated that selectivity strongly depended on the type of functional group, the substitutents and configurations at both the biaryl moiety and at the amine group, and the substrate type. For vinylarenes **S1**-**S5** and the heterocyclic olefin 2,5-dihydrofuran (**S6**), enantioselectivities (ee's up to 46%) were best with ligand **L67a**, whereas for 4,7-dihydro-1,3-dioxepin substrates (**S8** and **S9**) enantioselectivities (ee's up to 58%) were best with ligand **L67b**. These results extend the range of substrates for which monodentate phosphoroamidite ligands have proved to be promising and therefore open up new research lines on the use of monophosphoroamidites for the asymmetric hydroformylation of more challenging substrates such as heterocyclic olefins.

6.3.5. Experimental Section

6.3.5.1. General considerations

All experiments were carried out under argon atmosphere. All solvents were dried using standard methods and distilled prior to use. Ligands were prepared by previously described methods.[17] Commercial substrates **S1**-**S8** were used without further purification. *cis*-2,2-Dimethyl-4,7-dihydro-1,3-dioxepin (**S9**) was prepared according to the method in the literature.[18]

6.3.5.2. Typical hydroformylation procedure for vinylarenes S1-S5

In a typical experiment, the autoclave was purged three times with CO. The solution was formed from [Rh(acac)$(CO)_2$] (3.1 mg, 0.0125 mmol) and ligand (0.025 mmol) in toluene (10 mL). After pressurizing to the desired pressure with syngas and heating the autoclave to the reaction temperature, the reaction mixture was stirred for 16 hours to form the active catalyst. The autoclave was depressurized and a solution of substrate (6.25 mmol) in toluene (5 mL) was introduced into the autoclave, which was pressurized again. During the reaction several samples were taken from the autoclave. After the desired reaction time, the autoclave was cooled to room temperature and depressurized. The reaction mixture was analyzed by gas chromatography.[19]

6.3.5.3. Typical hydroformylation procedure for heterocyclic substrates S6-S9

The autoclave was purged three times with carbon monoxide. The solution of [Rh(acac)$(CO)_2$] (3.1 mg, 0.0125 mmol), ligand (0.025 mmol) and substrate (5 mmol for **S6** and **S7** and 1.25 mmol for **S8** and **S9**) in toluene (5 mL) was transferred to the stainless-steel autoclave. After pressurizing to 25 bar of syngas and heating the autoclave to the desired temperature, the reaction was stirred for the times shown in Tables 6.3.4-6.3.6. Conversions and selectivities of the reaction were determined immediately by ^{1}H NMR analysis of the crude reaction without evaporation of the solvent. The enantiomeric excesses and absolute configurations were determined using the procedures described in ref. 13b.

6.3.6. Acknowledgements

We thank the Spanish Government (Consolider Ingenio CSD2006-0003, 2008PGIR/07 to O. Pàmies and 2008PGIR/08 and ICREA Academia award to M. Diéguez), the Catalan Government (2009SGR116), COST D40 and the Swiss National Research Foundation (grant N° 200020-113332) for their financial support.

6.3.7. References

[1] See for example: a) Claver, C.; Diéguez, M.; Pàmies, O.; Castillón, S. in *Topics in Organometallic Chemistry;* Beller, M., Eds.; Springer: Berlin, 2006, *Chapter 2*, 35. b) Claver, C.; Godard, C.; Ruiz, A.; Pàmies, O.; Diéguez, M. in *Modern Carbonylation Methods*; Kollár, L., Ed.; Wiley-VCH: Weinheim, 2008, *Chapter 3*. c) Nozaki, K. in *Comprehensive Asymmetric Catalysis*; Jacobsen, E.N., Pfaltz, A., Yamamoto, H., Eds.; Springer: Berlin, 1999**,** *Chapter 11*, 382. d) Godard, C.; Ruiz, A.; Diéguez, M.; Pàmies, O.; Claver, C. in *Catalytic Asymmetric Synthesis*; Ojima, I., Eds.; Wiley: New Jersey, 2010, *Chapter 10*, pp 799.
[2] See for example: a) Diéguez, M.; Pàmies, O.; Claver, C. *Tetrahedron: Asymmetry* **2004**, *15*, 2113. b) Breit, B. *Top. Curr. Chem.* **2007**, *279*, 139. c) Klosin, J.; Landis, C. R. *Acc. Chem. Res.* **2007**, *40*, 1251. d) *Rhodium Catalysed Hydroformylation;* van Leeuwen, P.W.N.M.; Claver, C., Eds.; Kluwer Academic Press: Dordrecht, 2000. e) Claver, C.; Pàmies, O.; Diéguez, M. in *Phosphorous Ligands in Asymmetric Catalysis;* Börner, A., Ed.; Wiley-VCH: Weinheim, 2008, *Chapter 3*, vol. 2.
[3] See for example: a) Axtell, A. T.; Cobley, C. J.; Klosin, J.; Whiteker, G. T.; Zanotti-Gerosa, A.; Abboud, K. A. *Angew. Chem. Int. Ed.* **2005**, *44*, 5834. b) Huang, J.; Bunel, E.; Allgeier, A.; Tedrow, J.; Storz, T.; Preston, J.; Correll, T.; Manley, D.; Soukup, T.; Jensen, R.; Syed, R.; Moniz, G.; Larsen, R.; Martinelli, M.; Reider, P. J. *Tetrahedon Lett.* **2005**, *46*, 7831.
[4] See for instance: a) Clark, T. P.; Landis, C. R.; Freed, S. L.; Klosin, J.; Abboud, K. A. *J. Am. Chem. Soc.* **2005**, *127*, 5040. b) Thomas, P. J.; Axtell, A. T.; Klosin, J.; Peng, W.; Rand, C. L.; Clark, T. P.; Landis, C. R.; Abboud, K. A. *Org. Lett.* **2007**, *9*, 2665. c) Breeden, S.; Cole-Hamilton, D. J.; Foster, D. F.; Schwarz, G. J.; Wills, M. *Angew. Chem. Int. Ed.* **2000**, *39*, 4106. d) X. Peng, X.; Wang, Z.; Xia, C.; Ding, K. *Tetrahedron Lett.* **2008**, *49*, 4862.
[5] Yan, Y.; Zhang, X. *J. Am. Chem. Soc.* **2006**, *128*, 7198.
[6] See for instance: a) Reetz, M. T.; Mehler, G. *Angew. Chem. Int. Ed.* **2000**, *39*, 3889. b) Peña, D.; Minnaard, A. J.; Boogers, J. A.; de Vries, A.H.M.; de Vries, J. G.; Feringa, B. L. *Org. Biomol. Chem.* **2003**, *1*, 1087.
[7] See for instance: a) Biswas, K.; Prieto, O.; Goldsmith, P. J.; Woodward, S. *Angew. Chem. Int. Ed.* **2005**, *44*, 2232. b) Mata, Y.; Diéguez, M.; Pàmies, O.; Woodward, S. *J. Org. Chem.* **2006**, *71*, 8159.
[8] See for instance: a) Palais, L.; Mikhel, I. S.; Bournaud, C.; Micouin, L.; Falciola, C. A.; Vuagnoux-d'Augustin, M.; Rosset, S.; Bernardinelli, G.; Alexakis, A. *Angew. Chem. Int. Ed.* **2007**, *46*, 7462. b) d'Augustin, M.; Palais, L.; Alexakis, A. *Angew. Chem. Int. Ed.* **2005**, *44*, 1376. For a recent review on this topic, see also: Alexakis, A.; Bäckvall, J. E.; Krause, N.; Pàmies, O.; Diéguez, M. *Chem. Rev.* **2008**, *108*, 2796.
[9] Hua, Z.; Vassar, V. C.; Choi, H.; Ojima, I. *PNAS* **2004**, *101*, 5411
[10] It should be pointed out that related monophosphite ligands provided lower enantioselectivities (up to 43%) in the Rh-catalyzed hydroformylation of allyl cyanide. See: a) Cobley, C. J.; Klosin, J.; Qin, C.; Whiteker, G. T. *Org. Lett.* **2004**, *6*, 3277. b) Cobley, C. J.; Gardner, K.; Klosin, J.; Praquin, C.; Hill, C.; Whiteker, G. T.; Zannotti-Gerosa, A.; Petersen, J. L.; Abboud, K. *J. Org. Chem.* **2004**, *69*, 4031.
[11] See for example: a) Reetz, M. T. *Chimica Oggi* **2003**, *21*, 5. b) Minnaard, A. J.; Feringa, B. L.; Lefort, L.; de Vries, J. G. *Acc. Chem. Res.* **2007**, *40*, 1267. c) Diéguez, M.; Pàmies, O.; Ruiz, A.; Claver, C. *Phosphite ligands in asymmetric hydrogenation in Methodologies in Asymmetric Catalysis*; Malhotra, S. V., Ed.; ACS: Washington, 2004. Vol. 880. p. 161.
[12] See for instance: a) Lefort, L.; Boogers, J. A. F.; de Vries, A. H. M.; de Vries, J. G. *Org. Lett.* **2004**, *6*, 1733. b) Swennenhuis, B. H. G.; Chen, R.; van Leeuwen, P. W. N. M.; de Vries, J. G.; Kamer, P. C. J. *Org. Lett.* **2008**, *10*, 989.

[13] See for instance: a) Reetz, M. T.; Sell, T.; Meiswinkel, A.; Mehler, G. *Angew. Chem. Int. Ed.* **2003**, *42*, 790. b) Reetz, M. T.; Li, X. *Angew. Chem. Int. Ed.* **2005**, *44*, 2962.

[14] See for instance: a) Vietti, D. E. U.S. Patent 4376208, **1983**. b) Hoiuchi, T.; Ota, T.; Shirakawa, E.; Nozaki, K.; Takaya, H. *J. Org. Chem*. **1997**, *62*, 4285. c) del Rio, I.; van Leeuwen, P.W.N.M.; Claver, C. *Can. J. Chem.* **2001**, *79*, 560. d) Diéguez, M.; Pàmies, O.; Claver, C. *Chem. Commun.* **2005**,1221. e) Mazuela, J.; Coll, M.; Pàmies, O.; Diéguez, M. *J. Org. Chem.* **2009**, *74*, 5440. f) Gual, A.; Godard, C.; Castillón, S.; Claver, C. *Adv. Synth. Catal.* **2010**, *352*, 463. g) Chikkali, S. H.; Bellini, R.; Berthon-Gelloz, B.; van der Vlugt, J. I.; de Bruin, B.; Reek, J. N. H. *Chem. Commun.* **2010**, *46*, 1244.

[15] a) Polo, A.; Real, J.; Claver, C.; Castillón, S.; Bayón, J. C. *J. Chem. Soc., Chem. Commun.* **1990**, 600. b) Polo, A.; Claver, C.; Castillón, S.; Ruiz, A.; Bayón, J. C.; Real, J.; Mealli. C.; Masi, D. *Organometallics* **1992**, *11*, 3525.

[16] There are only two Rh-catalytic system that have provided better enantioselectivitites. One modified with the phosphine-phosphite BINAPHOS ligand (ee's up to 76% and 69% for **S8** and **S9**, respectively, see ref 14b) and the second modified with a furanoside diphosphite ligand (ee's up to 68%, see ref 14e).

[17] For the preparation of **L1-L4** see: Alexakis, A.; Polet, D.; Rosset, S.; March, S. *J. Org. Chem.* **2004**, *69*, 5660. For **L5-L7** see: Palais, L.; Alexakis, A. *Chem. Eur. J.* **2009**, *15*, 10473.

[18] Elliott, W. J.; Fried, J. *J. Org. Chem.* **1976**, *41*, 2469.

[19] a) Diéguez, M.; Pàmies, O.; Ruiz, A.; Castillón, S.; Claver, C. *Chem. Eur. J.* **2001**, *7*, 3086. b) Guimet, E.; Parada, J.; Ruiz, A.; Claver, C.; Diéguez, M. *APCATA* **2005**, *282*, 215.

6.4. Rh-catalyzed hydroformylation of 1,1'-disubstituted terminal enol esters

Javier Mazuela, Oscar Pàmies, Montserrat Diéguez *preliminary results*

6.4.1. Abstract

The first method for the highly regio- and chemoselective Rh-catalyzed hydroformylation of isopropenyl acetate has been developed. The screening of several achiral ligands (phosphine and phosphite) and the study of several reaction conditions have permitted the formation of desired 3-acetoxybutanal as a major product, minimizing the byproducts formation from hydrogenation and decomposition.

6.4.2. Introduction

Hydroformylation is one of the most important reactions widely used in industry that provides aldehydes directly from alkenes and *syngas* (CO/H_2) in one single step. The formed aldehydes are versatile intermediates and building blocks for various pharmaceuticals, agrochemicals, commodity and fine chemicals.[1] Despite the considerable interest from both industry and academia, the catalytic hydroformylation is still a challenging area in comparison with the rapid development of other catalytic reactions. One of the major problems is how to control chemo-, regio- and enantioselectivities while maintaining reasonable reaction rates ant moderately high temperatures. This is usually a difficult goal since at higher temperatures both regio- and enantioselectivities are often low. Although selectivity can be modulate to some extent by altering reaction parameters, the selection of the appropriate ligand is one of the most important factor in selectivity control.[1]

Most of the bulk examples on asymmetric hydroformylation have been devoted to the use of styrene derivatives as substrates which give rise to important building blocks for the synthesis of anti-inflammatory drugs.[1] More recently other type of substrates such as allyl cyanide, hetereocyclic olefins, bicyclic olefins and vinyl acetate have been successfully hydroformylated.[1] All these substrates are either monosubstituted olefins or 1,2-disubstitued olefins.[1] In these cases, α-chiral branched aldehydes are formed. In contrast the asymmetric hydroformylation of 1,1-disubstitued olefins to provide β-chiral linear aldehydes has been much less extensively investigated and has been proven to be a formidable challenge in terms of selectivity.[2,3] Recently, Buchwald and coworkers have hydroformylated α-alkylacrylates at high temperatures (90-100 ºC) with high enantioselectivities (ee's up to 94%), but regio- and chemo-selectivity is not completely satisfactory.[4]

Following our interest in asymmetric hydroformylation of challenging substrates, we herein report our preliminary results in the highly regioselective hydroformylation of one type of 1,1-disubstituted functionalized olefins: the enol ethers, whose hydroformylation has not been previously reported (Scheme 6.4.1). The hydroformylation of this substrate class will led to the formation of chiral β-hydroxyaldehydes which can be easily transform into β-hydroxyacids and 1,3-diols widely used as intermediates in the synthesis of natural products.

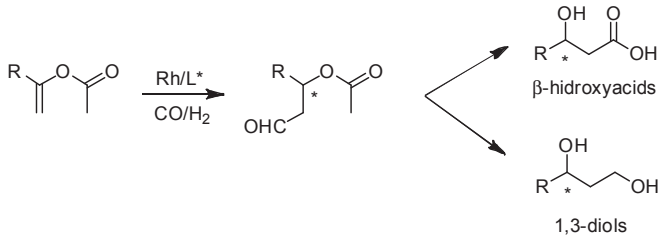

Scheme 6.4.1. Asymmetric hydroformylation of enol ethers. Application to the synthesis of chiral β-hydroxyaldehydes through asymmetric hydroformylation.

6.4.3. Results and Discussion

Initially, we studied the achiral hydroformylation of isopropenyl acetate (**S1**) using several achiral phosphite and phosphine ligands (Scheme 6.4.2). In this process as well as controlling the regioselectivity towards the desired product 3-acetoxybutanal (**1**), the chemoselectivity has also to be controlled. The latter is hampered by the formation of isopropyl acetate (**3**) by hydrogenation of the substrate and by the formation of acetic acid, butanal (**5**) and isobutanal (**4**) by decomposition of the acetoxyaldehydes through β-elimination or by decomposition of the substrate itself (Scheme 6.4.2).

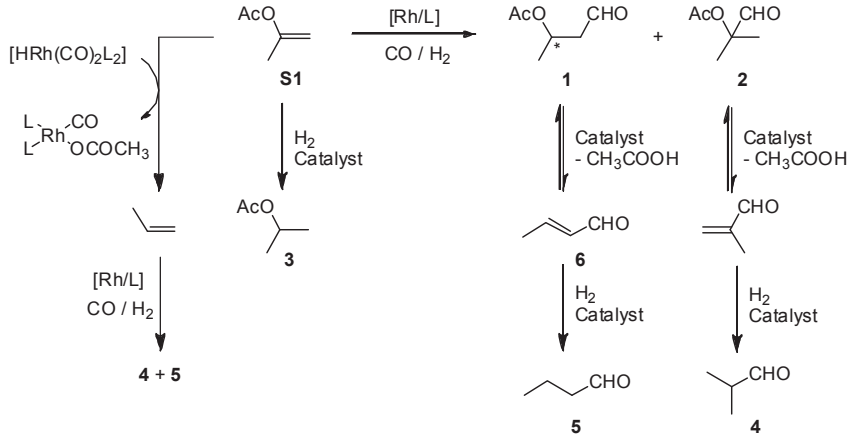

Scheme 6.4.2. Hydroformylation of isopropenyl acetate (**S1**). This scheme also shows the possible pathways for the formation of the observed side-products.

Initially, we determined the optimal reaction conditions by conducting a series of experiments with ligand P(O-2^{t}Bu-Ph)$_3$ in which the solvent, ligand-to-rhodium ratio and time were varied. The catalytic system was generated *in situ* by adding the corresponding ligand to a solution of [Rh(acac)(CO)$_2$] catalyst precursor. The results are shown in Table 6.4.1. We found that the efficiency of the process was strongly dependent on the nature of the solvent (dicloroethane (DCE), tetrahydrofuran (THF), dimethylformamide (DMF), toluene and acetonitrile (ACN)). Interestingly all the solvents except DMF provided the desired linear aldehyde **1** in high regioselectivity (up to 77%; Table 6.4.1, entries 1-2 and 4-5 vs 3). However, DCE was found to be optimal yielding the highest conversion on the desired aldehydes (Table 6.4.1, entry 1). The

use of THF, acetonitrile and toluene led to the formation of higher amounts of undesired side-products than when DCE was used (entries 2, 4 and 5). With the best solvent, we next investigated the effect of the ligand-to-rhodium ratio (Table 6.4.1, entry 1 vs 6). As expected due to the bulkiness of the phosphite ligand chosen,[5] excess of ligand is necessary for activities and selectivities to be optimal. Varying the reaction time showed that the chemo- and regioselectivity remains unaltered, which suggest that no decomposition of the catalyst takes place (entries 1 vs 7 and 8).

Table 6.4.1. Rh-catalyzed hydroformylation of **S1** using ligand P(O-2^{t}Bu-Ph)$_3$. Optimization of the reaction conditions[a]

Entry	Solvent	L/Rh	% Conv (h)[b]	%-(**1**+**2**)[c]	%-**3**	%-**4**	%-**5**	%-**6**	**1**:**2** ratio[d]
1	DCE	5	88 (8)	80	-	5	3	-	77:23
2[e]	THF	5	92 (8)	70	5	5	10	-	77:23
3	DMF	5	42 (8)	13		8	14	7	40:60
4	Toluene	5	72 (8)	57	-	8	7	-	75:25
5[f]	ACN	5	87 (8)	71	-	5	4	4	77:23
6[g]	DCE	1	64 (8)	47	-	6	4	2	77:23
7	DCE	5	80 (4)	71	-	6	3	-	77:23
8	DCE	5	48 (2)	41	-	4	3	-	77:23

[a] P = 100 bar, P_{CO}/P_{H2} = 1/2, [Rh(acac)(CO)$_2$] (0.2 mmol), **S1** (5 mmol), T= 80 ºC, solvent (15 mL). Conversions measured by GC. [b] Total conversion. Reaction time in hours shown in parentheses. [c] Total conversion into aldehydes. [d] Regioselectivity measured by GC. [e] 2% of unknown products. [f] 4% of unknown products. [g] 5% unknown products.

For comparative purposes, the rest of the ligands were tested under the conditions that gave the optimum trade-off between activity, chemo- and regioselectivity: that is to say, a ligand-to-rhodium ratio of 5 and dichloroethane as solvent. The results are summarized in Table 6.4.2. Comparing the results obtained using several phosphite ligands indicated that activity decreased considerably by decreasing the steric hindrance of the ligand, while chemo- and regioselectivity are less affected (Table 6.4.2, entries 1 vs 2 and 3). Next, we studied the hydroformylation of **S1** using several monophosphine ligands (entries 4-8). In all cases conversion was lower than when bulky P(O-2^{t}Bu-Ph)$_3$ was used. In contrast to the use of phosphite ligands, increasing the steric hindrance on phosphine ligands led to lower activities, chemo-and regioselectivities (Table 6.4.2, entries 4 vs 5 and 8). Interestingly, the introduction of electronwithdrawing substituents at the phosphine led to higher chemo- and regioselectivity (entries 4 vs 6). Having in mind that the most successful ligands developed for asymmetric hydroformylation are bidentated, we next screened achiral bidentated diphosphine ligands. We found that both chemo- and regioselectivity is highly affected by the chelate ring-size formed upon coordination to the metal center (Table 6.4.2, entries 9-11). Thus, while the use of dppb, which forms a seven-membered chelate ring, afforded comparable high regioselectivity than P(O-2^{t}Bu-Ph)$_3$, the use of dppe, which forms a 5-membered chelate ring, affords predominantly the undesired branched isomer. In addition the formation of undesired side-products is favored by using ligands with small chelate ring sizes (Table 6.4.2, entries 9 vs 10 and 11).

Table 6.4.2. Rh-catalyzed hydroformylation of **S1** using several ligands[a]

Entry	Ligand	L/Rh	% Conv[b]	%-(**1**+**2**)[c]	%-**3**	%-**4**	%-**5**	%-**6**	**1**:**2** ratio[d]
1	$P(O\text{-}2^tBuPh)_3$	5	88	80	-	5	3	-	77:23
2	$P(OPh)_3$	5	48	39	-	5	4	-	75:25
3	$P(O^iPr)_3$	5	38	33	-	3	2	-	73:27
4	PPh_3	5	32	26	1	3	2	-	71:29
5	$P(2\text{-}MePh)_3$	5	29	9	-	11	8		64:36
6	$P(4\text{-}CF_3Ph)_3$	5	32	30	-	1	1	-	81:19
7	$P(4\text{-}CF_3Ph)_3$	1	44	32	-	9	3	-	84:16
8	PCy_3	5	15	8	-	4	3	-	63:37
9	dppe[e]	1	25	10	-	10	5	-	13:86
10	dppp[f]	1	18	12	-	3	3	-	71:29
11	dppb[g]	1	19	10	-	5	4	-	76:24

[a] P = 100 bar, P_{CO}/P_{H2} = 1/2, $[Rh(acac)(CO)_2]$ (0.2 mmol), **S1** (5 mmol), T= 80 ºC, solvent (15 mL). Conversions measured by GC. [b] Total conversion. Reaction time in hours shown in parentheses. [c] Total conversion into aldehydes. [d] Regioselectivity measured by GC. [e] dppe= 1,2-bis(diphenylphosphino)ethane.[f] dppp= 1,3-bis(diphenylphosphino)propane [g] dppb= 1,4-bis(diphenylphosphino)butane.

6.4.4. Conclusions

We have developed the first method for the highly regio- and chemoselective Rh-catalyzed hydroformylation of isopropenyl acetate. The screening of several achiral ligands (phosphine and phosphite) and the study of several reaction conditions have permitted the formation of desired 3-acetoxybutanal as a major product, minimizing the byproducts formation from hydrogenation and decomposition.

6.4.5. Experimental Section

6.4.5.1. General considerations

All experiments were carried out under argon atmosphere. All solvents were dried using standard methods and distilled prior to use. Ligands and substrate **S1** were used as commercially available without further purification

6.4.5.2. Typical hydroformylation procedure of S1

The autoclave was purged three times with carbon monoxide. The solution of $[Rh(acac)(CO)_2]$ (84.6 mg, 0.2 mmol), ligand (1 mmol) and **S1** (0.55 mL, 5 mmol) in the desired solvent (15 mL) was transferred to the stainless-steel autoclave. After pressurizing to 100 bar of CO/H_2 (ratio 1/2) and heating the autoclave to the desired temperature, the reaction was stirred for the times shown in Tables 6.4.1 and 6.4.2. Conversions and selectivities of the reaction were determined by GC.

6.4.6. Acknowledgements

We thank the Spanish Government (Consolider Ingenio CSD2006-0003, 2008PGIR/07 to O. Pàmies and 2008PGIR/08 and ICREA Academia awards to M. Diéguez and O. Pàmies) and the Catalan Government (2009SGR116) for their financial support.

6.4.7. References

[1] See for example: a) Claver, C.; Diéguez, M.; Pàmies, O.; Castillón, S. in *Topics in Organometallic Chemistry;* Beller, M., Eds.; Springer: Berlin, 2006, *Chapter 2*, 35.b) Claver, C.; Godard, C.; Ruiz, A.; Pàmies, O.; Diéguez, M. in *Modern Carbonylation Methods*; Kollár, L., Eds.; Wiley-VCH: Weinheim, 2008, *Chapter 3*. c) Nozaki, K. in *Comprehensive Asymmetric Catalysis*; Jacobsen, E.N., Pfaltz, A., Yamamoto, H., Eds.; Springer: Berlin, 1999**,** *Chapter 11*, 382. d) Diéguez, M.; Pàmies, O.; Claver, C. *Tetrahedron: Asymmetry* **2004**, *15*, 2113. e) Breit, B. *Top. Curr. Chem.* **2007**, *279*, 139. f) Klosin, J.; Landis, C. R. *Acc. Chem. Res.* **2007**, *40*, 1251. g) *Rhodium Catalysed Hydroformylation;* van Leeuwen, P.W.N.M.; Claver, C., Eds.; Kluwer Academic Press: Dordrecht, 2000. h) Claver, C.; Pàmies, O.; Diéguez, M. in *Phosphorous Ligands in Asymmetric Catalysis;* Börner, A., Ed.; Wiley-VCH: Weinheim, 2008, *Chapter 3*, vol. 2.
[2] a) Nozaki, K.; Li, W.-G.; Horiuchi, T.; Takaya, H. *Tetrahedron Lett.* **1997**, *38*, 4611. b) Botteghi, C.; Corrias, T.; Marchetti, M.; Paganelli, S.; Piccolo, O. *Org. Process Res. Dev*. **2002**, *6*, 379. c) Ojima, I.; Takai, M.; Takahashi, T. Patent WO 078766, 2004.
[3] For diastereoselective hydroformylation of 1,1-disubstituted olefins by a catalyst-directing group, see: a) Doi, T.; Komatsu, H.; Yamamoto, K. *Tetrahedron Lett.* **1996**, *37*, 6877. b) Breit, B. *Angew. Chem., Int. Ed. Engl.* **1996**, *35*, 2835. c) Leighton, J. L.; O'Neil, D. N. *J. Am. Chem. Soc.* **1997**, *119*, 11118. d) Krauss, I. J.; Wang, C. C.-Y.; Leighton, J. L. *J. Am. Chem. Soc.* **2001**, *123*, 11514. e) Ren, L.; Crudden C. M. *J. Org. Chem.* **2002**, *67*, 1746. f) Breit, B.; Heckmann, G.; Zahn, S. K. *Chem. Eur. J.* **2003**, *9*, 425.
[4] Wang, X.; Buchwald, S. L. *J. Am. Chem. Soc.* **2011**, *133*, 19080.
[5] van Rooy, A.; Orij, E. N.; Kamer, P. C. J.; van Leeuwen, P. W. N. M. *Organometallics* **1995**, *14*, 34.

Chapter 7

Conclusions

7. Conclusions

1. Chapter 3. *Asymmetric catalyzed hydrogenation of minimally functionalized olefins*. The conclusions of this chapter can be summarized as follows:

- Five different phosphite-containing ligand libraries have been developed for their application in the asymmetric Ir-catalyzed hydrogenation of minimally functionalized olefins. The modular ligand design has shown to be crucial in finding highly selective catalytic systems for each substrate type.

- In the application of two large phosphite-oxazoline ligand libraries, we found the first successful application of phosphite-containing ligands in the reduction of a wide range of *E*- and *Z*- trisubstituted and challenging 1,1-disubstituted alkenes, including examples with neighboring polar groups (allylic alcohols, acetates, α,β-unsaturated esters and ketones, allylic silanes and vinylboronates). The results compete favorable with the best ones reported in the literature. The use of propylene carbonate as solvents allowed us to recover the catalyst up to 5 times maintaining the excellent enantioselectivities. DFT calculations agree with an Ir(III/V) catalytic cycle with migratory insertion of a hydride as selectivity-determining step. The catalytic results can be rationalized by a simple quadrant model.

- In the application of phosphite-thiazoline ligands, based on previous phosphite-oxazoline ligands, we found that the replacement of the oxazoline by a thiazoline moiety has been beneficial in terms of substrate scope. Enantioselectivities have therefore been increased (up to 99%) in the reduction of challenging *Z*-triubstituted olefins, α,β-unsaturated ketones and trifluoromethyl olefins.

- In the application of heterodonor-phosphite-nitrogen ligand libraries that include more robust N-donor groups (such as oxazole, thiazole and pyridine) than oxazolines, we found that again excellent activities and enantioselectivities were obtained in a wide range of *E*- and *Z*- trisubstitued olefins and challenging 1,1-disubstituted terminal olefins, including examples with neighboring polar groups. Both enantiomers of the hydrogenation product can be obtained in high enantioselectivity.

2. Chapter 4. *Asymmetric allylic substitution reactions*. The conclusions of this chapter can be summarized as follows:

- In the application of the phosphite-thiazoline ligand library, previously synthesized in chapter 3, and their related phosphite-oxazoline ligands, we have found that enantioselectivities depend on the ligand parameters and substrate structure. By the correct combination of substrate and ligand type (P-oxazoline or P-thiazoline) we have identified one of the few catalytic systems that provided high regio- and enantioselectivities in both enantiomers of the alkylation product for several hindered and unhindered mono-, di- and trisubstituted substrates using a wide range of carbon-nucleophiles (ee`s up to >99%).

- In the application of the previously described heterodonor-phosphite-nitrogen ligand libraries that include more robust N-donor groups (such as oxazole, thiazole and pyridine) than oxazolines, we found again excellent activities and enantioselectivities in Pd-catalyzed allylic substitution of several di- and trisubstituted substrates using a wide range of C-, N- and O-nucleophiles. In addition, the phosphite-pyridine ligand library not only performs well in traditional organic solvents but also in alternative environmentally friendly solvents such as propylene carbonate and ionic

liquids. Ionic liquids allowed the palladium catalyst to be reused while maintaining the excellent enantioselectivities. The Pd-π-allyl intermediate study allowed us to better understand the catalytic behavior obtained experimentally. We found that the nucleophilic attack take place at the allylic carbon *trans* to the phosphite moiety.

3. Chapter 5. *Asymmetric Heck reaction*. The conclusions of this chapter can be summarized as follows:

- In the application of a highly modular phosphite-oxazoline ligand library in the Pd-catalyzed intermolecular Heck reactions under thermal and microwave conditions, we obtained excellent activities (up to 100% conversion in 10 minutes), and regio- (up to >99%) and enantioselectivities (ee's up to >99%) in both enantiomers of the Heck-coupling products using a wide range of substrates and triflate sources. Reaction times were considerably shorter in microwave irradiation conditions (full conversion in a few minutes) and regio- and enantioselectivities were maintained. These results compete favorably with the best ones reported. This large modular ligand library contains three main ligand structures that have been designed by systematic modifications of one of the most successful ligand family (PHOX).

- In the application for the first time of phosphite-oxazole/imidazole ligands in the asymmetric intermolecular Pd-catalyzed Heck reactions under thermal and microwave conditions, we obtained excellent activities (up to 100% conversion in 30 minutes) and regio- (up to >99%) and enantioselectivities (up to 99% ee) using several triflate sources. Again the use of microwave irradiation conditions allowed considerably shorter reaction times maintaining excellent regio- and enantioselectivities.

4. Chapter 6. *Asymmetric hydroformylation*. The conclusions of this chapter can be summarized as follows:

- In the application a large series of diphosphite ligands in the Rh-catalyzed asymmetric hydroformylation of several hetereocylic olefins, we found that by carefully selecting the ligand components (ligand backbone, the length of the bridge and the substituents of the biphenyl moieties) high chemo-, regio- and enantioselectivities in different substrate types can be achieved. Unprecedentedly high enantioselectivities for five-membered heterocyclic olefins were therefore obtained. For the seven-membered heterocyclic dioxepines, our results are among the best obtained.

- In the application of a large biaryl-based monophosphoroamidite and aminophosphine ligand library in the Rh-catalyzed asymmetric hydroformylation of several vinylarenes and heterocyclic olefins, we found moderate enantioselectivities for vinylarenes and promising for the more challenging heterocyclic olefins.

- Finally, in the last chapter we have developed the first method for the highly regio- and chemoselective Rh-catalyzed hydroformylation of isopropenyl acetate. The screening of several achiral ligands (phosphine and phosphite) and the study of several reaction conditions have permitted the formation of desired 3-acetoxybutanal as a major product, minimizing the byproducts formation from hydrogenation and decomposition.

Chapter 8

Resum (Summary)

8. Resum (Summary)

Durant les últimes dècades, el desenvolupament de metodologies per l'obtenció de compostos enantiomericament purs ha estat un dels reptes més importants pels químics orgànics moderns. En aquest context, les reaccions asimètriques catalitzades per metalls de transició s'han mostrat com una de les principals eines per l'obtenció d'aquests compostos. La major part de la recerca feta es centra en el desenvolupament de nous catalitzadors organometal·lics modificats per lligands quirals. En aquest context, la síntesi de nous lligands quirals és essencial per descobrir bons sistemes catalítics en catàlisi asimètrica.

Inicialment, el lligands que contenien un grup fosfit estaven limitats a l'adició conjugada 1,4 catalitzada per coure i a la hidroformilació catalitzada per rodi. Durant les últimes dècades, el seu ús s'ha anat estenent a altres reaccions catalitzades per compostos organometal·lics, tals com la substitució al·lílica catalitzada per pal·ladi o la reacció de Heck. En comparació amb les fosfines o el fosfinits, els fosfits tenen un major caràcter π-acceptor i més resistència a l'oxidació i són fàcilment sintetitzables a partir d'alcohols quirals. Per l'altra banda, tenen major tendència a descomposar mitjançant hidròlisis, però aquest inconvenient es pot minimitzar introduint grups voluminosos biaril.

Els objectius d'aquesta tesi son el desenvolupament de noves llibreries de lligands fosfit (concretament fosfit-oxazolina, fosfit-tiazolina, fosfit-oxazol, fosfit-tiazol, fosfit-imidazol i fosfit-piridina) per la seva aplicació en diverses reaccions asimètriques catalitzades per metall de transició, tals com la hidrogenació d'olefines mínimament funcionalitzades catalitzada per iridi, les reacció de substitució al·lílica i Heck intermolecular catalitzades per pal·ladi, i la hidroformilació catalitzada per rodi.

Després de la introducció (**capítol 1**) i el objectius (**capítol 2**), el **capítol 3** es centra en l'aplicació de lligands fosfit-nitrogen en la hidrogenació d'olefines mínimament funcionalitzades catalitzada per iridi. Aquest capítol es divideix en 5 parts on es tracta la síntesi i aplicació de varies llibreries de nous lligands fosfit-nitrogen. La primera part inclou el treball titulat "*Pyranoside phosphite/phosphinite-oxazoline ligands for the highly versatile and enantioselective Ir-catalyzed hydrogenation of minimally functionalized olefins. A combined theoretical and experimental study*" on s'apliquen una libreria de lligands fosfit/fosfinit-oxazolina derivats de la *D*-glucosamina en l'hidrogenació d'olefines trisubstituïdes amb diferents propietats estèriques i electròniques, obtenint excessos enantiomèrics de fins al 99%. Aquests catalitzadors també es van aplicar en l'hidrogenació d'olefines terminals amb diferents propietats estèriques i electròniques obtenint excel·lents enantioselectivitats. En aquesta secció també es va realitzar un estudi computacional per esbrinar l'origen de l'enantioselectivitat. A partir de les estructures optimitzades, vam trobar que les enantioselectivitat obtingudes experimentalment es poden explicar a través d'un model de 4 quadrants.

La segona part està composada pel treball "*Iridium phosphite-oxazoline catalysts derived from hydroxyl aminoacids for the highly enantioselective hydrogenation of minimally functionalized alkenes*" on es va aplicar una llibreria de lligands fosfit-oxazolina derivada d'hidroxil aminoàcids en la hidrogenació d'olefines mínimament funcionalitzades. Es van obtenir enantioselectivitats superiors al 99% en l'hidrogenació de diferents olefines trisubstituïdes i terminals amb diferents propietat estèriques i electròniques. Les hidrogenacions asimètriques també es van realitzar

emprant carbonat de propilè com a solvent respectuós amb el medi ambient, el qual ens permet recuperar el catalitzador després de cada cicle. Emprant aquesta metodologia, es va poder reutilitzar fins a 5 cops el mateix catalitzador mantenint les excel·lents enantioselectivitats.

La tercera part està composada pel treball "*Expanded scope of the asymmetric Ir-catalyzed hydrogenation of minimally functionalized olefins using phosphite-thiazoline ligands*", on es va aplicar una llibreria de lligands fosfit-tiazolina, basats en els lligands fosfit-oxazolina descrits prèviament. La substitució de l'oxazolina per la tiazolina te efectes positius en termes de versatilitat. Es van incrementar les enantioselectivitats (fins al 99%) en la reducció de *Z*-olefines trisubstituïdes, cetones α,β-insaturades i d'olefines amb grups fluorats.

En les dues últimes parts, i per a comprovar el potencial dels lligands fosfit, es va decidir desenvolupar noves llibreries de lligands fosfit-nitrogen amb grups nitrogen dadors diferents de la típica oxazolina (oxazol, tiazol i piridina). Als treballs amb títol "*Adaptative biaryl phosphite-oxazole and phosphite-thiazole ligands for asymmetric Ir-catalyzed hydrogenation of alkenes*" i "*A phosphite-pyridine/iridium complex library as highly selective catalysts for the hydrogenation of minimally functionalized olefins*" es descriuen la síntesi i caracterització de tres lligandteques (fosfit-oxazol, fosfit-tiazol i fosfit-piridina) i s'estudia la seva aplicació a la hidrogenació d'olefines no funcionalitzades. Es van obtenir excel·lents enantioselectivitats (fins al 99%) en la reducció d'un gran nombre d'olefines trisubstituïdes i terminals amb diferents propietats estèriques i electròniques.

Per concloure, en aquest capítol s'han sintetizat i evaluat 5 llibreries de lligands fosfit-nitrogen obtenint excel·lents enantioselectivitats per un gran nombre d'olefines. Aquestes noves famílies competeixen favorablement amb les millors famílies de lligands desenvolupats fins a la data per aquest procés.

En el **capítol 4**, s'han aplicat les lligandteques fosfit-nitrogen, prèviament descrites al capítol 3, en la reacció de substitució al·lílica catalitzada per pal·ladi. Aquest capítol es divideix en 3 parts. En la primera part, titulada "*Phosphite-thiazoline vs phosphite-oxazoline ligands for Pd-catalyzed allylic substitution reactions. A case for comparison*" es va realitzar una comparativa entre els lligands fosfit-oxazolina i fosfit-tiazolina en la reacció de substitució al·lílica catalitzada per pal·ladi d'un ampli rang de substractes i nucleòfils.

La segona part està composada pel treball titulat "*A new class of modular P,N-ligand library for asymmetric Pd-catalyzed allylic substitution reactions. A study of the key Pd-π-allyl intermediates*". En aquest treball es van aplicar els lligands fosfit-oxazol i fosfit-tiazol descrits prèviament, en la substitució al·lílica catalitzada per pal·ladi. Es van obtenir excel·lents regio- i enantioselectivitats (ee's de fins al 96%) i bones activitats en un ampli rang de substrats mono-, di- i trisubstituïts lineals i substrats cíclics. L'estudi dels intermedis de reacció pal·ladi al·lil mitjançant espectroscòpia de ressonància magnètica nuclear i química computacional ha permès entendre el comportament catalític d'aquests compostos. L'estudi també ha indicat que l'atac nucleòfil té lloc preferentment al carboni al·lílic terminal localitzat *trans* al fosfit.

En la tercera part i per confirmar el potencial dels lligands fosfit en aquest procés, es va aplicar la lligandteca fosfit-piridina, descrita anteriorment, en l'alquilació al·lílica catalitzada per pal·ladi al treball "*A new modular phosphite-pyridine ligand library for asymmetric Pd-catalyzed allylic substitution reactions. A study of the key Pd-π-allyl intermediates*", obtenint selectivitats excel·lents per a un ampli rang de substrats al·lílics i nucleòfils. També es va realitzar un estudi de RMN dels intermedis pal·ladi π-al·lil.

En el **capítol 5**, en la primera part s'ha aplicat una lligandteca fosfit-oxazolina, composada per tres grups de lligands, en la reacció de Heck catalitzada per pal·ladi en el treball "*Biaryl phosphite-oxazoline from the chiral pool: Highly efficient modular ligands for the asymmetric Pd-catalyzed Heck reaction*". Després de l'optimització dels paràmetres dels lligands, es van obtenir regio- i enantioselectivitats excel·lents (superiors al 99%) amb elevades activitats per a un gran nombre de substrats en combinació amb diferents fonts de triflat. Per millorar encara més les activitats d'aquests sistemes, es van aplicar irradiacions de microones que van reduir considerablement els temps necessaris per obtenir conversions totals mantenint les excel·lents enantioselectivitats. Els resultats superen els millors publicats per aquest procés.

Amb l'objectiu de comprovar si el grup fosfit manté la seva efectivitat amb altres grups nitrogen dador, en la segona part del capítol es van aplicar els lligands fosfit-oxazol i fosfit-imidazol en la reacció de Heck en l'article "*Phosphite-oxazole/imidazole Ligands in Asymmetric Intermolecular Heck Reaction*", obtenint excel·lents activitats i selectivitats en la reacció de Heck del 2,3-dihidrofurà utilitzant diversos triflats amb diferents propietats estèriques i electròniques.

Finalment, en el **capítol 6**, s'ha estudiat la reacció d'hidroformilació catalitzada per rodi. En la primera part del capítol es van estudiar diversos paràmetres estructurals de lligands difosfit en l'hidroformilació catalitzada per rodi de diverses olefines heterocícliques en el treball "*Rh-catalyzed asymmetric hydroformylation of heterocyclic olefins using chiral diphosphite ligands. Scope and limitations*". Una selecció correcta dels paràmetres estructurals del lligand, han permès obtindre excel·lents quimio-, regio- i enantioselectivitats (fins al 76%ee) per a diferents tipus de substrats.

En la segona part del capítol es van aplicar lligands monodentats fosforoamidit i N-fosfina en l'hidroformilació catalitzada per rodi de diversos vinilarens i olefines heterocícliques en el treball "*Fine-tunable monodentate phosphoroamidite and aminophosphine ligands for Rh-catalyzed asymmetric hydroformylation*". Es van obtenir resultats prometedors en l'aplicació de lligands monodentats (enantioselectivitats de fins el 46%) que poden obrir noves línies de recerca en l'ús de lligand monodentas en la reacció d'hidroformilació catalitzada per rodi.

Finalment, es presenten els resultats preliminars en l'hidroformilació catalitzada per rodi d'enol esters terminals en el treball "*Rh-catalyzed hydroformylation of 1,1'-disubstituted terminal enol esters*". Aquest substrats poden ser posteriorment funcionalitzats i aplicats com a estructures bàsiques per a construir compostos de més complexitat. Es van obtenir resultats prometedors en l'hidroformilació del substrat acetat d'isopropenil, els quals obren les possibilitats d'un posterior estudi.

Chapter 9

Appendix

9. List of papers and meeting contributions

9.1. List of papers

1. Diéguez, Montserrat; Mazuela, Javier; Pàmies, Oscar; Verendel, J.Johan; Andersson, Pher G., "Chiral Pyranoside Phosphite-Oxazolines: A New Class of Ligand for Asymetric Catalytic Hydrogenation of Alkenes" *Journal of the American Chemical Society*, **2008**, *130* (23), 7208.

2. Diéguez, Montserrat; Mazuela, Javier; Pàmies, Oscar; Verendel, J.Johan; Andersson, Pher G., "Biaryl phosphite-oxazolines from hydroxyl aminoacid derivates: highly efficient modular ligands for Ir-catalyzed hydrogenation of alkenes", *Chemical Communications*, **2008**, (33), 3888.

3. Mazuela, Javier; Coll, Mercedes; Pàmies, Oscar; Diéguez, Montserrat; "Rh-Catalyzed Asymmetric Hydroformylation of Heterocyclic Olefins Using Chiral Diphosphite Ligands. Scope and Limitations", *Journal of Organic Chemistry,* **2009***, 74*(15), 5440.

4. Mazuela, Javier; Verendel, J. Johan; Coll, Mercedes; Schäfner, Benjamin; Börner, Armin; Andersson, Pher G.; Pàmies, Oscar; Diéguez, Montserrat, "Iridium Phosphite−Oxazoline Catalysts for the Highly Enantioselective Hydrogenation of Terminal Alkenes", *Journal of the American Chemical Society*, **2009**, *131* (34), 12344.

5. Mazuela, Javier; Paptchikhine, Alexander; Tolstoy, Päivi; Pàmies, Óscar; Diéguez, Montserrat; Andersson, Pher G., "A New Class of Modular P,N-Ligand Library for Asymmetric Pd-Catalyzed Allylic Substitution Reactions: A Study of the Key Pd-π-Allyl Intermediates", *Chemistry – a European Journal*, **2010**, *16*, 620.

6. Mazuela, Javier; Pàmies, Oscar; Diéguez, Montserrat. "Biaryl Phosphite-Oxazoline Ligands from the Chiral Pool: Highly Efficient Modular Ligands for the Asymmetric Pd-Catalyzed Heck Reaction". *Chemistry -a European Journal*, **2010**, *16*, 3434.

7. Mazuela, Javier; Paptchikhine, Alexander; Pàmies, Oscar; Andersson, Pher G.; Diéguez, Montserrat. "Adaptative Biaryl Phosphite-Oxazole and Phosphite-Thiazole Ligands for Asymmetric Ir-Catalyzed Hydrogenation of Alkenes." *Chemistry -a European Journal*, **2010**, *16*, 4567.

8. Mazuela, Javier; Pàmies, Oscar; Diéguez, Montserrat; Palais, Laetitia; Rosset, Stephane; Alexakis, Alexandre. "Fine-tunable monodentate phosphoroamidite and aminophosphine ligands for Rh-catalyzed asymmetric hydroformylation." *Tetrahedron: Asymmetry*, **2010**, *21*, 2153.

9. Mazuela, Javier; Tolstoy, Paivi; Pàmies, Oscar; Andersson, Pher G.; Diéguez, Montserrat. "Phosphite-oxazole/imidazole ligands in asymmetric intermolecular Heck reaction". *Organic & Biomolecular Chemistry*, **2011**, *9*, 941.

10. Mazuela, Javier; Norrby, Per-Ola; Andersson, Pher G.; Pàmies, Oscar; Diéguez, Montserrat. "Pyranoside Phosphite-Oxazoline Ligands for the Highly Versatile and Enantioselective Ir-Catalyzed Hydrogenation of Minimally Functionalized Olefins. A Combined Theoretical and Experimental Study" *Journal of the American Chemical Society*, **2011**, *133* (34), 13634.

11. Mazuela, Javier; Pàmies, Oscar; Diéguez, Montserrat. "Enantioselective Ir-catalyzed hydrogenation of minimally functionalized olefins using pyranoside phosphinite-oxazoline ligands" submitted to Tetrahedron: Asymmetry.

12. Mazuela, Javier; Pàmies, Oscar; Diéguez, Montserrat. "Phosphite-thiazoline vs phosphite-oxazoline ligands for Pd-catalyzed allylic substitution reactions. A case for comparison" in preparation.

13. Mazuela, Javier; Pàmies, Oscar; Diéguez, Montserrat. "Asymmetric hydrogenation of minimally functionalized olefins using Ir-phosphite-thiazoline catalyst precursors" in preparation.

14. Mazuela, Javier; Pàmies, Oscar; Diéguez, Montserrat. "A new modular phosphite-pyridine ligand library for asymmetric Pd-catalyzed allylic substitution reactions. A study of the key Pd-π-allyl intermediates" in preparation.

15. Mazuela, Javier; Pàmies, Oscar; Diéguez, Montserrat. "A phosphite-pyridine/iridium complex library as highly selective catalysts for the hydrogenation of minimally functionalized olefins" in preparation.

16. Mazuela, Javier; Pàmies, Oscar; Diéguez, Montserrat. "Rh-catalyzed hydroformylation of 1,1'-disubstituted terminal enol esters" in preparation.

9.2. Meetings contributions

1. **Authors**: Javier Mazuela, Oscar Pámies, Montserrat Diéguez, Alexander Paptchikhine, Paivi Kaukoranta, Pher G. Andersson
Title: New heterodonor P,N-ligands for Pd-catalyzed asymmetric allylic substitution reactions
Type of presentation: Pòster
Meeting: COST D40 Innovation II
Place: Tarragona, Spain
Year: May 2008

2. **Authors**: Javier Mazuela, Oscar Pàmies, Montserrat Diéguez, Alexander Paptchikhine, Paivi Kaukoranta, Pher G. Andersson
Title: Screening of P,N-Bidentate Phosphite Ligands in Pd-Catalyzed Asymmetric Allylic Substitution
Type of presentation: Pòster
Meeting: International Symposium on Homogeneous Catalysis XVI (ISHC 2008)
Place: Florence, Italy
Year: July 2008

3. **Authors**: Javier Mazuela, Montserrat Diéguez, Oscar Pàmies, Yvette Mata, Emmanuelle Teuma, Montserrat Gómez, Fabrizio Ribaudo, Piet W. N. M. van Leeuwen
Title: Palladium Nanoparticles in Allylic Alkylations and Heck Reactions: The Molecular Nature of the Catalyst Studied in a Membrane Reactor
Type of presentation: Pòster
Meeting: International Symposium on Relations between Homogeneous and Heterogeneous Catalysis XIV (ISHHC 2009)
Place: Stockholm, Sweden
Year: Setember 2009

4. **Authors**: Oscar Pàmies, Javier Mazuela, Mercedes Coll, Montserrat Diéguez
Title: Diphosphite Ligands for the Rh-Catalyzed Asymmetric Hydroformylation of Heterocyclic Olefins
Type of presentation: Pòster
Meeting: COST D40. Innovation IV meeting.
Place: Ankara. Turkey
Year: May 2010

5. **Authors**: Javier Mazuela, J.Johan Verendel, Mercedes Coll, Benjamin Schäffner, Armin Börner, Pher G. Andersson, Oscar Pàmies, Montserrat Diéguez,
Title: Iridium Phosphite-Oxazoline Catalysts for the Highly Enantioselective Hydrogenation of Terminal Alkenes
Type of presentation: Pòster
Meeting: International Symposium on Homogeneous Catalysis XVII (ISHC 2010)
Place: Poznan, Poland
Year: July 2010

6. **Authors**: Montserrat Diéguez, Javier Mazuela, Oscar Pàmies.
Title: Sugar-based Phosphite-oxazoline Ligands for Enantioselective Ir-catalyzed Hydrogenation of unfunctionalized Olefins
Type of presentation: Pòster
Meeting: International Symposium on Homogeneous Catalysis XVIII (ISHC 2012)
Place: Toulouse, France
Year: July 2012

Tetrahedron: *Asymmetry* 23 (2012) 67–71

Contents lists available at SciVerse ScienceDirect

Tetrahedron: *Asymmetry*

journal homepage: www.elsevier.com/locate/tetasy

Furanoside phosphite–phosphoroamidite and diphosphoroamidite ligands applied to asymmetric Cu-catalyzed allylic substitution reactions

Marc Magre [a], Javier Mazuela [a], Montserrat Diéguez [a,*], Oscar Pàmies [a,*], Alexandre Alexakis [b,*]

[a] Departament de Química Física i Inorgànica, Universitat Rovira i Virgili, Campus Sescelades, C/ Marcel·lí Domingo, s/n. 43007 Tarragona, Spain
[b] University of Geneva, Department of Organic Chemistry, 30, quai Ernest Ansermet, 1211 Genève 4, Switzerland

ARTICLE INFO

Article history:
Received 21 November 2011
Accepted 5 January 2012
Available online 8 February 2012

ABSTRACT

A phosphite–phosphoroamidite and diphosphoroamidite ligand library was applied in the Cu-catalyzed allylic substitution of a range of cinnamyl-type substrates using several organometallic nucleophiles. Results indicated that selectivity depended strongly on the ligand parameters (position of the phosphoroamidite group at either C-5 or C-3 of the furanoside backbone, as well as the configuration of C-3, the introduction of a second phosphoroamidite moiety, the substituents and configurations in the biaryl phosphite/phosphoroamidite moieties), the nature of the leaving group of the substrate and the alkylating reagent. Good enantioselectivities (up to 76%) and activity combined with high regioselectivities were obtained.

1. Introduction

Developing methods for enantioselective carbon–carbon bond formation is one of the key issues in organic synthesis. A versatile method for doing this is transition metal-catalyzed asymmetric allylic substitution with carbon nucleophiles.[1] Great effort has been put into controlling the chemo-, regio-, and enantioselectivities of the reaction. Most asymmetric allylic substitutions have been reported with soft nucleophiles (i.e., malonates and related stabilized anions) and Pd as the metal source, although Mo, W, Ru, Rh, and Ir catalysts have also proved to be effective for these nucleophiles.[1] In contrast, copper allows the use of hard, nonstabilized nucleophiles, such as small alkyl groups in the form of organometallic species.[2] Among the broad range of reagents available, the use of Grignard reagents in the catalyzed asymmetric allylic substitution reaction was first reported by Bäckvall and van Koten, with chiral copper thiolate **1** (Fig. 1), yielding moderate enantiomeric excesses.[3] This pioneering work was soon followed by that of Dübner and Knochel, who reported a highly enantioselective version using a different system based on diorganozinc reagents with ligand **2** (Fig. 1).[4] Since then, most efforts have been directed toward developing new efficient Cu catalysts for these organozinc reagents.[5] An important breakthrough in the use of Grignard reagents was made by Alexakis et al. They reported highly regio- and enantioselective Cu-phosphoroamidite catalyzed allylic substitution of di- and tri-substituted cinnamyl chloride substrates (Fig. 1, ligands type **3**).[6] Other successful ligands have been introduced for stereoselective allylic addition of organomagnesium reagents, such as chiral diaminocarbenes (Fig. 1, ligands type **4**) by Okamoto et al.[7] and more recently ferrocenic bidentate phosphines (Fig. 1, ligand type **5**) by Feringa et al.[8]

Apart from these latter bidentate phosphines, the most successful ligands developed for this transformation are monodentate. However, Alexakis et al. found that the successfully MeO-substituted phosphoroamidite monodentate phosphorus ligands **3** can act as bidentate P,O-ligands.[6b] On the basis of this finding we decided to study a library of bidentate furanoside phosphite–phosphoroamidite and diphosphoroamidite ligands **L1**–**L5a**–**f** in the Cu-catalyzed allylic substitution reaction. These ligands have the same advantages as carbohydrate and phosphite/phosphoroamidite ligands: that is, they are available at low cost, they have high resistance to oxidation, and they have simple modular constructions.[9] Therefore, with this library we fully investigated the effects of systematically varying the position of the phosphoroamidite group at both C-5 (ligands **L1** and **L2**) and C-3 (ligands **L3** and **L4**) of the furanoside backbone, as well as the effects of the configuration at C-3 of the furanoside backbone, the introduction of a second phosphoroamidite moiety (ligands **L5**), and the substituents/configurations in the biaryl phosphite/phosphoroamidite moieties (**a**–**f**). By carefully selecting the best of these elements and using a range of Grignard reagents, we achieved good regio- and enantioselectivities, and activities in different substrate types.

2. Results and discussion

Initially, we evaluated the phosphite–phosphoroamidite and diphosphoroamidite ligand library **L1**–**L5a**–**f** (Fig. 2) in the copper-catalyzed asymmetric allylic alkylation of cinnamyl chloride

* Corresponding authors.
E-mail addresses: montserrat.dieguez@urv.cat (M. Diéguez), oscar.pamies@urv.cat (O. Pàmies), alexandre.alexakis@chiorg.unige.ch (A. Alexakis).

0957-4166/$ - see front matter © 2012 Elsevier Ltd. All rights reserved.
doi:10.1016/j.tetasy.2012.01.003

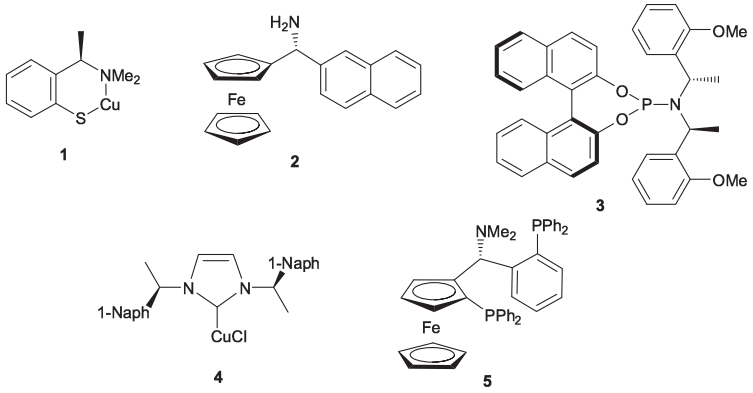

Figure 1. Ligands previously applied in asymmetric Cu-catalyzed allylic substitution reactions.

S1 using EtMgBr as the nucleophile (Eq. 1). The catalytic system was generated in situ by adding the corresponding ligand to a suspension of the catalyst precursor copper thiophene 2-carboxylate (CuTC).

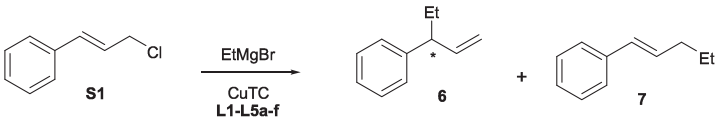

(1)

The results are shown in Table 1. They indicate that regio- and enantioselectivities are affected by the position of the phosphoroamidite group at either C-5 or C-3 of the furanoside backbone, and by the configuration of C-3, the introduction of a second phosphoroamidite moiety, and the substituents and configurations in the biaryl phosphite/phosphoroamidite moieties (**a**–**f**).

We first studied the effect of the position of the phosphoroamidite group at either C-5, ligands **L1** and **L2**, or C-3, ligands **L3** and **L4**, of the furanoside backbone and the configuration of C-3. We observed a cooperative effect between the position of the phosphoroamidite group and the configuration of carbon atom C-3 of the furanoside backbone. The results indicate that the best combination of these ligand parameters is achieved with ligands **L2**, whose phosphoroamidite moiety is attached to C-5 and which have an (*R*)-configuration of carbon atom C-3 on the tetrahydrofuran ring (Table 1, entries 1–4).

We then used ligands **L5** to study how catalytic performance was affected by replacing the phosphite moiety with a phosphoroamidite group in preferred ligands **L2**. The results indicated that the presence of a second phosphoroamidite moiety in the ligands had a negative effect on enantioselectivity (Table 1, entries 5 vs 2).

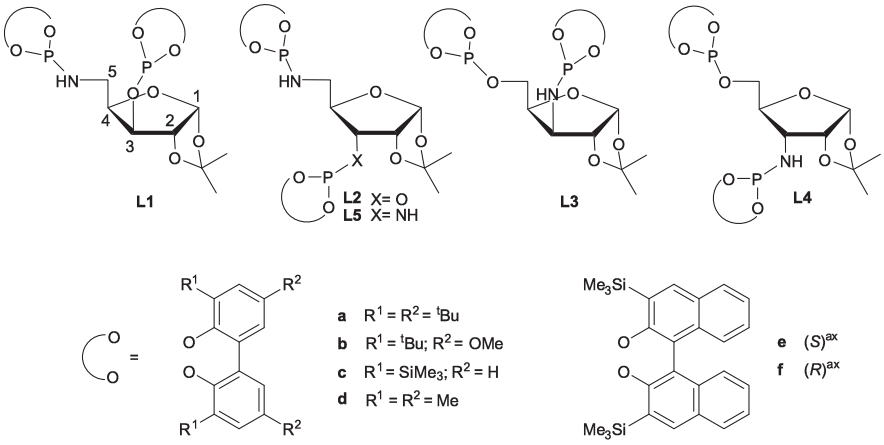

Figure 2. Furanoside-based phosphite–phosphoroamidite and diphosphoroamidite ligand library **L1**–**L5a**–**f**.

Table 1
Selected results for the Cu-allylic substitution of cinnamyl chloride with EtMgBr using ligands **L1–L5a–f**[a]

Entry	L	% Conv[b]	**6/7**[c]	% ee[d]
1	**L1a**	100	94/6	39 (*S*)
2	**L2a**	99	97/3	60 (*S*)
3	**L3a**	100	88/12	3 (*S*)
4	**L4a**	100	92/8	38 (*S*)
5	**L5a**	100	96/4	12 (*S*)
6	**L2b**	100	95/5	48 (*S*)
7	**L2c**	100	96/4	32 (*S*)
8	**L2d**	100	97/3	6 (*S*)
9	**L2e**	90	95/5	43 (*S*)
10	**L2f**	96	96/4	16 (*R*)
11[e]	**L2a**	99	98/2	70 (*S*)

[a] Reaction conditions: CuTC (1 mol %), ligand (1 mol %), EtMgBr (1.2 equiv, 1.2 mmol), **S1** (1 mmol), CH_2Cl_2 (2 mL), $T = -50$ °C.
[b] Conversion determined by GC after 1 h.
[c] Regioselectivity determined by GC.
[d] Enantiomeric excess determined by GC on a Supelco β-DEX 120 column.
[e] Reaction carried out at −78 °C.

We next studied the effects of the biaryl phosphite/phosphoroamidite moieties using ligands **L2a–f** (Table 1). We found that these moieties mainly affected enantioselectivity, while their effect on regioselectivity was less important. Results indicated that bulky substituents at both *ortho* and *para* positions of the biphenyl phosphite/phosphoroamidite moieties need to be present if enantioselectivities are to be high (Table 1, entries 2 vs 6–8). This indicates that bulky substituents are necessary to control the tropoisomerization of the biaryl phosphite/phosphoroamidite moieties in the catalytic active species. Similar behavior has been observed for other phosphite/phosphoroamidite based ligands in other metal-catalyzed asymmetric transformations.[10] Moreover, the presence of bulky enantiopure binaphthyl moieties (**e–f**) did not further improve enantioselectivity (Table 1, entries 2 vs 9–10). This suggests that in ligand **L2a**, the biphenyl moiety attached to the phosphoroamidite adopts a configuration that is different from that of the configuration of the biphenyl phosphite moiety.

To sum up, the best result was obtained with ligand **L2a**, which contains the optimal combination of ligand parameters. These results clearly show the efficiency of highly modular scaffolds in ligand design. Regio- and enantioselectivities can be improved by controlling not only the structural but also the reaction parameters. In this case, both regio- and enantioselectivities were further improved (98% regioselectivity with 70% ee) with ligand **L2a** by lowering the reaction temperature to −78 °C (Table 1, entry 11).

It has been shown that the catalytic performance for this transformation is highly dependent on a subtle balance between the nature of the leaving group, the type of organometallic reagent, and the copper source among other reaction parameters.[2] So we next investigated whether the performance of our CuTC/**L2a** catalytic system can be improved by using other leaving groups in the substrate and by using dialkylzincs instead of Grignard reagents. The results are summarized in Table 2. Using EtMgBr, we found that the replacement of the chloride leaving group by a bromide **S2** or phosphonate group **S3** leads to lower regio- and enantioselectivities (Table 2, entries 2 and 3 vs 1). On the other hand, the use of dialkylzincs instead of Grignard reagents for the allylic substitution of cinnamyl halides **S1** and **S2** leads to significantly lower regio- and enantioselectivities (Table 2, entries 4 and 5 vs 1 and 2, respectively). However, for phosphonate **S3,** enantioselectivity and to a lesser extent regioselectivity increased when $ZnEt_2$ was used, but at the cost of activity (Table 2, entry 6 vs 3). Finally, and on the basis of our previous results on Cu-catalyzed conjugate addition which show that for some substrates the combination of dialkylzincs with $CuOTf_2$ leads to higher enantioselectivities, we decided to assess the use of $CuOTf_2$ as a source of copper. Unfortunately, no improvement in the catalytic performance was observed (Table 2, entries 7 and 8 vs 4 and 5, respectively).

Finally, we investigated the allylic substitution of a range of cinnamyl type chlorides with various Grignard reagents. Cinnamyl chloride **S1** reacts with methyl and *n*-propyl Grignard reagents as EtMgBr does (Table 3, entries 2 and 3 vs 1). However, the use of a secondary Grignard reagent, ^{i}PrMgBr, decreases both regio- and enantioselectivities (Table 3, entry 4 vs 1). Regarding the substrate scope, Table 3 shows that electron-donating groups at the *para* position of the phenyl group, substrate **S4**, slightly decrease both regio- and enantioselectivities (Table 3, entries 5 and 6 vs 1 and 4, respectively), while electron-withdrawing groups, substrate **S5**, slightly increase enantioselectivities (Table 3, entries 7 and 8 vs 1 and 4, respectively). Interestingly, the allylic substitution of 2-(3-chloro-propenyl)-naphthalene **S6** provided the highest

Table 2
Selected results for Cu-catalyzed allylic alkylation of several cinnamyl halides **S1–S2** and phosphonate **S3** using EtMgBr and $ZnEt_2$[a]

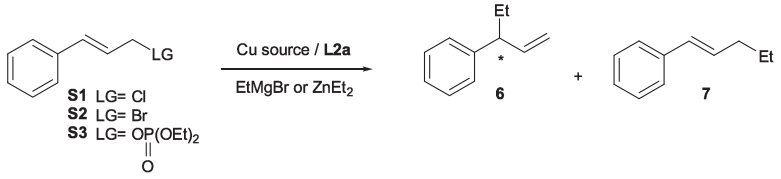

Entry	Cu salt	Substrate	Organometallic reagent	% Conv[b]	**6/7**[c]	% ee[d]
1	CuTC	**S1**	EtMgBr	99	97/3	60 (S)
2	CuTC	**S2**	EtMgBr	100	92/8	53 (S)
3	CuTC	**S3**	EtMgBr	85	70/30	42 (*S*)
4	CuTC	**S1**	$ZnEt_2$	100	84/16	39 (*S*)
5	CuTC	**S2**	$ZnEt_2$	100	78/22	44 (*S*)
6	CuTC	**S3**	$ZnEt_2$	40	75/25	55 (*S*)
7	$CuOTf_2$	**S1**	$ZnEt_2$	92	82/18	36 (*S*)
8	$CuOTf_2$	**S2**	$ZnEt_2$	85	70/30	46 (*S*)

[a] Reaction conditions: CuTC (1 mol %), ligand (1 mol %), EtMgBr (1.2 equiv, 1.2 mmol), **S1** (1 mmol), CH_2Cl_2 (2 mL), $T = -50$ °C.
[b] Conversion determined by GC after 1 h.
[c] Regioselectivity determined by GC.
[d] Enantiomeric excess determined by GC on a Supelco β-DEX 120 column.

Table 3
Selected results for the Cu-catalyzed asymmetric allylic substitution of a range of cinnamyl-type chlorides with various Grignard reagents[a]

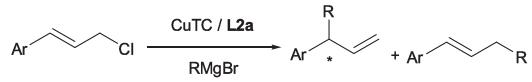

S1 Ar= Ph
S4 Ar= 4-Me-C_6H_4
S5 Ar= 4-MeO-C_6H_4
S6 Ar= 2-Naph

Entry	Substrate	R	% Conv[b]	γ/α[c]	% ee[d]
1	**S1**	Et	99 (95)	97/3	60 (*S*)
2	**S1**	Me	98 (94)	98/2	59 (*S*)
3	**S1**	^{n}Pr	99 (96)	97/3	59 (*S*)
4	**S1**	^{i}Pr	98 (92)	92/8	35 (*S*)
5	**S4**	Et	100 (93)	93/7	54 (*S*)
6	**S4**	^{i}Pr	100 (91)	88/12	32 (*S*)
7	**S5**	Et	99 (94)	97/3	62 (*S*)
8	**S5**	^{i}Pr	100 (90)	92/8	40 (*S*)
9	**S6**	Et	100 (92)	96/4	68 (*S*)
10	**S6**	Me	100 (94)	96/4	67 (*S*)
11	**S6**	^{n}Pr	100 (96)	95/5	67 (*S*)
12	**S6**	^{i}Pr	100 (92)	90/10	41 (*S*)
13[e]	**S6**	Et	100 (91)	96/4	76 (*S*)
14[e]	**S6**	Me	100 (95)	97/3	73 (*S*)

[a] Reaction conditions: CuTC (1 mol %), **L2a** (1 mol %), RMgBr (1.2 equiv, 1.2 mmol), substrate (1 mmol), CH_2Cl_2 (2 mL), $T = -50$ °C.
[b] Conversion determined by GC after 1 h. In parentheses the isolated yield of the mixture of regioisomers.
[c] Regioselectivity determined by GC.
[d] Enantiomeric excess determined by GC on a Supelco β-DEX 120 column.
[e] Reaction performed at −78 °C.

enantioselectivities (ee's up to 76%, Table 3, entries 9–14) while maintaining excellent regioselectivity.

3. Conclusion

A library of furanoside phosphite–phosphoroamidite and diphosphoroamidite was applied in the Cu-catalyzed allylic substitution of a range of cinnamyl-type substrates using several organometallic nucleophiles. Good enantioselectivities (up to 76%) and activity combined with high regioselectivities were obtained. Systematically varying the position of the phosphoroamidite group, at either C-5 or C-3 of the furanoside backbone, as well as the configuration of C-3 and several substituents and configurations in the biaryl phosphite/phosphoroamidite moieties had a strong effect on the rate and selectivity. Enantioselectivity was the best with the catalyst precursor containing ligand **L2a**, which has the optimal combination of ligand parameters.

Our results also showed that the nature of the leaving group of the substrate and the alkylating reagent also plays an important role in determining activity and regio- and enantioselectivities.

4. Experimental

4.1. General considerations

All syntheses were performed using standard Schlenk techniques under argon atmosphere. Solvents were purified by standard procedures. Ligands **L1**–**L5a**–**f**[11] and substrates **S3**–**S6**[12] were prepared by previously described methods. All other reagents were used as commercially available.

4.2. General procedure for the Cu-catalyzed enantioselective allylic substitution

A dried Schlenk tube was charged with the copper salt (1 mol %) and the chiral ligand (1 mol %). Dichloromethane (2 mL) was added and the mixture was stirred at room temperature for 30 min. The allylic chloride (1 mmol) was introduced dropwise and the reaction mixture was stirred at room temperature for a further 5 min before being cooled to −50 °C. Grignard reagent (2–3 M in diethyl ether, 1.2 equiv) in dichloromethane (0.5 mL) was added for 40 min via syringe pump. Once the addition was complete the reaction mixture was left at −50 °C for one hour. The reaction was then quenched by the addition of aqueous hydrochloric acid (1 N, 2 mL). Diethyl ether (10 mL) was added and the aqueous phase was separated and extracted further with diethyl ether (3 × 3 mL). The combined organic fractions were washed with brine (5 mL), dried over anhydrous sodium sulfate, filtered, and reduced in vacuo. Conversion and regioselectivity were determined by ^{1}H NMR, and enantiomeric excess was determined by GC.[6a] The absolute configuration of the alkylation products has been assigned by comparing the retention times with those obtained with enantioenriched samples prepared according to the literature.[6a] The oily residue was purified by flash column chromatography (eluent = pentane) to yield the product as a mixture of S_N2' and S_N2 regioisomers.[6a]

Acknowledgements

We thank Dr. Eva Raluy for her help on the preliminary catalyst results. We would also like to thank the Spanish Government for providing grants CTQ2010-15835, and 2008PGIR/07 to O. Pàmies and 2008PGIR/08 to M. Diéguez, the Catalan Government for grant 2009SGR116, and the ICREA Foundation for providing M. Diéguez and O. Pàmies with financial support through the ICREA Academia awards.

References

1. For reviews, see: (a) Trost, B. M.; Lee, C. In *Catalytic Asymmetric Synthesis*; Ojima, I., Ed., 2nd ed.; Wiley: New York, 2000; p 593; (b) Pfaltz, A.; Lautens, M. In *Comprehensive Asymmetric Catalysis I–III*; Jacobsen, E. N., Pfaltz, A., Yamamoto, H., Eds.; Springer: Berlin, 1999; p 833; (c) Trost, B. M.; van Vranken, D. L. *Chem. Rev.* **1996**, *96*, 395; (d) Johannsen, M.; Jorgensen, K. A.

Chem. Rev. **1998**, *98*, 1689; (e) Helmchen, G.; Pfaltz, A. *Acc. Chem. Res.* **2000**, *33*, 336; (f) Takeuchi, R. *Synlett* **2002**, 1954; (g) Trost, B. M.; Crawley, M. L. *Chem. Rev.* **2003**, *103*, 2921; (h) Miyabe, H.; Takemoto, Y. *Synlett* **2005**, 1641; (i) Martín, E.; Diéguez, M. C. R. *Chemie* **2007**, *10*, 188; (j) Lu, Z.; Ma, S. *Angew. Chem., Int. Ed.* **2008**, *47*, 258; (k) Diéguez, M.; Pàmies, O. *Acc. Chem. Res.* **2010**, *43*, 312.

2. For specific reviews on Cu-catalyzed allylic alkylation reactions, see: (a) Yorimitsu, H.; Oshima, K. *Angew. Chem., Int. Ed.* **2005**, *44*, 4435; (b) Kar, A.; Argade, N. P. *Synthesis* **2005**, 2995; (c) Alexakis, A.; Malan, C.; Lea, L.; Tissot-Croset, K.; Polet, D.; Falciola, C. *Chimia* **2006**, *60*, 124; (d) Alexakis, A.; Bäckvall, B.; Krause, N.; Pàmies, O.; Diéguez, M. *Chem. Rev.* **2008**, *108*, 2796; (e) Falciola, C. A.; Alexakis, A. *Eur. J. Org. Chem.* **2008**, 3765; (f) Harutyunyan, S. R.; den Hartog, T.; Geurts, K.; Minnaard, A. J.; Feringa, B. L. *Chem. Rev.* **2008**, *108*, 2824.
3. (a) van Klaveren, M.; Persson, E. S. M.; del Villar, A.; Grove, D. M.; Bäckvall, J. E.; van Koten, G. *Tetrahedron Lett.* **1995**, *36*, 3059; (b) Karlstrom, A. S. E.; Huerta, F. F.; Meuzelaar, G. J.; Bäckvall, J. E. *Synlett* **2001**, 923.
4. (a) Dübner, F.; Knochel, P. *Angew. Chem., Int. Ed.* **1999**, *38*, 379; (b) Dübner, F.; Knochel, P. *Tetrahedron Lett.* **2000**, *41*, 9233.
5. More recently, triorganomaluminum reagents and organoboronates have also been successfully applied to this process. See, for instance: (a) Bournaud, C.; Falciola, C.; Lecourt, T.; Rosset, S.; Alexakis, A.; Micouin, L. *Org. Lett.* **2006**, *8*, 3581; (b) Lee, Y.; Akiyama, K.; Gillingham, D. G.; Brown, K.; Hoveyda, A. H. *J. Am. Chem. Soc.* **2008**, *130*, 446; (c) Pineschi, M.; Del Moro, F.; Crotti, P.; Macchia, F. *Org. Lett.* **2005**, *7*, 3605; (e) Ito, H.; Ito, S.; Sasaki, Y.; Matsuura, K.; Sawamura, M. *J. Am. Chem. Soc.* **2007**, *129*, 14856.
6. (a) Alexakis, A.; Croset, K. *Org. Lett.* **2002**, *4*, 4147; (b) Tissot-Croset, K.; Polet, D.; Alexakis, A. *Angew. Chem., Int. Ed.* **2004**, *43*, 2426; (c) Falciola, C. A.; Tissot-Croset, K.; Alexakis, A. *Angew. Chem., Int. Ed.* **2006**, *45*, 5995; (d) Falciola, C. A.; Alexakis, A. *Angew. Chem., Int. Ed.* **2007**, *46*, 2619.
7. (a) Tominaga, S.; Oi, Y.; Kato, T.; An, D. K.; Okamoto, S. *Tetrahedron Lett.* **2004**, *45*, 5585; (b) Okamoto, S.; Tominaga, S.; Saimo, N.; Kase, K.; Shomoda, K. *J. Organomet. Chem.* **2005**, *690*, 6001.
8. Lopez, F.; van Zijl, A. W.; Minaard, A. J.; Feringa, B. L. *Chem. Commun.* **2006**, 409.
9. See for instance: (a) Feringa, B. L. *Acc. Chem. Res.* **2000**, *33*, 346; (b) Diéguez, M.; Pàmies, O.; Claver, C. *Chem. Rev.* **2004**, *104*, 3189; (c) Woodward, S.; Diéguez, M.; Pàmies, O. *Coord. Chem. Rev.* **2007**, *2010*, 254; (d) Diéguez, M.; Ruiz, A.; Claver, C. *Dalton Trans.* **2003**, 2957; (e) Diéguez, M.; Pàmies, O.; Ruiz, A.; Claver, C. In *Methodologies in Asymmetric Catalysis*; Malhotra, S. V., Ed.; American Chemical Society: Washington DC, 2004; (f) Diéguez, M.; Pàmies, O.; Claver, C. *Tetrahedron: Asymmetry* **2004**, *15*, 2113; (g) Minnaard, A. J.; Feringa, B. L.; Lefort, L.; de Vries, J. G. *Acc. Chem. Res.* **2007**, *40*, 1267; (h) Börner, A. *Phosphorus Ligands in Asymmetric Catalysis*; Wiley-VCH: Weinheim, 2008; (i) van Leeuwen, P. W. N. M.; Kamer, P. C. J.; Claver, C.; Pàmies, O.; Diéguez, M. *Chem. Rev.* **2011**, *111*, 2077.
10. The rapid ring inversions (tropoisomerization) in the biaryl phosphite/phosphoroamidite moieties are usually stopped upon coordination to the metal center when bulky substituents are present. See for example: (a) Buisman, G. J. H.; van der Veen, L. A.; Klootwijk, A.; de Lange, W. G. J.; Kamer, P. C. J.; van Leeuwen, P. W. N. M.; Vogt, D. *Organometallics* **1997**, *16*, 2929; (b) Diéguez, M.; Pàmies, O.; Ruiz, A.; Claver, C.; Castillón, S. *Chem. Eur. J.* **2001**, *7*, 3086; (c) Pàmies, O.; Diéguez, M.; Net, G.; Ruiz, A.; Claver, C. *Organometallics* **2000**, *19*, 1488; (d) Pàmies, O.; Diéguez, M.; Net, G.; Ruiz, A.; Claver, C. *J. Org. Chem.* **2001**, *66*, 8364; (e) Pàmies, O.; Diéguez, M. *Chem. Eur. J.* **2008**, *14*, 944.
11. (a) Diéguez, M.; Ruiz, A.; Claver, C. *Chem. Commun.* **2001**, 2702; (b) Diéguez, M.; Ruiz, A.; Claver, C. *Tetrahedron: Asymmetry* **2001**, *12*, 2827; (c) Raluy, E.; Claver, C.; Pàmies, O.; Diéguez, M. *Org. Lett.* **2007**, *9*, 49; (d) Raluy, E.; Pàmies, O.; Diéguez, M. *Adv. Synth. Catal.* **2009**, *351*, 1648; (e) Raluy, E.; Diéguez, M.; Pàmies, O. *J. Org. Chem.* **2007**, *72*, 2842.
12. Tissot-Croset, K. PhD Thesis, University of Geneva, 2005.